National Aeronautics
and Space Administration

The World's Largest Wind Tunnels

Their History, Contributions to Aeronautics, and Importance to Flight

A History of the NASA Ames 40- by 80-Foot
and 80- by 120-Foot Wind Tunnels

Kenneth W. Mort

U.S. AIR FORCE

The World's Largest Wind Tunnels

Their History, Contributions to Aeronautics, and Importance to Flight

A History of the NASA Ames 40- by 80-Foot and
80- by 120-Foot Wind Tunnels

Kenneth W. Mort

Cover Photos

National Full-Scale Aerodynamics Complex at top, original 40- by 80-Foot Wind Tunnel middle left, and Douglas BTD-1 aircraft in the 40- by 80-foot test section below it. McDonnell Douglas F-18 at high angle of attack in the 80- by 120-foot test section at middle right.

NASA/SP-20205009237

The World's Largest Wind Tunnels

Their History, Contributions to Aeronautics, and Importance to Flight

A History of the NASA Ames 40- by 80-Foot and
80- by 120-Foot Wind Tunnels

Kenneth W. Mort

National Aeronautics and
Space Administration

Ames Research Center
Moffett Field, California 94035-1000

December 2020

ISBN: 978-0-578-81608-1

Available from:

NASA STI Support Services
Mail Stop 148
NASA Langley Research Center, Hampton, VA 23681-2199
(757) 864-9658

National Technical Information Service
5301 Shawnee Road, Alexandria, VA 22312
info@ntis.gov
(703) 605-6050

This book is also available in electronic form at
http://ntrs.nasa.gov

Dedication

This book is dedicated to my wife, Irene, who for many years was exceptionally patient putting up with my boxes of files strewn all over the house and especially for putting up with the many hours I spent researching and writing this NFAC history.

Acknowledgments

There were many very important contributors to this book, however the author is solely responsible for all content and any errors that might have occurred. Mark Betzina contributed to the management history. Vic Corsiglia contributed to the section on wake-vortex effects and general aviation engine cooling. John Dusterberry wrote about the drive development. Jerry Kirk contributed to the sections on lift fans and lift jets, and the F-111 and F-16 forebodies. Paul Soderman wrote a section on the start of acoustics research. Others contributed comments and/or suggestions: Tom Aiken, Glenn Bugos, Mike Dudley, Bill Eckert, Michael Falarski, Hugh Feldmann, Louise Feldmann, T. J. Forsyth, April Gage, Jonathan Gesek, Roy Harris, Mike Herrick, Larry Meyn, Irene Mort, Tim Naumowicz, Dan Petroff, James Ross, Vernon Rossow, Joe Sacco, Nina Scheller, Keith Venter, and William Warmbodt. Layne Karafantis was a big help editing an early draft and offering many useful suggestions. Alyna Anderson was very helpful and did preliminary editing and worked on the test lists as well as on figure and reference numbering. Wayne Johnson added figures, added text describing rotorcraft, and laid out the photos for the cover. Catherine Dow was the professional editor and exhibited much patience, skill, and guidance in performing the final editing and formatting. Her efforts were much appreciated. Much help was received from Don Richey and Lynn Albaugh finding and scanning photographs and was greatly appreciated.

Table of Contents

Introduction 1

PART I. DESIGN AND CONSTRUCTION

Chapter 1. Design, Construction, and Modifications of the 40- by 80-Foot Wind Tunnel, 1941–1957 9
- Design 9
- Construction and Repairs 15

Chapter 2. Wind Tunnel Modifications and Repairs, NASA 1958–1980 31
- Repairs 31
- Modifications 34

Chapter 3. Major Upgrades, 1980–1987 39
- Background 39
- Modification of the 40- by 80-Foot Wind Tunnel: Repowering and the Addition of the 80- by 120-Foot Test Section 41
- Repair and Reliability Improvements 67
- Dedication of the National Full-Scale Aerodynamics Complex (NFAC) 70

Chapter 4. Additional Modifications and Repairs After 1987 71
- Acoustic Walls in 40- by 80-Foot Test Section 71
- Fan Blade Repair 72
- Drive Motor Repair 74
- Data Collection and Control Improvements 74

PART II. OPERATION AND MANAGEMENT HISTORY

Chapter 5. NACA Operation, 1944–1958 75
- Staffing, Organization, and Operations 75
- Model Design, Construction, and Instrumentation 78

Chapter 6. NASA Operation, 1958–2003 79
- Organizational Changes 79
- Full-Cost Accounting and Recovery 79
- NFAC Tunnels Shut Down October 2003 83

Chapter 7. U.S. Air Force Operation, 2005–Present 85
- Resumption of Tunnel Operation 85
- Facility Refurbishment 85

Table of Contents (cont.)

PART III. RESEARCH HISTORY

Chapter 8. NACA Research, 1944–1958 89
Overview 89
Calibrations 90
Fixed-Wing Aircraft and Large-Scale Models 91
Propellers 139
Rotorcraft 145
Chapter 9. NASA Research, 1958–1980 149
Overview 149
Airplanes and Large-Scale Airplane Models 149
Rotorcraft 180
V/STOL 201
Jet-Engine-Powered Lift 262
Space Related 278
Acoustics 298
Miscellaneous 302
Chapter 10. Research and Testing, 1987–2014 305
Overview 305
Rotorcraft 305
V/STOL 319
Conventional Fixed-Wing Aircraft 325
Space Related 338
Acoustics 343
Miscellaneous 347

PART IV. CONCLUDING REMARKS, REFERENCES, AND APPENDICES

Chapter 11. Concluding Remarks 359
Chapter 12. References 361
Bibliographic Essay 361
List of References 362
Appendix A. Dates of Important Events 381
Appendix B. List of NFAC Tests 383
Table B1. History of Tests in the 40- by 80-Foot Wind Tunnel 384
Table B2. History of Tests in the 80- by 120-Foot Wind Tunnel 407

Introduction

The Wright brothers, Orville and Wilbur, not only invented the airplane, they also pioneered the practice of doing systematic wind tunnel experiments on wing shapes for gliders and airplanes in a wind tunnel they built at their bicycle shop in Dayton, Ohio. They had found that airfoil or wing aerodynamic characteristics (based on simple experiments) in the scientific literature were limited, in error, or inconsistent, and gave them erroneous data when they designed and built their gliders and tried to fly them at Kitty Hawk, North Carolina, at the turn of the 20th century. It became evident to the brothers that aerodynamic experiments were required to acquire reliable data for their designs. As a result, the Wright brothers decided to perform some simple aerodynamic experiments on airfoils or wings.

After a few preliminary experiments using a simple balance mounted on the front of a bicycle and a crude wind tunnel made from a wooden box, they built a simple wind tunnel, 6 feet long with a 16-inch-square test section, in the back of their bicycle shop in 1901 (Fig. 1). A propeller at one end blew air down the duct to the test section in which they tested various wing shapes. Their model wings had various spans up to about a foot and were mounted to a simple balance system in the test section. The Wright brothers were much more focused, systematic, and comprehensive than previous experimenters had been. They varied angle of attack for airfoils with different aspect ratios (span-to-chord ratios), cambers, thicknesses, and planforms.

Wind tunnels had been used for determining wind loads on structures and various shapes for more than 30 years before the Wright brothers built their simple wind tunnel, but previous experimenters had been much less focused as far as airfoil or wing aerodynamics were concerned. The Wrights' procedures for using wind tunnel data for their glider and airplane-wing designs set a precedent for airplane design that continues to this day.

Today's wind tunnels are, of course, much more sophisticated than the Wright brothers' simple wind tunnel and are widely used for testing airplane models and airplanes. Various transducers and instruments are attached to the test models and then hooked up to measuring and recording instrumentation typically located external to the test section. Such instrumentation can be employed because most of the equipment is located out of the airstream and therefore not restricted in weight or size.

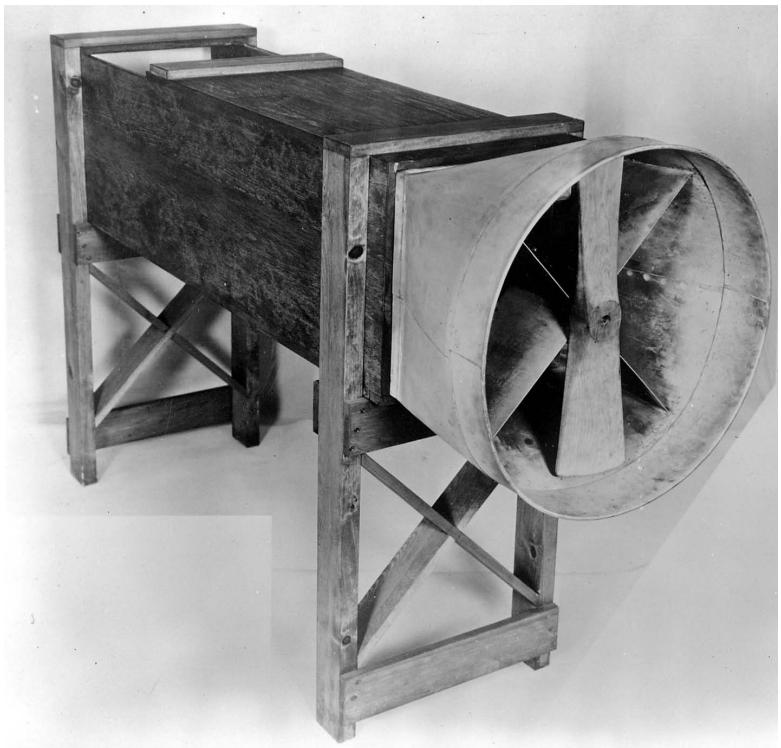

Figure 1. Wright Brothers' wind tunnel (1901).
(NASM-SI-2003-12979)

After the invention of the airplane in 1903, many European countries recognized the potential importance of the airplane before the United States did, and they took the lead in aircraft development. Subsequently recognizing the potential importance of aviation, the National Advisory Committee for Aeronautics (NACA) was created in 1915 by the United States Congress to advance the science of aeronautics in the United States. The first NACA research laboratory was the Langley Memorial Aeronautical Laboratory (now the Langley Research Center), which was built in Hampton, Virginia, in 1917. As wind tunnels had demonstrated their value in the development of aircraft, the NACA built several wind tunnels for aerodynamic research very early on. Reference [1] is an excellent summary of the history, need for, and use of wind tunnels. Several wind tunnels were built at Langley including the Full-Scale Wind Tunnel (or the 30- by 60-Foot Wind Tunnel—its test section was 30 feet high and 60 feet wide), which was completed in 1931, when biplanes and dirigibles were the dominant aircraft. The 30- by 60-Foot Wind Tunnel was later used for testing full-scale fighter aircraft and subsequently free-flight models of many aircraft until it was shut down and demolished in 2010. See reference [2] for a description of the tunnel and reference [3] for an excellent history of the tunnel from construction to demolition.

The second NACA laboratory constructed was the Ames Aeronautical Laboratory (now Ames Research Center), established on December 20, 1939, at Moffett Field, California. Moffett Field was a naval air base south of San Francisco and near Mountain View, California. It was judged prudent to locate the laboratory on the West Coast to be closer to the numerous airplane companies there and to be near sufficient land and electrical power. Moffett Field was an ideal site. Several history books have been written describing the evolution of the Center up to 2014. See reference [4] for a history of the Center from 1940 to 1965, and references [5-8] for updates to 2014.

The 40- by 80-Foot Wind Tunnel was conceived in the late 1930s as airplanes were getting bigger and faster. It was built at the newly established Ames Aeronautical Laboratory. The usable maximum test airspeed in the existing Langley Memorial Aeronautical Laboratory Full-Scale Wind Tunnel was considered too slow to test newer aircraft; it was less than 100 miles per hour (mph), and airplane landing speeds were increasing to well over this amount. In addition, a larger test section was needed because airplanes were getting larger, and whenever possible, the practice was to test actual airplane prototypes because small-scale model tests often suffered from Reynolds number or scale (size) effects. (Reynolds number is the ratio of inertial forces to viscous forces. Laminar flow occurs at low Reynolds numbers where viscous forces are dominant; turbulent flow occurs at high Reynolds numbers. For subsonic airflow, Reynolds number can be thought of as a scale effect.) Model experiments often excluded the effects of construction details such as rivets, gaps, and seams. Airplane configurations were often modified during construction of prototypes or production airplanes, which affected the aerodynamics after the model studies had been performed. For example, it was common for the military to add antennas and weapons to fighters that were very rarely modeled, or not modeled correctly, and these modifications could produce higher drag increases and therefore lower maximum airspeeds than were expected or required.

The 40- by 80-Foot Wind Tunnel was designed, and construction overseen, by a group at Langley Memorial Aeronautical Laboratory, led by Smith J. DeFrance. Many in the group had

worked on the design of the Full-Scale Wind Tunnel at Langley and had learned from this experience. The new, larger Ames tunnel was a marked improvement but still conservative in design. Its performance, however, exceeded all expectations. The tunnel began operation in the summer of 1944 (Fig. 2).

In the early days of its operation, much of the testing was on fighter and other military aircraft prototypes. After World War II more basic research was conducted including investigations to improve the landing and takeoff performance of aircraft. Landing and takeoff configurations were always a major design compromise. Even retracted landing gear can produce significant drag, and the wing flaps required for increasing lift at landing and takeoff cause complexities in the wing structure and can, if not carefully designed, increase drag when they are retracted. As aircraft airspeeds increased, wing sweep became important to reduce drag at the higher cruise speeds. Engineers found, however, that wing sweep reduced lift substantially at landing and takeoff airspeeds. Therefore, the effect of wing sweep on lift and drag and flap effectiveness at landing and takeoff conditions became very important for study.

Over the years, research emphasis slowly changed from drag cleanup and improved landing and takeoff performance for conventional landing aircraft, to vertical and/or short takeoff and landing (V/STOL) aircraft, rotorcraft, and space-related research. Because jet engines and gas turbines produce high energy and are relatively lightweight, V/STOL aircraft became more viable. If practical V/STOL aircraft could be developed, runway lengths could be reduced or possibly runways could even be eliminated. In addition, there was a goal to increase rotorcraft speed, improve reliability, and reduce vibration and noise, which warranted major research.

Figure 2. External overhead view of the completed 40- by 80-Foot Wind Tunnel. ***(NACA A-13516)***

The increased interest in space science resulted in tunnel research on recovery systems such as parachutes and drag devices, and on spacecraft such as lifting bodies and the Space Shuttle. Acoustic measurements became important, and after the feasibility of making acoustic measurements in the wind tunnel was established, many wind tunnel investigations included acoustic measurements and studies.

Comparing theoretical aerodynamics with experimental aerodynamics was a routine part of the research performed in the 40- by 80-Foot Wind Tunnel. Personnel at the tunnel included experts in theoretical aerodynamics such as John DeYoung, Bill Evans, Larry Olson, Vernon Rossow, and Wayne Johnson. Areas of investigation included defining wing stall boundaries, modeling multi-energy flows, modeling component interfaces, identifying boundary conditions, and developing theoretical aerodynamics and modeling for rotorcraft. In addition, theories were developed under contract for specialized problem areas to improve aeronautical expertise and to enable design of more effective experiments in the tunnel. Specific measurements that assisted in improving theories were an important element of the research performed in the wind tunnel. Investigations of rotorcraft, propellers, and wind turbines identified specific areas of inquiry for theoretical aerodynamics, many of which remain under investigation today.

It also became more important to perform research in areas where Reynolds number was an important variable, because many small-scale, low Reynolds number model experiments were of configurations that were sensitive to Reynolds number effects. This was especially true for most high-lift devices, V/STOL aircraft, and rotorcraft. As mentioned earlier, for subsonic airflow Reynolds number can be thought of as a scale or size effect. Going from low Reynolds number to high Reynolds number can result in significant changes in the flow characteristics such as going from laminar flow to turbulent flow. Increased turbulence typically delays flow separation and wing stall.

After about 30 successful years of performing research on a wide variety of models and aircraft, the limitations of the 40- by 80-Foot Wind Tunnel began to become evident during research and development of new aircraft. Its test section was judged too small for performing many V/STOL and rotorcraft tests at low speeds. At low speeds, the wake angles produced by rotors, propellers, and jets can be large and can produce large wind tunnel wall effects. Interaction of the wakes with the wind tunnel floor would occasionally produce flow recirculation at the models, which caused unrealistic airflows in the test section and at the model. In addition, there was heightened interest in increasing the flight speeds of rotorcraft. As a result, NASA studies considered the viability of constructing larger and faster subsonic wind tunnels (colloquially called “super tunnels” at the time), and also considered making modifications to existing wind tunnels. As a result of these studies, NASA management concluded (with encouragement from Ames) that it would be cost-effective to repower the 40- by 80-Foot Wind Tunnel for higher-speed testing of rotorcraft, and to add an 80- by 120-foot test section for testing larger aircraft, rotorcraft, and V/STOL aircraft at low airspeeds. The new test section would share the drive of the 40- by 80-Foot Wind Tunnel. New, larger wind tunnels were estimated to cost an order of magnitude more. NASA management believed that the modified 40- by 80-Foot Wind Tunnel would satisfy the majority of the large-scale low-speed aeronautic requirements well into the future.

The modified facility, which included two wind tunnels and an outdoor test facility, was renamed the National Full-Scale Aerodynamics Complex (NFAC). Figure 3 shows the wind tunnels, with the 40- by 80-foot test section on the left, and the 80- by 120-foot test section on the right. The

Outdoor Aerodynamic Research Facility (OARF) (Fig. 4) was used for checkout testing of powered models and aircraft before entry into the wind tunnels. It was, however, also capable of performing static and ground-effect studies using variable-height struts and was often used for this purpose. By using load cells or scales internal to the model, it had the capability for measuring the forces and moments on the aircraft.

During the repowering of the 40- by 80-Foot Wind Tunnel, a 6-inch-thick acoustic liner was installed on the inside of the test-section walls. As acoustic measurements were being taken during much of the wind tunnel aerodynamic research, reverberation from the steel walls was one of the limiting factors, and this step was designed to attenuate the problem.

Integrated systems testing (IST) began in December 1981 and was nearly completed when a serious accident occurred on December 9, 1982. The vane set upstream of the drive collapsed, which destroyed the fan blades and caused significant damage to the wind tunnel. An accident board was convened. The accident board recommended repairs as well as implementation of significant upgrades that had been identified during the IST. NASA headquarters (HQ) agreed to fund the repairs and upgrades, and the facility was significantly improved as well as repaired. After these actions were performed, the IST was resumed and then completed. Research began in the NFAC after it was dedicated on December 11, 1987.

Several years later, because of the agency's dedication to the importance of acoustic research, research engineers successfully advocated replacing the walls of the 40- by 80-foot test section with special 42-inch-thick acoustically treated walls to further improve the acoustic properties

Figure 3. NFAC with the 40- by 80-foot test section on the left and the 80- by 120-foot test section on the right. ***(NASA AC84-0712-28)***

Figure 4. The OARF. ***(NASA AC84-0176-35)***

of the test section. The existing steel-plate walls were removed from the structural-steel bents and placed on the outside of the 36-inch-deep steel bent rings to allow for the acoustic treatment. The 6-inch treatment was placed on top (inside surface) of the bent rings maintaining the previous test section size of 39 by 79 feet resulting from the previous acoustic liner.

Scientists performed a wide variety of experiments on powered-lift models, V/STOL aircraft and models, many rotorcraft, and miscellaneous aircraft and models. Some included the F-111 airplane pilot recovery cockpit capsule, a Boeing 757 vertical tail with boundary layer control (BLC), wind turbines, trucks, and a full-scale reproduction of the Wright Flyer. Acoustic experiments were a major element of the research, and studies included efforts to reduce airframe noise, propulsive-device noise, and rotorcraft noise. It was common to perform acoustic measurements at the same time that aerodynamic measurements were being taken.

The NFAC was shut down in 2003 because of changing NASA mission priorities. NASA was becoming more interested in space exploration and less interested in aeronautics for a variety of reasons, particularly in the context of the constrained total budget of the agency. As a result, the NASA aeronautics budget was drastically reduced to about one-third of its original level. This had a major impact on the Centers performing aerodynamic research—Ames, Langley, and Glenn (Lewis). Full-cost recovery had been implemented for facilities, which resulted in NASA

wind tunnels no longer being free for use by other government agencies; nor were they free for programs performed by contractors for the benefit of the government. In addition, buying NFAC test time was excessively expensive because of Ames Research Center's overhead expenses regarding normal wind tunnel operations. The fewer the customers, the higher the overhead costs. This model became unsustainable and essentially eliminated paying customers for the NFAC. Because of the lack of customers, NASA and Ames Research Center management decided to close down the NFAC—ignoring NACA and NASA charters requiring aerodynamic research both for the benefit of the aviation industry and for advancing the field at little or no cost to the industry. This was done unilaterally by NASA and Ames upper management without sufficient notice to the Department of Defense (DoD) upper management, which contradicted the understandings and agreements between NASA and the DoD.

The U.S. Army needed to develop advanced rotorcraft, which resulted in strong advocacy for retaining the NFAC for the benefit of both the Army and the helicopter industry. As a result, the facility was restored and returned to operation in 2007. The NFAC was critical for the development of advanced rotorcraft because small-scale model experiments and theoretical modeling were not able to adequately deal with the many aerodynamic and aeroelastic problems of advanced rotorcraft. The U.S. Air Force leased the NFAC from NASA and took responsibility for the facility's restoration, maintenance, and operation for the DoD. (The Air Force has the DoD charter for the operation of major ground-test facilities.) The Air Force sold wind tunnel test time at much more reasonable rates that reflected actual costs and overhead. The Air Force based rates on direct overhead costs and recouped some fraction of overhead expenses from non-DoD customers. Experiments were not only performed on rotorcraft for the Army, but on V/STOL aircraft for NASA, wind turbine studies, and other NASA investigations as well. Wind tunnel test time has also been purchased by many other organizations for proprietary experiments. The NFAC has become a facility for hire, rather than a NASA research facility as it had been in the past.

This book describes the history of the facility in some detail. Modifications to the tunnel are described along with much of the research and development testing performed over the years. Often models or aircraft were studied in the facility and then modified and tested again, such that many models and aircraft were tested numerous times over a period of several years. Descriptions generally cover investigations of models that occurred for several years, rather than descriptions of tests performed chronologically. The goal has been to make the descriptions understandable and not particularly technical, but yet clearly state their purposes. Not all tests are described because of the large number of tests performed (on the order of 700), but many representative tests are described that are intended to illustrate the variety and importance of the models and aircraft investigated over the years. A comprehensive list of references is included for those who are interested in more technical details. It should be noted that after the implementation of full-cost recovery, the interest of NASA in producing traditional reports on aerodynamics was substantially reduced. As a result, there were fewer NASA aeronautical reports in later years. This was a disappointing development because of the importance and high quality of the NASA reports and the importance of archiving results of unique experiments. Dates of important events are provided in Appendix A and a list of NFAC tests are provided in Appendix B.

This book is organized in four parts: Part I. Design and Construction; Part II. Operation and Management History; Part III. Research History; and Part IV. Concluding Remarks, References, and Appendices.

PART I. DESIGN AND CONSTRUCTION

Chapter 1. Design, Construction, and Modifications of the 40- by 80-Foot Wind Tunnel, 1941–1957

Design

Overview

Designers took advantage of experience gained at the Langley Aeronautical Laboratory where they had constructed several 7- by 10-Foot Wind Tunnels (7- by 10-foot rectangular test section); the 20-Foot Propeller Research Tunnel (PRT), which had a 20-foot-diameter test section; and the 30- by 60-Foot Wind Tunnel, called the Full-Scale Wind Tunnel, which had a flat-oval-shaped test section [2]. Many engineers on these design teams helped design the 40- by 80-Foot Wind Tunnel at the Ames Aeronautical Laboratory, led by Smith J. DeFrance. Reference [3] is an excellent history of NACA wind tunnel designs leading up to the design of the 40- by 80-Foot Wind Tunnel. Many lessons had been learned through trial and error. For example, the inlet contraction shape for the 30- by 60-Foot Wind Tunnel had to be reworked and its turning vanes had to be made adjustable to achieve the correct flow turning. The 30- by 60-Foot Wind Tunnel had an open test section (that is, it had a floor but no walls or ceiling) that was prone to pulsing and reduced efficiency. Solving these issues informed the design of the 40- by 80-Foot Wind Tunnel: the contraction shape did not require rework, nor did the turning vanes need to be adjustable, and its test section was closed.

Circuit

The tunnel was designed as a closed circuit with a total centerline length of 1,932 feet. The contraction ratio—that is, the largest cross-sectional area (called the settling chamber), divided by the test-section cross-sectional area—was 8:1 for good flow quality as well as increased airspeed in the test section. The contraction ratio is a major element in establishing wind tunnel flow quality as well as performance, but high contraction ratios increase the structural cost, therefore a trade-off is required. (For contrast, the contraction ratio of the 30- by 60-Foot Wind Tunnel was about 5:1 and for the 7- by 10-Foot Wind Tunnels it was about 14:1.)

The 20-Foot PRT and the 30- by 60-Foot Wind Tunnel had dual return circuits. The flow would leave the test section, be split in two, go around in two return ducts, and then come together upstream of the test section. Dual return circuits, however, were not necessary. It is not clear why the designers thought that dual return circuits were necessary, but several wind tunnels in the 1920s and 1930s had that configuration. The 7- by 10-Foot Wind Tunnels, in comparison, were single return and had very good flow quality (that is, very uniform flow velocity). Upon inspection, they were judged to have relatively larger circuits than necessary for the size of the test section, so the 40- by 80-Foot Wind Tunnel was designed with a single return and was relatively more compact. Designers also decided that the tunnel did not need an open test section like the 30- by 60-Foot Wind Tunnel. This choice substantially reduced aerodynamic losses and eliminated the flow pulsing (much like an open sunroof in automobiles) in open-jet wind tunnels. Reducing the wind tunnel circuit losses was a primary ambition. Designers wanted to minimize the drive power required, as achieving maximum airspeed was an important goal despite the tunnel's size.

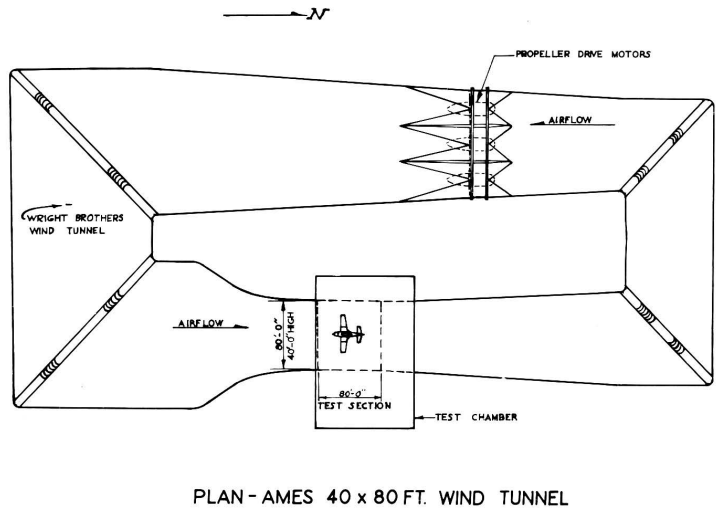

Figure 5. Early sketch of the 40- by 80-Foot Wind Tunnel circuit with a line showing the length of the Wright brothers' wind tunnel. ***(NACA ARC A-7612)***

Figure 5 is an early sketch of the wind tunnel circuit. To illustrate the size, a very small line drawn in the settling chamber represents the Wright brothers' 1901 wind tunnel.

Wind tunnel performance is commonly measured by the energy ratio, which is the test-section dynamic pressure divided by the total-pressure rise produced by the drive fans. The energy ratio of the 30- by 60-Foot Wind Tunnel was less than three, whereas the energy ratio of the 40- by 80-Foot Wind Tunnel exceeded eight—more than was expected. The power required to drive the wind tunnel is a direct function of the reciprocal of the energy ratio (as well as a direct function of the test-section size and the velocity cubed). A higher energy ratio results in lower energy or power required by the drive system for a given size and speed. The requirement for the 40- by 80-Foot Wind Tunnel had been to achieve a maximum airspeed of 200 knots (or 230 mph) at a total power of 36,000 horsepower (hp); this goal was readily achieved.

Drive

The drive system consisted of six 40-foot-diameter drive fans in a three-wide by two-high arrangement. The availability of electric motors and the limits of large-fan-blade construction essentially dictated the number and size of the drive units. The motor nacelles or drive housings were 14 feet in diameter. Each fan motor was 6,000 hp, for a total system power of 36,000 hp. The Langley 30- by 60-Foot Wind Tunnel, in contrast, had two drive fans, each 35 feet in diameter, and used two 4,000-hp electric motors for a total drive power of 8,000 hp.

The larger test-section dimensions and higher maximum airspeed of the Ames 40- by 80-Foot Wind Tunnel required substantially more power than the Langley Full-Scale Wind Tunnel. The availability of large amounts of electrical power was one of the criteria used in the selection of the San Francisco Bay Area site for the Ames Aeronautical Laboratory. Comparing the power requirements and control schemes of the two wind tunnels illustrates the technical advances in wind tunnel drive design.

Owing to its economical upfront investment, the Langley 30- by 60-Foot Wind Tunnel used two 4,000-hp wound-rotor induction motors to power its two drive fans. Slip rings on the motor shafts carried the electricity for the rotor windings off-board to a bank of resistors. Together with a motor pole change, the components of this resistor bank could be switched in 24 steps to control the motor speed and thus the wind tunnel airspeed. The initial airspeed range was 25 to 118 mph in 24 discrete steps. Since it was built during the Great Depression in 1930,

construction costs strongly dictated this tunnel's design. This brought with it the disadvantages of the airspeed control not being continuous and of the energy in the resistor bank being wasted. It was, however, relatively low cost to build.

The 1940 design of the Ames 40- by 80-Foot Wind Tunnel used a modified Kramer system for the fan drive. This system used wound-rotor drive motors, but instead of a resistor bank several machines were used to allow continuous control of the rotational speed of the drive motors and fans and therefore the airspeed in the wind tunnel. The portion of the fan-motor rotor power that is not used in turning the fans is returned to the power grid through the other machines. While the initial cost of the Kramer system is higher than some other wound-rotor systems, it has the advantages of lower operating costs and continuous speed control.

The six drive motors were mounted in streamlined nacelles that were supported by two struts. The fans were mounted on the motor shafts close to, and downstream of, the drive-support struts. This arrangement caused unsteady loading on the fan blades because of the struts' aerodynamic wakes impinging on the fan blades. Because the stress levels in the wood blades were low (only a couple hundred pounds per square inch (psi)) the loading was not a structural problem. It did, however, cause the drive to be noisier than it would have been if the fans had been mounted upstream of the supports. This problem was not well understood at the time the tunnel was designed and constructed, but research performed in the tunnel on propeller-powered models and airplanes after it was built helped reveal and define the problem.

The fan blades were made from laminated spruce, similar to the construction used for the fans in the Langley 30- by 60-Foot Wind Tunnel. Downstream, or stator, blades were not required.

Initially there was a small hole in the center of the fan nacelle nose cone to let in wind tunnel air to cool the motors. Unfortunately, when powered airplanes were tested, engine exhaust deposited soot on the motor windings. The nose cone inlets were subsequently closed, and outside air was ducted up inside the motor support struts to cool the motors.

The drive system heats up the air in the tunnel; all of the drive power produces heat as a result of the internal airflow overcoming the aerodynamic losses of the circuit elements, such as friction drag. Initially the 40- by 80-Foot Wind Tunnel was to have an air exchange system for cooling the tunnel air like the NACA 7- by 10-Foot Wind Tunnels. To maintain the wind tunnel air temperature, that system scooped up and exhausted hot tunnel air and brought in cooler outside ambient air downstream of the exhaust. The 40- by 80-Foot Wind Tunnel air exchanger was to be located in the leg opposite the test-section leg, as it was in the 7- by 10-Foot Wind Tunnels. Designers subsequently decided, however, that because of the large size and high cost (which would have been over $1 million; the entire tunnel cost a little more than $7 million), a similar air exchanger would not be required. Test runs of an hour or so of unpowered models could be performed without requiring an air exchanger or air-cooling system; experience at Langley indicated that test runs of an hour duration were typical and, as a result, were assumed likely for the new wind tunnel. A simple venting system was installed for ventilation during and after propeller-engine or jet-powered models and aircraft tests. Off-the-shelf adjustable ventilation louvers were installed in the walls of the north and south legs (also known as the wind tunnel cross legs). The louvers in the north leg served as the air intake because the tunnel would be at a negative pressure at this location, and external air would be sucked in. The louvers in the

south leg served as the exhaust because the tunnel would be at a positive pressure at this location. (It is typical for closed-circuit wind tunnels that the tunnel wall pressure is negative upstream of the drive and positive downstream of the drive unless there is additional venting.) This was a very simple and economical system, but it had limited effectiveness as an air exchange system and was not efficient from a performance standpoint.

Model Installation

Models were installed in the test section through a pair of double-hinged overhead clamshell doors that opened the full width of the test section. The doors were 49 feet long, resulting in an access opening at the top of the test section that was 49 feet long and 80 feet wide. A 15-ton overhead crane, which was mounted to the ceiling of the building enclosing the test section, was used for model lifting, handling, and installation. Typically, models or aircraft were picked up on the shop floor below the test section and lifted about 110 feet overhead, transported over the test section, and then lowered into the test section and mounted on the model-support struts. The models were nominally mounted in the center of the wind tunnel or about 20 feet above the test-section floor. There was also a door in the side of the test section for personnel access and to bring in model access ladders and workstands. Initially, tall ladders (that looked like those used in orchards) were used for model access, but later workstands with wheels were used, which were more stable and safer. Two of the workstands were custom made and could support three to four mechanics and/or test engineers at a time working on the models. They could be folded down for rolling in and out of the test section through the door and then readily tilted up for model access.

After long runs or runs with powered models the tunnel could be aired out by opening the test-section overhead doors, opening the air exchange louvers, and running the tunnel at very low airspeeds.

Model Supports

Generally, the models were supported by three struts attached to the balance frame, which was below the test-section floor: two fixed-length main struts, the tread of which could be adjusted for the models, and a telescoping tail strut that could be adjusted fore and aft for the models. The initial intent was that the main struts would attach to the aircraft's main landing gear, and the tail strut would attach to the tail landing gear. Since the purpose of the scale system was to only measure the aerodynamic forces on the models, it was important to not include the aerodynamic forces on the model-support struts. Therefore, the support struts had windshields that shielded the supports from the wind. The windshields were supported independently of the struts by the test-section floor. Data corrections were required for the exposed part of the strut tips that extended above the strut shields. Runs were used to measure the forces on the exposed portions of the support-strut tips for corrections to the data (tare runs).

It was important that the struts not contact the windshields or "foul" the aerodynamic data measured by the balance system. Therefore, a fouling system was used that would indicate if the struts and windshields or fairings contacted each other causing an error in the indicated forces. Fouls were detected by electrically isolating the floating or balance frame from the surrounding

structure. Initially, and for many years, a low-voltage direct-current system was used to indicate contact or fouling. Occasionally the tail strut would cause a foul that would have to be corrected. The tail strut was very complicated. To change model angle of attack, the tail strut would move up and down and drag its fairing with it using extendable/retractable dogs. At the desired angle of attack, the fairing would be released by the dogs and held in place with two rear slave-support struts.

For powered models with large, high-powered (up to 1,500-hp) electric motors, electrically isolating the model and floating frame was a potential safety hazard, therefore a grounding system was used that would provide an electrical path to ground in case of an electrical problem. The grounding system would be used when working on models or changing the model angle of attack during a test run. Before data were taken, the grounding system would be turned off to enable the fouling system to indicate if there was a foul. If there was a foul during a run, the run would be terminated and the source of the foul identified and corrected.

Control Room

The control room was located below the test section, at the same level as the balance system scale heads and next to the scale heads. When the tunnel was built, access to the scales was necessary to take visual readings during testing. By necessity—because the model supports that were attached to the balance system could not interfere with the test-section floor, so there was clearance between the supports and floor—the control room was vented to the test section. Therefore, airlock doors were required to enter the control room during wind tunnel operation, because the test-section static air pressure was negative and significantly below atmospheric pressure. (The maximum could be on the order of 100 pounds per square foot (psf) lower than atmospheric pressure.)

Platform-Balance System and Steady-State Aerodynamic Data Acquisition

The tunnel was designed with a mechanical, platform-balance scale system to measure the forces and moments on the models—similar in principle to truck scales. It was under the test section, and patterned after the scale systems successfully used in the 30- by 60-Foot Wind Tunnel and the 7- by 10-Foot Wind Tunnel, as well other wind tunnels. It had four lift posts that supported the balance frame at each corner. There were various balance system levers, and large “knife edges” were used for pivots or bearings. The balance frame contained the yaw system and supported the model-support struts. The scale system was built by Toledo Scales, and was very accurate and reliable with a large range and did not require frequent calibrations as electronic load cells did (especially those at the time). The accuracy in the lift direction was on the order of 0.02 percent. The scales were also very durable and could withstand the unsteady forces generated by rotorcraft. The levers were linked mechanically to scale-head dials that indicated the wind forces on the models.

Figure 6 is a schematic diagram of the balance and model-support system. The drag-scale lever system is illustrated. The heart of the system is a balance frame or floating frame (illustrated). The model yaw system is contained in the balance frame. The model-support struts were attached to the yaw system.

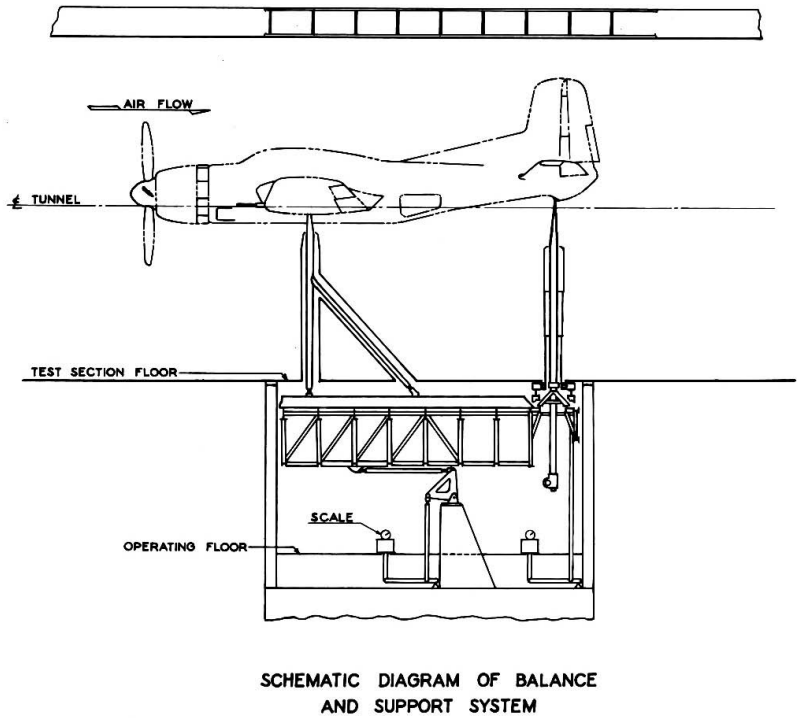

Figure 6. Sketch showing a schematic of the model support and the linkage for the drag scale. *(NACA ARC A-7614*)

There were eight scale heads: four for lift, two for side force, one for drag, and one for dynamic pressure. The dynamic pressure scale head (required to calculate airspeed) was driven by a pressure transducer that measured the static pressure difference in the settling chamber and test section. This was a convenient and reliable measurement that gave the test-section dynamic pressure within a few percentage points because of the 8:1 contraction ratio that resulted in a large difference in static pressures. This difference in static pressures was close to the magnitude of the dynamic pressure in the test section. Calibrations were used to correct this pressure to give very accurate test-section dynamic pressures. The measured test-section static pressure, which was often used as a reference pressure for pressure measurements and surveys, was also corrected using test-section static pressure surveys.

The balance scale heads had paper-tape printers that were used for recording data. A toggle switch on the control bench board allowed the operator to control all eight scale heads simultaneously. Typically, five recordings were taken at each test condition, 5 seconds apart. After a run, the paper tapes were collected and given to the computer staff for calculating forces and moments and their coefficients. All six force and moment components (lift force, drag force, side force, pitching moment, yawing moment, and rolling moment) were usually determined and coefficients calculated for the research engineers by the computer staff, which was nominally about half a dozen young women who used mechanical calculators instead of slide rules for good accuracy. The computer staff were generally referred to as “computers” and they often had degrees in mathematics and science. Up until the late 1950s the tunnel did not have a mainframe computer, and many other computations were performed by the computers in support of theoretical studies by the researchers.

For many years the scale system was maintained by John Curd, a machinist assigned to the tunnel from the machine shop. Curt Holzhauser and later William Tolhurst were the tunnel research engineers assigned to monitor the condition of the scales. If there was a serious accident that could compromise or damage the scales, calibrations were performed after repairs using

many 50-pound lead weights. A lot of physical labor was required by the wind tunnel mechanics to lift and move the weights for the scale calibrations. Fortunately, this process was not required very often.

Wing Surface Pressures

Up until about the mid-1960s much data from wing surface pressures and pressure surveys were collected using 80-tube water manometer boards. Many experiments used half a dozen of these 80-tube manometer boards. Pictures were taken of the manometer board readings using 70-millimeter (mm) cameras. It was routine for these types of tests to collect the film magazines in the morning at the start of the day shift after a night of running and send them to the photo lab for development. A custom-designed projector was used for reading the film. Often the computers were tasked with reading the film, which was a very tedious and not well-liked task. Sometimes the film was read by the research engineers if they were anxious to see the data. After the film was read, the readings were recorded and pressure coefficients calculated by the computers. Detailed wing loading distributions were often determined from wing surface-pressure surveys that were very important for evaluating wing design, especially in the early days of aircraft research and development. Wing pressure distributions were typically used to adjust the wing shapes for higher lift, lower drag, and optimum pitching moment or optimum center of pressure locations.

Dynamic Data

Dynamic data were monitored and recorded using analog oscillographs. Early on, the source of the data was primarily strain gages used to monitor strains on propellers and rotors. Oscillographs recorded the data on special paper that was developed at the oscillograph with either a chemical bath or by a fluorescent light. Neither system was very convenient, and the fidelity was not very good. It was very difficult to observe the traces while conducting the tests, which made monitoring critical strains during a test a serious problem. The traces were hard to observe via a small window on the oscillograph. Engineers would often use short pieces of card stock with scales drawn on them to estimate critical loads. This process was crude, slow, and often inaccurate.

Construction and Repairs

Site test piles were driven in July 1940, and construction of the 40- by 80-Foot Wind Tunnel began in 1941. The tunnel became operational the summer of 1944. Staff at the Ames Laboratory monitored construction and reported progress to the designers, some of whom were still at Langley and some at Ames. This wartime effort was completed amazingly fast and efficiently. Much of the structural design work was done by folks at Ames, under the supervision of Harvey Allen and Don Wood, who would become world-class aerodynamic researchers.

Circuit

Figure 7 is an aerial view of the Ames Laboratory in March 1943. Figure 8 is a view of the structure looking down the test-section throat from the contraction structure showing some of the structural framing. Three of the test-section structural bents are shown in Figure 9. Installation of a test-section bent is shown in Figure 10, illustrating the flat-oval shape of the test section. Figure 11 is a view of some of the construction looking through the contraction. Figure 12 is a view from the east of the test section with a U.S. Navy blimp flying overhead in the background. The concrete structure that is below the location of the test section is shown. This was a substantial structure that was well supported by many piles. It was important that this structure be as rigid as reasonably possible because it was the foundation for the balance system and model supports; for maximum data accuracy, it was important that the balance system be very well supported.

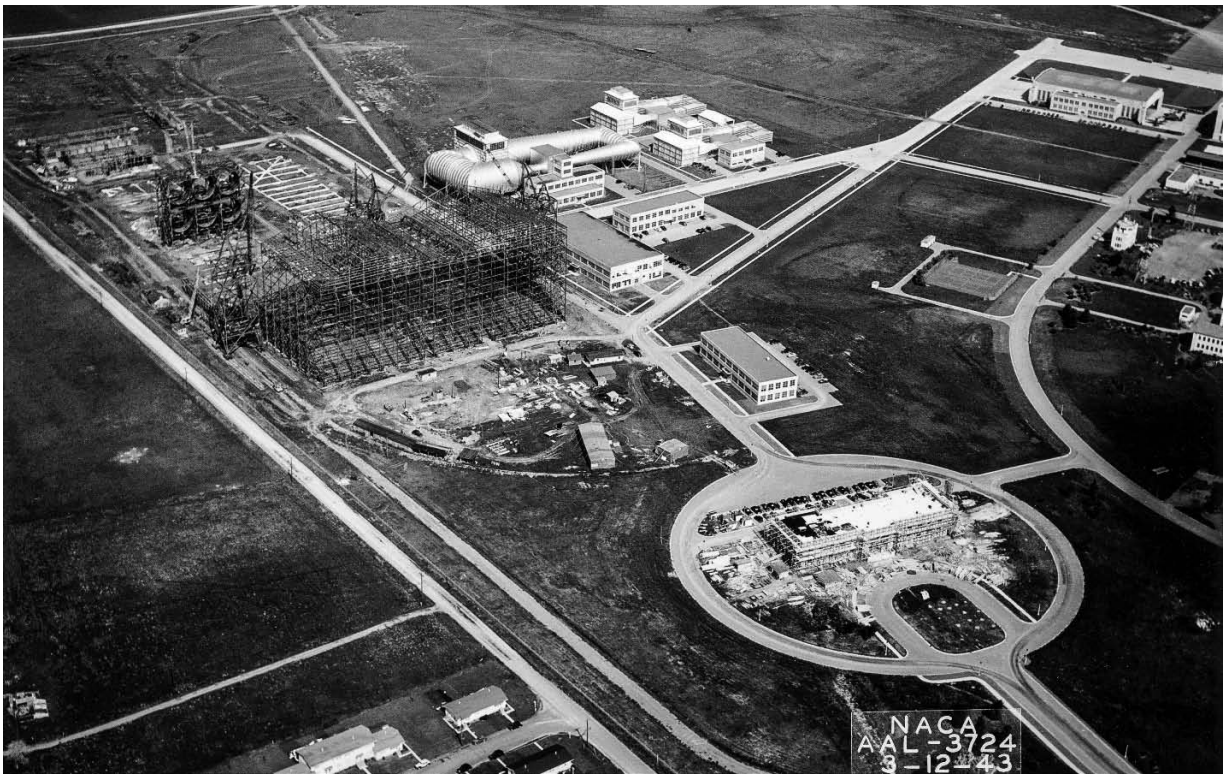

Figure 7. Aerial view of the Ames Lab in March 1943. The start of the framing for the big end of the 40- by 80-Foot Wind Tunnel is shown, as well as the framing for the six drives in the upper left. The 16-Foot Wind Tunnel and two 7- by 10-Foot Wind tunnels are shown in the upper center. The administration building under construction is shown in the lower right. ***(NACA AAL-3724)***

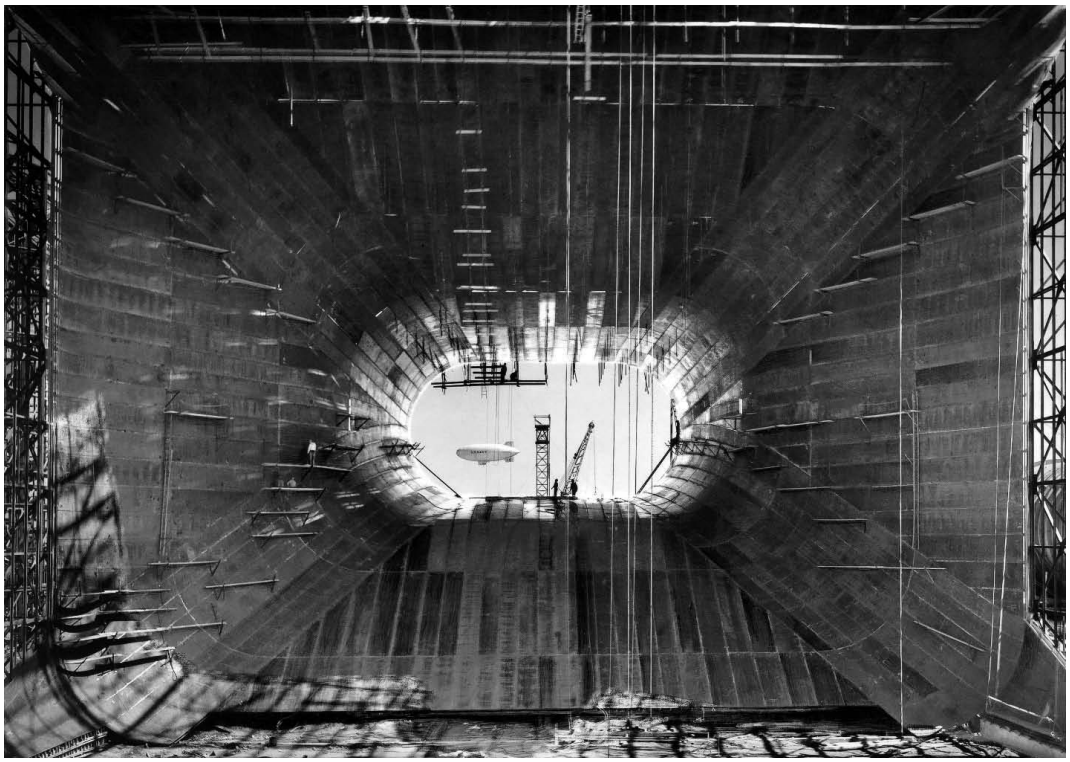

Figure 8. Wind tunnel structure looking down the test-section throat from the contraction structure showing some of the structural framing. A Navy blimp is shown in the center. *(NACA AAL-4270*)

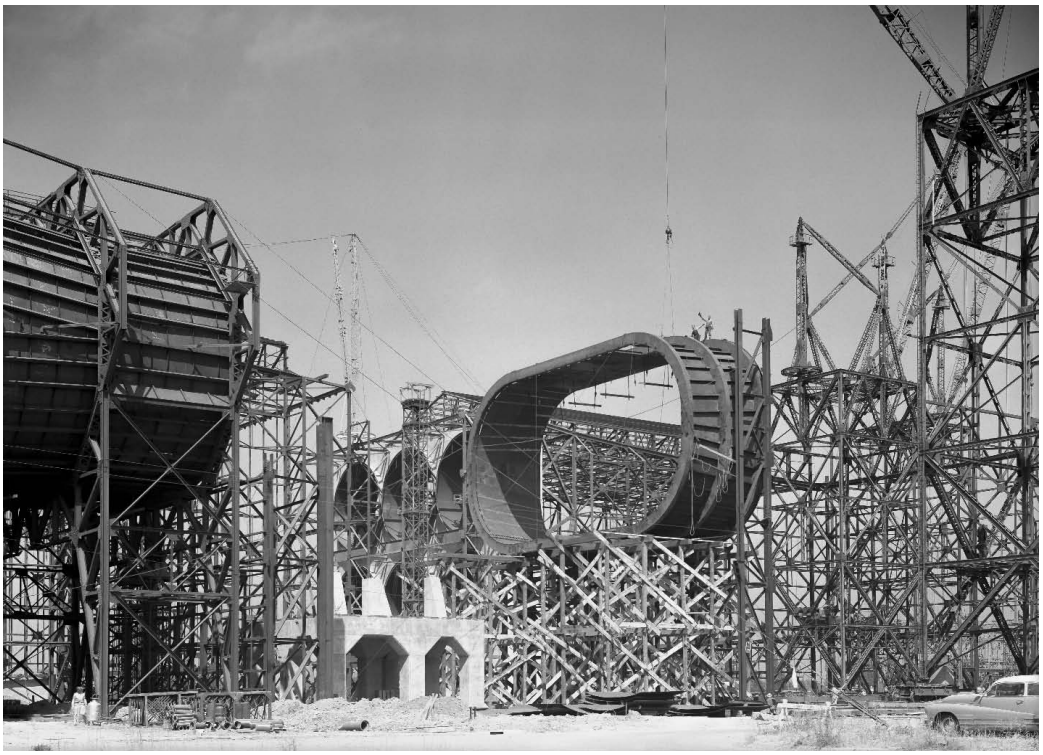

Figure 9. Three of the primary diffuser structural bents assembled. The concrete support structure for the model supports and balance is shown in the lower left. *(NACA AAL-4478)*

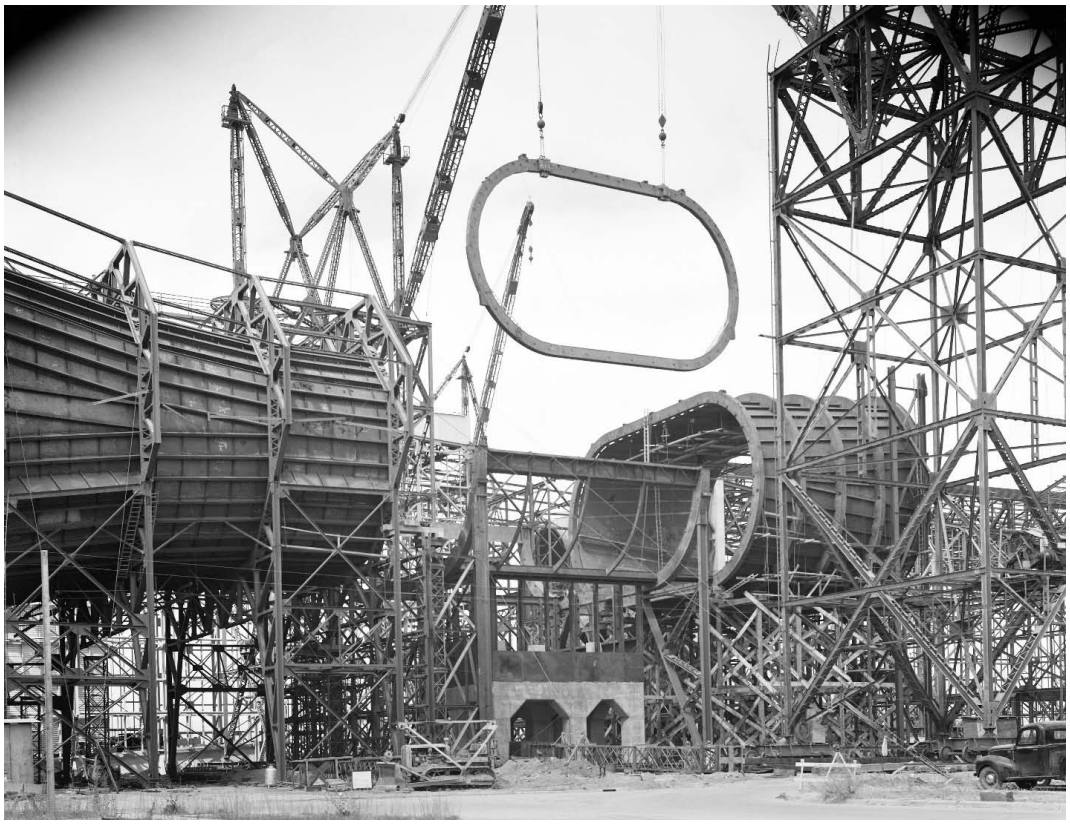

Figure 10. Installation of a test-section bent showing the flat-oval shape of the test section.
(NACA AFST 40)

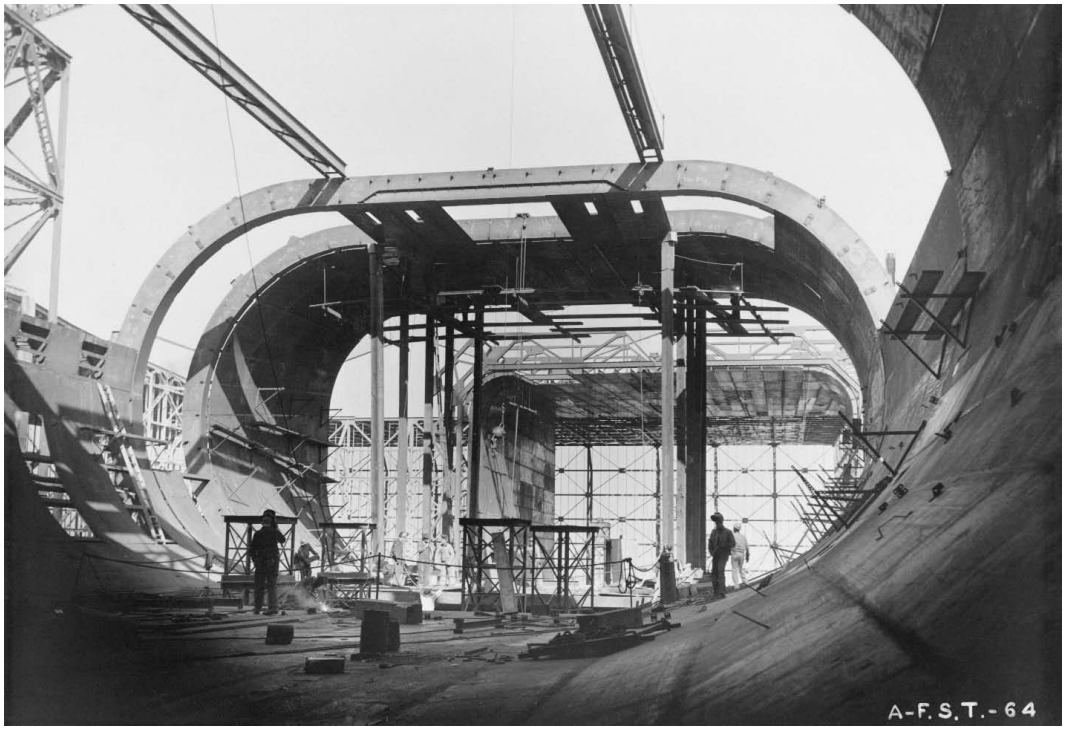

Figure 11. Some of the test-section construction looking through the contraction.
(NACA AFST 64)

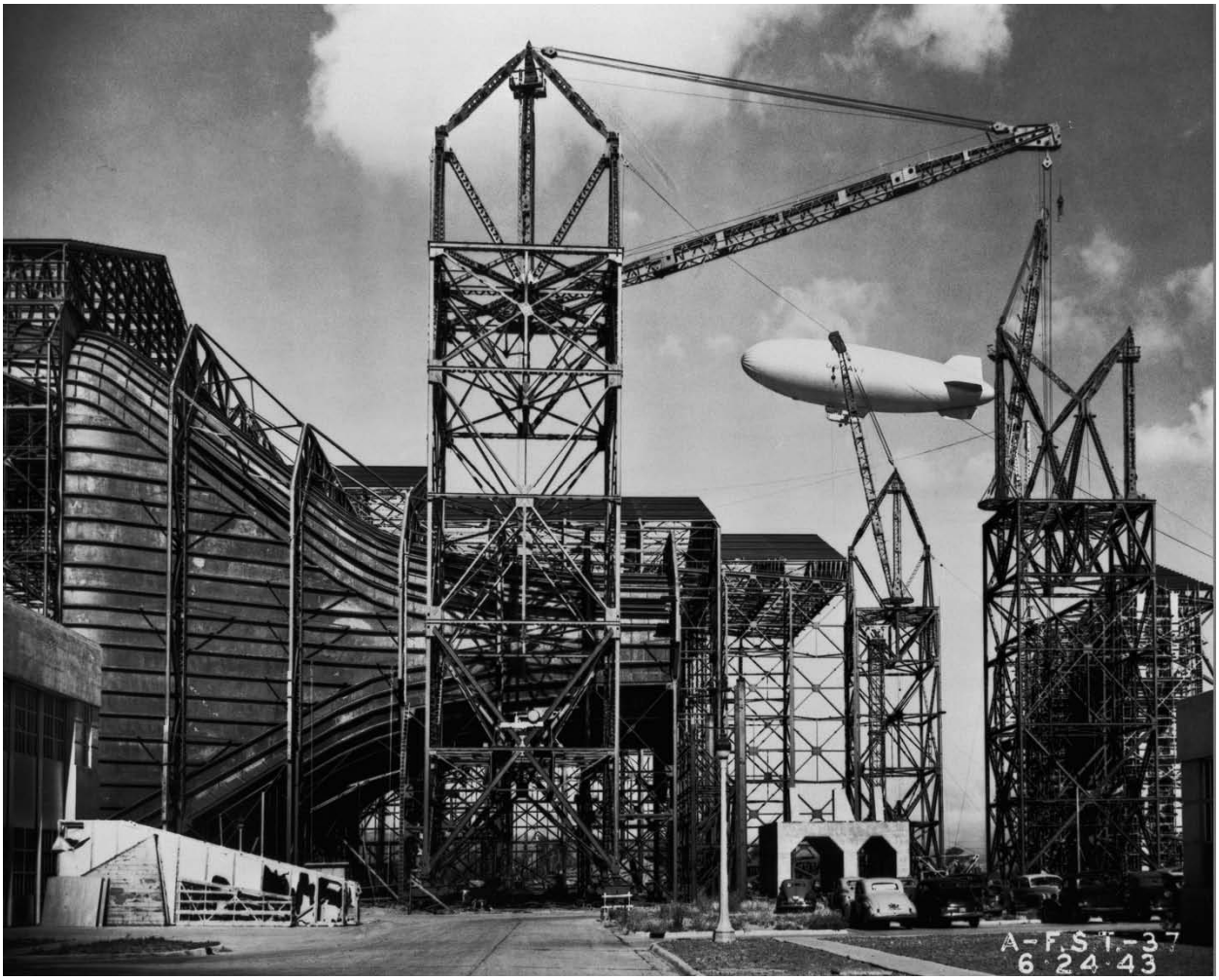

Figure 12. View of the test-section construction from the east with a Navy blimp flying overhead in the background. ***(NACA AFST 37)***

Figure 13 is an aerial view taken on November 4, 1943, showing substantial progress in the wind tunnel structure. Figure 14 is a side view from the east showing the structure with a Navy blimp overhead in the background. (The photographers loved taking pictures with Navy blimps in the background.) Figure 15 is an external view of the tunnel.

Figure 13. Aerial view taken on November 4, 1943, showing substantial progress in the wind tunnel structure with cladding. ***(NACA AAL-4801)***

Figure 14. Side view of the tunnel structure from the east with a Navy blimp in the background. ***(NACA AFST 60)***

Figure 15. External overhead view of the completed tunnel. The 12-Foot Pressure Wind Tunnel is shown in the foreground, the 16-Foot Wind Tunnel is shown above middle, and two 7- by 10-Foot Wind Tunnels are shown to the right. ***(NACA A-13516)***

Drive

To be conservative, a substantial steel structure was built to support the drive. Figure 16 shows the drive-support structure looking from the big end of the tunnel. There were two primary structural-steel bents that, after being built, were encased in concrete (Fig. 17). This was a very conservative approach and would later be a significant advantage when the tunnel was repowered. Figure 18 shows assembly in-place of one of the drive motors, and Figure 19 is a view of the motor from the floor of the nacelle. The completed six-fan drive is shown in Figure 20, and one of the drive units is shown in Figure 21. The photo with the single drive unit shows the access to the motors in the individual nacelles with the ladder up the side of one of the support struts. There were six blades per fan.

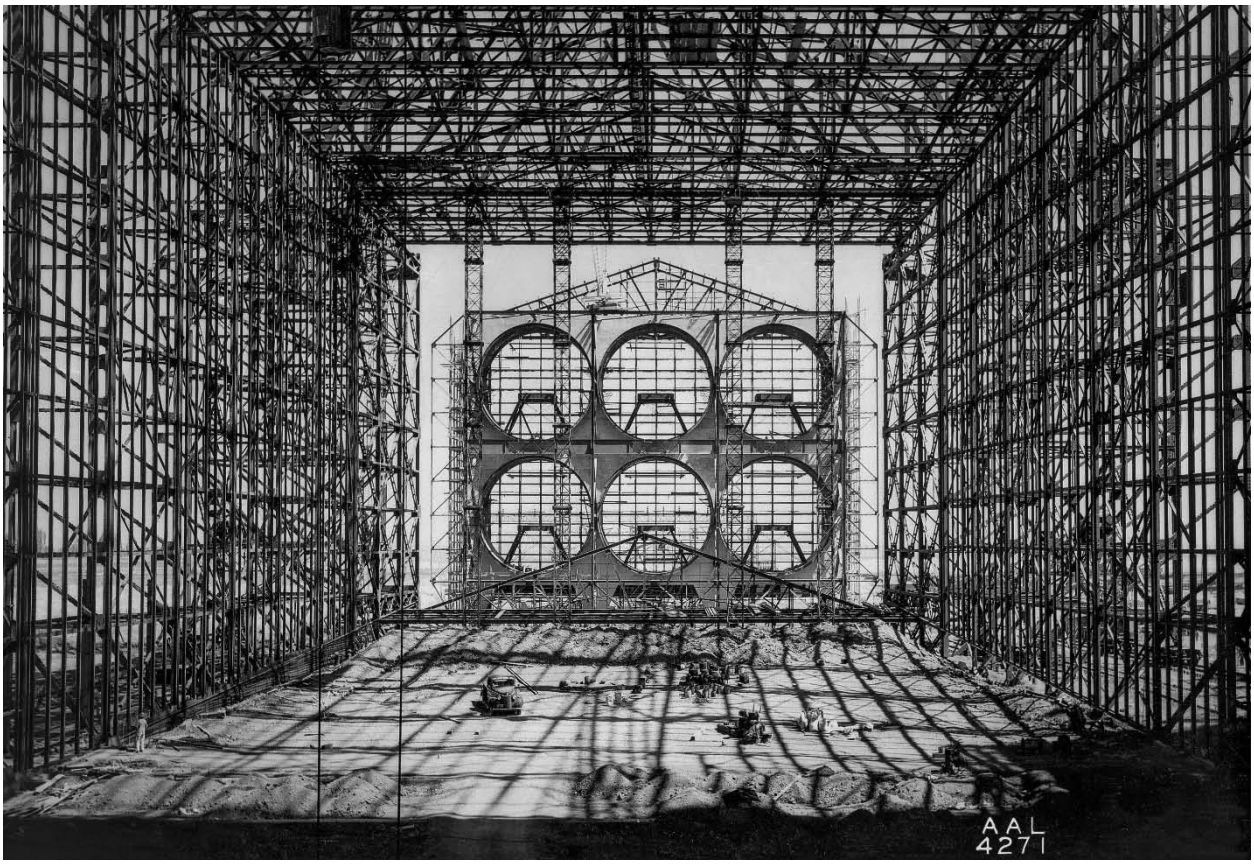

Figure 16. Wind tunnel drive-support structure looking from the big end of the tunnel. ***(NACA AAL-4271)***

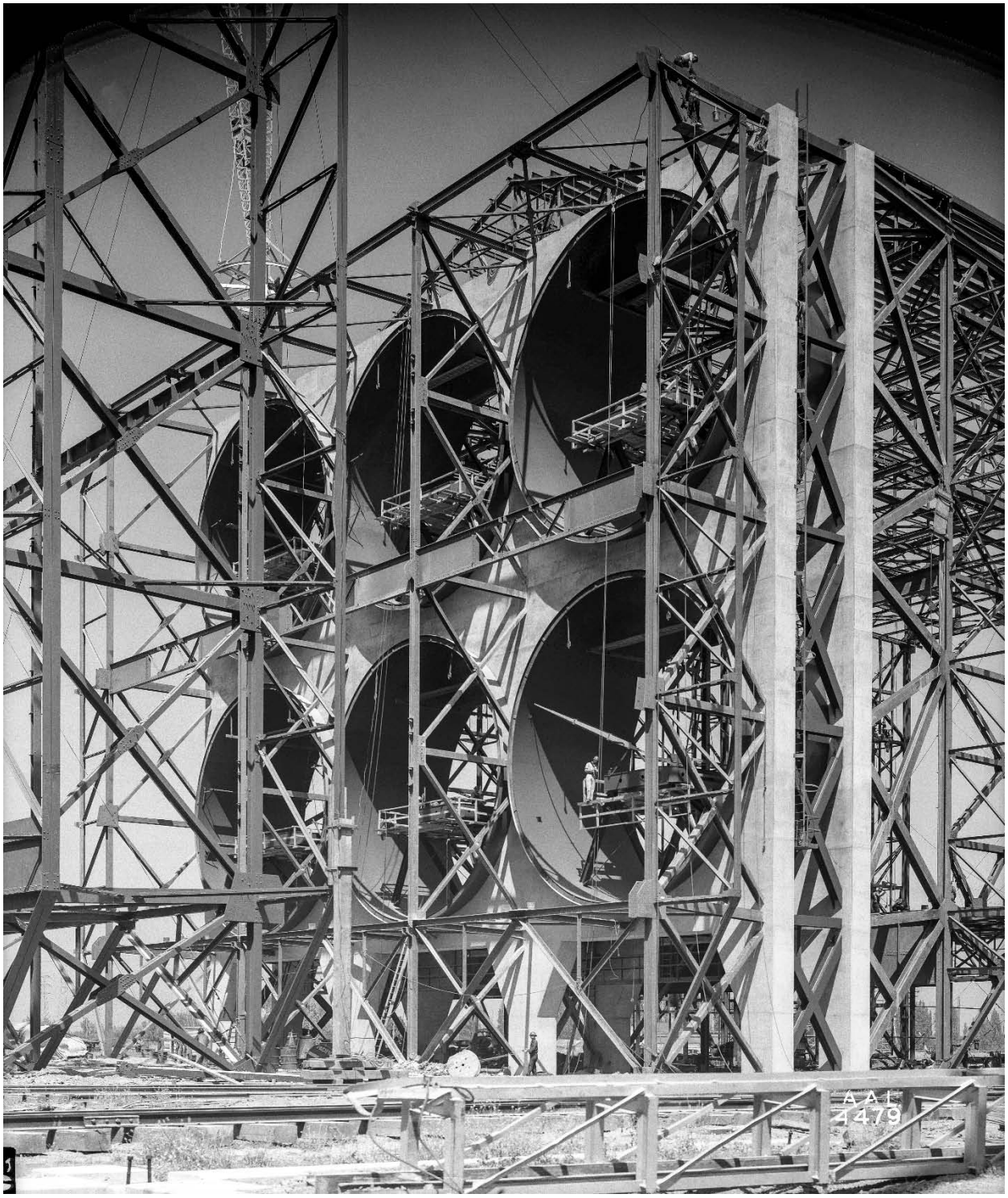

Figure 17. The two drive bents encased in concrete for conservatism. ***(NACA AAL-4479)***

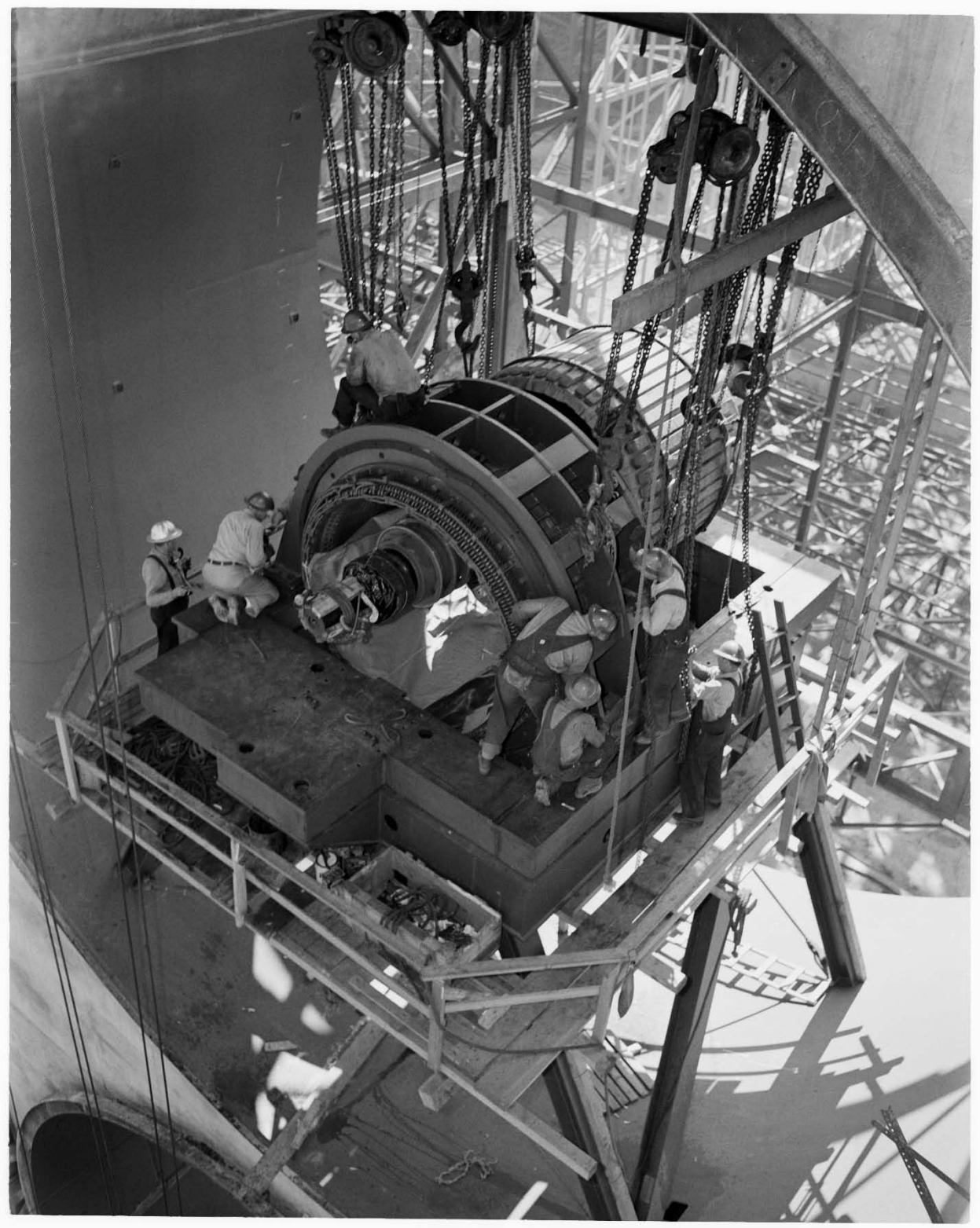

Figure 18. Installation of one of the tunnel drive motors. ***(NACA AFST 50)***

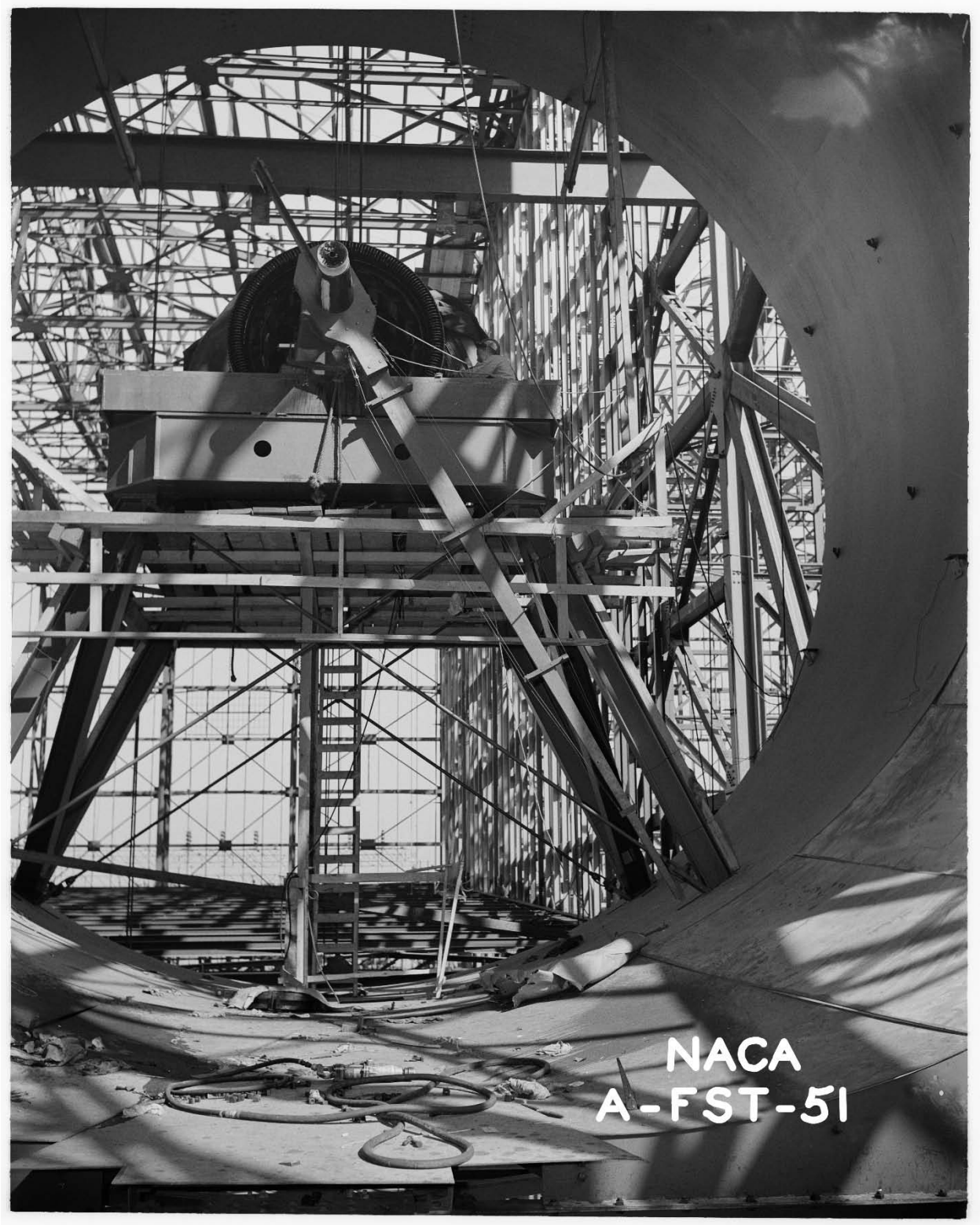

Figure 19. View of a drive motor from the floor of the nacelle. ***(NACA AFST 51)***

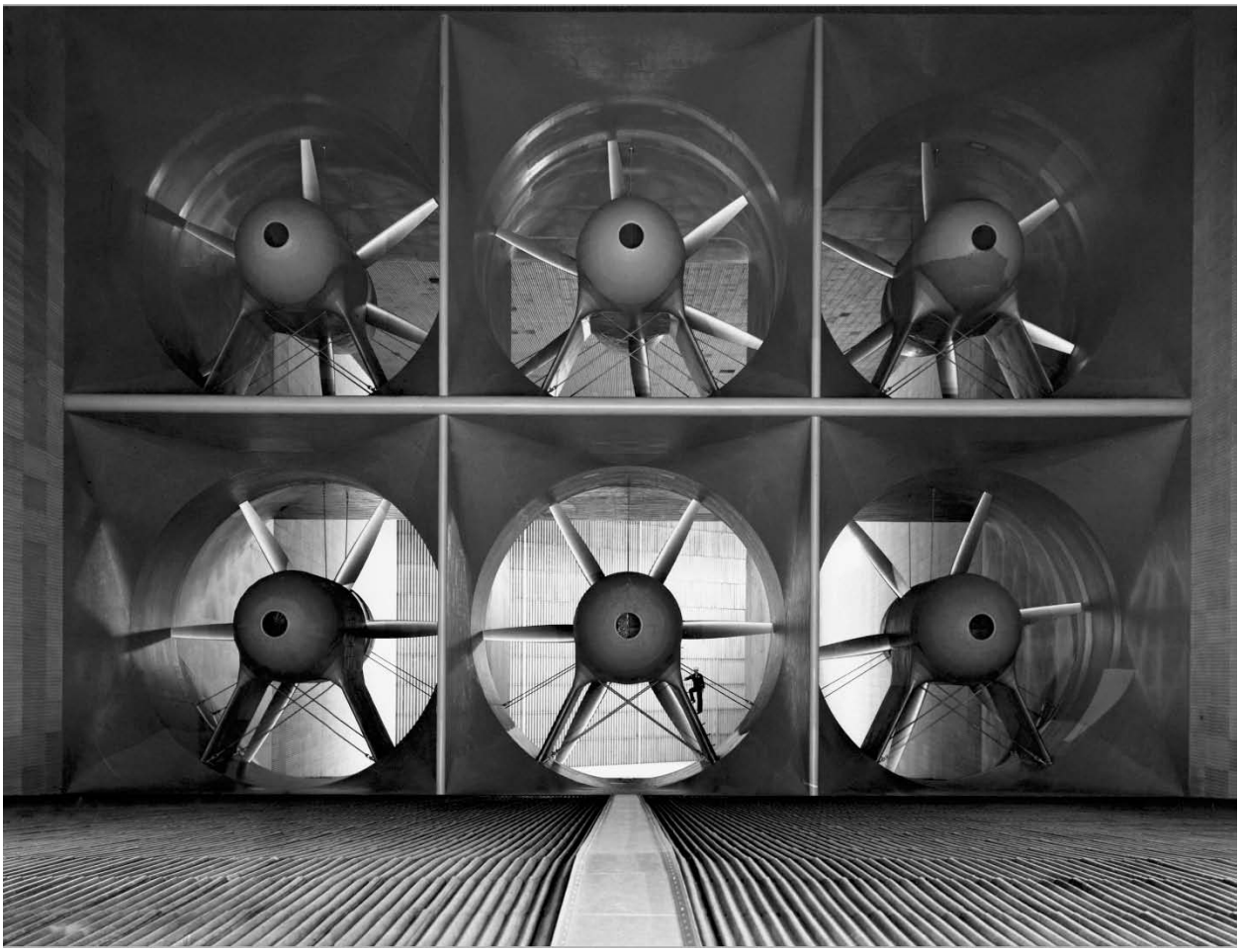

Figure 20. Completed six-fan drive. ***(NACA AAL-5993)***

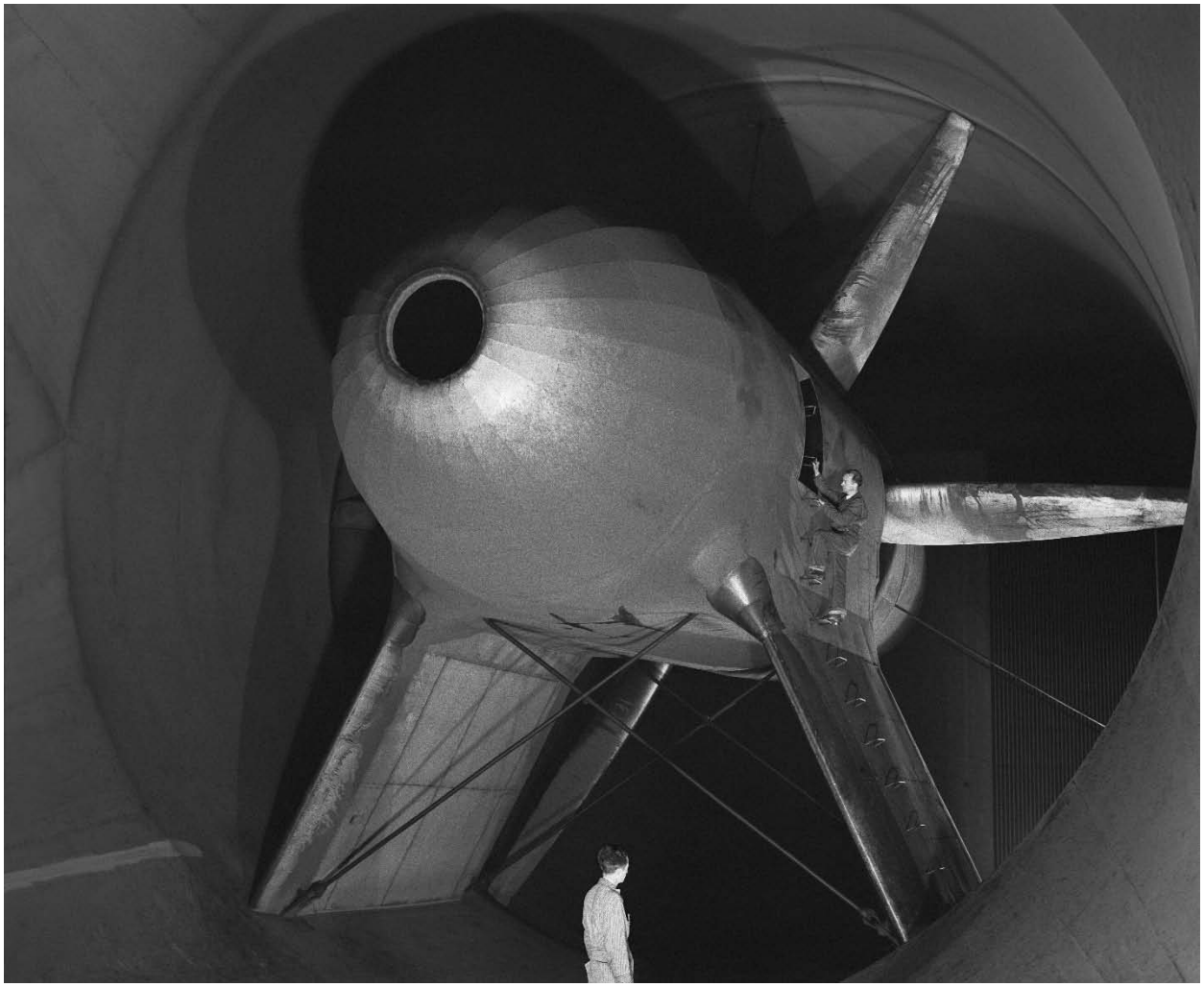

Figure 21. One of the completed drive units showing access to motors; the hole in the center for motor-cooling air was later abandoned and closed. ***(NACA A-9591)***

Control Room

Figure 22 shows the control room bench board (the control panel was called the bench board). The tunnel was controlled from the bench board. This was at the same level as the wind tunnel scale heads; five are shown in this picture. The wind tunnel operator and the research engineer would be in this room. The research engineer would read the appropriate scale heads for his experiment and plot preliminary results during the test in order to intelligently manage the test. This room was vented to the test section therefore its static pressure was below atmospheric pressure necessitating an air-lock door system for access when the tunnel was operating.

Figure 22. Control room bench board. Five of the scale heads are shown. ***(NACA A-15219)***

Flow Survey Rig

A couple of years after the tunnel became operational, a survey rig was built and installed. The purpose of the survey rig was to survey the flow on the models and aircraft. The 30- by 60-Foot Wind Tunnel had a survey rig that was extensively used, but as it had an open test section, it could be mounted to the ceiling structure of the surrounding building. The survey rig for the 40- by 80-Foot Wind Tunnel had to be mounted on tracks on the inside and on the ceilings of the test section and primary diffuser (Fig. 23). The rig could be driven and parked at the end of the primary diffuser just ahead of the first turning-vane set when it was not in use to minimize tunnel loss due to its blockage and drag. The rig caused significant test-section blockage, and significantly more power was required to drive the tunnel when the survey rig was in the test section. Flow blockage corrections were required when the survey rig was used because of its size and its required location in the test section with respect to the model.

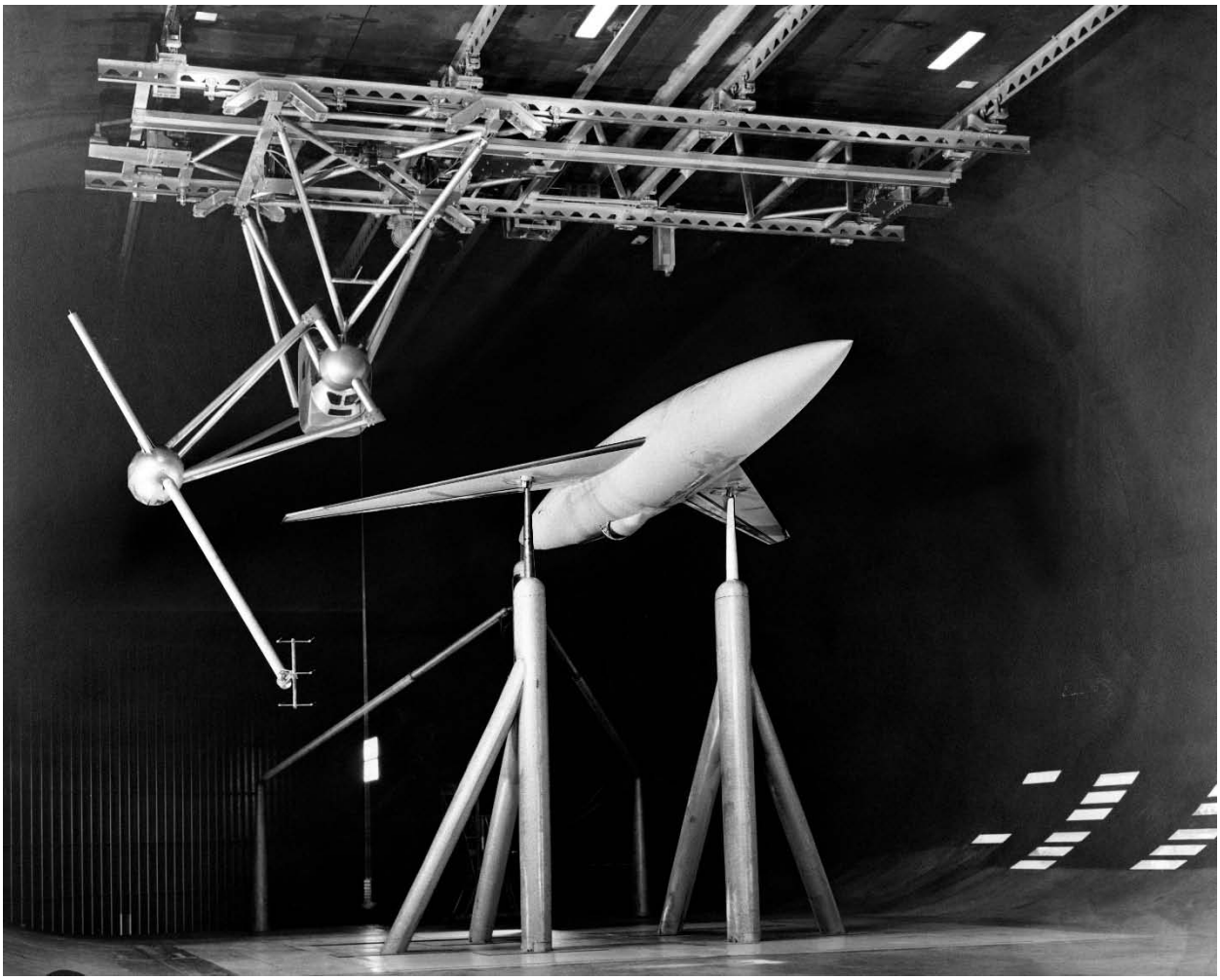

Figure 23. View of 63-degree swept wing with survey rig in the background to the left. ***(NACA A-16650)***

The survey rig had six pitot-static direction probes at the end of its arm. The flow total pressure, static pressure, dynamic pressure (for determining velocity), and flow angle could be measured at essentially any location in the test section by rotating and translating the arm and driving the survey rig forward or aft as required. The capability to perform flow surveys was very important in the early days. It was especially important to survey the flow at candidate airplane tail locations. The effects of wakes from different wings and propulsive devices, especially propellers, could be studied to allow optimum tail locations, sizes, and configurations. Surveys were also performed at candidate propeller locations to enable propeller inflow measurements and estimates of propeller loads. When the pitot-static direction probes were not being used, they were removed from the survey rig and put in a special box and retained in the branch chief's office.

An operator rode inside the survey-rig cab. The operator controlled the survey-rig location and the survey-rig arm position using switches and counters that had been calibrated for the particular test. In the cab behind the operator there was a water manometer board for indicating the survey pressures and a 70-mm camera for photographing the manometer board readings. The operator accessed the survey-rig cab through a hatch in the top of the test section using a permanent ladder that led to the side of the cab. It was not a lot of fun to climb down the ladder, which was 40 feet above the test-section floor (this was before the Occupational Safety and Health Administration (OSHA)—the ladder was uncaged) and go into the cab and drive the survey rig. The cab visibility was poor and occasionally an operator would run into the model with the probes. Driving the survey rig was often one of the tasks typically assigned to new, young research engineers.

Repairs

The siding and cladding used for much of the tunnel was a commercial corrugated sheet cement product, named Transite, that encapsulated asbestos cloth. It was used for the airflow passages except for the contraction, test section, and the primary diffuser. It was also used for the outside walls of the building that enclosed the wind tunnel test section and primary diffuser. The contraction, test section, and primary diffuser had steel cladding. The rest of the tunnel used Transite. It was a good product, especially during wartime when there was a steel shortage. However, because of the vibration caused by the drive, some of the floor and ceiling Transite panels upstream of the drive failed and damaged some of the fan blades. As a result, the floor and ceiling cladding upstream of the drive was replaced with a galvanized and coated corrugated iron product. Since the fan blades were wood, they were readily repaired by the Ames model shop, which was experienced in fabricating sophisticated wood structures. (The blades had been fabricated at the Langley Aeronautical Lab model shop and were very similar to the fan blades of the 30- by 60-Foot Wind Tunnel.)

Chapter 2. Wind Tunnel Modifications and Repairs, NASA 1958–1980

Repairs

Upper-Drive-Motor Bearing Failures and Repair

The original tunnel drive motors used spherical roller bearings that were lubricated with oil from 50-gallon tanks in the nacelles. There was an oil tank in each nacelle to supply oil for lubrication of the two motor bearings. Access to the upper nacelles was limited; there was no elevator, and maintenance was always a challenge. The only personnel access was by a caged ladder at the end of the drive nacelles that was about 90 feet downstream of the fans. The tunnel lighting, from a single light bulb at the top of the ladder, was very poor at the end of the drive (it was not much better at the fans). There was only a very small handrail and platform at the top so that wind tunnel and maintenance staff could get around the upper nacelle vertical partitions; there were no handrails at the front and rear of the nacelles. It was very scary because it was at least 50 feet above the floor of the tunnel, it was dark, and the floor was always very oily. This was long before OSHA! To change the oil, rigging and a small crane had to be temporarily installed so that 50-gallon oil drums and pumps could be lifted to the upper three drives.

A motor bearing in the upper middle drive (FM2) failed because of oil contamination in 1965. The bearing seized and damaged the motor shaft. The motor rotor subsequently dropped before rotation stopped completely, and significant damage was done to the motor windings. Fortunately, the fan was not seriously damaged and could be readily repaired.

Repairs required that a large access hatch be cut in the top of the tunnel. Special rigging was assembled on top of the tunnel; a custom track and trolley with a crane were installed. Repairs were first done by removing the fan by unbolting it (not an easy task) and then moving it aft while supported by the temporary crane. Special temporary supports were installed so the damaged shaft could be rotated and machined in place. After the shaft was machined, a sleeve was then pressed onto the shaft to build up the shaft surface to its original diameter. The bearings were a press fit and were installed by cooling the shaft and heating up the bearings in an oil/water solution per the directions of the bearing manufacturer, SKF. The bearings were then pressed onto the shaft before the shaft warmed up and the bearings cooled down. The motor repairs were done by Westinghouse Electric; the motors had been built by Westinghouse. While waiting for parts and repairs, the tunnel was run with five drive fans on a noninterference basis. The flow quality was compromised but some useful tests were performed by using special test-dependent flow-quality calibrations.

In December of 1971, another drive-motor bearing failure occurred. This time it was in the upper east motor (FM1). The approach to the repair was similar to what was done in 1965, however this time motor damage did not occur. Figure 24 shows the top of the drive where the hatch was cut and the trolley with the portable crane was mounted. Figure 25 shows the fan removed from the motor shaft.

Figure 24. Top of drive that was to be repaired with hatch cut, and installation of a portable trolley and crane to enable fan removal. ***(NASA A71-8826)***

Figure 25. Fan has been removed. Fan hub plate is shown with all of the bolt heads, and tapered drive shaft with keyway end is shown on the left. ***(NASA A71-8832)***

Tunnel Repairs and Armor-Plate Installation

During testing of the Lockheed AH-56 Cheyenne helicopter (Test 348) in September 1969 a catastrophic accident occurred. Due to a rotor instability at an airspeed of about 100 knots, the rotor began to oscillate and impacted the fuselage and was destroyed. One of the 20-pound rotor tip-weights went through the test-section wall, which was 3/8-inch-thick steel. The tip-weight knocked down a light fixture from the ceiling that injured one of the test engineers in the model control and observation room, which was upstairs of the balance house and wind tunnel control room. This was the first time an injury had occurred during testing in the 40- by 80-Foot Wind Tunnel. As a result, wind tunnel staff, with the help of armor-plate experts, made the decision to install armor plate to protect personnel. A 5/8-inch-thick armor plate was installed inside the tunnel walls in the planes of propellers and rotors to protect the operating personnel. After the accident, branch management required a risk analysis for all models in the tunnel with high-energy components that were a potential hazard such as helicopter rotors, propellers, and fans.

Modifications

Model Supports

In the 1950s many experiments were being performed using different height model-support struts to perform ground-effect studies for V/STOL models. This was an inefficient process so variable-height struts were designed and built to be used for this type of testing. The struts were part of a ground board system that could be installed and removed after ground-effect testing. This system was designed and fabricated at Ames in the early 1960s. Load cells were employed at the strut tips to measure forces and moments so that strut fairings would not be required to eliminate strut drag.

The original model-support system could only yaw the models about 10 to 20 degrees, depending on the size and geometry of the model. The system was slow-moving and the support machinery did not move precisely the same way each time, so there was a lot of scatter in the static runs performed when varying the yaw angle at a constant angle of attack because of the inconsistent shift in weight. (Static runs are required to correct the moment data due to weight shifts of the model-support system and are run with wind and model motors off.) As a consequence, much of the testing to obtain lateral-directional data was done with the yaw angle fixed and the angle of attack varied. This was not satisfactory for all experiments, and as a result a large turntable was designed and built at Ames and installed in 1974. Figure 26 shows the turntable in the shop, and Figure 27 shows the top and the strut T-frame. It allowed a 290-degree rotation of the models. Static runs varying the yaw angle were much more repeatable, and the magnitude of the weight variation was much smaller.

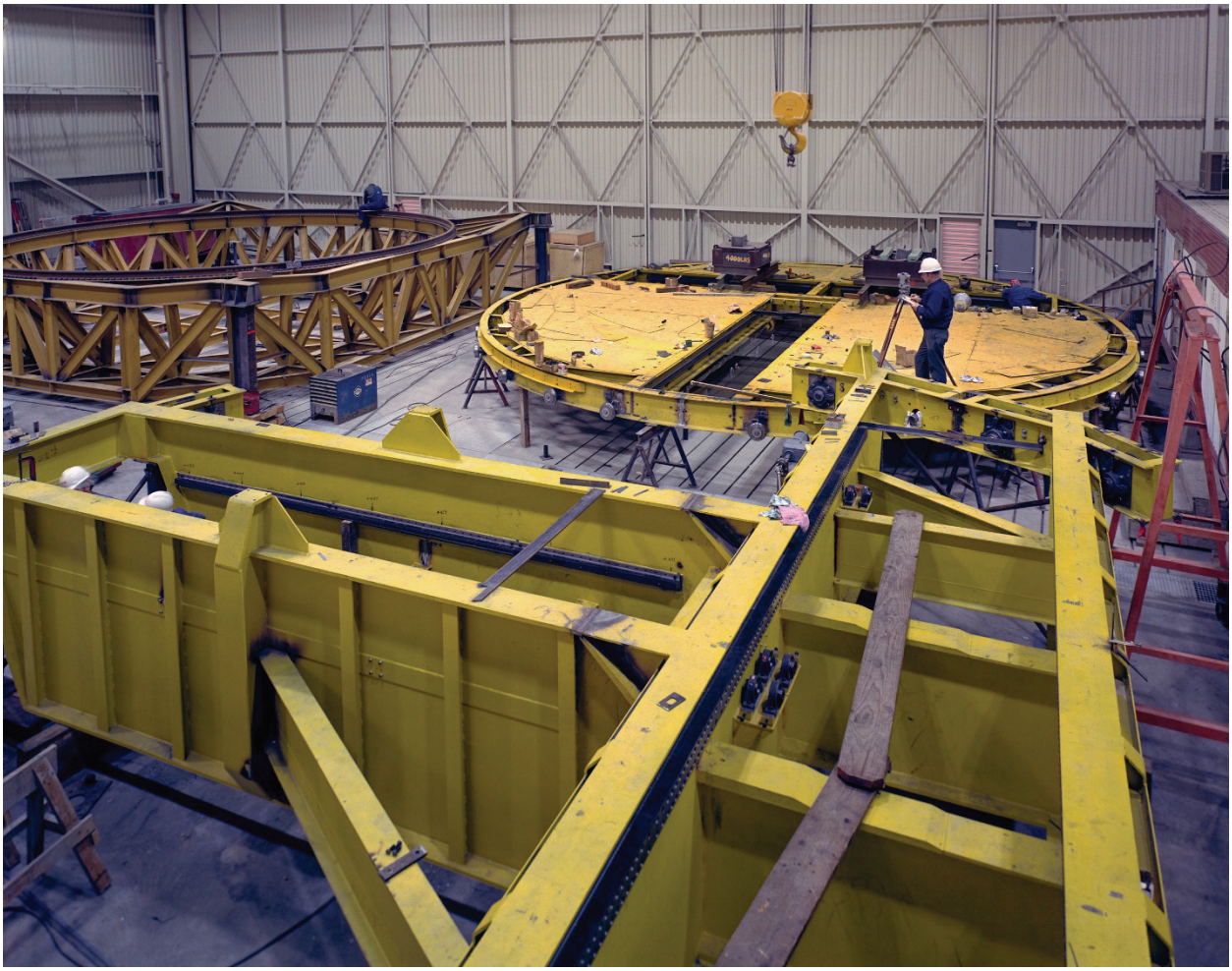

Figure 26. Turntable in the shop. Balance frame at upper left, T-frame in the foreground, and turntable floor shown upper right. ***(NACA AC74-0665)***

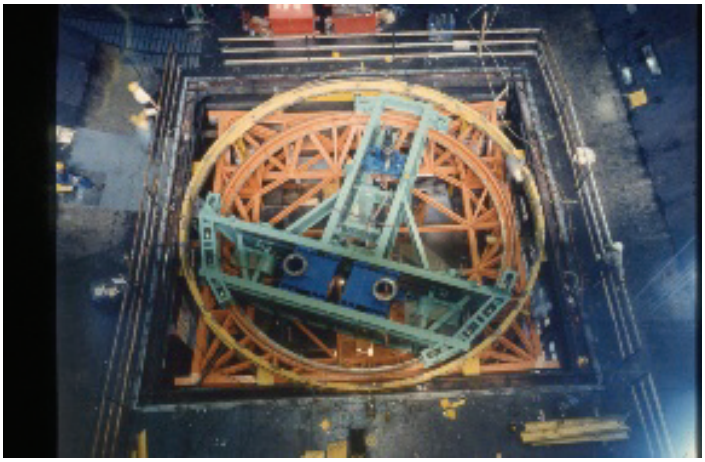

Figure 27. Top of the new turntable and T-frame installed in 40- by 80-foot test section.
(T. J. Forsyth collection, TJ2)

Air Exchange Roll Doors Installed on South Wall

A vertical flight simulator mounted on the outside of the south wall of the wind tunnel was removed because it was no longer needed by the Ames simulation organization. It had been used for supersonic transport (SST) landing and takeoff simulations, which were no longer of interest to NASA. In 1974 roll doors were installed on the south wall to reduce the time required to air out the wind tunnel after performing powered tests. The test-section overhead doors would be opened after a test along with the roll doors on the south wall. Fresh air would enter the test section and hot, contaminated air would be exhausted out the roll doors while the tunnel was operated at very low speeds. The roll doors reduced the time to air out the tunnel nearly an order of magnitude.

Data Acquisition System and Instrumentation Development

Data reduction. As mentioned earlier, the data acquisition system was not very sophisticated when the tunnel was first built. Printed paper tapes from the balance scale heads were collected after each run and given to the computers for manual data reduction. The computers were women who averaged the tape information and then calculated the required force and moment coefficients per instructions and equations from the research engineers. It was a slow, time-consuming process; generally, a couple of days were required for data reduction.

In the early 1970s, the computers would punch cards after the tapes were read and averaged. The cards would then be sent to the Ames central computing center, where calculations and data reduction were performed using the Center's mainframe computer. Mainframe computers were expensive, and most test facilities did not have their own mainframe computers at this time. (This, of course, was also well before the advent of the personal computer.) The computed data were printed out and sent back to the tunnel for the engineers to plot and analyze as required. The turnaround time was still 1 or 2 days, but the reduced data tended to be more consistent and accurate. At this stage, there was still no online data reduction, which was a major obstacle to running an efficient test. Research engineers in the balance house would read the scale heads and do manual calculations using slide rules during testing. (New engineers were issued a 2-foot-long slide rule for improved accuracy.) The engineers would do plots of the data during the tests to more efficiently conduct the test and plan for the next test conditions or runs or both. This was an inaccurate process, but it was generally adequate, and it was more efficient than waiting a couple of days for reduced data. Estimating pitching and rolling moments by hand was especially difficult.

A few years later, load cells were installed in the scale heads, and optical digitizers were mounted on top of the scale heads, which would digitize the load-cell data. The digitized data were then processed by special equipment and punched paper tapes were created. After a run, test engineers would feed the punched tape into another machine that sent the data electronically to Time Share in Palo Alto for data reduction. The data would be reduced and rapidly sent back to the tunnel electronically over a phone line. It would be printed out at the tunnel for plotting by the test engineers. This was a major improvement since data turnaround time was reduced from a few days to 1 or 2 hours.

As computers became cheaper, the tunnel got its own computer, printer, and plotter so that online data could be obtained, reduced, and plotted during the course of a run, producing more accurate data and more efficient testing. Pressure data were captured by electronic-scanning pressure transducers and were included in the data acquisition system, as well as rotorcraft steady and dynamic data. Wind tunnel operational functions (for example, model angle of attack and angle of yaw) were included in the data acquisition system. Punched cards were used to set up the computer system for different test requirements. This was a major advancement, and it made testing and research much more efficient and effective. The balance-scale paper tapes were retained as a backup. Punched cards and tapes were also used as backup. The system could also communicate with the Center's central computer facility (CCF). References [9] and [10] provide detailed descriptions of the data system.

High-speed data acquisition. As mentioned earlier, originally oscillographs were used for "high-speed" data acquisition and recording. It was common to install strain gages on rotor and propeller blades. The oscillographs recorded the strain-gage data on 12-inch-wide paper rolls. After the run or after the test, the data curves had to be read by hand, most often by the test engineers. Eventually this system was upgraded, and data were included in the tunnel's computer system with a tape system used as backup.

Hot-wire instrumentation. Hot-wire probes were introduced into the tunnel for measuring unsteady velocities and turbulence in the late 1960s. The probes were small and therefore had a minimal effect on the airflow and had a relatively fast response. Hot-wire instrumentation utilizes a very small hot wire held at the end of a small fork. The wire temperature is maintained as the airstream acts to cool the wire. The voltage required to maintain the wire temperature is proportional to the air (or fluid) velocity, which is then measured and recorded and converted to velocity. Hot-wire probes were extensively used for measuring lift-generated wake vortices because the wakes were small and unsteady.

Laser velocimetry. Laser velocimetry was later developed in the early 1970s for measuring velocities. Laser velocimetry has no effect on the flow field, therefore it was used for many experiments in place of pitot-static or hot-wire probes. It allows velocities to be measured on the airfoils of spinning helicopter rotors and in lift-generated wake vortices without interfering with the model or the model flow field. Typically, two laser beams are aimed at the location where the air velocity is to be measured. Complex flows can be investigated. Before its use in the 40- by 80-Foot Wind Tunnel, early trial experiments were performed in the Ames 7- by 10-Foot Wind Tunnel to gain experience with operation of the equipment. References [11] and [12] describe how laser velocimetry works, and describe measurements of velocity distributions at the tip of a spinning rotor and measurements of lift-generated wake vortices. Subsequently, large systems were developed for the 40- by 80-Foot and 80- by 120-Foot Wind Tunnels [13-15].

Closed-circuit TV. During testing, especially rotorcraft and propeller testing, it became very desirable to monitor the status of the model with a closed-circuit TV system in the event of a model failure. The closed-circuit TV system was a great help in diagnosing problems and failures as they occurred. It became routine to continuously record TV images of the model during tests with rotating machinery. Even though there was closed-circuit TV, the practice of using an observer with an emergency stop button was maintained.

Fouling system upgrade. Often fouls would occur and the simple fouling system was not good in helping to determine the source. There would be significant delays in conducting the test if a foul occurred; occasionally delays could last for a couple of shifts. Because of these delays, a different system was implemented [16]. This new fouling system allowed work to continue on powered models if the grounding system was not turned on. Fouls could be detected while work was being performed on the models, which was essential for early detection of fouls and their subsequent correction.

Chapter 3. Major Upgrades, 1980–1987

Background

New Large-Scale and Higher-Speed Subsonic Wind Tunnel Studies

Tunnel shortcomings became evident during vertical and/or short takeoff and landing (V/STOL) model and rotorcraft studies at transition airspeeds between takeoff and cruise airspeeds. The 200-knot maximum airspeed of the tunnel limited research on high-speed rotorcraft. It was becoming increasingly more important to test at higher airspeeds for rotorcraft as well as for V/STOL aircraft. In addition, fighter aircraft were becoming larger, so 3/4-scale models were typically used instead of full-scale models or prototype aircraft. Tunnel wall effects became an issue at low speeds because of the large downwash angles from V/STOL aircraft and rotorcraft at transition and low speeds. Model wake interference with the walls, and especially with the floor, would occur, requiring large data corrections. Occasionally the model wake flow would impinge the tunnel floor and cause recirculation of the tunnel flow that would result in unrealistic test-section flow.

Because of evolving wind tunnel shortcomings, studies of new full-scale subsonic wind tunnels were performed at Langley, Lewis (Glenn), and Ames Research Center (the three Office of Aeronautics and Space Technology (OAST) Centers) from about 1967 to 1974. The prospective new tunnel was unofficially called the Super Tunnel. H. Clyde McLemore and William Gilbert of Langley; Roger Luidens, Douglas Breunlin, and Noel Sargent of Glenn; and Bill Eckert, Joe Piazza, and Kenneth Mort of Ames worked on the studies (as well as others). Cost reduction studies were performed because of the large size of the prospective tunnels. The feasibility of non-return wind tunnels (no return legs) as well as tunnels with shorter wide-angle diffusers was studied at Ames in the hopes of reducing construction costs. Models of the wind tunnels were built and used for studies. There was friendly competition among the three Centers. At Ames a complete model (about 1/106 scale) was built for wind-effect studies in the 40- by 80-Foot Wind Tunnel (Fig. 28, Test 402). The model was designed and built in a very short time using off-the-shelf air-cooled angle-grinder motors for drive motors and cut down British Motors Sprite automobile radiator fans for the drive fans. There were eight drive fans in a two-by-four arrangement [17]. The full-scale wind tunnel was designed to have 18 drive units in a three-by-six arrangement because of the limitations of designing and building large fans and motors. The 18 drive units were simulated by downstream transition ducts as can be seen in the photo (Fig. 28) that shows the six vertical rows.

From the wind-effect studies in the 40- by 80-Foot Wind Tunnel, engineers concluded that a non-return circuit was feasible and that flow quality could be made acceptable using screened areas in front of the inlets, along with a vertical exit. The flow quality could be comparable to that of closed-circuit wind tunnels, regardless of wind conditions, using screened chambers in front of the contraction inlet for tunnels with equal performance. Regardless of location, they determined that a non-return wind tunnel could be built with the same flow quality as a closed-circuit wind tunnel with at least 20 to 30 percent lower construction cost and with the same performance or power required and flow quality [18, 19]. However, a clear area in front of the inlet would be required so that the effects of upstream structures would not adversely affect the flow quality. The trade-off was wind tunnel structural cost versus real estate in front of the inlet.

The judgment at all three Centers was that non-return wind tunnels would be acceptable and cost-effective, and that the tunnel temperature would not need to be precisely controlled. Temperature was not controlled in the 40- by 80-Foot Wind Tunnel nor in the Langley 30- by 60-Foot Wind Tunnel. Data were simply corrected for the small temperature variations. Therefore, temperature variations would not be a problem for a non-return wind tunnel. In addition, a non-return wind tunnel would, of course, not need airing out after engine-powered model and aircraft investigations.

From the diffuser experiments performed, it was evident that wide-angle diffusers were not feasible because of excessively high total-pressure losses. Model studies were performed on diffusers with internal vanes that could be much shorter than conventional diffusers. Vaned diffusers could achieve the required pressure recovery and be a lot cheaper, but the losses were much too high. Wide-angle diffusers with bleed air to energize the boundary layer were also considered. These diffusers, however, could not be made to work consistently. In general, the diffuser studies performed validated the diffuser research described in the literature.

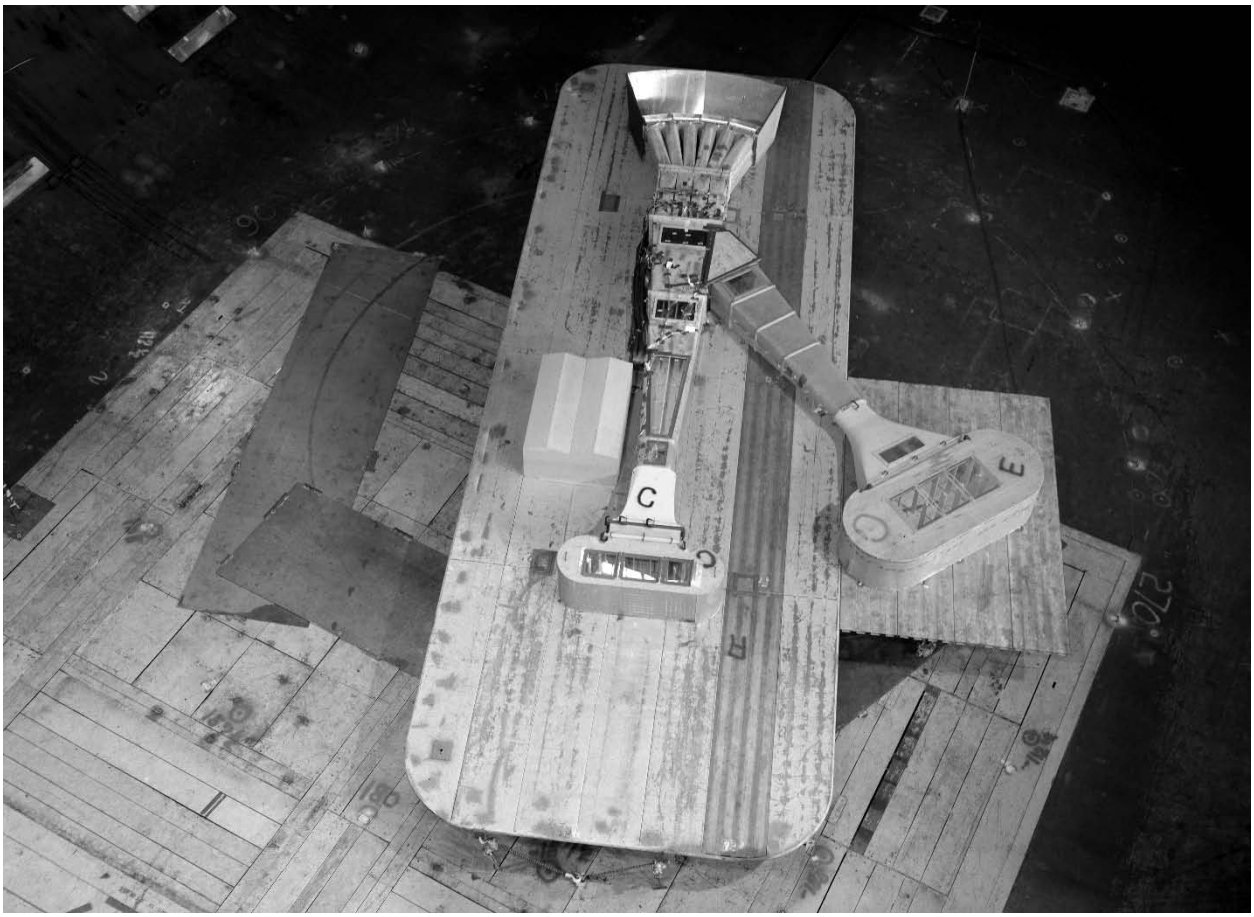

Figure 28. Super Tunnel model mounted on a ground board used for wind-effect studies in the tunnel. Y-configuration, high-speed test-section screened inlet in lower center, low-speed test-section screened inlet to the right, and vertical exhaust at top of figure. ***(NASA A72-2687)***

Two open-circuit test sections in a Y-configuration that shared a common drive appeared to be the most cost-effective configuration for an entirely new large-scale facility. Engineering studies were completed by August 1973.There was a low-speed leg with a 133- by 200-foot flat-oval test section with a maximum airspeed of 150 knots for performing research on V/STOL aircraft and rotorcraft at low speeds and for performing research on miscellaneous large aircraft/models. A high-speed leg with a 75- by 150-foot flat-oval test section and a maximum airspeed of 300 knots would be used for research on high-speed rotorcraft and propulsive devices. The flat-oval-shaped test section was the same shape as the test section in the 40- by 80-Foot Wind Tunnel and the 30- by 60-Foot Wind Tunnel. Studies had indicated that wall effects would be minimal and circuit losses would be somewhat lower than with a rectangular test section of the same cross-sectional area.

The shared drive with 18 drive fans would require a total power of about 400,000 hp. The 18 drive units were determined—at the time—to be cost-effective because of the practical size limitations of electric motors and construction of large custom-built fans. Extensive drive studies were performed in-house, as well as by General Electric and Westinghouse and others. Variable-pitch drive fans appeared to be cost-effective. Solid-state equipment would be used to start the synchronous motors and get them up to synchronous speed at flat pitch or low-fan-blade angles to minimize the power required [17-21].

In parallel with studies of new wind tunnels, modifications of existing wind tunnels were studied, including modification of the 40- by 80-Foot Wind Tunnel. As a result, it became evident that repowering the 40- by 80-Foot Wind Tunnel and adding an 80- by 120-foot test section sharing a common drive would be cost-effective and meet the majority of the research requirements for the near future. The cost was estimated to be an order of magnitude less than for the new larger wind tunnel. The decision was made by NASA HQ (with much encouragement from Ames) to modify the 40- by 80-Foot Wind Tunnel rather than build a new wind tunnel.

Modification of the 40- by 80-Foot Wind Tunnel: Repowering and the Addition of the 80- by 120-Foot Test Section

Studies and Configuration Development

First project team. The first project team was established by the Center Director, Dr. Hans Mark, by memo to the Center on September 26, 1973. Benjamin H. Beam was the Project Manager, James M. Silver was the Deputy Project Manager for engineering, and Kenneth W. Mort was the Deputy Project Manager for aerodynamics. In addition, fan system design was managed by Wayne O. Hadland, electrical and drive system design was managed by Conrad W. McCloskey, project control was managed by Virgil R. Page, and safety was managed by Lewis W. Hughes.

Geometry development. Figure 29 illustrates the operation of the facility in the 40- by 80-foot and 80- by 120-foot modes. Design details were developed using a 1/50-scale model of the entire facility, a 6-foot-diameter fan model (15 percent scale) of the drive, 1/10-scale models of new vanes and louvers, and full-scale acoustic louvers in the Ames 7- by 10-Foot Wind Tunnel. The 1/50-scale model was tested in the 40- by 80-Foot Wind Tunnel to study wind effects on flow quality on the model of the 80- by 120-Foot Wind Tunnel. The arrangement of the inlet for the

80- by 120-foot test section took advantage of the prevailing winds, which were from the northwest and approximately aligned with the proposed inlet. New wind tunnel studies had found that wind effects were much less for winds aligned with, and heading into, the inlet.

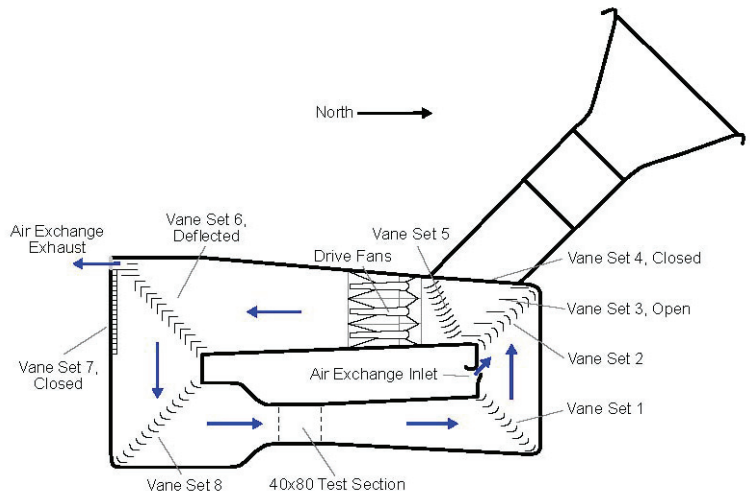

40- by 80-Foot Test Section

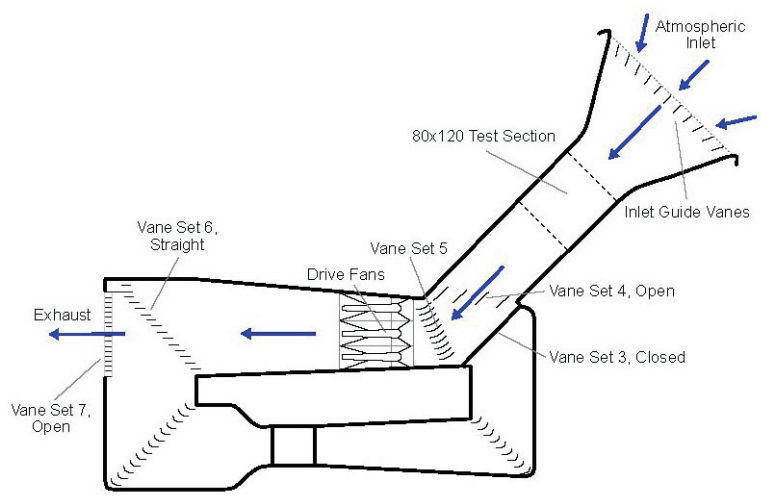

80- by 120-Foot Test Section

Figure 29. Illustration of the NFAC operating in 40- by 80-foot and 80- by 120-foot modes. Vane sets three, four, six, and seven are moved to change the flow between modes. ***(NFAC 40x80; NFAC 80x120)***

This model was also used to verify performance and wall pressure estimates. Air exchangers for cooling during operation of the 40- by 80-foot test section were studied. (Air exchangers cause a portion of the hot inside air to be exhausted and cool outside air injected into the tunnel.) The 1/50-scale model was used to study the exhaust during operation of the 80- by 120-foot test section. Fan inflow was measured during operation of both test sections. The model was also used for acoustic studies. Model results were corrected for Reynolds number effects as required. The drive motors were 10-hp model motors borrowed from Langley Research Center (they were never returned to Langley), and custom fans were designed at Ames Research Center and built using laminated spruce in the Ames model shop. See reference [22] for the rationale and design features for the facility. The model was mounted to a rotatable ground board in the 40- by 80-foot test section (Figs. 30 and 31).

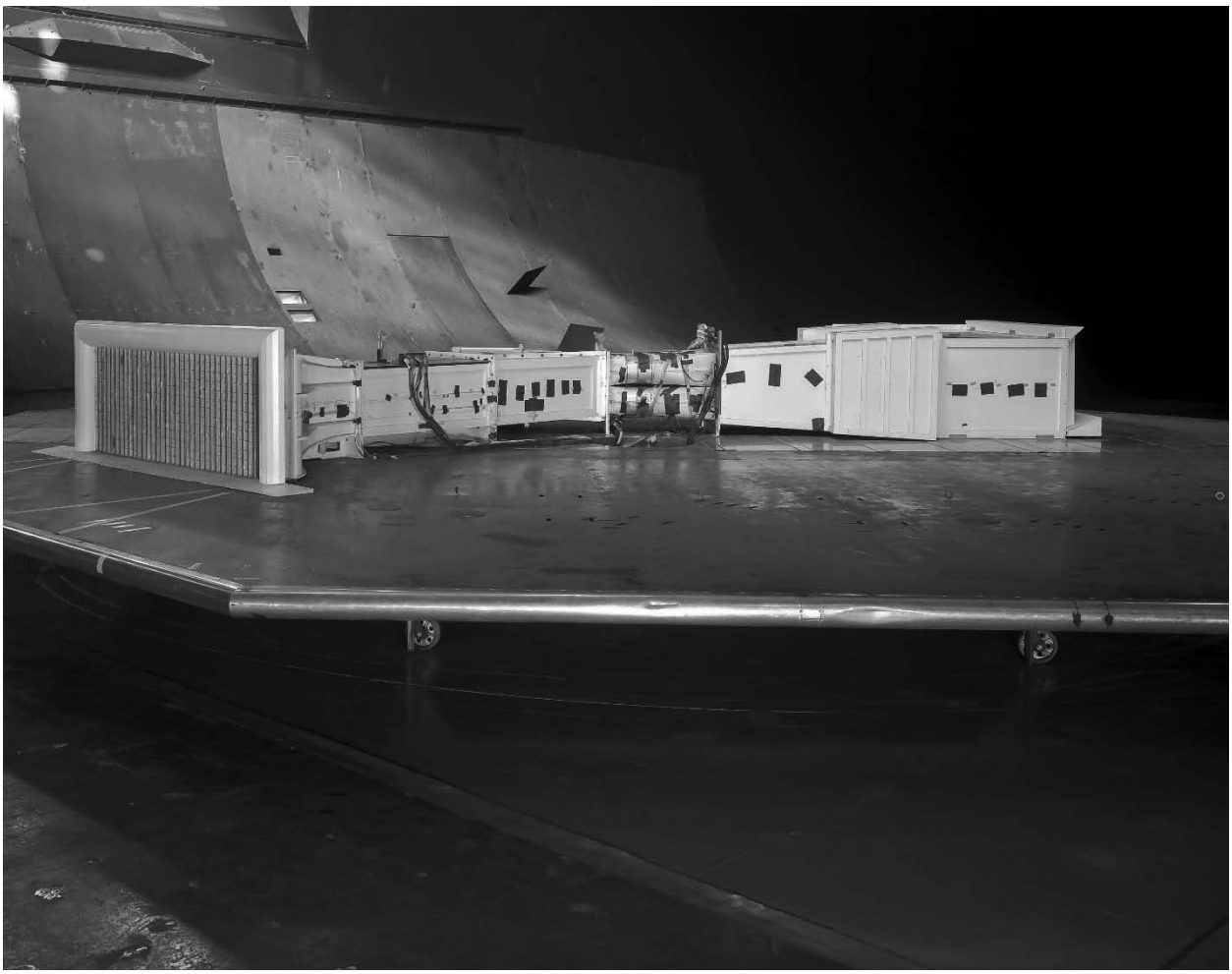

Figure 30. Side view of NFAC wind tunnel model in the 40- by 80-foot test section mounted on a ground board. Inlet for the 80- by 120-foot test section on the left and drive in the center. ***(NASA A76-0634)***

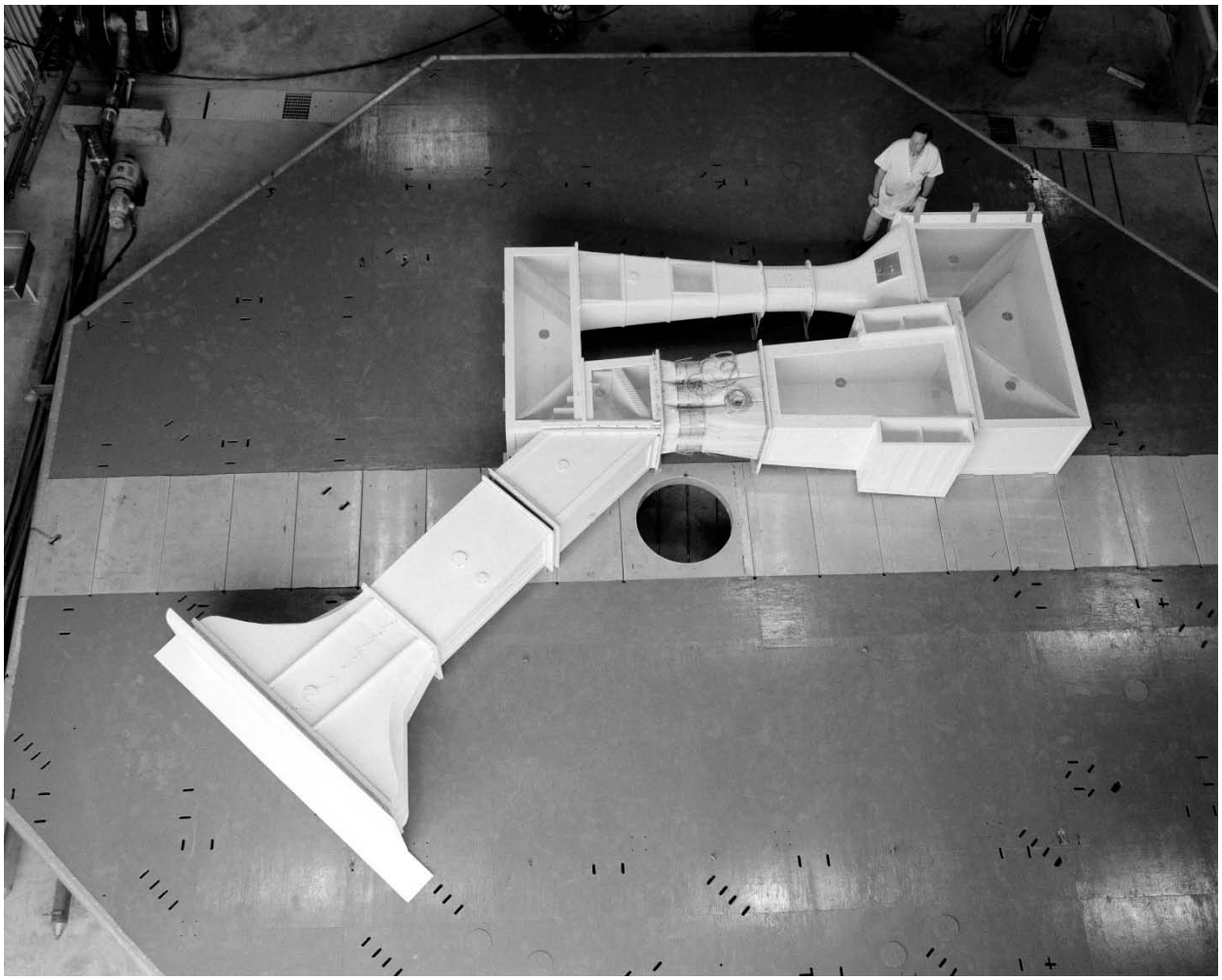

Figure 31. Top view of NFAC wind tunnel model in 40- by 80-foot test section with Gene Thomas, model builder, in photo. The 80- by 120-foot test-section inlet is shown at lower left. ***(NASA A74-4514)***

Drive development. Numerous in-house and contractor studies of the drive system were performed; it was important to achieve both high efficiency and low noise. The 6-foot-diameter fan model included the entire drive nacelle and diffuser and was used to verify fan performance and noise level estimates, as well as fan diffuser loss estimates. A high-speed-fan (627 feet per second (fps) tip speed) and two low-speed-fan (377 fps tip speed) designs were tested. Results showed the low-speed fans had the same performance but lower noise than the high-speed fan, although they required 15 fan blades compared to 9 blades; in addition, 23 stators were required to straighten the flow. It was found that the noise from the low-speed fans was much less sensitive to inflow disturbances, which is very desirable for a wind tunnel drive because of possible model-caused flow disturbances. A low-speed fan with the highest efficiency was selected because of its lower noise for both lower community (or environmental) noise and because low background noise was important when performing acoustic studies in the facility [23-26].

The final drive fan design was state of the art. Modified 65 series airfoil shapes were used instead of Clark Y airfoils (as had been used in the original fans). Drive studies were completed by the Applied Mechanics Branch of the Power Generation and Propulsion Laboratory, Corporate Research and Development, at General Electric Company in Schenectady, New York. The fan was designed by the GE Aircraft Engine Business Group's Advanced Turbomachinery Aerodynamics subsection under the direction of Dr. Leroy H. Smith, Jr. [23]. The principal contributors were Harold Lown; M. R. Simonson; Dr. Leroy H. Smith, Jr.; and Richard J. Wells of General Electric. The motor diameter was minimized with some fan and motor design effort for a hub/tip ratio of 0.4375 to reduce the drive nacelle losses [23]. The motors and the drive control system were designed by Westinghouse. Dealing with the fan-inflow-velocity variation due to the wind tunnel boundary-layer buildup, which was on the order of 20 feet thick, complicated the fan design. It is interesting to note that the original fan design had assumed uniform fan inflow, which, of course, was not the case. However, at the time the inflow velocity distribution was unknown, and a wind tunnel drive with six fans was unique.

Fan diffuser measurements verified studies that indicated reduced fan diffuser loss if residual swirl was introduced that was about the same as the equivalent cone angle of the fan diffuser; that is, about 10 degrees [27]. This was accomplished by reducing the camber of the stators and was especially important for operation of the 80- by 120-foot test section because the fan diffuser accounted for about 25 percent of the total circuit aerodynamic losses. It was expected that the swirl would be taken out by the downstream wind tunnel vane sets (vane sets six and eight) during operation of the 40- by 80-foot test section.

Drive controls. The higher test-section air velocity and the new wind tunnel drive fans of course required larger fan drive motors. Synchronous motors were the first choice because of their relatively low cost and their high efficiency. Six 18,000-hp motors (22,500 hp, 2-hour rating) were required to power the revised wind tunnel. Such motors are not usually designed to be started by connecting them directly to the electrical grid; they must be brought up to synchronous speed by some other means, usually a separate variable-speed motor. The existing large motor-generator (MG) sets used in the modified Kramer drive system represented a large investment, and rebuilding the rotor of one of the machines made it possible to convert the machine to a frequency changer. The frequency changer driven by the MG set could provide enough power to start the fan drive motors and operate them over the lower part of the airspeed range. When the speed, and thus the load, on the fans approached the power limit of the MG set, the frequency changer could be brought to 60 Hz, and the drive motors connected directly to the power grid. Higher test-section air velocities could then be attained by increasing the fan blade angle with the blade-pitch control system.

Responsible design of the new facility dictated retention of any usable existing equipment, and reusing the large MG sets resulted in effective cost savings. The original speed control of the fan motors used a motor-operated "multi-rheostat," (six rheostats ganged together and remotely positioned by the wind tunnel operator). This 10-foot-long, largely handmade apparatus, in turn, controlled the field currents of the large MG sets, directly and through a six-unit exciter MG set. These early 20th-century devices gave way to late-20th-century substitutes. Advances in solid-state electronics made it possible to replace these electromechanical devices with solid-state power supplies and to attain a true closed-loop speed control system, as opposed to the test-section speed loop closed by the operator.

Vanes and louvers. A special test facility was fabricated and was driven by a 4-foot-diameter fan to test candidate vanes and louvers for the new facility. Figure 29 illustrates the wind tunnel configuration. The most important new vane set comprised the vanes that were upstream of the drive and had to direct the flow from either the 40- by 80-foot or the 80- by 120-foot test section. This was the fifth vane set downstream of the 40- by 80-foot test section, so it was called vane set five. Vane sets one and two were the original 40- by 80-Foot Wind Tunnel turning vanes. Vane sets three and four were the louvers that were added to close off the circuits as required. Several configurations were tried for vane set five. Both losses and turning efficiency were determined. The selected configuration had nose sections that could be deflected during operation of the 80- by 120-foot test section and a fixed tail section [28].

The vane set downstream of the drive, which deflected the flow out the exhaust during operation of the 80- by 120-foot test section, was named vane set six. The forward part of the vane set was fixed and consisted of acoustic baffles. The downstream part of the vane set was a panel that could be deflected. It was essentially straight during operation of the 80- by 120-foot test section and deflected to serve as turning vanes during operation of the 40- by 80-foot test section.

Vane set seven was the louvers that were on the south wall that opened and closed depending on which circuit was operational. They served as the exhaust louvers during operation of the 80- by 120-foot test section and diffused and deflected the exhaust flow upward about 25 to 45 degrees. Vane set eight was the turning vane set upstream of the 40- by 80-foot test section and was the original vane set.

Wind effects. Extensive research had been done in support of studies for a new wind tunnel, which was beneficial to the development of the modified 40- by 80-Foot Wind Tunnel. Wind measurements were done at the site using an anemometer mounted on a tower upstream of the inlet location for the 80- by 120-foot test section. In addition, data the Navy had collected for many years at Moffett Field were useful for analysis. Because of the prevailing winds and the favorable orientation, it was judged that minimal inlet treatment would be acceptable, and a 5:1 contraction ratio would be acceptable. As mentioned earlier, engineers had found that flow directly into the inlet was the easiest to deal with in minimizing wind effects on the wind tunnel flow quality. Inlet flow straighteners were required, which also served as acoustic baffles. A small honeycomb screen was located near the leading edge of the baffles to help improve the flow and to serve as a bird screen. Based on experiments with the 1/50-scale model, the flow quality in the 80- by 120-foot test section was judged to be acceptable for testing V/STOL and rotorcraft models [29, 30].

Winds into the exhaust were more of a problem; fortunately winds from that direction were very rare. It was judged that minimum treatment would be required at the exhaust. The exhaust air was deflected upward at an angle by vane set seven to avoid the existing roadway and buildings downstream of the exhaust. Studies were also done concerning the exhaust velocity decay so there would not be a problem for low flying, low-wing-loading aircraft.

Acoustics. Acoustic characteristics of the tunnel were estimated from acoustic measurements of the existing tunnel, the 1/50-scale model, and the 6-foot-diameter fan model. Full-scale acoustic baffles were developed in the NASA Ames 7- by 10-Foot Wind Tunnel; four baffles were simulated [31, 32]. Noise contours were developed for the proposed wind tunnel. In general, the

community noise was determined to be significantly less (about 10 dB) than the noise from the original 40- by 80-Foot Wind Tunnel at full-power conditions.

Detailed Design

Architect-engineering (A/E) team. An A/E team was selected on March 12, 1973, to perform detailed design analysis and write the preliminary engineering report (PER) and the environmental impact statement (EIS). A contract was signed by the A/E team on June 13, 1973. The A/E team consisted of URS/John A. Blume and Associates, Parsons Corporation, and FluiDyne Engineering. This team furnished all of the expertise required to design a very large and unique wind tunnel. Blume was well known for designing large structures that were excellent in withstanding large earthquakes. Parsons' expertise was in designing large rotating machinery, and FluiDyne was experienced in designing aerodynamic facilities.

Unfortunately, NASA HQ became short of money for design, so partway through design they wanted Ames to descope the design contract. The scope of work was reduced, and then later restored, but the activity of descoping and then restoring at the same contract funding level took unproductive resources from both the Ames team and the A/E team.

Geometry. The aerodynamic flow path—the internal shape of the wind tunnel—was developed by NASA and furnished to the A/E team. A design document was developed and furnished to the A/E team that described the shapes required and the design loads. William Eckert and Jean Jope developed software to derive the wind tunnel performance and wind tunnel wall pressures. The procedures for estimating wind tunnel performance were subsequently described in reference [33], which includes design guidelines and is widely used by many wind tunnel designers.

Drive and controls. The drive system was a significant departure from the original drive. The original drive used fixed-pitch fans and variable rotational speed to control wind tunnel airspeed. As a cost-saving approach, the new drive used the modified Kramer Set to start the synchronous motors and bring the motors up to synchronous speed. Operation in this phase allowed absorption of total power up to 30,000 hp. At synchronous speed, the variable fan-blade angle was used to vary the airspeed. The blade angle could be varied under all conditions within the power limits. At the maximum rotational speed of 180 revolutions per minute (rpm), the airspeed could be varied from about –10 knots to the maximum capabilities of the two test sections—that is, 100 knots in the 80- by 120-foot test section and 300 knots in the 40- by 80-foot test section at the maximum total drive power of 135,000 hp (2-hour motor rating). The tunnels were designed to achieve these airspeeds with test-section blockages representative of typical models and their supports.

Studies of the original drawings indicated that the design of the two structural-support bents for the drives was exceptionally conservative, which proved a major advantage, and additional support structure was not required. The steel bent structure had been conservative; to improve strength and damping, the entire steel structure of the two bents had been encased in concrete.

Model handling. A more-or-less-standard 75-ton-capacity gantry crane was obtained to lift and install models in the 80- by 120-foot test section. There are two access doors on the northeast side of the test section to allow the gantry crane to enter into the test section from the side. To install or remove models, these doors open and then floor access panels open to allow the legs of

the gantry crane to pass into the test section. The floor of the test section is about 25 feet above ground level. Models are at ground level when they are transported to the side of the test section. The gantry crane lifts the models up from this level, transports the models into the test section, and then sets them down on the support struts where they are attached to ball joints at the strut tips.

Model supports. The model-support system in the 80- by 120-foot test section was patterned after the model-support system in the 40- by 80-foot test section. The balance frame contains a turntable onto which the model-support struts were mounted. The tail strut was telescoping. The main strut tread could be varied, and the distance between the main struts and tail strut could be varied depending on the model size requirements. There were several lengths of main struts so the model height above the test-section floor could be changed for ground-effect testing.

Platform balance. A platform balance was used in the 80- by 120-foot test section to measure model forces and moments. It was essentially scaled up from the platform balance in the 40- by 80-foot test section because of the success of that balance. Platform balances are exceptionally reliable mechanical balances that had been used in several NACA wind tunnels. The balance was built by Toledo Scale Company. William Tolhurst was the technical monitor for the contract because of his expertise with the 40- by 80-foot test-section balance.

Data acquisition systems. The data systems for both test sections were upgraded and standardized. Several computers were employed, and data reduction and online plots of reduced data were standardized for efficient test conduct.

Preliminary Engineering Report (PER) and Environmental Impact Statement (EIS)

A PER for the modified tunnel was issued in August 1974. The tunnel would have at least a maximum airspeed of 300 knots in the 40- by 80-foot test section and at least 100 knots in a new 80- by 120-foot test section. The two test sections would share a common 135,000-hp drive (2-hour rating, 111,000-hp continuous rating). As before, the drive consisted of six 40-foot-diameter drive units in a three-by-two arrangement; however, the 2-hour rating for each motor would be 22,500 hp rather than the original 6,000 hp. Appropriate vanes and louvers were designed so that the two test sections could be used, one at a time, with the shared drive. The intention was to increase productivity by being able to do model preparation work in one test section while research was being conducted in the other test section.

An EIS was completed by the A/E team. A series of meetings with the neighboring communities (Mountain View, Sunnyvale, Palo Alto, Los Altos, etc.) were held describing the proposed modifications to the 40- by 80-Foot Wind Tunnel. Predicted noise levels were presented: at maximum airspeed the new drive was predicted to be significantly quieter than the existing drive (on the order of 10 dB) even though the maximum drive power was to be increased nearly four times. This was due to lower fan-blade tip speed and placement of the fans upstream of the motor supports instead of downstream. The wakes of the support struts had had a major impact on the fan loading and on the noise of the original fans. It was emphasized to the communities that not only was low noise important from the community standpoint, it was also very important from an acoustic research standpoint. The reactions of the communities to the presentations were very favorable, and they were very supportive of the planned project.

Construction

Groundbreaking for construction of the 80- by 120-Foot Wind Tunnel occurred in November 1978, and the 40- by 80-Foot Wind Tunnel was shut down in July 1980 for repowering. Prior to the shutdown, more than 600 research tests in the 40- by 80-Foot Wind Tunnel had been performed and hundreds of reports written. The 40- by 80-Foot Wind Tunnel was well established as a national treasure and a major contributor to the advancement of aeronautics; it helped establish aeronautics as a so-called mature science.

An Ames team served as the general contractor, with the aid of a construction manager, to save construction costs. An Ames review board was also established to periodically review safety, engineering, performance, cost, and schedule.

More than 50 contractors were required for construction, all low bidders that ranged in quality from excellent to marginally acceptable. The drives alone needed about a dozen contractors. This made construction management very complex. The motors and their control system were built by Westinghouse. Synchronous motors were used and the existing MG set, which had been built by Westinghouse, was modified for starting the motors and for controlling the frequency so that the rotational speed of the synchronous drive motors could be precisely varied at low rpm and low power for low-speed research. Studies at the time indicated that it would be cost-effective to use the modified MG set rather than buy a new starting system that would have been solid-state. Also, at the time, large solid-state equipment had to be custom designed and built and was very expensive. A variable-pitch hub was designed and built for varying airspeed with the motors at their maximum synchronous speed of 180 rpm and to achieve maximum airspeed. Variable blade pitch could also be used at lower rotational speeds to provide more flexibility for controlling the character of the drive's background noise when performing acoustic research at low airspeeds.

NASA HQ was a strong and continual advocate for value engineering. (If bids come in higher than expected, design studies are performed to explore revisions that have the potential to reduce construction cost, however in-house staff are typically required.) Value engineering was frequently performed to minimize construction cost. For example, initially a fan spinner (fan nose cone) was to be used to maximize fan performance. The first concept was an aluminum spinning, 17.5 feet in diameter. At the time there was only one company in the country that could manufacture spinnings that large. When fixed-price bids were limited and excessive, a second concept design for a composite spinner was put out for bid. Bids for the composite spinner were also excessive. There was a lot of construction uncertainty, which resulted in very few bidders. A fixed steel nose cone was finally selected and designed in-house to reduce cost and uncertainty. Struts were required for support, but they were streamlined to reduce inflow disturbances to the fans.

The fan inlet-contraction duct length was reduced by half to lower construction cost. Compound curves were used for the contraction to improve fan inflow. Because of the complexity of the shapes, the Ames designers produced many of the shop drawings, in addition to design drawings, for the fabricator. Many design details were completed and furnished by Wilbur Vallotton of Ames.

Most of the special vanes and louvers were redesigned in-house to reduce construction cost and to simplify operation. Instead of adding acoustic baffles upstream of vane set six, reinforcing the old vane set six and adding a trailing-edge vane to turn the flow for 80- by 120-Foot Wind Tunnel operation as originally planned, a new vane set six was designed in which the upstream part was fixed and constructed as acoustic baffles with a panel or flap attached to the trailing edge. This was not only cheaper, but it was an improvement aerodynamically and acoustically.

Engineers also determined that it would be acceptable to have support columns for the ceiling and roof structure going down the center of the primary diffuser of the 40- by 80-Foot Wind Tunnel circuit. The columns were streamlined to ensure acceptably low drag. These columns eliminated the reinforcement required for the ceiling steel-support bents, which provided a major cost savings.

To further reduce cost, the 80- by 120-Foot Wind tunnel exit area was reduced. The maximum airspeed penalty was estimated to be 5 to 10 percent. Ames management decided that a maximum airspeed of 100 knots was sufficient for the tunnel. In addition, the ramp for the 80- by 120-Foot Wind Tunnel exhaust was eliminated; its needs would be determined during full-scale wind tunnel operation to better define the requirements. At about the same time, the model preparation building for the 80- by 120-Foot Wind Tunnel—which had been intended to improve productivity—was eliminated from the project to reduce costs. NASA HQ had mandated that the total construction cost not exceed $85 million, despite the acknowledgement that the price of steel had increased substantially after early estimates had been made, and that unforeseen events were very likely when repowering and extensively modifying the world's largest wind tunnel.

Several figures show some of the construction of the 80- by 120-Foot Wind Tunnel model support and balance system. Figure 32 shows the beginning of the foundation for the model support and balance frame, Figure 33 shows the completed octagonal concrete foundation, Figure 34 shows installation of the round balance frame into the foundation, Figure 35 shows lifting the T-frame prior to installation in the balance frame, and Figure 36 shows the installation of the turntable floor. Sketches of the assembly of the model support and balance system are shown in Figures 37 and 38, respectively.

The beginning of the test leg framing is shown in Figure 39. The view is from the top of the 40- by 80-Foot Wind Tunnel. The beginning of the structure for the inlet is shown in Figure 40 from the same location, and completed framing is shown in Figure 41. The completed leg is shown in Figure 42 viewed from the east and in Figure 43 viewed from the north. The model-handling gantry crane is shown in both views. Figure 44 shows the model-handling gantry crane in the 80- by 120-foot test section with the doors and the floor access panels open.

Figure 32. Beginning of concrete forms for construction of the foundation for the 80- by 120-foot test-section model support and balance. ***(Author's collection, KM31)***

Figure 33. Completed octagonal concrete foundation for the model support and balance. ***(Author's collection, KM34)***

Figure 34. Lowering the turntable into the octagonal foundation. ***(Author's collection, KM38)***

Figure 35. Lifting the model support T-frame. ***(Author's collection, KM39)***

Figure 36. Lifting the turntable floor for installation. ***(T.J. Forsyth collection, TJ3)***

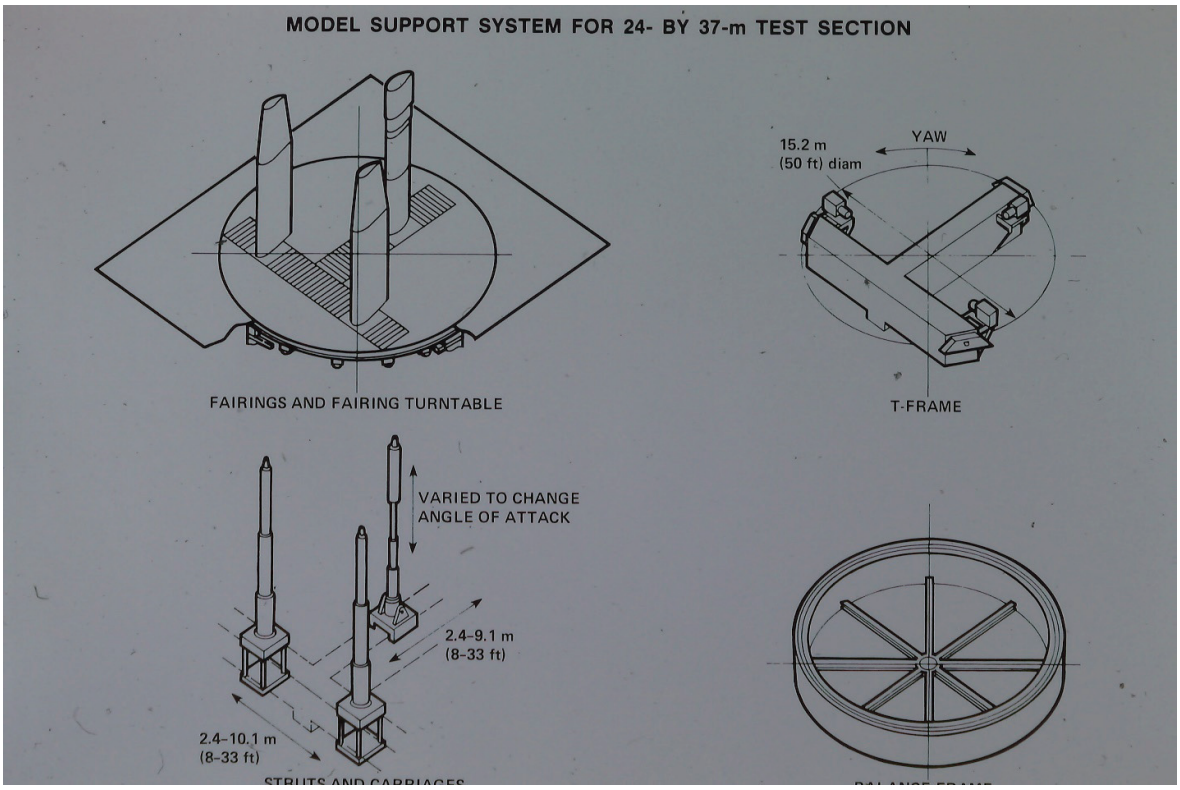

Figure 37. Sketch of the model support. ***(Author's collection, KM35)***

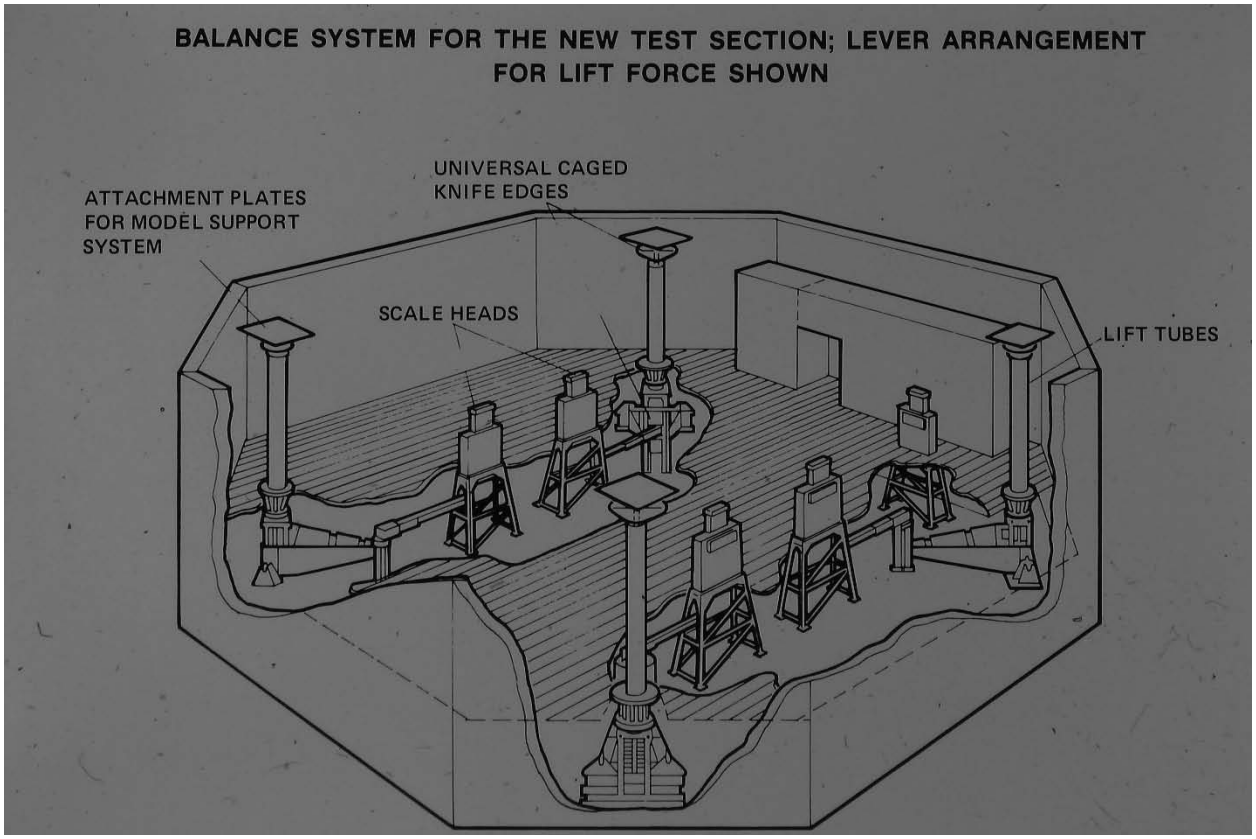

Figure 38. Sketch of the model balance system. ***(Author's collection, KM43.1)***

Figure 39. Beginning of the 80- by 120-foot test-section test leg framing. ***(NASA AC81-8017-25)***

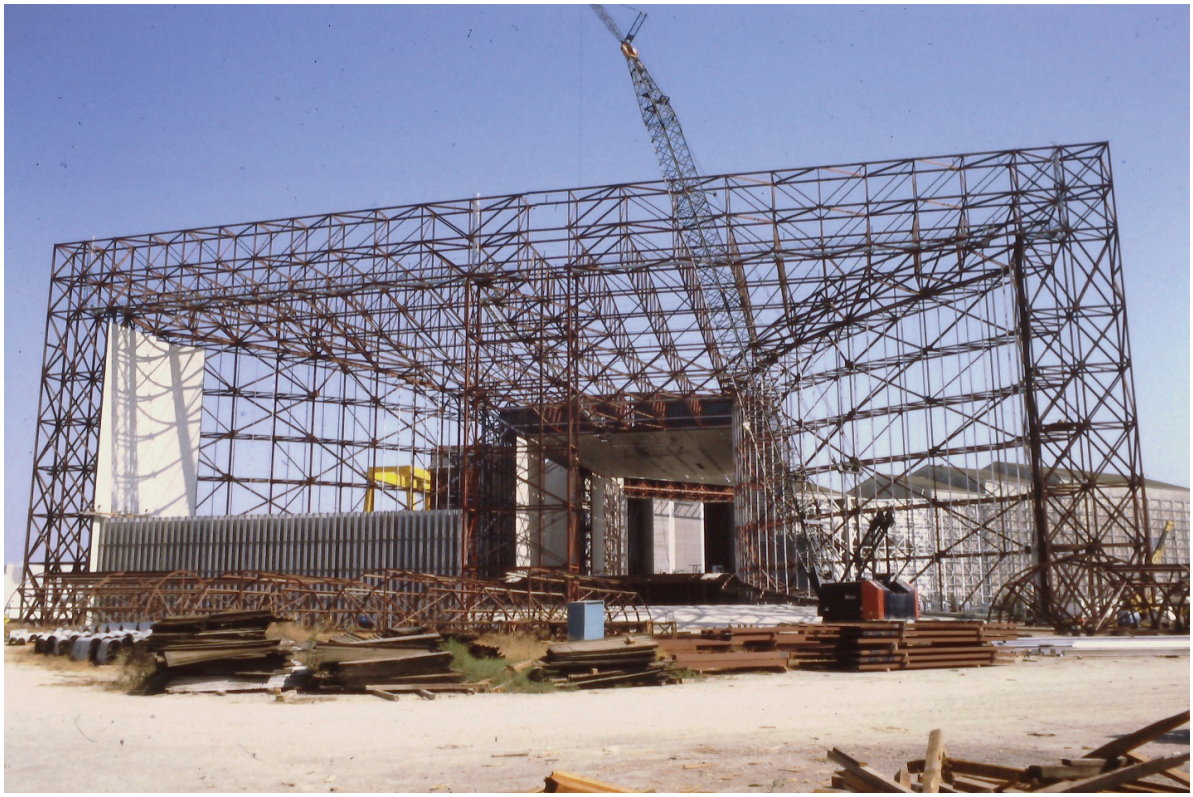

Figure 40. Beginning of the inlet framing. ***(Author's collection, KM50)***

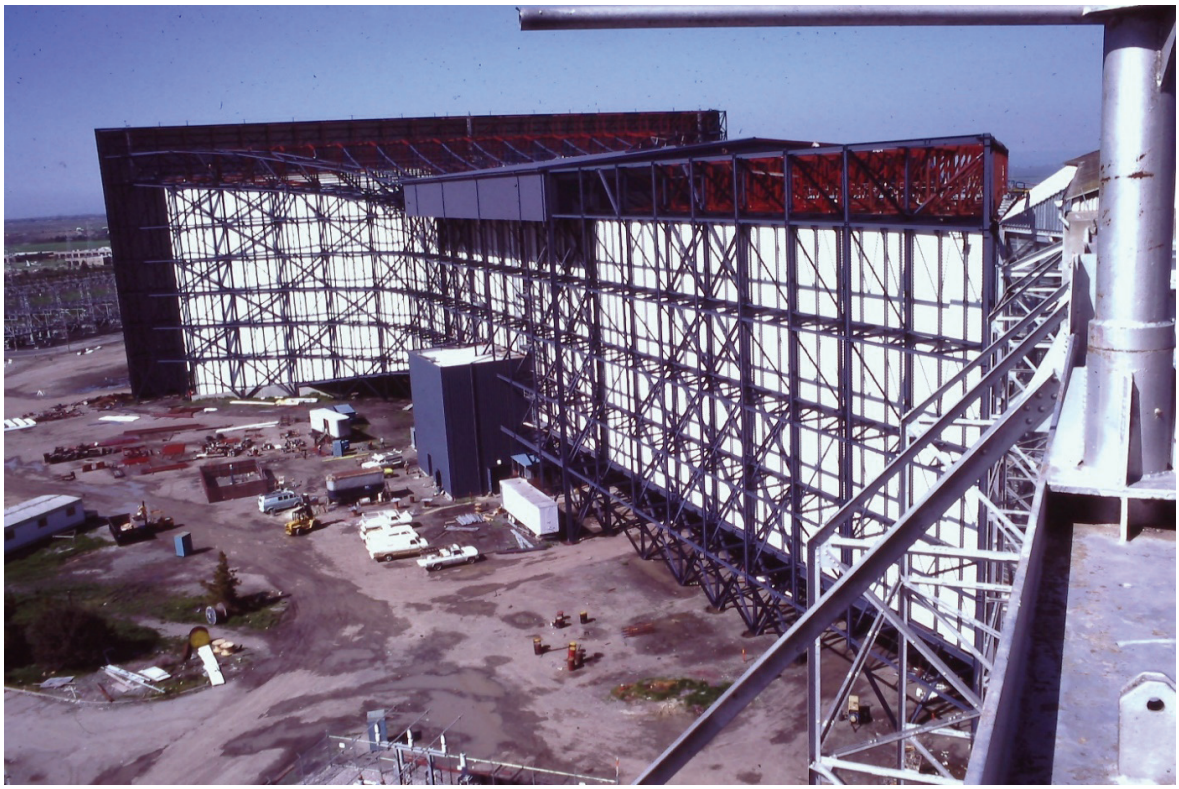

Figure 41. Completed new leg framing. ***(Author's collection, KM54)***

Figure 42. Completed NFAC viewed from the east. Yellow gantry crane for the 80- by 120-foot test section is shown outside the test section to the right. ***(NASA AC84-0712-28)***

Figure 43. Completed NFAC viewed from the north. ***(NASA AC84-0712-15.1)***

Figure 44. Model-handling gantry crane in the 80- by 120-foot test section with the test-section doors and floor access panels open. ***(Author's collection, KM76)***

Two fixed-price bids were received for the design and construction of the drive fan blades: one design had a cast aluminum spar covered with foam and fiberglass, and the second was a wood composite. The wood composite was selected as it was about half the cost. The fan blades were made in England by Permali-Gloucester Ltd. The root sections were composed of a proprietary material named Hydulignum, which consisted of a stack of 0.035-inch-thick birch veneers glued together and compressed with heat into boards about three-quarters of an inch thick, having about three times the strength of natural birch with a specific gravity of 1.31. The root sections were threaded into steel adapters. This was a process developed by Permali to build airplane propellers during World War II when metal was scarce; some Spitfire Airplane propeller blades had been built this way. Laminated spruce was used farther out on the blades. A balsa wood tip was used for ready repair if foreign object damage (FOD) occurred at the tip. Some balsa wood was also used internally to control weight and the center-of-gravity (c.g.) location. The wood was covered with several layers of fiberglass for protection. Covering the blades with fiberglass was the approach successfully developed to protect the laminated spruce fan blades in the original drive. Figure 45 shows a row of blade blocks before shaping, Figure 46 shows the shaping process with a pattern as a guide and a following router, and Figure 47 shows a blade ready for covering with fiberglass.

Figure 45. Row of drive fan blade blocks awaiting shaping. ***(Author's collection, KM7)***

Figure 46. Fan blade shaping process showing the pattern on the left with follower and cutting router on the right. ***(Author's collection, KM8)***

Figure 47. Fan blade ready for covering with fiberglass. ***(Author's collection, KM10)***

The stator blades were laminated out of 3/4-inch-thick spruce boards. The construction approach was very similar to the original 40- by 80-Foot Wind Tunnel fan blade construction. The stator blades were also covered with several layers of fiberglass for protection.

To minimize wind tunnel downtime, engineers decided to remove the old drives as complete units and install the new drives as complete units as much as was practical. The fan blades of the old drives were cut off at the blade roots, and the nose cones and tail cones were unbolted before drive removal. The new drives were installed without the blades and without the nose and tail cones. Major construction challenges were removal of the old drives, which weighed about 70 tons each, and installation of the new drives that weighed more than 200 tons each. The old drives were removed and the new drives installed using a very large elevator constructed downstream of the concrete support bents at the concrete floor upstream of the settling chamber. A large bridge, approximately 200 feet long, was constructed that extended from the elevator to the concrete drive-support bents. The bridge was constructed with twin 7-foot-deep steel girders. An intermediate support was installed between the fan mounting location and the elevator. This approach allowed the complete drive units to be removed (except for the fan blades, nose cones, and tail cones), and the assembled new drive units to be installed complete (except for the blading and nose and tail cones). It was spectacular to see the old drive units removed and the new units installed. Figure 48 shows the motor mounted on the chassis in the shop, and Figure 49 shows the drive unit being transported to the wind tunnel. Figure 50 shows installation of the last drive partially lifted with the elevator, and Figure 51 is a rear view of the completed drive. Figure 52 is a front view of the completed drive. There are 15 rotor blades and 23 stator blades for each of the six drive units.

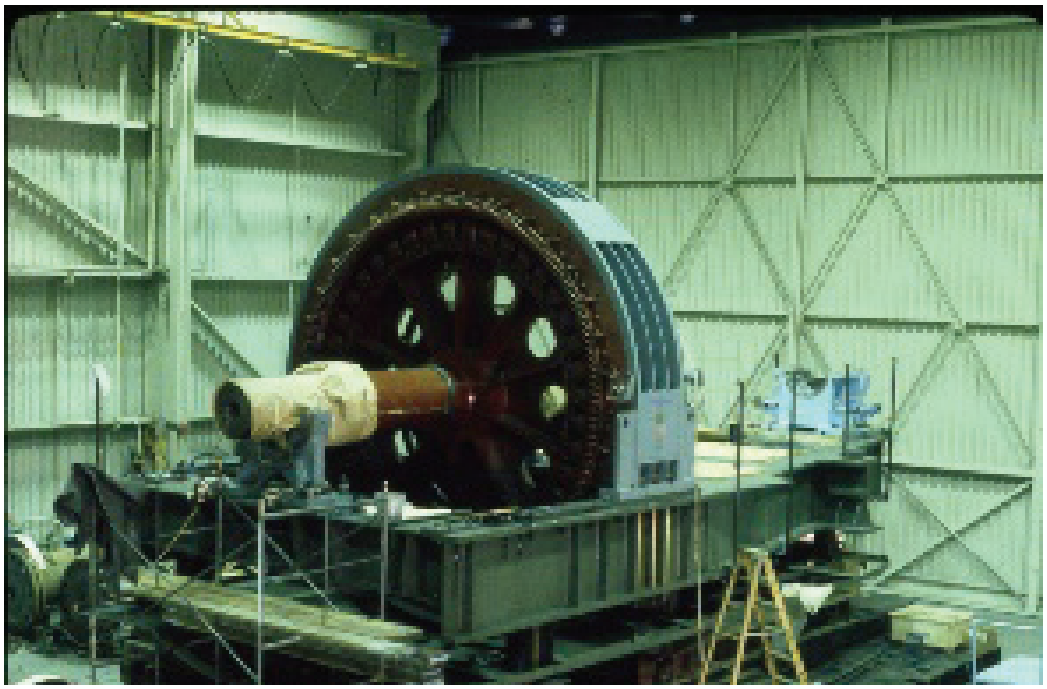

Figure 48. New drive motor mounted on its chassis in the shop.
(T. J. Forsyth collection, TJ8)

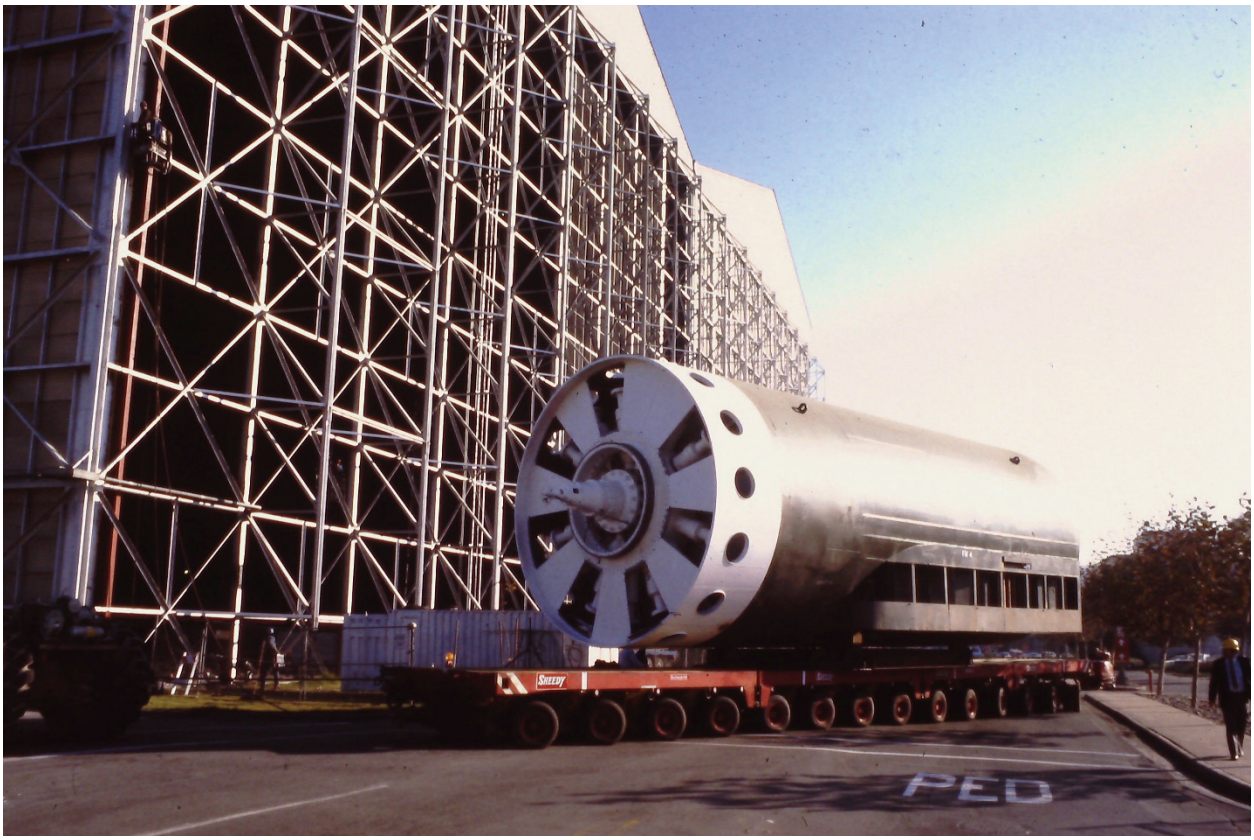

Figure 49. Dive unit being transported to the wind tunnel. ***(T. J. Forsyth collection, TJ10)***

Figure 50. Last drive unit partially lifted with the elevator. ***(Author's collection, KM25)***

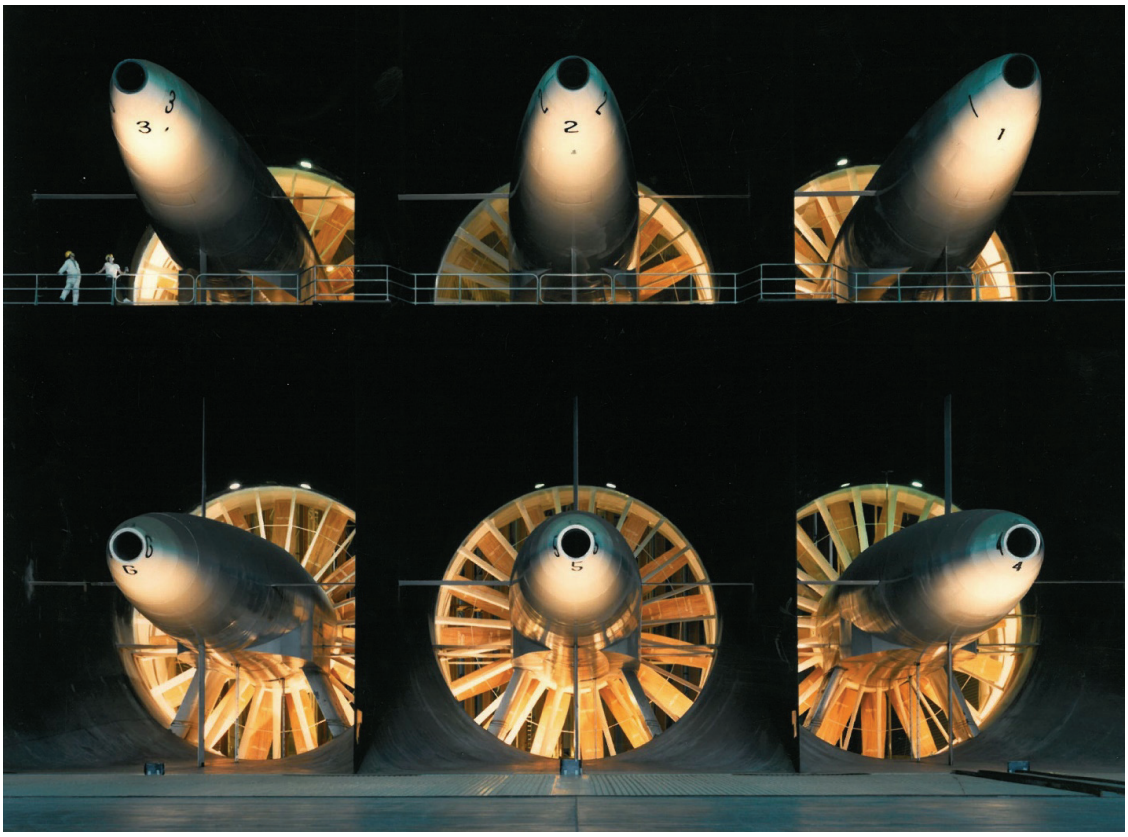

Figure 51. Rear view of completed drive showing cooling air exhausts. ***(Author's collection, FD2)***

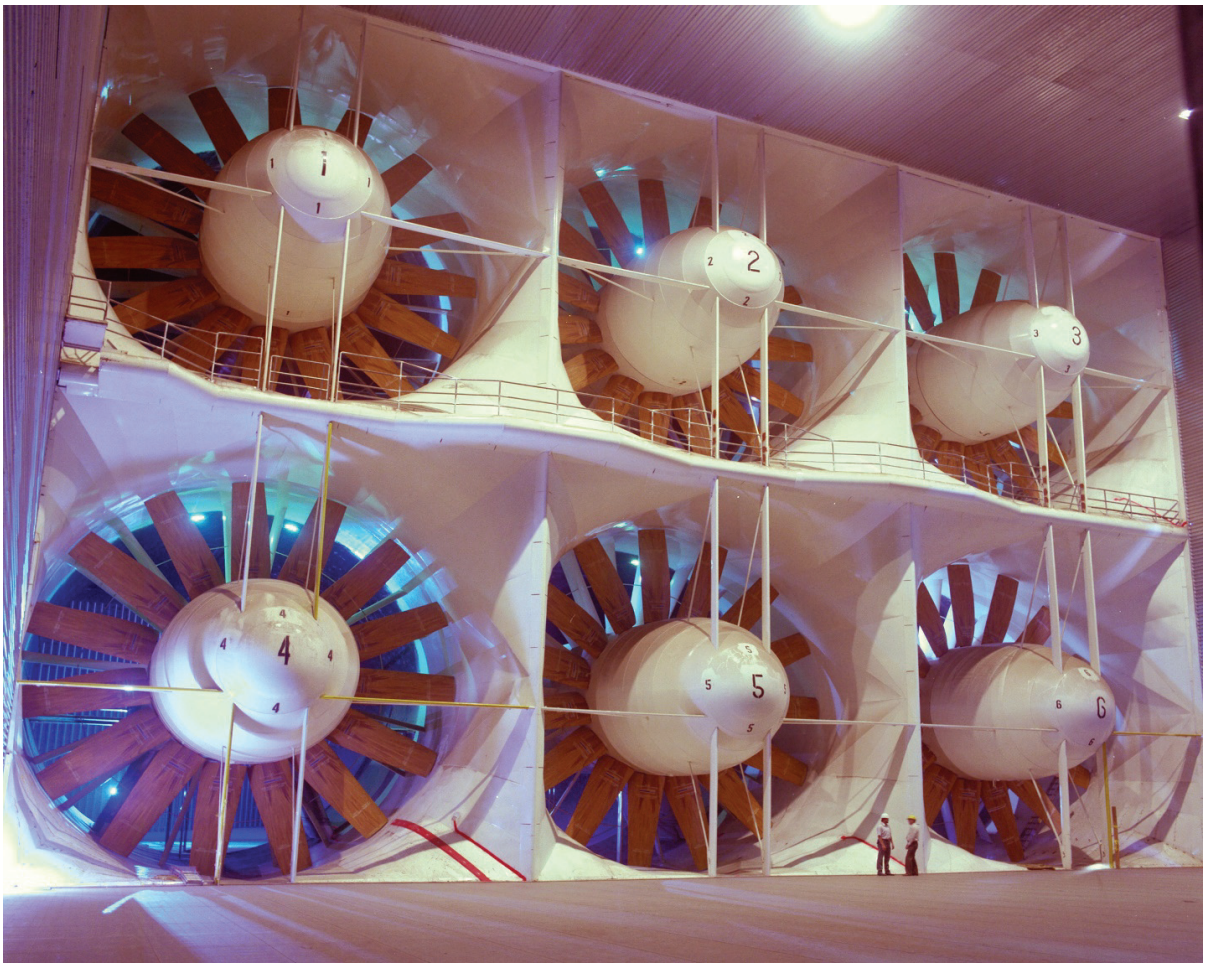

Figure 52. Front view of completed drive. There are 15 rotor blades and 23 stator blades for each of the 6 drive units. ***(NASA AC86-8016-7)***

A central motor-bearing oiling system that served all six drives was designed and built because of oil contamination problems with the original drive-lubrication system. The oil tank was located at ground level under the tunnel, which allowed readily monitoring the condition of the oil. It is a complex system that involved a significant amount of plumbing. There are three tilt-pad journal bearings for each drive motor, and each required lift pumps as well as circulation pumps. If required, the bearing pads can be replaced without removing the fans. The oil-system design and construction were managed by James Hallam of Ames.

A 6-inch-thick acoustic liner was installed in the 40- by 80-foot test section, and vortex generators that had been installed previously at the start of the primary diffuser were removed to enable the acoustic liner to be installed. This liner was not part of the repowering project. It was done under the management of the research staff using separate funds on a noninterference basis with the overall modification and repowering project. The purpose of the installation was to take advantage of the shutdown period.

References [34] and [35] are summaries of the design and construction of the modified facility as well as the testing capabilities.

Integrated Systems Testing (IST)

After construction was completed, integrated systems testing (IST) was performed from December 1981 to December 1982. The drive system was checked out, vanes and louvers were operated, performance measurements were made, flow quality was determined, and acoustic measurements were made. Performance and acoustic requirements were met. However, the flow quality in the 80- by 120-foot test section was not as good as desired at the time of the testing; the turbulence was somewhat higher than desired because of flow separation on the inlet-acoustic-baffle trailing edges and in the corners of the side walls at about the location of the acoustic baffles.

Fan blade loads were measured and were found to be somewhat higher than the loads given to the blade vendor. Limited fan-inflow velocities had been used to estimate fan blade loads during operation of the 40- by 80-foot test section, and model fan-inflow velocities had been used to estimate blade loads during operation of the 80- by 120-foot test section, which resulted in uncertainties in the blade load estimates.

Expected shortcomings of the air exchange system during operation of the 40- by 80-foot test section were confirmed. The original air exchanger system was simple and consisted of venting using adjustable, off-the-shelf louvers in the north and south legs. Because of budget constraints, this system was simply augmented to accommodate the additional heating due to the higher power. It was not an efficient nor very effective system. In addition, the inflow at the north leg came in normal to the wind tunnel flow, which thickened the boundary layer and worsened the already poor flow into the two drive fans next to the inside of the circuit (east side, fans number one and four).

The fan inflow was also worsened during 40- by 80-foot test-section operation by the 6-inch-thick acoustic liner installed in the test section, because it increased the boundary layer thickness in the primary diffuser, which in turn increased the boundary layer thickness of the flow entering the fan. The fan inflow was also worsened because of the removal of the vortex generators (to allow installation of the acoustic liner in the test section). They had not been replaced. As a result, unsteadiness during operation of the 40- by 80-Foot Wind Tunnel was increased because of intermittent flow separation in the primary diffuser. This had been the reason for the installation of the original vortex generators. Unacceptable intermittent fan stall was encountered during some operating conditions.

The exhaust flow from the 80- by 120-Foot Wind Tunnel was unacceptably high and very turbulent at ground level. This had been predicted from 1/50-scale-model studies. Because of cost restraints, Ames management deferred the implementation of an exhaust ramp until the requirements could be more definitive.

Accident

On December 9, 1982, an accident occurred during the drive-motor acceptance test that was part of the 80- by 120-Foot Wind Tunnel IST. The IST was nearly completed when it occurred. The variable-geometry vane set immediately upstream of the drive (vane set five), which could either direct the flow from the 40- by 80-foot test section or from the 80- by 120-foot test section into the drive, collapsed (Fig. 53) and destroyed the drive fans (Fig. 54) and caused significant damage to the tunnel as well.

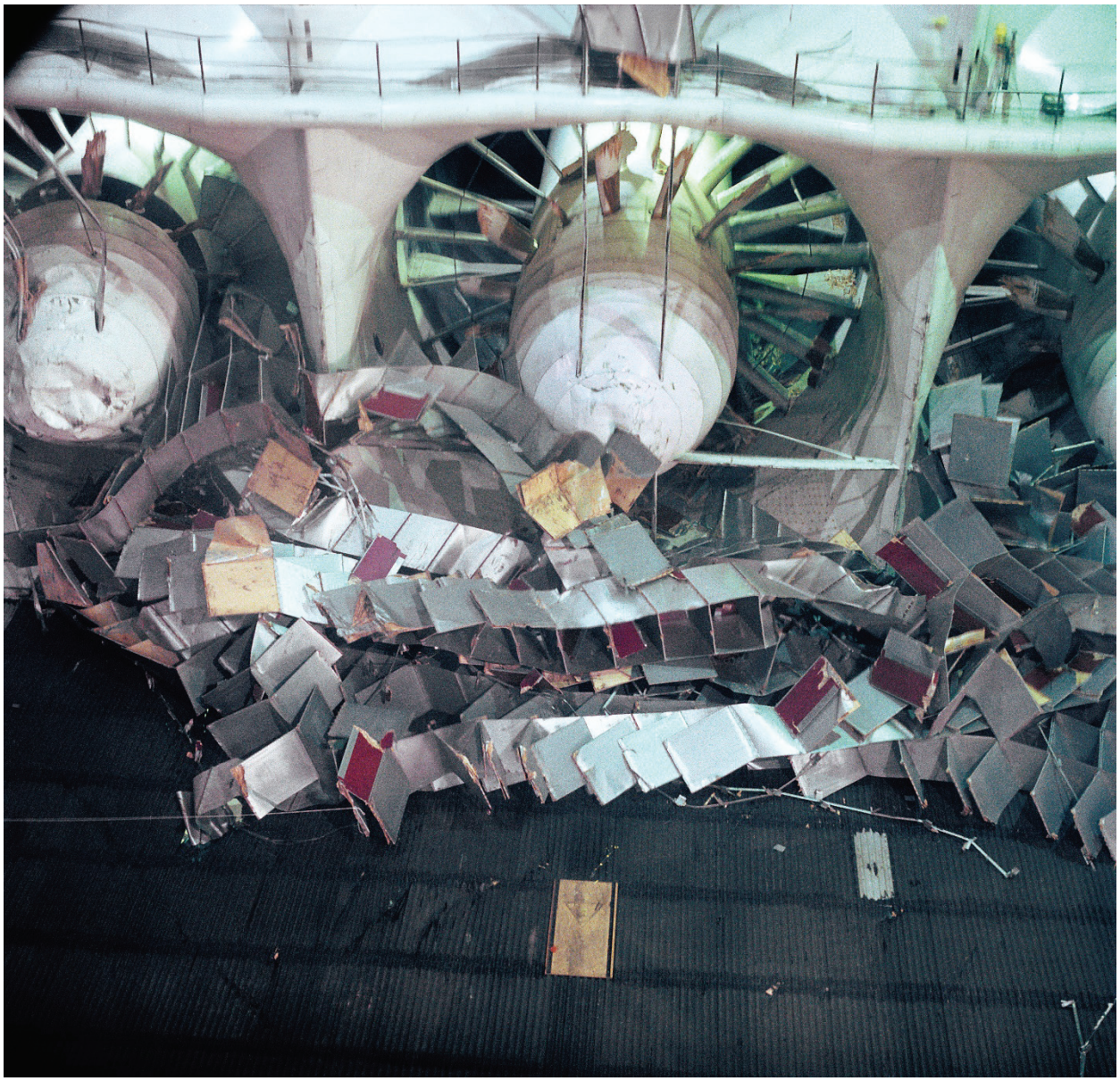

Figure 53. Results of the 1982 accident showing collapsed vane set five in front of the drive.
(NASA AC82-0875-183)

Figure 54. Results of the 1982 accident showing fan blade destruction. ***(NASA AC82-0875-155)***

An accident investigation board was convened and included representatives from other NASA Centers. It was chaired by Robert L. Swain of Langley Research Center; the Vice Chairman was Frank H. Nichols of Ames Research Center. Members were Daniel J. Keliher of Glenn (ex-Lewis) Research Center, Cecil E. Kirby of Langley Research Center, Peter A. Minderman of Kennedy Space Center, Richard C. Monaghan of Ames Research Center at Dryden, and Michael J. Rutkowski of U.S. Army AVRADCOM. There were also five consultants: Donald A. Buell, Roy W. Hampton, and Howard G. Nelson of Ames Research Center; Alan L. Carter of Ames Research Center at Dryden; and Arthur Henderson of HQ (OAST).

Their accident report was issued on February 28, 1983 [36]. The board determined that the linkage for the movable forward-section of vane set five failed, and the vane nose sections moved and closed off the flow very rapidly. This increased the loads on the vanes, which caused the entire vane set to fail catastrophically. The vane debris damaged the wind tunnel and destroyed the drive fan blades. Retention bars with friction slip joints had been used so the movable nose sections could be readily adjusted in an attempt to reduce the loads on the nose sections while still maintaining acceptable inflow to the fan drives. The slip joint was designed for about 10 degrees of adjustment. Budget restraints at the time caused construction funds to be insufficient to allow for reinforcing the vane set. In retrospect, reinforcing the vane set would have been the best approach. The optimum settings as far as performance was concerned had been determined, but the nose-section loads had not been minimized. Fortunately, no one was hurt.

Repair and Reliability Improvements

Based on the recommendations of the accident board, and with concurrence of NASA HQ, the tunnel was repaired and improvements were incorporated. A new project team was established to manage the project under the leadership of Lee Stollar and Frank Nichols; John Peterman led the engineering group. A large aerodynamic group was assembled under the leadership of Vic Corsiglia and later Larry Olson, and a new review board was established.

Fixed-Geometry Vane Set Five

A new fixed-geometry vane set five was developed at the insistence of Ames upper management. Excellent theoretical aerodynamic design assistance was provided by Glenn Research Center. Theories were verified and small adjustments were made to the design using 1/10-scale-model experiments. The newly designed vanes could accommodate inflow variations of up to 60 degrees without significant flow separation [37], which was a major accomplishment. Revised wall shapes were developed for the inside or west wall to prevent flow separation during operation of the 80- by 120-Foot Wind Tunnel [38, 39].

The as-built implementation of vane set five incorporated additional conservative details. Each vane was constructed of Douglas fir planks laminated into a single floor-to-ceiling beam. The beams were shaped into airfoils and finished on-site before installation. Teflon pads were installed at the ends to prevent excessive stress loads from being transferred into the structure when the wood expands and contracts. Two horizontal splitter plates were installed across the full width of the vane set to ensure vane set rigidity.

80- by 120-Foot Wind Tunnel Inlet Improved for Better Flow Quality

The inlet to the 80- by 120-foot test section was extensively modified to improve the flow quality [40-48]. It was found that the flow was separating part way along the inlet-acoustic-baffle trailing edges. The flow was also separating in the corners of the inlet's inside walls at essentially the baffle location. Subsequent studies in the 7- by 10-Foot Wind Tunnel verified baffle flow separation [40, 41]. In addition to theoretical studies [42-44] experiments were done using a new, larger-scale model that was also driven by the 6-foot-diameter fan model; the scale was about 1/15. A screen with higher loss than the inlet honeycomb "bird screen" was put across the baffle trailing edges to reduce turbulence, the acoustic baffles were replaced, and the side

walls were modified to eliminate flow separation. The new baffles had longer chords (16 feet vs. 10 feet), were thinner (12 inches vs. 16 inches), and were installed closer together (27 inches vs. 36 inches apart at the trailing edges). The baffles were splayed across the inlet and adjusted from the theoretical streamlines to achieve adequate velocity distributions in the test section [45, 46]. Engineers judged this approach as more effective and practical than attempting to develop a variable-loss screen attached to the original baffle trailing edges [47], especially since the inlet tended to be more two dimensional (2D) than three dimensional (3D). Splaying the baffles across the inlet and adjusting their angle settings to control the test-section velocity distribution was a unique approach developed by James Ross [47, 48].

80- by 120-Foot Test-Section Acoustic Liner

A 10-inch-thick acoustic liner was installed on the 80- by 120-foot test-section walls and 6-inch-thick liners were installed on the floor and ceiling. The inside dimensions therefore became 79 feet by 118 feet, 4 inches. This liner improved the ability to perform acoustic testing in the 80- by 120-foot test section, and also reduced community noise when operating the 80- by 120-foot test section, especially with powered models or aircraft.

Improved Air Exchanger

A new air exchanger intake was developed using the 1/50-scale model, which consisted of a large movable panel that allowed adjustment of the air exchange flow rate. The inlet flow was introduced essentially parallel to the flow at the wall, and it significantly reduced the boundary layer thickness on the south wall of the cross leg. The maximum air exchange rate achievable was about 10 percent [49]. The air exchange exhaust remained the same using louvers in the south leg (vane set seven); three panels were left off on the west row of exhaust louvers.

Exhaust Ramp for Operation of the 80- by 120-Foot Wind Tunnel

An exhaust ramp was developed using the 1/50-scale model [50, 51]. Results without the ramp correlated well with the full-scale results. The developed ramp consisted of a 30-percent perforated plate tilted up from the ground at a 45-degree angle. Based on model experiments, the predicted flow at ground level with the ramp would be acceptable, and the ramp cost would be minimal. Exhaust flow measurements were made with the ramp, including the decay rate as the flow exhausted upward [50]. Studies also determined the potential impact of the exhaust flow on low flying, low-wing-loading aircraft. Using simulations, it was found that the flow would probably not be a problem at altitudes above about 1,000 feet. Aerodynamicists recommended that aircraft flight-tests be performed to verify the model-based experiments, which had predicted that conditions would also be sensitive to atmospheric winds [51].

Vortex Generators Added to the 40- by 80-Foot Wind Tunnel Primary Diffuser

Replacement vortex generators were developed for the 40- by 80-Foot Wind Tunnel primary diffuser using a new 1/10-scale testing facility driven by the 6-foot-diameter fan model. The entire primary diffuser was modeled. The developed vortex generators were designed to replace the vortex generators that had been removed when the 6-inch-thick acoustic liner was installed. New and improved vortex generators were installed in the tunnel. These new vortex generators were Clark Y airfoils, whereas the original vortex generators were simply flat plates that had been placed at the end of the test section—at the farthest aft location that the test-section

overhead crane could reach for convenience. They had been designed without the benefit of any experiments but proved very effective. The purpose of the vortex generators was to energize the primary-diffuser boundary layer flow, which tended to be unsteady in the corners downstream from the test section and cause pulsing in the test section. That was the reason that the original flat-plate vortex generators were installed in 1974. As a further benefit, they improved the inflow to the drive fans.

Improved Vane Sets One and Two

Vane sets one and two (the first two sets of vanes downstream of the 40- by 80-foot test section) were replaced with vanes with lower drag (using computational fluid dynamics (CFD) help from Glenn Research Center) and improved structure. The original turning vanes were simply galvanized sheet metal nailed to wood formers. CFD analysis was verified, and the design was adjusted based on 1/10-scale-model experiments. The new vanes had about the same maximum thickness (about 15 percent of chord) and chord as the old vanes, but with less camber in the forward part of the airfoil. The loss (total pressure drop) was about three-quarters of that of the original vanes [38].

Reinforced North Leg of the 40- by 80-Foot Wind Tunnel Circuit

The north leg of the tunnel was reinforced. Joseph Hurlbut performed a NASA Structural Analysis (NASTRAN) of the north leg structural framing and designed a cost-effective reinforcement. NASTRAN is a finite element analysis (FEA) code developed for NASA. NASTRAN, of course, was not available when the tunnel was originally designed; slide rules were used for engineering calculations instead of computers, however the designs were typically conservative because of uncertainties and low accuracy of the calculations. The reinforcement allowed higher wall-pressure magnitudes, which meant that the wall pressures would not need to be monitored as precisely as before. Reinforcement had not been done during the original project because of a lack of funds, and wall pressures had to be carefully monitored during operation to ensure that "over pressurization" (large negative pressure on the north leg and large positive pressure on the south leg) did not occur by carefully adjusting the air exchange intake-louvers in the north leg.

Fan-Blade Stall Margin Improved

The destroyed drive fan blades were replaced with new blades that had modified airfoils to give a higher maximum lift coefficient and therefore a higher stall margin; the modification increased the local thickness on the upper surface near the blade's leading edge a small amount. Theoretical work was done at Ames by Ray Hicks, 2D airfoil experiments were done at The Ohio State University, and verification studies were done at Ames using the 6-foot-diameter fan model [52-54]. Intermittent fan blade stall had been encountered in the lower-east drive, fan motor four (FM4), during the IST because of poor fan inflow that was due to the old air exchanger, the thicker boundary layer caused by the acoustic liner, and the absence of vortex generators at the inlet to the primary diffuser. In addition to modifying the wind tunnel to improve the fan in-flow, it was considered prudent to increase the fan stall margin to accommodate possible future large-blockage research models.

Integrated Systems Testing (IST)

After tunnel repairs were completed and replacement components installed, the 40- by 80-foot test-section IST began in January 1987, and the 80- by 120-foot test-section IST followed on October 21, 1987. The total cost of the wind tunnel facility, which included two test sections and a ground check-out facility, had become about $122 million, the amount that had been originally requested [7]. The drive system was checked out, vanes and louvers were operated, performance measurements were made, improved flow quality was confirmed, the air exchange system was deemed very effective, and blade loads were measured. The drive motors were run for 2 hours at maximum power to satisfy the 2-hour maximum power rating of 22,500 hp each. Acoustic measurements were made to establish the community noise footprint and the acoustic goals were met or exceeded. Additional performance goals were also met or exceeded [55-59].

The flow on the new vane set five did not appear to be separated during operation of either test section. However, the fan blade loads for fan motors three and six (which are on the west side and the closest drives to the vanes) appeared to be somewhat higher during operation of the 80- by 120-foot test section. The fairing on the west-side wall of the tunnel appeared to be keeping the flow attached [38]. Vane set five appeared to be under-turning the flow slightly during operation of the 80- by 120-foot test section. This did have a small adverse effect on fan blade loads but was small enough that modifications were not contemplated.

Dedication of the National Full-Scale Aerodynamics Complex (NFAC)

The National Full-Scale Aerodynamics Complex (NFAC) was the name given to the 40- by 80-Foot and 80- by 120-Foot Wind Tunnels and the outside aerodynamic research facility (OARF). Dedication of the NFAC occurred on December 11, 1987.

Chapter 4. Additional Modifications and Repairs After 1987

Acoustic Walls in the 40- by 80-Foot Test Section

The test-section wall plate and 6-inch-thick acoustic liner in the 40- by 80-foot test section were replaced with a 42-inch-thick acoustic wall system from July 1996 to November 1998 [60-63]. The original steel wall plate was removed, but the flat-oval steel bents were retained. New steel wall plate, which was the pressure shell, was installed on the outside of the 36-inch-deep steel bents, rather than on the inside, to allow acoustic treatment to be added to the inside. This was in addition to a 6-inch-thick acoustic treatment on top of the bents, which resulted in the 42-inch thickness of the acoustic treatment. The new acoustic wall interior was a complex structure designed to improve wall acoustic characteristics, especially at low frequencies (Fig. 55). The primary justification for the new wall treatment was for research on high-speed civil transport (HSCT) models; engine noise at landing and takeoff conditions was an important issue with the HSCT. The tunnel was being used extensively for acoustic research on a variety of full-scale and large-scale models. Many experiments were done to develop improved acoustic properties of the liner while maintaining minimum skin friction [60-63]. The 6-inch-thick acoustic liner that had been installed during the tunnel shutdown for repowering caused the inside dimensions to be 39 feet by 79 feet. The inside test-section wall dimensions were retained at 39 feet by 79 feet after the new wall system was installed, which allowed for a 6-inch-thick acoustic liner to be placed on top of the structural-bent inside surface.

During the same shutdown, the variable-frequency drive set was modified to produce higher variable-speed power and improve reliability. The available power was increased from about 28,000 hp to 33,500 hp during the variable-frequency or variable-fan-speed mode. This project

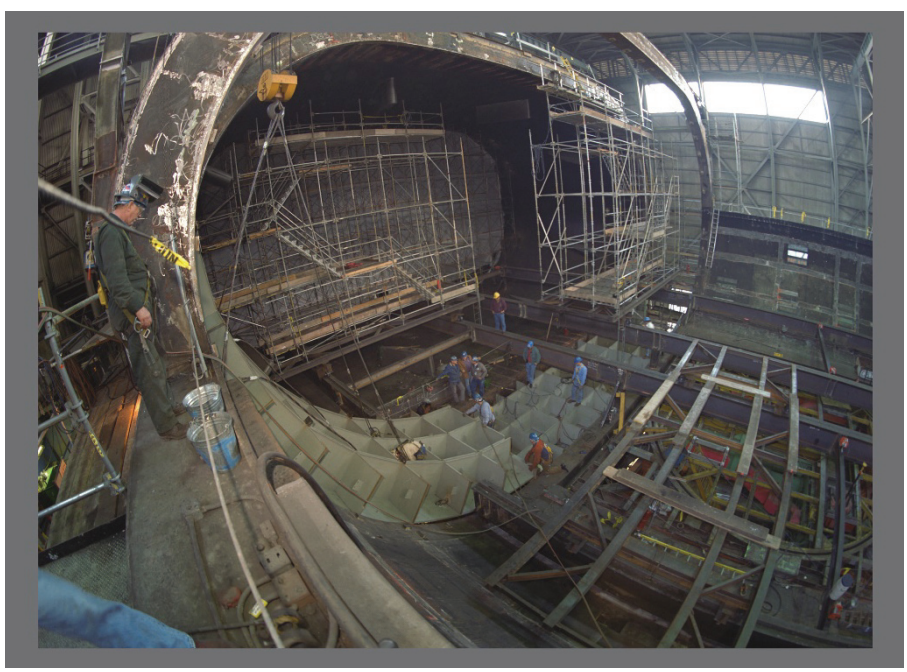

Figure 55. Construction and installation of the 42-inch-thick acoustic walls in the 40- by 80-foot test section showing partial framing. ***(NASA AC94-0071-395)***

also included a control system work package. Seven programmable logic controllers were installed to replace old analog control systems for fan drive operation and model-support-system movement in both test sections. This allowed operators to control all wind tunnel test conditions with a custom graphical user interface using computers that could more easily be updated when necessary.

The 40- by 80-Foot Wind Tunnel IST was performed in the fall of 1998 and included measurements of the boundary layer in the test section as well as blade loads. The boundary layer was thinner than it had been with the previous 6-inch-thick acoustic liner; this was the successful result of extensive research and development of the 42-inch-thick acoustic wall system. Developments had included experiments of a sample full-scale test panel that was tested in the 40- by 80-foot test section. The new wall system met the acoustic requirements. The operational readiness review (ORR) was completed on November 21, 1998 [64].

Fan Blade Repair

Fan Blade Cracking

Blade cracking was discovered in March 1996 during routine inspections, and the causes were soon established. The measured loads were somewhat higher than the loads furnished to the blade vendor, and they were also increased because of the wakes from the new vane set five during operation of the 80- by 120-Foot Wind Tunnel. The wakes from the two splitters for vane set five were determined to cause large aerodynamic load spikes. The splitter plates were required to react the vane turning loads, but they were not faired. In addition, the natural frequency of the blades was closer to 12 Hz than desired, such that the blade response at four times per revolution (4 p) was higher, causing the blade loads to be higher at 4 p. They essentially became the same magnitude as the loads at 1 p. This was a significant problem because the original blade loads were specified at 1 p, so the rate for fatigue loads was at least four times the original rate.

Blade Repair and Reinforcement

Blade repair and reinforcement were completed between August 1997 and January 1998. Cracks were filled with high-strength epoxy. The reinforcement consisted of a carbon-fiber-composite wrap about 0.2 inches thick, which extended from approximately the 93-inch radius to the 140-inch radius (39 to 58 percent of the 20-foot-maximum radius) on the blade. At the time the repairs were considered temporary because the intent was to purchase improved replacement blades.

Blade Fatigue Tests

Blade fatigue tests were performed from January 1997 to February 1999; the tests demonstrated at least a 30-month life, which was the goal at the time. Tests were not done to failure because funding for new blades had been obtained, and new blades had been ordered. Testing was performed on six repaired blades and on one unrepaired blade. Five repaired blades and the unrepaired blade were cut up for forensic investigations after fatigue testing. The character and growth of the cracking was consistent with the cracking during the blade contractor's structural and fatigue tests.

Fatigue testing was resumed on the remaining partially fatigued blade in February 2007 because the order for the new blades had been cancelled by Ames management. The blade fatigue test setup and composite reinforcement are shown in Figure 56. Fatigue failure of the blade occurred on April 2009, which allowed an estimation of fan blade life. Circumferential cracking of the composite wrap and subsequent increased cracking in the wood was the failure mode causing blade compliance to become excessive. Blade life was estimated and the likely failure mode during tunnel operation was determined. It was likely that blade failure would not result in catastrophic failure if the planned periodic inspections were maintained and the drive vibration system was monitored on schedule, because the "failed" blade was still able to react to the entire centrifugal force despite having substantially increased compliance and resultant increased vibration. There is, however, significant uncertainty in blade life predictions because only one blade was actually tested to failure. Blade life depends on blade construction, blade location (which drive motor), and tunnel operations (model effects, speeds, and test-section operation). Engineers estimated that blade life would be infinite if the airspeed were restricted to about 80 percent of the maximum, which was more of a problem during operation of the 80- by 120-foot test section than during operation of the 40- by 80-foot test section because of planned facility usage.

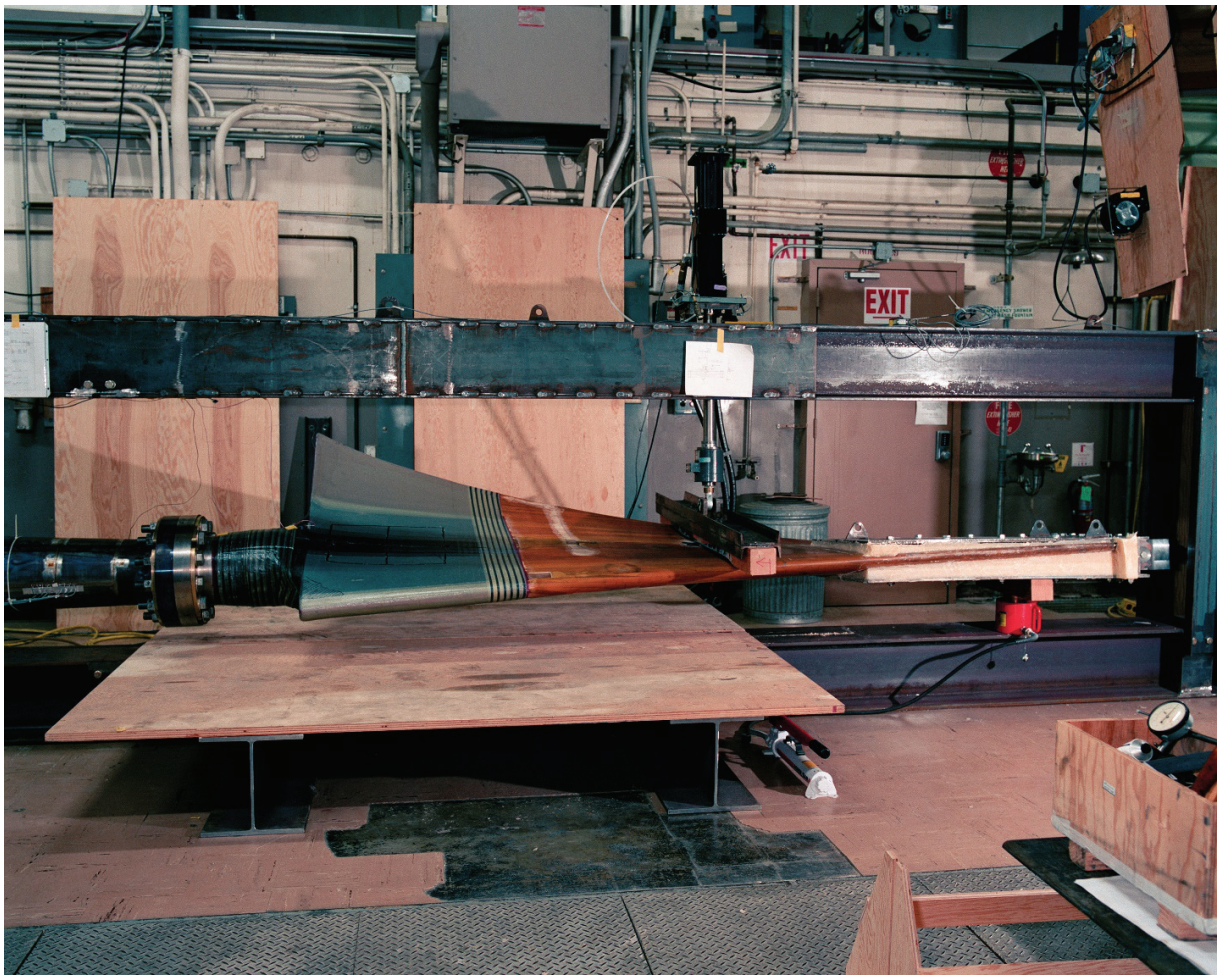

Figure 56. Repaired blade mounted horizontally, with reinforcement using composite wrap in blade root area, undergoing fatigue tests. ***(NASA AC96-0338-96)***

New Blades Ordered, Then Cancelled

A contractor had been selected to perform design and construction of new carbon-fiber-composite blades in June 1998; carbon-fiber composite had been judged the best choice for high-strength, lightweight blades. A request for proposal (RFP) was issued and three offerers were selected. Each offerer was given $270,000 to produce a preliminary design. The selection from the three offerers was based on a combination of preliminary design and proposed cost. The selected contractor, Advanced Technologies Incorporated (ATI), was judged to have submitted an acceptable preliminary design and proposed cost ($9.35 million including the $270,000). After ATI was selected, a fixed-price contract was issued for 108 blades, which included 18 spares. The rationale for 18 spares was that if there were a catastrophic accident destroying the 90 blades in the tunnel, the tunnels could still be operated with three blades per fan at airspeeds up to about 30 percent of the maximum airspeed while replacement blades were obtained. (It was expected that funding for 90 spares would never be approved by NASA HQ based on past experience; the original blade contract had included only 1 spare blade!)

The order for the replacement blades was canceled in November 2001, before the design was completed. Detailed design of the root attachment had not been completed because of design challenges such as high design loads and physical restraints. To be conservative, the loads furnished to ATI were much higher than the loads furnished to the original blade manufacturer. Compounding the design problem, the constraints of the hub system were very physically and structurally restrictive. However, two options for the root detail design appeared feasible. Remaining design/construction money was withdrawn by Ames Research Center management because of changes in NASA and Ames missions and funding priorities; aeronautics, in particular, was being deemphasized and limited by the agency and funding was being drastically reduced. Aeronautic programs were being eliminated or reduced in scope despite the importance to the nation. Several NASA wind tunnels were shut down, deactivated, or demolished.

Drive Motor Repair

In 1999, a motor design defect was discovered during routine preventive maintenance inspections of the six drive motors. All 960 pole-retaining bolts had to be replaced with new bolts and special custom washers. Simultaneously, 19 damaged rotor pole pieces (weighing 675 pounds each) had to be removed, repaired, and then reinstalled, which required use of special rigging. This was a major job, but it was performed in about 2 months, including checkout testing, with the excellent participation of many in-house staff members [64].

Data Collection and Control Improvements

When the NFAC went back online after the shutdown in 2003, which lasted until about 2007, a major part of the reactivation was the design, installation, and checkout of a new state-of-the-art data acquisition system. The system was personal-computer-based, similar to systems at Arnold Engineering and Development Complex (AEDC), and was intended to handle all of the expected rotorcraft and fixed-wing experiments. The system included the capability to accommodate data from a large number of rotor-blade strain gages and pressure transducers. The system also included model and NFAC health-monitoring systems. The design requirements and descriptions of the architecture are described in references [65] and [66]. The instrumentation staff at AEDC made major contributions to the design.

PART II. OPERATION AND MANAGEMENT HISTORY

Chapter 5. NACA Operation, 1944–1958

Staffing, Organization, and Operations

When the 40- by 80-Foot Wind Tunnel first became operational, some of the aeronautical research and wind tunnel operations staff came from the 7- by 10-Foot Wind Tunnels at Ames, some came from the Langley Full-Scale Wind Tunnel, and many were new college graduates. However, because of the size of the new tunnel and its uniqueness, it was a learning experience for everybody. The staff from the 7- by 10-Foot Wind Tunnel and from Langley were considered veterans, even though for the most part they only had a couple of years of wind tunnel experience. Later on, staff at Ames who were experienced in theoretical aerodynamics, thermodynamics, and wind tunnel research would conduct training sessions for the new Ames hires. R. T. Jones, John Spreiter, Sy Syvertson, Morris Rubesin, and many other world-class scientists conducted the training sessions, which were a great experience for new hires. Lectures would be given on the research performed as well as descriptions of the support organizations available at the Center. The new hires would write summaries of the lectures for review and comment by the lecturers.

The support staff at the 40- by 80-Foot Wind Tunnel made up a branch with a branch chief, assistant branch chief, head mechanic, head computer, and secretary. There was on the order of a couple dozen research engineers, a dozen mechanics, and half a dozen computers. Engineers were organized into small groups of typically three or four, which were led by a senior engineer. One or two fresh-outs, or new hires, were assigned to a group to gain experience. The groups were responsible for preparing, performing, and reporting on experiments performed in the tunnel. Each group was responsible for several experiments. New engineers were issued a 2-foot-long slide rule to perform calculations.

Table 1 charts the organization from 1944 to 1984. The division chiefs are included, as well as the head wind tunnel mechanics. Generally, organization management did not change very frequently, and it remained intact when NACA facilities formed the nucleus of NASA in 1958. Figure 57 is a photo of several of the early managers, taken during the December 11, 1987, dedication of the NFAC. From left to right: Brad Wick, Vic Stevens, Mark Kelly, Harry Goett, Bill Harper, Woody Cook, Paul Yaggy, and Dave Hickey.

Generally the branch staff performed, or was responsible for, cradle-to-grave activities required for the experiments, including initial planning (occasionally even including advocacy of experiments to Ames and NACA HQ) and model design, experiment planning, conducting experiments, collecting data, and analyzing and reporting the test results. Branch mechanics prepared and installed the models or aircraft in the tunnel, and operated the wind tunnel under the direction of the research engineers.

Table 1. 40- by 80-Foot Wind Tunnel Management History, 1944–1984

Year	Division Chief	Assistant Division Chief(s)	Branch Chief(s)	Assistant Branch Chief(s)	Master Mechanic
1944			H. Goett	S. Davidsen	A. McEwin
1945					
1946	H. Goett	L. Clousing	B. Harper	V. Stevens	
1947					
1948					
1949					
1950					
1951					
1952				B. Wick	
1953					
1954					W. Ferris
1955					
1956				W. Cook	
1957					
1958					
1959	B. Harper		W. Cook	M. Kelly	
1960					
1961					
1962					
1963					
1964	L. Clousing	W. Cook N. Johnson	M. Kelly	P. Yaggy	
1965				D. Hickey	
1966					
1967	B. Wick	N. Johnson L. Clousing			
1968					
1969					
1970					R. Stuart
1971					
1972					
1973					
1974	C.T. Snyder				
1975					
1976					
1977				D. Hickey J. Kirk	
1978					
1979					
1980	W. Deckert	K. Edenborough D. Few	D. Hickey J. Kirk	W. Johnson V. Corsiglia M. Falarski	
1981					
1982					
1983				W. Warmbrodt V. Corsiglia M. Shovlin (Acting)	
1984					

Figure 57. Early wind tunnel managers at the December 11, 1987, dedication of the NFAC. From left to right: Brad Wick, Vic Stevens, Mark Kelly, Harry Goett, Bill Harper, Woody Cook, Paul Yaggy, and Dave Hickey. ***(NASA AC87-0785-9)***

In the early days, communications with organizations outside of Ames and NACA were primitive. All outside correspondence went through the Center director. Even data would be sent to the director, attached to memorandums. If approved, the data could then be sent to the customers such as airplane companies and other NACA Centers. These were the days before copiers so all correspondence was typed with multiple carbon copies; it was very demanding work for the secretaries.

The staff did not have office phones, and there were only three telephone extensions in the branch for general use. There were two phones in the office hallways, and three phones in the tunnel area: one downstairs in the shop area, one upstairs in the control room, and one upstairs near the observation station. The branch chief and assistant each had a phone and a dedicated extension number. An intercom with a buzzer system was used by engineers, and each had their own code. If you got a call, the secretary would answer the phone and then buzz you so you knew to locate and pick up a phone. There was an additional phone and extension in the motor-generator (MG) building for communications during troubleshooting the Kramer wind tunnel drive system. (The Kramer system produced the variable-frequency electricity required for the drive motors.) It was a primitive system, but it served effectively and was used for many years.

Model Design, Construction, and Instrumentation

Many models for aerodynamic testing in the wind tunnel came from airplane companies; they could be large-scale models, prototype aircraft, or production aircraft. Other models were designed and constructed at the Center. Model design could be done by the research engineers or by staff in one of the other branches in the research facilities and equipment division. As time went on, it occasionally became desirable for fast turnaround to supplement the design effort, and a small design group was created and managed at the branch by Joe Piazza.

There were several shops on-site at Ames that could construct wind tunnel models of various sizes. There was a model shop that used wood, foam, plastic, and fiberglass; a sheet-metal shop; a structural-steel fabrication shop; a machine shop; and an instrumentation shop. The shop workers took pride in their work and rightfully so—they were excellent at building high-quality models in a timely fashion with minimal instructions and drawings. The models to be tested in the 40- by 80-Foot Wind Tunnel typically had structural-steel frames that were covered with blocks of foam. The foam could be readily shaped to the required contours, then covered with fiberglass and painted. This was a very cost-effective and unique approach for building large models for the tunnel.

Jet-powered models used surplus jet engines, typically from the DoD, which had a short remaining life and were not acceptable for aircraft use, but proved excellent for use in wind tunnel models. This was an acceptable practice during wind tunnel testing because a typical jet-powered wind tunnel test only required that the jet engines run on the order of 100 hours. Skilled aircraft mechanics from the flight branch maintained the engines and kept them operational. Surplus propeller gear-boxes were used when required for propeller experiments in a similar fashion—that is, they had limited life but were acceptable for wind tunnel use.

Model instrumentation was designed by the tunnel research engineers or by the electronic branch, depending on the complexity and requirements. Implementation was completed by electronic-branch technicians and/or by aircraft mechanics with the guidance of the research engineers. As required, one or two instrumentation technicians were assigned to the tunnel to implement the instrumentation design and to troubleshoot any problems that arose. As instrumentation requirements became more complicated and extensive, a small dedicated group was established at the tunnel to design, install, and maintain model instrumentation.

After testing, many of the models were stored outside near the flight line, and subsequently modified in the shops for follow-on experiments. This was an efficient and cost-effective approach. Eventually, subsequent Center directors insisted on removal of the old models because, in their estimation, it looked like a junkyard at the flight line. A few models were stored under the wind tunnel and in a small warehouse. Because of the size of the models, storage remained a problem.

Chapter 6. NASA Operation, 1958–2003

Organizational Changes

The 40- by 80-Foot Wind Tunnel was operated as its own branch until the tunnel was repowered and the 80- by 120-foot test section was added. The modified facility was named the National Full-Scale Aerodynamics Complex (NFAC) and included an outdoor checkout facility called the Outside Aerodynamic Research Facility (OARF); the NFAC was dedicated on December 11, 1987. In addition to checking out powered models, the OARF was capable of measuring all six components of forces and moments. The ground height could be varied for ground-effect studies. Recognizing the future needs of the NFAC, a new division was created to allow more effective management of the facilities. Tables 2 to 5 list the organizations in the division.

In October 1994 a major reorganization was implemented that combined all Ames wind tunnel operations and separated research management from operations management. Later, all of the Center's wind tunnel operations were further combined, including simulator operations, in an attempt to reduce overhead expenses at Ames. Subsequently, much of the wind tunnel operations and support functions were performed by contracted support service staff rather than by civil service staff. Table 6 shows the research management organizations. In 1997, rotorcraft research was moved to a separate division and combined with the U.S. Army organization at Ames. In 1998 a reorganization eliminated the Applied Aero Division. NASA closed the NFAC in October 2003.

Full-Cost Accounting and Recovery

Full-cost accounting was implemented in 2001 to allow for examination of Center budgets by Ames management and NASA HQ. NASA was in the process of drastic reductions in the aeronautics budget [67]. There was an emphasis on space science and projects. Full-cost recovery was soon implemented as well. The purpose of full-cost recovery was to recover all wind tunnel operating costs and overhead from customers. This initiative was started at the beginning of FY 2004. Each Center could develop their own plan for full-cost recovery. This was a large change in the use of the tunnels, especially the NFAC, which had never done "fee" testing—that is, charging users for wind tunnel test time. (The unitary plan wind tunnels at Ames had long done "fee" testing.) Aeronautical research that had been generated and funded by NASA successfully for so many years in the past, as described in the NACA and NASA charters, was drastically reduced; many important programs were eliminated such as high-speed commercial flight, V/STOL, wake vortex effects, and rotorcraft research. The tunnels had been designed as world-class research facilities. Their unique research capabilities were essential and emphasized, but productivity was of secondary importance and was not emphasized at any of the NASA Centers. Generally, recommended upgrades to increase productivity were rejected by NASA management. In addition, because of a decline in new aircraft designs and manufacturers (during the 1990s), there was a declining use of the NASA wind tunnels by potentially paying customers, which further resulted in higher overhead costs. Coupled with lower usage by NASA—because of reduced funding for aeronautics research—these factors resulted in overhead costs that were much higher than the actual operating and overhead costs of wind tunnel operation. Under the newly mandated accounting process, the annual cost of maintenance and overhead expenses was amortized over the number of hours of operation planned for one year.

The customers were expected to pay for the direct operating cost plus these amortized fees. If there was only one customer, they were expected to pay for all of the annual maintenance and overhead expenses for that year.

The NACA, and subsequently NASA, aeronautics role had been to perform basic research that could not be performed by private industry, or to solve identified and especially common industry problems such as deep-stall and high-speed aircraft-related research. Much of the basic research was long-term research, which was important for future advances in aeronautics. Much basic research was still in widespread use as long as 50 years after it had been performed. The private sector was never able (for a variety of reasons) to perform this sort of research, which was one of the major reasons for the creation of the NACA and for the retention of aeronautics in NASA [68]. After all, the first 'A' in NASA is aeronautics. Unfortunately, many politicians (and much of the later NASA HQ management) have never understood the importance of this and have tended to focus on near-term budgets instead of long-term consequences. Aircraft companies have not been consistent supporters of NASA aeronautics. This has primarily been the case because of their corporate near-term goals rather than far-term goals, as well as the mistaken argument that they could and should perform basic research if it were required and funded.

Table 2. NFAC Management History, 1986–1989

	Date	Mar-86	Jan-87	Oct-87	Apr-89	Oct-89
Full-Scale Aero Research Division						
	Chief	Vacant	F. Schmitz	F. Schmitz	F. Schmitz	F. Schmitz
	Asst. Chief	H. K. Edenborough	H. K. Edenborough	H. K. Edenborough J. Kirk (Operations)	H. K. Edenborough J. Kirk (Operations)	H. K. Edenborough J. Kirk (Operations)
Fixed Wing Branch						
	Chief	Vacant	R. Margason	R. Margason	L. Olson	V. Corsiglia
	Asst. Chief	V. Corsiglia	V. Corsiglia	V. Corsiglia	V. Corsiglia	P. Soderman
Rotary Wing Branch						
	Chief	W. Warmbrodt	W. Warmbrodt	W. Warmbrodt	W. Warmbrodt	W. Warmbrodt
	Asst. Chief	M. Betzina	M. Betzina	M. Betzina	M. Betzina	Vacant
NFAC Operations Branch						
	Chief	J. Kirk	J. Kirk	F. Nichols	F. Nichols	M. Betzina
	Asst. Chief	M. Falarski M. Shovlin (Acting)	M. Falarski M. Shovlin (Acting)	M. Shovlin	M. Shovlin	M. Shovlin
NFAC Data Systems Branch						
	Chief			M. Falarski	E. Maynard	E. Maynard
	Asst. Chief			E. Maynard	Vacant	Vacant

Table 3. NFAC Management History, 1991–1994

	Date	Feb-91	Nov-91	Nov-92	Jan-94
Full-Scale Aero Research Division					
	Chief	F. Schmitz	F. Schmitz	F. Schmitz	F. Schmitz
	Asst. Chief	H. K. Edenborough J. Kirk (Operations)	H. K. Edenborough J. Kirk (Operations)	H. K. Edenborough J. Kirk (Operations)	H. K. Edenborough J. Kirk (Operations)
Fixed Wing Branch					
	Chief	L. Olson	L. Olson	L. Olson	L. Olson
	Asst. Chief	V. Corsiglia	D. Riddle	D. Riddle	D. Riddle
Rotary Wing Branch					
	Chief	W. Warmbrodt	W. Warmbrodt	W. Warmbrodt	W. Warmbrodt
	Asst. Chief	D. Signor (Acting)	S. Dunagan (Acting)	M. Mosher (Acting)	S. Kottapalli (Acting)
NFAC Operations Branch					
	Chief	M. Betzina	M. Betzina	M. Betzina	M. Betzina
	Asst. Chief	J. Allmen	J. Allmen	J. Allmen	R. McMahon
NFAC Data Systems Branch					
	Chief	E. Maynard	E. Maynard	E. Maynard	E. Maynard
	Asst. Chief	O. Jung	O. Jung	O. Jung	O. Jung

Table 4. NFAC Management History, 1995–1997

	Date	Jan-95	Jun-96	Aug-97
Aero Test and Simulation Division				
	Chief	L. Presley	L. Presley	M. Betzina (Acting)
	Deputy Chief	Vacant	Vacant	M. Betzina (Acting)
	Asst. Chief Wind Tunnels	M. Betzina	M. Betzina	M. Betzina
Aero Facilities Engineering Branch				
	Chief	Vacant	D. Petroff	D. Petroff
	Deputy Chief	R. Ashford	Vacant	R. Johnson
Wind Tunnel Systems Branch				
	Chief	Vacant	L. Alderete	H. Finger
	Deputy Chief	L. Alderete	E. Maynard	E. Maynard
Wind Tunnel Operations Branch				
	Chief	Vacant	D. Banducci	D. Banducci
	Deputy Chief	D. Banducci	R. McMahon	Vacant
	Test Engineering Section Head	R. McMahon	T. Aiken	T. Aiken
	Mech. Operations Section Head	Vacant	W. Doty	W. Doty

Table 5. NFAC Management History, 1998–2003

	Date	Oct-98	Oct-99	Jul-01	Apr-03
Wind Tunnel Operations Division					
	Chief	G. Mulenburg (Acting)	M. George	M. George	M. George
	Deputy Chief	D. Petroff (Acting)	J. Allmen (Acting)	D. Bufton	D. Bufton
	Asst. Chief	Vacant	Vacant	Vacant	D. Banducci
Wind Tunnel Engineering Branch					
	Chief	D. Bufton (Acting)	D. Petroff (Acting)	F. Kmak	Branch Eliminated
	Deputy Chief	Vacant	Vacant	S. Ord	
Wind Tunnel Systems Branch					
	Chief	H. Finger	H. Finger	H. Finger	H. Finger
	Deputy Chief	E. Maynard	E. Maynard	M. Liu	M. Liu
	Asst. Chief	Vacant	J. Bader	J. Bader	J. Bader
Wind Tunnel Operations Branch					
	Chief	D. Banducci	D. Banducci	D. Banducci	F. Kmak
	Deputy Chief	Vacant	Vacant	T. Aiken	S. Ord
	Test Engineering Section Head	T. Aiken	T. Aiken	Position Eliminated	
	Mech. Operations Section Head	W. Doty	Position Eliminated		

Table 6. Research Management History, 1995–2003

	Applied Aero Division			Low Speed Aero Branch		Rotorcraft Aeromechanics Branch	
Date	Chief	Deputy Chief	Asst. Chief	Chief	Asst. Chief	Chief	Asst. Chief
Jan-95	F. Schmitz	J. Flores	H. K. Edenborough	L. Olson	D. Riddle	W. Warmbrodt	Vacant
Jun-96	F. Schmitz	J. Flores	H. K. Edenborough	L. Olson	D. Riddle	W. Warmbrodt	G. Yamauchi

	Applied Aero Division		Low Speed Aero Branch		Army/NASA Rotorcraft Division		Aeromechanics Branch	
Date	Chief	Asst. Chief	Chief	Asst. Chief	Chief	Deputy Chief	Chief	Deputy Chief
Aug-97	J. Flores (Acting)	J. Flores	L. Olson	D. Riddle	E. Aiken (Acting)	W. Stephens	W. Warmbrodt	C. Tung

	Aero Projects and Programs Office		Advanced Aircraft and Powered Lift Branch		Army/NASA Rotorcraft Division		Aeromechanics Branch	
Date	Chief	Deputy Chief	Chief	Asst. Chief	Chief	Deputy Chief	Chief	Deputy Chief
Oct-98	L. Olson	Vacant	J. Flores	Vacant	E. Aiken (Acting)	M. Rutkowski	W. Warmbrodt	C. Tung
Oct-99	L. Olson	Vacant	J. Flores	D. Wardwell	E. Aiken (Acting)	M. Rutkowski	W. Warmbrodt	C. Tung
Jul-01	L. Olson	D. Bencze	J. Flores	D. Wardwell	E. Aiken	M. Rutkowski	W. Warmbrodt	C. Tung
Apr-03	L. Olson	D. Bencze	J. Flores	D. Wardwell	E. Aiken	M. Rutkowski	W. Warmbrodt	C. Tung

NFAC Tunnels Shut Down October 2003

The NFAC was shut down in October 2003 because of NASA's changing missions and priorities. The tunnels were to be "mothballed." Other NASA wind tunnels were shut down or demolished, including the 14-Foot Wind Tunnel and 7- by 10- Foot Wind Tunnel number two at Ames, and at the other Office of Aeronautics and Space Technology (OAST) Centers for this reason. As a result of this unfortunate shutdown, the very knowledgeable aeronautics staff was essentially eliminated at the NFAC. This staff had often helped solve major problems encountered by industry in a timely way because of their unique knowledge, and comprehensive and extensive experience. Among many examples, common problems such as landing and takeoff performance and drag reduction were frequently solved in the wind tunnels. Occasionally problems would arise that required a rapid response because of flight-safety issues and resulting fatalities, such as deep-stall and propeller-whirl instability, as well as other vertical flight and helicopter-related issues. Ames research staff were especially proficient at solving these kinds of problems, and this knowledge base and problem-solving ability had been an important part of the NACA and NASA aeronautics charters.

Unfortunately, many NASA wind tunnels went from research wind tunnels to wind tunnels for hire because of the drastic reductions in NASA aeronautics funding and elimination of knowledgeable staffing. The ongoing reduction in the NASA aeronautics budget has been dramatic; as of 2009 it has been reduced from a high of over $1.8 billion to less than $600 million dollars in 2008 [67]. Both the wind tunnel operating budgets and the wind tunnel staffing budgets have been drastically reduced [68]. As a result of this decline, funds have been insufficient to operate NASA's many wind tunnels in the ways that had been so successful in the past.

Chapter 7. U.S. Air Force Operation, 2005–Present

Resumption of Tunnel Operation

In 2005 the Department of Defense (DoD) decided to resume NFAC operation because of pressing Army rotorcraft research needs [69, 70]. The American Helicopter Society (AHS) Executive Director, Rhett Flater, and Army Aeroflightdynamics Director, Andy Kerr, received special recognition awards from the American Institute of Aeronautics and Astronautics (AIAA) for their successful campaign to save the NFAC. The Air Force would now operate the NFAC for the Army and lease it from NASA. The Air Force currently has the DoD charter to operate wind tunnels, as well as utilize other aeronautical testing and research facilities. The NFAC is uniquely qualified to perform research on full-scale or large-scale rotorcraft. Small-scale model studies of rotorcraft are limited because of conflicting aerodynamic and aeroelastic requirements. Both Reynolds number and Mach number must be matched, and correctly modeling aeroelastic effects is essential. On the advancing blade of a rotorcraft there are compressibility and shock-wave effects. On the retreating blade, high angles of attack and dynamic stall are encountered; dynamic stall is very sensitive to Reynolds number. (Dynamic stall is the term for blade stall that occurs as the blades rotate and stall and then recover during each revolution. The resulting blade dynamic loads can exceed static loads achieved by the blade airfoils.) These problems are compounded by the dynamic behavior of the rotor blades. Theoretical models and computational fluid dynamics (CFD) have had limited success consistently dealing with these problems, especially for advanced designs in which there is no previous experience nor related empirical aerodynamic and aeroelastic data.

The Air Force cost rates were much lower than what the NFAC was required to charge under NASA management because of full-cost recovery with very high overhead rates. Under Air Force operation, government users pay for direct operating costs including labor, electrical power, and special test hardware. Commercial users pay the same cost plus a 59-percent surcharge for maintenance and overhead [69]. The rate that the NFAC had to charge under NASA's full-cost recovery requirement was about five times as much for tunnel time as the Air Force rate. This estimate may be high, but it certainly reflects the industry perception.

Facility Refurbishment

Restoration, repair, maintenance, and checkout testing of the tunnels occurred from 2005 to 2007. Significant work was required to return the NFAC to operational status after years of being offline. The data acquisition system was extensively refurbished, especially to improve data acquisition for rotorcraft experiments. The Air Force implemented a new personal-computer-based system that had been developed at the Arnold Engineering and Development Complex (AEDC) and was based on their experience performing aeronautical research. People with knowledge of the facility were brought out of retirement, and from other Ames organizations, to help manage and guide the refurbishment. NASA staff included Tom Aiken, Mark Betzina, Michael Herrick, Reg King, Al Lizak, Joseph Sacco, Robert Scott, and Morgan Wright. Operational status was successfully restored in 2007, and the NFAC has been performing a variety of research investigations since refurbishment for the government as well as for many commercial customers.

The NFAC transition from management by NASA to management by the Air Force is well described by Mark Betzina:

> After the NFAC was unilaterally closed by NASA in October 2003 (due to declining use resulting from the "full-cost recovery" mandate), the Army Aeroflightdynamics Directorate (led by Andy Kerr) was very unhappy. The Army had been a major customer of the NFAC and had a number of tests planned in conjunction with the NASA Rotorcraft group at Ames. Shockingly no one in NASA management had contacted the Army prior to the closure. The relationship between the Army and NASA Rotorcraft research groups had been a large part of the success of the Army/NASA agreement, one that went back more than 40 years and had always been touted as a prime example of the benefits of cooperation between the organizations. The availability of the NFAC was the primary reason that a large number of Army researchers were co-located at Ames, and Andy Kerr believed that it would be difficult to justify that the Army remain at Ames without the NFAC, especially considering the impact to ongoing research. Kerr carried this message up the Army chain of command, and Bill Warmbrodt and Mark Betzina provided him with information to make a case for transferring the NFAC to the Department of Defense (DoD).
>
> It took some time, but representatives of the OSD (Office of the Secretary of Defense) were supportive of keeping the NFAC operational as a national capability. I remember putting together cost and staffing estimates for reactivation of the NFAC under Army management. At the time, NASA rotorcraft research was threatened with losing all of its funding, as the NASA Aeronautics budget was being severely cut. At one point, the Army had a plan to hire many of the NASA rotorcraft staff; for a while it looked like this was a likely scenario. It was a time of much uncertainty about the future of rotorcraft research at Ames. The NFAC became a focal point for the survival of both the Army and NASA rotorcraft groups at Ames. I put together a small group of NASA people with NFAC experience to create an NFAC Activation Plan, which was led by Tom Aiken.
>
> Finally, in September 2005, the OSD made a determination that the NFAC was mandatory for future rotorcraft development, and directed the Air Force to take over management of the facility, reactivate it, and operate it. They allocated significant funding to the Air Force to accomplish this—a higher level of funding than NASA had ever been willing to provide. This was a bit of a surprise, since we had been working on a model where the Army would operate the facility, but I believe it was a much better approach. The Air Force had Arnold Engineering Development Complex (AEDC) in Tullahoma, TN, which housed many other wind tunnel facilities and had operational experience with a large contract workforce. The plan was for the NFAC to be a remote site of AEDC. Being part of AEDC provided a vast amount of support for DoD processes, engineering expertise, procurement, and an existing contract mechanism for acquiring staffing needed for the NFAC.
>
> While some brass at higher levels of the Air Force were not pleased with this decision (because Air Force programs did not often use the NFAC), the AEDC supporters readily accepted the challenge. They sent a large team to Ames, led by Ron Polce, to create an activation plan. We met with them and gave them the activation plan that we had already developed. They were very thorough and were not afraid to allocate funding as required to make sure all systems were inspected, refurbished as necessary, and activated properly. In other words, they believed in doing things right and not cutting corners on cost. This was a welcome change after working under NASA's constrained budgets for so many years.
>
> One of the first things required was for the lawyers to figure out how to transfer responsibility for the facility. This took longer than you would think, and I remember thinking, "Do not these guys all work for the same government?" They were finally successful in working out a long-term lease arrangement where the Air Force would annually pay for the lease to cover their share of institutional support, such as base security, fire services, and road maintenance.

In addition, as a tenant organization, the Air Force would be allowed to purchase demand services (at full cost) from NASA, including services such as design, fabrication, engineering, and facilities maintenance. The lease was signed in February 2006, and the OSD provided authority to proceed with staffing and reactivation.

When the OSD made their determination in the fall of 2005, Colonel Vince Albert, Vice Commander at AEDC, was designated the NFAC Director. As a major customer of the NFAC, the Army wanted to participate in its management and proposed that the Deputy Director be from the Army. Andy Kerr asked me to transfer from NASA to the Army to fill this position, and I agreed. I met with Col. Albert at AEDC, and the Air Force appointed me to this position. Col. Albert and I began identifying key personnel for the NFAC and assisted lawyers with the lease development. Col. Albert moved permanently to Ames in December 2005, and by the time the lease was signed in February, we had identified Nick Jize (a previous facilities manager at the NFAC) to be the contract Site Manager. The plan was to use the Jacobs Technology, Inc. group at Ames on the NASA wind tunnel contract as a vehicle for hiring a separate Jacobs group for the NFAC, and Jize was already a Jacobs employee at Ames. Jacobs was part of the ATA (Aerospace Testing Alliance) contract at AEDC that operated all the AEDC facilities. Having a Jacobs group already at Ames made things a lot easier because they could locally support administrative functions, like payroll. This group just needed to be kept separate from the NASA contract, so the funding went from the Air Force to ATA to Jacobs.

With Nick Jize on board, we started identifying and hiring the rest of the contract staff. We hired Mike Herrick who retired from NASA some years earlier but had critical knowledge of the electrical systems. Jeff Johnson was hired as the Test Operations group leader. He had rotor test experience in the NFAC and had been working with the NASA Rotorcraft Branch as a contractor. I succeeded in getting NASA to assign Joe Sacco and Tom Aiken to work full time at the NFAC as NASA employees, although the Air Force had to pay their full cost to NASA. Aiken had been Assistant Chief of the Wind Tunnel Operations Branch and Sacco had been the facility manger prior to its shutdown.

Jeff Johnson was given the task of refurbishing the NFAC office space and buying furniture. The Air Force did this in first class fashion, providing carpet throughout the office area and new furniture. When this was completed, it definitely looked different than a typical sparse NASA facility. Jize continued to hire personnel with NFAC experience as often as possible, including NASA retirees. The Army assigned two aircraft mechanics, Gene DeVargas and Rick McIlmoil, and one instrumentation technician, Larold Pruett, with NFAC rotorcraft experience to work full time at the NFAC. Vendors were contracted to perform much of the inspection and refurbishment work required to reactivate the facility.

While management was clearly Air Force, experienced NASA and Army personnel provided the majority of the reactivation team. This collaboration allowed for a very successful reactivation in a minimal amount of time. Looking back, I think the decision to have the Air Force take over the facility was the best outcome that could have happened. The facility was brought back on line for the nation's benefit (including for the benefit of NASA) with ample funding support from the Air Force. The Air Force has continued to invest millions of dollars in upgrading the capabilities of the facility. The DoD's direct cost charging policy makes large-scale testing affordable, allowing the facility to continue its long history of valuable contributions to aerospace research and development.

After Col. Albert retired in August 2007, I became Acting Director for almost a year while waiting for AEDC to select another Director. I participated in the selection process and David Duesterhaus, a civilian Air Force engineer at AEDC, was chosen. I continued as Deputy Director until I retired in December 2010. At that time, Joe Sacco took my place as Deputy Director. He had been Chief Engineer prior to that as a NASA employee and continued working under the auspices of NASA. Rick Shinoda became the Chief Engineer. He had been

working full time with the NFAC as an Army engineer and NFAC rotor systems expert. We originally had an Air Force Director, Army Deputy Director, and NASA Chief Engineer. After I retired, the NFAC had an Air Force Director, NASA Deputy Director, and an Army Chief Engineer, continuing the management involvement of all three organizations. When David Duesterhaus went back to AEDC in September 2012, they chose Scott Waltermire to take his place as Director, once again having a military background, retired Navy, as Director.

The 25th Anniversary of the NFAC was celebrated on December 11, 2012.

PART III. RESEARCH HISTORY

Chapter 8. NACA Research, 1944–1958

Overview

Initially, the aircraft investigated in the tunnel were propeller-driven military aircraft. For example, there were propeller slipstream (downstream propeller wake) issues at the tail or at the wing. Scientists surveyed the airflow at candidate tail locations so that tail sizes and positions could be optimized. The effect of air inflow variations on propeller loads was also an issue and therefore extensively studied by researchers.

It was common for these early aircraft to have higher drag than expected. Reducing the drag of military fighters was an important research area needed to improve performance. Even though the aircraft typically had higher maximum airspeeds than the wind tunnel was capable of, the drag coefficients (as well as the other aerodynamic coefficients) were found to be valid because the wind tunnel Reynolds number was high enough to readily allow small corrections of the aerodynamic coefficients to be made for the higher airspeeds, up to reasonably high subsonic Mach numbers—at least up to the cruise speeds of these early aircraft.

Prototype fighter aircraft were tested; wing trailing- and leading-edge devices (flaps and slats) were studied to increase lift at landing and takeoff conditions. Later, the development of the jet engine, and the desirability of wing sweep to reduce the drag of high-speed aircraft at cruise conditions, introduced a new set of landing and takeoff problems. Wing sweep changed the airflow on the wings, which affected the aerodynamics of the wing and the high-lift devices (flaps and slats) required for landing and takeoff. The effects of wing sweep on wing airflow were extensively studied for different wing shapes and high-lift devices.

Generally, only research of interest to the government and the NACA (and subsequently, NASA) was performed. Research on non-government aircraft or models was only performed if the research was judged to be of general interest to the aircraft industry as well as to the government, and the test results could be analyzed and published by the government. The tunnel was heavily used; it typically operated two shifts a day and sometimes three shifts. The tunnel was usually scheduled for several years in advance.

It was important for the researchers to report the test results, and distribute the data and results of data analysis in a systematic and permanent way to the aeronautical industry; that was part of the NACA charter (and subsequently the early NASA charter). The quality of the reports was exceptionally high. After a branch review of the reports, there was always a review by an editorial committee made up of peers from other branches at the Center. The reports were then submitted to Ames Center management for additional review. The goal was always to write reports that would be of maximum use to the government and industry, and that were of high enough credibility and accuracy to be useful well into the future. The reports were generally complete enough that they could stand alone. The test models or aircraft were carefully described in the reports, and original and reduced data were given along with analyses. References were

verified and checked for accuracy and appropriateness. Excellent, clear writing was valued, and technical writing classes were often given to newly hired engineers to improve their technical report writing skills.

Calibrations

Once the 40- by 80-Foot Wind Tunnel was operational in the summer of 1944, engineers performed flow surveys in the test section and tested a standard Clark Y 2D airfoil wing section (Fig. 58). Test results were compared to similar test results from the Langley 30- by 60-Foot Wind Tunnel to verify consistency of the data and flow quality. The Clark Y airfoil was a popular early standard airfoil that was extensively used. It had a flat lower surface and a simple, curved upper surface that was relatively easy to accurately construct, and it had reasonably good subsonic longitudinal (lift, drag, and pitching moment) aerodynamic characteristics.

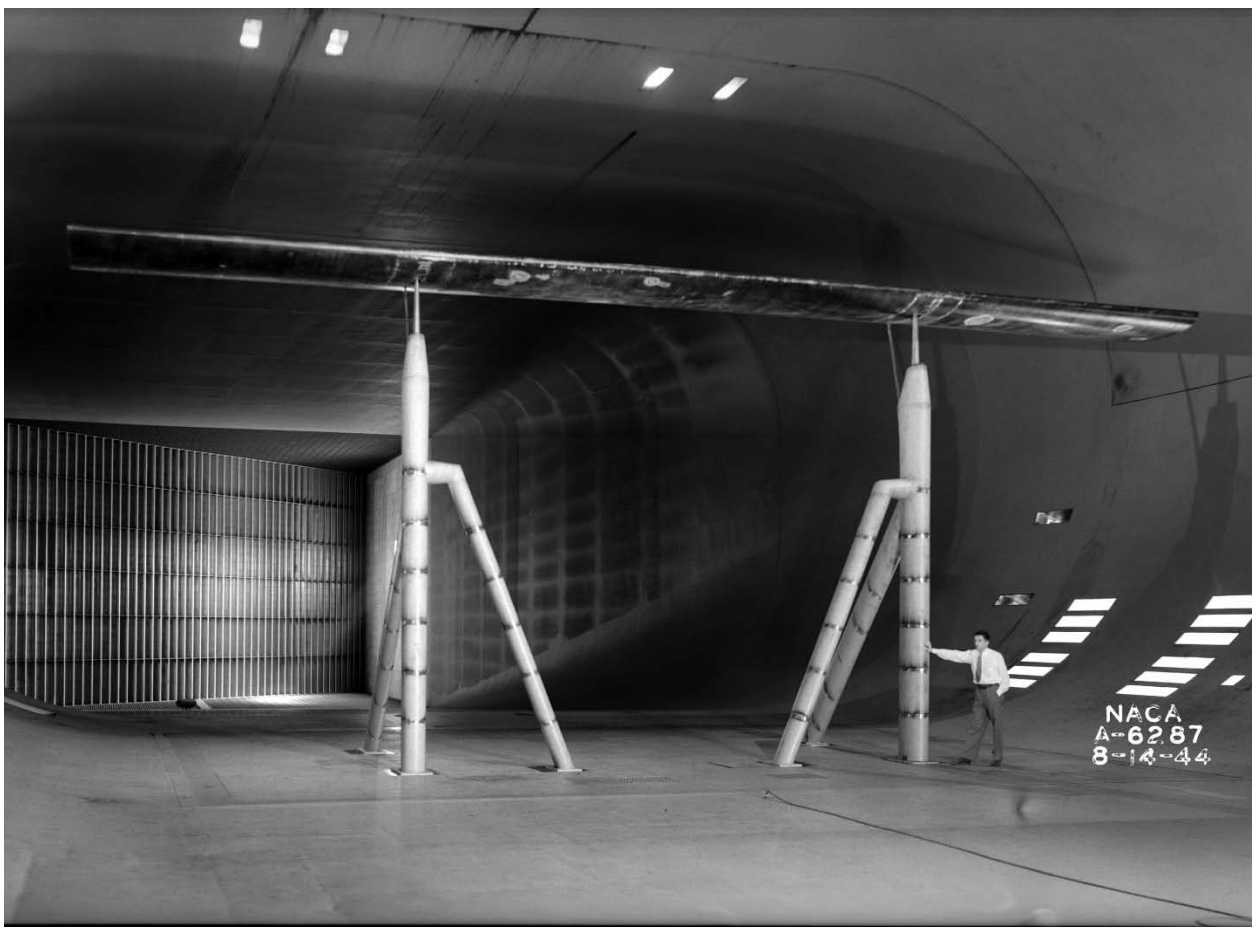

Figure 58. Calibration of the 40- by 80-foot test section using a Clark Y 2D airfoil. ***(NACA A-6287)***

Fixed-Wing Aircraft and Large-Scale Models

Flying Qualities

Many of the early experiments performed on aircraft and models determined their basic aerodynamic characteristics and flying qualities. There was a lot of uncertainty in the aerodynamic characteristics of aircraft, and optimum design procedures and requirements had not yet been well established by the aircraft industry. There were significant uncertainties in both longitudinal data and lateral-directional data (side force, yawing moment, and rolling moment). When testing began in the tunnel World War II was still underway, and much of the research was classified as it was war-related with tight schedule requirements. The first few tests were of prototype or experimental aircraft, mostly fighter-type aircraft.

Douglas XSB2D-1. The first airplane in the tunnel was the Douglas XSB2D-1, which was a dual-seat experimental fighter airplane with a gull wing. It was shown extensively in early photos (Figs. 59 and 60). The first figure shows the aircraft being installed in the wind tunnel through the doors above the test section. The second figure shows the aircraft being mounted on the support struts. The overhead doors are open and their edges are shown near the sides of the photo. Tall ladders were used by the mechanics to access the strut tips for attachment of the aircraft. Ball joints were used at the strut tips to serve as pivots when the angle of attack was varied by changing the length of the tail strut. There has been some question as to whether aerodynamic data were actually collected on this specific airplane since it was not given a test number, and it was installed as soon as possible for photos. However, experiments were, in fact, performed and the results reported [71]. These experiments allowed for the study of methods for estimating the required takeoff runway length for aircraft. Subsequent investigations were done on the Douglas BTD-1 (Fig. 61 and 62, Test 1), which was essentially the same airplane with a single seat. It was an advanced Navy dive-bomber that started production but was terminated shortly after the end of World War II. Engineers found that the aircraft had disappointing performance.

Flight-tests were performed by Ames on the XSB2D-1 [72]. Its last flight-test ended in a Sunnyvale, California, prune-orchard crash due to an engine fire. George Cooper was the pilot and Welko Gasich was the passenger and research engineer. Because of Cooper's amazing skill, they made a crash landing between rows of trees and were not injured. They walked away from the crash landing, although the airplane's wings were torn off and a lot of orchard trees were destroyed. Their flight-test results would be compared with the wind tunnel test results and predictions.

Grumman F7F-1 Tigercat. The F7F-1 was to be a carrier-based single-seat twin-engine high-powered fighter-bomber with a 52.5-foot wingspan. This was designated as Test 2. During one of the early test runs the flaps were inadvertently left deflected, which would produce high lift. As the airspeed in the tunnel was slowly increased, the plane started to lift up, lifting the support struts and balance frame. Fortunately, the wind tunnel mechanic, who was the test observer, pushed the emergency stop button before any damage was done. (This was well before closed-circuit TV in the tunnel.) The procedure during all tests was to have an observer watching the test model so that if there were a model failure or problem, the observer could push the emergency stop button that was next to the observation window. This procedure was maintained

even after closed-circuit TV was installed. The primary purpose of the F7F-1 test was to investigate the propeller slipstream effects on a wing-inlet oil-cooler ducting system. During flight-testing the oil cooler was not as effective as required, causing the aircraft engines to run excessively hot. As a result of the wind tunnel experiments, the ducts were modified. An additional significant result of the wind tunnel tests was that the size of the vertical tail was increased for improved directional stability [73]. After the studies in the 40- by 80-Foot Wind Tunnel were completed, flight-tests were performed at Ames. The flight-tests verified the wind tunnel tests. The plane was never operational on aircraft carriers as originally intended, but it was effective as a land-based aircraft for the Navy and Marine Corps. During the tests, the airplane started to lift the support struts because large knife edges were used as pivot bearings for low friction at the ends of the balance-frame lift posts. Subsequently, the lift-post knife-edge ends were caged to prevent large high-lift airplanes and models from inadvertently partially lifting the model-support struts and balance frame.

Figure 59. The first airplane tested in the 40- by 80-Foot Wind Tunnel was a Douglas XSB2D-1; it is shown being lowered into the test section on June 12, 1944. The edge of the overhead doors can be seen. This was a so-called gull-wing aircraft. ***(NACA A-6031)***

Figure 60. Douglas XSB2D-1 being mounted on the support struts. Initially, tall ladders (as shown) were used by the mechanics to access the strut tips for attachment of the aircraft. Ball joints at the strut tips served as pivots when the angle of attack was varied using the telescoping tail strut. ***(NACA AAL-6032)***

Figure 61. Front view of the Douglas BTD-1, which was a single-pilot version of the XSB2D-1. ***(NACA A-6462)***

Figure 62. Rear view of the Douglas BTD-1; the two telescoping tail-strut support struts are shown.
(NACA A-6463)

Northrop N9M-2 tailless airplane (flying wing). The N9M-2 aircraft was a flying model (about 35 percent scale) of the proposed XB-35 flying-wing bomber and was designated as Test 3. The aircraft did not have a conventional fuselage or tail; it was controversial, and there were questions about its stability and controllability. Power-off tests were performed in the 40- by 80-Foot Wind Tunnel prior to flight-tests to verify small-scale-model test results (Fig. 63). The flying model was to be propelled with two pusher propellers, whereas the full-scale bomber was to be propelled by four pusher propellers. The wind tunnel tests determined that manned flight-tests could be safely performed with the flying model without incurring undue risk [74]. The control system was evaluated; it was deemed acceptable and the airplane would be controllable. Lift, drag, and pitching moment were comparable to conventional airplanes that had tails. As a result of the wind tunnel experiments, confidence was gained, and successful flight-tests were safely performed.

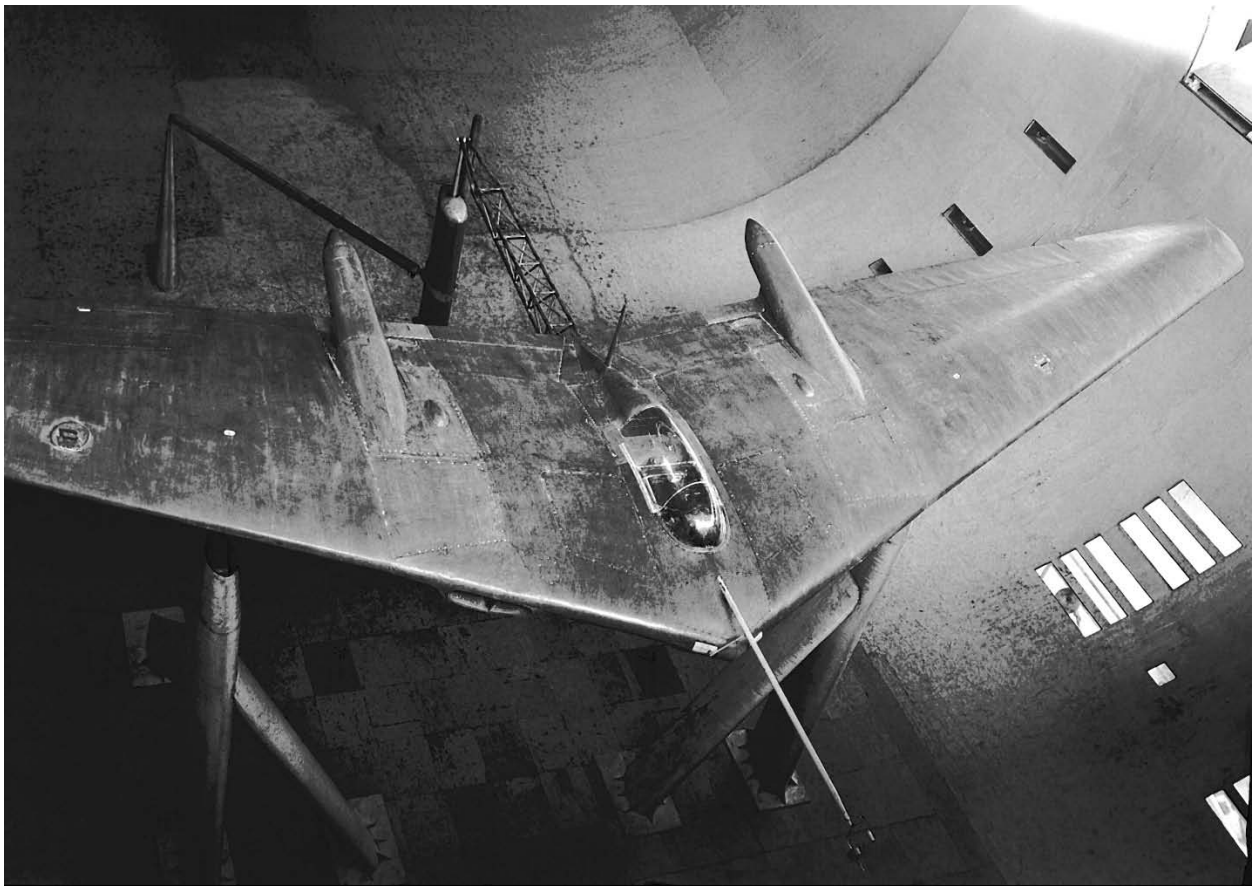

Figure 63. Top view of the Northrop N9M-2 tailless airplane or flying wing. The temporary framework shown in top center allowed the tail strut to be used to vary angle of attack. ***(NACA A-6643)***

GM Fisher XP-75 Eagle. The XP-75 was initially intended to be a high-powered, long-range interceptor, and then subsequently it was to be used as an escort fighter. The aircraft was investigated in the 40- by 80-Foot Wind Tunnel in December 1944 (Fig. 64, Test 4). At the time, much research on interceptor-type aircraft was being done because of concerns about an air invasion on the homeland during World War II. The airplane was assembled in a very short time with many off-the-shelf parts by the Fisher Body Company, a division of General Motors, a well-known automobile manufacturer. Because it was important for interceptor aircraft to achieve a high rate of climb, it was powered with an experimental configuration that used two Allison V-12 engines put together providing 24 cylinders with a common crank case and crank shaft that produced about 2,600 hp, which was exceptional at the time. The goal was to produce very high thrust since it was to be an interceptor. It used two counter-rotating propellers to reduce the net torque on the airplane to minimize control problems during high-powered ascents. The main landing gears were from an F4U Corsair, the outer wing panels were from a P-40 Warhawk, and the tail assembly was from a Douglas SBD Dauntless. It was a disappointing airplane with stability problems, and the experimental liquid-cooled engine would overheat. The program was cancelled.

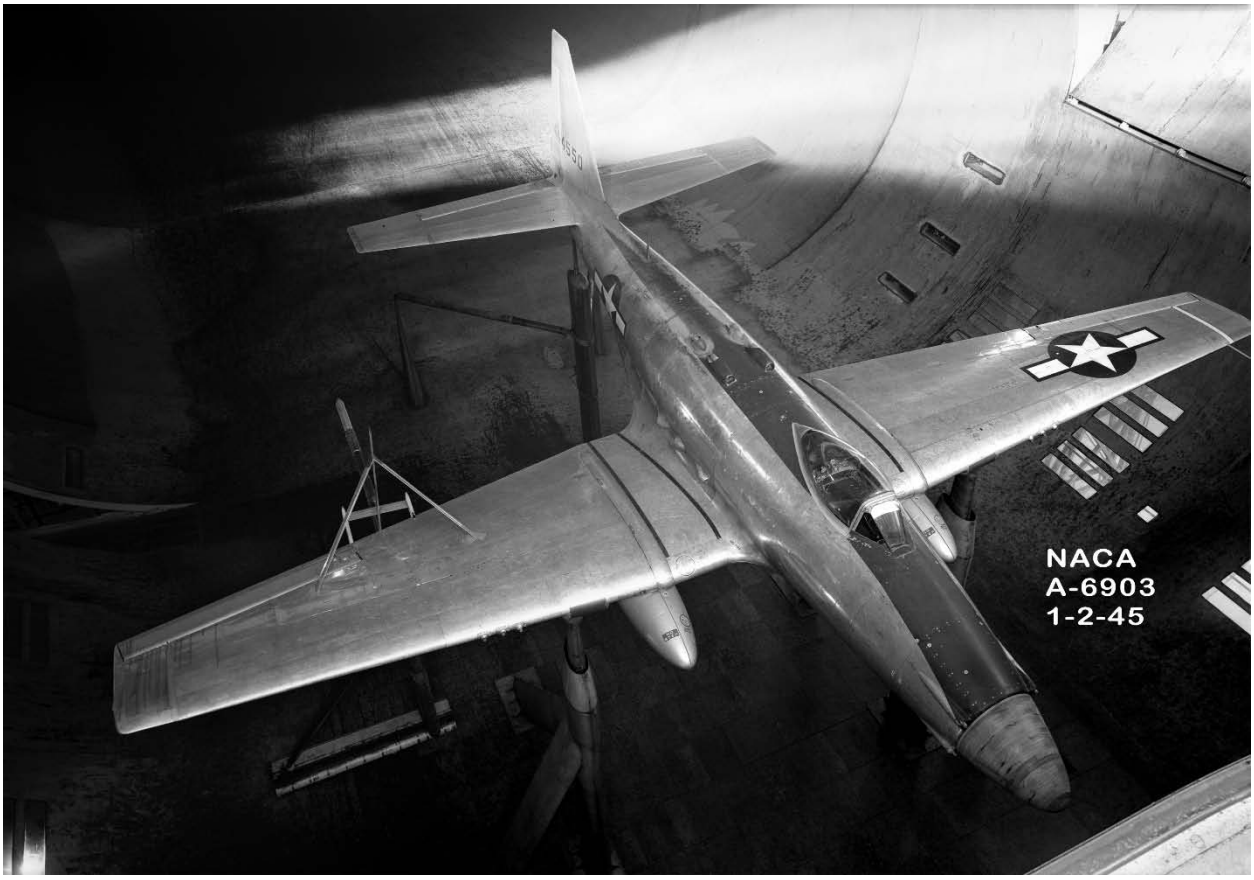

Figure 64. GM Fisher XP-75 Eagle interceptor. ***(NACA A-6903)***

Douglas A-26. The Douglas A-26 was a twin-engine midwing airplane powered by two radial air-cooled engines. This was a large airplane for the tunnel; it had a wingspan of 70 feet. Figure 65 shows the airplane (without its nose cone and propellers) being lifted over the test section prior to opening the overhead test-section doors. Figure 66 shows the airplane in the wind tunnel without propellers and with weapons attached to the bottom of the wings. The purpose of the wind tunnel investigation was to reduce the airplane's high-speed-maneuvering control forces. Pilots had complained about excessive control forces at high speeds. The goal was to make the airplane suitable for high-speed ground-support attack operations. As a result of the wind tunnel investigation, it was recommended that Douglas replace the original fabric-covered straight-sided elevators with metal-covered contoured elevators incorporating a balance tab (a small aerodynamic device that reduces the hinge moments of the control surface therefore reducing the force required to move the control surfaces for pitch control). The fabric-covered elevator surfaces would bulge in high-speed flight. In addition, researchers made several recommendations that were intended to reduce airplane drag and significantly increase airspeed; it was a very successful investigation [75]. The A-26 was the fastest bomber in World War II and many (about 2,500) were built and flown.

Figure 65. Douglas A-26 attack bomber being lifted into the tunnel without its fuselage nose and propellers. The aircraft is above the test section in this view. ***(NACA A-7950)***

Figure 66. Douglas A-26 in the wind tunnel without propellers. ***(NACA A-8051)***

Republic XF-91 airplane model. The Republic XF-91 airplane was to be a jet-engine and rocket-powered interceptor fighter; it had four small rocket engines in addition to its jet engine. It had 37.5-degree swept-back and inverse-tapered wings; that is, the tip chord was longer than the root chord (the ratio of tip chord to root chord was 1.63), which was, and still is, very unusual. However, it is just one example of the many configurations studied because of the uncertainties involved when designing high-speed airplanes in this era. Because of the radical design, full-scale models of the wing, and then the wing and fuselage, were studied in the 40- by 80-Foot Wind Tunnel (Fig. 67) before a flying mock-up was built and tested (Fig. 68) and subsequently flown. In addition to the unusual wing shape and propulsion system, the landing gears were also unusual as can be seen in Figure 68; there were tandem wheels in each main gear. Longitudinal and lateral-directional characteristic were determined along with the characteristics of the ailerons. (Ailerons are like flaps near the wingtips and are used for roll control; one side goes up and the other side goes down to produce roll.) Damping (aerodynamic restorative-forces generated by wing motion) in roll of the wing alone was investigated. Various high-lift devices were also studied. One of the purposes of the reverse taper was to reduce the effects of sweep, which it was successful in doing. The reverse taper resulted in a more uniform spanwise distribution of lift forces, which was one of the goals of the tests [76]. The airplane became the XF-91 Thunderceptor and was flight-tested using a jet engine. It could achieve supersonic airspeeds in level flight with both the rocket engines and jet engine operating; it was the first jet to exceed Mach 1. However, the decision was made that an airplane with the jet-rocket combination would not be practical for operational use.

Figure 67. Front view of the Republic XF-91 experimental airplane. The reverse taper is shown (that is, the wingtip chord is greater than the wing root chord). ***(NACA A-12886)***

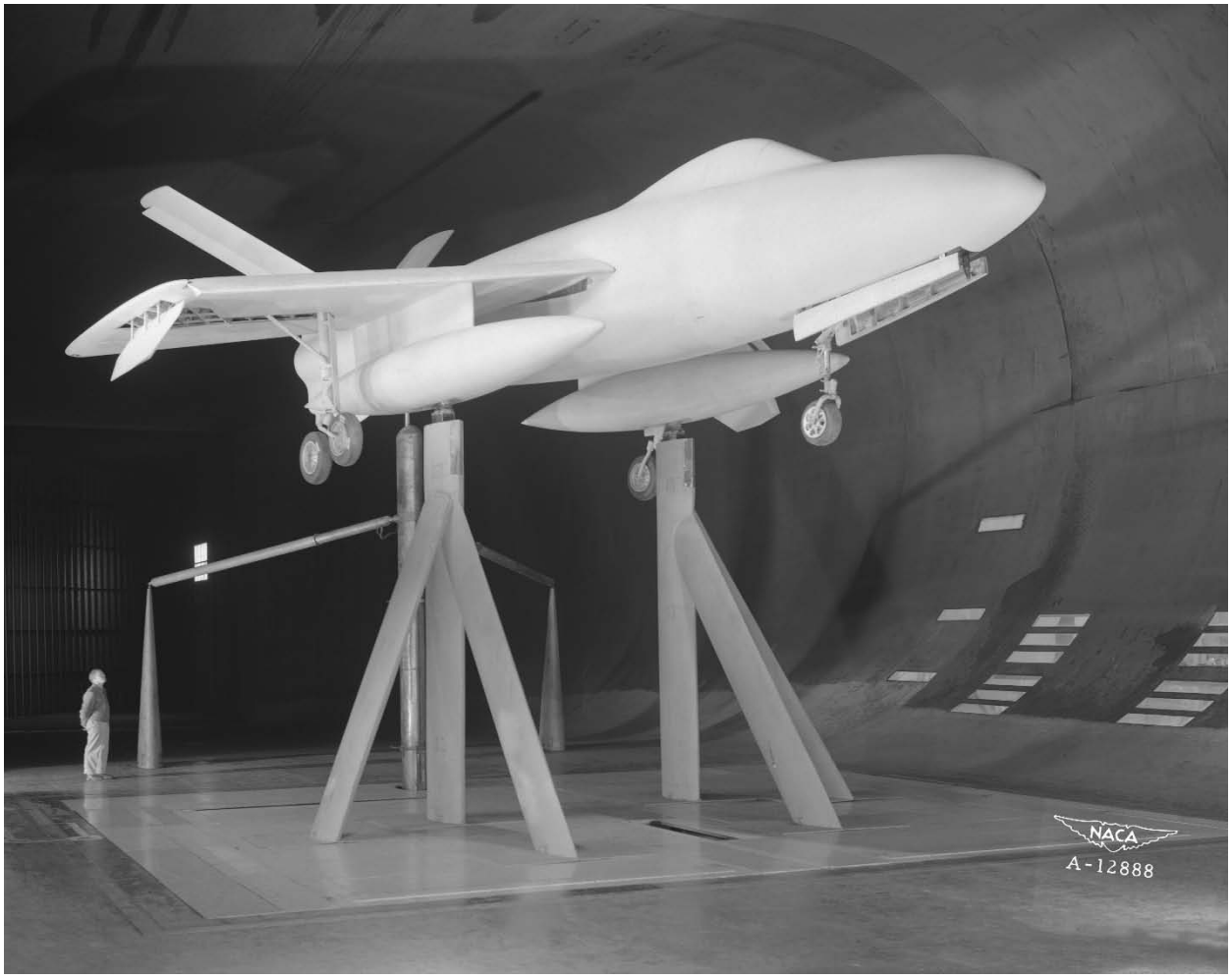

Figure 68. Republic XF-91 experimental airplane with landing gear down. Note the tandem main landing gear. ***(NACA A-12888)***

Boeing XB-47 full-scale tail. An investigation of the Boeing XB-47 bomber full-scale empennage was conducted in the 40- by 80-Foot Wind Tunnel, prior to initial flight-tests of the airplane, to allow development of the control surfaces. Actual prototype tail surfaces were incorporated in the model that was furnished by Boeing (Fig. 69). The XB-47 airplane was to be a jet-propelled medium bomber with wing and tail surfaces swept back 35 degrees. This successful investigation illustrates some of the unusual testing done in the wind tunnel [77]. The XB-47 was powered by 6 turbojet engines and was a very successful Air Force program; more than 2,000 aircraft were built.

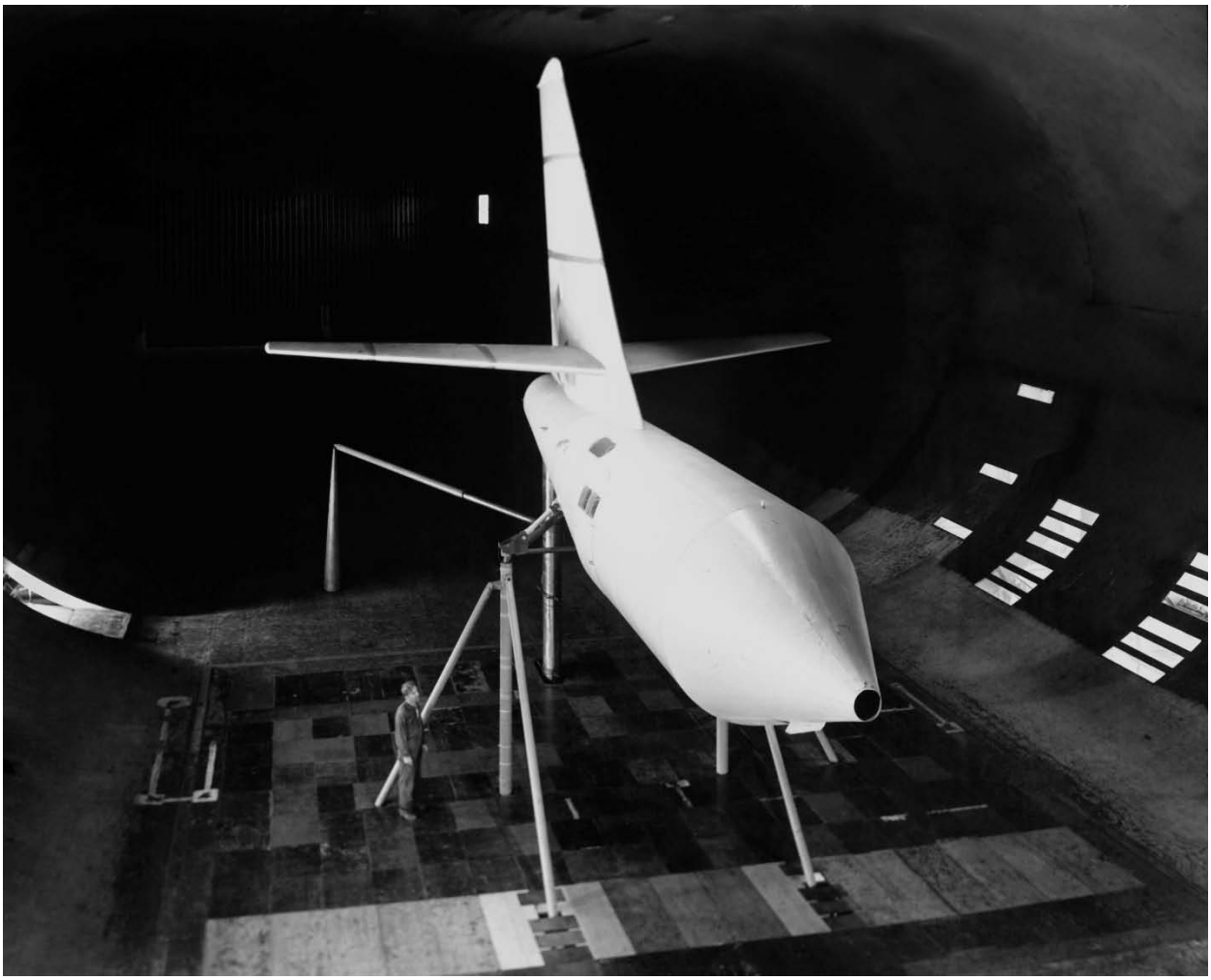

Figure 69. Boeing XB-47 full-scale tail mounted to a special forward fairing to give proper inflow to the tail. ***(NACA A-11732)***

McDonnell XP-85 Goblin jet fighter. The McDonnell XP-85 was a jet-propelled parasite aircraft that was intended to be operated from a proposed B-36 bomber for air-to-air takeoff and recovery, and used for defense of the bomber. The planned approach was to install the airplane in the forward bomb bay of the B-36. The XP-85 was a stubby little airplane, and at the time, the smallest jet-propelled fighter ever built. It had a very unusual tail system (Fig. 70). The airplane wings were swept 37 degrees. The wingtips could be folded upward to allow stowage of the airplane in the B-36. Both force and pressure-distribution measurements were taken. Longitudinal, lateral, and directional stability characteristics and control-effectiveness data were obtained. In addition, there was an extensive investigation of the effects of the extended skyhook in front of the cockpit on the directional stability of the airplane. The skyhook was to be used to hook onto the trapeze on the bomber for retrieval. It was found that the extended skyhook caused a 75-percent reduction in directional stability because the skyhook had such a large projected area; this was contrary to small-scale model results. Several modifications were studied; an aft ventral fin was recommended as the simplest fix for the stability problem [78]. The aircraft had five tail fins, but the stability and control were still marginal.

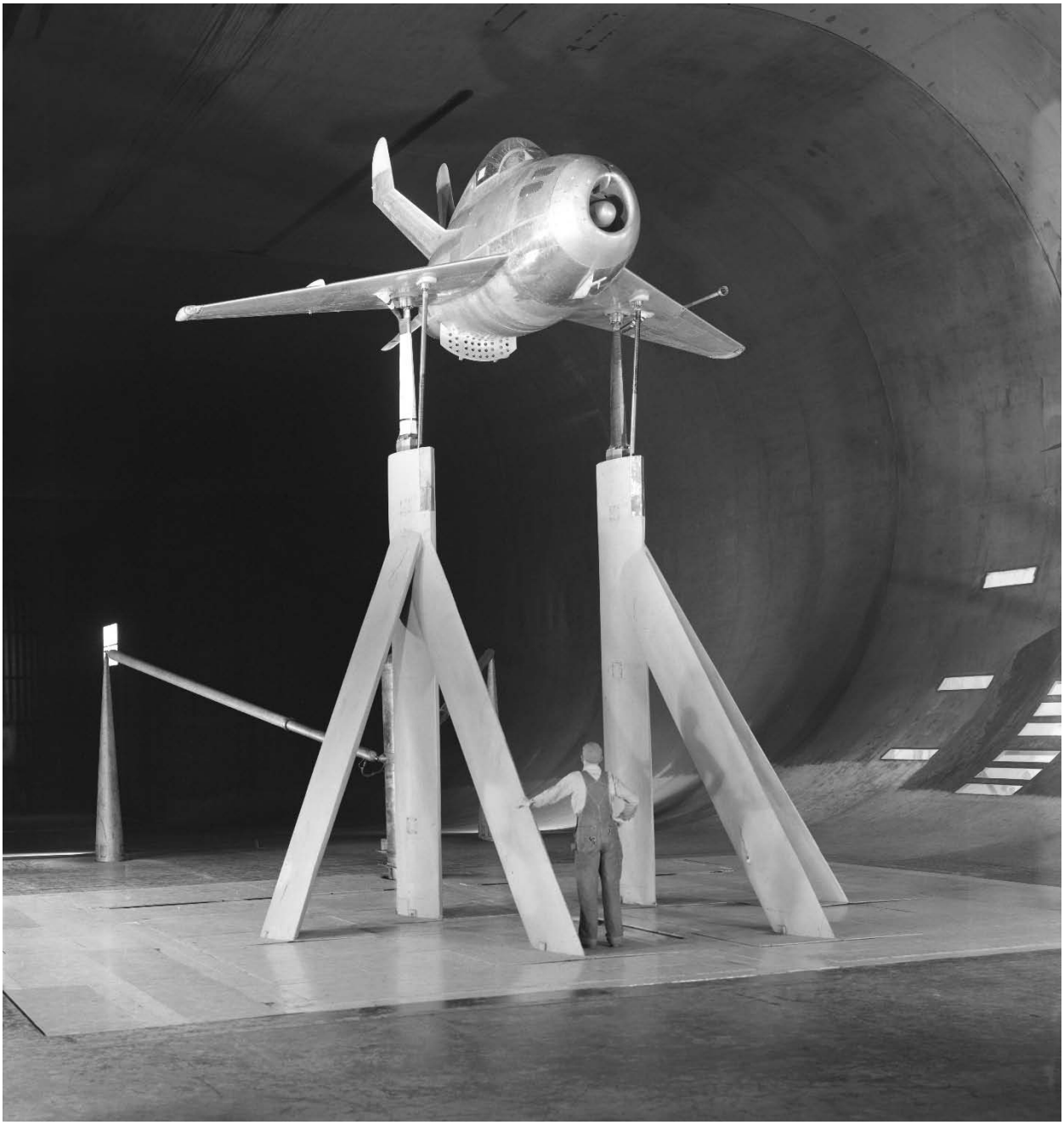

Figure 70. Three-quarter front view of the McDonnell XP-85 Goblin jet fighter. Note the lowered, perforated drag plate on the bottom and near the rear of fuselage for drag control. ***(NACA A-12703)***

When the aircraft was being lifted into the tunnel, the folding lift hook on the aircraft failed, and the aircraft dropped about 40 feet to the floor. The hook that failed was to be the actual hook used for retrieving the aircraft in flight. Therefore, one very important wind tunnel entry result was that redesign of the hook was mandatory if the XP-85 were to be used as a parasite aircraft. The aircraft was replaced in the wind tunnel, and the damaged aircraft was returned to McDonnell.

Minimal flight-tests were subsequently performed. Prior to flight-tests, vertical wingtip fins were installed to improve lateral-directional characteristics. During the flight-tests, pilots had difficulty engaging the trapeze that was temporarily mounted to a B-29 airplane for feasibility tests. When it failed to engage the trapeze, the airplane had to make belly landings on skids because of the lack of landing gear. The idea was eventually abandoned after minimal flight-testing because of the difficulty pilots had in engaging the trapeze.

Republic F-84A Thunderjet. The F-84A was a straight-wing jet-powered fighter-bomber aircraft with a nose inlet, built for the Air Force. It was tested in the wind tunnel after flight-tests at Ames Research Center had identified shortcomings (Fig. 71). The airplane had longitudinal stability issues. Significant development work was required. The plane was eventually used extensively by the U.S. Air Force, and it was the first airplane to be flown by the USAF Thunderbirds.

Chance Vought F6U-1 Pirate. The F6U-1 was designed for the Navy for aircraft-carrier operations. It was the first turbojet-powered aircraft designed by Vought, and it had an afterburner. It had a straight wing with about a 33-foot wingspan. It was found to be underpowered; the Navy had ordered 65 aircraft, but 35 were subsequently cancelled. Early on, straight wings were proposed for Navy jet aircraft because high-lift wings were thought to be required for carrier takeoff and landings, and at the time there was much uncertainty concerning the ability to achieve sufficient low-speed lift with swept wings. The plane was subsequently judged unsuitable for combat.

Figure 71. Republic F-84A Thunderjet in the wind tunnel. ***(NACA A-13695)***

North American F-86A. The F-86A was essentially treated as a generic jet fighter and was used for many experiments in the wind tunnel as well as in flight at Ames for numerous years. The F-86A had a 35-degree swept wing. Often wind tunnel experiments were performed and then results verified during flight-testing. Figure 72 shows the airplane being installed in the test section, and Figure 73 shows the F-86A in the wind tunnel (Test 62). The effects of wing modifications and horizontal-tail location were investigated [79]. The effects on low-speed static longitudinal characteristics were investigated. The wing leading-edge radius was increased and the wing camber was modified to increase the maximum lift of the wing to eliminate the need for leading-edge slats; however, with the modified wing, the airplane was longitudinally unstable beyond maximum lift. Lowering the horizontal tail had a stabilizing effect.

The F-86A was a highly successful fighter airplane for the Air Force and was used for many years with many modifications during its service life. It was the first swept-wing subsonic jet fighter to serve in the Air Force.

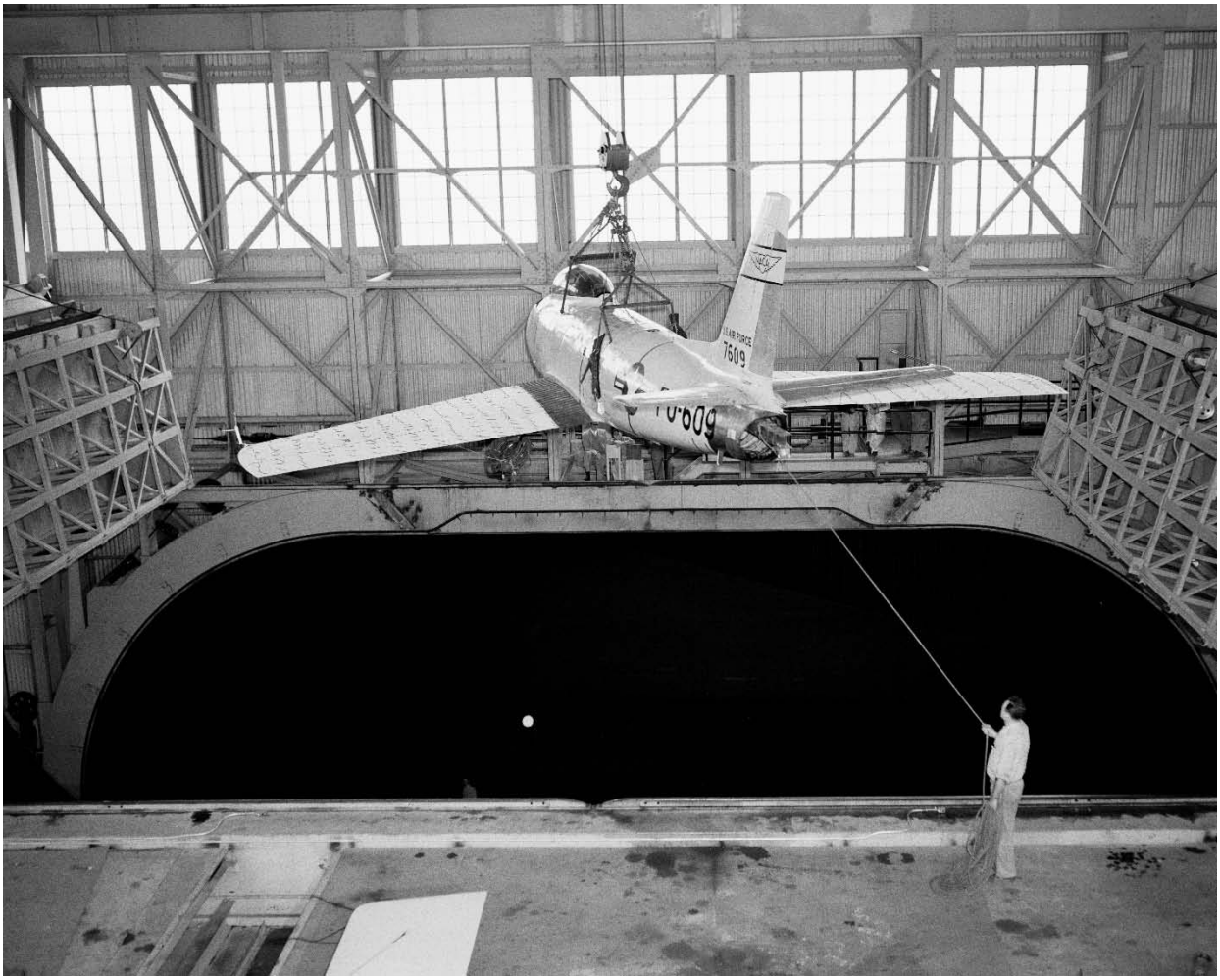

Figure 72. North American F-86A being installed in the wind tunnel. The aircraft is above the open test section. The overhead doors are shown, and Bud Farris is holding the guide line. ***(NACA A-15957)***

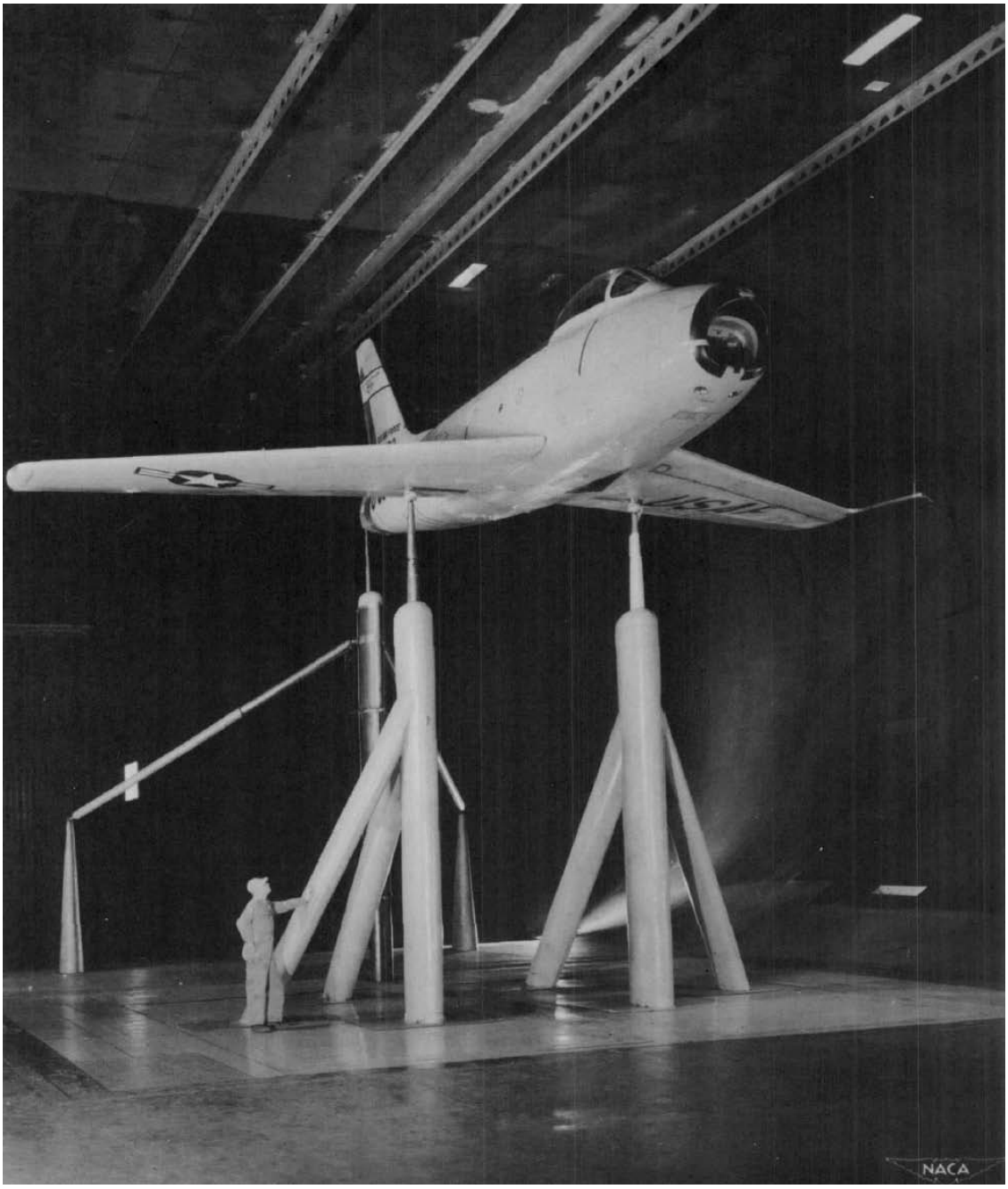

Figure 73. North American F-86A in the wind tunnel. ***(NACA A-15939)***

Lockheed F-94C airplane. The aerodynamic characteristics as a function of angle of attack for an F-94C airplane in the 40- by 80-Foot Wind Tunnel were determined, with emphasis on ascertaining the drag of various surface irregularities, ports, and component parts of the production airplane (Fig. 74, Test 70). The characteristics of the airplane in the landing configuration were also studied [80]. The airplane was designed to be a two-seat all-weather radar-equipped fighter with the radar operator in the back seat. This was the first Air Force turbojet-powered all-weather interceptor. It served primarily with the Air Defense Command for national defense and was used for many years.

Figure 74. Lockheed F-94C—the first Air Force turbojet-powered all-weather interceptor. ***(NACA A-17029)***

Lockheed XFV-1, 1/4-scale tail-sitter VTOL airplane model. A 1/4-scale model of the Lockheed XFV-1 Salmon airplane was remotely test flown in the settling chamber (the large section of the tunnel upstream of the contraction and test section) of the 40- by 80-Foot Wind Tunnel; see Figures 75 and 76 (Test 71). The airplane was a so-called tail-sitter that was propelled by two counter-rotating propellers. This was one of the earliest proposed vertical takeoff and landing (VTOL) airplanes. The model was dynamically similar to the proposed full-scale airplane and was remotely flown to assess its low-speed and landing qualities. The model was powered by two 38-hp electric motors, each driving a propeller. The model was flown from hover up to 70 fps forward speed. The model flights were recorded by motion pictures. Landings and takeoffs were found to be difficult from the tail-sitting position [81].

The full-scale airplane was to be powered by an Allison T-40 gas turbine engine driving a specially designed six-blade counter-rotating Curtiss-Wright propeller. A temporary conventional undercarriage was to be fitted to the full-scale test airplane so it could be flown as a conventional airplane during test flights. The XFV-1 was never flown vertically as a tail-sitter.

Another very similar aircraft that had the same propulsion system, the Convair XFY-1 Pogo, was flown vertically from the tail-sitter position although pilots found it difficult to do.

The VTOL tail-sitter concept worked, but it was abandoned because pilots agreed it was too difficult to land and takeoff from the tail-sitter position. To complicate matters, it was to be flown off of ships, and at the time it did not appear practical to land and takeoff vertically from a moving ship. The two airplanes were subsequently sent to Hiller Aircraft so that the engines and propellers could be used to power the experimental twin-engine X-18, a tilt-wing VTOL airplane.

North American FJ-3 Fury. The FJ-3 was a Navy jet fighter designed for carrier operations. It had a swept wing based on the F-86 Sabre and was part of the evolution of jet-powered Navy aircraft built by North American that included the FJ-1, FJ-2, FJ-3, and FJ-4. (The FJ-1 had a straight wing, but the remaining aircraft in the series had swept wings.) The FJ-3 was very similar to the F-86, but it had a larger jet engine and modified landing gear to make it more appropriate for aircraft-carrier operations. Several hundred aircraft were built for carrier operation after successful investigations in the 40- by 80-Foot Wind Tunnel (Test 94).

Chance Vought F8U Crusader fighter model. The F8U was used by both the Air Force and the Navy. It was designed to be carrier-based for the Navy. One version of the aircraft had boundary layer control (BLC) on the flaps (high energy air blown over the knee of the flaps to increase lift). See Figure 77 (Test 115) for a photo of the model in the tunnel. This aircraft was unique in that it had variable wing incidence to improve the landing and takeoff attitude for better visibility by the pilot. The wing could be tilted up about 7 degrees for landing and takeoff. It was a highly successful aircraft and was used for many years.

Figure 75. A 1/4-scale Lockheed XFV-1 tail-sitter VTOL airplane model in the settling chamber, which is the largest area of the wind tunnel. ***(NACA A-17167)***

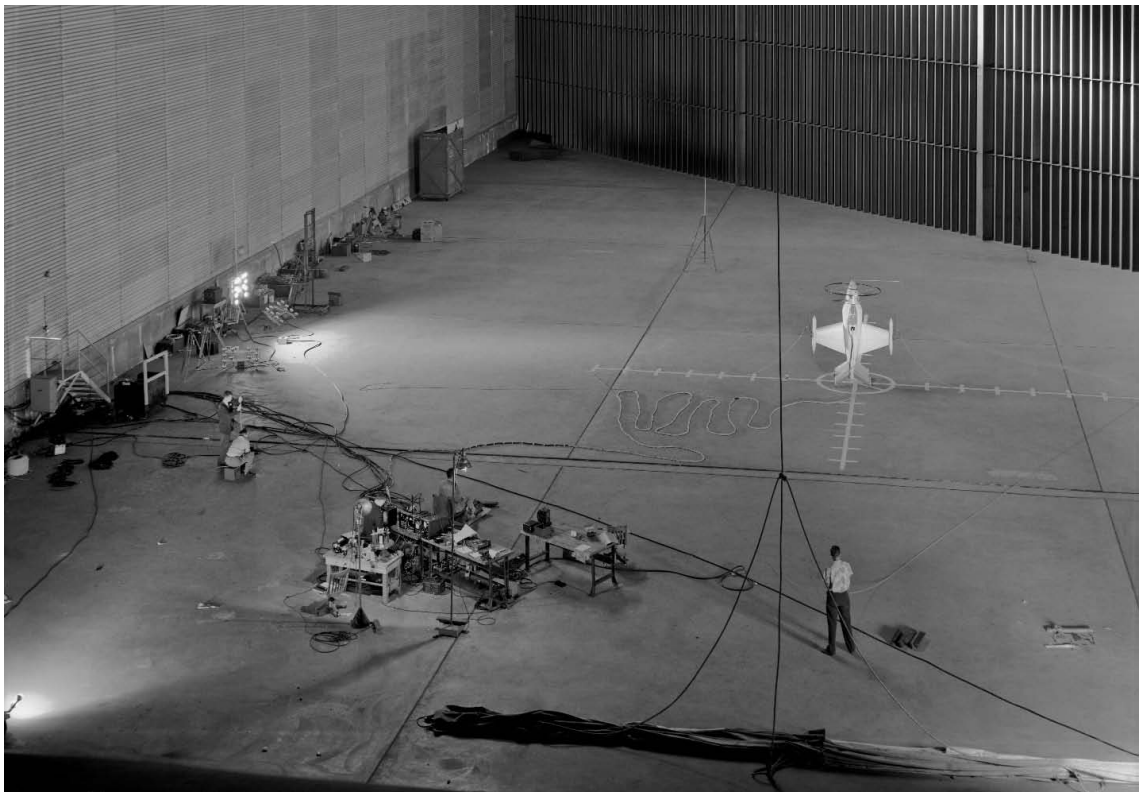

Figure 76. A 1/4-scale Lockheed XFV-1 tail-sitter VTOL airplane model in the settling chamber of the wind tunnel showing the overall arrangement of the remote-controlled flight-testing. The wind tunnel turning vanes upstream of the test section are shown at the upper right. ***(NACA A-17168)***

Figure 77. Chance Vought F8U Crusader fighter model with wing tilted upward.
(NACA A-23318)

Jet-Engine-Inlet Locations

Early on there was a lot of uncertainty concerning the optimum location for jet-engine inlets. At first the inlets were in the nose of the airplane, but that location became undesirable since the engine was aft of the cockpit, and the nose was the ideal location for weapons and photo equipment. Therefore, experiments were performed on different jet-engine-inlet locations at the wing roots or on the sides or bottoms of the fuselage.

Ryan FR-1 Fireball. The FR-1 was a mixed-powered aircraft intended for use by the Navy for carrier operations. It had a 1,350-hp radial engine driving a propeller as well as a 1,600-pound-thrust turbojet engine. The piston/propeller power was thought to be required because jet engines at the time did not produce enough low-speed thrust for carrier takeoff. The jet-engine intakes at the wing roots are evident in Figure 78, and the jet-engine exhaust is shown in the rear view in Figure 79. This was the first aircraft with a jet engine built for the Navy. Less than 100 were built because the aircraft was determined to be structurally unacceptable for aircraft-carrier operation.

Figure 78. Ryan FR-1 Fireball experimental aircraft intended for carrier operations using both propeller and jet-engine thrust. The jet-engine inlets are at the wing roots next to the fuselage. The overhead doors are still open. ***(NACA A-7309)***

Figure 79. Rear view of the Ryan FR-1 Fireball showing the jet-engine exhaust. ***(NACA A-7310)***

An investigation of the intake installation required for the jet engine was conducted to determine the full-scale aerodynamic characteristics of this intake design. The investigation was at the request of the Bureau of Aeronautics, Navy Department. Small-scale testing had been done, but the full-scale airplane did not have the same inlet geometry. Wind tunnel testing was done with the propeller and jet engine removed. An electric-motor-driven compressor was installed to simulate the intake airflow of the jet engine for research convenience and better airflow control. Flow surveys were done at the intake. It was found that there were excessive pressure losses in the intake ducts. Minor revisions within the airplane's structural constraints significantly improved the intake airflow. Additional design revisions were recommended [82, 83] (Tests 5, 8, and 12). Subsequent flight-tests were performed. It was found that the combined thrust of both engines was too great to permit the use of both engines, and the program was discontinued.

Submerged-inlet model studies. Experiments on a full-scale model of a fighter-type airplane were performed to determine the large-scale aerodynamic characteristics of several submerged air-intake configurations and to compare results with small-scale model results [84]. The intakes were forward and above the wing root on the sides of the fuselage. The inlets were termed submerged but were essentially flush along the sides of the aircraft (Fig. 80, Test 26). Longitudinal aerodynamic characteristic were obtained. The same favorable characteristics indicated at small scale were also indicated at full scale. The inlet pressure recoveries at full

scale were somewhat higher than those indicated at small scale; this was caused by differences in the boundary layer thickness, which is a typical Reynolds number effect. As the Reynolds number is increased, boundary layers typically get thinner, which is usually desirable.

Experiments on single and twin submerged inlets at several angles of sideslip for the above full-scale model were also performed [85]. The concern was that sideslip would affect the performance of the engine inlets because of the potential blockage by the aircraft's nose on the downstream inlet. It was found that the effect of sideslip on pressure recovery was greater for a single-nose intake than for a twin submerged-intake installation. Therefore, within the usual flight operating range, the variation with sideslip of the pressure recovery of submerged side intakes was found to be acceptable.

Experiments were also performed on submerged inlets located further aft and on the bottom of the fuselage. Results were similar to those for the forward submerged inlets [86].

Figure 80. Submerged jet-engine inlet model in tunnel. The inlet is shown in the fuselage above the leading edge of the wing. ***(NACA A-11851)***

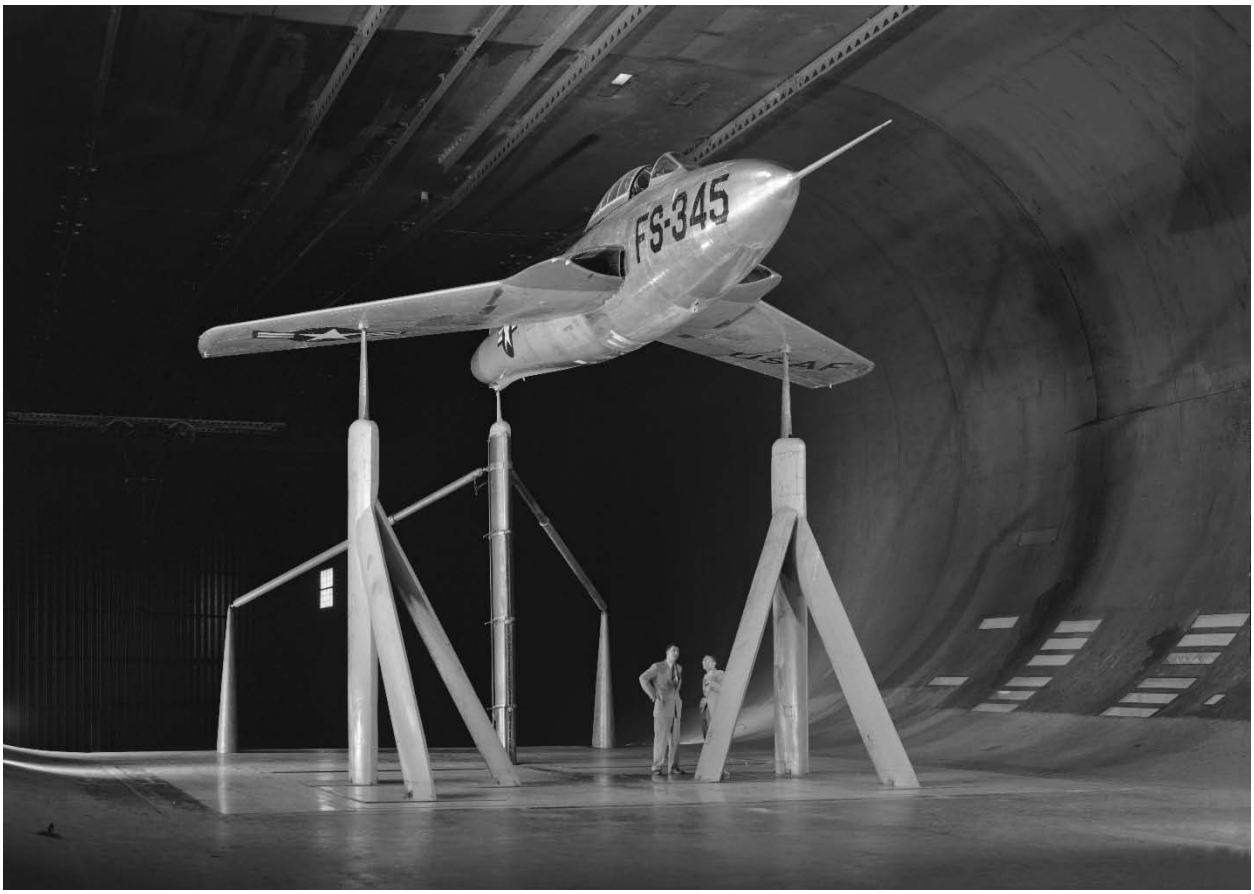

Figure 81. Republic RF-84F Thunderflash jet aircraft with wing-root inlets. ***(NACA A-16937)***

Republic RF-84F Thunderflash with wing-root inlets. The longitudinal aerodynamic characteristics of the Republic RF-84F were investigated in the 40- by 80-Foot Wind Tunnel to determine the origin of, and a suitable remedy for, a pitch-up tendency the airplane encountered at moderate lift coefficients. This airplane was a derivative of the Republic YP-84A-5 but had swept wings and jet-engine inlets at the wing roots. The airplane was a high-performance 40-degree swept-wing jet aircraft designed for photo reconnaissance (Fig. 81, Test 69). Cameras were to be mounted in the nose. Results indicated that the pitch-up at moderate lift coefficients was caused by an abrupt change in downwash at the tail. It was thought that this was traceable to flow conditions associated with an inlet-to-wing leading-edge discontinuity. Several devices intended to fix the problem were not wholly successful. However, it was found that significant gains in performance could be achieved in the upper lift range. Several fixes delayed the onset of wing-flow separation to higher lift coefficients and provided major improvements in the stability of the airplane in the upper lift range [87].

Missiles

In the late 1940s and early 1950s the Air Force was interested in developing jet-engine-powered surface-to-surface cruise missiles that were like conventional jet-engine-powered aircraft. This was before Intercontinental Ballistic Missiles (ICBMs) had been completely developed and

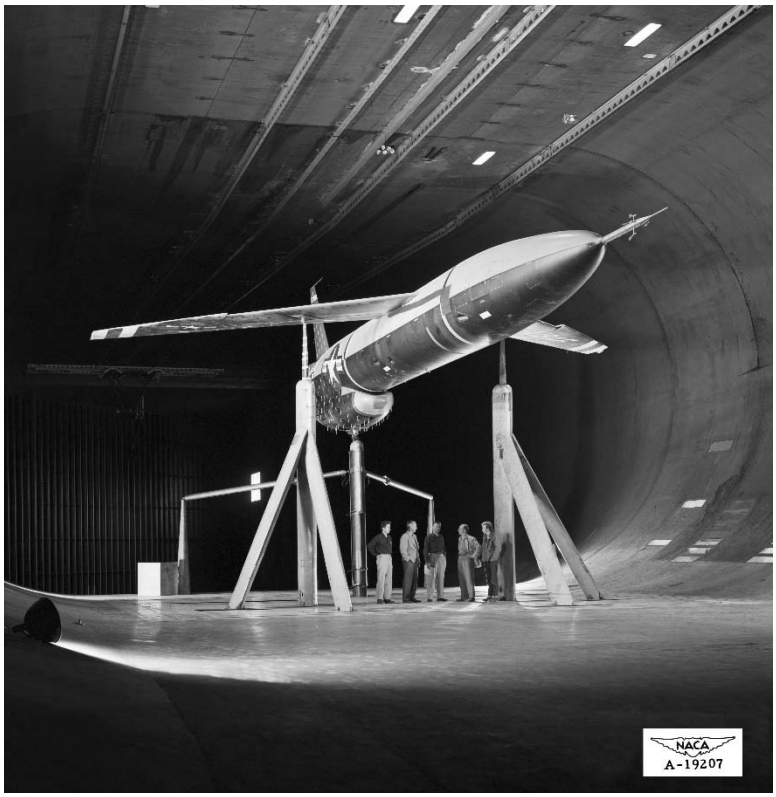

Figure 82. Northrop XB-62 cruise missile; jet-engine inlet shown at the bottom of the fuselage near the rear. ***(NACA A-19207)***

became operational. The jet-powered cruise missile was considered an interim weapon system that would cruise at high subsonic Mach numbers. Northrop was awarded contracts to develop cruise missiles. Two of the missiles were investigated in the tunnel [88, 89]. They had the same dimensions but differed in weight and jet-engine size. The first missile was designated XSSM-A-3. Small-scale studies had indicated that there would be stall near the wingtips. The purpose of the full-scale investigation was to determine the effects of wing modifications to delay stall and to extend the angle-of-attack range for stable pitching moment. Various lift-enhancing modifications were studied including leading-edge flaps and increased wing leading-edge radius. As a result of the experiments, the decision was made to increase the leading-edge radius of the wing. In addition, the low-speed stability and control characteristics were determined in the tunnel. The effects of landing skids were also investigated since the missile was required to undergo flight-tests that included landings. During the wind tunnel tests, the model was unpowered and the engine intake was covered with a fairing.

The Northrop XB-62 missile was the second missile studied in the 40- by 80-Foot Wind Tunnel (Fig. 82, Test 87). The missile was to have a range of about 6,000 miles with a larger payload and a larger engine with a larger air intake. The purpose of the test was to investigate a flight problem at the request of the Air Force. The XB-62 exhibited a directional out-of-trim problem during flight-tests; that is, yawing and rolling moment existed at otherwise trimmed conditions. It was found that the directional out-of-trim condition was caused by cross flow on the vertical tail induced by engine operation. It did not occur when the engine was not operating. In addition, the aerodynamic characteristics were to be correlated with additional small-scale model results obtained by Northrop [89].

Large-Scale Model Studies of Common Low-Speed Problems of High-Speed Aircraft

Systematic basic research was performed at low speeds on models of supersonic aircraft. Models were used to make the testing more economical, systematic, and convenient. The models would have swept wings or delta wings to minimize drag at cruise airspeeds. It was important to investigate common potential landing and takeoff problem areas for high-speed aircraft.

The Effect of Wing Sweep

Wings swept forward and backward. Theory indicated, and high-speed wind tunnel experiments verified, that sweeping the wings either forward or backward was desirable to reduce drag as aircraft speeds increased and to delay compressibility effects to higher Mach numbers. However, at low speeds or landing and takeoff speeds, wing sweep tends to reduce lift; consequently, an increase in landing and takeoff speeds or an increase in wing size is required to maintain sufficient lift for landing and takeoff, both of which are undesirable. Increased landing speed makes landings more hazardous, and increased wing size increases drag at cruise conditions. Wing sweep tends to cause the wing airflow to go spanwise and affect the way wings and flaps produce lift, so development of wing shapes and flaps and high-lift devices on swept wings was very important to reduce the required landing and takeoff speeds to acceptable levels.

Experiments of five large-scale tapered wings that had angles of sweep of 0, ±30, and ±45 degrees were conducted in the 40- by 80-Foot Wind Tunnel to determine the effects of sweep on damping in roll [90]. Rolling moments and pressure distributions were measured while in steady roll for an angle-of-attack range of –1 to 29 degrees. Experimental results were compared with theoretical results, and the theoretical results did not agree for the swept wings investigated. As a result, additional experiments were performed on these models [91].

Wing stall was studied on a model with 45-degree swept-forward wings (Fig. 83). The causes of undesirable longitudinal characteristics at moderate- and high-lift conditions were studied. Detailed flow studies were performed and force data collected to enable a detailed correlation between flow separation phenomena and longitudinal aerodynamic characteristics. In the moderate-lift range, the occurrence of turbulent separation caused a chordwise redistribution of load over the inboard sections of the wing. An increase in drag resulted along with a rearward shift of the aerodynamic center, but there was no loss in lift. In the high-lift range, leading-edge separation caused a loss of lift that occurred first over the inboard sections and then progressed outward over the wing as angle of attack was increased. This was accompanied by a large increase in drag, a decreased lift-curve slope, and a very large forward shift of the aerodynamic center [92].

The effect of the wingtip shape for swept wings was studied [93]. In addition, the swept-back wing was tested with bodies of revolution mounted on the wingtips. The goal of these experiments was to attenuate the development of leading-edge stall that began at the wingtip and progressed inboard because of the wing sweep. The results indicated that none of the modifications produced major changes in the characteristics of the swept wings. Tuft studies (tufts are small pieces of yarn taped to surfaces) indicated that the unstable pitching-moment characteristics of swept-back wings at high angles of attack are caused by a rapid development of leading-edge stall, beginning at the wingtip and progressing inboard [93].

One of the problems when designing horizontal tails for swept-wing airplanes was the effect of the wing wake on the tail. Downwash characteristics of large-scale swept (up to 45 degrees) and unswept wings were studied [94]. It was found that the spanwise distribution of downwash was affected by sweep in a manner similar to span loading; that is, downwash was increased toward the wing root by sweepforward and increased toward the wingtip by sweepback. After stall occurred the downwash near the root of the swept-forward wing decreased markedly, while the downwash near the root of the swept-back wing increased.

Low-speed high-Reynolds-number longitudinal characteristics were investigated at landing conditions on a model with a 63-degree swept wing that would be appropriate for an airplane designed for speeds up to about 1.5 Mach number [95-97]. The model is shown in Figure 84 (Test 27A). Smaller models of this configuration were studied in other wind tunnels at Ames at higher speeds. This study was part of a large effort to define the aerodynamic characteristics of a 63-degree swept-wing configuration at all appropriate speeds. Studies of the same model were done at low speeds and high Reynolds numbers with the model in sideslip [96]. Investigations of a swept vertical tail with rudder were included in the studies.

Flow surveys were also done for the large-scale 63-degree swept-back-wing and fuselage model. Downwash characteristics and vortex-sheet shape were studied (Fig. 23, Test 56). In addition to the model, the survey rig, which had been moved into the test section, is shown in this figure. Results were compared with theory, and some desirable modifications to theory became apparent.

Figure 83. Wing model used for swept-wing studies; wings are swept forward. ***(NACA A-12509)***

Figure 84. A 63-degree swept-wing model. ***(NACA A-11996)***

Semispan models. To reduce the cost of the models, engineers would often use semispan models for studies of low-speed-lift characteristics for swept wings when tail effects were not of interest. The models consisted of a wing panel and sometimes a half fuselage, but not always. The effects of wing camber and twist on the aerodynamic loading and stalling characteristics were typically studied on semispan models. In addition to longitudinal aerodynamic characteristics (lift force, drag force, and pitching moment) wing pressure distributions were often obtained. It was found that camber and twist significantly improved the upper surface loading of the wing, and the onset of leading-edge flow separation on the wing could be significantly delayed. Comparisons with theory generally gave good agreement at moderate lift coefficients. At higher lift coefficients the agreement was not as good [98-102].

The effects of double-slotted flaps and wing leading-edge modifications on the low-speed characteristics of a semispan 45-degree swept-back-wing and fuselage model with and without camber and twist were studied (Fig. 85) [99]. It was found that the flaps substantially increased the maximum lift coefficient. The wing with camber and twist attained higher lift coefficients before drag increased abruptly. Results indicated that theory was satisfactory for predicting the lift increase at zero degrees angle of attack because of the double-slotted flaps.

An investigation of a large-scale, semispan, 45-degree swept-back-wing and fuselage model with double-slotted flaps and ailerons was performed [100]. Longitudinal force and moment characteristics and rolling-moment data were obtained as well as wing pressure distributions.

The effects of finite span on the wing-section characteristics of two 45-degree swept-back wings of aspect ratio 6 were investigated in the tunnel [101]. One wing had symmetrical airfoil sections and the other was twisted and had cambered airfoil sections. Two-dimensional data for the airfoil sections used had different stall characteristics. The goal was to evaluate the use of simple aerodynamic theories that used 2D data. It was found that at low lifts the finite span effects were restricted to the root and tip of the wing. At higher lifts, spanwise flow was evident. This effect tended to delay flow separation and thus increase maximum lift. The effect was greatest near the root and diminished gradually spanwise moving toward the tip.

The wing on one of the semispan 45-degree swept-back-wing models [99] was swept back to 60 degrees. The effects of high-lift devices were studied such as double-slotted flaps, ailerons, leading-edge slats, and a split flap [102]. In addition to forces and moments, surface-pressure-distribution data were obtained in order to precisely determine flow-separation characteristics.

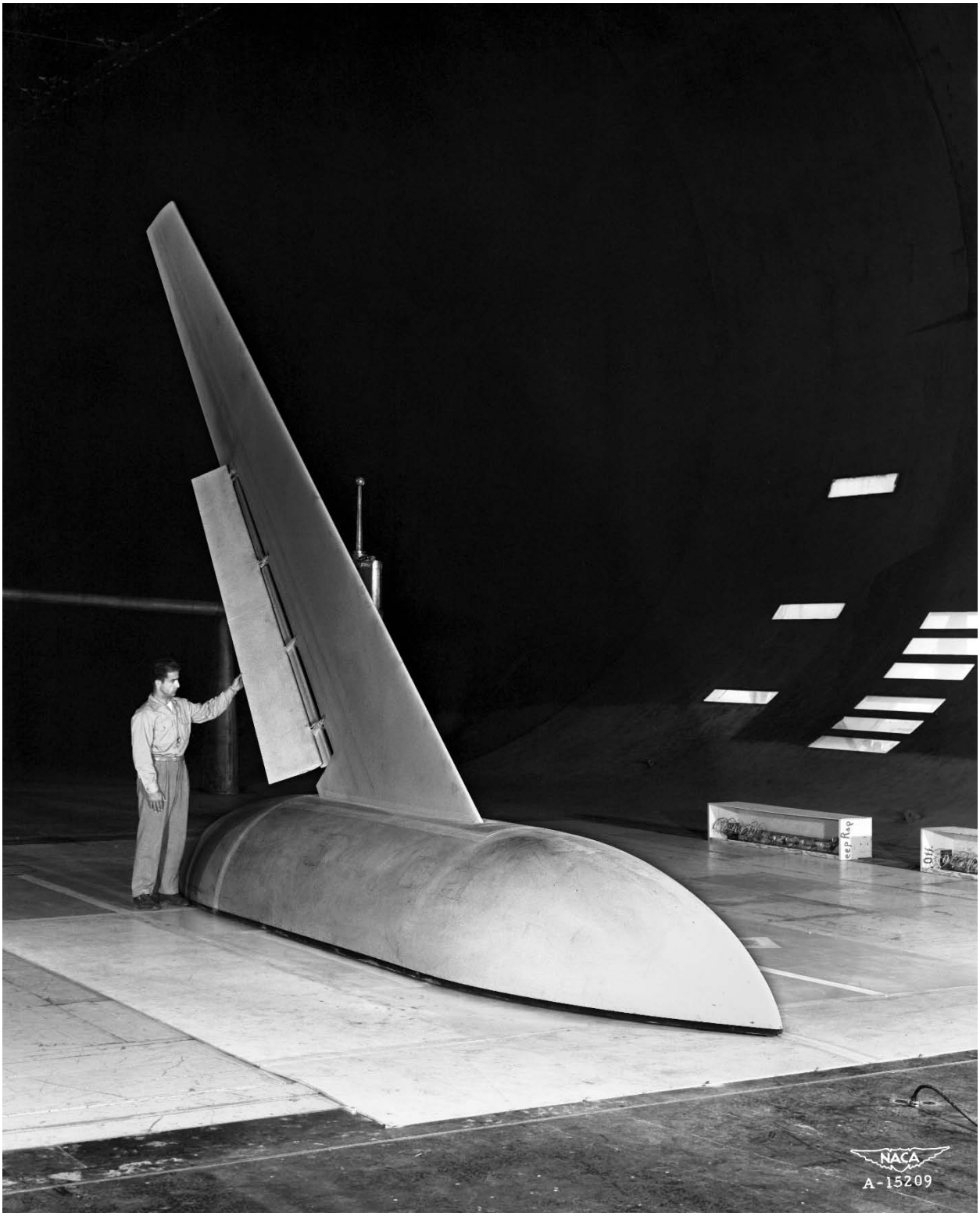

Figure 85. A 45-degree swept-wing semispan model. ***(NACA A-15209)***

Delta Wings

Delta or triangular wings are used on some high-speed aircraft, and the flow over the wing is significantly different than it is for straight and swept wings, making the design requirements for high-lift devices such as flaps and slats different. Delta wings have relatively low high-speed drag similar to swept wings, but they can have high low-speed lift at high angles of attack. Many flap and high-lift devices were investigated on models and aircraft with delta wings. Systematic studies were performed on large-scale models to establish a comprehensive database for use by designers. Aerodynamicists discovered that high-energy vortices occurred at the leading edges of thin delta wings near the fuselage as soon as the angle of attack was increased. These vortices would energize the flow over the delta wings. As a result, lift would continue to rise, up to high angles of attack. This would become an important factor in the development of supersonic aircraft with delta wings. Many experiments were performed on delta-wing models; only a few are described.

Consolidated Vultee XP-92 flying mock-up. An investigation of the flying mock-up of the XP-92, which was an early experimental delta-wing airplane, was conducted in the 40- by 80-Foot Wind Tunnel to determine the limits of stability and controllability (Fig. 86, Test 28) [103]. In addition, pressure distributions were measured on the wing [104]. An engine was not installed, and pressure losses through the engine ducting were obtained. The airspeed indicators were calibrated in addition to the angle of attack and sideslip-angle indicator vanes. The XP-92 was originally intended to be a pursuit-type airplane designed for flight at moderate supersonic speeds. Its triangular planform wing had 60 degrees of leading-edge sweep. The operational airplane was to have a combination of a ram-jet and a rocket engine for propulsion. The flying mock-up was intended to investigate subsonic flight characteristics of delta-wing aircraft and was to be powered with a turbojet during subsonic flight-tests; therefore, there were attendant small differences in geometry between the flying mock-up and the planned aircraft. Small-scale data were available, but there were uncertainties as to Reynolds number (scale) effects. Since applicability of the small-scale data was in question, it was important that full-scale wind tunnel studies be performed prior to flight-tests. The flying mock-up, intended to be a research airplane and subsequently designated the Consolidated Vultee XF-92A, made its first flight in September 1948. This was the world's first delta-wing jet flight. It was flight-tested at Edwards Air Force Base in Southern California and was re-engined and modified during the course of the flight-test program. It was found that because of the strong vortex energizing the wing flow, lift was maintained at high angles of attack (up to 45 degrees angle of attack). This was subsequently found to be a unique feature of delta wings.

Large-scale model experiments. Many systematic large-scale model experiments were performed because of the potential of delta-wing aircraft to have low high-speed drag and high low-speed lift. Models were used because of the ease of making configuration changes and studying their effects. Experiments included delta-wing-alone [105-108] and wing and fuselage models with different wings and tails [109-118].

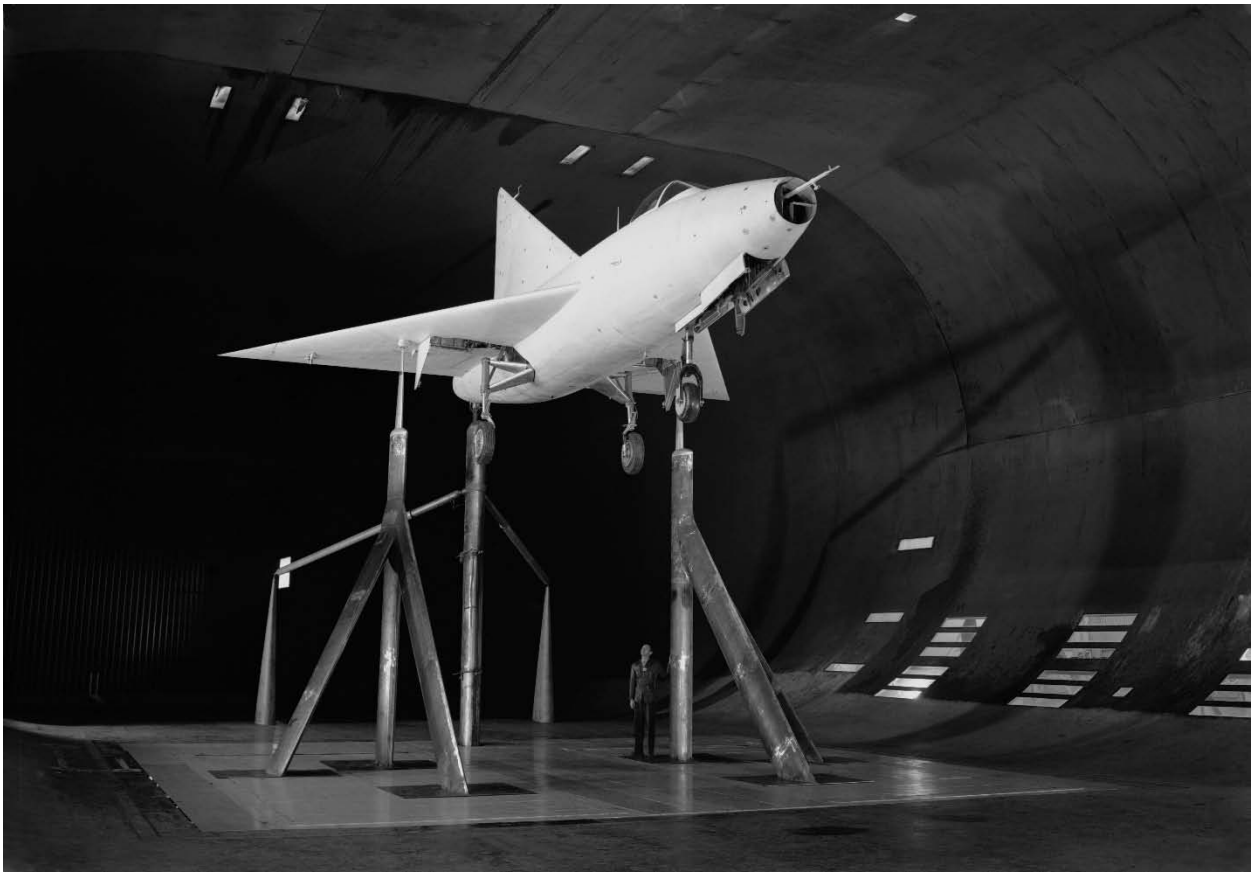

Figure 86. Flying mock-up of the Consolidated Vultee XP-92 delta-wing aircraft in the tunnel with landing gear down. The flying mock-up was going to have a turbo-jet engine, but the airplane was intended to have both ram-jet and rocket power plants. ***(NACA A-12352)***

Low-speed experiments were performed on a large-scale triangular-wing-alone model with an aspect ratio of 2 and a thin double-wedge wing-airfoil section (Fig. 87, Test 20A) [105]. The wingspan was 25 feet. Because triangular-shaped wings with thin double-wedge airfoil sections were of interest for supersonic flight, and most experiments had been done at small scale, large-scale experiments at landing and takeoff airspeeds became important. Thin double-wedge airfoils tend to have low maximum lift that can make takeoff and landing problematic because higher landing and takeoff speeds are required. In addition to longitudinal aerodynamic characteristics, force and moment data were obtained at several angles of sideslip for various configurations with split flaps and ailerons. It was found that there were two regimes of force and moment characteristics indicated by breaks in the force and moment curves. It was believed that these breaks indicated an intense separated flow at the sharp leading edge of the wing and the creation of a strong vortex. This was a major finding warranting further study. Airfoil-section modifications and wake downwash were also studied on this model [106], along with chordwise and spanwise loadings [107]. Additional pressure distributions were obtained on a thin subsonic-type airfoil section [108].

Figure 87. Triangular-wing- (delta-wing-) alone model with an aspect ratio of 2 and a wingspan of 25 feet; flaps are down. ***(NACA A-15261-010)***

Many delta-wing and fuselage experiments were performed [109]. The characteristics of the delta wing with body and vertical tail were studied on the model shown in Figure 88. Aerodynamic characteristics in sideslip were investigated. In addition, an exploratory investigation of the effect of skewed, plain nose flaps was performed on the model [110]. Results were promising and warranted additional experiments on the concept.

Longitudinal characteristics were studied with an aspect-ratio-2 triangular-wing and fuselage model with an all-movable, unswept horizontal tail (Fig. 89) [111]. (Aspect ratio is wingspan squared/wing area; for a rectangular wing this is wingspan/wing chord; for reference, the Concorde airplane had an aspect ratio of 1.55.) Three vertical positions of the horizontal tail were studied. Results indicated that the most desirable location from a low-speed longitudinal stability standpoint was to locate the horizontal tail in the wing-chord plane.

Longitudinal characteristics were investigated for a triangular-wing model with an aspect ratio of 4 and an all-movable horizontal tail [112]. The horizontal tail was tested in three vertical positions, and the results were similar to those described above for the model with the aspect-ratio-2 triangular wing; that is, the most desirable position for the horizontal tail was the wing-chord plane. The same model was also studied with high-lift devices and lateral and directional controls. A three-quarter front view of the model is shown in Figure 90 [113]. The above mentioned fuselage model was also tested with an aspect-ratio-3 triangular wing. The intent was to supplement previous studies with triangular wings with aspect ratios of 2 and 4 to produce a systematic and complete set of basic data for high-speed delta-wing aircraft [114].

Figure 88. Three-quarter front view of delta-wing model with body and vertical tail; aspect-ratio-2 wing shown with flaps down. ***(NACA A-11948)***

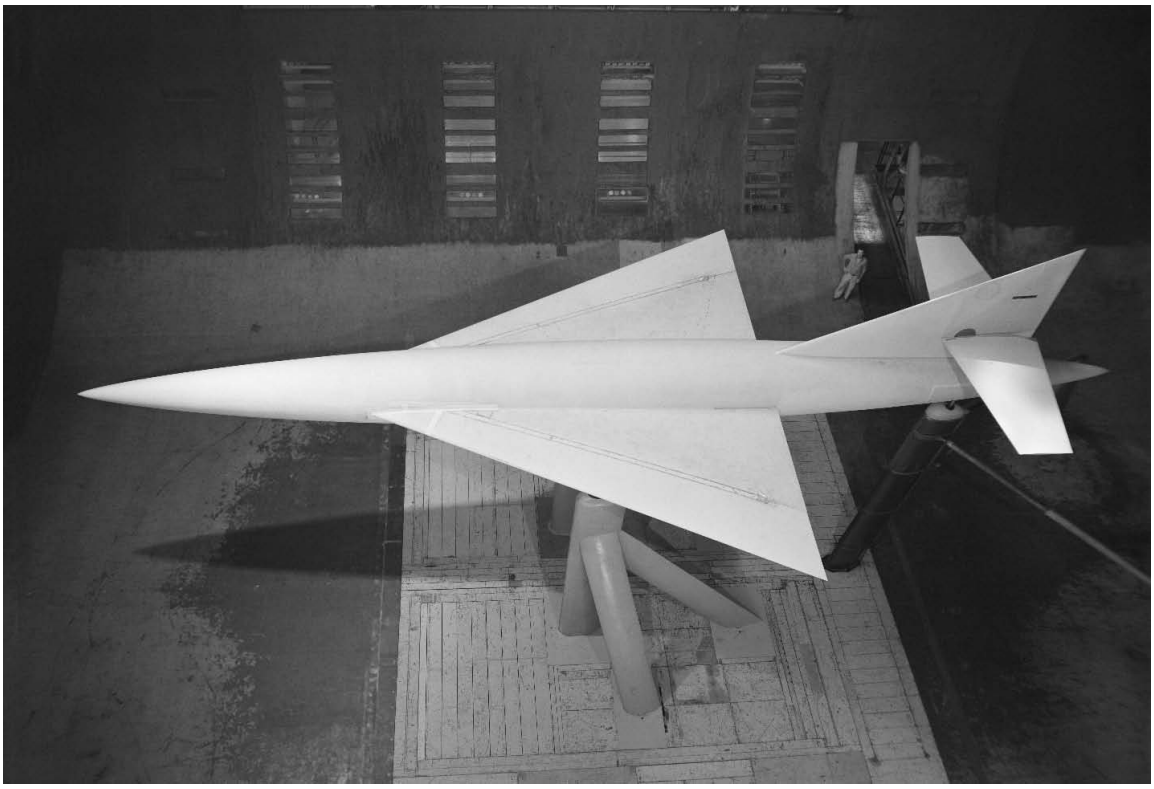

Figure 89. Top view of aspect-ratio-2 delta-wing model with fuselage and all-movable, unswept horizontal tail. ***(NACA A-15630)***

The models above were subsequently modified to have trapezoidal wings. A trapezoidal wing was created by cutting off a section of the wingtip. Two airplane models were tested with aspect-ratio-2 trapezoidal wings. The model wings were the aspect-ratio-3 and -4 wings described above with the tips cut off to achieve aspect-ratio-2 wings. The experiments were parallel to the above experiments [115, 116]

Studies were performed on a model with a variable-incidence aspect-ratio-2 triangular wing and an all-movable horizontal tail. The purpose of the variable-incidence wing was to reduce the angle of attack of the airplane at landing and takeoff conditions when the wing is at high angles of attack to produce high lift. The intent was to take advantage of the delta-wing's capability of producing increased lift at high angles of attack. The wing would be tilted up while the fuselage remained at a lower angle of attack for optimum pilot visibility during landing and takeoff. The model is shown in the tunnel in Figure 91. Based on these experiments, a variable-incidence wing did not appear to hold significant advantage over a fixed wing. Also, it had a small adverse effect on the aerodynamic characteristics of the tail [117] .

Investigations were also performed with modifications to a triangular wing on a wing-fuselage model with and without horizontal tails. The purpose was to eliminate the destabilizing changes in pitching moment through the use of wing modifications for two airplane models having triangular wings of aspect ratios 2 and 3. (Destabilization is when the pitching moment increases with increasing angle of attack, causing the model to want to pitch up further with increasing

angle of attack.) Wing-chord extensions and fences were studied. The destabilizing effects were not entirely eliminated, but considerable improvement was realized by modifying the wing. Delta-wing airplanes have been designed and built without separate horizontal tails [118].

Figure 90. Three-quarter front view of triangular-wing model with an aspect-ratio-4 wing with flaps down. ***(NACA A-16603)***

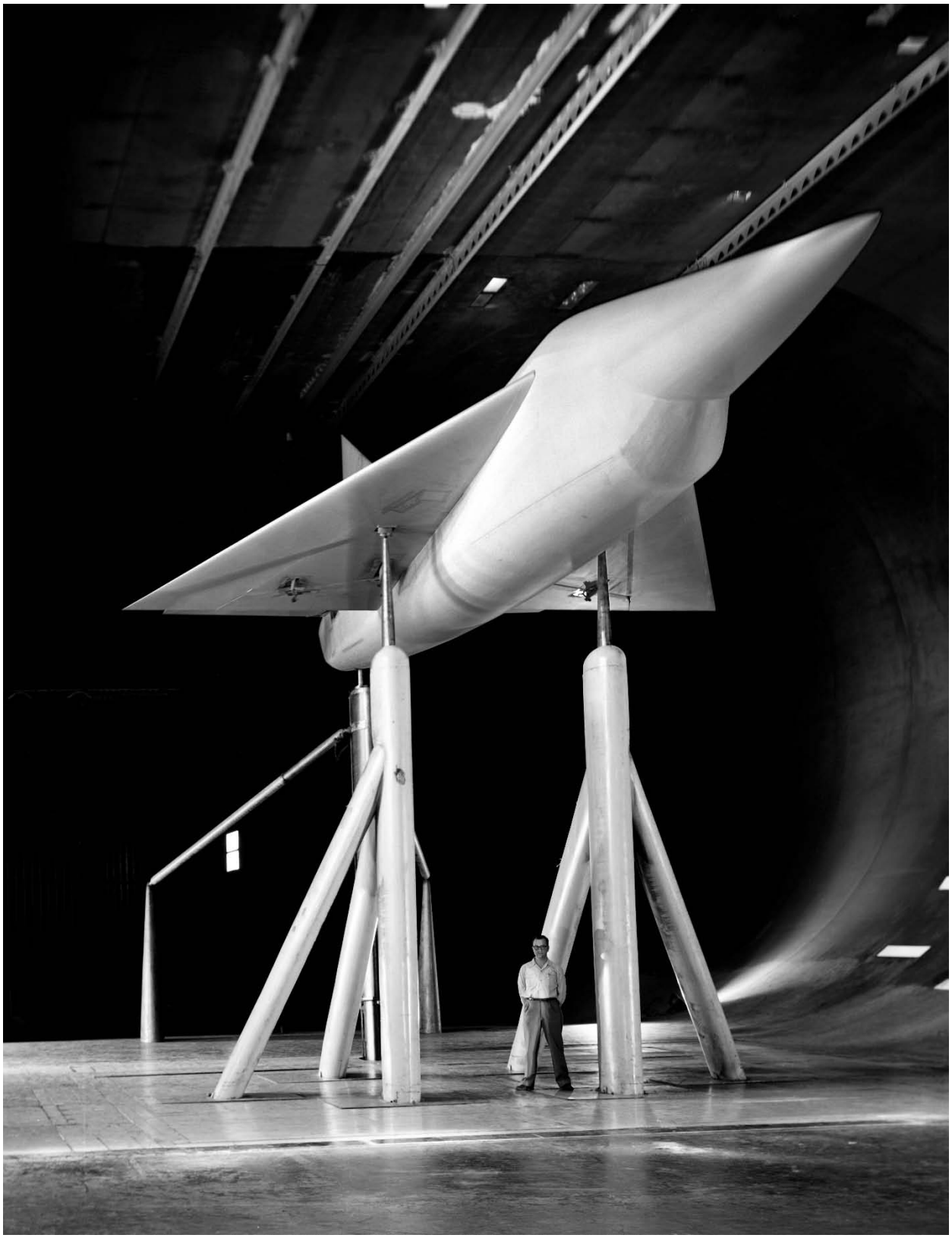

Figure 91. Three-quarter front view of model with an aspect-ratio-2 variable-incidence triangular wing on the fuselage with a vertical tail. Engineer William T. Evans in photo. ***(NACA A-17102)***

Boundary Layer Control (BLC)

The boundary layer flow is the airflow very close to aerodynamic surfaces such as wings, flaps, tail, and fuselage. The boundary layer is typically thin (a fraction of the wing chord for wings, for example) and is the area where the relative airflow velocity is slowing down to zero at the surface from the free-stream velocity. (In the wind tunnel, the velocity at the model surfaces would be zero; for an airplane in flight, the airflow next to the aerodynamic surface would be at the same velocity as the aerodynamic surface such as the wing.) The boundary layer thickness is a function of viscosity, surface roughness, geometry, and Reynolds number, and was first explored during aerodynamic research shortly after the Wright brothers' invention of the airplane. The character of the boundary layer flow determines when the flow on a wing surface will separate and cause a decrease in lift and an increase in drag. Interest in controlling and energizing the boundary layer became important to try to delay separation of the flow on wings and flaps to increase maximum wing lift. Increasing lift would allow landing and takeoff airspeeds to be reduced. Controlling separation could also reduce the variation in pitching moment and control requirements. Wing boundary layer control (BLC) became practical with the use of jet engines because of the high-energy airflow available from the jet-engine compressors. High-energy flow could be blown over the wing and/or the wing high-lift systems, such as wing leading-edge slats or trailing-edge flaps, to energize the boundary layer flow over these surfaces. Alternatively, suction BLC could also be used to remove the low-energy boundary layer flow to achieve a similar result. Early on it was thought that utilizing suction to remove the low-energy boundary layer air would require less energy than utilizing blowing to energize the boundary layer. Later, after many experiments, researchers found that suction was limited in its capacity to remove low-energy air in the boundary layer.

Many configurations were studied in the tunnel; both blowing and suction experiments were done. In the wind tunnel, blowers powered by electric motors were often installed in unpowered models to produce high-energy airflow to simulate the effects of using jet-engine compressor bleed air. Suction could also be produced by using blowers with their intakes connected below aerodynamic surfaces that were composed of some sort of porous material that would allow suction air to pass. The goal was to develop the most efficient and cost-effective means of BLC to increase wing lift.

Large-scale model investigations. The effects of suction BLC on the longitudinal characteristics of a 45-degree swept-forward-wing and fuselage model were investigated [119]. In addition to longitudinal characteristics, wing surface pressures were obtained to determine wing-loading distributions. The experiments were based on results of previous experiments that guided the suction locations. Suction was applied to the fuselage as well as the wings. The model is shown in Figure 92 (Test 22). With suction applied, airflow separation on the wing was delayed and longitudinal characteristics improved with increasing angle of attack. The aerodynamic pressure-center variation (therefore pitching-moment variation) with angle of attack was essentially eliminated until close to the maximum lift coefficient. Drag was reduced 50 to 60 percent.

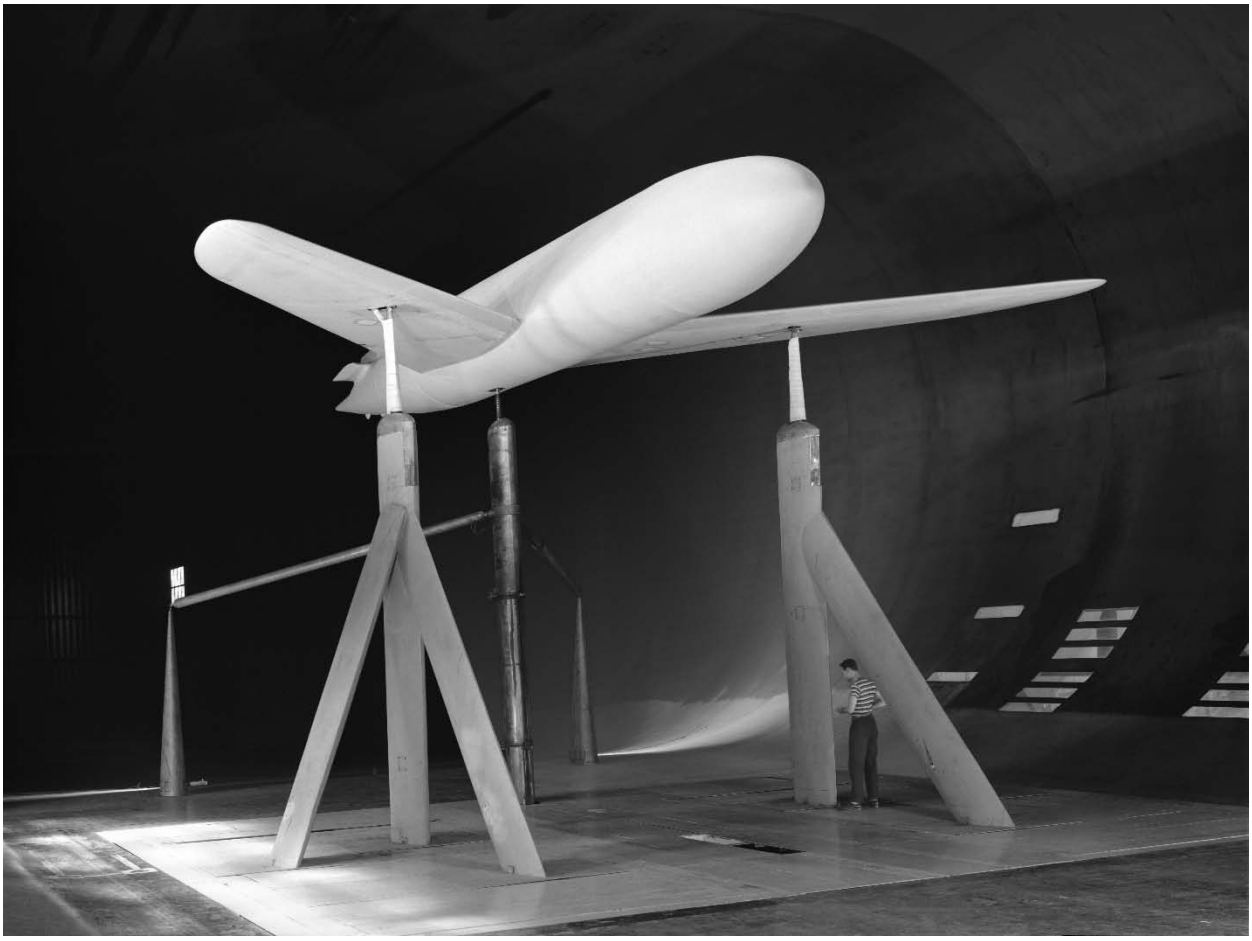

Figure 92. Three-quarter front view of a 45-degree swept-forward-wing model with suction BLC.
(NACA A-13064)

The use of area suction to delay separation of the airflow at the leading edge of a 63-degree swept-back wing was also studied. Substantial improvements in lift were achieved [120, 121] (Tests 27, 40). Suction through streamwise slots in the outboard portion of the wing was also studied. This represented a simplified version of BLC but was still successful in significantly increasing the maximum lift of the wing. Additional experiments were performed to improve the efficiency of the suction [122].

Experiments were performed with area suction on the constant-chord trailing-edge flaps of a delta-wing model [123]. It was found that with small amounts of suction applied near the leading edge of the flap, high lift at relatively low attitudes could be achieved. The purpose was to eliminate the necessity of going to extremely high angles of attack to attain the high-lift coefficients required at landing and takeoff conditions. Suction applied near the leading edge of the flaps was effective in doing that.

North American F-86 Sabrejet fighter with BLC. Many experiments were done on F-86 models and aircraft using BLC to increase lift. The wing was swept back 35 degrees. Since the F-86 was jet powered, the jet-engine compressor was a ready source of compressed air for BLC, especially with engine operation during landing and takeoff. However, before experiments were done on the airplane, experiments were done on a full-scale model with a 35-degree swept wing with an air compressor mounted inside the model to supply air for BLC (Fig. 93). Suction BLC improved the effectiveness of trailing-edge flaps and was effective in delaying separation of airflow from the leading edge of the wing. The investigation results were very favorable [124, 125].

Figure 93. Model for investigation of BLC on a 35-degree swept wing. ***(NACA A-17275)***

After the favorable model experiments, many tests were done on F-86 airplanes in the wind tunnel. Reference [126] gives results of high-velocity blowing over the trailing-edge flaps of the F-86. Blowing over the deflected trailing-edge flaps produced large flap-lift increments. It was found that the amount of air required to prevent flow separation on the flaps was significantly less than that estimated from published 2D data. In addition, it was found that the increased lift was relatively insensitive to the location of the flap BLC nozzle. It was also concluded that installation of this system on an F-86 airplane was feasible and a desirable modification.

In addition to high-velocity blowing over the flaps, area suction near the leading edge of the wing was investigated [127]. This investigation was performed first with the 35-degree swept-wing model in the wind tunnel and then with the operational F-86F airplane that was modified in accord with the wind tunnel model. Wind tunnel and flight-tests indicated that the maximum lift coefficient was increased by more than 50 percent with the use of area suction. Good agreement was obtained between wind tunnel and flight-test results [127].

Additional experiments were done on the F-86D airplane with high-velocity blowing over the trailing-edge flaps [128]. Longitudinal and lateral stability and control results were obtained. It was found that blowing over the deflected flaps increased the average downwash angle at the horizontal tail, however the horizontal tail was not near stall at trim conditions of interest during takeoff and landing conditions; therefore, it was judged not to be a major problem. There was an increase in directional stability with blowing over the flaps. Additional experiments were also performed on lateral control devices. Experiments for blowing-type BLC applied to the trailing-edge flaps are described in reference [129], and experiments of area-suction BLC also applied to the trailing-edge flaps are described in reference [130].

The F-86 was a very successful fighter aircraft and was used for many years. It was modified numerous times and used for a variety of roles by the military. As mentioned earlier, it was treated as a generic jet-powered airplane for many years of wind tunnel and flight experiments.

North American YF-93A. The North American YF-93A was developed from the F-86 and was originally designated the F-86C. It was somewhat bigger than the F-86, and had side-mounted inlets for the jet engine instead of a nose inlet. It was wider to accommodate a larger engine, and had a longer range and greater load carrying capability than the F-86.

Wind tunnel tests of blowing BLC with jet pressure ratios up to 9.5 on the trailing-edge flaps of the F-93A airplane were performed [131]. Pressure ratios were varied. It was found that good correlation could be obtained by using either high mass flows and low jet velocities or low mass flows and high jet velocities as long as the momentum of the air jet was not changed. This was of considerable practical importance. It indicated that the flow and pressure ratio requirements of a blowing BLC system could be satisfied by a wide variety of airplane jet engines, and in addition, the amount of wind tunnel testing could be considerably reduced and simplified.

Preliminary circulation control investigation. The use of circulation control to increase the lift of a 45-degree swept-back-wing model by suction through trailing-edge slots was investigated [132] (Test 76). Increasing circulation of the air about an airfoil could potentially increase the lift of an airfoil or wing without increasing the airfoil angle of attack. Suction was also applied at the leading edge of the wing to prevent leading-edge separation at increasing angles of attack. It was found that considerable increases in lift could be achieved with circulation control. The study was very preliminary and was mainly conducted to determine the feasibility of the circulation

control method of increasing lift on swept-back wings. Results were correlated with 2D model results and reasonable correlation was found. Apparently, even though circulation control was found to be very effective, it did not hold significant advantages over simpler BLC systems and was not employed in production aircraft.

Variable flap spans. Experiments were performed in the 40- by 80-Foot Wind Tunnel using area suction to increase the effectiveness of trailing-edge flaps of various spans on a wing with 45 degrees of sweepback and an aspect ratio of 6 (Test 84). The results defined the effectiveness of flap area suction for a range of conditions to help complete the aerodynamic characteristics database. Area-suction flaps achieved the flap lift increments predicted by inviscid-flow theory for the smaller flap deflections and shorter flap spans, however at greater flap spans and deflections, the lift increments were somewhat lower than predicted because of local flow separation. Limited tests were made with area suction applied to the leading edge of the wing [133].

Supersonic fighter model. Small-scale high-speed studies had been performed on models of supersonic fighters that employed thin, straight wings of low aspect ratio. As pointed out, sufficient lift at landing and takeoff conditions was an important and critical issue for high-speed aircraft. In view of this, studies of a large-scale model representing a fighter with a thin (4.2-percent wing-chord maximum thickness) straight wing with an aspect ratio of 3 were performed in the 40- by 80-Foot Wind Tunnel to study improvements in low-speed lift due to BLC (Test 89). Experiments with suction on leading- and trailing-edge flaps were performed [134]. Substantial gains in lift were achieved. This was an effective method of substantially increasing the lift of the small, thin wings of supersonic fighters to reduce landing and takeoff airspeeds to acceptable or manageable levels.

Suction requirements. Experiments were performed on a 44-degree swept-wing model with area suction applied to the leading- and trailing-edge flaps [135]. The aspect ratio was 3.74 and the wing taper ratio was 0.4. The purpose of the experiments was to determine the effects on the longitudinal characteristics of BLC and to determine the suction requirements for the flaps. The use of area suction at the knees of the leading- and trailing-edge flaps was very effective with the flaps deflected; it essentially doubled the maximum lift coefficient.

BLC on models of the McDonnell Douglas F-4 Phantom. A series of experiments were conducted on F-4 models to develop the BLC system for the aircraft [136-138] (Tests 97, 97B, and 104). The models used two different fuselages, but the wing planforms (and the drooped horizontal tail) were the same. The wing had a 45-degree sweep and an aspect ratio of 2.8. Initially the model had a straight horizontal tail, but it was found that drooping the tail reduced the adverse pitching-moment variations in the medium- to high-lift range. Reference [136] describes the results with area suction applied to trailing-edge flaps and with several wing leading-edge modifications. It was found that area suction was effective in increasing flap lift to within 90 percent of theoretical values. However, it was also found that the lift advantage of the flap installation was greatly penalized at high angles of attack by leading-edge flow separation. Some leading-edge devices delayed leading-edge separation, allowing higher lift coefficients to be achieved [136]. Additional experiments were performed on the same model by improving the wing leading-edge lift capability in order to increase the total lift of the wing [137]. Area suction was employed to the leading-edge flaps as well as other modifications. Substantial improvements in lift coefficient were achieved.

Figure 94. Follow-on experiments of F-4 model wing with flaps and BLC but with a different fuselage. Empennage with drooped horizontal tail; flaps and slats down. Engineer Leo Hall in photo. ***(NACA A-22148)***

Follow-on experiments were done on an F-4 model with the same wing and horizontal tail but with a different model fuselage and blowing BLC (Fig. 94) [138]. The second fuselage model used a fuselage with a nose inlet as opposed to the two inlets on the fuselage sides, which resembled the actual F-4 inlets. High-velocity blowing was employed over the leading- and

trailing-edge flaps. The effects of several variables were studied. It was found that leading-edge blowing BLC significantly increased maximum lift and improved stability near maximum lift. Lift and stability generally were sensitive to spanwise variations of leading-edge flap deflection and the extent of blowing BLC. Comparisons with the results from the model with the same wing and area-suction BLC showed blowing-type BLC produced larger lift increments with approximately the same airflow. The trailing-edge flaps caused a relatively small gain in maximum, usable lift when compared to the leading-edge flaps.

The F-4 Phantom was a popular airplane and many were built. It was used for many years by the Navy, Air Force, and Marines, as well as several other countries.

Lockheed T-33 airplane model. The T-33 model was investigated to determine the effectiveness of area suction to increase the lift of a moderately thick (maximum thickness of 13 percent of wing chord) straight wing that encountered flow separation near the trailing edge, as opposed to separation near the leading edge that typically occurred on thinner wings. It had been demonstrated that area suction could improve the maximum lift coefficient of thin wings that are susceptible to leading-edge flow separation, but the question became whether area suction could be effective for thick, straight wings that normally experience trailing-edge separation rather than leading-edge separation at high angles of attack. The model was unpowered and did not have a tail (Fig. 95, Test 91). To power the suction airflow in the model, a compressor driven by a variable-speed electric motor was installed. The wing had a partial-span trailing-edge flap and a full-span leading-edge flap, both with porous areas and suction at the knee of the flaps. The maximum lift coefficient was increased substantially using area suction [139].

The Lockheed T-33 was a two-seat trainer with a single jet engine. It was adopted as the standard jet trainer for the Air Force and remained in construction for 10 years. It was a very successful airplane.

Douglas A3D airplane. Wind tunnel studies of the static-longitudinal characteristics at low speeds of a Douglas A3D airplane were performed in the 40- by 80-Foot Wind Tunnel (Fig. 96, Test 96C). The purpose was to study the effects of both suction and blowing BLC on the trailing-edge flaps and leading-edge slats. The A3D was the largest and heaviest airplane designed for operation from an aircraft carrier. It was an attack bomber with twin turbojets and 36-degree swept wings with a 72.5-foot wingspan. This was a big airplane for the wind tunnel, however the investigation was successful. It was found that BLC increased lift enough to reduce the takeoff and landing airspeeds adequately to allow aircraft-carrier operations [140, 141]. The A3D and its variants were used for many years for a variety of roles by the Navy.

BLC on a model of the North American F-100 Super Sabre. Blowing BLC was investigated on a full-scale model of the F-100 fighter aircraft (Test 108). BLC on both the leading- and trailing-edge flaps was investigated. The F-100 was a 45-degree swept-wing aircraft with an engine inlet in the fuselage nose, and it was the first Air Force fighter capable of supersonic speeds in level flight. The principal purpose of the test was to determine the effects of leading-edge flap deflection and BLC on maximum lift and longitudinal stability. Leading-edge flap deflection alone was sufficient to maintain static longitudinal stability without trailing-edge flaps. However, leading-edge flap blowing was required to maintain longitudinal stability by delaying leading-edge flow separation when trailing-edge flaps were deflected either with or without blowing. These preliminary studies were used to define aerodynamic characteristics

prior to planned flight-tests of the F-100 airplane [142]. Several variants of the F-100 were used by the Air Force for many years.

Figure 95. Three-quarter front view of a Lockheed T-33 airplane in the tunnel with BLC on wing.
(NACA A-19841)

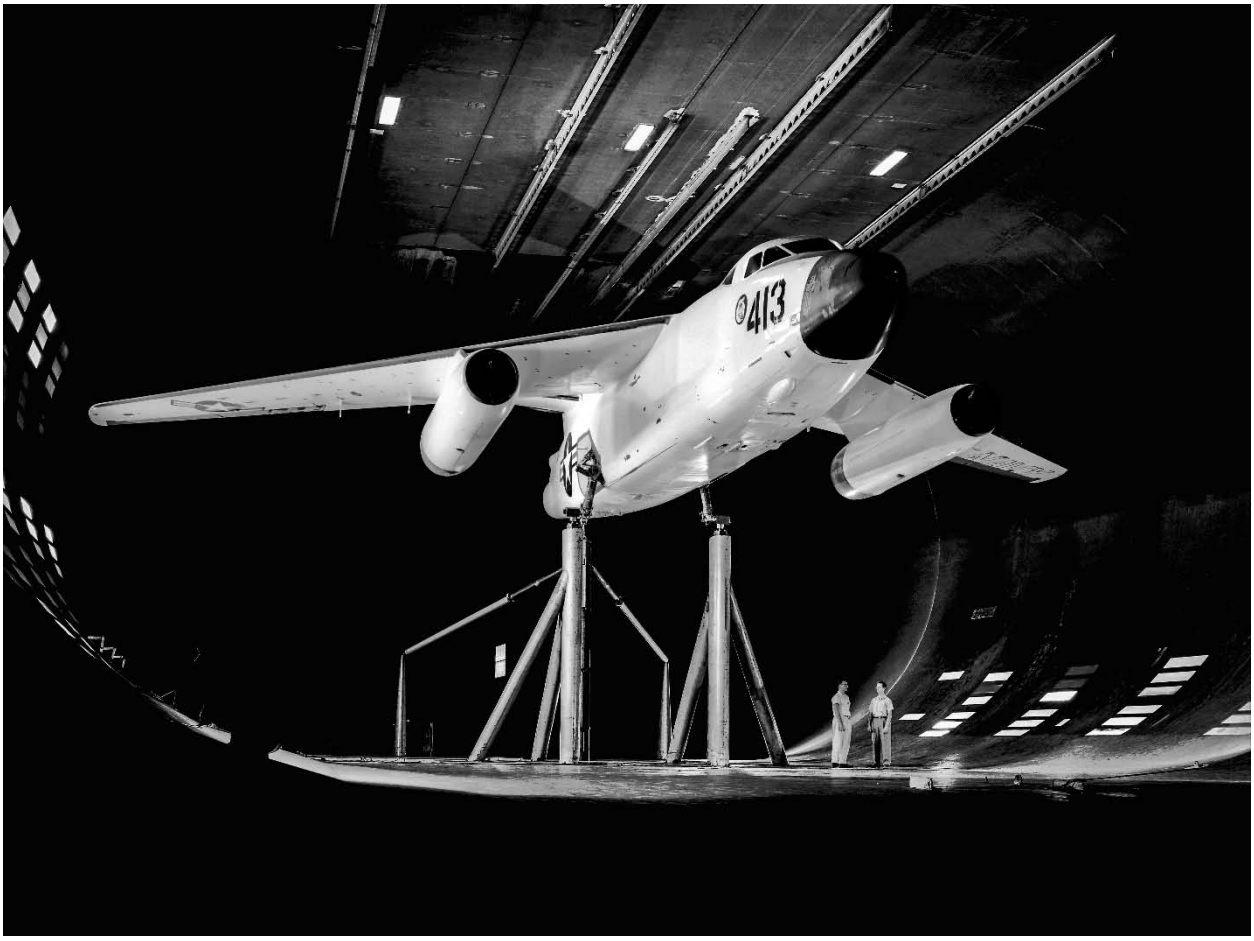

Figure 96. Douglas A3D attack bomber (one of the largest airplanes tested in the tunnel) with BLC on wing. ***(NACA A-20573)***

BLC on the Lockheed F-104 Starfighter. The F-104 fighter was designed to be a high-performance interceptor; it had a very small, thin straight wing with a wingspan of only 22 feet and a wing area of only 195.9 square feet. The maximum wing thickness was only 3.6 percent of the wing chord. The maximum wing loading (airplane weight divided by wing area) was close to 150 psf, which is high. It had a maximum speed of 2.2 Mach number and a high landing speed because of the small wing. Because of the high landing speed, investigations were performed in the 40- by 80-Foot Wind Tunnel to develop blowing BLC on the flaps in order to increase lift and reduce the landing and takeoff airspeeds (Fig. 97, Test 123). The experiments with BLC were successful in increasing lift and reducing landing and takeoff airspeeds to manageable levels—about the same levels as those of typical subsonic jet fighters. The necessity for engine operation required the pilot to eject if the engine failed. The F-104 was used for many years and by several countries.

High-Lift Wing Systems Without BLC

As aircraft cruise speeds increased, it became important to improve the lift at landing and takeoff speeds without having to rely on BLC for many aircraft. The concerns with BLC were its complexity, reliability, and potential for failure. It was often desirable to improve lift without

BLC in the event of engine failure and consequent loss of BLC on landing and takeoff. As pointed out, smaller wings reduce drag at higher speeds, but large wings with more lift are required for landing at lower airspeeds. Flap systems are an excellent method to help meet low-speed requirements for airplanes with small wings. Flaps are retracted for cruise and extended for landing and takeoff. It is important to design the flap systems for minimum drag when retracted and high lift when extended. Many basic studies were performed on different flap systems.

Swept-wing fighter model. Various studies were performed on high-lift devices for swept-wing aircraft models that did not employ any form of BLC (Fig. 98, Test 77). Studies were performed on a fighter model in the tunnel that had a 45-degree swept wing with a 3.5 aspect ratio. The purpose was to design the wing so that stalled flow would be delayed until the maximum lift coefficient was achieved. The airplane was intended to have a landing speed as low as 120 mph at an angle of attack of 14 degrees and a wing loading (airplane weight divided by wing area) of 50 psf. A wing lift coefficient of 1.4 was required to satisfy these conditions. Airfoil modifications, slats, and trailing-edge flaps were investigated. The experiments were successful and demonstrated that the design goals could be met and existing theoretical approaches were satisfactory [143].

Figure 97. Lockheed F-104 Starfighter with BLC on wing. ***(NACA A-24097)***

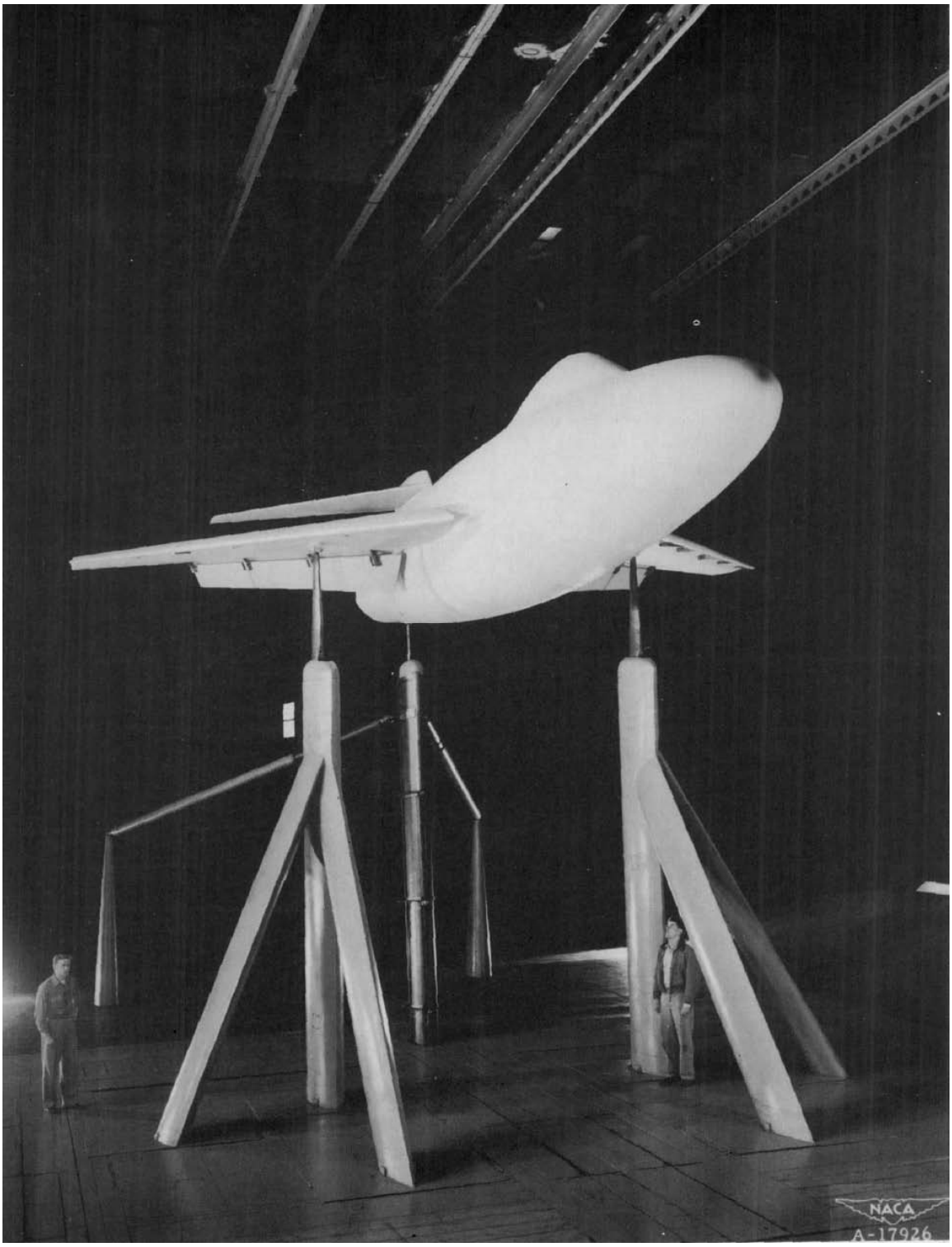

Figure 98. Model for investigation of high-lift devices for swept-wing aircraft. ***(NACA A-17926)***

Jet transport model. Experiments with a generic four-jet transport model were performed with various wing leading- and trailing-edge high-lift devices to increase lift at landing and takeoff conditions. The model had a 35-degree swept wing with an aspect ratio of 7 and four pylon-mounted nacelles (Test 119). Several wing leading-edge configurations were studied in conjunction with double-slotted trailing-edge flaps. Reference [144] describes the increase in lift possible. Airplane designers judged that it was important for commercial transport aircraft to have good lift capabilities without requiring some sort of BLC. Commercial aircraft are typically not designed to be dependent on BLC for landing and takeoff because of the possibility of engine failure; the loss of the bleed air (from the failed jet engines) used for BLC results in loss of wing lift during landing and takeoff.

Thin-Wing Airfoil Studies

Thin wings are desirable for high-speed aircraft to minimize drag at high speeds, but generally thicker wings are more effective at producing high lift at lower landing and takeoff airspeeds. Thin wings tend to stall sooner than thicker wings because of flow separation from the thin leading-edge of the wing. As a result, airfoil development was undertaken. An approach that was extensively studied was to thicken the wing near the leading edge, producing what was termed "a bulbous nose." Both theoretical studies and experiments were performed to develop airfoils that had low drag at high speeds and high lift at low speeds. These airfoils tended to be thin but had more camber or curvature and modified thickness distributions at or near the leading edge. The modifications were well forward of the wing's maximum-thickness station. Flow separation is affected by scale or Reynolds number, so large-scale studies were very important when determining the onset of flow separation.

Since it was important to not compromise supersonic performance with wing modifications, studies were performed at both subsonic and supersonic airspeeds to ensure good performance at both conditions. Several studies were performed at low speeds in the 40- by 80-Foot Wind Tunnel on configurations that had low drag at supersonic speeds during high-speed wind tunnel experiments [145-147]. A representative large-scale interceptor-type configuration model was tested in the wind tunnel. It had a thin (6-percent chord thickness), 45-degree swept wing with an aspect ratio of 3, and a taper ratio (wingtip chord/wing root chord) of 0.4. Tests of the same configuration had also been performed in high-speed wind tunnels on small-scale models to determine the performance penalties, at cruise conditions, of the airfoil modifications. An excellent summary of the results is presented in reference [147]; the results were very promising and warranted additional research as described in this reference.

Propellers

Flow Surveys

Many flow surveys were performed at potential propeller locations for propeller-powered aircraft to allow for estimation of steady and unsteady propeller loads for propeller design. A few representative studies are described.

Flow surveys were done at the plane of the propeller of a twin-engine airplane, the Grumman XF7F-1 (Fig. 99, Test 31). The purpose of the experiments was to provide flow measurements at the propeller location to enable propeller loads and vibratory stresses to be estimated. It was important to determine the effect of the propeller nacelle and wing, as well as the effect of angle of attack. Measured upwash angles were compared with wing-induced angles calculated by wing lifting-line theory. The effect of the measured flow field on the oscillating aerodynamic loading on a propeller was estimated, and the method used in calculating such loadings was described [148-150]. Vibratory stresses in the propellers are provided in reference [149]. Three- and four-blade steel propellers, about 13 feet in diameter, were used in the studies. It was found that with the known oscillating air load, an accurate prediction of nonresonant, first-order vibratory stresses on propellers could be obtained.

The effects of the propeller nacelle on the flow at the propeller location for the above airplane were studied [150] by performing flow surveys with only the nacelle on the wind tunnel supports (Fig. 100, Test 51). The study allowed separation of the nacelle effects from the effects of the rest of the airplane. The purpose was to allow improvement in the theory for predicting the flow field at a representative propeller location. It was expected that the methods described could be applied to a similar class of airplanes.

The effect of wing sweep on the flow upwash at the propeller planes of multiengine airplanes was investigated [151]. Both straight wings and swept wings were included in the semispan study. It was found that the effects of sweep on the spanwise distribution of upwash were appreciable. Nacelle-axis inclination was found to be a powerful factor in the reduction of the overall upflow angles at the propeller disks. The asymmetry of the upflow distribution for airplanes having swept wings indicated that the propellers would be subjected to higher-order (higher than once per revolution (1/rev)) excitations.

Surveys of the flow fields at the propeller planes of six 40-degree swept-back-wing fuselage-nacelle semispan models were performed [152]. The semispan model with two nacelles is shown in the tunnel in Figure 101 (Tests 46 and 65). The surveys showed that the variations of the flow parameters with angular position are predominantly first-order sinusoidal for the models tested.

Detailed analysis of 1/rev oscillating aerodynamic thrust loads at zero yaw were done for the above models [153]. Analyses for other geometries with multiple nacelles and swept wings were also included.

Figure 99. Flow surveys at the left propeller plane of the Grumman XF7F-1. Vertical flow-measuring rake on top of left nacelle. ***(NACA A-13436)***

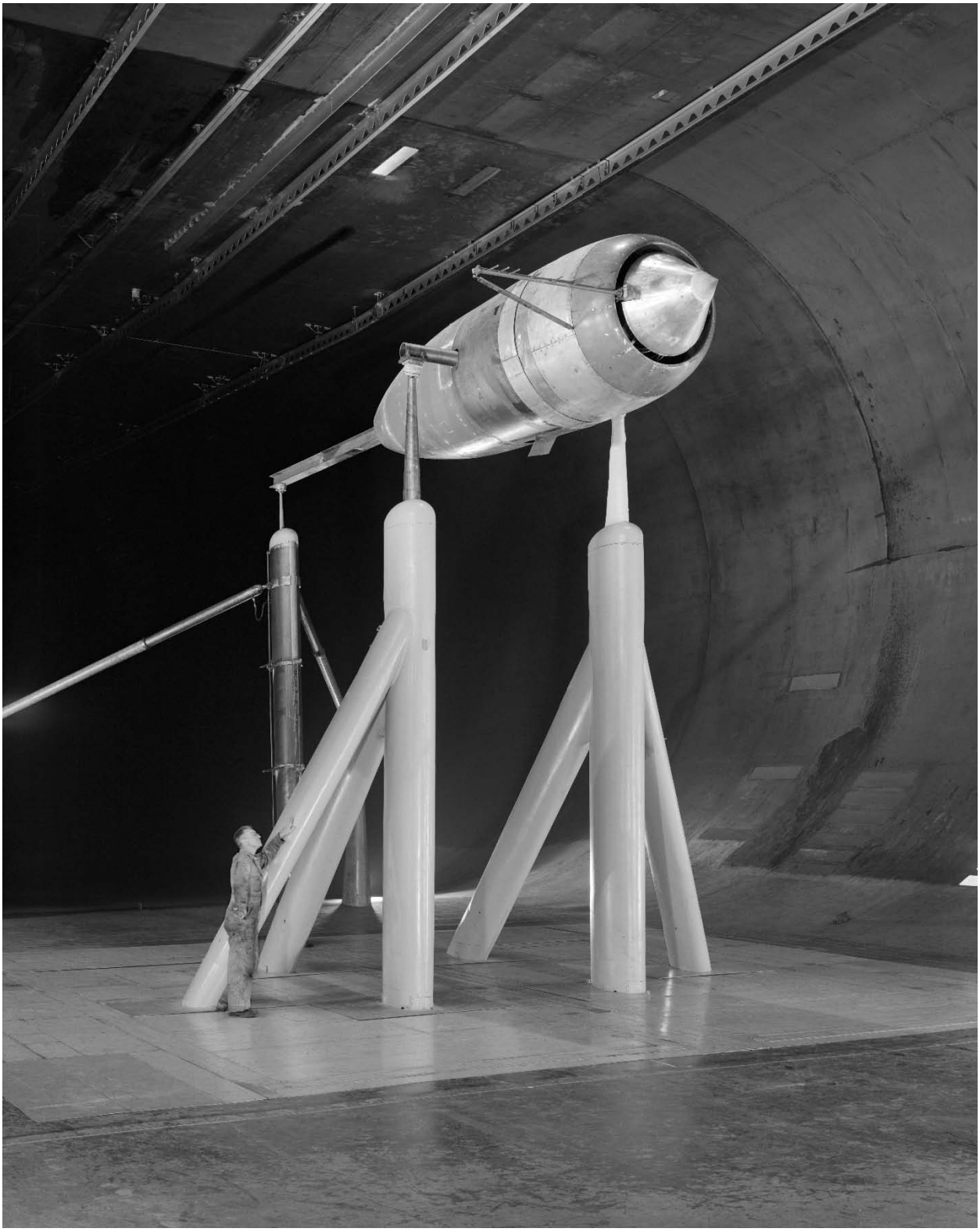

Figure 100. Propeller nacelle used for surveying the flow at the propeller location. Horizontal flow-measuring rake on right side. ***(NACA A-15561)***

Figure 101. Semispan swept-wing model used for flow surveys at propeller locations. Engineer Vern Rogallo in photo. ***(NACA A-16397.1)***

Propeller Decoupler and Controlled-Feathering Device

A YT-56A turboprop engine was investigated with a propeller decoupler and a controlled-feathering device to determine their effectiveness in reducing the high negative thrust (drag) that accompanies a power failure of this type of engine and propeller (Fig. 102, Test 85). It was an automatic system that had a much faster response than a pilot would have using manual control. This sort of device had never been tested in a wind tunnel before. It was a safety system intended to prevent large drag and yaw on the airplane in the event of a power failure. When there is a power failure, torque sensors cause the propeller blades to go to the feather blade angle, which essentially eliminates the drag of the windmilling propeller. (The feather blade angle is a blade angle in which the blades are aligned with the airstream to minimize drag.) In the tunnel, power failures were simulated by shutting the fuel off. It was found that with neither device free to operate, the propeller drag levels after power failures at airspeeds above 150 knots would impose vertical tail loads higher than those allowable for the YC-130, the airplane for which the test equipment was intended. (The YC-130 was a four-turboprop military transport airplane that was used for many years.) The drag levels were reached in about 1 second, which was much faster than manual operation of a decoupler and feathering device by a pilot. With the automatic decoupler and controlled-feathering device, the drag was reduced to very low levels in 1 or 2 seconds. It was determined to be a successful system and very important for safety of flight [154].

The only problem with the use of the decoupler, which mechanically disconnects the propeller from the engine, is that it complicates and slows attempts to air-start the engine while in flight. For an air-start, the propeller would have to be reconnected to the engine and then the blade angle would need to be adjusted in order to attempt a restart.

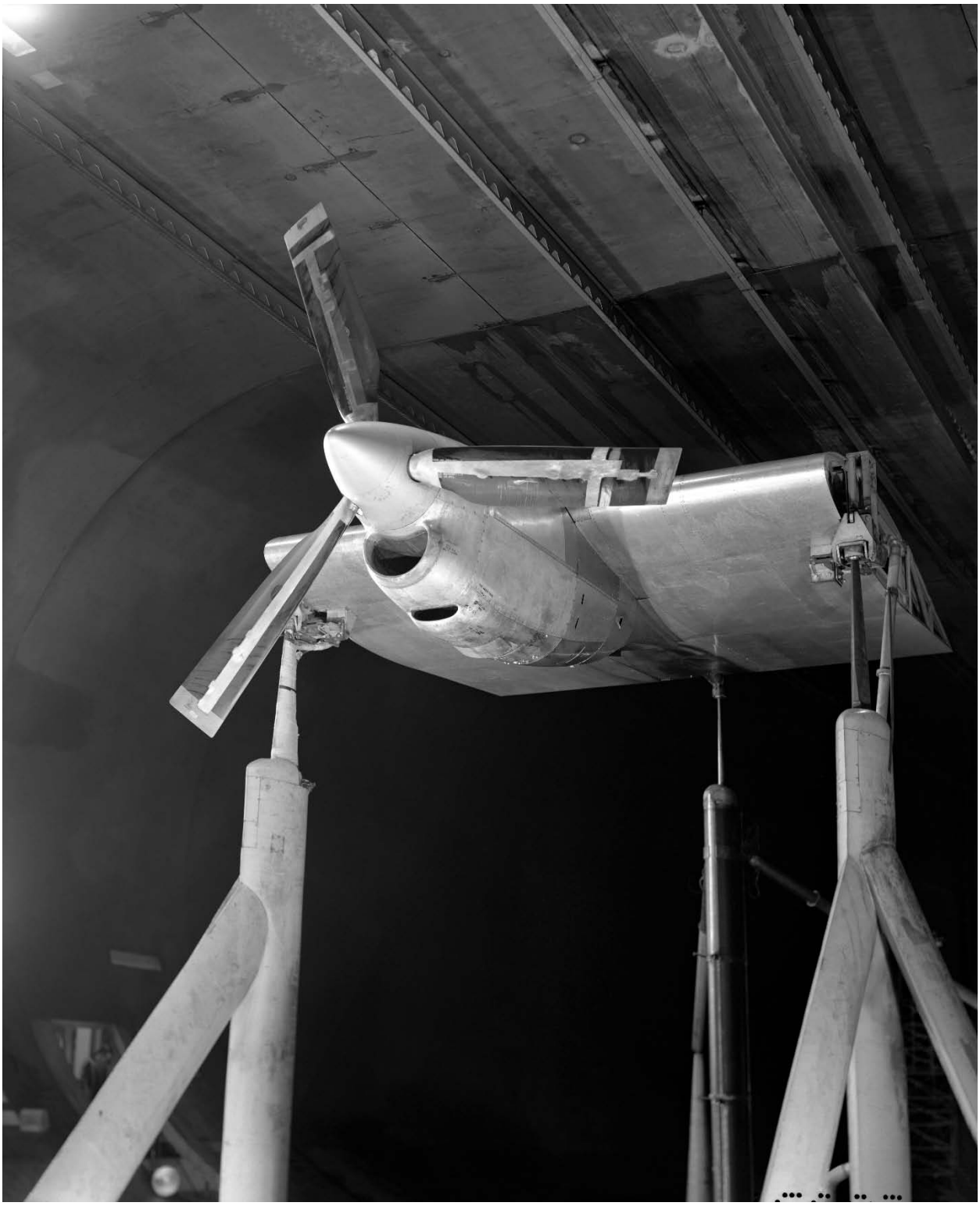

Figure 102. Nacelle with propeller decoupler and controlled-feathering device mounted on partial wing.
(NACA A-18957)

Rotorcraft

McDonnell Aircraft Corporation XV-1 Convertiplane

The XV-1 was a unique experimental compound-aircraft designed for vertical takeoff and landing (VTOL) using a helicopter-type rotor. It used a tip-jet-driven rotor for VTOL and a wing for lift to unload the rotor during cruise. It was driven by a pusher propeller powered by a 550-hp internal combustion engine. During hover and low forward speeds, the same engine drove two compressors that supplied air to the rotor-tip jets. The aircraft used the rotor for takeoff and landing and for forward speeds up to about 80 knots. Transition-flight mode (autogiro mode) was from about 80 knots to about 115 knots forward speed in which the rotor produced the majority of the lift. Airplane-mode flight was at airspeeds greater than 115 knots in which the wing produced most of the lift, and the rotor produced only about 15 percent of the lift.

Two experimental studies were performed in the 40- by 80-Foot Wind Tunnel. The first study involved a full-scale model that had a rotor and a very simple fuselage, and a simple wing but with the required area. This study was used for development of the aircraft rotor system. Small-scale tests had been done, but it was recognized that full-scale development was crucial. The second study was done on the actual aircraft (Figs. 103 and 104, Tests 83 and 88).

The purpose of the second test on the actual aircraft in the 40- by 80-Foot Wind Tunnel was to continue development experiments and to determine the stability and control of the aircraft in autorotative conditions—that is, with no power to the rotor [155]. The experiments were also used to develop the transition strategy from hover to forward flight and vice versa. The aircraft was mounted on the three wind tunnel struts shown in Figure 104. The wind tunnel experiments demonstrated the feasibility of the concept and resulted in many improvements. In addition, drag reduction studies resulted in significant drag reduction and improved cruise performance, because the aircraft's drag was significantly higher than small-scale model data had indicated. The full-scale wind tunnel experiments were considered by McDonnell Aircraft Corporation to be equivalent to many months of flight-testing, with much less risk and expense, and were expected to be a big help in expediting flight-testing, which they subsequently did. This development work was an important use of the tunnel.

Flight-tests were performed, and the aircraft successfully executed transitions from hover to cruise and achieved relatively high speeds. It achieved a top speed of a little more than 200 mph, which was the highest airspeed achieved by any rotorcraft in the U.S. at the time. However, the aircraft was judged to be too complex and noisy by the program sponsors, the Army and Air Force, and the program was cancelled in 1957.

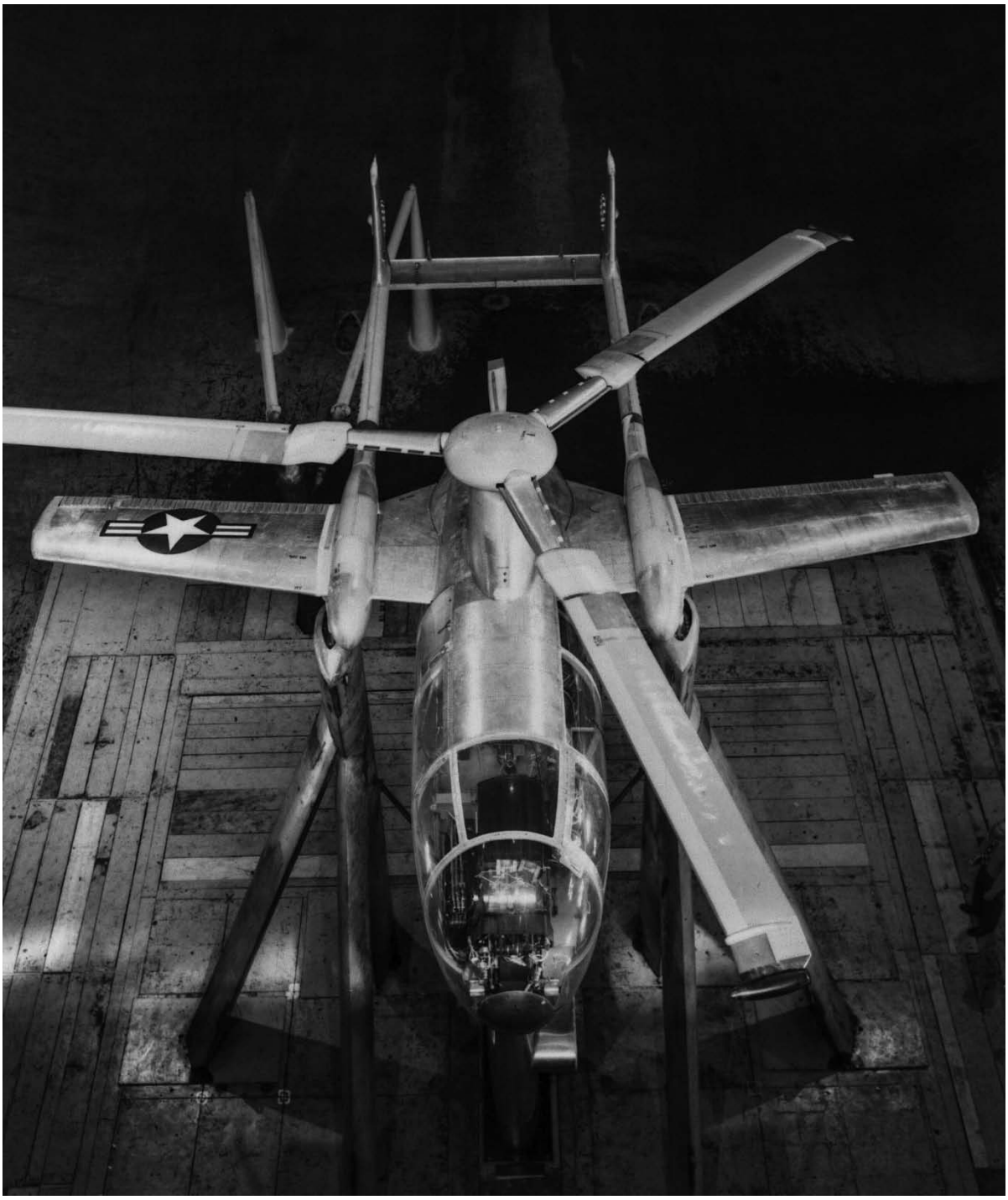

Figure 103. Top front view of the McDonnell Aircraft Corporation XV-1 convertiplane.
(NACA A-19328)

Figure 104. Three-quarter rear view of the XV-1 convertiplane. The small rotors used for yaw control at low forward speeds are shown behind the vertical tails. *(NACA A-19237*)

Rotors With Symmetric and Cambered Airfoils

John McCloud and George McCullough essentially pioneered helicopter research in the 40- by 80-Foot Wind Tunnel. An early, January 1957, test was an investigation of helicopter blades comparing symmetric and cambered airfoil sections. At the time, most helicopter blade sections were symmetrical. Figure 105 shows the 44-foot-diameter three-bladed model in the tunnel (Test 105). The cambered airfoil had a higher maximum lift coefficient than the symmetrical airfoil. The intent was to delay retreating blade stall using the cambered airfoil and to therefore increase the maximum airspeed capability of the helicopter. It was found that the rotor using the cambered airfoil did have increased lifting capacity at a given forward speed. Forward speed capability for a given lift was increased 20 to 25 percent [156]. Nowadays most helicopters use cambered airfoils for the rotor blades.

Rotor Blades With BLC

The configuration described above with the cambered blades was tested with BLC on the rotor blades to further increase lift and forward-speed capability. It was found that blowing from a nozzle near the leading edge of the blades further delayed retreating-blade stall. Results also indicated that delay of retreating-blade stall could be obtained by cyclic blowing with a lower flow rate than that required for continuous blowing. The experiments demonstrated that retreating-blade stall could be delayed significantly by blowing near the blade's leading edge. Blowing applied through a mid-chord nozzle was not found to be effective [157].

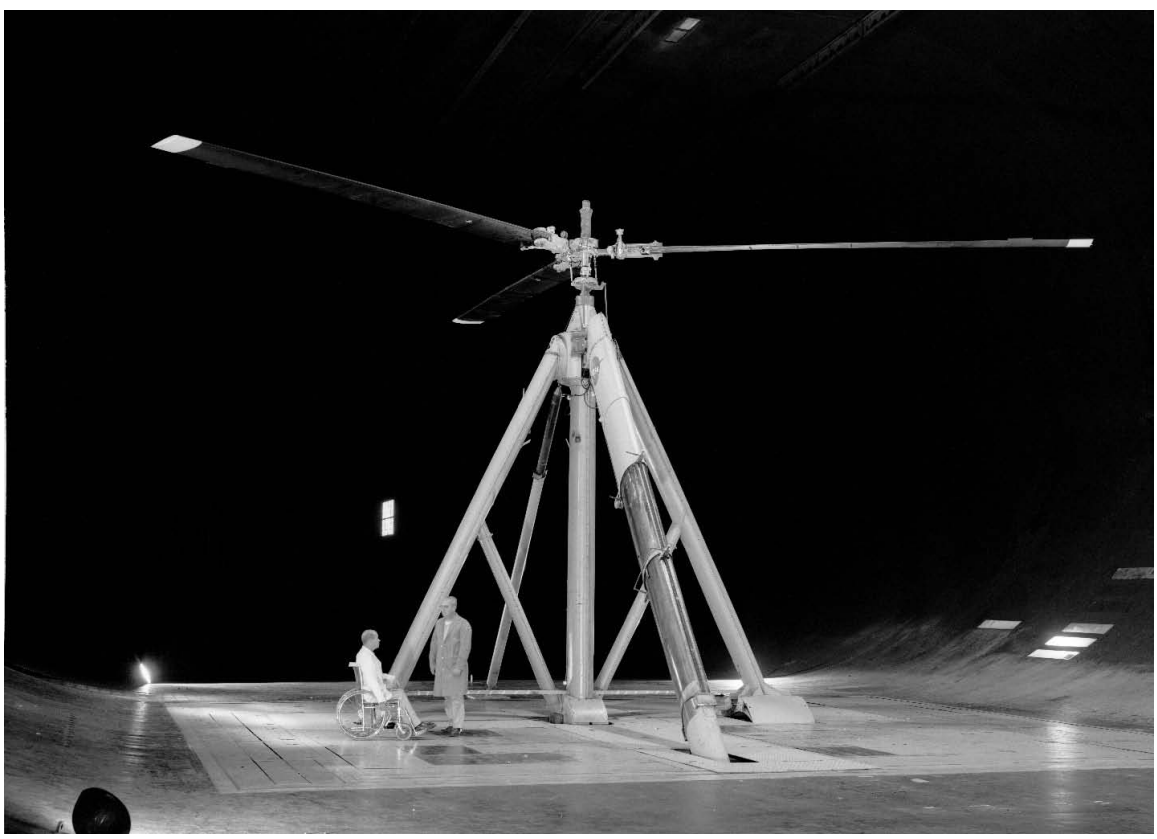

Figure 105. Three-bladed 44-foot-diameter helicopter rotor with John McCloud (in wheelchair) and Marcus Zieger in photo. ***(NACA A-33071)***

Chapter 9. NASA Research, 1958–1980

Overview

Testing emphasis slowly changed during the years after the end of the NACA and the Ames Aeronautical Laboratory's new designation as NASA Ames Research Center. There was a gradual transition over several years in the type of research performed in the 40- by 80-Foot Wind Tunnel. Research on conventional aircraft and rotorcraft continued, but research on supersonic transport (SST) models became important, as well as space-related research such as gliding parachutes for spacecraft recovery, lifting bodies, and a space shuttle model. For many years there was a major interest in V/STOL and powered lift, as well as high-speed rotorcraft, that continues to this day.

Airplanes and Large-Scale Airplane Models

Airplane Flying Qualities and Performance

Despite the shift in emphasis, much research was still performed on conventional airplanes, primarily for the military.

Grumman YAO-1 Mohawk. The Grumman YAO-1, which was the prototype of the Mohawk airplane for the U.S. Army, was tested in the 40- by 80-Foot Wind Tunnel; a drag reduction study was performed to resolve differences between the propeller manufacturer and the airplane manufacturer because the maximum airspeed required had not been achieved. The 48-foot-wingspan airplane had twin turboprops (Fig. 106, Test 152). It had various appendages such as antennas that significantly increased drag and reduced airspeed; the investigation was successful in identifying the various sources of drag. The airplane was intended to be an Army reconnaissance and attack aircraft, designed for battlefield surveillance and light strike capabilities. The aircraft flew for several decades for the Army. It had low stall speed and was capable of short takeoffs and landings on rough airstrips.

North American OV-10 Bronco. The twin turboprop OV-10 was tested in the 40- by 80-Foot Wind Tunnel (Figs. 107 and 108, Tests 271 and 320). The two-seat aircraft was intended to be used by the U.S. Marine Corps as a night observation and attack plane (light armed reconnaissance airplane (LARA)). The unusual empennage allowed a half dozen paratroopers to exit the airplane out of a door at the rear of the fuselage. It had a wingspan of 40 feet with twin turboprops. It was a successful program and many aircraft were built and flown.

General Dynamics F-111B. The DoD, under Secretary Robert McNamara, decided to design and build a supersonic fighter/bomber that would fill the needs of both the U.S. Air Force and the U.S. Navy, however the Navy did not want the aircraft that resulted from this decision. The Air Force designation for the F-111 was the "A" model and for the Navy it was the "B" model. The F-111 was a dual-seat "swing wing" aircraft; that is, it had variable-sweep wings. The Navy was not happy with the handling characteristics and response to control inputs during carrier landing operations. With the wings unswept and full forward for low-speed flight, the wingspan was 76 feet. There was much controversy when it came to decisions concerning the aircraft-carrier suitability of the F-111, and the aircraft was heavy. The number five aircraft off of the pre-production line was a "B" model, and Ames was requested to test its handling characteristics

in the 40- by 80-Foot Wind Tunnel. There were many critics of this test program (and rightfully so) because of the large size of this aircraft in relation to the wind tunnel. Despite this, the test program was approved and test plans initiated. The number five aircraft was flown in to Moffett Field Naval Air Station. The engines were removed to reduce weight, and the aircraft was prepared for testing. It was a challenge to place the aircraft in the tunnel because of its size. When the aircraft was mounted on the wind tunnel struts, there was only 2 feet of clearance from the wingtips to the tunnel walls (Fig. 109, Test 333). The fuselage was so long that a maximum angle of attack of only about 12 degrees could be attained. Wind tunnel boundary corrections were extremely large. The test, however, was very successful and produced unexpected results. Both the A and B models were designed with a very complex wing-leading-edge slat system with multiple motions that would be deployed during low-speed flight to increase lift for landing and takeoff. The system had been developed using small-scale wind tunnel studies. During full-scale studies, it was found that full-scale lift was significantly higher than small-scale lift, and that the slat motion could be significantly simplified, reducing construction costs and maintenance. As a result of the tests, modifications were implemented on the production aircraft [158]. This was a prime example of the great benefits of full-scale wind tunnel testing of actual aircraft.

Figure 106. Three-quarter front view of the Grumman YAO-1 Mohawk. ***(NASA A-28005)***

Figure 107. Three-quarter front view of the North American OV-10 Bronco. ***(NASA AC-41121)***

Figure 108. Three-quarter rear view of the North American OV-10 Bronco showing the unusual empennage that allowed up to six paratroopers to jump from the rear fuselage door. ***(NASA AC-41122)***

Figure 109. Three-quarter front view of the General Dynamics F-111B fighter/bomber with wings unswept and landing gear down—another very large aircraft in the tunnel. ***(NASA A-42117-040)***

The Navy won the battle, and the F-111B never went into production. However, the A model became one of the Air Force's premier fighter-bombers after early flight and structural problems were corrected. It was only very recently retired from inventory.

Navy/Grumman F-14A Tomcat. A 3/4-scale unpowered model of the F-14A was studied in the 40- by 80-Foot Wind Tunnel. The F-14A is a twin-engine airplane with variable wing sweep intended to be carrier based. Because the wingspan of the airplane in the high-lift unswept configuration was 64 feet, a 3/4-scale model was built for the wind tunnel investigation to minimize wind tunnel wall effects. The variable-sweep model was built in the Ames Research Center shops. It was tested in the high-lift configuration; that is, with the wings unswept (Fig. 110, Tests 365 and 370). Both longitudinal [159] and lateral-directional characteristics were obtained [160]. The primary purpose of the test was the determination of lift and stability levels and landing approach attitude required for the airplane in its high-lift configuration. The test angle of attack ranged between –2 and 30 degrees. The model configuration was varied to

determine the effects of wing-leading-edge glove slat, wing slat leading-edge radius, flow ducting for the engines, flap deflections, spoilers for direct-lift control, a horizontal tail, a speed brake, landing gear, and missiles.

The variable-sweep wing has the potential advantage of low sweep and high aspect ratio to aid in meeting low-speed landing and takeoff requirements for aircraft-carrier operations. However, the vortex flows from the highly swept fixed-inboard section of the wing and the projecting sharp-edged nacelle inlets could not be handled by existing low-speed theory, and there were questions about using small-scale wind tunnel test results. Small-scale tests are notoriously poor at accurately indicating stall or maximum lift for full-scale aircraft. Because of these deficiencies, the large-scale F-14 model was built and tested.

Figure 110. Three-quarter front view of the 3/4-scale model of the Grumman F-14A Tomcat variable-wing-sweep fighter with the wings unswept. ***(NASA A70-1376)***

Figure 111. A 3/4-scale model of the McDonnell Douglas F-15 Eagle fighter undergoing construction in the Ames model shop. ***(NASA AC71-5717)***

McDonnell Douglas F-15 Eagle. A 3/4-scale model of the F-15 was investigated in the 40- by 80-Foot Wind Tunnel (Tests 378 and 381). The model was unpowered and had a fixed 45-degree swept wing. The model is shown in the Ames shop during construction in Figure 111. The effects of various configuration changes were studied [161]. Ground-effect experiments were also performed. At the time of the experiments the test was classified Confidential because the F-15 was to be an advanced and dedicated air-superiority fighter with maneuvering capability greater than any existing or foreseeable fighter. The turning capability of the aircraft was to be outstanding, and it had a thrust-to-weight ratio well in excess of 1. This was to be a single-place, dual-engine, all-weather fighter and the most potent fighter aircraft in the Air Force. This was a successful program and hundreds of aircraft were built.

High-Lift Studies

To achieve reasonable and reliable high lift for landing and takeoff, aircraft employ multi-element wings. Trailing-edge flaps and leading-edge slats and flaps are typically deployed for landing and takeoff to increase wing lift. After liftoff or during cruise the devices are retracted to reduce drag; they are only used to increase lift during low speeds because they also increase drag when deployed. Basic theoretical and experimental studies of multi-element wings were performed including the effects of sweep to evaluate the theories used in the 40- by 80-Foot Wind Tunnel. A large-scale (52.5-foot-wingspan), constant chord, 2D model was mounted on the

three wind tunnel struts using a simple frame (Fig. 112, Test 476). For the studies, the model employed a leading-edge slat and a single, trailing-edge slotted flap. In addition to the total forces and moments, surface-pressure distributions were obtained to allow detailed comparisons to be made between theory and experiment. The comparisons indicated reasonable agreement where flow-separation effects were negligible for zero and moderate sweep angles. The studies included comparing the theoretical optimum slat position with the optimum experimental slat position. It was concluded that the agreement was good enough that theoretical predictions had the potential to significantly reduce wind tunnel test time [162, 163].

Boundary Layer Control (BLC) for Transports to Reduce Runway Length

Much work was done in the wind tunnel to increase wing lift and reduce runway length using BLC on transports [164-167]. A variety of configurations were studied.

BLC on a straight wing with an aspect ratio of 10 with two propellers. The BLC consisted of high-energy air blown over the trailing-edge flaps and ailerons. With sufficient BLC to prevent flow separation, flap deflections up to 80 degrees were enabled that substantially increased lift. Lift was also increased with increasing propeller thrust coefficient. The BLC required for attached flow on the flaps was not significantly affected by propeller thrust coefficient, angle of attack, or blowing nozzle size. Details of the investigation are described in references [164] and [165] (Tests 110 and 113).

Figure 112. Two-dimensional wing model with a single-slotted flap and a leading-edge slat used for high-lift studies; Mark Betzina in photo. ***(NASA AC76-0011)***

BLC on a straight wing with an aspect ratio of 10 with four propellers. This model is very similar to the above model but with four propellers instead of two (Fig. 113). Interest in obtaining short takeoff and landing (STOL) performance for transport aircraft led to the wind tunnel experiments of this large-scale propeller-driven transport-type model. The results indicated that the landing and takeoff distances could be more than halved by the use of highly effective flaps with BLC along with large amounts of engine power. At the lowest speeds studied (about 50 knots), adequate longitudinal stability was obtained, but the lateral and directional stability were unsatisfactory. This problem was alleviated by BLC on the control surfaces. Details are provided in reference [166] (Test 118).

BLC on a jet transport with a 35-degree swept wing. An investigation was conducted to determine the effect of trailing-edge flaps with blowing-type BLC and leading-edge slats. The 35-degree swept wing had an aspect ratio of 7. It was found that blowing-type BLC applied to trailing-edge flaps, and used in conjunction with leading-edge slats, could improve takeoff and landing performance substantially. Results are described in reference [167] (Tests 119 and 126).

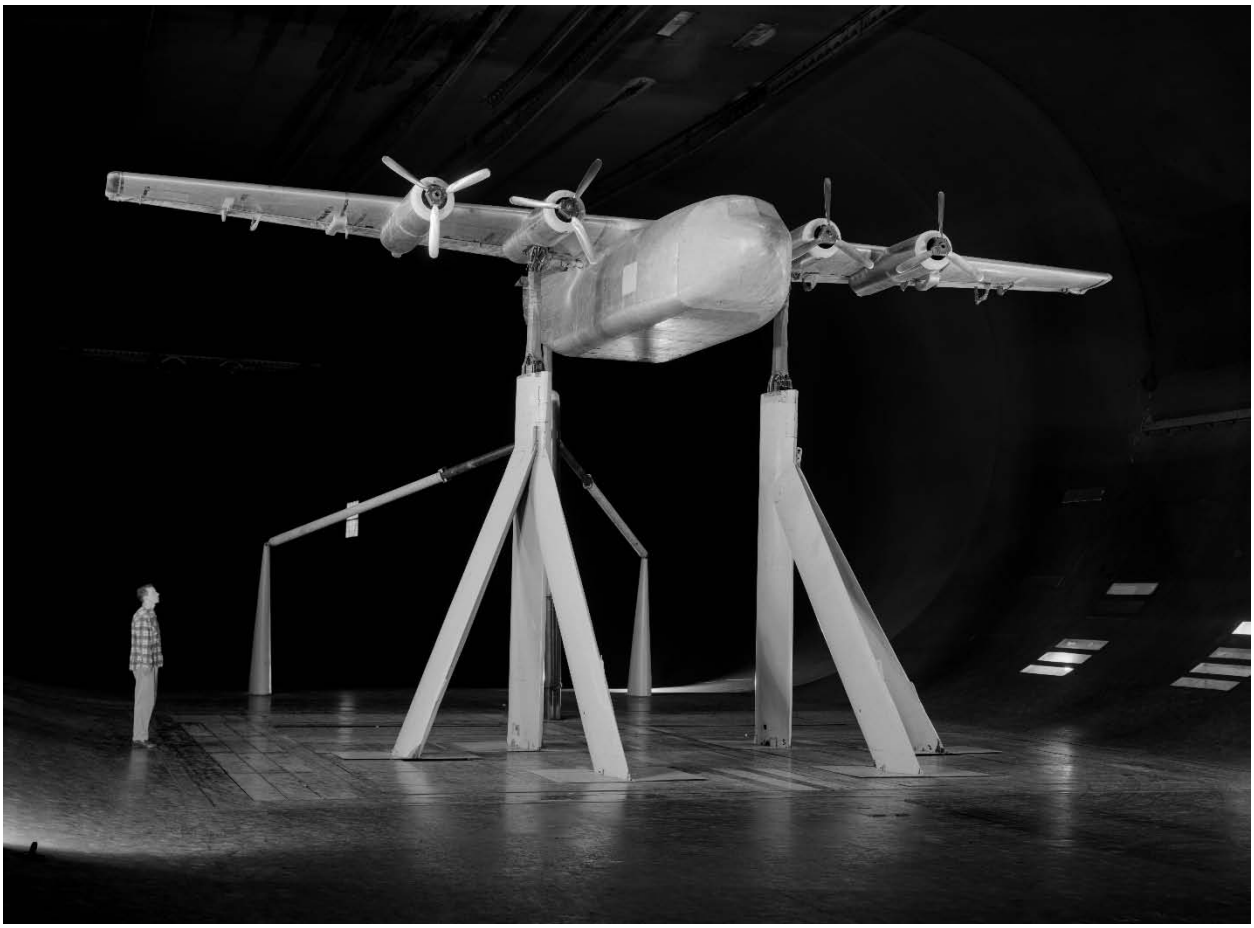

Figure 113. Transport model with a straight, aspect-ratio-10 wing with four propellers and wing BLC; Tom Wills in photo. ***(NASA A-23743)***

Airplane Deep or Post Stall

Aircraft with T-tails are susceptible to a condition in which the aircraft can be trimmed at high angles of attack (30 to 40 degrees, or so) and low speeds after the wing has initially stalled, such that the aircraft would be unable to recover from the condition and suffer catastrophic results. (Tails with the horizontal tail, or elevator, attached at or near the top of the vertical tail are called T-tails.) The aircraft would essentially fly into the ground at trimmed, high angles of attack and low forward speeds. There were several fatal crashes of T-tail aircraft. The condition was caused by the wakes from the stalled wing, and sometimes also from engine nacelles located aft of the wing, substantially reducing the air velocity at the horizontal tails. There would be insufficient pitching-moment control by the elevator for recovery because of the low-velocity air at the elevator caused by the wakes. Experiments were conducted in the 40- by 80-Foot Wind Tunnel to better understand and quantify the problem, and to provide recommendations for design improvements and to identify possible control strategies for recovery [168-170].

Figure 114. Subsonic jet transport model with aft fuselage-mounted engines and a T-tail, used for deep-stall studies. ***(NASA A-36210)***

Generic unpowered model. A generic unpowered model with a thin (4.2-percent-thick) wing and T-tail was studied very early on. The configuration was representative of typical T-tail fighter aircraft. The experiments included flow surveys at tail locations as well as force and moment data. Angles of attack up to 30 degrees were investigated. At high angles of attack, surveys indicated a region of a large wing-wake with low dynamic pressures and rough flow that extended high above the wing-chord plane and further aft. The low-energy flow enveloped the horizontal tail and elevator. As a result, there was a severe loss of longitudinal-control effectiveness at angles of attack that exceeded the angle of attack at which the wing initially stalled. The model was trimmed, but at a high angle of attack at which control effectiveness would be insufficient for the longitudinal control needed for aircraft recovery. Study results are provided in reference [168].

Subsonic transport model. Deep-stall studies of a large-scale model of a subsonic transport with aft engine nacelles and a high T-tail were performed (Fig. 114) [169]. At the time of the research this was a popular configuration for commercial jet transports. The model had a

35-degree swept wing with an aspect ratio of 5.38. The static longitudinal stability and control effectiveness of the model were reduced substantially at angles of attack above that for wing stall. The engine nacelles did not decrease the longitudinal stability and control effectiveness of the model, compared to that without nacelles, for angles of attack up to 30 degrees. At larger angles of attack, the nacelle wakes did reduce the stability of the model.

Business jet. A full-scale business jet airplane (Lear Jet Model 23) with a T-tail was also studied. The aircraft wing had 13 degrees of sweep and an aspect ratio of 5.02 (Figs. 115 and 116, Test 340). The tests were power off. The angle of attack was varied from –2 to 42 degrees. It was found that the aircraft had static longitudinal stability through initial stall. Above initial stall the aircraft had pronounced pitch-up, characteristic of T-tail configurations. A stable trim point was possible at angles of attack between 30 and 40 degrees depending on the center-of-gravity (c.g.) location. Details are provided in reference [170].

Figure 115. Lear Jet Model 23 used for deep-stall studies. ***(NASA A-40938)***

Figure 116. Lear Jet Model 23 at high angle of attack. ***(NASA A-40937)***

Large-scale experiments were important to enable Reynolds number effects to be evaluated, which would allow corrections for the many small-scale experiments that were being performed because of the seriousness of the problem. The small-scale models would have low Reynolds numbers, and as pointed out, conditions for flow separation and wing stall are often very sensitive to Reynolds number. The large-scale experiments were very successful and helped develop flight control strategies as well as clarify airplane design requirements.

It should be mentioned that there have been several cases of catastrophic deep stall of airplanes without T-tails, however they were caused by aircraft failures, pilot error, or both. Failure of the aircraft airspeed indicating system has, at times, been catastrophic because erroneous data were input to the automatic flight control system and airspeed instruments.

Lift-Generated Vortex Wakes

Airplanes produce lift-generated tip-vortex wakes. When aircraft are producing lift, these wakes are caused by airflow going around the wingtips from the relatively high-pressure area under the wing to the low-pressure area above the wing; the flow curls around the wingtip creating a vortex that is shed from the wingtip. Generally, the larger the airplane, the higher the energy in the airplane's tip-vortex wakes. These wakes spread out and can persist for many miles. During certain weather conditions, vortex wakes shed from aircraft can be observed from the ground for many miles. These turbulent wakes can be a serious problem for aircraft that are following too closely, especially small aircraft with low-wing loadings. (Low-wing-loading airplanes are more sensitive to disturbances than high-wing-loading airplanes.) Fatal accidents have occurred when small aircraft have followed large aircraft too closely. Safe distances are prescribed by air traffic controllers, however the data these distances are based on has significant uncertainty. In addition, pilots have some discretion once they are airborne. Airport runway spacing has also been determined because of lift-generated tip-vortex wakes. There are many variables involved, and there have been many experimental studies performed in the 40- by 80-Foot Wind Tunnel supported by theoretical studies.

With the introduction of heavy, jumbo jet aircraft in about 1970—such as the Boeing 747, Lockheed L1011, and Douglas DC-10—there was special concern about high-energy vortex wakes trailing behind such large aircraft encountering smaller, follower aircraft during landing and takeoff. The resulting government regulations for safe operating distances resulted in a limitation on the use of airport runways at a time when the growth of the commercial airline industry required an increasing number of transport aircraft to use the existing runways.

NASA initiated a program that included both flight and wind tunnel research. The objectives were to understand the vortex-wake flow field, to define the safe operating distance behind a vortex-wake-generator aircraft for follower aircraft, and to identify possible modifications to the vortex-generator aircraft that would result in reduced vortex-wake strength. Tests in the 40- by 80-Foot Wind Tunnel were conducted to support this program. This wind tunnel was especially well suited for these tests because of the size of the test section. For example, a 6-foot-span model of the Boeing 747 transport (3 percent scale) could be used with the follower aircraft at a maximum scaled downstream distance of 1/2 mile, which is 81feet in the wind tunnel.

The upset rolling moment was measured in the follower-aircraft models. In addition, both hot-wire anemometry and laser velocimetry were used to perform detailed velocity surveys [171-178].

Follower-wing rolling moment tests. The wind tunnel installation for follower-wing rolling moment tests is shown in Figure 117. Rolling moment measurements were made on follower wings for three wake-producing models: a 747 model (3 percent scale, Fig.118), an idealized swept-wing vortex-generator model (Tests 398, 405, and 413), and a Concorde transport model (6 percent scale, Fig. 119) [171-173]. The follower wings were mounted on an instrument tower (Fig. 119).

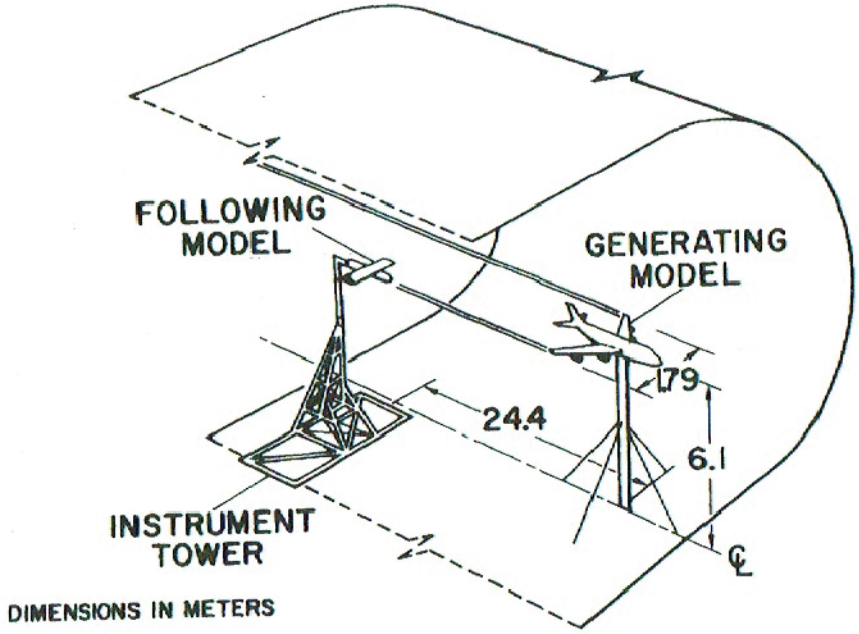

Figure 117. Sketch showing lift-generated-wake model arrangement. ***(Author's collection, F1)***

Figure 118. Vortex-wake testing with a 747 model as a wake generator. ***(NASA AC74-2201)***

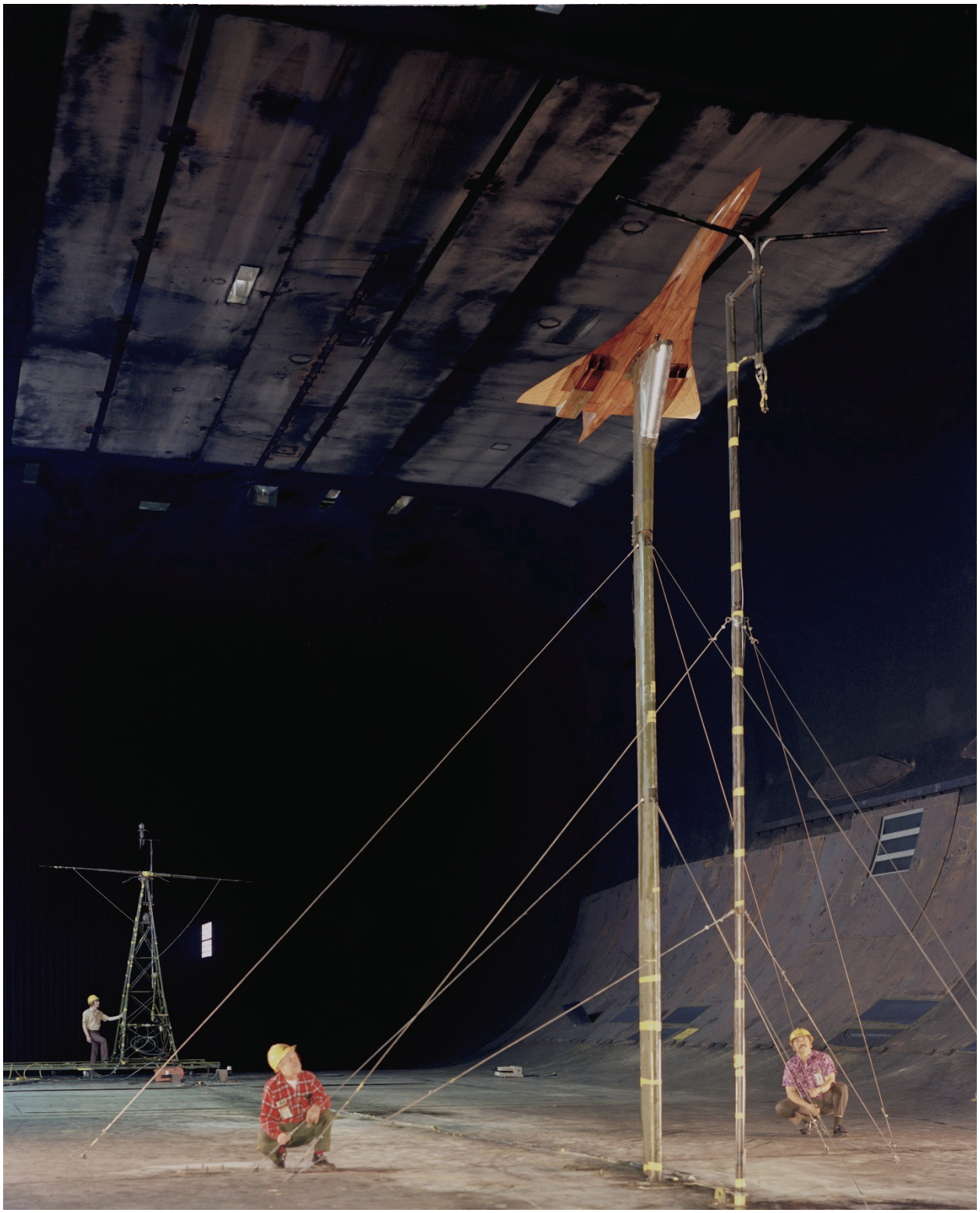

Figure 119. Vortex-wake testing with a Concorde model as a wake generator. ***(NASA AC74-1153)***

Use of hot-wire anemometry and laser velocimetry. A hot-wire probe was used to measure the wake velocities. It was attached to the end of a rotating arm that was mounted on the instrument tower. The rotating arm moved the probe through the vortex flow field, and by moving the tower laterally in increments, passes of the hot-wire probe were made directly through the center of the wingtip vortex [174]. The reason that a rapid-scanning technique was used is that the vortex wakes would meander because of wind tunnel turbulence. It was important to obtain a survey over the complete vortex flow field. Measurements were made at several downstream distances from close to the vortex-wake-generator aircraft to the maximum-measurement station (81 feet).

Detailed velocity surveys of the vortex wake were also accomplished using a laser velocimeter [175]. For these tests, the same 747 aircraft model and the same rectangular follower-wing model that was used in the 40- by 80-Foot Wind Tunnel were installed in the Ames 7- by 10-Foot Wind Tunnel. The downstream measuring location for these wake surveys was 1.5 spans of the model 747 wing.

The rapid-scanning hot-wire anemometer was found to be an effective way of overcoming the natural meander of the trailing-wake vortices in the wind tunnel. The data provided velocity distributions that were in good agreement with theory and the maximum swirl velocities that were measured at various downstream distances in the 40- by 80-Foot Wind Tunnel. The data agreed well with the values found using the laser velocimeter at the short distance used in the 7- by 10-Foot Wind Tunnel. The vortex velocities in the wake of the 747 model were found to be in good agreement with those predicted using vortex-lattice theory on the vortex-generator model along with a wake structure consisting of the superposition of four axisymmetric vortices with finite cores.

Most of the theoretical and experimental work in the tunnel was performed under the leadership of Vernon Rossow over many years (Tests 420, 424, 427, 432).

Modifications to the aircraft creating the vortices have been tried and developed to attenuate the turbulent wakes [176]. The effect of changing the inboard and outboard flap settings to vary the vortices across the wingspan—that is, to change the span-loading distribution—was extensively studied [177]. Experiments using porous spoilers as well as various fins on top of the 747 model were performed [178]. The results were promising and warranted additional experiments.

In principle, the roll control of the following aircraft could be increased, however this is not a practical solution for small aircraft because of the magnitude of the roll control required.

Flight-tests have been performed, but it is very difficult to control the conditions during flight, and flight-testing is more hazardous than wind tunnel testing. Accurate data are harder to obtain during flight-testing, however, it is obviously necessary to perform flight-testing to verify model wind tunnel study results and to verify recommended control strategies and configurations. The goal of the wind tunnel tests is to reduce the number of variables and to reduce the number of possible aircraft improvements. It is much more efficient, safe, and cost-effective to perform these studies in the tunnel whenever possible. The purpose of the flight-tests is to verify the model experiments and to refine the promising results. Comparisons have been made between wind tunnel model test results and flight-test results, and in general, agreement has been reasonably good.

Airport runway spacing has been a major issue, and studies of wake character and decay have been, and will continue to be, very important. If the wakes can be significantly attenuated, runways could be closer together, and landing and takeoff aircraft spacing could be reduced, increasing the use of existing runways.

Thrust Reversers

Thrust reversers are devices that are familiar nowadays to everyone who travels in a commercial airplane. They are mechanical devices at the exhaust of the jet engines that are deployed to reverse the jet-engine thrust at landing touchdown. They cause a large increase in noise. Typically, they are deployed to reduce the braking required to slow down the aircraft. In addition to reversing the thrust at landing touchdown, studies were done to investigate the practicality of using thrust reversers in flight for rapid thrust control because jet engines have slow thrust response. The thrust-reverser effects on the flow at the tail were studied along with the effects on lift and pitching moment.

Many exploratory and development experiments were done in the 40- by 80-Foot Wind Tunnel, which is ideally suited for these types of experiments since actual jet engines can be used. Experiments were performed on single-engine fighter-type aircraft and on various transports. Generally, target-type thrust reversers (essentially two large clamshells that close off the exhaust) and cascade-type thrust reversers (many small vanes that close off the exhaust flow) were studied [179-182].

Thrust reverser on a North American F-100F fighter. A thrust reverser was tested on the F-100F fighter (Fig. 120, Test 129). The F-100F was the last of the century series of fighters. The F version was a lengthened, tandem, two-seat operational trainer and tactical attack aircraft. It was a successful program, but a thrust reverser was apparently never used on the production aircraft.

Thrust reversal on a four-engine jet-transport model in ground effect. Experiments were conducted to study the factors affecting exhaust gas ingestion into the engine inlets when thrust reversal is used during ground roll. As described, the purpose of the thrust reversers is to slow the aircraft down at landing touchdown, which is the typical use for commercial aircraft. As the aircraft is slowed down, there is potential for the engine exhaust gases to be sucked into the engine inlets, which is undesirable. A picture of the model in the wind tunnel is shown in Figure 121 (the thrust reversers are not well shown in this view; Test 135). Both cascade- and target-type reversers were studied. The minimum free-stream velocity at which exhaust gases were ingested in the outboard engines was determined, as well as the increment of drag due to thrust reversal for various modifications of the thrust-reverser configuration. Motion picture films of smoke flow studies were obtained to supplement the data. It was found that the free-stream velocity at which ingestion occurred in the outboard engines could be reduced considerably by simple modifications to the reversers without reducing the effective drag due to reversed thrust. Results are presented in reference [179].

Thrust reversal on a four-engine jet transport with controllable thrust reversers. The same model as described above was studied with controllable target-type thrust reversers. The thrust reversers were designed to provide thrust control ranging from full forward thrust to full reverse thrust. The use of thrust control during landing approach was the primary purpose of the study.

Results were obtained with both leading- and trailing-edge high-lift devices on the wings. It was found that significant improvements in landing-approach performance could be achieved before deterioration of longitudinal characteristics occurred. Details are provided in reference [180].

Safety devices on multiengine aircraft are often used to prevent thrust-reverser operation during flight because of safety considerations. A major concern is sudden and unexpected deployment of a thrust reverser on one side of a multiengine aircraft during flight, which would produce large airplane yawing moments. There are only a few multiengine aircraft that use thrust reversers during flight.

Figure 120. North American F-100F fighter used for thrust-reverser tests; landing gear down and Mark Kelly in photo. ***(NASA A-24788)***

Figure 121. Four-engine jet-transport model used for thrust-reverser experiments. ***(NASA A-25585)***

Delta-wing supersonic transport (SST). Large-scale low-speed studies of a delta-wing SST model with forward or reverse thrust were performed (Fig. 122, Test 187) [181]. The model was tested with various wing trailing-edge flap deflections and various horizontal-tail incidence angles. The temperature of the horizontal tail was measured. It was found that at forward thrust the engine effects on the model were small, however with reverse thrust, the engine effects on the aerodynamic characteristics were significant. Full reverse thrust caused a reduction in

longitudinal stability when the wing trailing-edge flaps were undeflected and a loss in stability when the flaps were deflected to 30 degrees.

Cessna A-37B airplane with experimental thrust reversers. Thrust reversers did not always work for some aircraft. For example, thrust reversers were tried on the Cessna A-37B airplane (Fig. 123, Test 322). The airplane was tested with and without a ground plane. This was a very successful and highly used jet-aircraft trainer with side-by-side seating. The airplane was propelled by two J-85-17A turbojet engines with experimental target-type thrust reversers. It was found that operation of the reversers caused large decreases in longitudinal stability and control, and severe airplane buffeting. In addition, exposure to the exhaust-gas plumes caused failure of the flap and reverser control mechanisms and caused major skin distortion. The thrust-reverser runs were, by necessity, kept very short because of potential damage to the airplane [182]. As a result of the experiments in the wind tunnel, thrust reversers were not used on the A-37 aircraft.

Figure 122. Delta-wing SST model used for thrust-reverser experiments; Tom Wills in photo.
(NASA A-31004)

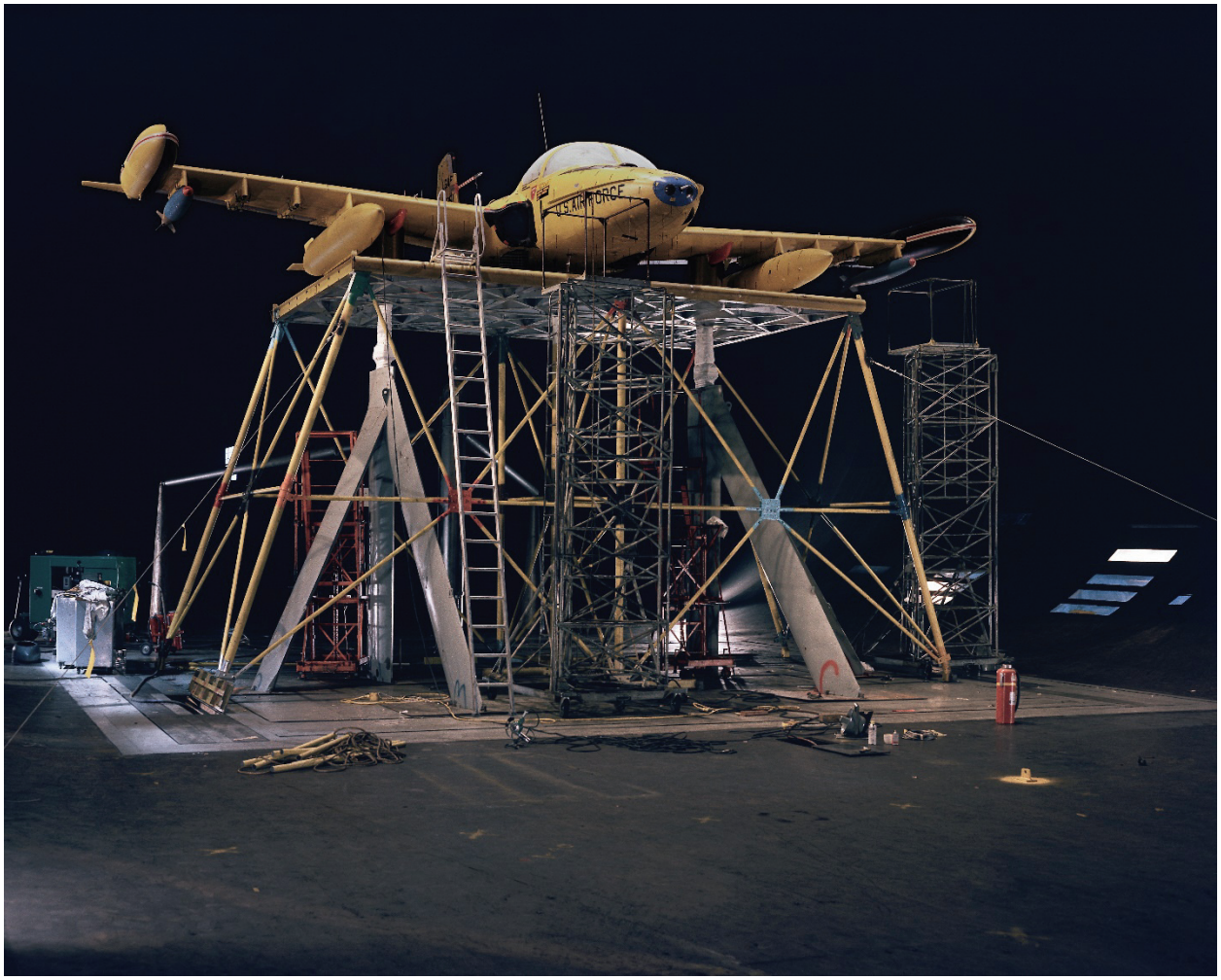

Figure 123. Cessna A-37B airplane with experimental thrust reversers with a temporary ground board being installed. *(NASA AC-41258)*

Supersonic Transport (SST) and High-Speed Aircraft Research (HSR) Programs

At one time the United States was committed to a major program to develop a supersonic (Mach number 2 to 3 at cruise) commercial transport. See reference [183] for a summary, and reference [184] for a more detailed description of the NASA Supersonic Transport (SST) and High-Speed Research (HSR) programs. Much research and development work was done by NASA, including low-speed investigations in the 40- by 80-Foot Wind Tunnel; on the order of 25 tests were performed in the 40- by 80-Foot Wind Tunnel studying landing and takeoff requirements for several aircraft configurations. Landing SSTs and hypersonic transports can be a serious technical challenge. Many models of proposed SSTs were investigated to aid in development of the required high-lift systems for landing and takeoff as well as for low-speed flight required for landing approach. Different wing shapes and airfoils were investigated with different flap configurations. With the flaps in the retracted position, it was very important that the drag not be significantly increased by the retracted flaps during cruise flight.

Commercial SST aircraft had many technical problems, as well as undesirable social impacts such as environmental effects and noise. However significant progress was being made in all areas when the HSR program was cancelled at NASA in about 1998. Some of the research would have likely benefitted subsonic commercial aircraft as well.

Aerodynamicists at Langley Research Center were strong advocates of SSTs with variable-sweep wings. Variable-sweep wings have the advantage of higher lift at unswept conditions for landing and takeoff, however they add significantly more complexity and weight to the airplane. Eventually NASA and the airplane companies settled on the fixed wing—a so-called double-delta wing. Landing and takeoff configuration investigations were performed on models of many of the NASA SST versions in the 40- by 80-Foot Wind Tunnel. Landing and takeoff was a serious problem for SSTs because the low-speed lift tended to be low, requiring high landing speeds, and the aircraft engines could be very noisy. In addition to the NASA models, one model studied in the 40- by 80-Foot Wind Tunnel had a modified delta wing that was very similar to the wing used on the supersonic Aérospatiale/BAC Concorde airplane. The Concorde and the Russian Tupolev Tu-144 were the only SSTs to see regular service. A few representative investigations are described.

Research on a delta-winged SST model with a delta-canard control surface, both out of ground effect and in ground effect, was performed [185, 186]. This model was very similar to the SCAT 17 (supersonic commercial air transport number 17) configuration. Stability and control were investigated as well as various high-lift devices. See Figure 124 (Test 161) for a photo of the model in the wind tunnel.

Figure 124. Delta-wing SST model with a delta-canard (forward) control surface.
(NASA A-28474)

Experiments with variable-sweep wings were performed with the wing swept and unswept (Fig. 125). Reference [187] describes low-speed results for an SST with variable-sweep wings. This was a 1/5-scale model of a 200-passenger aircraft that was designated SCAT 14. Wing sweepback and aspect ratio were varied along with leading-edge slat deflection and geometry, trailing-edge flap deflection, and horizontal-tail geometry and location. It was found that all configurations tested except one were longitudinally unstable at high lift. The configuration that was not unstable had the horizontal tail in a low horizontal position and a wing sweepback angle of 25 degrees with a large portion of the fixed-wing leading edge deflected as a leading-edge flap.

The top view of another variable-sweep model is shown in Figure 126 (Test 237), the Boeing variable-sweep supersonic model. In addition to various experiments performed to study and improve the landing and takeoff performance, experiments were performed with the wings still swept back to study failure modes with the sweep mechanism. In the event of failure of the wing-sweep actuators, landings would have to be performed at higher speeds if the wings could not be unswept. Experiments with models both in and out of ground effect were also performed. Results are described in reference [188].

Figure 125. SST model with variable-sweep wings in forward position and engine pod in center underneath. ***(NASA A-30876)***

Figure 126. Top rear view of Boeing variable-sweep SST model with wings in forward position.
(NASA A-35511)

Another large-scale investigation to improve the low-speed longitudinal stability at high lift of an SST with variable-sweep wings was performed [189]. Special efforts were made to minimize the adverse effects of the vortex flow from the strake, which was the highly swept inboard fixed-portion of the wing. Modifications and flow-control devices tested on the strake included increased leading-edge radius, leading-edge flaps, and upper-surface vortex generators, as well as fences on both the strake and the movable wing panel. It was found that the model with a sharp strake leading edge had a pitch-up tendency at an angle of attack as low as 5 degrees, which was very undesirable. The use of a larger strake leading-edge radius, together with a strake leading-edge flap and a wing fence, produced essentially linear pitching moments up to 18 degrees angle of attack, with a stable break at stall that was a major improvement. A combination of vortex generators on the strake's upper surface, and a wing fence outboard of the pivot, also produced acceptable pitching-moment characteristics.

Large-scale investigations of an SST model with a double-delta wing of aspect ratio 1.66 were also performed in the 40- by 80-Foot Wind Tunnel [190]. The model had no horizontal tail or canard; elevons (flap-like devices on the wings) were used for longitudinal and lateral control. Longitudinal and lateral characteristics and ground effect were studied. The model is shown in the tunnel with short support struts in Figure 127 to study ground effect during landing and takeoff. It was found that there was no large reduction in static longitudinal stability at high angles of attack. The ground effect was positive at the angle of attack required for takeoff or landing.

Figure 127. Ground-effect testing of a double-delta SST model. ***(NASA A-37700)***

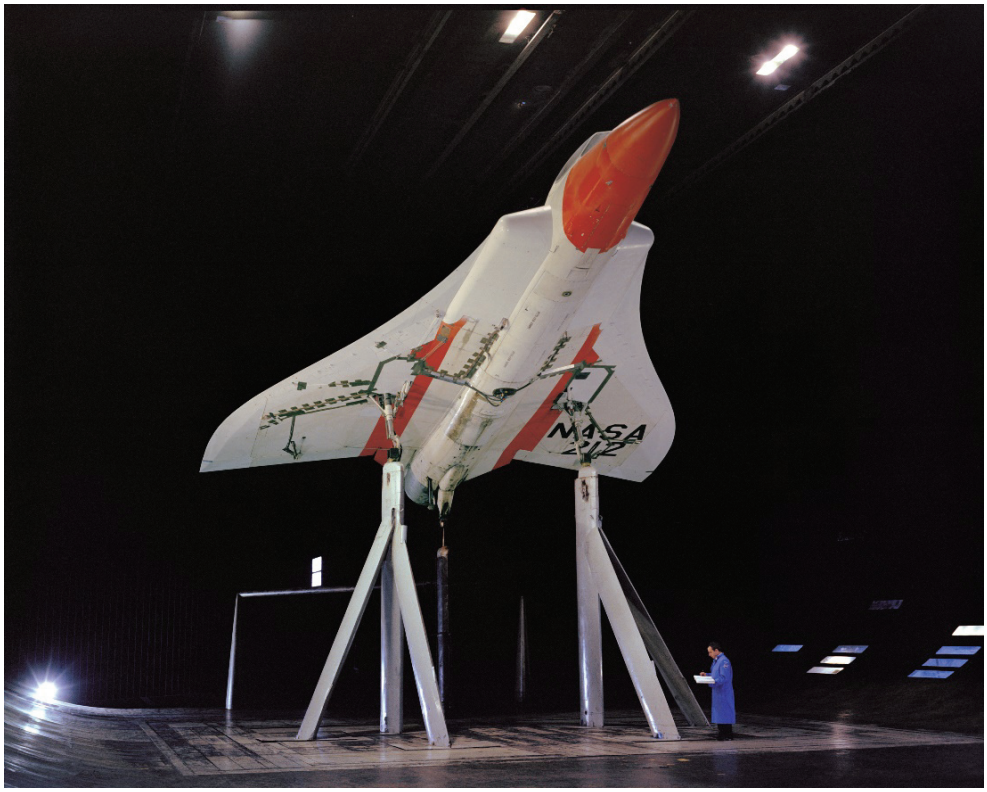

Figure 128. Front lower view of Douglas F5D-1 aircraft with ogee-shaped wing; the wing was modified to simulate a Concorde SST wing. ***(NASA AC-31304)***

The wing on a delta-wing Douglas F5D-1 aircraft was modified to become an ogee-shaped wing that was very similar to the wing on the Concorde SST airplane. The ogee-shaped wing was a modified delta wing with increased curvature on the leading edges. Experiments were performed in the 40- by 80-Foot Wind Tunnel to study landing and takeoff performance [191, 192]. After the wind tunnel tests, flight-tests were performed at Ames. Figure 128 (Test 192) shows the aircraft in the wind tunnel on the normal support struts. The results of the wind tunnel and flight-tests out of ground effect are presented in reference [191], and wind tunnel and flight-test results in ground effect are presented in reference [192]. It was found that the ogee shape had improved low-speed aerodynamic characteristics compared to the delta shape; the landing approach speed could be safely reduced by about 10 knots with the ogee wing.

Subsequent extensive theoretical work was done on the original SCAT 15 at Langley Research Center, and it was converted to a fixed-wing configuration with much improved aerodynamic characteristics. It was designated the SCAT 15F. Large-scale experiments were performed on the configuration in the 40- by 80-Foot Wind Tunnel (Fig. 129). According to studies at Langley [193], the configuration had a pitch-up problem at moderate angles of attack and the potential for deep-stall trim that would be unrecoverable, however it represented the most efficient supersonic configuration to date.

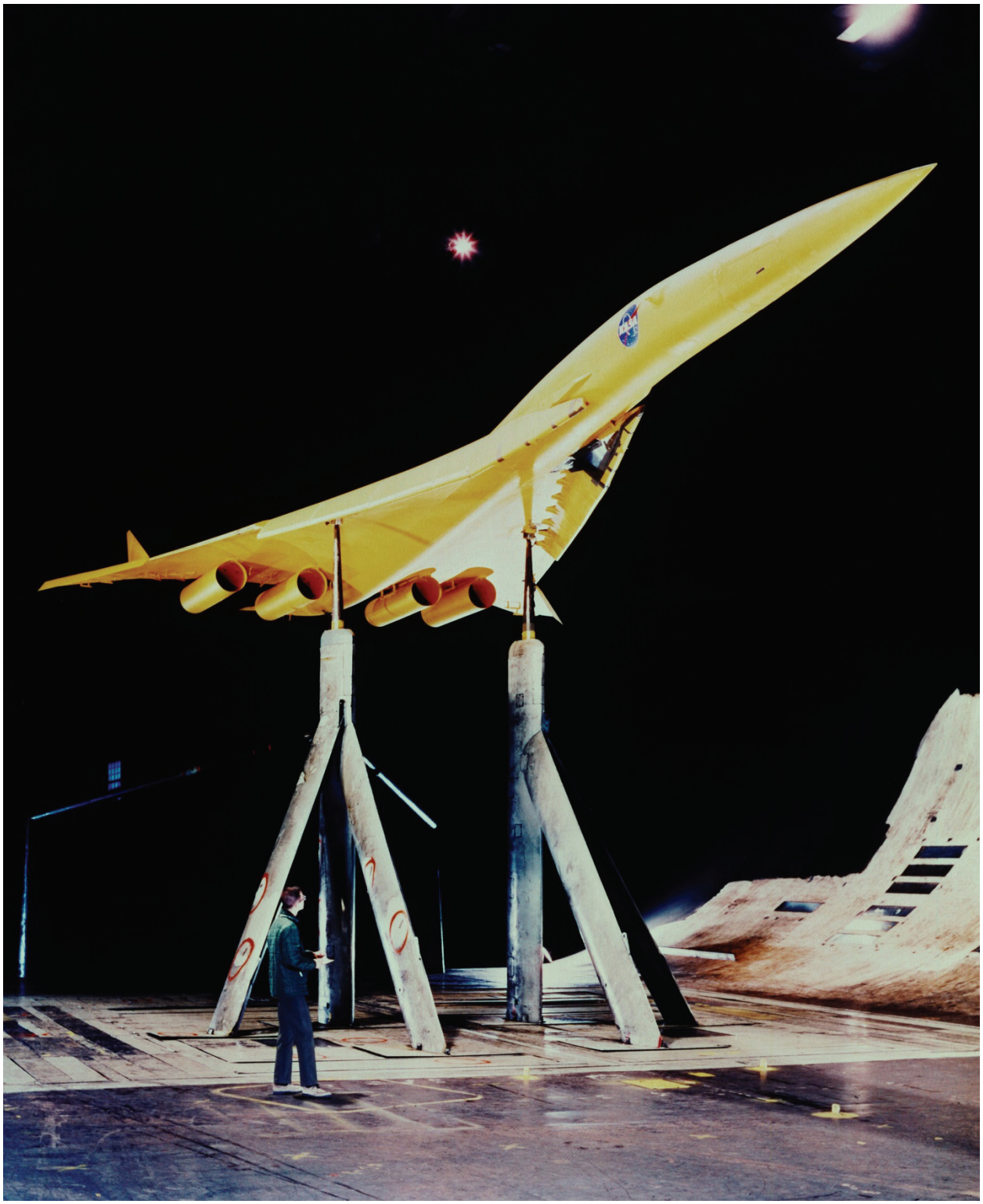

Figure 129. SCAT 15F SST model. ***(NASA AC42062)***

Hypersonic Transport Model

Landing characteristics of a proposed hypersonic transport model were investigated in the 40- by 80-Foot Wind Tunnel. Hypersonic aircraft have cruise speeds on the order of a Mach number of 5. The model had a delta wing and is shown in the tunnel in Figure 130 (Tests 305 and 314). Increasing the lift during landing and takeoff of hypersonic aircraft configurations is even more of a challenge than during landing and takeoff of SSTs because of the increased importance of reducing drag during cruise when the high-lift devices are retracted. Also, the wings tend to be smaller and swept more, aggravating the problem of having sufficient lift for landing and takeoff. Unfortunately, this was a relatively short-lived NASA program and not a lot of work was done on hypersonic transports because of reduced interest by NASA.

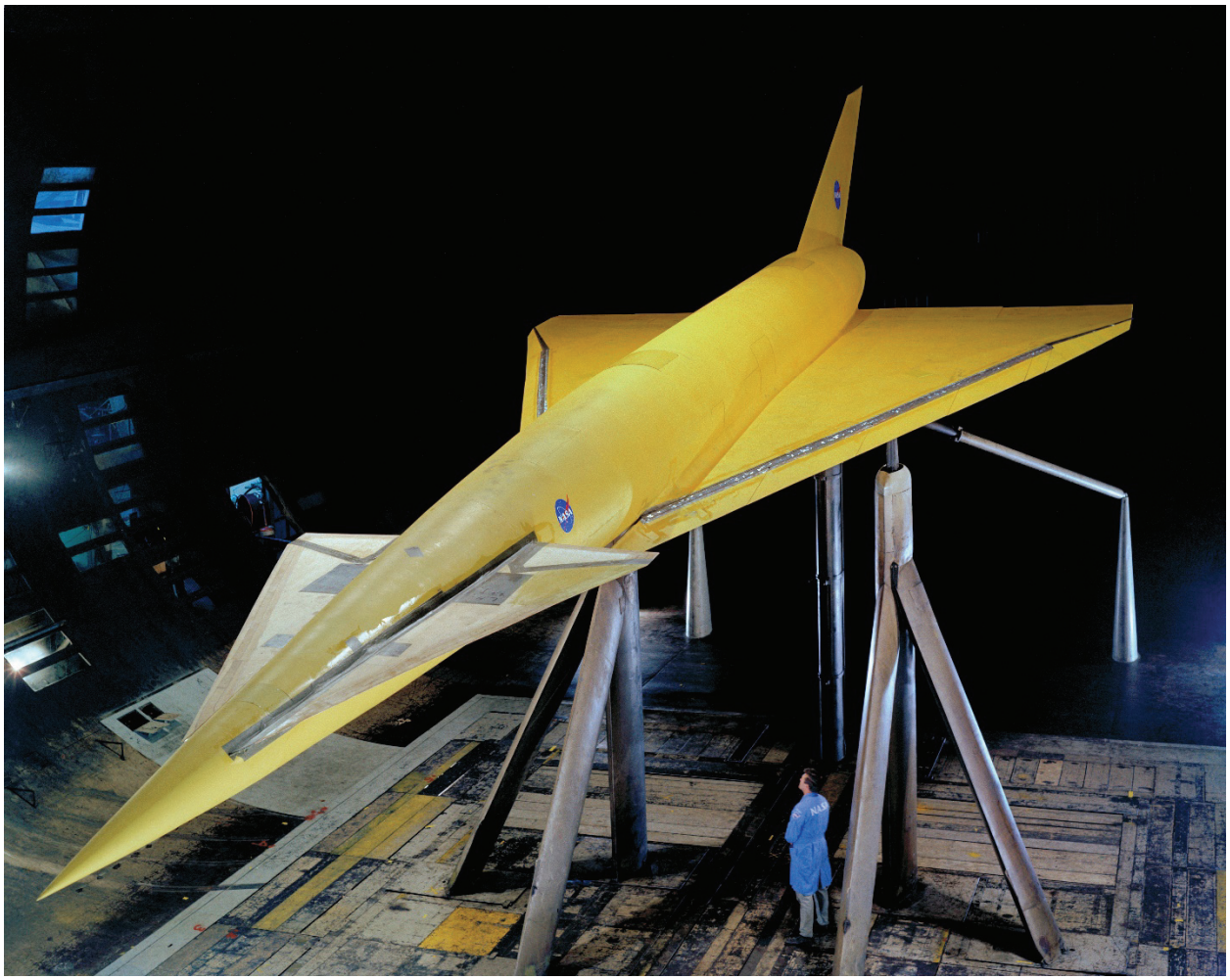

Figure 130. Three-quarter front view of a hypersonic transport model with delta-wing canard.
(NASA AC-40028)

General Aviation

General aviation is defined as all civilian aviation operations except scheduled passenger airlines. General aviation aircraft range from gliders and powered parachutes to corporate business jets. However most general aviation aircraft are small propeller or jet-powered aircraft that carry two to six passengers. Experiments were performed on this type of general aviation aircraft in the 40- by 80-Foot Wind Tunnel.

General aviation stall-spin studies. Experimental stall-spin studies were performed on a Beechcraft Musketeer, Model 23A [194]. Spin can occur on many airplanes when the wing stalls and wing lift drops more on one side than the other side causing the start of a spin. This is a potentially very dangerous situation because spins can be difficult to recover from, depending on the airplane. The airplane can keep rotating until it crashes. The approach was to add modifications to the wing that would result in a nearly constant lift coefficient after stall so there would not be a large drop in lift at stall conditions. The airplane is shown in the 40- by 80-Foot Wind Tunnel in Figure 131. Gloves were added to the wing with the goal of decreasing the drop in lift coefficient after stall. The gloves did decrease the drop in lift coefficient up to the limit of the test angle of attack, which was 40 degrees. The drop without the gloves was on the order of 50 percent compared to about 20 percent with the gloves. More details are presented in reference [194]. This was judged to be an acceptable approach to mitigating the possibility of spin.

General aviation aircraft cooling drag. A series of experiments were conducted in the 40- by 80-Foot Wind Tunnel to provide design information for the engine-cooling systems on a propeller-powered general aviation aircraft with twin air-cooled engines [195-198]. The objectives of these tests were to measure the drag on the aircraft due to the engine-cooling air (termed “cooling drag”) and to provide design information for the nacelles to provide adequate cooling for the engines. An additional objective was to identify the sources of cooling drag and to identify concepts to reduce the drag due to engine cooling so that better flight efficiency could be achieved.

Prior to this program, aircraft designers used the results of test programs conducted by the NACA from 1920 to 1950. The aircraft in this earlier period were mostly radial piston-engine powered. Also, in these earlier studies, cooling drag was not the primary focus; the primary focus was to provide adequate cooling for the engines that were multi-cylinder and high powered. In the experiments described herein, a full-scale semispan wing was mounted in the 40- by 80-Foot Wind Tunnel (Fig. 132; Tests 536, 544, and 548). This wing was an actual wing from a commonly used general aviation twin-engine piston-powered aircraft. Tests were conducted both with and without the actual horizontally opposed six-cylinder engine. When the engine was not installed, tests were conducted with and without the propeller, which was driven by an electric motor. For these tests, the engine-cooling-flow blockage was simulated by using calibrated orifices between the upper and lower plenums inside the nacelle. (Intake air entered the upper plenum and flowed downward through the engine into the lower plenum and then out a rear exhaust.) The wind tunnel airspeed during the experiments was the actual cruise flight speed for the aircraft. Three cooling-flow-inlet sizes and two designs of cowl flap were studied. Some novel concepts for improved engine-cooling design were explored.

Figure 131. Stall studies using a Beechcraft Musketeer, Model 23A. Note the wing-leading-edge glove on the inboard half of the wings. ***(NASA AC79-0973-2)***

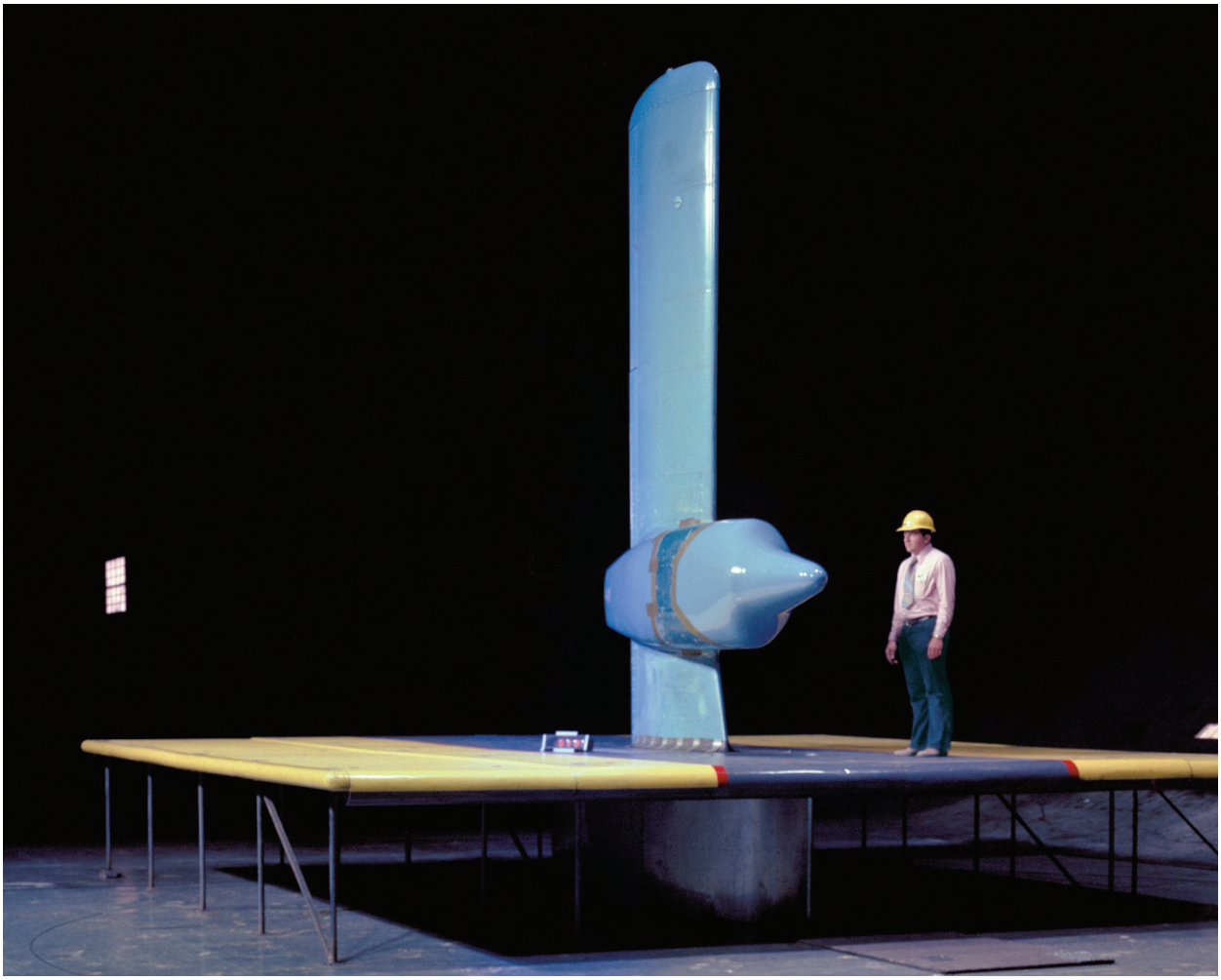

Figure 132. Engine-cooling studies using a semispan model with the intake and exhaust faired in.
(NASA AC79-0046-1)

In addition to the data from the wind tunnel scale system, a total-pressure rake was used to measure the spanwise distribution of the section drag coefficient, and there were numerous surface pressures external to the nacelle. Total pressure measurements were made in the upper and lower plenums inside the engine nacelle (that is, above and below the engine location).

In tests without the engine, cooling drag was measured by comparing the drag of a reference configuration with the drag of the actual configuration with air flowing through the nacelle. The reference configuration was obtained by smoothly fairing over the nacelle inlet and exit (as shown in Figure 132) so that there was no flow through the nacelle. When the cooling air was flowing, the interior of the nacelle consisted of an upper and lower plenum with several orifice openings between the plenums to simulate the flow resistance of the actual engine. The airflow through the nacelle was calibrated using a venturi meter attached to the nacelle exit.

The results of the tests without the actual engine but with the simulated engine blockage showed that the cooling drag was about 13 percent of the total airplane drag. In the climb condition, about 40 percent of this drag was associated with nacelle internal flow. Inlet pressure recovery

was found to be low by about 63 percent. The use of a cowl flap to lower the pressure in the lower plenum, and thereby increase the cooling flow rate to the level required to cool the engine, was a significant contributor to cooling drag. The drag associated with the airflow external to the nacelle was increased because of the poor efficiency of the internal airflow in the nacelle. This coupling came from the inlet spillage because of the poor upper plenum pressure recovery. The effect of adding the propeller was to improve the flow both internal and external to the nacelle. The pumping action of the propeller improved the inlet efficiency, and the added slipstream reduced flow separation on the aft portion of the nacelle. With the propeller operating, however, there was still substantial room for improvement in the cooling system design. When the actual operating engine was installed, it was found that the use of calibrated orifices to measure the internal flow characteristics was a good simulation of the internal flow with the actual engine.

Several exploratory tests were conducted to address the shortcomings of the cooling flow system. Improvements were recommended for reducing the cooling drag while maintaining cooling requirements [195-198].

Wing-fuselage interaction. Wing-fuselage-interaction studies were performed in the tunnel and results compared with theory on a Beech Sundowner airplane [199] (Test 547). The effects of three different wing airfoil contours on the aft fuselage drag were studied. The airplane had a low wing with a wingspan of 33.75 feet. Low-wing airplanes tend to have more adverse wing-fuselage interactions (lower maximum lift and higher drag) than mid-wing or high-wing aircraft. Measured changes in the locations of the fuselage pressure contours with airfoil sections correlated well with the changes predicted by an inviscid computer code. A criterion based on the code was proposed as an indicator for possible adverse viscous interactions at the wing-fuselage juncture.

Rotorcraft

Overview

There were many rotorcraft experiments done in the 40- by 80-Foot Wind Tunnel before the repowering and addition of the 80- by 120-foot test section [200-202]. Reference [200] is an excellent summary describing rotorcraft research from about 1953 to 1984. The test facilities and research capabilities are described. Only a sample of the testing done is described herein.

Harris [201] is an excellent history of rotorcraft and contains much more technical detail than what is presented in this book. It contains superb descriptions of the various rotorcraft details and defines the jargon used by the industry. Johnson [202] describes rotorcraft and presents helicopter theories as well as excellent descriptions and backgrounds for the theories.

Tilt-Rotor Aircraft

Tilt-rotors are treated separately from helicopters in this book.

Development of tilt-rotor aircraft was a major activity in the 40- by 80-Foot Wind Tunnel. Researchers and management at Ames were major advocates for the development of tilt-rotor aircraft technology because of its great potential both for military and commercial use. Tilt-rotor aircraft have the potential to be able to hover nearly as efficiently as helicopters with low downwash velocities and yet have a much higher cruise-speed capability than conventional

helicopters—at least double. The concept was to use wingtip-mounted rotors for vertical lift similar to helicopters, and to tilt the rotors forward for forward flight and to use the wing for lift at cruise conditions. At cruise, the rotors would become large-diameter thrust-producing propellers (commonly referred to as proprotors). Because of the size of the rotors, they would have to be tilted up when landing as a conventional aircraft because they would not clear the ground at the cruise angle. More commonly, they would be tilted up to 90 degrees for vertical landings as a helicopter. Tilt-rotors could autorotate in the event of a power failure assuming sufficient altitude was available, much like a helicopter, for a safe landing. If the aircraft was in the cruise mode, the proprotors could be tilted up, and then autorotation initiated in the event of a power failure. Generally, the main problem areas for tilt-rotor aircraft were in transition from hover to forward flight, and from forward flight to hover, as well as when the rotors were in the propeller mode at cruise and higher airspeeds. This was because the large proprotors were more flexible than propellers and subject to potential aeroelastic problems during these conditions.

Bell XV-3. The XV-3 was the first tilt-rotor aircraft to be developed and tested in the 40- by 80-Foot Wind Tunnel [203, 204]. Bell had been working on the concept since the late 1940s. The initial configuration used rotors with three blades. Bell built two research aircraft and started performing flight-tests in 1955. In 1956 an accident caused by blade oscillations occurred during flight-testing. The aircraft suffered from wing/pylon/rotor instabilities. Whirl-flutter instability was first experienced on a tilt-rotor aircraft during these flight-tests. Modifications were made and flight-tests were resumed. Higher speeds were achieved, but problems persisted so Bell decided to make major modifications. The modified aircraft was then sent to Ames for investigations in the 40- by 80-Foot Wind Tunnel (Fig. 133). Problems with the three-bladed rotors were confirmed, and the decision was made to replace the three-bladed rotors with two-bladed rotors. Semirigid-type rotors were employed and were mounted on shorter masts. During the wind tunnel investigations, there were additional modifications. Conversion to forward flight was much improved, but shifting gears for forward flight was time consuming. The gear-shift capability was important to lower the rotor speed to about half of the hover rotational speed for forward flight, while the blade angle was increased to improve propulsive efficiency during cruise flight.

Flight-testing was resumed and was quite successful. The aircraft performed autorotation during simulated engine failures, and it flew well as a helicopter. However, another rotor oscillation was encountered in flight at a 40-degree pylon angle (the rotor pylon angle is about 90 degrees in the hover mode and close to 0 degrees during cruise). The decision was made to perform additional wind tunnel testing. This was done and additional modifications were made as a result of the testing in the 40- by 80-Foot Wind Tunnel.

Flight-testing was again resumed after more modifications, and the aircraft achieved about 120 knots and demonstrated the viability of the tilt-rotor concept. After much flight-testing and analysis and improvements, the aircraft was returned to the 40- by 80-Foot Wind Tunnel for high-speed tests. The aircraft successfully demonstrated simulated flight up to the maximum wind tunnel speed of about 200 knots. During the last data point of the experiments at maximum airspeed, the wings failed in fatigue and both rotors tore loose destroying the aircraft without significant damage to the wind tunnel. This was the fourth and final wind tunnel test of the aircraft.

Figure 133. Bell XV-3 tilt-rotor aircraft with two-bladed proprotors in forward-flight mode. ***(NASA A-37006-5)***

This was the end of the XV-3, but the aircraft had successfully demonstrated the viability and potential advantages of the tilt-rotor concept. The vehicle was able to hover efficiently—comparable to a helicopter—and to achieve cruise airspeeds with good propeller efficiency at airspeeds on the order of double that of a helicopter. One of the aircraft was restored and put on display in the National Museum of the U.S. Air Force at Wright-Patterson Air Force Base near Dayton, Ohio.

XV-15 tilt-rotor aircraft. The XV-15 was a larger tilt-rotor aircraft and had improved rotors. It was developed because of the success of the XV-3, and the lessons learned from the XV-3 were used in its design. The 40- by 80-Foot Wind Tunnel was heavily used for the development of the XV-15, and it was a very successful program [205, 206]. See Figures 134 and 135 (Test 525). The complete airplane was tested in the 40- by 80-Foot Wind Tunnel prior to flight-tests. Reference [205] describes the early wind tunnel tests. Reference [206] is an excellent book that chronicles the development of the XV-15 from the lessons learned and improvements made based on experiments with the XV-3. The development and design of the XV-15 was as thorough as that for any prototype aircraft even though it was only intended to be used for research. The aircraft was able to achieve 300 knots airspeed in level flight—much faster than a conventional helicopter. Some of the rationalization for, and the beginning of, the V-22 tilt-rotor program is also described in this book.

Figure 134. XV-15 tilt-rotor research aircraft in lifting mode. ***(NASA AC78-0579-1)***

Figure 135. XV-15 tilt-rotor research aircraft in forward flight or cruising mode. ***(NASA AC78-0579-3)***

Advanced Helicopters

Helicopters have been improved over the years, and theories have improved [207]. Wind tunnel experiments, principally in the 40- by 80-Foot Wind Tunnel, have been done that have contributed to helicopter improvements. Helicopters have become faster, quieter, safer, and easier to fly and with longer range. Some of the representative studies performed in the 40- by 80-Foot Wind Tunnel are described next; the studies ranged from exploratory to developmental.

Jet-flap rotor. A 40-foot-diameter jet-flap rotor was studied in the 40- by 80-Foot Wind Tunnel; the rotor was two bladed (Fig. 136, Test 239). The rotor was built by the French firm Giravions Dorand under contract to the Army. The jet-flap rotor was driven and controlled by the jet itself, which was incorporated in the outer 30 percent radius of each blade. The blades were fixed in pitch, and varying the jet-flap deflection angle—both cyclically and noncyclically—controlled the rotor force output. Aerodynamicists compared the force-producing capabilities of the jet-flap rotor with those of conventional rotors. The jet-flap rotor produced very large lift and propulsive forces. It was found that the jet-flap rotor could be operated well beyond standard rotor-blade-stall boundaries, and the investigation did not expose any inherent limitations of the concept. The increased load-carrying capability of the jet-flap rotor was quite substantial, reaching as high as 2 to 2-1/2 times the capability of a conventional rotor. Engineers concluded that additional investigations were warranted to evaluate this concept at higher advance ratios (airspeeds). It was also found that correlations between measured and calculated results showed generally good agreement [208].

Lockheed stoppable rotor. Experiments were performed on a Lockheed stiffened, hingeless, 33-foot-diameter rotor on a wing-fuselage model (Figs. 137 and 138). The vehicle would take off as a helicopter and then transition to forward speed. At sufficient speed, the rotor blades would fold back and the wing would produce the required lift. On an actual aircraft, there would also be a propulsive device such as a propeller or jet engine for thrust. The purpose of the wind tunnel experiments was to investigate the transition from helicopter lift mode to cruise flight mode with the rotors folded back and stowed [209].

Figure 136. Giravions Dorand jet-flap helicopter rotor with Sam Yacco, aircraft mechanic, in photo. The jet engine on the floor of the test section produces compressed air for the jet flap. ***(NASA A-34960)***

Figure 137. Lockheed stoppable rotor in lifting mode. ***(NASA A-36028)***

Figure 138. Lockheed stoppable rotor with blades folded back for cruise mode. ***(NASA A-36030)***

Sikorsky high-speed rotors. A series of Sikorsky high-speed rotors were studied in the wind tunnel (Fig. 139) [210]. The goal was to increase the maximum airspeed capability of single-rotor helicopters.

Figure 139. Sikorsky high-speed rotor. ***(NASA A-37645)***

Hughes OH-6A Light Observation Helicopter (LOH) experiments. The Hughes LOH was studied in the wind tunnel (Fig. 140). This helicopter was used for personnel transport, escort and attack missions, and observation. Comparisons were made of wind tunnel results, flight results, and computer estimates. The studies were done at the request of the Naval Air Systems Command (NAVAIR), Department of the Navy. In general, agreement was reasonably good [211].

Figure 140. Hughes LOH. ***(NASA A-40832)***

Lockheed AH-56 Cheyenne. The AH-56 Cheyenne was an advanced-technology compound helicopter with a pusher propeller for thrust, a small wing (26-foot wingspan), and a "rigid" rotor that was about 50 feet in diameter. It was expected to satisfy the Army's need for a fast and heavily armed helicopter for escort and attack. It was intended to be capable of high speeds for a helicopter because of its pusher propeller and wing; it was designed to cruise at about 175 knots and have a top speed of about 220 knots. Preliminary flight-tests were performed, and 10 aircraft were built and delivered to the Army for further tests and evaluation by July 1968. During flight-testing, there was a fatal crash in March 1969. Rotor oscillations had caused the rotor to impact the fuselage. Despite Lockheed's objections because of the rigid wind tunnel mounting, wind tunnel tests were requested by the Army to study the rotor oscillation problem. (Lockheed contended that the rigid supports in the tunnel would not allow the aircraft to respond to rotor disturbances.) A Cheyenne aircraft was installed in the 40- by 80-Foot Wind Tunnel (Figs. 141 and 142, Test 348). Research tests were started on September 17, 1969. A catastrophic accident occurred at about 100 knots airspeed shortly after the testing had started. The rotor impacted the

Figure 141. Three-quarter front view of the Lockheed AH-56 Cheyenne compound helicopter.
(NASA AC-42561-1)

fuselage during oscillations and destroyed the aircraft. The Cheyenne used rotor-hub-moment feedback to a control gyro to eliminate adverse handling qualities and gust response characteristics of the rigid rotor. The pilot commanded moments on the gyro in order to fly the aircraft. The gyro was actually seeing pitching moments from the blades, with the blades swept, so in free flight the pitching moment was a measure of hub moment. When collective was increased in the wind tunnel, the rotor stalled, producing high blade aerodynamic pitching moments. The gyro interpreted these pitch loads as hub moments, and tried to eliminate them by tilting the rotor, until the blades struck the tail boom. The damaged aircraft came off of the wind tunnel support struts and ended up at the end of the primary diffuser at the first set of wind tunnel turning vanes (Fig. 143). As described earlier, when the rotor impacted the fuselage, a 20-pound tip-weight broke off of one of the blades and it went through the wind tunnel wall at the top of the control room.

Figure 142. Three-quarter rear view of the Lockheed AH-56 Cheyenne showing the pusher propeller.
(NASA AC-42561-2)

Figure 143. Lockheed AH-56 Cheyenne accident. ***(NASA A-42557-10)***

Lockheed aerodynamicists subsequently solved the Cheyenne rotor oscillation problems using newly developed theory and some flight-testing, but it was too late to save the program. The Cheyenne had a lot of potential, but the program was cancelled in August 1972 because of cost overruns and energetic criticism from the Air Force (apparently because the Army aircraft infringed on the Air Force charter). The total cost had been $400 million for research and development of 10 aircraft.

Advancing Blade Concept (ABC) rotor. A potential approach to increasing the high-speed capability of helicopters is to delay stall of the retreating blade and delay compressibility effects of the advancing blade. A conventional helicopter rotor operates with only small hub roll moments, requiring balance of retreating side and advancing side blade lift. The retreating blade lift is limited by stall, and loading balance keeps the advancing blade from lifting as much as it could. In the ABC, retreating blade stall is reduced by carrying a hub roll moment with stiff rotors, so the blade can use the lifting potential of the advancing side. In addition, with coaxial, counterrotating rotors, the two rotors cancel the torque on the aircraft so the traditional antitorque tail rotor is eliminated. If a thrust-producing jet engine or propeller is used, the aircraft has the

potential for speeds much higher than conventional helicopters. The rotors would still need to produce lift but they would not need to produce thrust, which they do not do as efficiently as propellers or jet engines at cruise speeds. Experiments were performed in the 40- by 80-Foot Wind Tunnel on a 40-foot-diameter coaxial-rotor model. The rotors were three bladed and built by Sikorsky. The blades were very stiff in torsion, and in flatwise and chordwise bending, so the two rotors were not likely to impact each other and the rotor spacing could be minimized. The rotor spacing was 30 inches at the hub, and the testing was limited such that the clearance at the rotor tips would not be less than 10 inches. Each rotor had a feathering bearing to allow the blade angle or pitch to be varied. Experiments with only the upper rotor were also performed. The rotors were driven by two 1,500-hp electric motors located in the faired body (Fig. 144, Test 362). Aerodynamic and acoustic results of the wind tunnel investigation are provided in reference [212].

Figure 144. ABC rotor model. ***(NASA AC70-2604)***

Because of the success of the wind tunnel investigation, two ABC helicopters were built by Sikorsky (XH-59A) under Army sponsorship. ABC helicopters were considered a possible alternative to compound helicopters to achieve higher airspeeds. The rotor diameter was 36 feet, and the rotor spacing was 30 inches at the hub. Auxiliary propulsion was expected to provide forward thrust. Shortly after flight-testing was initiated, a low-speed accident occurred. Neither pilot was injured. The damaged aircraft was rebuilt for extensive wind tunnel testing in the 40- by 80-Foot Wind Tunnel (Fig. 145, Test 554). Performance and aerodynamic loads data were measured as well as acoustic data [213, 214].

The aircraft subsequently had a successful flight-test program and completed essentially all technical objectives. A maximum level flight speed of 240 knots was achieved, making it the first rotary-wing aircraft to achieve this speed without the use of an auxiliary wing.

X-wing. Experiments were performed on a stoppable helicopter rotor with blade-circulation control in the 40- by 80-Foot Wind Tunnel from March through May 1979 (Fig. 146) [215]. The four-bladed rotor was designed to stop at a preset orientation to allow the blades to act as wings during cruise. The aircraft would be supported by the stopped rotor blades acting as wings, and propulsion would be supplied by suitable means such as jet engines or propellers. The rotor-blade airfoil sections were symmetric ovals with flat bottoms, and with nozzles for airflow possible from both leading edges and trailing edges along the entire blade span. The airflow out the nozzles provided circulation control and resultant lift during the helicopter or vertical lift mode. The model was tested as a rotating wing and a fixed wing, and during transition of the start-stop sequences. The objectives were to determine the capability of the model's control system to maintain pitching- and rolling-moment balance during the start-stop sequences and to determine the steady-state data of the model as both a helicopter rotor and as a fixed-wing aircraft. The test objectives were successfully met. The X-wing control system was able to maintain pitch and rolling-moment control and balance in the rotary-wing mode and during the start-stop sequence. The blades were able to withstand the loads encountered in the starting and stopping procedures.

Bearingless main rotors (BMRs). BMRs are currently being investigated as a possibility to simplify rotor hubs. All hub bearings are eliminated and composite flexbeams are used at the blade roots instead of bearings. Blade angles are set by twisting flexures with pitch actuators. Materials development have made this technology possible. However, because the elasticity tends to be nonlinear and difficult to predict, full-scale experiments are required. One set of early experiments [216] involved a 32.2-foot-diameter rotor for the BO-105 modified by Boeing-Vertol under sponsorship of the Army (Figs. 147 and 148, Test 550). The rotor was mounted in the tunnel on the rotor-test apparatus. Operating characteristics were investigated in hover and at airspeeds up to 165 knots. The primary objective of the test was to determine the aeroelastic stability of the fundamental flexbeam-blade chordwise bending mode. The investigation was successful, and the rotor was found to be stable for all flight conditions.

Figure 145. Sikorsky ABC helicopter with Al Lizak in photo. ***(NASA AC80-0453)***

Figure 146. Overhead view of the X-wing helicopter model. ***(NASA AC79-0367-1)***

Figure 147. Boeing-Vertol BMR model. ***(NASA A80-0120-2)***

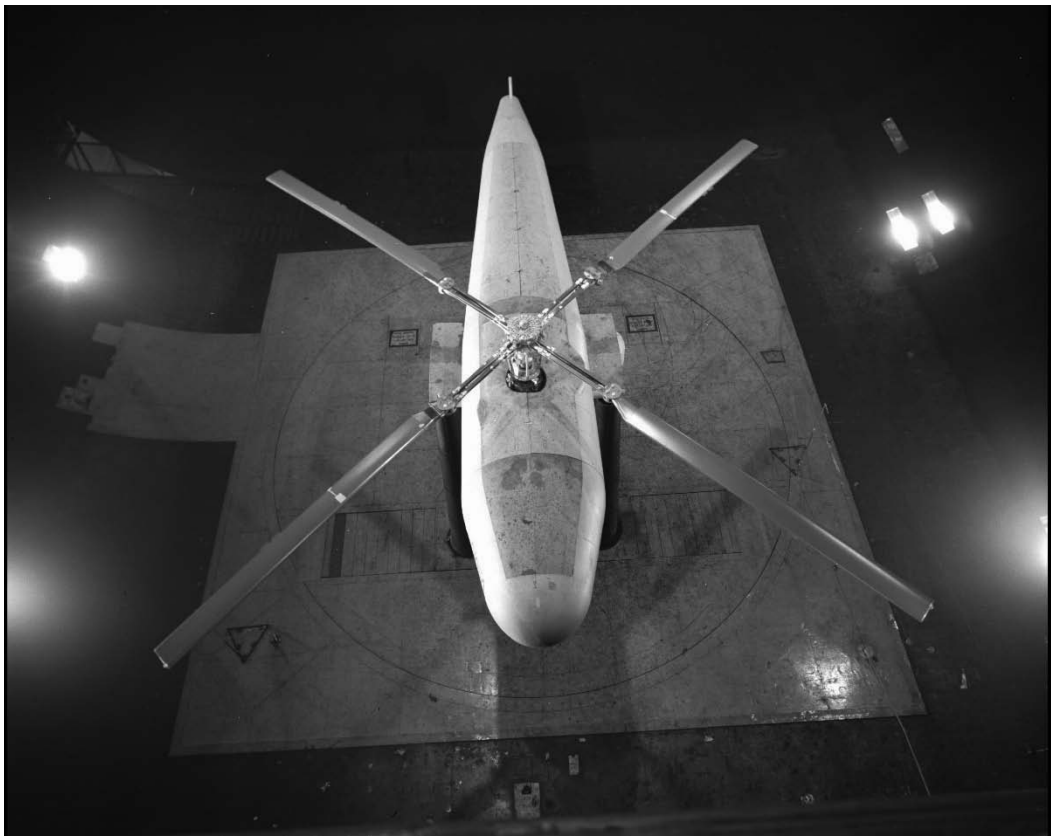

Figure 148. Overhead view of Boeing-Vertol BMR model. ***(NASA A80-0120-3)***

Sikorsky S-76 helicopter. Experiments were performed in the 40- by 80-Foot Wind Tunnel on an S-76 rotor to allow comparison with 1/5-scale-model wind tunnel test results as well as comparisons with flight-test results (Fig. 149, Test 502). Additionally, Sikorsky was interested in evaluation of their theoretical analysis. The four-bladed rotor was 44 feet in diameter and had elastomeric bearings for flapwise, chordwise, and blade-pitch motion. Elastomeric bearings are an advanced concept for helicopters and have an elastic material instead of balls or rollers between the inner and outer bearing races. The approach was intended to reduce vibration and maintenance.

It was found that the small model had Reynolds number effects (scale effects) as well as effects due to fabrication differences. However, developed analytical corrections were able to account for most of the differences between the 1/5-scale model and the full-scale model.

The full-scale experiments also included evaluation of different rotor-tip configurations. Blade-tip sweep and, to a lesser extent, tip planform taper were found to be effective in reducing rotor power requirements and blade vibratory loads with forward speed [217]. Acoustic data were also obtained for the four tip shapes [218].

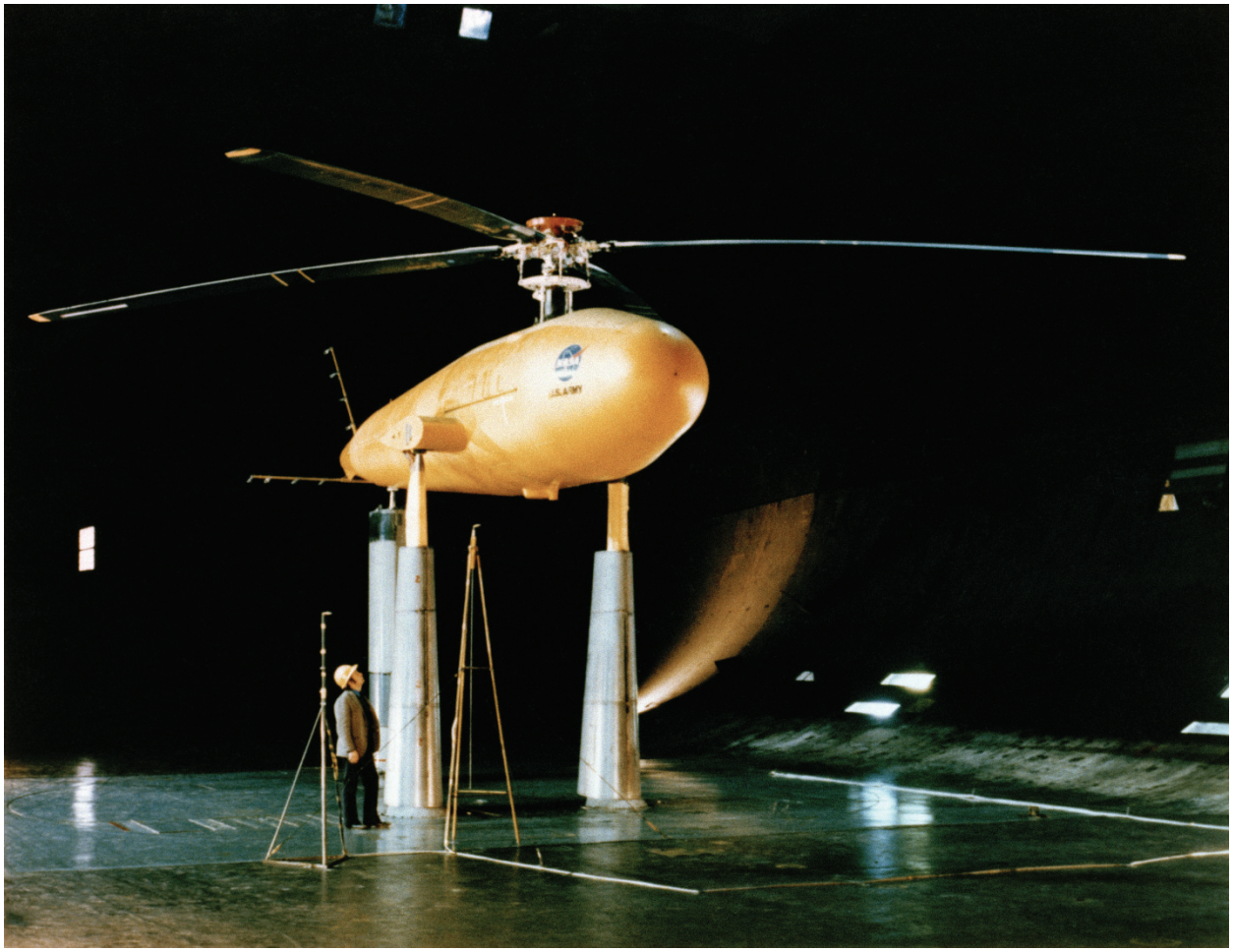

Figure 149. Sikorsky S-76 helicopter rotor test. ***(NASA AC77-0405)***

V/STOL

For many years vertical and/or short takeoff and landing (V/STOL) research was actively performed at Ames Research Center, especially in the 40- by 80-Foot Wind Tunnel. (V/STOL is generally considered separately from rotorcraft in this book, as is commonly done.) There were many concepts proposed. Jet engines and gas turbines were becoming more readily available, and were relatively lightweight, making V/STOL more practical. It was an exciting time for low-speed wind tunnel research. Runway lengths could potentially be greatly reduced, or possibly runways could be eliminated. It was generally thought that these aircraft could be much simpler, have lower vibration, and fly much faster than rotorcraft. Maintenance could potentially be significantly lower than for rotorcraft. Many of the experimental aircraft were sponsored by the Department of Defense Tri-Services (Army, Navy, and Air Force). Low-speed studies of both subsonic and supersonic V/STOL aircraft were performed in the tunnel.

A variety of V/STOL models and aircraft were investigated in the tunnel, from low-disk-loading rotors and fans to high-disk-loading fans and lift engines, starting in the 1950s [219]. For verification of wind tunnel tests, comparisons were made with flight-test results. Model size limitations and wall effects had been established for conventional aircraft models and aircraft, but V/STOL testing introduced new considerations, and verification and test-limit establishment for V/STOL wind tunnel testing was very important [220]. Later on (in the 1980s to 1990s) lessons learned from V/STOL testing were developed for rotors, propeller-powered models such as tilt wing and deflected slipstream, lift fans, ducted fans, jet flaps, and lift jets. Configuration requirements such as model size and thrust levels were determined [221]. Surveys of lift-fan technology were done as well as design guides for lift-jet engines [222-224]. A few of the representative investigations are described next.

Lift Fans, Lift Jets, and Lift Engines

Avrocar flying saucer. The Avrocar was an 18-foot-diameter flying saucer that had a centrally located fan that was to be used for lift and thrust. The airflow was ducted to the periphery of the disc for efficient lift in ground effect. A ring at the exhaust periphery was used to divert the flow aft for thrust for forward flight [225]. It was a very clever system, but it did not produce enough pitching moment for trim and control. There was also a problem when hovering. At very low altitudes (less than a disc diameter) there was favorable ground effect, but as the vehicle rose, the peripheral jet air would converge to the center resulting in a loss of lift. The transition from ground-effect hover to out-of-ground-effect hover was unstable. The transition from hover to forward flight (in or out of ground effect) was also unstable with an attendant very strong and uncontrollable pitch-up moment that increased with forward speed.

There was a lot of initial publicity when the aircraft was brought to Ames Research Center for testing even though the aircraft was classified Secret. Newspaper articles said that Ames was about to test a secret flying saucer (which was true). Overhead pictures had been taken of it from a very high altitude, so it was hard to tell what it was, except that it was round. A security screen was kept around it when it was in the wind tunnel model-preparation area; once installed in the wind tunnel, there was a full-time armed guard.

During the course of the testing, the aircraft was declassified and test engineers determined that it was unflyable. It was unstable and could not be trimmed. As a result, some experiments were done with a tail installed so that it could at least be trimmed and controlled in pitch (Figs. 150 and 151, Test 141) [225, 226]. Small-scale pilot-model wind tunnel testing had been performed before the large-scale experiments. It was found that round wings are not very efficient; that is, their lift-to-drag ratio (L/D) was low.

Figure 150. Three-quarter front view of the Avrocar flying saucer on variable-height support struts.
(NASA A-27748)

Figure 151. Three-quarter rear view of the Avrocar with a T-tail added for stability. ***(NASA A-27749)***

Lift fans. Systematic lift-fan research began in 1960 with the development of the x373-5 lift fan by General Electric. This was a single scroll, 1.1-pressure-ratio fan that was powered by a 2,500-pound-thrust J-85 turbojet engine. (Fan pressure ratio is defined as the ratio of the exit-to-inlet total pressure.) The lift fan was driven by the exhaust of the turbojet using a peripheral fan-tip turbine. The first tests in the 40- by 80-Foot Wind Tunnel were completed with the fan mounted in the fuselage of a 1/2-scale model (Fig. 152; Tests 143, 145, and 151). Two test programs were conducted, one in 1960 and one in 1961 [227, 228]. The test programs were very successful and offered promise of a future lift-fan aircraft. The 40- by 80-Foot Wind Tunnel was uniquely capable of producing test results that were verifiable and closely matched the estimates and theoretical data produced by the manufacturer.

Figure 152. Lift fan mounted in the fuselage of 1/2-scale model. ***(NASA AC-27149-B)***

Fan-in-wing models. The Army became interested in the lift-fan-in-wing concept, and negotiations began to construct two aircraft with General Electric as the prime contractor and Ryan Aircraft of San Diego, California, as the airframe contractor. To obtain preliminary results of the concept, a full-scale model of the proposed aircraft configuration (the aircraft was designated the XV-5A) was constructed in-house at Ames and tested in the 40- by 80-Foot Wind Tunnel. The model had two x376 lift fans, one in each wing. The model was powered by two J-85 turbojet engines with exhaust flowing into diverter valves that would exhaust the flow for conventional flight or direct the flow into the lift-fan tip-turbines for VTOL performance. The model was designated the VZ-11 (Fig. 153, Test 173). Each of the lift fans had exit vanes that could direct the fan flow from –10 to 45 degrees to allow transition from hover to wing-borne flight. Yaw control was obtained by differential movement of the fan exit vanes. Roll control was obtained by increasing or decreasing the lift from the fans as required [229]. There were no other control features involved. This test program was very successful, however the model did not have a means for pitch control, which necessitated the installation of a small, 36-inch lift fan in the nose of the model. The nose fan had control doors that could be rapidly moved to provide the necessary control function. Control effectiveness was investigated during a second test program of the VZ-11 in ground effect [230].

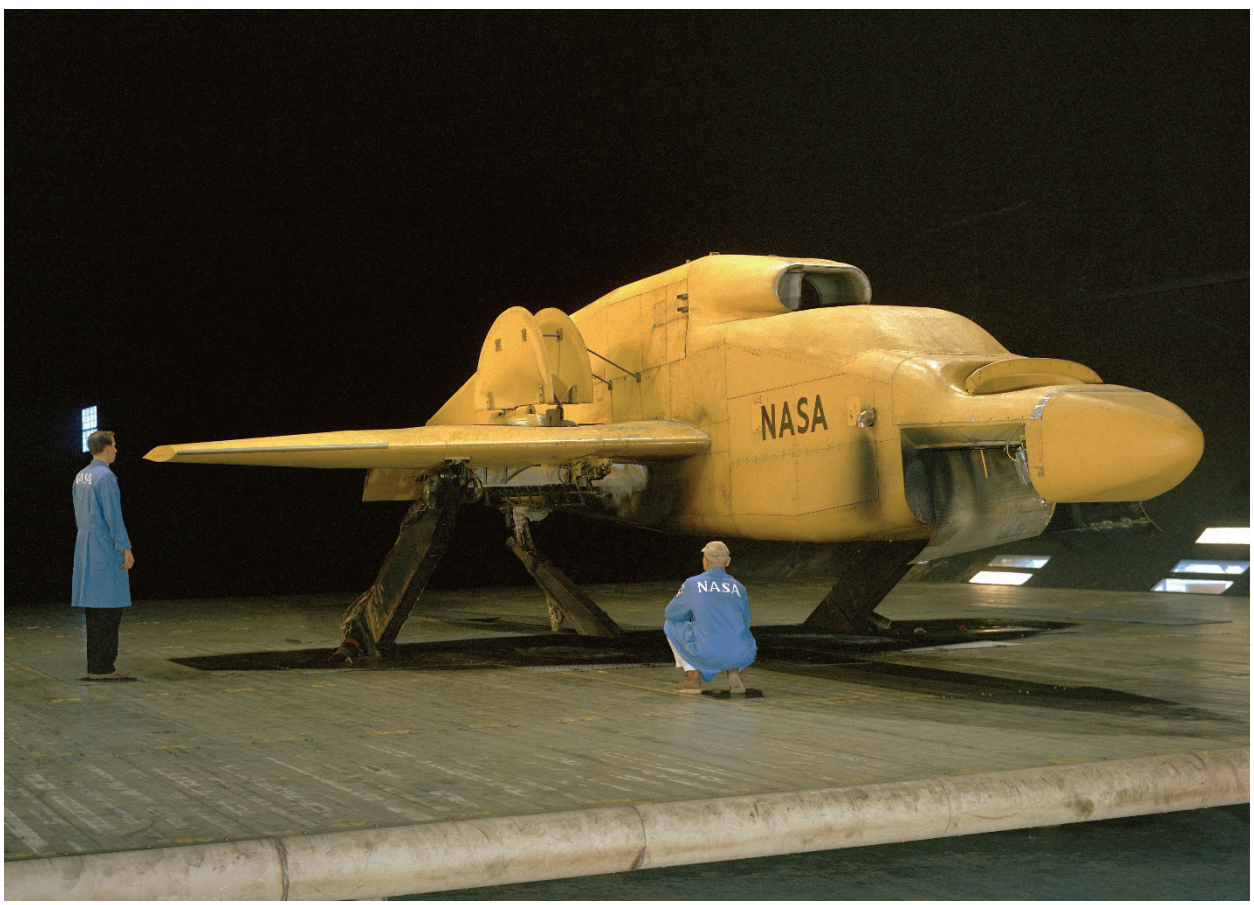

Figure 153. VZ-11 lift-fan-in-wing model on variable-height struts for ground-effect tests. ***(NASA AC-30211)***

Testing of the VZ-11 provided valuable design information for stability and control and construction of the XV-5A. Two test-aircraft were constructed by Ryan Aircraft. A stipulation in the contract was that one of the aircraft would be wind tunnel tested prior to flight-testing, which was to be done at Edwards Air Force Base. One of the aircraft arrived by barge at Ames in April 1964 and was prepared for testing in May 1964. During the wind tunnel testing (Fig. 154, Test 210), the XV-5A aircraft displayed (for the most part) the handling qualities exhibited by the VZ-11 model [231].

A minor difference between the model and the aircraft was insufficient turning of the fan inflow over the wing into the lift fans. Considerable time was consumed in the tunnel attempting to remedy this problem with limited success. Data from the wind tunnel test program were used extensively to provide simulation algorithms for the transition from fan-borne hover to wing-borne cruise flight. This was a major concern because the transition control was a "bang-bang" affair—that is, with the diverter valves moving from one method of flight to the other in less than 3 seconds.

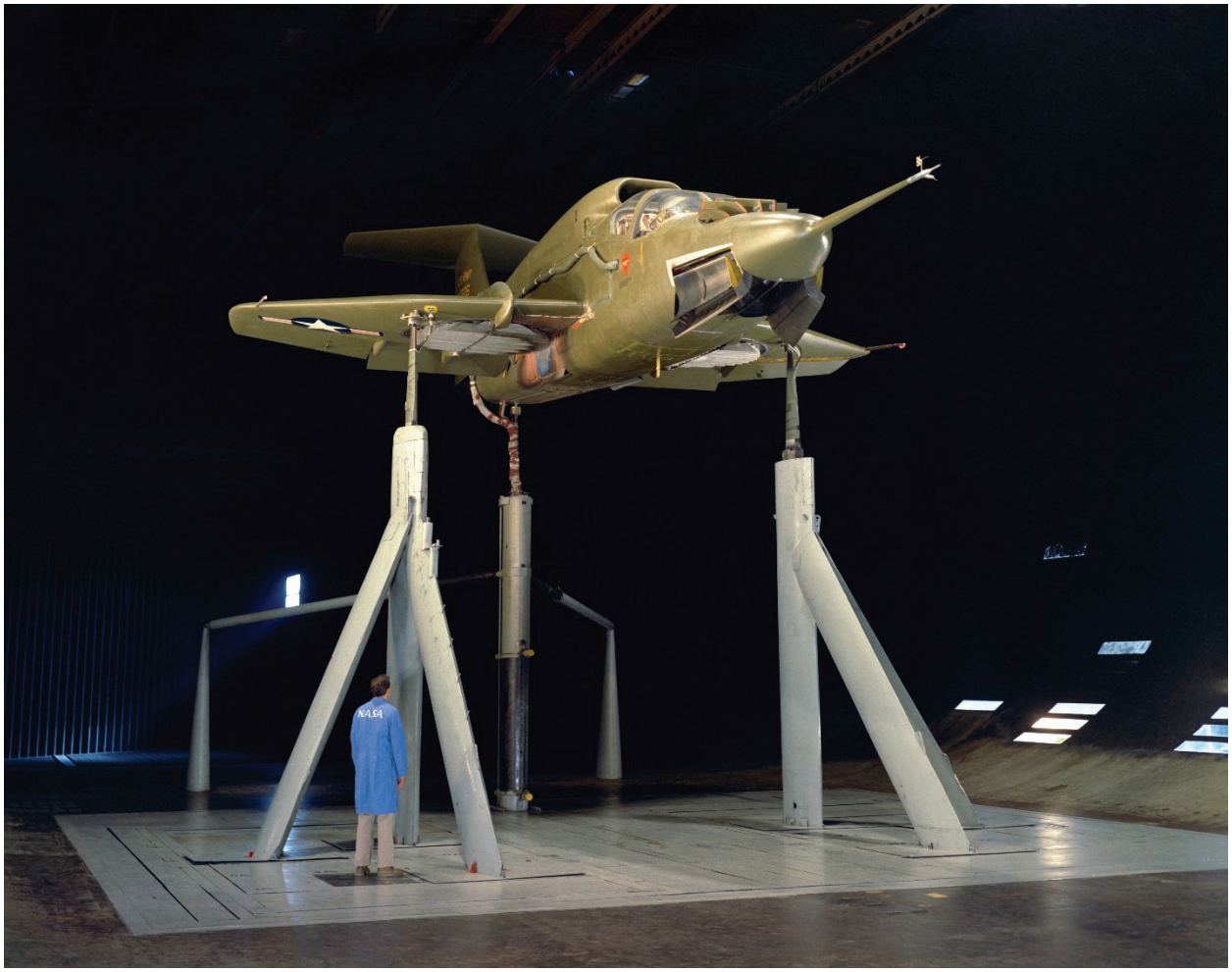

Figure 154. Three-quarter front view of the XV-5A fan-in-wing experimental aircraft; note the fan in the nose of the airplane for pitch control at hover and low speeds. ***(NASA A-32745)***

The flight-test program at Edwards Flight Research Center was not successful; both aircraft crashed and two pilots were killed. The second aircraft was salvaged and returned to Ryan to be modified as the XV-5B; modifications were based on the wind tunnel testing and flight-testing results. This aircraft was transferred to NASA, and after wind tunnel testing (Fig. 155, Tests 406 and 445) it underwent a long and successful flight-test program at Ames Research Center.

This aircraft is presently on display at the U.S. Army Aviation Museum, in Fort Rucker, Alabama.

Figure 155. XV-5B fan-in-wing prototype V/STOL fighter. ***(NASA AC72-3530)***

Subsequent to the XV-5A program, lift-fan research was judged a viable and attractive method for vertical and short field aircraft, both for the military and for civil applications. The majority of the research was conducted in-house with vigorous support from branch and division management. Woodrow Cook, Mark Kelly, and David Hickey were strong advocates and offered critical support for lift-fan research.

Three jet-engine tip-driven lift-fan systems were used in the research effort: the X353-5B, the X376-B, and the LF336. The X376-B and LF336 had a diameter of 36 inches and design pressure ratios of 1.1 and 1.3, respectively. The X353-5B had a rotor diameter of 62.5 inches and a design pressure ratio of 1.1. The fans were driven by either J-85 or T-58 turbojets. One T-58 propelled one X376 fan. One J-85 propelled one X353-5B, one LF336, or four X376-B fans. It was fortunate that surplus Army and Air Force engines (J-85 and T-58) were available in sufficient numbers for this research. (The surplus engines were ideal for wind tunnel models because they had enough life left for the wind tunnel experiments, yet they were no longer suitable nor acceptable for flight.)

Lift-fan and lift-cruise-fan transports. Many transport configurations were explored with fan-in-wing lift fans. Lift fans and lift-cruise fans were studied on a transport model with lift fans mounted forward of the wing in three different locations and rotating lift-cruise fans located aft of the wing on either side of the fuselage (Figs. 156 and 157; Tests 301, 309, 325, 359).

The lift increase due to fan-flow interaction with the aircraft's flow field was found to be a small percentage of the installed fan thrust, but it was adequate to provide significant increases in payload for simulated STOL operation. Isolated fan operation could cause either large positive or negative induced wing-lift depending on the forward-fan location. The overall induced lift was positive with all lift fans operating. Longitudinal trim requirements of both complete configurations were moderate. Both configurations were directionally unstable over a portion of the transition speed range [232].

One model had six LF-376B lift fans mounted in the wing and engines mounted forward of the wing on the fuselage (Figs. 158 and 159). Combinations of two, four, and six fans were investigated as well as two chordwise positions of the fans in the wing to determine the interaction of the fan-flow field with the airframe flow field. The effects of operating two engines forward of the wing in conjunction with six fans operating had generally acceptable aerodynamic characteristics [233].

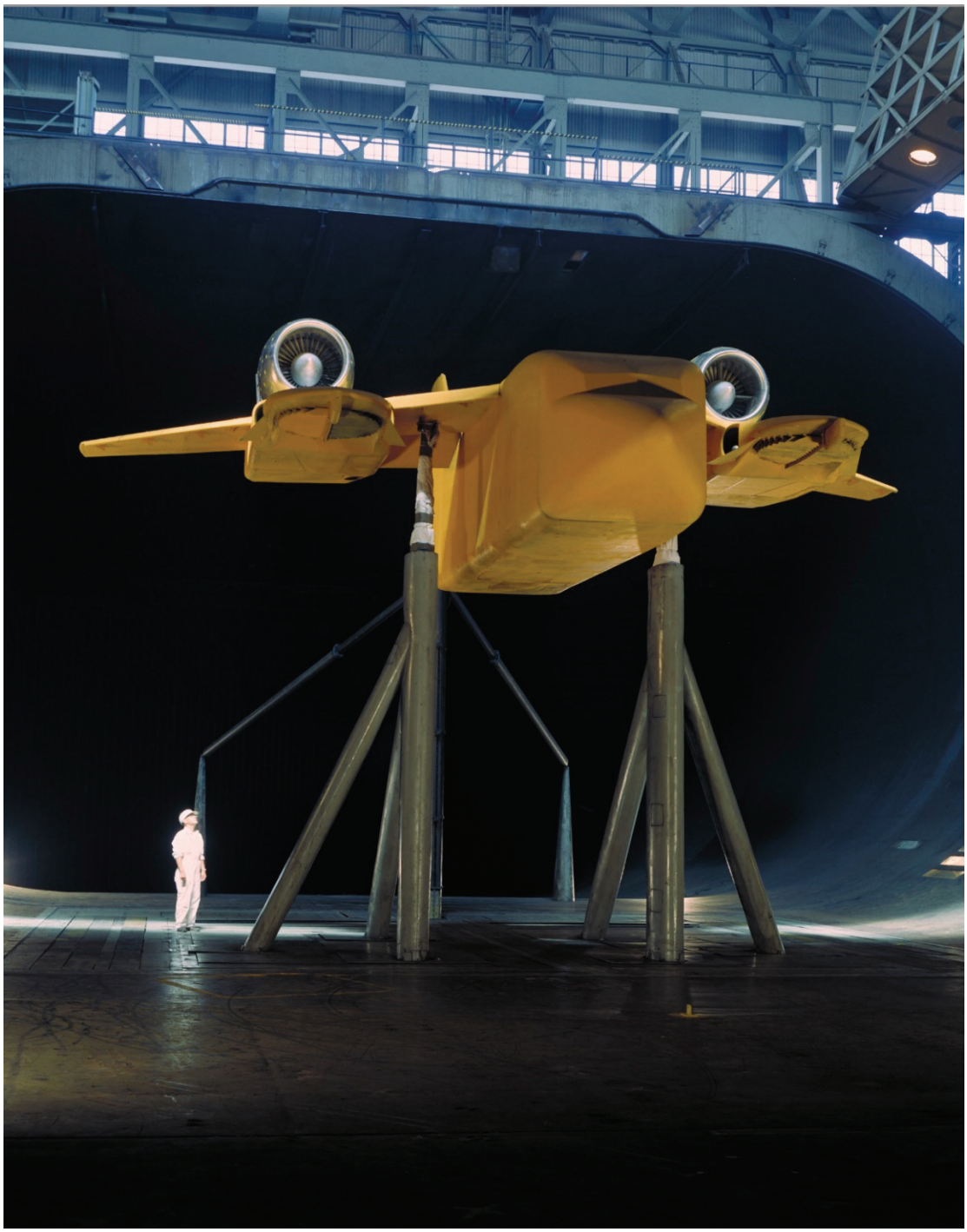

Figure 156. High-wing transport model with lift fans and lift-cruise fans. ***(NASA AC-41550)***

Figure 157. Low-wing transport model with lift fans forward of wing. ***(NASA AC70-1604)***

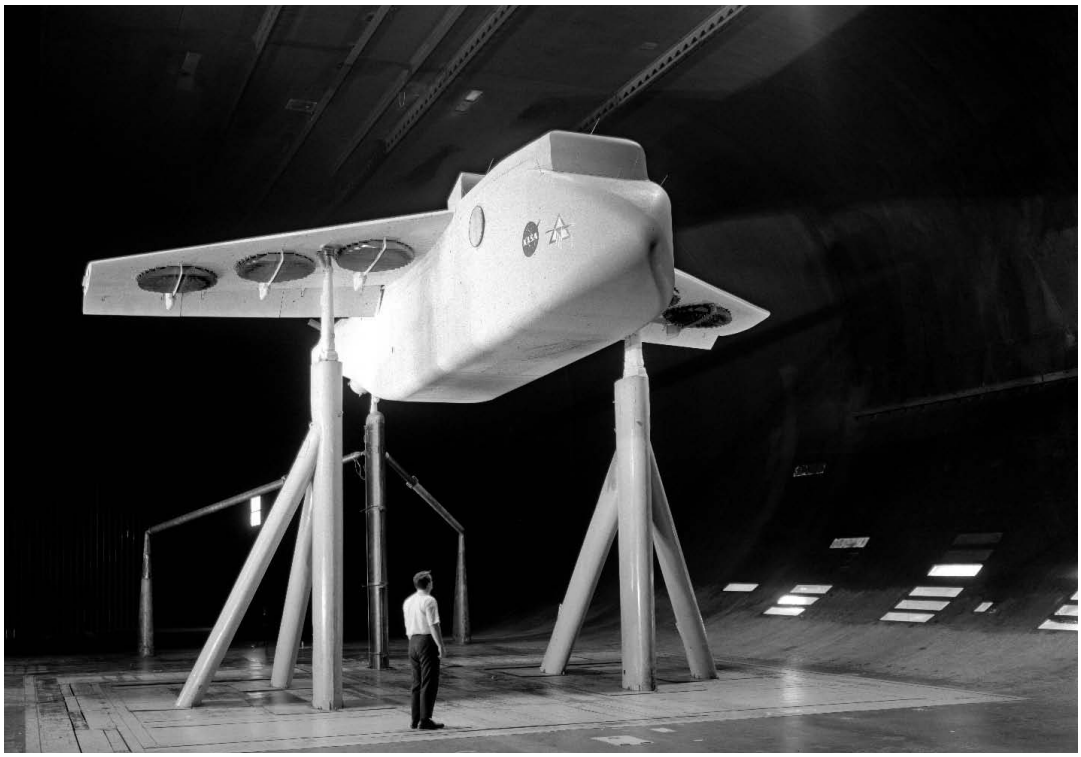

Figure 158. Three-quarter front view of a lift-fan transport model with six wing lift fans.
(NASA A-37161)

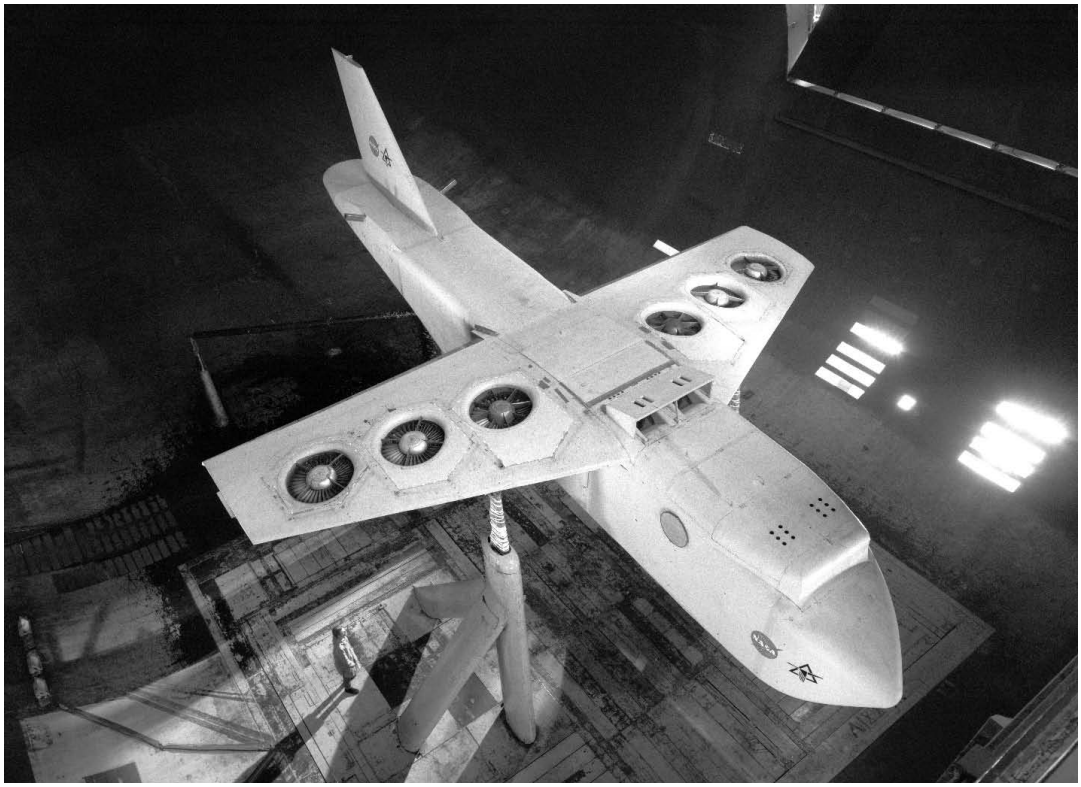

Figure 159. Overhead view of a lift-fan transport model with six wing lift fans.
(NASA A-37207)

Studies also explored the possibilities of modifying existing transports by adding lift fans. One such configuration is shown in Figure 160. The concept was to add lift fans to a DC-9 aircraft to achieve STOL performance. Previous large-scale studies conducted in the 40- by 80-Foot Wind Tunnel investigated the aerodynamic and propulsion system performance of fan-in-wing, fan-in-fuselage, and podded-fan configurations. Lift-fan configurations for the most part have had shallow fan inlets (e.g., XV5A/B), which may give poor inlet performance. The subject model had two fans mounted side-by-side in the nose section of the fuselage (Fig. 160, Tests 359 and 392). This permitted a reasonably deep inlet on the inboard side of each fan while the outboard side had a fairly shallow inlet. Lift-cruise fans were installed on the aft section of the fuselage, which was a representative commuter-transport configuration. Hood-type deflection ducts were used to turn the fan flow from the cruise direction to the lift direction for STOL performance. Four X-376B lift fans were propelled by four T-58 gas generators. The test results are presented in reference [234]. Results showed that podded lift-fan configurations can produce induced lift approaching the magnitude of the better fan-in-wing configurations while significantly reducing the variation in pitching moment with forward speed. The results also showed that significant overload STOL operation would be very attractive.

Lift-fan fighters. Figures 161 and 162 show lift fans mounted in a 5-percent-thick wing of a supersonic fighter model. Normally lift-fan depth required a maximum wing thickness of about 10 percent of the wing chord. Research was subsequently conducted on a thinner version of the X353-5 lift fan, which included removing the fan stator blades (Test 301). The lift fans were completely enclosed within the wing with the exception of the fan hub that, because of mechanical complexity, was not modified to fit within the wing's contour. The fan inlet was modified by removing the conventional bell-mouth-inlet and circular-inlet guide vanes from the outboard 180 degrees of the fan. This inlet section was then replaced by an inlet section of varying radii that blended with the local contours of the wing. A blowing nozzle for BLC was incorporated into the inlet to prevent flow separation. Results showed that BLC applied to the fan inlet substantially increased fan thrust, indicating a reduction of inlet flow separation, and a subsequent improvement in total-pressure recovery. The effects of fan operation on model performance showed no large adverse deviations from general delta-wing characteristics, therefore V/STOL capability provided by lift fans for this supersonic configuration appeared feasible [235].

Figure 160. STOL transport model with lift fans and cruise fans. ***(NASA AC75-1002)***

Figure 161. Three-quarter front view of lift fans in a 5-percent-thick wing of a supersonic fighter model. ***(NASA A-37808)***

Figure 162. Rear view of a wing lift-fan model with a 5-percent-thick wing. ***(NASA A-37809)***

Figures 163 and 164 show the front and rear views of a lift/cruise-fan fighter. Flow was deflected downward to produce lift with a nozzle evident in the rear view, and then the nozzle was retracted to produce thrust for cruise. The lift fan in the nose of the airplane required to produce pitching moment is evident in the front view.

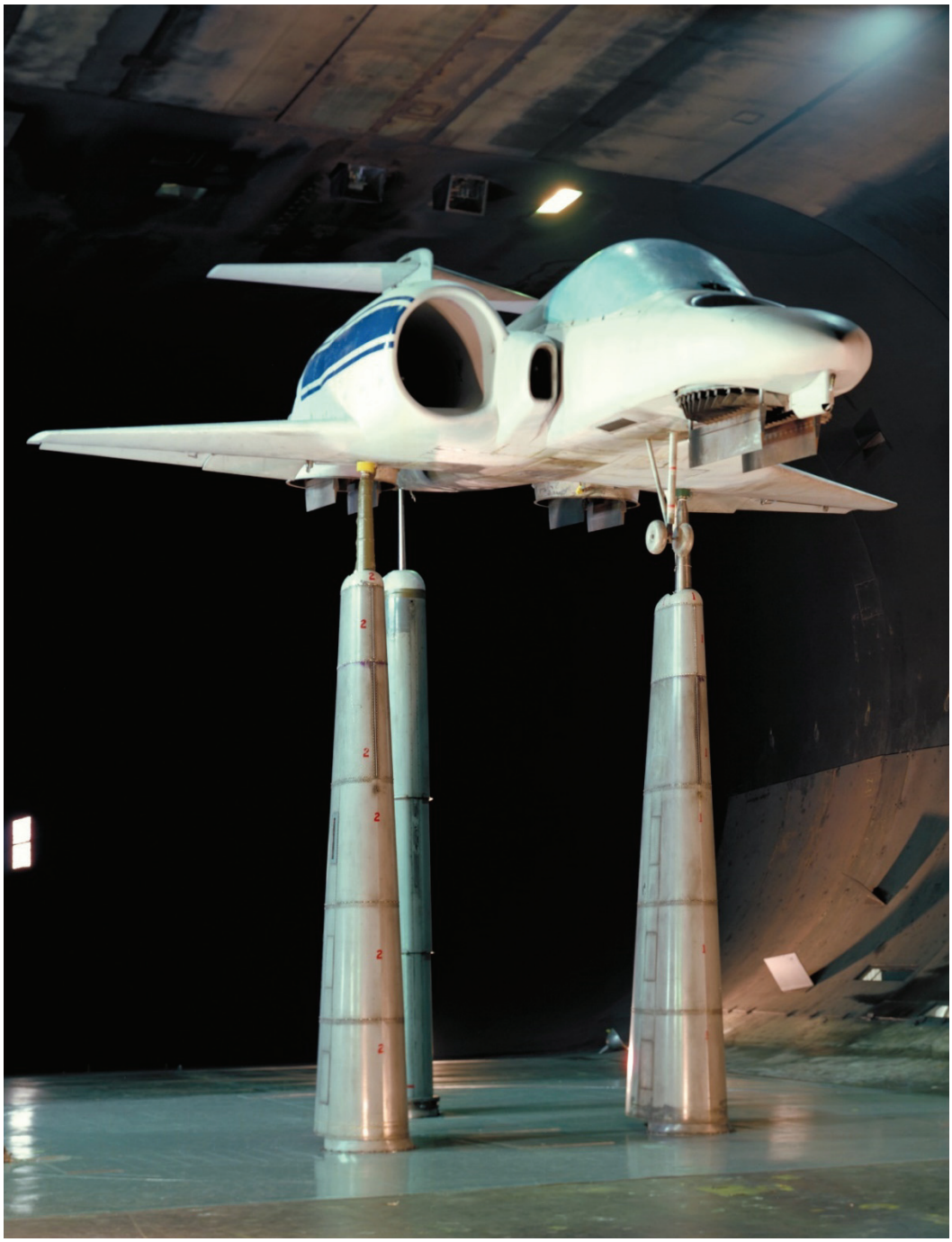

Figure 163. Three-quarter front view of lift/cruise-fan fighter. ***(NASA AC 76-1060)***

Figure 164. Three-quarter rear view of lift/cruise-fan fighter showing fan nozzle deflected downward. ***(NASA AC76-1061)***

Lift-fan pressure ratio. It was found that the 1.3-pressure-ratio lift fan (LF-336), based on installed thrust to weight and thrust to volume, was about optimum for maintaining an augmentation ratio of 2.5 (total aircraft lift divided by fan-alone lift). To determine the cross-flow performance of the 1.3-pressure-ratio fan, a semispan model was employed (Fig. 165), and the fan was placed in the same location as a previously tested 1.1-pressure-ratio fan. The tests were conducted at equivalent velocity ratios to ensure comparable results. The 1.3-pressure-ratio-fan thrust did not decay significantly with forward speed, and it performed slightly better than the 1.1-pressure-ratio fan over the entire velocity range. The highly loaded, 1.3-pressure-ratio fan was tested over a large velocity range and model angle-of-attack range; it stalled only once during a test specifically programmed to induce lift-stall, and the stall occurred well beyond the velocity ratio ranges typically required for transition from hover to forward flight [222], (Test 371).

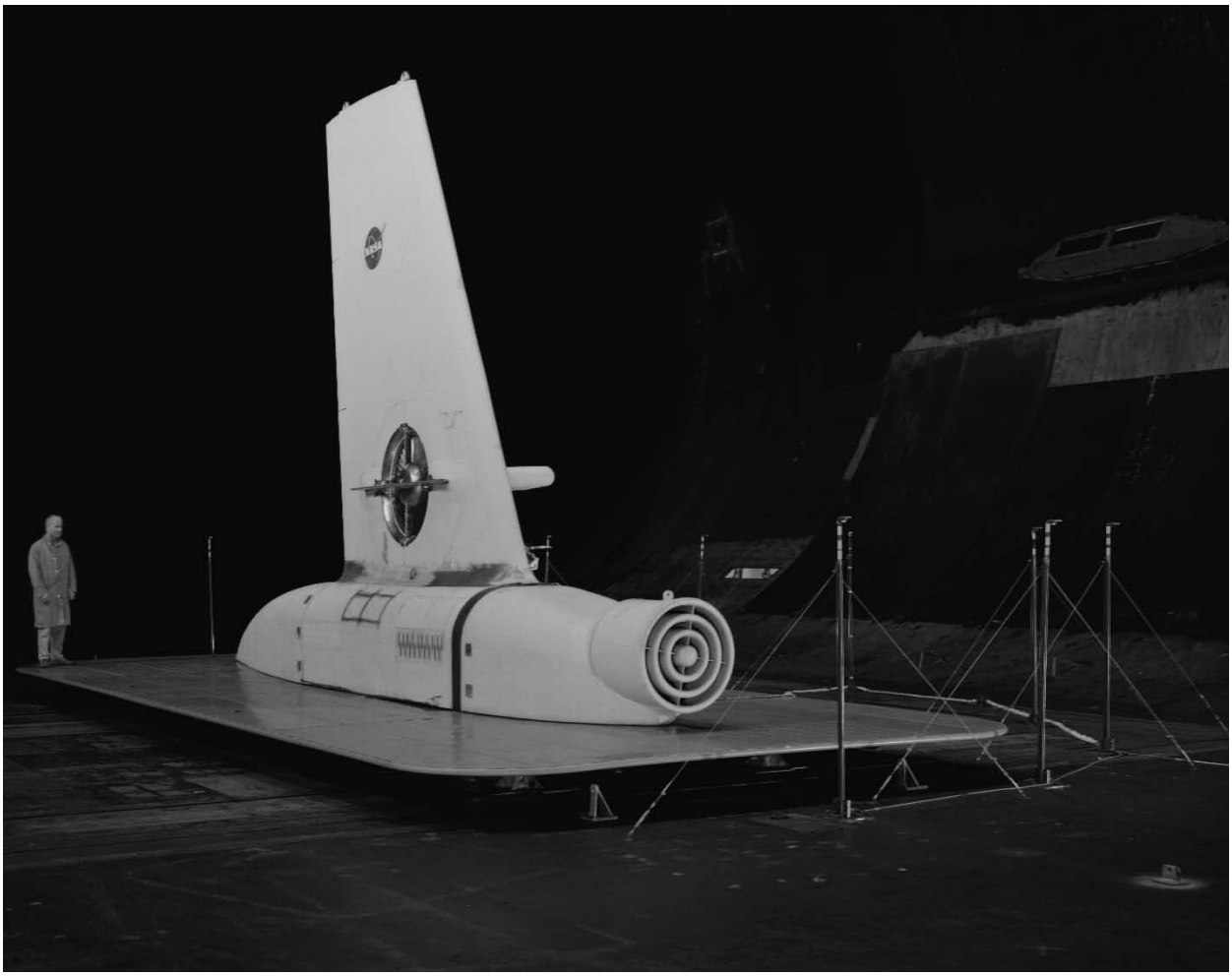

Figure 165. Quiet lift-fan (1.3-pressure-ratio) semispan model with mechanic Ray Schmoranc in photo.
(NASA A70-4654)

Lift-fan applications. It was found that lift-fan aircraft are competitive throughout the powered-lift spectrum, i.e. STOL, VTOL, V/STOL, and short takeoff and vertical landing (STOVL) [223]. They are applicable to supersonic aircraft, fighters and subsonic aircraft, civil and military aircraft, transports, and personal aircraft. The lift-fan research conducted in the 40- by 80-Foot Wind Tunnel over a prolonged period of time is a tribute to the vision of NASA, and to the many engineers and craftsmen associated with the 40- by 80-Foot Wind Tunnel who made it possible.

Low-disk-loading fan-in-wing model: Vanguard Omniplane. The Vanguard Omniplane fan-in-wing VTOL was a low-disc-loading (12 psf versus greater than 200 psf for the above lift fans) fan-in-wing experimental aircraft that had structural issues but had the potential to produce useful research data contributing to understanding the effects of disk loading. Low-disc-loading fans have to be larger in diameter than high-disc-loading fans (higher pressure ratio) to produce the same lift, however low-disk-loading fans produce lower jet velocities and higher efficiency (thrust per power) at hover, which would be desirable for some applications that require prolonged hovering and lower-downwash velocities. Vanguard Air and Marine Corporation designed and built the Model 2C Omniplane that used a 265-hp Lycoming engine. Wing compliance of the model was excessive and the fan-tip clearance was several inches, which would cause a significant reduction in thrust. The fans were 6 feet in diameter and had three blades with flapping hinges. Louvers were used to close off the fans during conventional horizontal flight, and a 5-foot ducted fan was used for propulsion. The Ames model shop was tasked with filling the space inside of the ducts to reduce the tip clearance to improve performance prior to the wind tunnel tests. The tunnel tests were performed (Figs. 166 and 167, Tests 140 and 159) [219], and it was found that the model was underpowered. Comparisons with above fan-in-wing data indicated that the change in lift, drag, and moment with speed is more pronounced for low-disk-loading configurations. After the wind tunnel tests, the airplane was extensively modified. It was repowered with an 860-hp Lycoming turboshaft engine, and the nose was extended so that a lift fan could be added. The aircraft was redesignated as Model 2D. This version of the aircraft was tested in the tunnel in early 1962. Ground trials were performed, but the aircraft was never flown.

Figure 166. Three-quarter front view of the Vanguard Omniplane low-pressure-ratio fan-in-wing experimental aircraft with engineer Ralph Maki in photo. ***(NASA A-26189)***

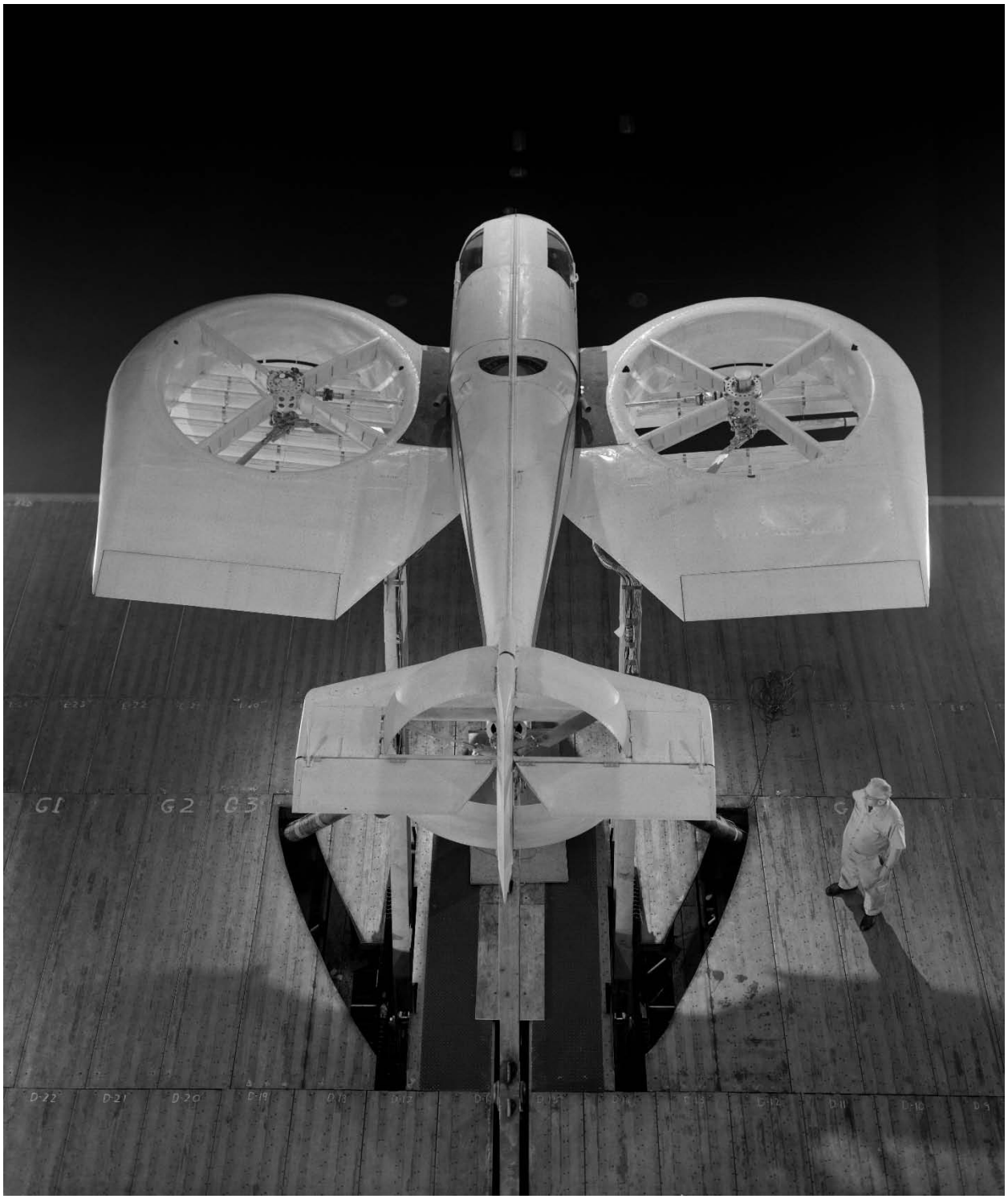

Figure 167. Overhead view of the Vanguard Omniplane fan-in-wing experimental aircraft.
(NASA A-26192)

Generic lift-engine research. Lift-engine research was conducted in the late 1960s and early 1970s. During these tests, exhaust gas ingestion into the engine inlets during hover and engine-inlet flow distortion were studied using a large-scale generic lift-engine fighter model powered by J-85-5 turbojet engines [236] (Tests 219 and 225). Exhaust gas ingestion during hover was tested on a static-test facility in free air, while inlet flow distortion and total pressure loss were measured at forward speeds in the 40- by 80-Foot Wind Tunnel. These tests included internally fixed and swiveling, retractable arrangements of the lift engines (Figs. 168 and 169; Tests 281, 287, and 308). Three different lift-engine exhaust nozzles were studied: conical, bifurcated, and slotted. They were examined for the internally fixed engine configuration and did have different effects on hover inlet temperature rise and thrust loss.

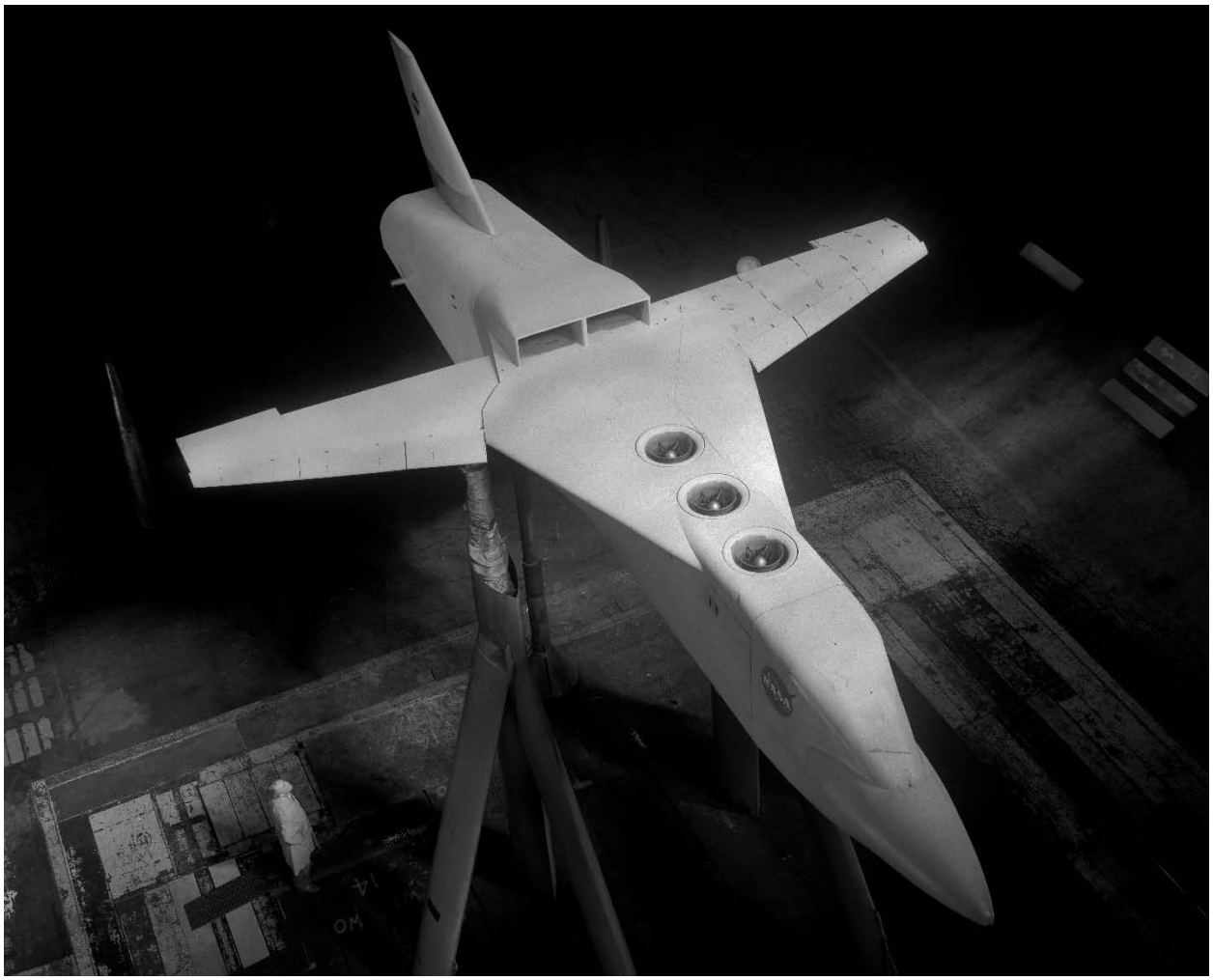

Figure 168. Overhead view of lift-engine model with three engines in fuselage. ***(NASA A-38524)***

Figure 169. Three-quarter front view of lift-engine model showing exhaust louvers. ***(NASA A-38534)***

It was found in references [224] and [236] that the effects of exhaust vectoring on temperature rise and thrust loss with the swiveling, retractable configuration indicated that the largest temperature rise, and loss of thrust and lift in ground effect, occurred with the thrust angle 90 degrees from horizontal (hover mode). Vectoring the lift engines to a small forward angle and the rear lift engines aft from vertical to balance the aircraft would alleviate exhaust gas ingestion and thrust loses. The aircraft could take off and land with decelerating approaches surrounded by exhaust but relatively free of ingestion effects and losses.

All configurations tested, both swiveling and internally fixed lift engines, experienced excessive thrust loss and compressor stall when the thrust was vectored 90 degrees from horizontal. Of the three exhaust nozzles with the internally fixed lift engines, the slotted nozzles produced somewhat lower temperature gradients and average inlet temperatures and less lift loss than the conical or bifurcated nozzles, but at angles of 80 to 90 degrees to the horizontal, engine stall occurred regardless of the exhaust nozzle installation.

Bell Aircraft X-14. The X-14 was an experimental V/STOL aircraft powered by two GE J-85 jet engines. There were movable vanes in the jet exhaust that could control the direction of the jet exhaust to achieve VTOL and transition to forward flight. Reaction controls were used for aircraft control at hover and low forward speeds. The X-14 was extensively used as a flying simulator; the control system could be reconfigured to allow study of flying qualities criteria for specifications for different V/STOL aircraft. To support the flight-tests, experiments were performed in the wind tunnel at 0 degree yaw angle (Fig. 170, Test 290) and 90 degrees yaw angle (Fig. 171, Test 289). The aircraft was flown for many years until it crashed in May 1981. The pilot was not injured, but the aircraft was not repaired. Years later it was restored for display by the Ropkey Armor Museum in Crawfordsville, Indiana.

McDonnell Douglas AV-8B Harrier II. The AV-8B was an extensively modified Harrier AV-8A. It had a larger wing, a more powerful Rolls-Royce Pegasus engine, improved engine inlets, an elevated cockpit for improved pilot visibility, and a redesigned fuselage. The original Harrier was built by Hawker Siddeley, a group of British manufacturing companies. Vertical lift was achieved by the special Pegasus engine that had four synchronized vectorable nozzles—two in the front and two at the rear of the aircraft. The nozzles were directed downward to produce vertical lift. The aircraft also had smaller valve-controlled nozzles in the nose, tail, and wingtips to provide control at low airspeeds. Investigations were performed in the 40- by 80-Foot Wind Tunnel in August and September 1976 (Figs. 172 and 173, Test 493). The modified Harrier was a successful aircraft used extensively by the Marines. Approximately 340 were built.

Figure 170. Bell lift-jet X-14 aircraft at zero sideslip in tunnel. ***(NASA A-38814)***

Figure 171. Bell X-14 at 90 degrees sideslip in tunnel. ***(NASA A-38761)***

Figure 172. Three-quarter front view of the McDonnell Douglas AV-8B Harrier II lift-jet V/STOL aircraft.
(NASA A76-1269-9)

Figure 173. Three-quarter rear view of the McDonnell Douglas AV-8B Harrier II lift-jet V/STOL aircraft.
(NASA A76-1269-10)

Highly maneuverable supersonic V/STOL fighter. A model of a highly maneuverable, supersonic V/STOL fighter was built in the NASA Ames Research Center shops and then studied in the 40- by 80-Foot Wind Tunnel. Interest in military application of V/STOL technology had revived in the 1970s, but there were technology uncertainties, especially at low speeds, that persisted; the model was designed and built for low-speed studies to address those uncertainties. It had a 24-foot wingspan and was powered by two J-97 turbojet engines (Figs. 174 and 175, Test 537) representing approximately a 0.7-scale model. The model combined upper surface blowing (USB) and spanwise blowing to improve the lift characteristics over a wide angle-of-attack range. The model used a close-coupled canard to create a highly maneuverable aircraft. The model was designed to be adapted to different V/STOL propulsion concepts. Lift coefficients greater than 4 were achieved, and spanwise blowing delayed wing stall [237].

Vertical attitude takeoff and landing (VATOL) fighter. There was renewed interest by the Navy in jet-powered tail-sitter aircraft because they tend to be simpler than normal (horizontal) attitude VTOL aircraft, and modern fighters have sufficiently high thrust for vertical takeoff. A special retrieval system for ships was proposed that was intended to reduce the pilot landing and takeoff workload that had been the problem with previous proposed tail-sitter aircraft. Fighter aircraft were being developed with thrust-to-weight ratios greater than 1, so fighter aircraft had enough thrust to take off vertically in a vertical attitude. An additional advantage of fighter aircraft with thrust-to-weight ratios greater than 1 is improved combat maneuverability. Experiments were performed in the 40- by 80-Foot Wind Tunnel on a sting-mounted 0.38-scale model (Fig. 176). Twelve-inch fans were used to simulate the engines. A report describing the advantages of VATOL and the planned experiments in the 40- by 80-Foot Wind Tunnel was produced [238].

Figure 174. Three-quarter front view of a highly maneuverable, supersonic V/STOL fighter model.
(NASA AC79-0110-1)

Figure 175. Three-quarter rear view of a highly maneuverable, supersonic V/STOL fighter model.
(NASA AC79-0110-2)

Figure 176. VATOL fighter model mounted sideways on a sting so it could be rotated in horizontal plane to increase the angle of attack to high values. ***(NASA AC80-0623-1)***

Ducted Fans

Several ducted fan models were studied in the 40- by 80-Foot Wind Tunnel. Ducted fans have a smaller diameter than propellers for the same static-thrust-to-horsepower ratio, however the duct drag is a penalty at relatively high forward speeds. On the other hand, the duct can serve as a safety shield and can be used to house noise-attenuation treatment.

Collins Lippisch Aerodyne. The Collins Lippisch Aerodyne VTOL was an invention of Alexander M. Lippisch, who was very imaginative and proposed many very unusual aircraft configurations [239]. Lippisch's career spanned working in Germany from 1919 through World War II and in the U.S. from 1946 to 1975. The Aerodyne was essentially a very large duct with a couple of propellers inside. It was initially intended to be a flying experimental aircraft. It had exit vanes that were arranged at about a 45-degree angle. The vanes could be deflected downward to produce vertical lift or deflected rearward to produce thrust. Çollins ran out of government funding so the aircraft was finished with wood beams and fabric covering—essentially like a scaled-up model airplane. It was mounted on the variable-height struts in the tunnel (Fig. 177, Test 139). The aircraft was found to be underpowered [240]. During the wind tunnel testing one of the Ames test pilots, Fred Drinkwater, was asked if he would be willing to fly the aircraft. His reply was that it needed a few more rubber bands—it did indeed.

Doak VZ-4DA. The VZ-4DA had 4-foot-diameter ducted fans mounted on the wingtips. The fans had eight blades. There were initially seven inlet guide vanes and nine stator blades and an exit vane to augment pitching-moment control. The ducts were positioned for hover (90 degrees) and then rotated forward for transition to forward flight. The pressure ratio of the fans was low; it was on the order of 1.03.

A 4-foot-diameter ducted fan from the Doak VZ-4DA airplane was studied in the tunnel mounted on a wingtip as a semispan model. The model was assembled with a fan mounted on the tip of a semispan wing panel that was identical to the airplane wing (Fig. 178, Test 132). The ducted fan was driven by an electric model motor at the base of the wing. At certain transition conditions the flow on the duct lip, which would be the lower lip in flight, would separate causing poor fan inflow, a decrease in fan thrust and duct lift, and a significant increase in noise [241-243]. The separation boundary was defined during the wind tunnel tests. The flow would also separate on the outside of the upper lip, but it was hardly perceptible and did not significantly affect fan performance nor cause an increase in fan noise. Based on the experimental results, predictions indicated that the aircraft could accomplish level, 1-g transition from hover to forward flight with some lip-stall margin. These results were verified during flight-tests. To improve the duct-lip stall margin for descent cases, the exit vane was used. The exit vane allowed the duct to be set at lower angles with respect to the horizon [241].

The airplane used seven variable-angle inlet guide vanes to vary thrust for roll control. Later, the effect of double the number of inlet guide vanes was also studied in the tunnel as a potential modification to increase airplane roll control. As expected, the increased number of inlet guide vanes would increase the roll-control moment of the airplane [241].

Figure 177. Collins Lippisch Aerodyne VTOL model on variable-height struts with Dave Koenig in photo. Front propeller in duct can be readily seen. ***(NASA A-26150)***

Figure 178. Doak VZ-4DA 4-foot-diameter ducted-fan semispan model. ***(NASA A-25140)***

The airplane used engine exhaust through a vaned duct exit at the tail for pitch and yaw control at hover and low speeds. In addition, the airplane had a conventional tail for control during conventional forward flight. The airplane and ducted fans were exceptionally well made by Doak—the quality was notable in comparison with most of the V/STOL aircraft of the era. The Doak VZ-4DA was one of the more successful early VTOL aircraft and was a tribute to the small company.

Additional experiments were done with several duct exit-vane configurations in the 4-foot ducted fan for possible applications for helicopter tail rotors and other V/STOL configurations (Fig. 179, Test 166). The idea was to fix or minimize the duct rotation and deflect the exit vanes for side force or lift depending on the application [244]. The experiments were a success and defined the capability of several vanes sets. As expected, 90 degrees of flow turning with the exit vanes was not achieved nor was that the goal.

Figure 179. Four-foot-diameter ducted-fan semispan model with variable-exit-vane cascade.
(NASA A-28982)

Basic experiments were done to define the propulsive performance of the ducted fan. The fan had a fixed blade angle, but the blade angle could be changed by loosening the hub bolts and rotating each blade in the hub. It was modified for the tunnel tests with an index system so that each blade angle could be reliably set and its position repeated as required for the experiments. Basic performance of the ducted fan at zero angle of attack was determined [245].

Deflected slipstream ducted fan. Occasionally "amateur" inventors would visit the tunnel offices with new ideas for aircraft, and especially V/STOL aircraft, configurations. A notable visitor was Harlan D. Fowler who had invented the Fowler Flap that was used on most commercial aircraft. One set of discussions led to the testing of a semispan model with two ducted fans mounted on a wing with an external airfoil or flap that could be deflected about 90 degrees and lined up with a deflected triple-slotted wing flap system. It was intended that the deflected flaps and auxiliary wing would deflect the duct exhaust flow 90 degrees for vertical lift. Two of the 4-foot-diameter Doak ducted fans were used for the model (Fig. 180, Test 339). The model was tested with two ducted fans and a single ducted fan. It was found that the flow was not turned a full 90 degrees. The performance was comparable with other fan and ducted-fan models that used large-chord flap systems to turn the flow (deflected slipstream configurations). In addition, the externally mounted auxiliary flap would increase drag somewhat at cruise conditions [246].

Four-ducted-fan model. Four of the Doak ducted fans were used for a simulation of the Bell X-22A (57 percent scale), which was an experimental VTOL aircraft that used two ducted fans at the front and two at the rear of the fuselage. The front two ducted fans were mounted to the sides of the fuselage, and the rear two ducted fans were mounted to the tips of short wings. All four ducted fans could be rotated for transition from hover to forward flight. The model used the ground-adjustable-blade-angle Doak fans, but the X-22A used variable-pitch fans, and each ducted fan had an exit vane. The X-22A aircraft had four gas turbines mounted on top of the aft wing for redundancy, however the model ducted fans were powered by electric model motors. The model was used to predict performance as well as definition of the boundaries for duct-lip separation that would not necessarily match the stall boundaries of the X22A [247]. Ground-effect studies were also performed using this model (Fig. 181, Test 226) [248].

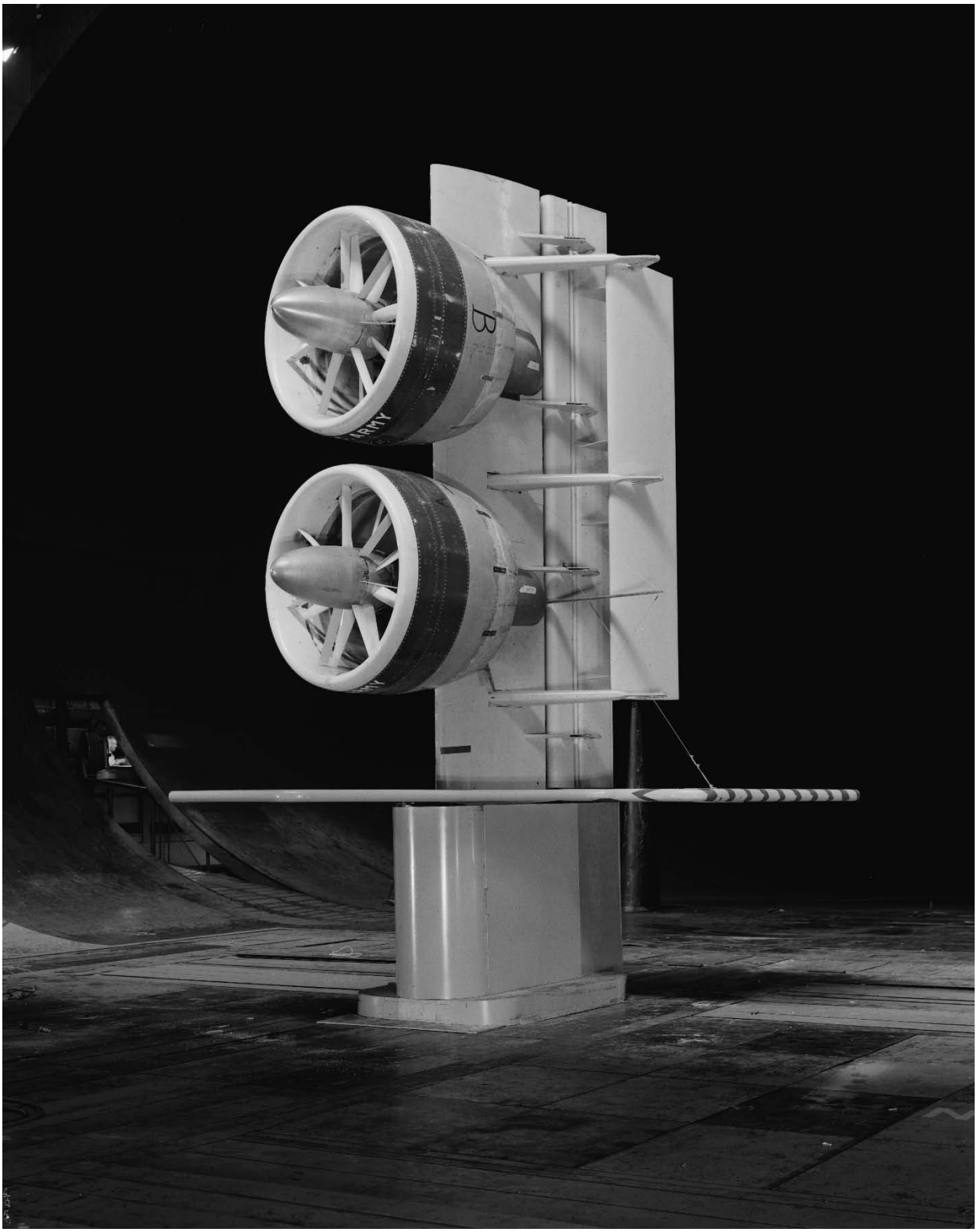

Figure 180. Deflected slipstream semispan model with two 4-foot-diameter ducted fans.
(NASA A-42303)

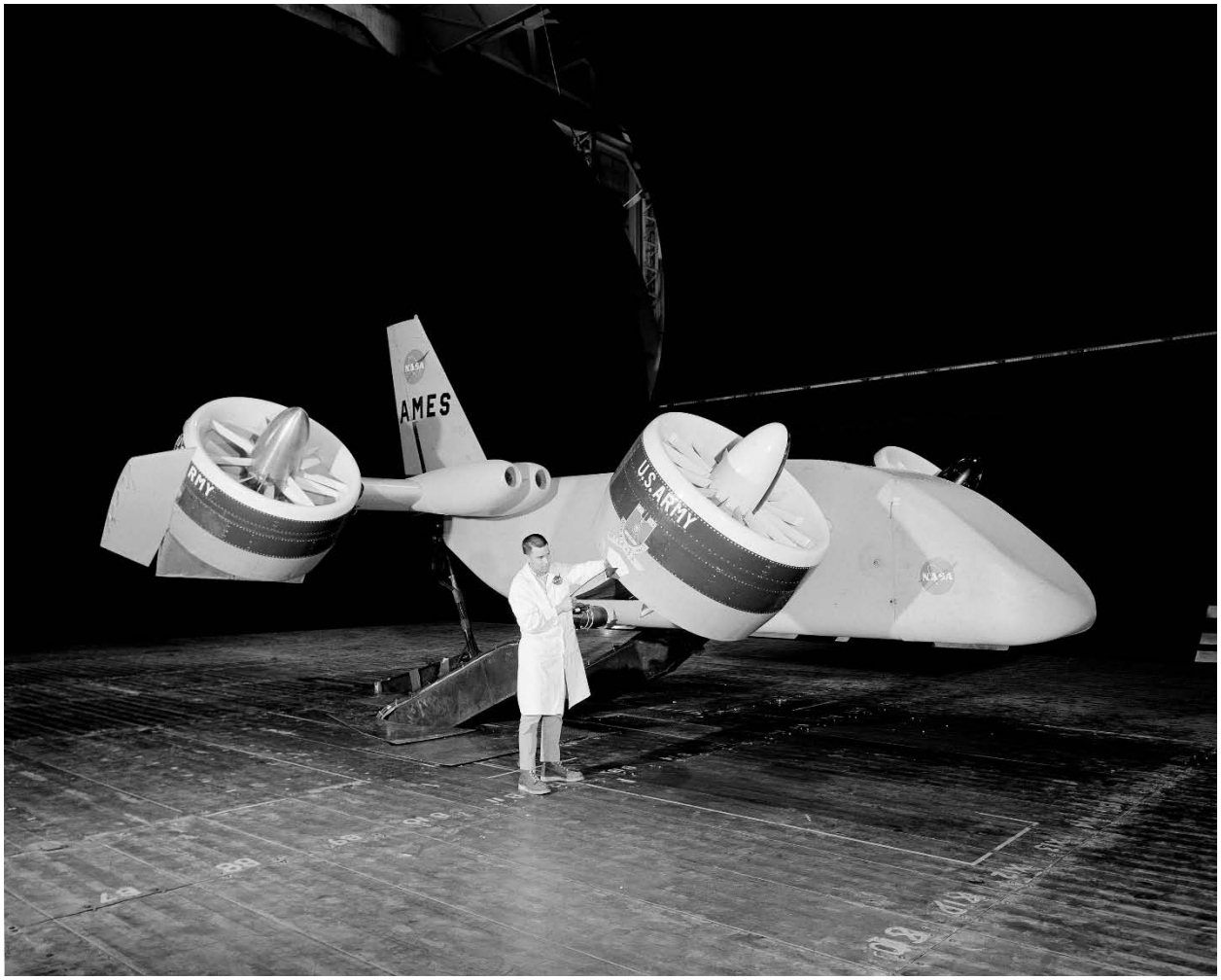

Figure 181. Four 4-foot-diameter ducted-fan wind tunnel model used to simulate the Bell X-22A VTOL airplane, shown on variable-height struts with Vic Bravo in photo. ***(NASA A-34112)***

X-22A ducted fan. A single, 7-foot-diameter full-scale Bell X-22A ducted fan was tested in a semispan arrangement in both the forward-fan configuration and the aft-fan configuration of the X-22A; that is, on the tip of a short wing (Fig. 182, Test 212). The three-bladed fan had variable pitch. The duct had an exit vane for pitching-moment control. Duct-lip separation boundaries were defined [249]. Some experiments were performed with vortex generators mounted to the upstream duct lip (lower lip for the airplane) to delay flow separation and improve the duct-lip stall-margin during descending transition flight of the aircraft (Fig. 183, Test 282). The vortex generators were successful in delaying flow separation. The aerodynamic characteristics from the four-ducted-fan model and the single, full-scale ducted-fan model were used to predict flight and transition characteristics for the X-22A aircraft. The wind-tunnel-based predictions were very close to the actual transition flight conditions for the airplane.

The Bell X-22A airplane was able to perform level, 1-g transitions from hover to forward flight and with a reasonable duct-lip flow-separation margin. It was one of the more successful early VTOL experimental aircraft.

Figure 182. Bell X-22A 7-foot-diameter ducted-fan semispan model with Chuck Greco in photo checking the blade angle. ***(NASA A-32844)***

Figure 183. Bell X-22A 7-foot-diameter ducted fan with vortex generators on upstream duct lip (left side) with Mike Falarski in photo. ***(NASA A-38036)***

Lift-cruise fans. Studies were performed on a full-scale ducted lift-cruise fan with a pressure ratio of about 1.1 and a fan diameter of 62.48 inches. The fan was tip-turbine driven by a turbojet engine enclosed in a nacelle mounted on top of the ducted fan. The fan was fixed pitch, but the internal duct area could be varied by changing the diameter of the centerbody. The angle of attack ranged from –4 to 80 degrees. The ducted fan was designed for V/STOL aircraft with high subsonic-cruise-speed ranges of 0.6 to 0.8 Mach number [250]. Boundaries for stall of the lower duct lip were established similar to what had been done for the 4- and 7-foot-diameter ducted fans that had lower pressure ratios [251].

Grumman 698 tilt-nacelle V/STOL model. A full-scale powered model of a subsonic, tilt-nacelle V/STOL aircraft concept was tested in the 40- by 80-Foot Wind Tunnel and at the Outside Aerodynamic Research Facility (OARF). The model was tested at three ground heights at the OARF, i.e. 18 feet, 7 inches; 6 feet; and 4 feet, 2 inches (landing gear height). Figures 184, 185, and 186 show the model at both locations [252, 223].

Figure 184. Grumman 698 tilt-nacelle V/STOL model during outside static testing. ***(NASA AC80-0455-6)***

Figure 185. Grumman 698 tilt-nacelle V/STOL model with nacelles tilted upward about 60 degrees during outside static testing. ***(J. Sacco collection, tilt_nacelle)***

Although the aircraft could be trimmed over the transition range, large nose-up pitching moments reduced the control available for maneuvering to about half of what was determined as acceptable. This trim problem was mainly caused by the shift in the c.g. location due to tilting the large nacelles. Another reason for the large pitching moment was due to the long inlet at the high position above the c.g. and to the large area of the unprotected wing center section over the fuselage between the nacelles. It was concluded that reducing the inlet length by 1 foot would reduce the pitch-up moment sufficiently to provide acceptable pitch-down control moments for maneuvering; however, during the ground-effect and inlet-ingestion tests at static conditions, the lack of ingestion and thrust losses were attributed in some degree to the high location and length of the inlet, and it was determined that any reduction of the inlet length would probably increase the ingestion problem at hover and low forward speeds during transition.

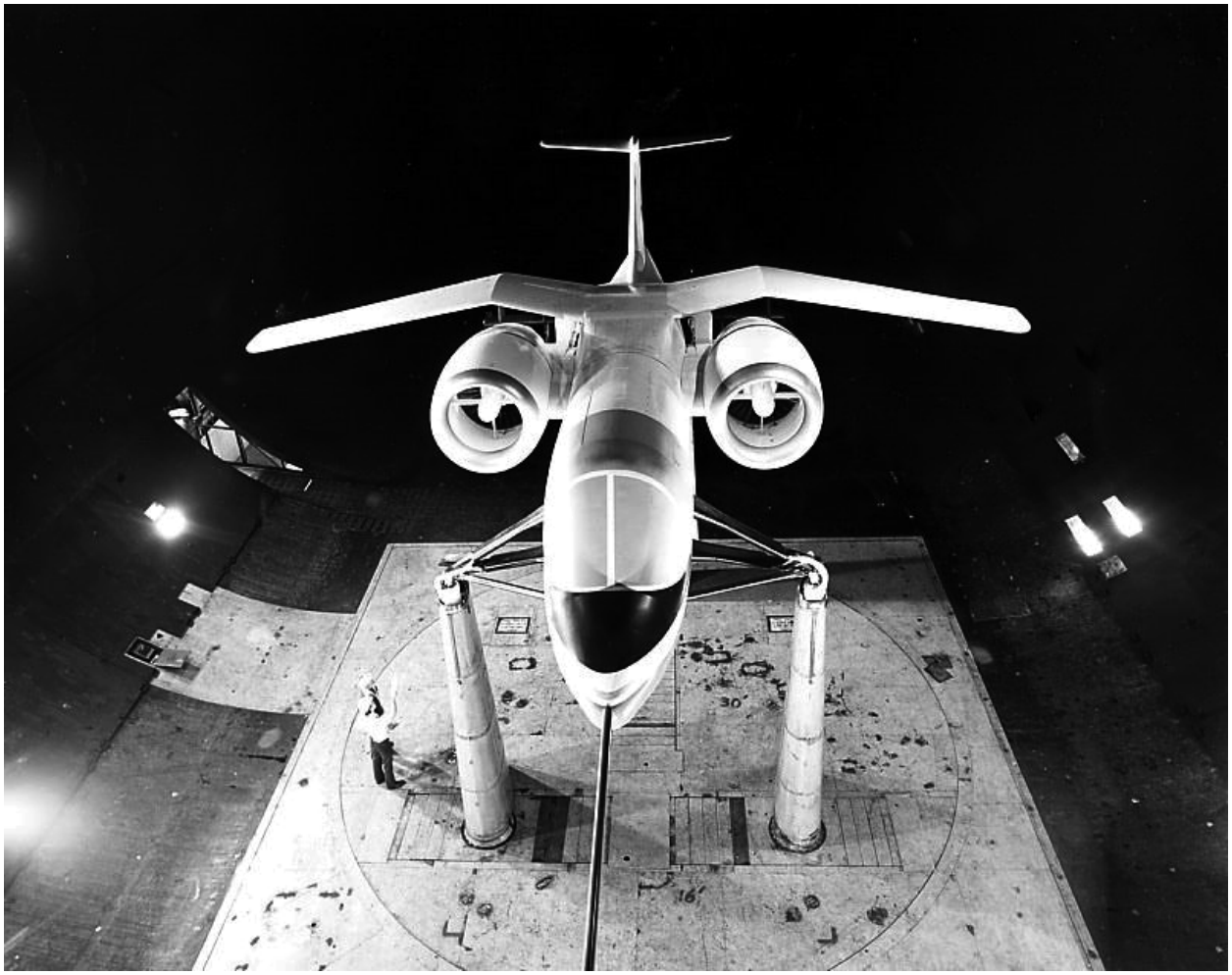

Figure 186. Overhead front view of Grumman 698 tilt-nacelle V/STOL model in the wind tunnel.
(J. Sacco collection, gru698_4X80)

Propellers and Propeller-Powered Aircraft

There were many propeller-powered V/STOL aircraft proposed over the years. There was a large variety ranging from deflected slipstream to tilt-wing and tilt-propeller configurations.

Deflected slipstream configurations were thought to be relatively simple for V/STOL aircraft. Larger propellers could be used with more power, and the wing flaps could have longer chords to deflect the propeller slipstream 90 degrees downward so that vertical lift could be achieved. The goal was an aircraft that would be simpler and quieter than a helicopter, yet have significantly higher (at least double) cruising airspeed.

Ryan VZ-3RY. The Ryan VZ-3RY deflected slipstream airplane was tested in the tunnel before flight-tests—it was intended to be an experimental flight-test VTOL. It used very large double-slotted flaps that were intended to deflect the slipstream from the propellers for vertical lift (Fig. 187, Test 122). The propellers were variable pitch. Differential pitch of the variable-pitch propellers was used for roll control. The engine exhaust was ducted to the tail and deflected with

small vanes for pitch and yaw control. Initially, the airplane cockpit was enclosed and there was not an ejection seat. To exit the plane during emergencies, the pilot had to get out of the seat and go out through a hatch in the floor behind the seat—not a very safe arrangement for an experimental aircraft.

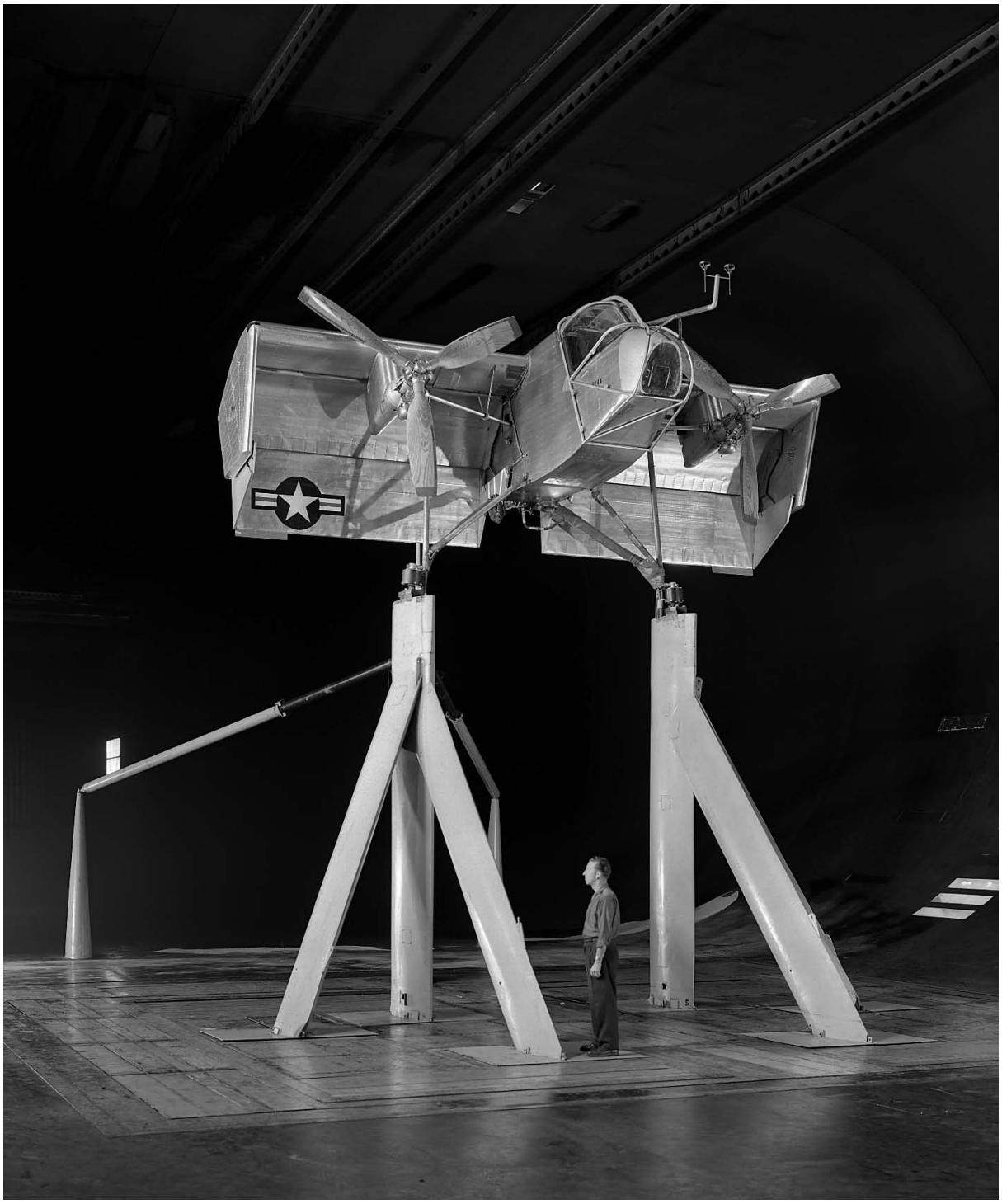

Figure 187. Ryan VZ-3RY deflected slipstream experimental VTOL aircraft. ***(NASA A-23991)***

The last run of the initial wind tunnel tests was during the graveyard shift (11:30 p.m. to 8:00 a.m.) on a Friday morning at about 3 a.m. After the last scheduled run (the author was running the shift at the time as a very junior engineer), the Ryan test pilot, Pete Girard, requested that the flaps be fully deflected and then the wind tunnel airspeed slowly increased until the first sign of failure. This was done and the limiting airspeed with the flaps fully deflected was determined—the flaps began to deflect excessively but did not fail catastrophically. Because of its lightweight construction, it was important for the test pilot to determine the actual structural limitations of the airplane before the first flight-tests. It is hard to imagine that this approach would be allowed in today's environment, however it was an excellent safety-of-flight experiment.

After the tunnel investigation, simulator studies and pilot practices were performed. Preliminary flight-tests were then started. During one of the early flights, there was a hard landing because of a mechanical failure of the blade pitch system, and the pilot was seriously injured. The aircraft was extensively damaged, but was repaired and modified with an ejection seat installed as well as modifications to the cockpit to make it open. Tunnel tests were again performed to determine changes in aerodynamic characteristics from the initial test. Extensive flight-testing was then performed. The airplane could not quite achieve level, 1-g transition. During one of the test flights, the plane got into an inverted spin, and the NASA pilot ejected. The pilot was injured but recovered. The plane was retrieved and repaired for additional flight-testing. The airplane successfully demonstrated the potential of the propeller deflected slipstream concept and its limitations [253].

Large-scale four-propeller models. Several studies of large-scale deflected slipstream models were performed in the 40- by 80-Foot Wind Tunnel (Figure 188 shows one of the models during ground-effect experiments; Tests 299, 304, and 307). These models represented a STOL transport concept [254] with wings of various aspect ratios (5.7 to 8.1). Variables studied were wingspan, full-span leading-edge slats, full-span triple-slotted trailing-edge flaps deflected 0 to 100 degrees, two directions of propeller rotation, and spanwise variation of propeller thrust. It was found that the lift coefficient increased and drag coefficient decreased as the wingtips were extended outboard. Maximum lift coefficient appeared to be limited by flow separation between the nacelles on all configurations, even though the flow on the wingtips of the high-aspect-ratio configuration were not energized by the propeller slipstream. Wing-leading-edge slats controlled the progression of flow separation and extended the angle of attack for maximum lift approximately 10 degrees. It was found that spanwise variation of propeller thrust improved descent capability most effectively for the short span wing [254].

Stability and control characteristics of the large-scale deflected slipstream STOL model (described above) with a wing of 5.7 aspect ratio were determined [255]. Variables included aileron geometry, spoiler geometry, spanwise variation of propeller thrust, and two vertical heights of the horizontal tail. It was found that a 0.2 wing-chord slot-lip aileron was an effective roll control device when installed on a wing fully immersed in the propeller slipstream. Large downwash angles were induced in the vicinity of the horizontal tail by the propeller slipstream. Downwash effects were greatest with a low tail position and caused longitudinal instability to develop as thrust was increased. Both horizontal tail and rudder were more effective when the horizontal tail was mounted in the high position. This model was very similar to the Bréguet 941 STOL airplane [255, 256].

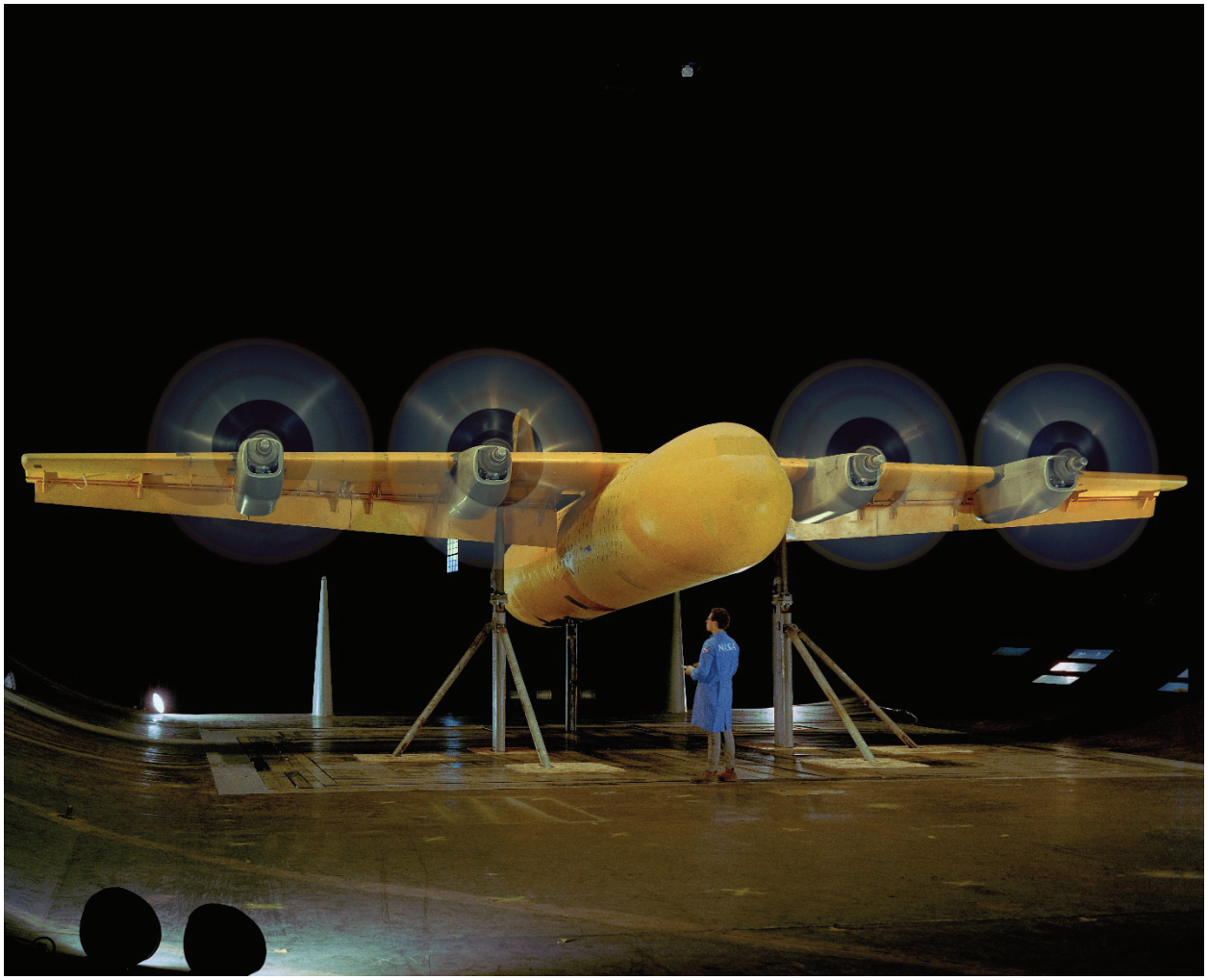

Figure 188. Large-scale four-propeller deflected slipstream transport-aircraft model during ground-effect tests. ***(NASA AC-39636)***

Tilt-wing research model. There was a lot of NASA interest in tilt-wing V/STOL aircraft very early on. On these aircraft, the wing and engines, or propellers, would tilt up for vertical lift and then rotate back to the horizontal position for wing-supported flight. The goal was to achieve reasonably efficient hovering and much higher cruise speeds than helicopters. A major problem was wing-leading-edge flow separation, especially during descent conditions. A concept with a lot of potential was a combination of a tilt wing and deflected slipstream using large-chord flaps. Extensive research was done on a four-engine transport model with a wing aspect ratio of 5.5 that employed both wing tilt and deflected slipstream in the 40- by 80-Foot Wind Tunnel (Figs. 189 and 190, Test 138). Figure 189 shows the model in the tunnel on the normal struts and figure 190 shows the model during ground-effect tests. The wing tilt was limited in an attempt to improve descent characteristics of the wing sections not directly in the propeller slipstream. Results with trailing-edge flaps with BLC and a leading-edge flap were studied, as well as the effects of various heights above ground [257, 258].

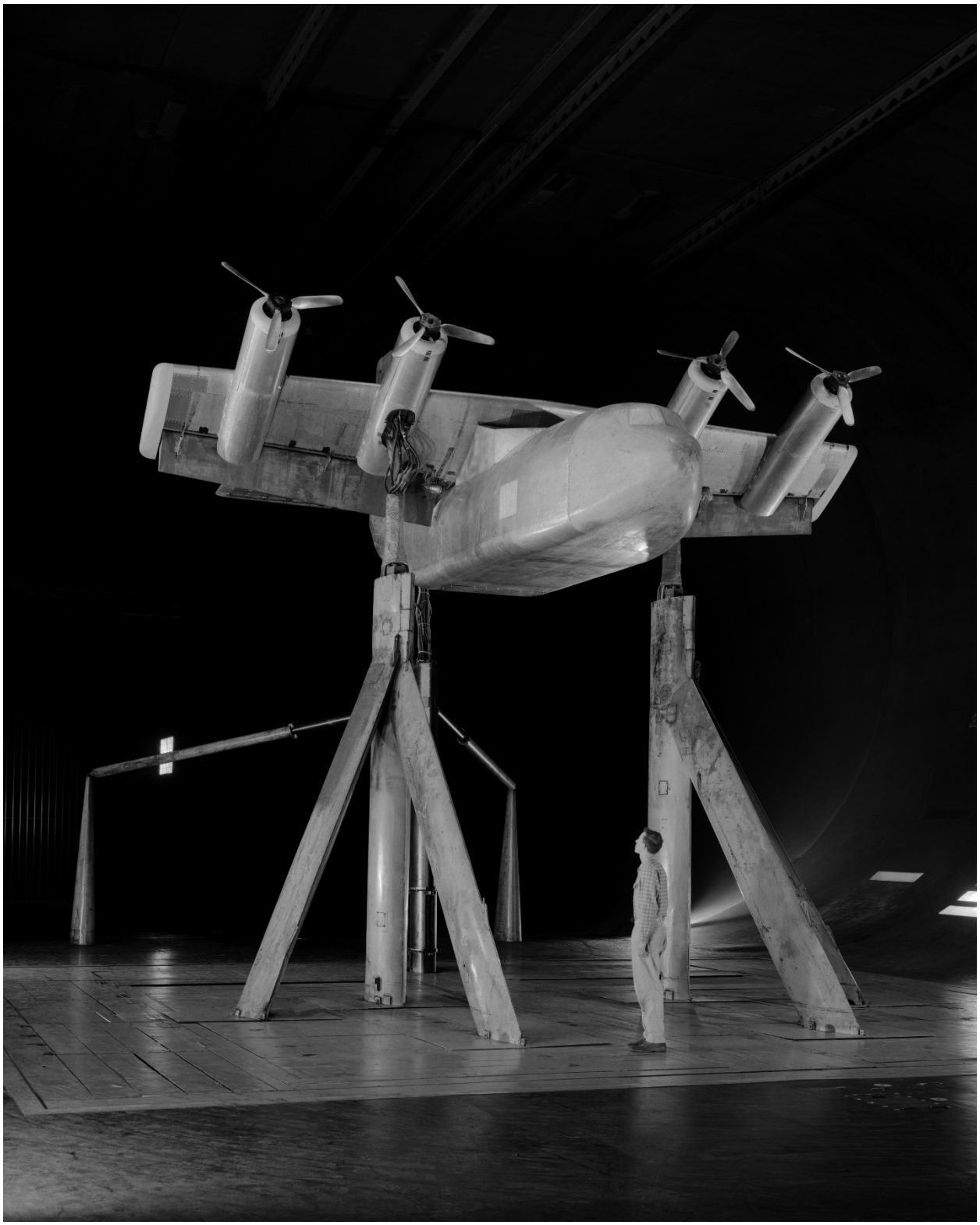

Figure 189. Large-scale four-propeller tilt-wing V/STOL transport model with Tom Wills in photo.
(NASA A-25998)

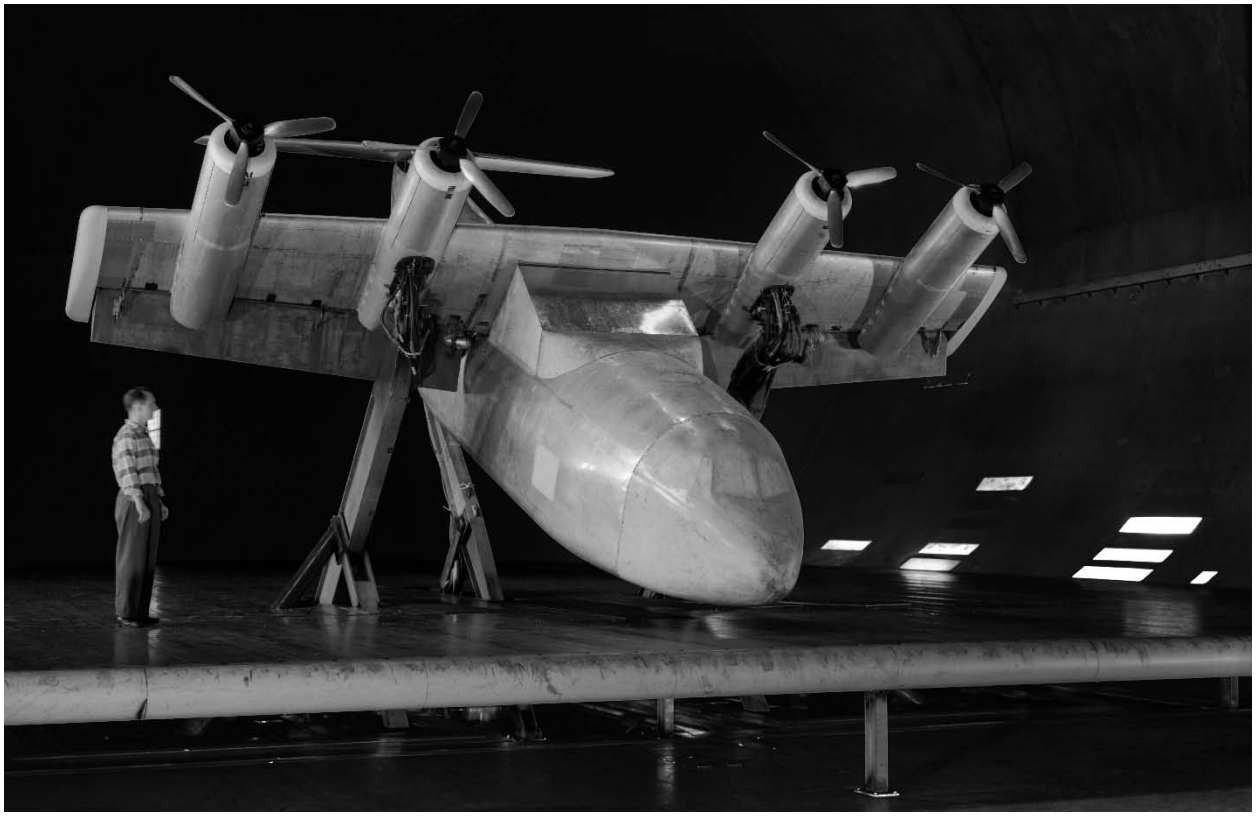

Figure 190. Large-scale four-propeller tilt-wing V/STOL transport model on variable-height struts and ground plane with Leo hall in photo. ***(NASA A-26612)***

Studies of the same model were conducted with various devices to delay wing stall during descent [259]. The effects of wing-leading-edge slats, trailing-edge flaps, wing-fuselage ramp fairing and propeller rotation on the flow separation, buffeting, and descent characteristics were studied. It was found that wing stall and resulting buffeting could be significantly delayed by these modifications during descending flight.

Ling-Temco-Vought XC-142A model. Subsequently a 60-percent model of the Ling-Temco-Vought XC-142A Tri-Service tilt-wing airplane was studied in the 40- by 80-Foot Wind Tunnel (Figs. 191 and 192, Test 229). The aspect ratio of this four-propeller airplane model was 8.4. In addition to normal aerodynamic characteristics, descent characteristics were studied because, as pointed out, this had been identified as a potential problem area for tilt-wing aircraft. The focus was on the wing tilt required for the transition flight regime [260]. In addition, differential propeller thrust was studied; the inboard propellers were set at higher thrust in order to improve the flow over the wing above the fuselage section. Both full-span slats and differential propeller thrust significantly improved descent capability.

Ground-effect studies were also done on the XC-142A model as shown in Figures 191 and 192. The model was tested at various heights above the ground plane. Wing tilt angles were studied from 0 to 90 degrees, and flap deflections varied from 0 to 60 degrees. It was found that ground effect decreased lift, decreased drag, and increased nose-down pitching moment [260].

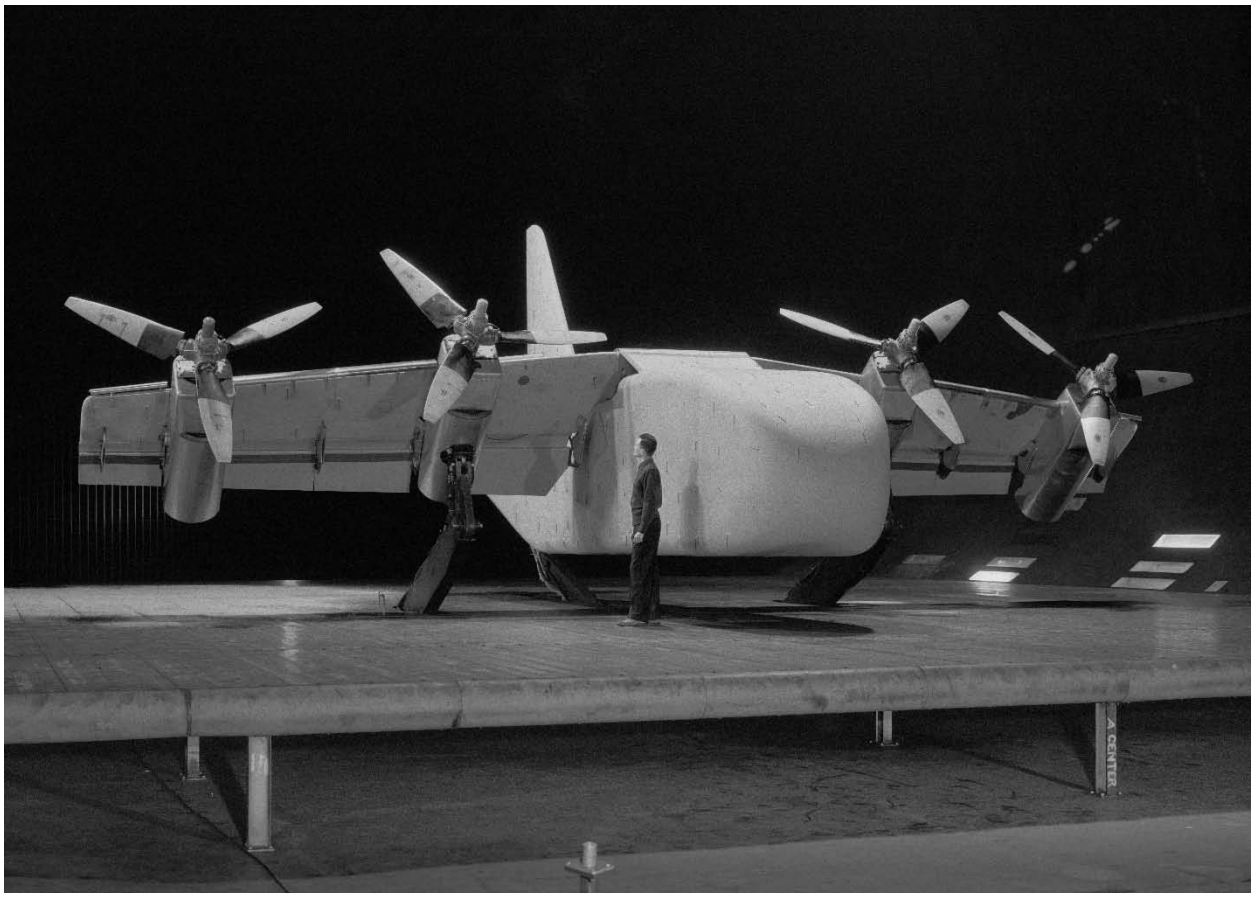

Figure 191. Three-quarter front view of XC-142A V/STOL transport model on variable-height struts with Jim Biggers in photo. ***(NASA A-30364)***

The XC-142 aircraft had an extensive flight-test program, however it did encounter hardware and pilot workload problems, and there were several crashes. Five prototypes were built. A tail-rotor driveshaft failure caused a fatal accident. The aircraft propellers were interconnected, and a tail rotor in the horizontal plane was also interconnected. The tail rotor was required for pitch control at low-speed conditions; at cruise conditions, it was declutched and braked. The cross-shafting required was complicated and was interconnected such that all propellers were operational even if three engines were shut down. Aerodynamicists judged that if the mechanical problems had been solved, the plane could well have achieved operational status.

Kaman K-16B tilt-wing aircraft. The K-16B was a combination tilt-wing and deflected slipstream aircraft sponsored by the Navy. Kaman Aviation Corporation was tasked by the Navy to build a V/STOL aircraft on a very small budget. Kaman built the wing but used existing parts and fuselage from a Grumman JRF Goose flying boat. Needless to say, it was an unusual aircraft. The wing was designed to tilt 50 degrees and incorporated large flaps that could be deflected sufficiently to produce enough lift to enable VTOL. The airplane was to be propelled by two 4.5-meter-diameter propellers, each of which was driven by a T58-GE-2A turboprop engine. The aircraft was tested in the 40- by 80-Foot Wind Tunnel to determine flight characteristics (Figs. 193 and 194, Test 175). There is no record that it was ever flown.

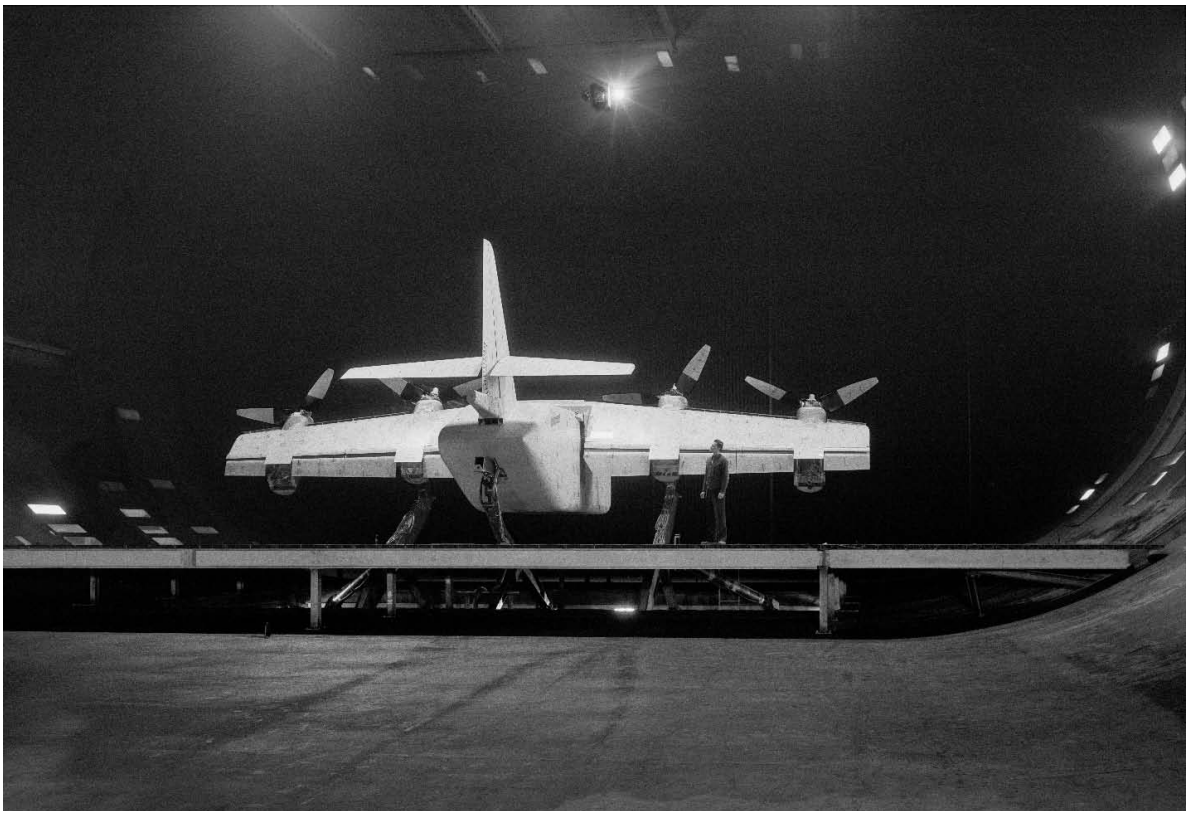

Figure 192. Rear view of XC-142A model. ***(NASA A-30365)***

Figure 193. Kaman K-16B experimental tilt-wing seaplane being lifted into tunnel.
(NASA A-29884-005)

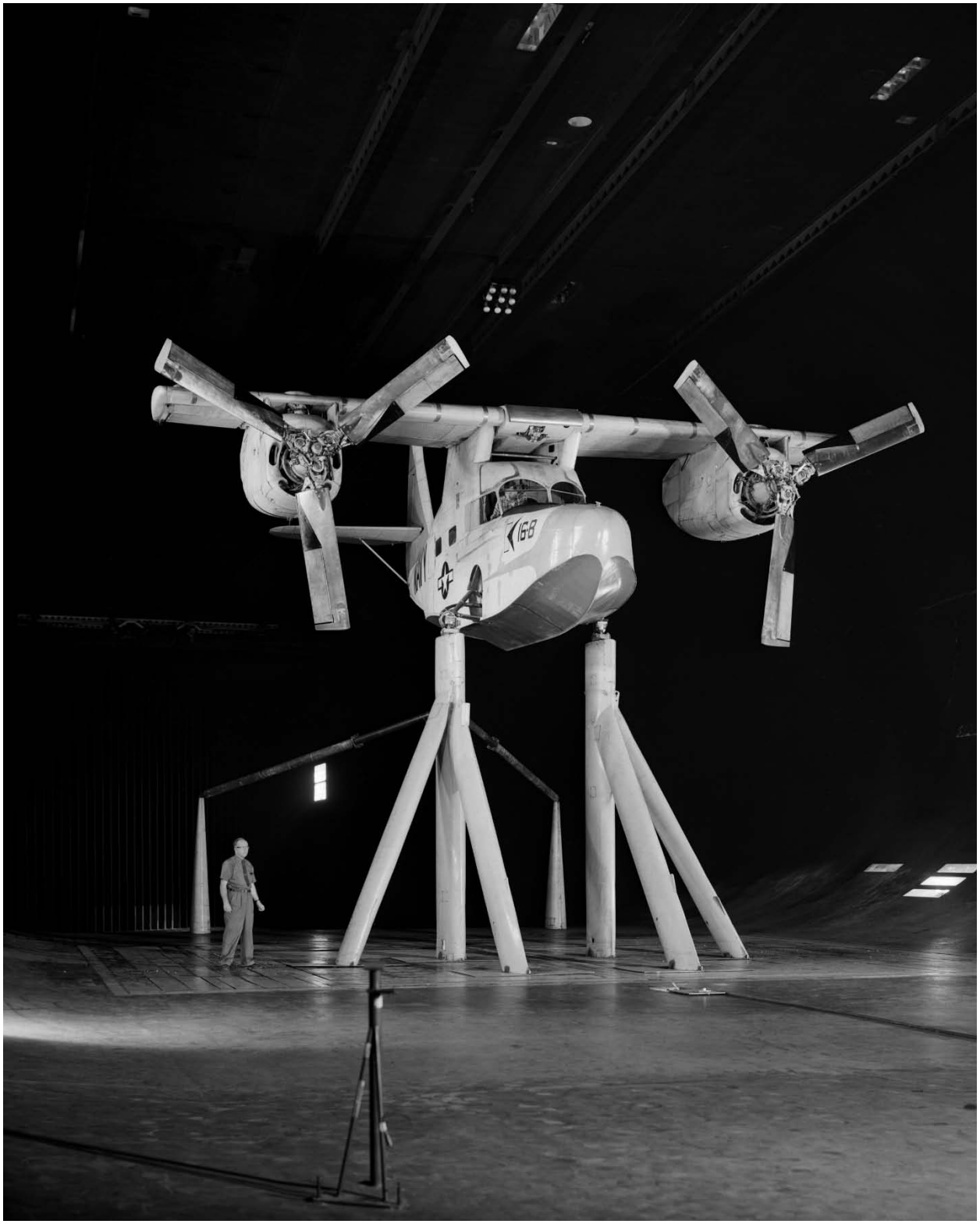

Figure 194. Three-quarter front view of the Kaman K-16B in tunnel. ***(NASA A-29884-1)***

Propeller tests through angles of attack of 85 degrees. Three propellers were tested through 85 degrees angle of attack to obtain basic propeller data at high angles of attack. The propellers were tested using the propeller test rig (Fig. 195, Test 120). Two were Curtiss-Wright propellers and one was a Vertol 76 propeller. The results are presented in reference [261]. The data were useful for design of tilt-wing and tilt-propeller aircraft.

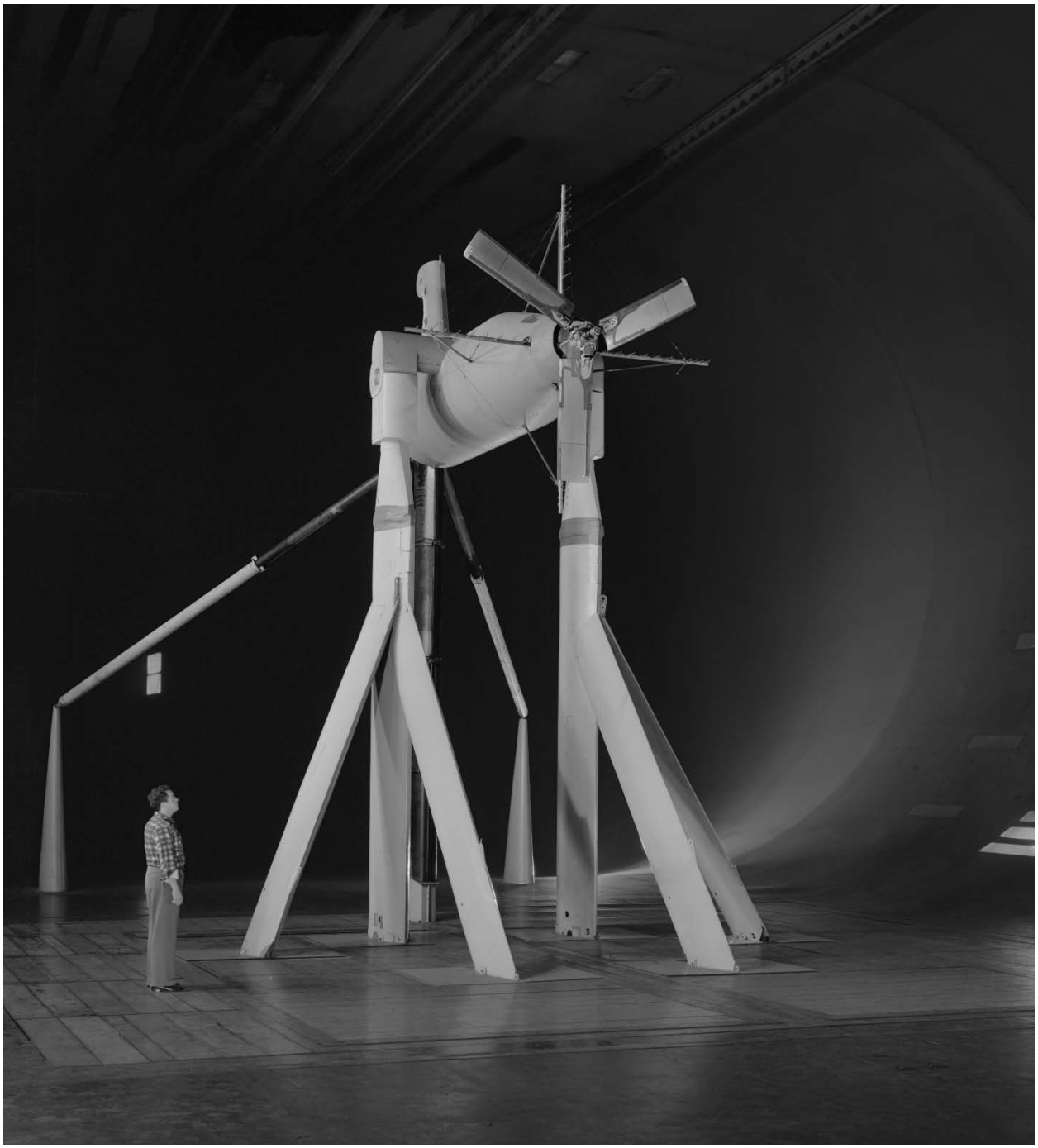

Figure 195. Vertol 76 propeller on test rig at zero angle of attack with Demo Giullianetti in photo; total-pressure rakes are shown behind propeller. ***(NASA A-23635)***

Vertol 76 V/STOL aircraft propeller descent tests. Descent tests of the Vertol 76 aircraft propeller were performed in the 40- by 80-Foot Wind Tunnel to define the vortex-ring state for the tilt-wing Vertol 76 V/STOL aircraft that was being flight-tested at Langley Research Center (Fig. 196, Test 157). The vortex-ring state is a condition during high-descent velocities that produces a large, propeller ring vortex and results in very unsteady flow through the propeller. The airspeed in the tunnel could be reversed at low speeds for low descent airspeeds, however for these experiments the propellers were mounted backwards from the normal mounting to achieve higher simulated descent speeds. Descent velocities as high as 6,000 feet per minute were tested, and the propeller disc loadings ranged from 0 to 36 psf. Thrust oscillations of as high as ±75 percent of the steady-state thrust occurred [262].

The Vertol propeller had flapping hinges, but a reinforced version was also tested without flapping hinges. Vortex-ring states were defined for both configurations, and boundaries were established for the version with the flapping hinges in support of the Langley Research Center flight-tests.

Flapping and non-flapping effects on control for the airplane were determined in the wind tunnel. The effect of varying blade angle was included. The non-flapping version of the blades had significantly higher control effectiveness—which was the goal of eliminating the flapping hinges—but of course the bending stresses were much higher [263].

Curtiss-Wright propellers and VTOL aircraft. Curtiss-Wright had not built an aircraft since 1952 after failing to earn any significant post-war (WWII) military contracts. However, engineers in the propeller division developed an innovative approach to designing a propeller-driven VTOL using the radial or normal force produced by propellers.

The object was to design a propeller that would have significantly higher radial or normal force (normal to the thrust axis) for VTOL applications during transition flight conditions, and yet still not have significantly reduced propulsive efficiency at cruise conditions. If higher radial forces could be achieved, wings could be reduced in size—maybe even sized for cruise conditions—and therefore result in lower cruise drag for the aircraft. The normal force was increased by increasing the propeller-blade chord (Fig. 197). The effectiveness of the developed propeller to produce more normal force was compared with a normal propeller designed by Curtiss-Wright during investigations in the 40- by 80-Foot Wind Tunnel [261] (Test 120). These developed propellers did produce more normal force without an unacceptable reduction in propulsive efficiency. As a result, the propellers were used on the Curtiss-Wright X-100 experimental aircraft. This experimental aircraft was intended only to demonstrate the propeller normal-force concept at transition airspeeds. The X-100 was successfully flight-tested and then tested in the 40- by 80-Foot Wind Tunnel for comparison with flight-test results and to obtain data on propeller loading (after it had been used for ground-effect testing at Langley Research Center). Figure 198 (Test 184) shows the airplane at the Ames flight line prior to checkout testing.

Figure 196. Vertol 76 tilt-wing V/STOL aircraft propeller with wing on propeller test rig at 85 degrees angle of attack. ***(NASA A-28486)***

Figure 197. Downstream flow surveys of Curtiss-Wright VTOL propeller on propeller test rig at zero degree angle of attack. Note the wide-chord blades. ***(NASA A-24304)***

Figure 198. Curtiss-Wright X-100 V/TOL experimental aircraft on flight line for checkout prior to wind tunnel tests. ***(NASA A-30770)***

The Curtiss-Wright X19A was subsequently built and flight-tested in the early 1960s. It employed the high-normal-force propellers. It was intended to be developed into a business VTOL with about a 350-knot cruising speed. It had two, short, tandem wings with wingtip-tiltable propellers. Problems developed during the flight-tests. In addition, the problem of engine-out operation became an issue. Because the propellers had higher disc loading than helicopter rotors, vertical-descent velocities during autorotation were judged excessive and therefore not safe for flight. The program was ultimately cancelled after an accident occurred during flight-testing. Reference [264] provides an excellent, detailed description of the entire program to employ propeller normal force for V/STOL aircraft.

Rotating-cylinder-flap models. Rotating cylinders located at the knees of flaps were proposed to energize the flow and increase the effectiveness of the flap. Rotating-cylinder flaps were installed on a two-propeller airplane model (Figs. 199 and 200) and on a four-propeller model shown in Figure 201. Figure 201 shows the model in the tunnel and Figure 202 shows details of the rotating-cylinder flap. The rotating cylinder is shown at the knee of the flap.

Figure 199. Three-quarter front view of two-propeller model with rotating-cylinder flap.
(NASA A-41389)

Figure 200. Three-quarter rear view of two-propeller model with rotating-cylinder flap.
(NASA A-41390)

Figure 201. Three-quarter front view of four-propeller model with rotating-cylinder flaps.
(NASA A-39267)

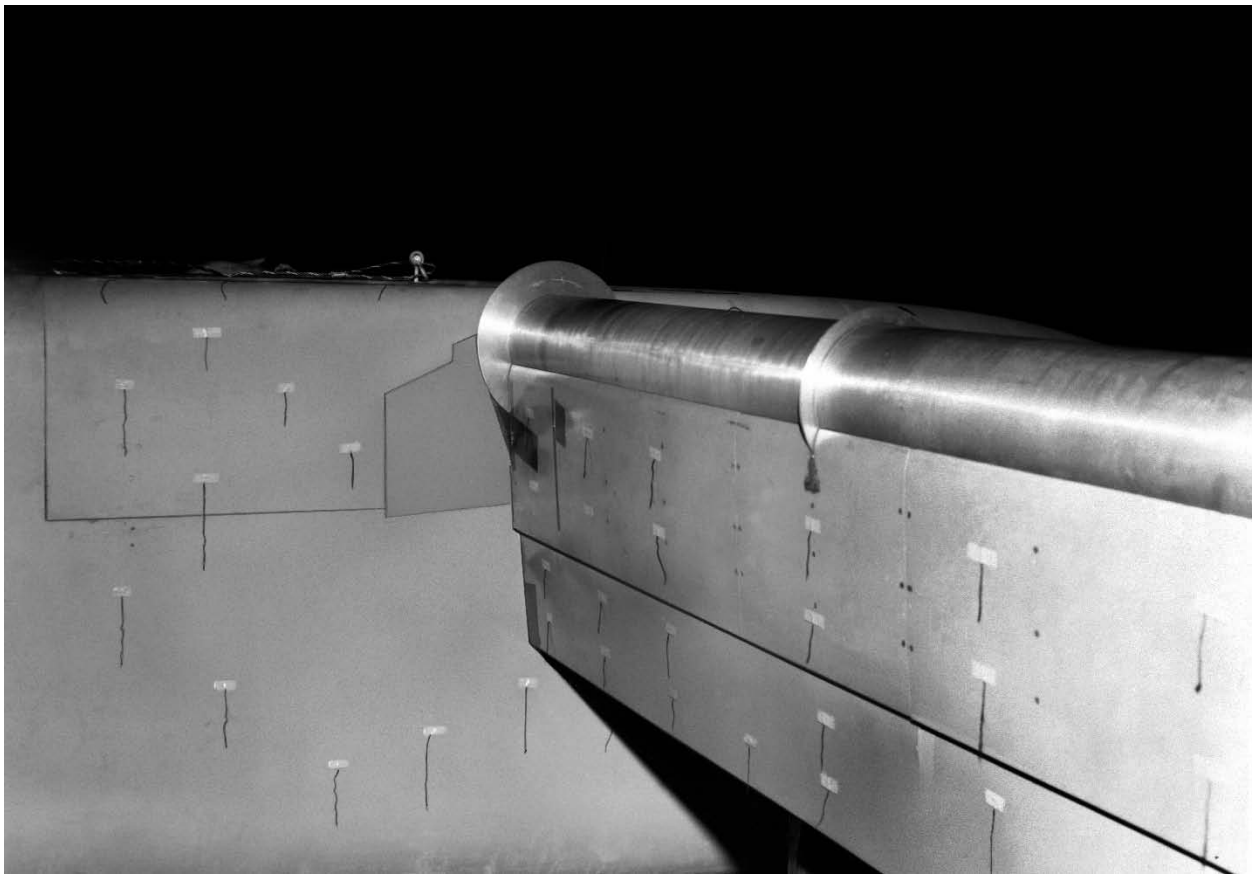

Figure 202. Details of the rotating-cylinder flap. ***(NASA A-39266-001)***

The cylinder was composed of two segments with an electric motor driving each. The large-diameter disks on the cylinder are end plates for each cylinder segment. The semispan of the cylinder was 11 feet. The smooth aluminum cylinders were 10.9 inches in diameter. Flap chord, including the cylinder, was 46 percent of the wing chord. A full-span slat with a chord of 22 percent of the wing chord was installed on the leading edge of the wing. The model had 9.3-foot-diameter three-bladed propellers that were driven by electric motors. The straight wing had an aspect ratio of 3.5 and a span of 25 feet. A 44-percent-chord double-hinged conventional flap was also evaluated on the model for comparison with the rotating-cylinder flap. A maximum lift coefficient of 9.1 was obtained with the rotating-cylinder flap compared to 7.5 for the double-hinged flap. The power required to operate the rotating cylinder sufficiently to energize the boundary layer was found to be low; it was less than for a comparable blowing flap BLC system. Pitching moments were found to be significantly less than those for a plain double-hinged flap. Results were reported in references [265] and [266].

Jet-Engine-Powered Lift

Many schemes to increase lift employing jet-engine exhaust were studied in the tunnel. Generally, the purpose was to increase lift and thereby reduce landing speed and the runway length required. The goal was to develop systems that were relatively simple yet very effective in increasing lift. Jet augmentation intended to induce secondary airflow and hence increase thrust and/or lift was investigated. Jet flaps that use engine exhaust ducted through flaps were studied. Externally blown flaps (EBFs) were implemented by directing the jet-engine exhaust at deflected flaps, which was intended to increase flap effectiveness and increase lift during low-speed flight. Upper surface blowing (USB) was implemented by directing the jet-engine exhaust to the upper surface of the wing. The purpose was to increase wing and flap lift by energizing the circulating flow about the wing and flaps.

Augmented Lift Models

Augmentor wing model. The augmentor wing is essentially an ejector system with engine air ducted spanwise along the wing and ejected through a nozzle. Secondary air is induced in from the upper surface of the wing and the mixed flow is ejected downward through the augmentor flap. The straight wing had an aspect ratio of 8 and a span of 42.2 feet. The maximum lift coefficient achieved was about 6 [265]. The de Havilland model is shown in Figure 203 during ground-effect experiments (Test 260). Front and overhead views (Figs. 204 and 205) show a swept-wing augmentor model out of ground effect.

Semispan augmentor wing models were also investigated (Figs. 206 and 207).

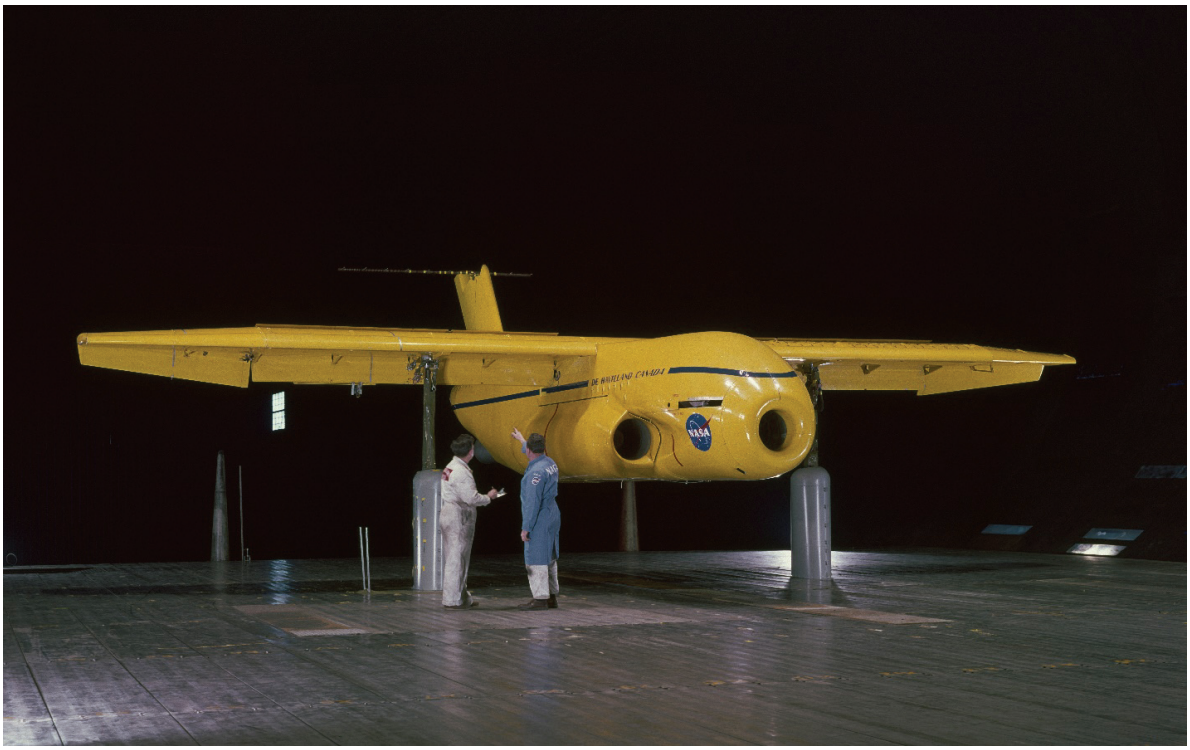

Figure 203. Three-quarter front view of de Havilland augmentor wing model during ground-effect experiments. ***(NASA AC-36486)***

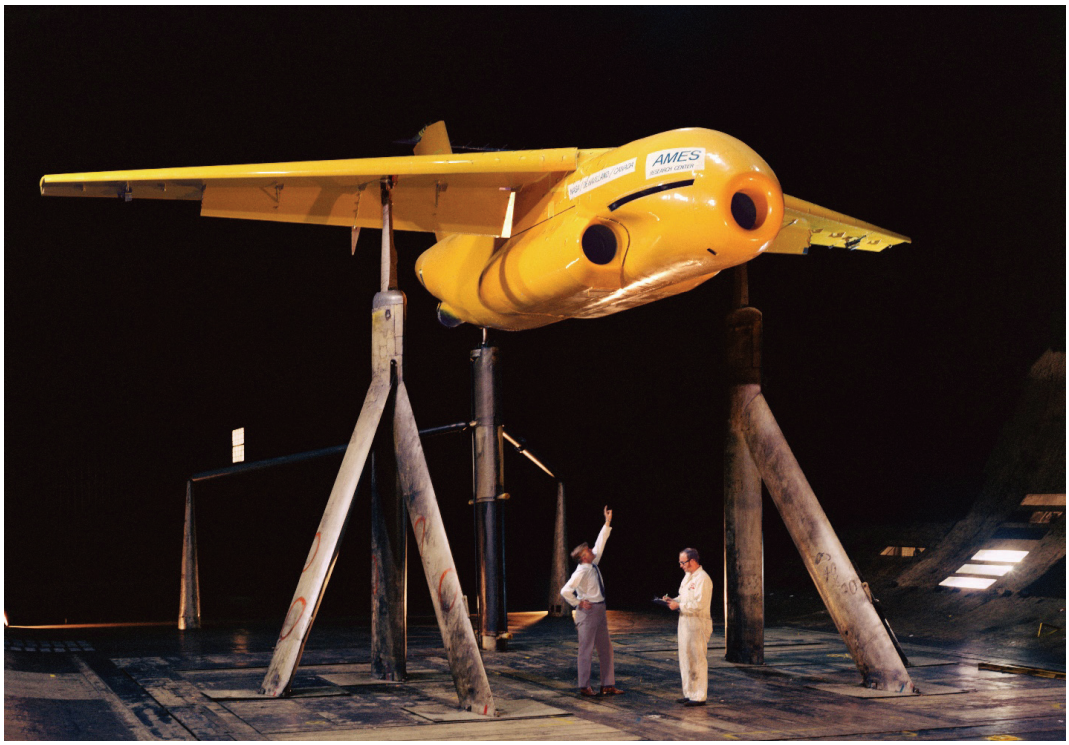

Figure 204. Three-quarter front view of de Havilland augmentor wing model.
(NASA AC71-2500)

Figure 205. Overhead front view of de Havilland augmentor wing model.
(NASA AC71-2502)

Figure 206. Three-quarter front view of semispan augmentor wing model with Edwin Verrette making model changes. ***(NASA AC74-1799)***

Figure 207. Three-quarter front view of semispan augmentor wing and fuselage model with John Bouldt in photo. ***(NASA AC75-2276)***

Fuselage ejectors. Fuselage ejector models and aircraft were also extensively investigated. The Lockheed XV-4A Hummingbird experimental VTOL aircraft was an early concept investigated in the 40- by 80-Foot Wind Tunnel (Test 215). It was a twin jet-engine airplane that employed a jet-ejector augmentation system contained in the fuselage as shown in Figure 208. The maximum static augmentation ratio measured (that is, the lift produced divided by the engine thrust) was 1.19; the ratio increased with forward speed. The investigation included hover up to and

including wing-supported flight conditions. Two experimental aircraft had been built. Flight-tests were performed and there was a fatal crash before the wind tunnel tests. Results from full-scale wind tunnel tests, flight-tests, and small-scale tests were compared and generally agreed favorably [267]. Subsequent flight-testing was also performed on this airplane by Lockheed. The program was terminated after another crash during flight-testing.

Figure 208. Three-quarter front view of the Lockheed XV-4A Hummingbird experimental jet-ejector augmentor VTOL aircraft. The augmentors were in the fuselage; open augmentor exhaust doors are shown. ***(NASA A-33194)***

De Havilland VTOL ejector fighter model. Figures 209 and 210 show the model that had ejectors at the wing root. It was powered by a J-97 jet engine. Much development work was done on this model in the wind tunnel.

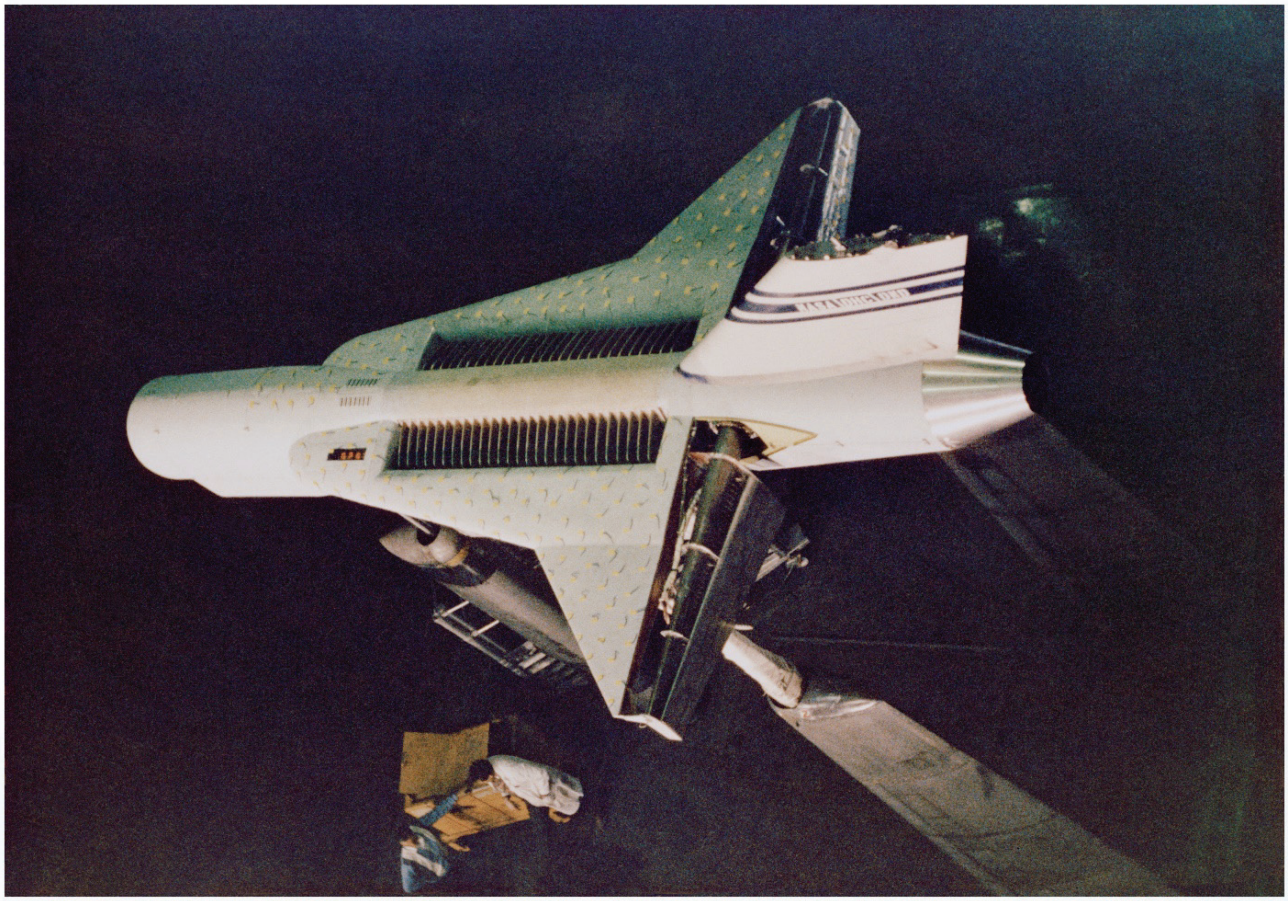

Figure 209. Overhead view of augmentor model with ejectors at the wing root. ***(NASA AC78-0255-4)***

Figure 210. Three-quarter front view of augmentor model with ejectors at the wing root.
(NASA AC79-0197-1)

Jet-Flap and Blown-Flap Aircraft

Lockheed expanding jet-flap wing model. This model employed a special flap system to achieve expanding flow for a jet flap and is shown in Figure 211. The experiments were performed at the request of the Lockheed-Georgia Company and the Flight Dynamics Lab of the Department of the Air Force. Both aerodynamic and acoustic data were obtained [268, 269].

Hunting H.126 jet-flap experimental aircraft. The Hunting H.126 was tested in the 40- by 80-Foot Wind Tunnel after extensive flight-testing in the United Kingdom. The aircraft was only intended to perform research on the jet-flap principle at transition airspeeds and therefore had fixed landing gear because aircraft drag was not a concern (Fig. 212, Test 343). Model tests had also been done at Ames in the 7- by 10-Foot Wind Tunnel [270]. Static longitudinal, lateral, and directional characteristics were measured on the aircraft. The jet-control power and the aerodynamic characteristics were measured. A portion of the exhaust gas from the engine was blown through full-span converging nozzles over the flap and aileron upper surfaces to provide the air jet for lift. The remainder of the exhaust gas was ducted to two thruster nozzles and the control reaction jets. At maximum lift conditions, 55 percent of the mass flow was distributed to the jet-flap nozzles for lift, 30 percent to the thruster nozzles, and 15 percent to the control jets.

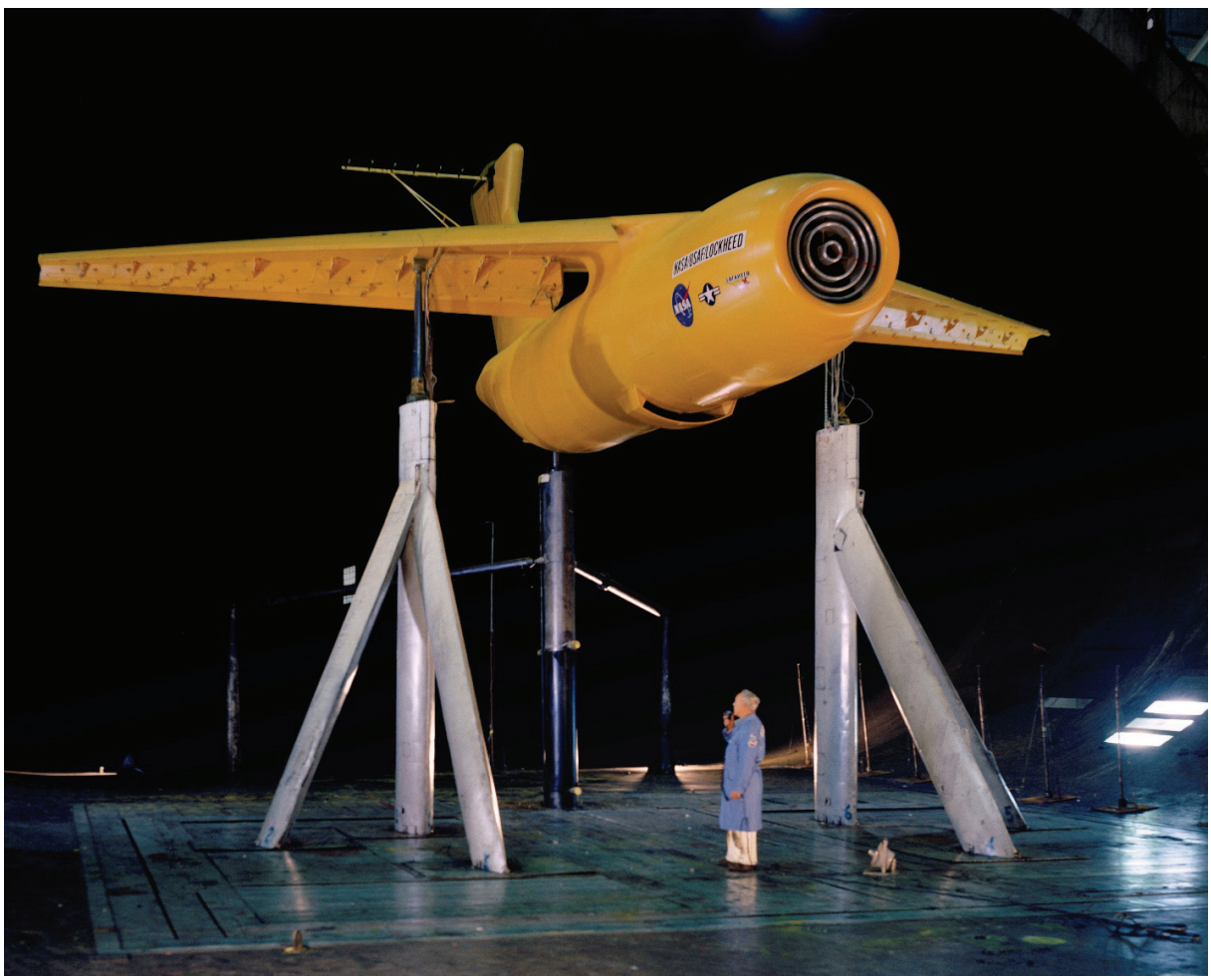

Figure 211. Three-quarter front view of the Lockheed expanding jet-flap model. ***(NASA AC72-6482)***

Figure 212. Three-quarter front view of the Hunting H.126 jet-flap experimental aircraft. ***(NASA AC-42409)***

The maximum lift coefficient achieved was nearly 7 (lift coefficient is a nondimensional coefficient that is a measure of lift; typical wings have a lift coefficient of less than 2). It was found that stall was rather abrupt and lift dropped abruptly. One wing would always stall first causing roll, but it was not always the same wing [271]. However, it was pointed out that this was not necessarily a characteristic of jet-flap aircraft and that the H.126 had a thick, straight wing with uniform loading with very little taper. Modifications to the wing to improve the stall characteristics of the airplane were not done but would have had the potential for significant improvements in the stall characteristics.

Ball-Bartoe Jetwing experimental aircraft. This aircraft was investigated in the 40- by 80-Foot Wind Tunnel in December 1976 after it was built and before flight-testing. It had a wingspan of 21.75 feet. Supercirculation lift was achieved by using a unique system that ducted all engine air through the leading edge of the wing and ejected it over the top of the wing through a slot nozzle that extended along approximately 70 percent of the wingspan. A Coandă flap was mounted at the trailing edge of the blown portion of the wing. A smaller wing panel was mounted above the slot nozzle. The air passage between the main wing and the smaller upper wing acted as an ejector to increase mass flow. Front and rear views of the aircraft are shown in the tunnel in Figures 213 and 214, respectively (Test 498). The wind tunnel results indicated that lift coefficients in excess of 5 could be achieved. The wind tunnel results also indicated that the

aircraft was neutrally stable to unstable longitudinally at the c.g.'s where it was likely to be flown. As a result, about 300 pounds of lead ballast were added to the nose of the aircraft prior to flight-tests. After the wind tunnel tests, the aircraft was flight-tested at Mojave, California. The aircraft was then taken back to the company facility for additional flight-testing. Later the aircraft was donated to the University of Tennessee for Navy-sponsored flight and ground testing by the university [272].

Figure 213. Overhead front view of the Ball-Bartoe Jetwing experimental aircraft.
(NASA AC76-1716-3)

Figure 214. Three-quarter rear view of the Ball-Bartoe Jetwing experimental aircraft. ***(NASA AC76-1716-2)***

EBF models. A model with two jet engines with an exhaust deflector and flaps in the engine exhaust was investigated. The purpose was to investigate the potential increase in lift with this sort of scheme. The engines were J-85 turbojets set parallel to the wing chord with paddle deflectors to deflect the exhaust toward the wing trailing edge and flaps. The quarter chord of the wing was swept about 35 degrees. A maximum lift coefficient of 4.3 was obtained, and it was found that a small auxiliary flap had the potential for direct flightpath control. The research aerodynamicists judged that the concept warranted further study; it was likely that the lift coefficient could be improved and landing and takeoff distances reduced [273].

A model with four jet engines with external augmentors used to simulate high-bypass engines is shown in an overhead view in Figure 215. As can be seen, the engines are forward with the engine augmentors just forward of the wing leading edge. A lower front view of this model is shown in Figure 216. A rear view of another model with high-bypass jet engines (bypass ratio of 3), which would be more appropriate, is shown in Figure 217. The purpose of both of these models was to study the EBF concept.

Figure 215. Overhead front view of EBF model using augmented jet engines. Bell-mouth inlets of augmentors are shown close to the leading edges of the wings. Exhaust flow is directed to flap trailing edges to increase lift. ***(NASA A-42494-001)***

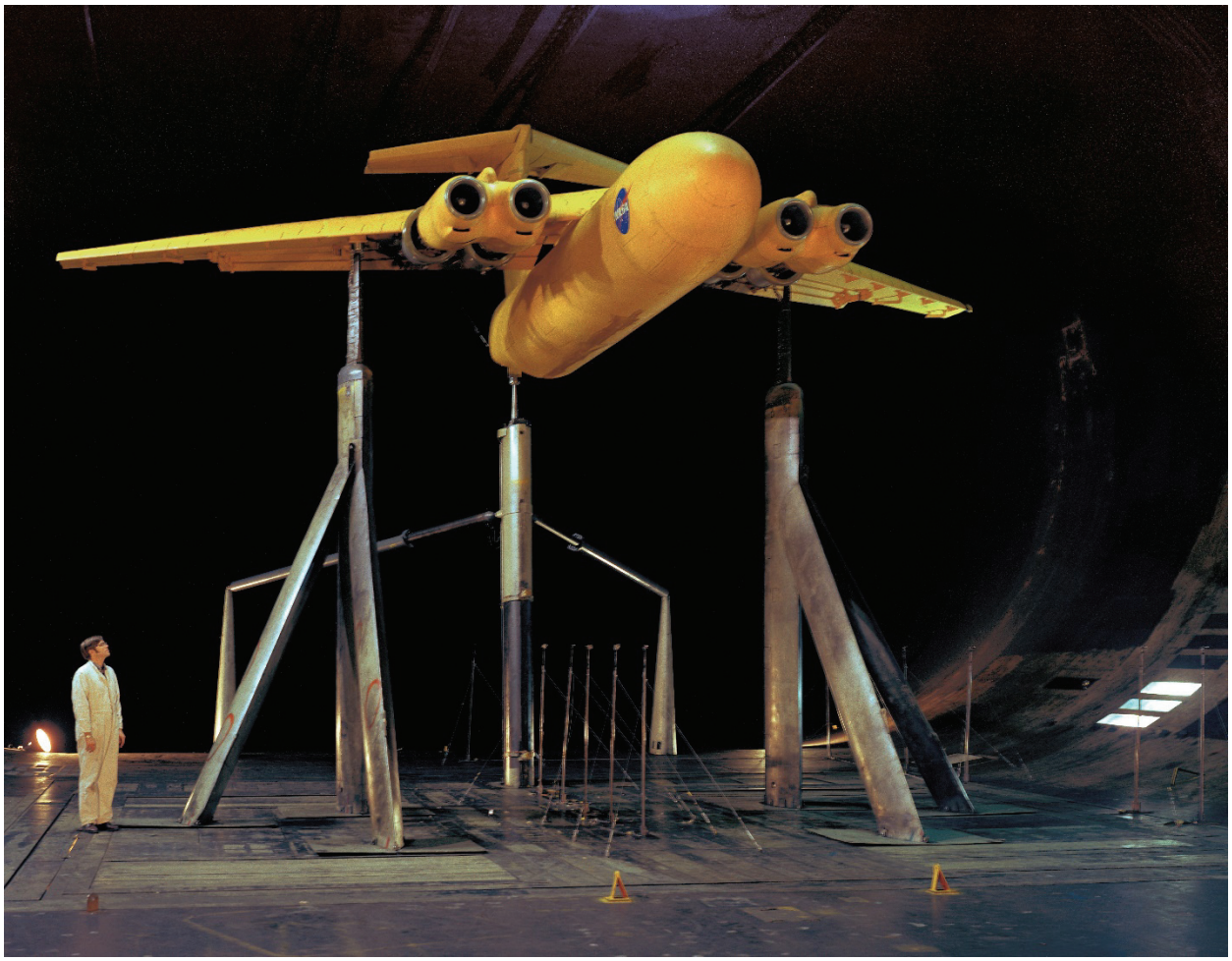

Figure 216. Three-quarter front view of EBF model using augmented jet engines. ***(NASA AC70-5677)***

Figure 217. Three-quarter rear view of EBF model using bypass-ratio-3 jet engines.
(NASA AC72-4376)

USB models. Several models were studied with both two jet engines and four jet engines for USB. Performance with two jet engines is described in reference [274]; acoustic characteristics for this model are presented in reference [275]. Figures 218 and 219 show the four-jet-engine model. The test results are presented in reference [276]. The concept was such that the flow over the wing and flaps would be energized by the jet-engine exhaust. Placing the engine exhaust over the top of the wing was intended to reduce noise at ground level; it was successful doing that.

Figure 218. Overhead view of USB model with four jet engines. Jet-engine exhaust is directed over the top of the wing flaps. ***(NASA AC74-2756)***

Figure 219. Rear view of USB model with four jet engines. ***(NASA AC74-0958)***

Space Related

Lifting Bodies

NASA began an extensive study of lifting bodies in the 1950s and 1960s. Lifting bodies were aircraft, intended to return from orbit or space, that did not have wings but relied on the lift produced by the body or fuselage for landing. The original NASA Ames Research Center concept was to take a symmetric space capsule, cut it in half, and thereby increase the L/D. Several lifting-body flight machines were built. All but one of the lifting-body flight machines were investigated in the 40- by 80-Foot Wind Tunnel prior to flight-tests. There were several books and reports written about the program [277-280].

M2-F1. The first flying lifting body was designated the M2-F1 and was proposed by Dale Reed at Dryden Research Center. It was a modification of the basic shape developed at Ames Research Center. The M2-F1 was a lightweight glider that was purposely built with a low "wing loading" (weight divided by projected area of the body) for low landing speeds. Control surfaces were added. The wing loading was about 9 psf. The structure was designed at Dryden Research Center where the flight-test studies were to be performed. The body was built by the Briegleb Glider Manufacturing Company, which built lightweight plywood gliders. The company, which was owned by Gus Briegleb, built the shell in about 4 months for $10,000. After studies in the 40- by 80-Foot Wind Tunnel (Fig. 220, Test 181) [281] and simulator studies using the wind tunnel test results, the glider was initially towed and released (the aircraft is towed up to flight speeds and then the tow cable is released) using a modified, souped-up car, and then subsequently towed and released using a C-47 airplane at Dryden Flight Research Center.

M2-F2 model. Because of concerns about possible damage during flight-tests, two fiberglass shells were made at Dryden using the glider as a mold. One was to be a spare for the flying machine, and the other was sent to Ames to build a wind tunnel model for configuration studies [282]. The internal structure for the Ames model was fabricated by the structural fabrication shop at Ames. An internal steel frame was fabricated such that the fiberglass shell could be attached. This was a very unusual approach to building a wind tunnel model; that is, it was built from the outside in. However, the Ames shops were always excellent at meeting construction challenges and did so very often in a timely manner with a minimum of engineering sketches and drawings and the absence of computer assistance. Many experiments were performed in the wind tunnel, especially on devices to improve low-speed lift [282]. Figure 221 shows the model with elevons similar to the M2-F1, and Figure 222 shows the model with quasi-wings. The idea was to explore the possibility of using the landing-gear doors as quasi-wings prior to landing to increase the lift at landing.

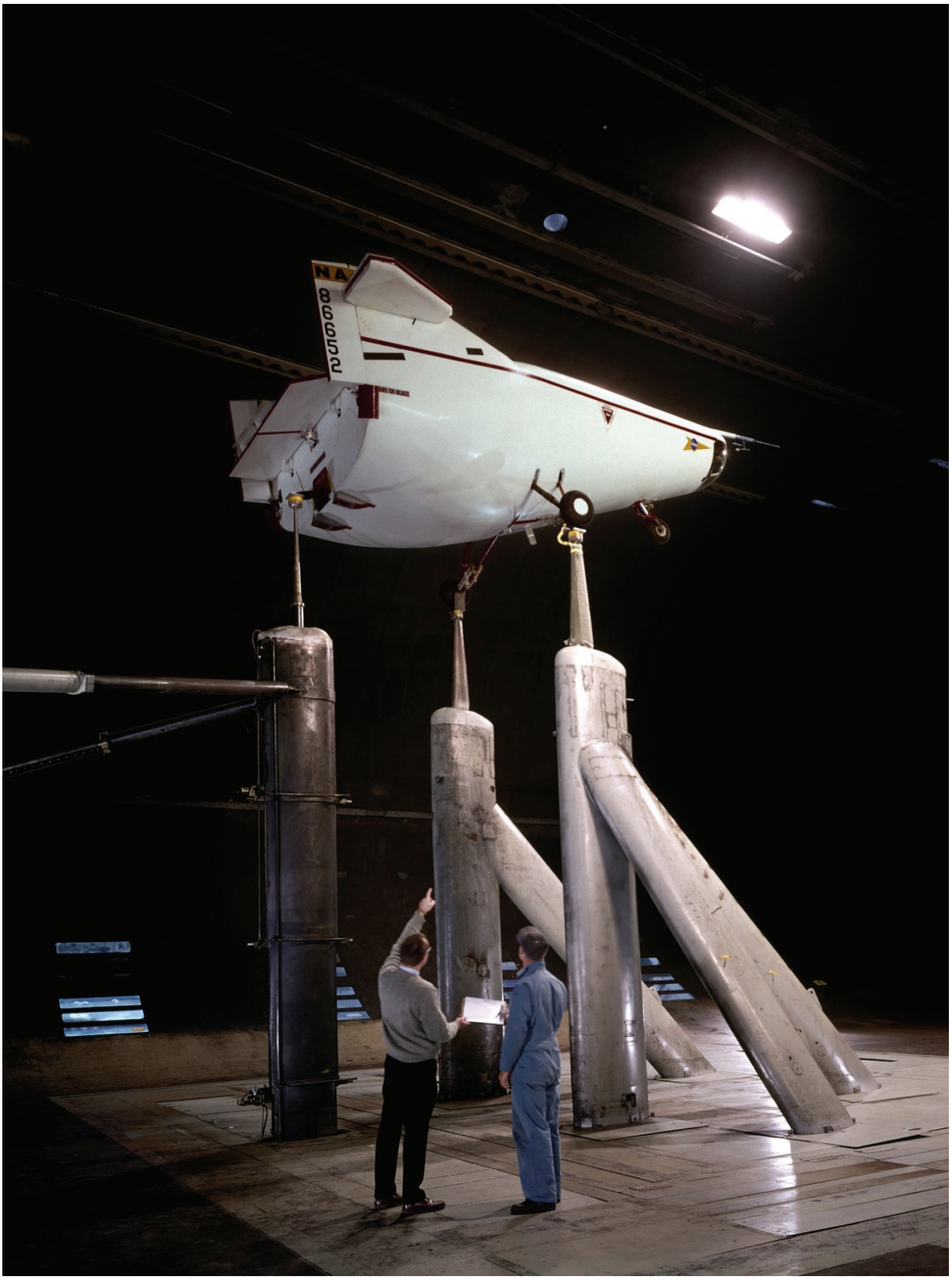

Figure 220. M2-F1 lightweight lifting-body experimental aircraft. ***(NASA A-33717)***

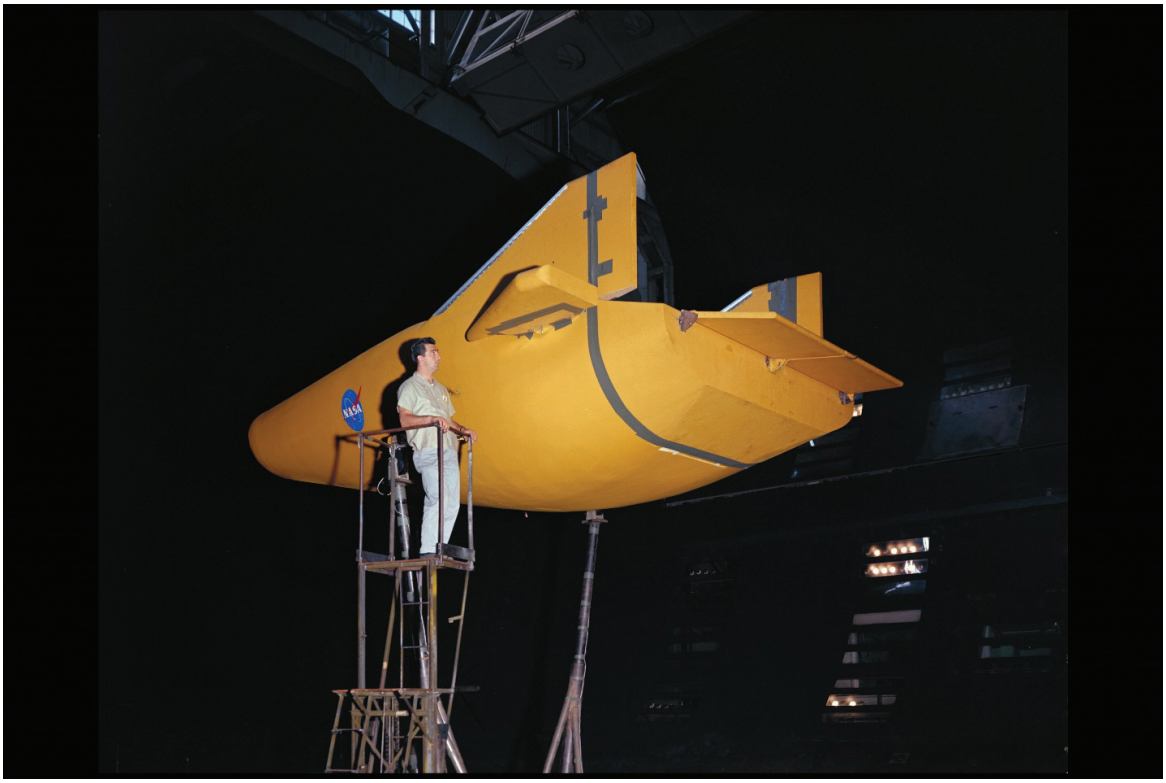

Figure 221. M2-F2 lifting-body model showing elevons on sides that were similar to the M2-F1, with Chuck Greco in photo. ***(NASA A-31465)***

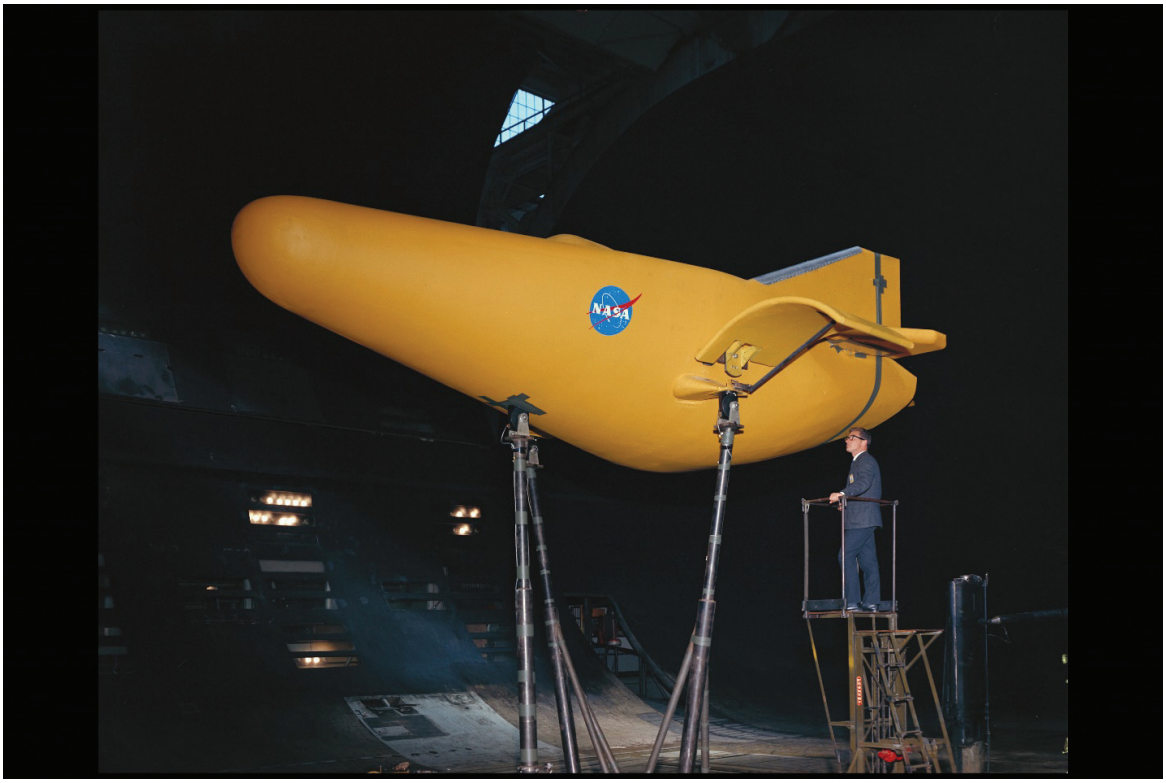

Figure 222. M2-F2 lifting-body model showing landing-gear doors that potentially could serve as quasi-wings (although they were not used), with Berl Gamse in photo. ***(NASA A-31467)***

M2-F2 aircraft. After a very successful program of flight studies at Dryden using the M2-F1, NASA decided to build a so-called "heavy M2" that became the M2-F2. It was built by Northrop. The wing loading (weight/body projected area) was 43.2 psf. It was intended for higher speeds and was to be launched from the B-52 aircraft that was used for X-15 aircraft launches. Wind tunnel studies were performed in the 40- by 80-Foot Wind Tunnel (Fig. 223, Test 240) [283] prior to flight-tests, as were subsequent simulator studies using the wind tunnel data.

The vehicle had retractable landing gear. The gear-down drag worsened the already low L/D, which was on the order of 3. At trimmed conditions, the L/D was reduced by about 0.7 when the gear were down [283]. Because of this, the gear were deployed only a few seconds before touchdown during test flights. It had been determined that the L/D had to be at least 3 for the machine to be landable.

Comparing the wind tunnel test results of the M2-F2 flight vehicle with the test results from the model made from the fiberglass shell indicated some differences, with the result that the flight vehicle had a lower L/D. There were small physical differences that caused the aerodynamic differences and that reduced the L/D by about 0.5. The model was smoother, it had no air leakage, and it did not have a nose boom (Test 217) [282, 283].

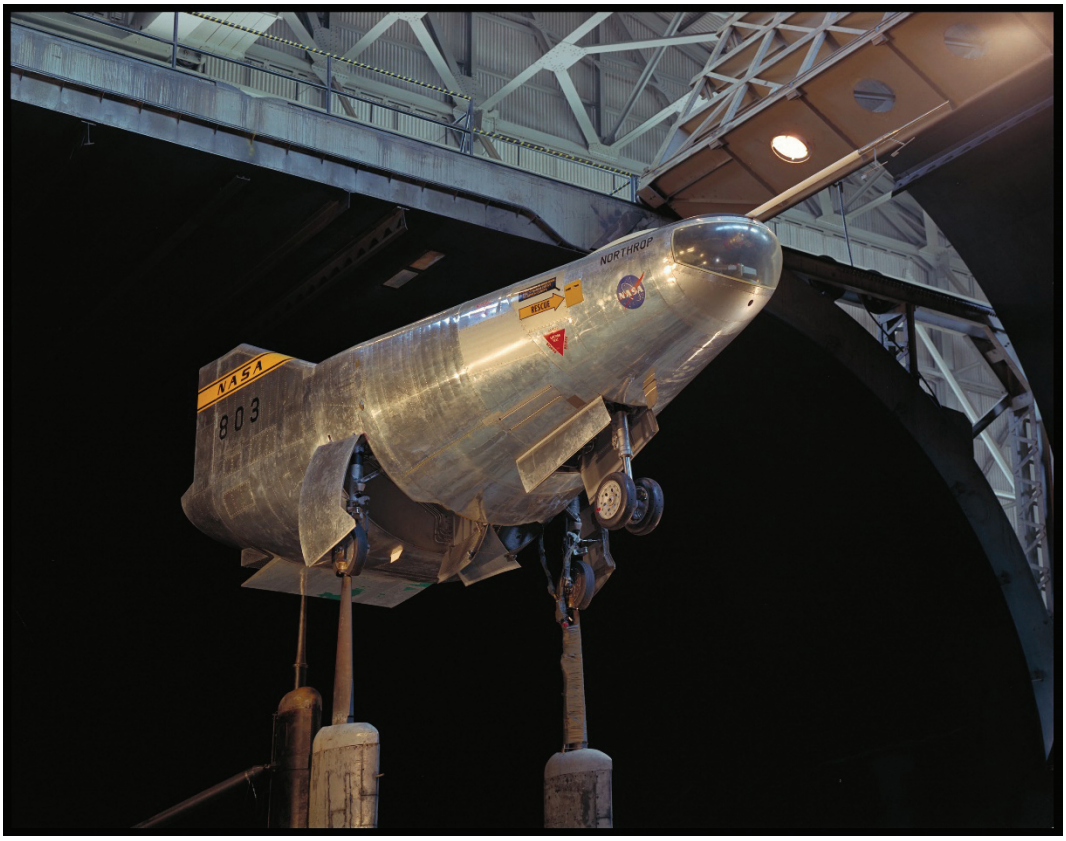

Figure 223. Three-quarter front view of M2-F2 lifting-body experimental aircraft with landing gear down. ***(NASA A-35069)***

During flight-tests at Dryden there was a major crash with the vehicle tumbling end over end; the M2-F2 was extensively damaged. (The film from the crash was used at the beginning of *The Six Million Dollar Man*, a popular TV show in the 1970s.) The pilot was distracted during the landing maneuver and did not deploy the landing gear quite soon enough. The pilot, Bruce Peterson, survived but lost his sight in one eye. The aircraft was rebuilt with a center fin, which had been found in wind tunnel studies to improve lateral-directional-control characteristics. The lateral-directional characteristics had proven problematic without the center fin. The rebuilt vehicle was called the M2-F3.

The M2-F2 wind tunnel model was used to evaluate the use of reaction control for the aircraft. Reaction control would be used at high altitudes where aerodynamic controls would lose effectiveness because of the low-density air. An electric model motor and blower were installed in the model to produce the flow for the reaction-control jets. Studies in the 40- by 80-Foot Wind Tunnel indicated that reaction control would be effective and would not adversely affect the basic aerodynamics or handling of the M2-F3.

HL-10 lifting body. The HL-10 lifting-body flight vehicle was the next lifting body to be studied in the 40- by 80-Foot Wind Tunnel (Figs. 224 and 225, Test 262) [284]. This flight vehicle was also built by Northrop. The HL-10 configuration was developed at Langley Research Center using model studies that included a large-scale model tested in the 30- by 60-Foot Wind Tunnel. This model was somewhat larger than the aircraft (28 feet long versus 22.2 feet) to increase the Reynolds number. Comparisons between the flight-vehicle data from the 40- by 80-Foot Wind Tunnel and the large-scale-model wind tunnel data from the 30- by 60-Foot Wind Tunnel were initially confusing; the vehicle drag was significantly higher than the model drag in the landing configuration. It was subsequently discovered, after discussions with the Langley Research Center research engineers (principally with George M. Ware), that there had been some minor modifications to the outboard fins that had not been incorporated into the flight vehicle. Flow separation occurred on the outboard fins when the movable trailing-edge fins were in the landing configuration, which was intended to minimize drag and maximize L/D. With the fins deflected in the landing configuration, a sharp corner was created that caused separation that did not occur on the Langley model because the corner had been radiused during the 30- by 60-Foot Wind Tunnel Tests. Early on it had been judged a minor difference by the Langley engineers, but this example illustrates the possible effects of small differences between models and actual aircraft, and the importance of performing wind tunnel testing of actual aircraft whenever possible. Unfortunately, during the first flight, additional fin aerodynamic problems were discovered. The flight program was put on hold, and the decision was made at Langley to perform additional wind tunnel studies (at Langley) and to develop modifications to the outboard fins. The fins were subsequently extensively modified after a year or so of studies. After the fin modifications, the flight-test program was successfully resumed and completed [278, 285].

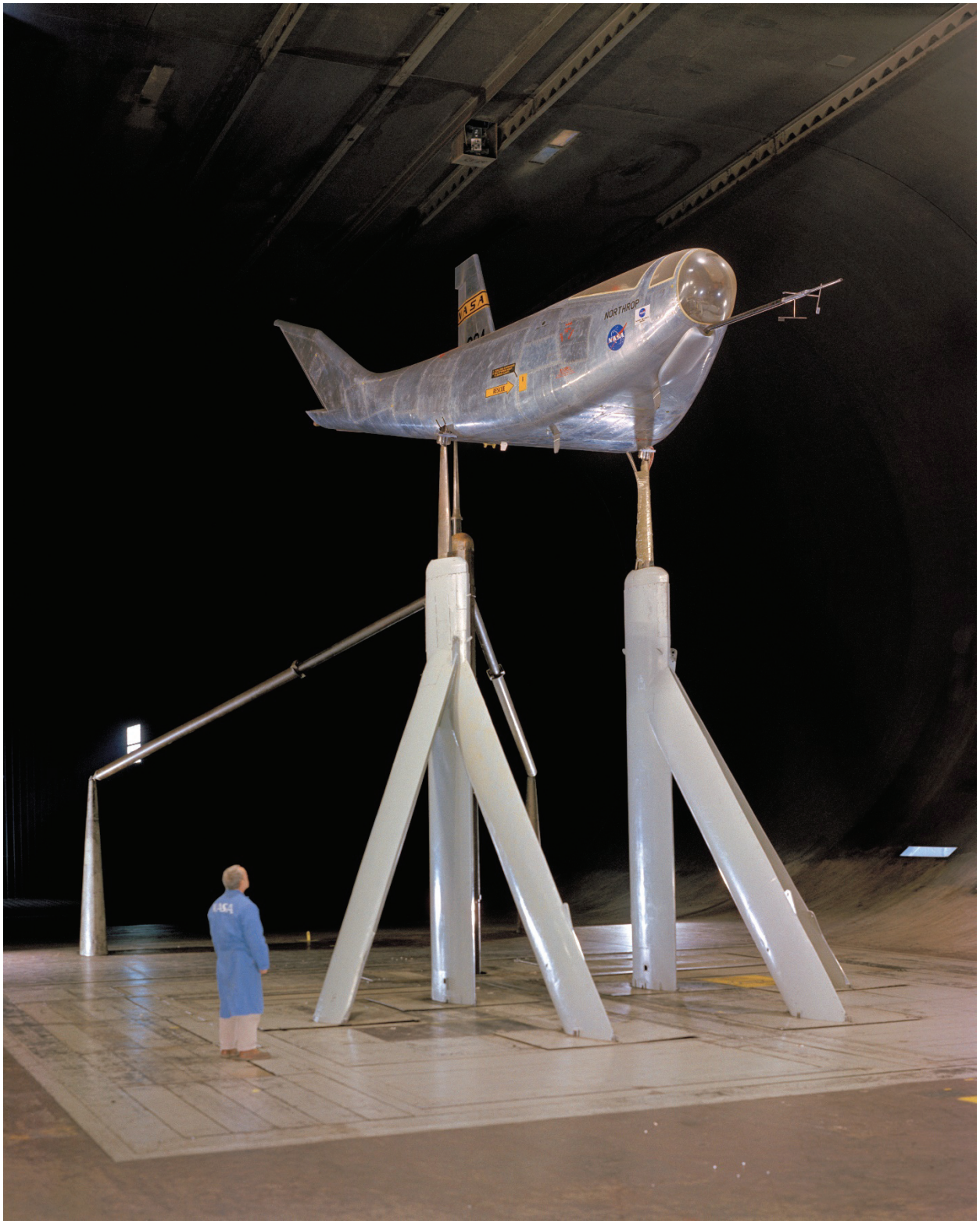

Figure 224. Three-quarter front view of HL-10 lifting-body experimental aircraft with Edwin Verrette in photo. ***(NASA AC-36601)***

Figure 225. Three-quarter rear view of HL-10 lifting-body experimental aircraft.
(NASA A-36621)

X-24A lifting body. The last lifting-body flight vehicle to be studied in the 40- by 80-Foot Wind Tunnel was the X-24A (Martin SV-5P) lifting-body aircraft, designed and built by Martin Marietta for the Air Force. As with the other lifting bodies, this aircraft was tested in the 40- by 80-Foot Wind Tunnel prior to simulator studies and flight-tests [286]. Figure 226 (Test 313) shows a three-quarter front view of the aircraft on the normal struts, and Figure 227 shows the aircraft mounted as it would be attached to the B-52 airplane for launching for flight-tests. The X-24A had a trimmed L/D that was a few tenths higher than the M2-F2 and the HL-10. Very good agreement was found with the 1/5-scale-model wind tunnel studies performed by Martin Marietta. Separation of the airflow on the outboard fins occurred at angles of attack near 20 degrees. This separation was very similar to that which had occurred on the HL-10 aircraft outboard fins. Abrupt changes in the lateral-directional characteristics occurred with this separation, however, the angle of attack at which this separation occurred was larger than the angle of attack at maximum L/D. Because of this, aerodynamicists judged that this separation would probably not occur during normal-trimmed flight but might occur during maneuvering flight, which would be acceptable. After the flight program was completed, the aircraft was modified and called the X-24B. The modified vehicle was not tested in the 40- by 80-Foot Wind Tunnel because the modifications were not considered significant enough as far as landing was concerned [286].

Figure 226. Three-quarter front view of Martin Marietta X-24A lifting-body experimental aircraft with Francis Malerick in photo. ***(NASA AC-40423-001)***

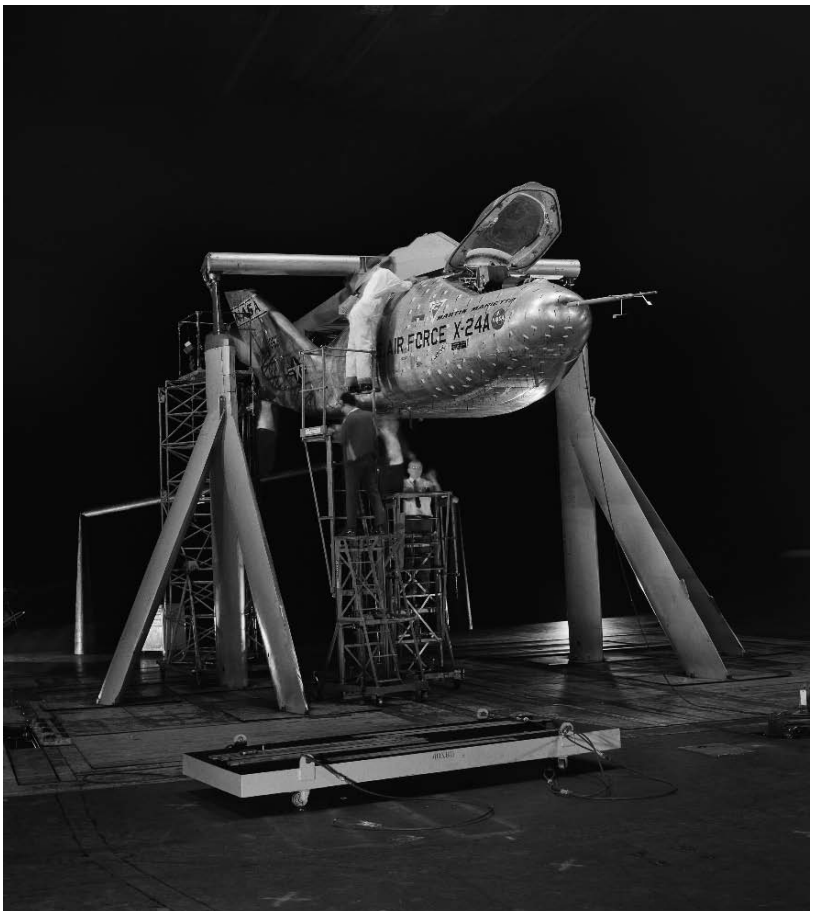

Figure 227. Martin Marietta X-24A mounted as it would be on the B-52 airplane for launching flight-tests. ***(NASA A-40423-009)***

M1-L lifting body. In addition to studies of the lifting-body aircraft, research was performed in the 40- by 80-Foot Wind Tunnel on a lifting-body model that had a higher volumetric efficiency than the M-2 and other lifting bodies. It was a 30-degree cone that was cut down to a shape that would produce increased lift (Figs. 228 and 229; Tests 186, 211, 247). It was to use an inflatable afterbody to increase L/D for landing. The configuration was called the M1-L. The original shape had been proposed by Ames Research Center in the early days of the lifting-body program. The model was built by Goodyear Aerospace Corporation that built airships with inflatable control surfaces. Deployment of the inflatable afterbody was successfully performed in the wind tunnel; the maximum L/D went from about 1 to greater than 2. It did successfully demonstrate the concept, but the L/D of the M1-L was judged to be too low for successful landings. In addition to the inflatable afterbody, the model was also tested with a rigid afterbody to evaluate the effects of the afterbody's flexibility on the aerodynamic characteristics. The model with the inflatable afterbody had an L/D about 15 to 20 percent lower than the model with the rigid afterbody because of bulging and wrinkles, etc. [287].

The lifting-body program was a great success in defining the minimum aerodynamic control and performance requirements required for landing an unpowered, wingless aircraft with low L/D.

Figure 228. Three-quarter front view of M1-L lifting-body model with inflatable afterbody.
(NASA A-35755)

Figure 229. Three-quarter rear view of M1-L lifting-body model with inflatable afterbody and vertical fins.
(NASA A-35756)

Space Shuttle

The success of the lifting-body program demonstrated that unpowered aircraft with low L/Ds, on the order of 3, could be reliably landed. This encouraged development of the space shuttle without an auxiliary engine for landing, which would save weight and be safer because engine fuel for landing would not have to be carried during space flight. Studies were performed in the 40- by 80-Foot Wind Tunnel on a 36-percent-scale model of the shuttle. Figure 230 shows the model being installed in the tunnel. Figure 231 is a three-quarter front view of the model, and Figure 232 is a three-quarter rear view of the model that shows mock-ups of the large engine nozzles. This was the largest model of the shuttle that could be practically tested in the tunnel without unacceptable wind tunnel wall effects. The model was built in the Ames shops. It was found that the L/D was somewhat higher than that of the lifting bodies; it was about 4-1/2.

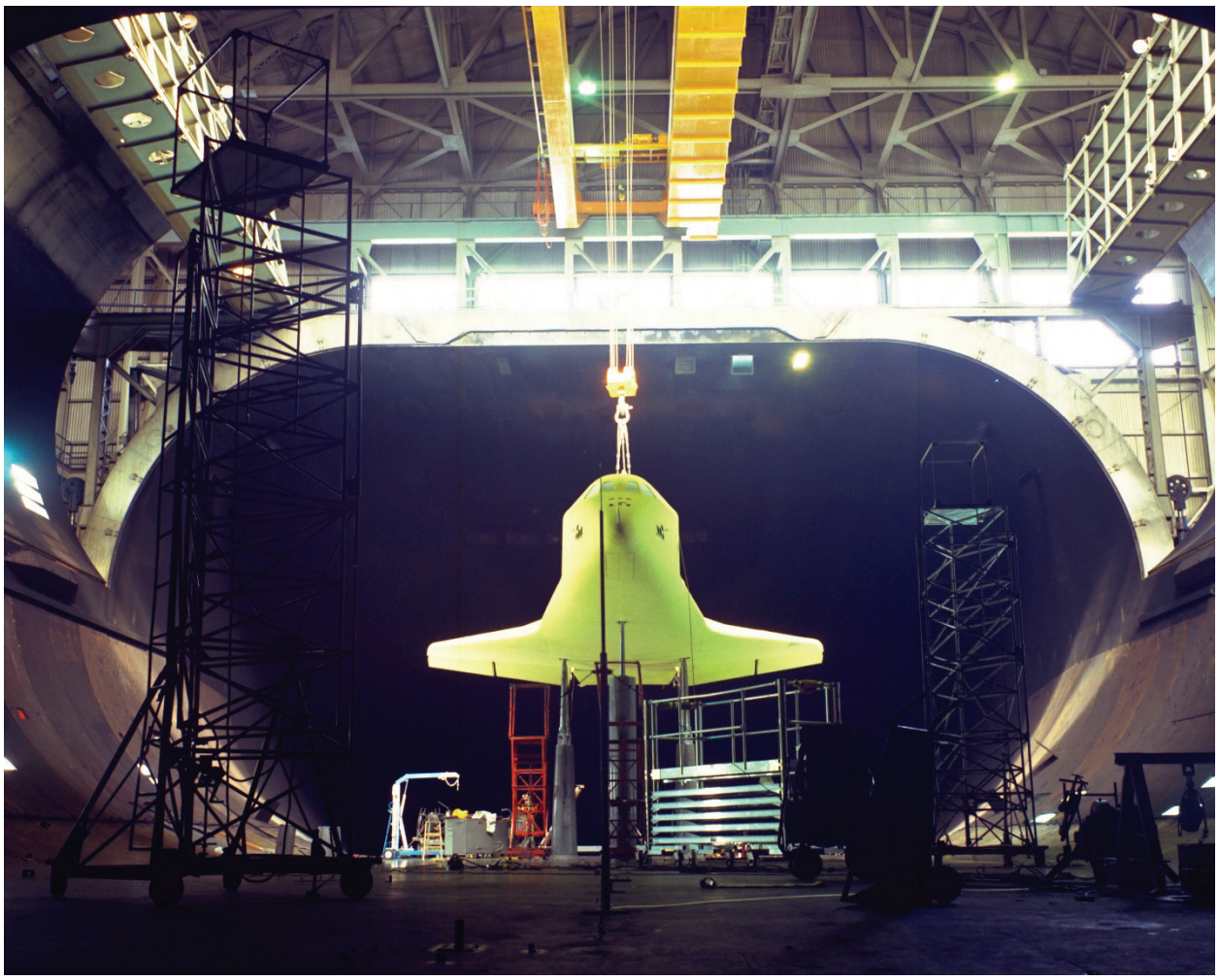

Figure 230. Installation of the 36-percent-scale space shuttle model. ***(NASA AC75-2584)***

Figure 231. Three-quarter front view of the space shuttle model in the wind tunnel. ***(NASA AC75-1161-004)***

Figure 232. Three-quarter rear view of the space shuttle model in the wind tunnel showing mock-ups of engine nozzles. ***(NASA AC75-1161-003)***

Predictions were validated, and the effects on drag of the surface roughness due to the ablation tiles were assessed in the tunnel. The effects of afterbody fairings, required when transporting the shuttle on the 747 airplane, were determined. Since the shuttle was to ride on top of a 747 for transport, the concern was that the wake from the shuttle might have an unacceptable effect on the vertical tail of the 747, so afterbody fairings were developed for the shuttle. In addition, development of the air data system (required for airspeed, angle of attack, and other considerations at subsonic speeds) was performed for the low Mach number portion of the shuttle landing. Stability and control data were obtained for use in landing simulation studies at the tunnel prior to flight. Prior to each shuttle flight, the shuttle pilots practiced landings using the Vertical Motion Simulator (VMS) at Ames, which utilized the data from the 40- by 80-Foot Wind Tunnel investigations.

Parachutes and Paragliders

A long-term goal at NASA was to develop gliding parachutes and paragliders for various applications, including space-capsule recovery. At one point, studies were done on the feasibility of a land landing for the Gemini program. If successful, gliding parachutes would also be used for the Apollo program. Over the years, various drag parachutes were also tested in the 40- by 80-Foot Wind Tunnel.

Early on, gliding parachutes were fabricated by merely cutting a vent in one side of a symmetric parachute and converting part of the canopy into a sort of flap (Fig. 233, Test 156) [288]. This produced an L/D of more than zero, but it was low, on the order of about 0.5, which was much less than the goal that was on the order of 3. Experiments were performed on clusters of three parachutes (Fig. 234). Engineers later developed more sophisticated parachute geometry, including rectangular shapes that had aspect ratios greater than 1 and had better L/Ds (Test 269) [289]. Some parachute configurations used ram air to maintain their shape. The Rogallo parawings were triangular shaped (Fig. 235) and were also a major improvement over round shapes [290]. The improved parachutes tended to have an L/D on the order of 2. Increasing the aspect ratio resulted in L/Ds of close to 3. One of the concerns with the early attempts to develop gliding parachutes was that the leading edge would often collapse or tuck under, making the parachute hard to reinflate during descent and gliding, and therefore very dangerous. This was extensively studied in the tunnel. Gliding parachutes developed later did not have this problem to the extent that the early parachutes did. Current gliding parachutes used by sky divers have L/Ds of on the order of 2.5 and are very reliable. Reference [290] (Test 312) presents wind tunnel results for several parawings.

A paraglider with large-diameter inflatable booms was constructed by North American for possible use in NASA's Gemini program. If successful, it would have also been considered for the Apollo program. Wind tunnel tests were performed with a 1/2-scale model (Fig. 236, Test 196). An L/D on the order of 4 was achieved, which was sufficient for a land landing [291]. However, the wing exhibited extensive aeroelastic effects; it was unsteady at high and low extremes in angles of attack. During deployment, the partially deployed wing was intended to act as a drogue chute, but it was very unsteady. The unsteadiness was so violent that the partially deployed paraglider would self destruct. This contributed to the judgment that the concept was

unacceptable for land landing the Gemini capsule. The sail cloth used for the canopy had very low porosity and there was no venting, which probably contributed to the unsteadiness at partial deployment. Drag parachutes usually require significant venting to prevent or minimize unsteadiness.

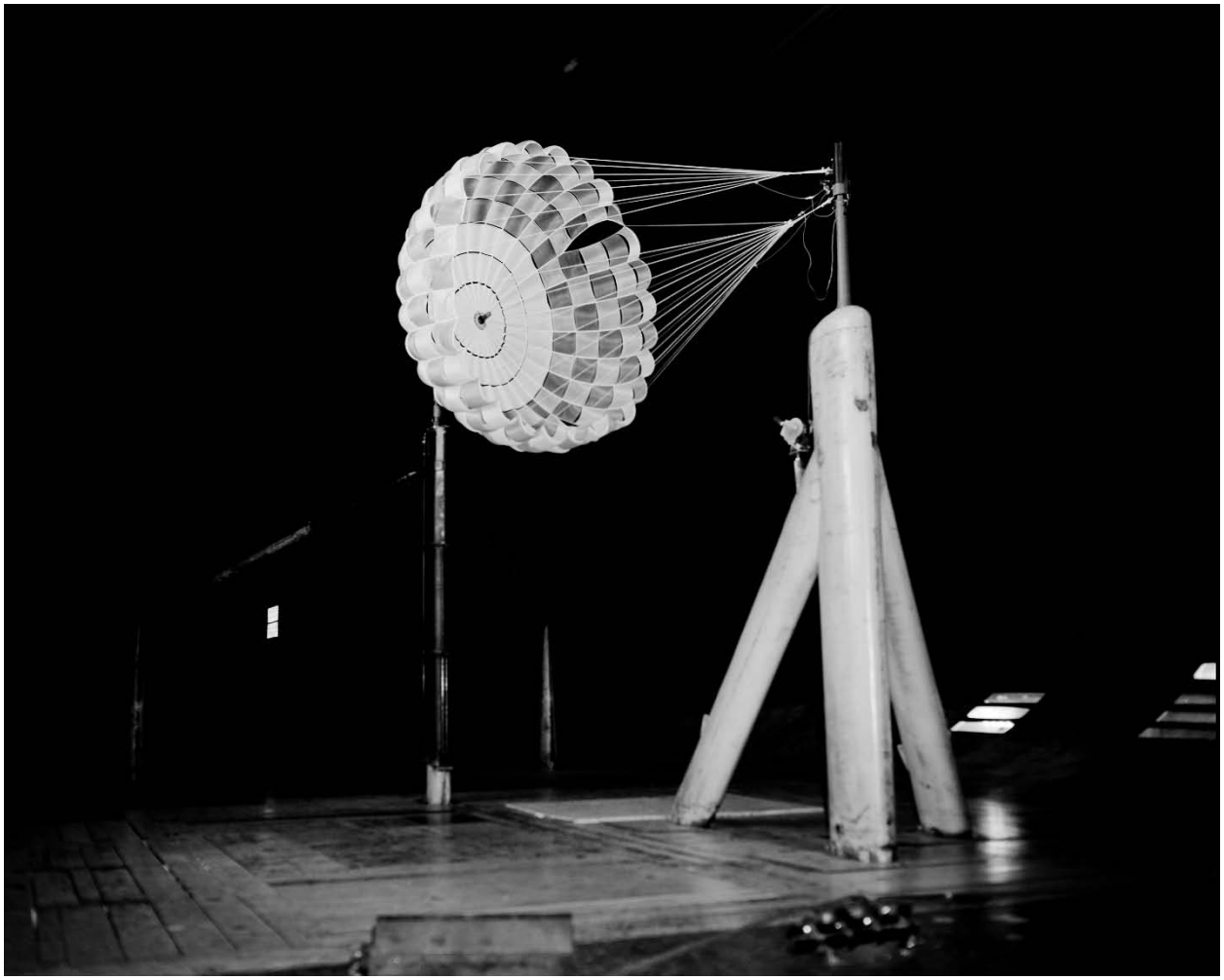

Figure 233. Early parachute experiments in the wind tunnel with horizontal orientation; tail-strut sting in the central vent hole. The sting could be translated side-to-side for performing stability experiments. ***(NASA A-29215)***

Figure 234. Cluster of three parachutes in vertical orientation. ***(NASA A-32159)***

Figure 235. Dual-keel parawing in wind tunnel with vertical orientation. ***(NASA A-40414)***

Figure 236. A 1/2-scale paraglider model with inflatable booms; suspension lines attached to capsule model. ***(NASA A-29418-6)***

Acoustics

Early on, the feasibility of performing acoustic research in the 40- by 80-Foot Wind Tunnel was explored. Acoustic instrumentation was developed that could offset the effect of tunnel wall reverberation. The background noise of the wind tunnel drive was corrected for by using acoustic measurements of drive-alone noise. The microphone and support self-noise were reduced. It subsequently became routine to frequently make acoustic measurements of models in the tunnel during aerodynamic testing. At least half of the research tests included acoustic measurements.

The following is an interesting history of the acoustic research performed in the 40- by 80-Foot Wind Tunnel, written by Paul Soderman, who started the program.

> The genesis for acoustic research in the 40- by 80-Foot Wind Tunnel, the fruits of which have spread to aeronautic and automotive wind tunnels around the world, can be attributed to Mark Kelly—40- by 80-Foot Wind Tunnel Branch Chief in the 1960s and 1970s. In 1967, Mark walked into the office of a newly minted aero engineer, Paul Soderman, and asked Paul to find a way to measure noise from a helicopter being readied for a test in the 40- by 80-Foot Wind Tunnel. Kelly recognized that helicopter noise was a serious problem, so with his usual can-do attitude decided that while we were putting the model through its paces aerodynamically, why not measure the noise as well. To our knowledge that had never been done before in a wind tunnel. Soderman had never studied acoustics, but realized that aerodynamic noise—unsteady pressures, propagating waves, etc.—must be a subset of aerodynamics and therefore amenable to aero-physics analysis. So he signed out a sound level meter* from the Instrumentation Branch and installed a microphone in the 40- by 80-Foot Wind Tunnel with a signal cable connected to the meter outside the test section and commenced to measure helicopter noise. The signal was quite strong but confusing [292, 293].
>
> It was found that the measurement of aircraft noise in the 40- by 80-Foot Wind Tunnel was handicapped by three important problems. First, the steel test-section walls created very strong reflections and a reverberant sound field that tended to mask and confuse the aircraft noise. Second, the six drive-fans generated a very loud noise that easily followed the circuit—a noise that was compounded by the 1940ish fan design that placed large motor-support struts just upstream and close to the rotors thereby feeding strong wakes into the fans. Third, microphones and microphone support struts in flow create turbulence noise that can mask sound from all but the noisiest models. Despite these challenges, the 40- by 80-Foot Wind Tunnel had the advantage of size—microphones could be placed in the far field of many noise sources. And the wind tunnel was well equipped for powered model testing with real propulsors. Thanks to outstanding mechanical-engineer designers at Ames and first-rate machine shops, traversing microphone systems, calibrated loud speakers, and other special apparatus were soon developed and available for exploring the acoustic environment. Thus, began a long research and development program by Soderman and his Acoustics Group comprised of Clifton Horne, Chris Allen, Julie Hayes, Steve Jaeger, Nate Burnside, Adolph Atencio, Srba Jovic, and others tasked to solve those problems and perform acoustic research.
>
> The reverberant- and background-noise problems were addressed by developing phased microphone arrays that could beam form and selectively scan the model's acoustic sources while rejecting unwanted sound. Of course, acoustic antennas can be traced back to the early days of World War I and more recently to Bell Labs in New York, but they had never been

* R. T. Jones, aerodynamic pioneer of the swept wing and swing wing aircraft, asked to borrow the same sound level meter from Soderman for development of advanced violins and guitars. Soderman was ribbed by his colleagues for making the celebrated Jones sign a loan receipt. Bureaucratic protocol was preserved.

used in wind tunnels until Soderman and Noble installed simple four- and eight-microphone versions [294, 295] in the 40- by 80-Foot Wind Tunnel. Those simple devices used electronic delay circuits to control signal-phase (delay and sum), but with the rapid development of computer technology and high-speed analog-to-digital converters, phased arrays became more complex and more effective in wind tunnel applications. With these instruments, researchers can visualize sound radiation from aircraft or automotive components in wind tunnels using computer graphics at the same time aerodynamic investigations are being performed. The real-time synergism of acoustics and aerodynamics is a powerful tool for aerodynamic noise reduction and is now used in many research facilities worldwide. The original beam forming algorithms for this work were based on the theoretical work of Marianne Mosher of Ames [296] and were implemented by many fine software developers such as Srba Jovic, Mike Barnes and others at Ames. We also collaborated with Boeing researchers—notably Bob Dougherty and Jim Underbrink—who were eager to adapt phased arrays for studies in Boeing facilities as well as in Ames facilities (see chapters two and three of reference [297]).

Wind Tunnel Noise

Noise studies were performed to define and document the noise produced by the wind tunnel. In addition to data taken at various locations inside the tunnel for possible acoustic research, noise surveys were performed on the outside and around the tunnel at various distances from the tunnel. It was important to define the noise impact at other locations at the Center as well as at the neighboring communities.

Airplane Flyover Noise to Verify Wind Tunnel Acoustic Measurements

Airplane noise measured on the ground with airplanes flying overhead at 50 feet was compared with noise measured in the wind tunnel. The microphones were lined up on the ground, similar to the wind tunnel configuration, and the aircraft would fly overhead. The purpose was to verify the acoustic measurements made in the wind tunnel.

YOV-10A STOL aircraft. Comparisons of wind tunnel and flyover noise measurements were performed using a modified North American YOV-10 propeller-driven Navy airplane. The plane was modified to increase its low-speed performance. A high-lift flap system was used with rotating cylinders to keep the airflow attached over the wing to enable a larger speed range and a larger angle-of-attack range than allowed with a convention flap system, and thereby reduce the landing speed. Instrumentation on the ground along the airplane flightpath was used to define the airplane noise. The airplane was flown over the ground at an altitude of 50 feet. The purpose of the experiments was to determine the validity of wind tunnel acoustics experiments. It was found that the agreement between corrected wind tunnel data and flight data was good [298].

XV-5B V/STOL aircraft. Comparisons of wind tunnel and flyover noise measurements were performed using jet-engine-powered lift-fan V/STOL experimental aircraft. The airplane had 5-foot-diameter lift fans in the wings and a 3-foot-diameter lift fan in the nose. The plane was flown at 50 feet altitude in conventional jet mode over the microphone array on the ground. The data were compared with data taken during a test of the same aircraft in the Ames 40- by 80-Foot Wind Tunnel. The corrected data showed good agreement [299].

Quiet Lift Fans

Fairly late in the lift-fan research program conducted at NASA Ames Research Center, the LF-336, a 1.3-pressure-ratio lift fan, was built by General Electric. Two fans were designed and assembled at Edwards Air Force Base in Southern California. This fan was not originally designed as a quiet fan, but fan noise was becoming an area of concern. The fan was modified to reduce noise and was designated LF-336/B. Extensive noise measurements were conducted as part of a contract with General Electric at their outdoor complex at Edwards Flight Research Center. Modifications to the fan that gave the greatest noise reduction were:

- Incorporating a 90-vane stator with 30 degrees of lean in the direction of rotation.
- Increasing the rotor-stator spacing to two fan-blade chords.
- Placing acoustic material at the hub and tip walls, and adding an acoustic splitter.

This quiet fan was tested in the 40- by 80-Foot Wind Tunnel in a semispan wing with both aerodynamic and acoustic measurements taken to compare with the outdoor measurement at Edwards. The acoustic modifications were shown to be very effective, and the agreement between outdoor measurements and wind tunnel measurements was reasonably good (Fig. 165, Tests 371 and 373) [300].

STOL Aircraft Configuration Studies

The acoustics of various STOL transport aircraft configurations were studied in the tunnel including EBF configurations, the augmentor wing, jet-flap configurations, and USB configurations [269, 275, 301-304]. STOL transports have the potential for operation near community centers, and low noise is very important.

Airframe Noise

Extensive experiments were performed to define airframe noise. High-lift devices cause increased noise when they are deployed at landing and takeoff. A triple-slotted-flap system is shown in Figures 237 and 238 on a semispan wing model as an example of experiments on high-lift systems. The microphone stands are shown in the photo.

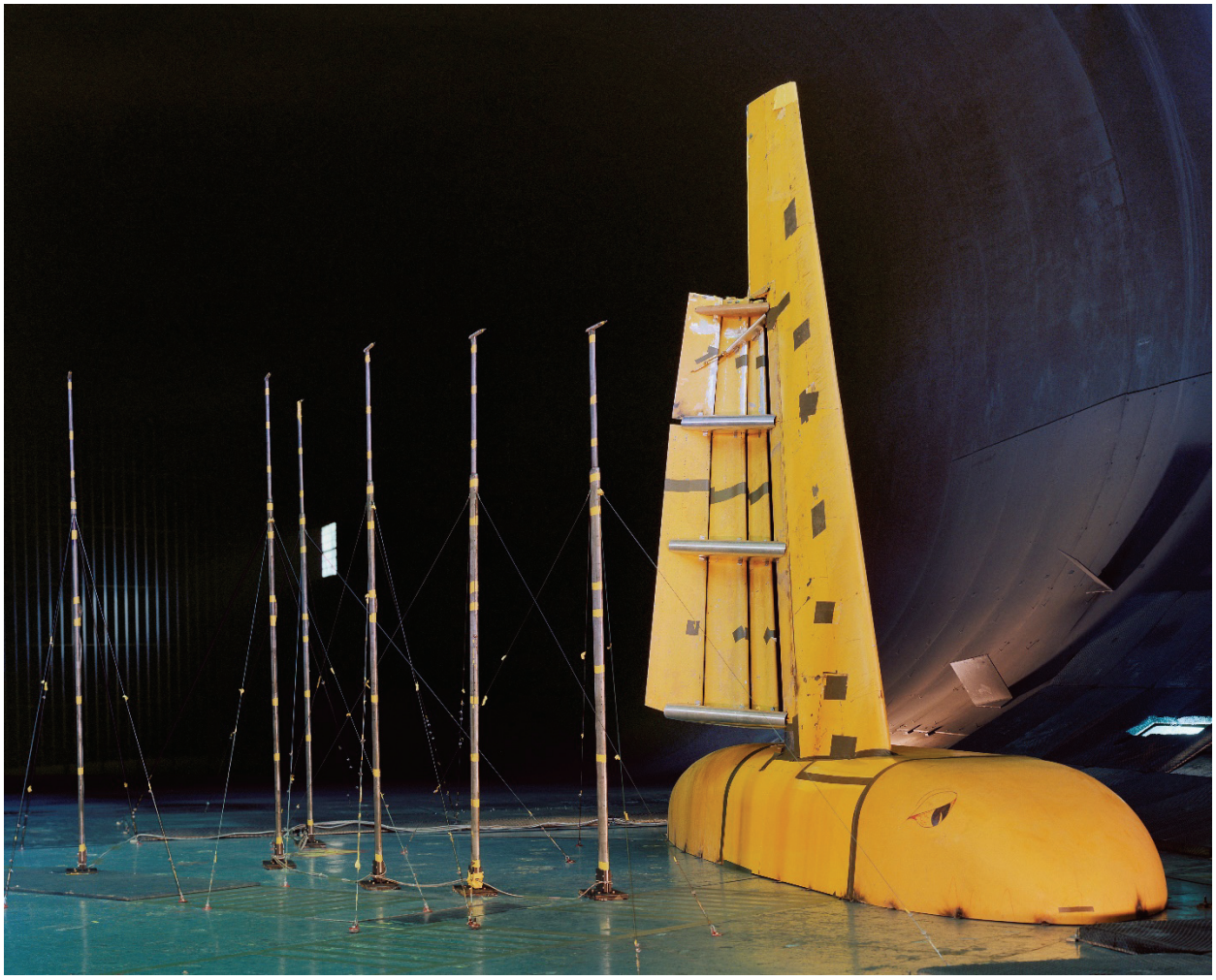

Figure 237. Airframe noise semispan model with triple-slotted flap. ***(NASA AC78-1062-1)***

Figure 238. Airframe noise semispan model with close-up of triple-slotted flaps. ***(NASA78-1062-2)***

Miscellaneous

Wind Tunnel Pressure Surveys

Over the years the maximum airspeed in the 40- by 80-Foot Wind Tunnel had decreased. At various opportunities, different measurements were taken in an attempt to discover the reason. Runs with and without the model-support struts were made. Flow surveys were made in the primary diffuser and the first cross leg (north leg) by using a pitot-static probe designed by Joe Piazza with a streamlined fairing that looked like a missile. It was guided up and down cables strung from floor to ceiling at various locations in the primary diffuser. Pressure readings were taken at various locations to allow velocity distributions to be derived. In addition to these measurements, rakes were installed diagonally at the end of the primary diffuser in the four corners and upstream of the first set of turning vanes (first set downstream of the test section). Static pressures were measured down the floor of the primary diffuser and along the floor of the north cross leg. It was found that pressure recovery was still occurring in the constant area cross

leg, but intermittent separation was occurring in the corners of the primary diffuser. The boundary layer was many feet thick at the end of the primary diffuser. It was determined that the gradual maximum-airspeed reduction was due to a number of causes, such as holes in the tunnel walls, and soot buildup on turning vanes and drive-fan blades, and was not due to a single cause.

Wind Tunnel Wall Effects

Despite the large size of the tunnel, wind tunnel wall effects were often a concern, especially when performing experiments on V/STOL models. Occasionally, experiments were performed to define wall effects. One such set of experiments was performed on a small fan-in-wing model that had been tested in the 7- by 10-Foot Wind Tunnel. Since the model only had a wingspan of 42 inches, the experiments in the 40- by 80-Foot Wind Tunnel were performed to define the interference-free aerodynamic characteristics. These data were used, along with the data from the 7- by 10-Foot Wind Tunnel, to define the wall effects for this model that was essentially a generic fan-in-wing model. The data contributed to the understanding of the wall corrections required.

Oblique-Wing Remotely Piloted Research Aircraft

NASA Ames theoretician R. T. Jones had proposed that wing sweep forward on one side and aft on the opposite side would be as effective at supersonic speeds as the more usual symmetric sweep back (or forward) on both sides. This had the potential for making supersonic aircraft simpler than aircraft with variable sweep back on both sides because of simplification of the wing-sweep mechanisms. To study the low-speed implications of this concept, a flying remotely piloted aircraft was built for low-speed flight-tests. Before flight-tests, the model was tested in the 40- by 80-Foot Wind Tunnel (Fig. 239, Test 455 and 468). The wing swivels in the center about the ducted propeller, which was designed to propel the model. The wing could swivel with the left wing 45 degrees forward and the right wing 45 degrees aft. The program was successful, and subsequently a jet-powered, piloted experimental aircraft was built with a swiveling wing.

B-77 Lifting Parachute

The B-77 parachute was intended for weapons delivery by the B-1A bomber. The potential conditions for the delivery were to be from supersonic speeds at altitudes of 60,000 feet to subsonic speeds at altitudes as low as 100 feet. The parachute was tested in the wind tunnel to determine its flying orientation and forces. It was mounted to a floor mounting (Tests 467, 489, and 494). This was an unusual parachute test for the wind tunnel because it was not for spacecraft recovery, as were the majority of the parachute tests in the tunnel. The experiments were successful, but the program was cancelled because of cancellation of the B-1A bomber.

Figure 239. Oblique-wing remotely piloted research model with the wing in the straight orientation.
(NASA AC75-2410)

Chapter 10. Research and Testing, 1987–2014

Overview

Research testing resumed in 1987 after the repowering and addition of the 80- by 120-foot test section and continued until the tunnel's temporary shutdown in 2003. The research included rotorcraft, V/STOL, conventional aircraft, and space-related recovery devices such as parafoils and large parachutes [305, 306]. Early research on the joint strike fighter (JSF), which evolved into the F-35, was performed. A principle rationale for building the 80- by 120-foot test section was to perform research on V/STOL models and aircraft like the JSF, which are very expensive to develop, and large-scale or full-scale wind tunnel experiments can significantly reduce development cost. Special large-scale or full-scale propulsive devices could also be studied at landing and transition airspeeds before flight-tests.

The tunnel was shut down from 2003 to 2007. After refurbishment, the tunnel was started back up in 2007. In addition to Army aviation research on rotorcraft after the startup in 2007, tunnel test time was sold to a variety of customers by the U.S. Air Force at rates that were much more reasonable than what NASA Ames had been charging under "full-cost recovery." The rates were more reflective of the actual operating and overhead costs. Research was resumed on rotorcraft, V/STOL aircraft, recovery devices, and drag-related test devices. NASA research was also performed (paying fees to the Air Force) because of the unique capability of the NFAC. Mars Science Laboratory (MSL) parachutes were studied and developed.

Rotorcraft

Tilt-Rotors

As mentioned previously, NASA Ames and especially the 40- by 80-Foot Wind Tunnel Branch have always championed the tilt-rotor aircraft concept, from the XV-3 and XV-15 to the V-22 and future civil and military tilt-rotor concepts. When size permits, actual aircraft have been studied in the tunnel, as well as candidate rotors (proprotors), which are designed for tilt-rotor aircraft. Rotor investigations have frequently been performed on proprotor-wing semispan models and on helicopter test rigs to investigate candidate rotors at large scale. As mentioned, research on tilt-rotors is described separately from research on advanced helicopters in this book.

XV-15 tilt-rotor. Full-scale isolated XV-15 rotor experiments were performed in the 80- by 120-Foot Wind Tunnel in the helicopter orientation. Because of its size, the 80- by 120-Foot Wind Tunnel accommodated larger sizes and lower test speed investigations with minimal tunnel-wall interference. The design of the XV-15 rotors was a compromise between hover and airplane mode in forward flight. The 25-foot-diameter rotors are twisted to provide good performance in forward flight, but as a result are not optimum for edgewise flight in helicopter mode. Consequently, many experiments were done with one of the rotors in the helicopter mode. The right-hand XV-15 hub and rotor on the rotor test apparatus (RTA) is shown in Figure 240 (Tests 828 and 80-0048). Performance results are presented in reference [307] and acoustic results in reference [308]. It was found that, because of the high blade twist, the inboard portion of a proprotor generally produces more thrust than a helicopter rotor. In some descending flight

Figure 240. Isolated proprotor experiments for the XV-15 tilt-rotor aircraft in hover orientation in the 80- by 120-foot test section. ***(NASA AC98-0261-6)***

conditions, the tip of the proprotor may be negatively loaded, producing a pair of counterrotating trailing vortices that makes it difficult to derive accurate performance predictions using analytical codes.

Acoustic experiments were performed on the XV-15 rotor to study blade vortex interaction (BVI) noise. Rotor blades produce tip vortices, much like a wing, that are encountered by the following blade causing increased noise. Several noise reduction concepts were studied [309]. One of the concepts studied was to use four blades instead of three. Adding another duplicate blade increased rotor solidity and allowed for reduced rotational speed, which reduced the rotor-tip Mach number and resulting noise.

Higher harmonic control (HHC) was also investigated to reduce noise and vibration produced by the XV-15 rotor. The higher harmonic blade-root pitch (higher than once per revolution (1/rev)) was generated using swashplate oscillations. It was found that the HHC was highly effective in reducing BVI noise, achieving a 12-dB reduction in peak noise level within the noise footprint [310].

V-22 rotor model. The V-22 was the first tilt-rotor aircraft to go into production; it was a logical follow-on to the XV-15 research aircraft and was significantly larger than the XV-15. There were many rotor experiments performed in the 40- by 80-Foot Wind Tunnel in support of the V-22 program; experiments were performed on a 2/3-scale model of the rotor and wing. The principal objectives were to measure the wing download in hover and to measure rotor performance in forward flight. In addition, limited data were obtained in vertical-climb conditions (Fig. 241, Tests 568 and 579). Wing surface pressures were measured. It was found that the wing flaps can produce substantial lift loads in hover. Sample wind tunnel hover results are presented in reference [311], and forward-speed results as well as hover results are provided in reference [312]. Experiments under the Joint Vertical Experimental (JVX) program were also performed on a 0.656-scale preliminary V-22 proprotor. This rotor differed from the V-22 rotor in several minor respects [313]. The experiments were performed on a single rotor on the propeller test rig (Test 579).

Figure 241. A 2/3-scale V-22 tilt-rotor aircraft proprotor in cruise orientation in the 40- by 80-foot test section. ***(NASA AC88-0182-2)***

The Dream Machine, the Untold History of the Notorious V-22 Osprey by Richard Whittle [314] is an excellent book; it is very comprehensive and contains a detailed description of the development of the V-22 tilt-rotor aircraft. In addition to the research and development descriptions, the book describes much of the politics that went on during the course of the development and subsequent flight-testing and production.

Figure 242. TRAM test stand; approximately 1/4-scale model V-22 in the 40- by 80-foot test section. ***(J. Sacco collection, T40-0062)***

The tilt-rotor aeroacoustic model (TRAM). The TRAM consists of two test stands: an isolated-rotor test stand and a large-scale full-span model with dual rotors and a complete airframe [315]. The baseline test stands are a nominally 1/4-scale model of the V-22 Osprey aircraft (Fig. 242, Test 40-0062), designed to investigate tilt-rotor aircraft technologies. These test stands were developed for research on tilt-rotor aircraft because of the unique and outstanding potential of tilt-rotors for future subsonic-transport aircraft for both military and civil applications. An overview is presented in reference [316], along with a description of the initial testing in the 40- by 80-Foot Wind Tunnel. As of 2014, many experiments have been performed, and extensive studies are planned for the future [317].

Advanced Helicopters

No tail rotor (NOTAR). The NOTAR system eliminates the tail rotor by using a fan, driven by the main rotor transmission, which blows air down the inside of the tail boom and out of two tail-boom slots. These slots use the Coandă effect to induce airflow over the aft part of the tail boom to create an anti-torque moment, which balances the torque created by the main rotor. This is augmented by a direct-jet thruster that provides flow normal to the tail boom. The purpose of the NOTAR system was to eliminate the personnel hazard caused by the normal helicopter tail rotor. Vertical stabilizers were also used for rotor-torque control during forward flight. Hughes Helicopters originally began concept development. Currently, MD Helicopters, Inc. (formerly McDonnell Douglas Helicopter Systems) produces three helicopters that employ the concept.

McDonnell Douglas advanced rotor technology (MDART). The MDART has a bearingless main rotor (BMR), which uses composite flexbeams at the blade root instead of bearings in its hub. BMRs have been continually studied because of their potential for making helicopter hubs simpler, more reliable, safer, and with lower maintenance. Experiments on the MDART are described in reference [318]. The bearingless hub is simpler than a conventional hub, but the analysis of rotor aeroelasticity is complicated because of redundant load paths, complex bending-torsion, geometrical couplings, and material nonlinearities. Reliable predictions are often dependent on comprehensive databases, but for bearingless rotors this is a special problem

because of the structural complexity and lack of sufficient existing data. The 34-foot-diameter rotor had five blades and is shown in the 40- by 80-Foot Wind Tunnel in Figure 243 (Test 583).

Figure 243. MDART rotor in the wind tunnel. ***(NASA AC92-0078-9)***

In addition, the MDART rotor was the first full-scale rotor to have HHC implemented. This system is designed such that the swashplate can be tilted at frequencies higher than 1/rev. The actuators, which are part of the nonrotating system, traditionally tilt the swashplate 1/rev, but the HHC is designed to tilt the swashplate at higher frequencies but at smaller amplitudes. The purpose is to reduce vibration and noise, and thereby allow somewhat higher forward airspeeds.

Sikorsky S-76 BMR. The S-76 was a proof-of-concept five-bladed full-scale main rotor tested in the 40- by 80-Foot Wind Tunnel at speeds from hover up to 200 knots. The rotor was 44 feet in diameter and was sized for the Sikorsky S-76 helicopter. It was mounted on the RTA, which has two 1,500-hp electric motors to drive the rotor (Fig. 244). The test provided a comprehensive set of data for better understanding of the BMR concept and for assessing the state-of-the-art of aeroelastic rotor analyses. It was found that the rotor was stable at all test conditions [319].

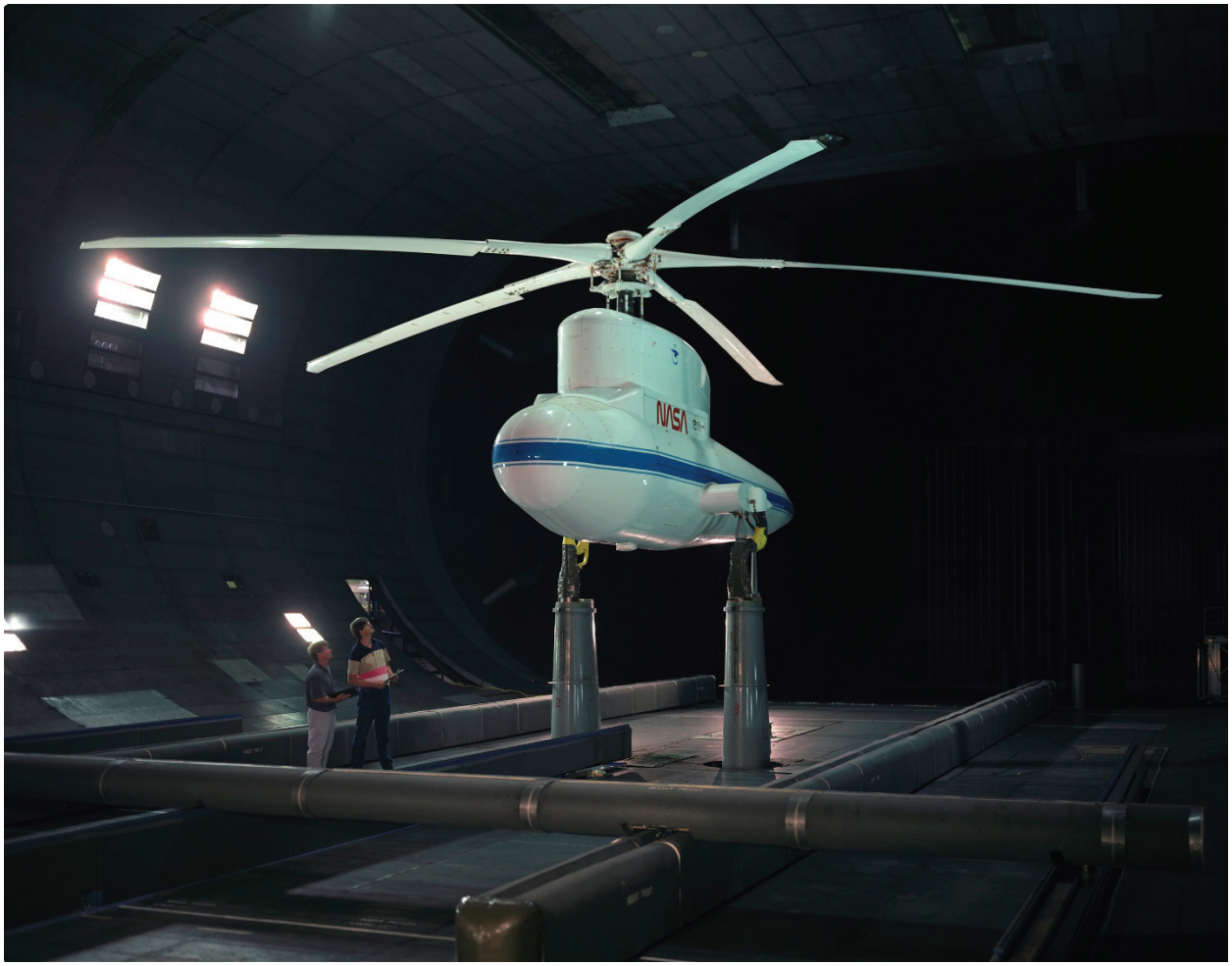

Figure 244. Sikorsky S-76 proof-of-concept BMR. ***(NASA AC92-0323-117)***

MBB Bo-105 hingeless main rotors. So-called "hingeless" rotors do not have flapping bearings nor lead-lag bearings, but use composite flexbeams to allow blade flapping with damping. They still have pitch (feathering) bearings. A full-scale Messerschmitt-Bölkow-Blohm (MBB) Bo-105 hingeless rotor system was tested in the 40- by 80-Foot Wind Tunnel (Fig. 245, Test 587). The rotor had four blades and was 32.2 feet in diameter. The test was performed in support of the rotor data collection task under the U.S. Army-German Memorandum of Understanding (MOU) on cooperative research in helicopter aeromechanics. The primary purpose was to create a database for full-scale hingeless rotor performance and structural blade loads. A secondary purpose was to produce wind tunnel data that was appropriate for comparison with flight-test data. Data from hover up to 170 knots were collected. The test results are presented in reference [320].

Figure 245. MBB Bo-105 hingeless main rotor mounted on the RTA. ***(NASA AC93-0035-13)***

Sikorsky Aircraft S-76 rotor—basic performance, loads, and acoustics. Experiments were performed in the 80- by 120-Foot Wind Tunnel on the Sikorsky S-76 helicopter rotor to obtain data at speeds ranging from 0 to 100 knots. The objectives were to acquire data for comparison with theoretical results, to allow comparison with results obtained in the past in the 40- by 80-Foot Wind Tunnel (previous experiments had not been done at velocities below 60 knots because of potential wind tunnel wall effects), to evaluate the acoustic capability of the 80- by 120-Foot Wind Tunnel for obtaining BVI noise for comparison with flight-test data, and to evaluate the capability of the 80- by 120-Foot Wind Tunnel test section as a hover facility [321, 322]. In addition, one of the goals was to assess wall-effect corrections. The rotor was the same as the one tested in the 40- by 80-Foot Wind Tunnel, but modifications had been made to the RTA; a rotor balance was installed at the top of the apparatus that required an additional enclosure at the top of the rig (Fig. 246, Test 815). A shadowgraph flow visualization technique was also investigated [323]. Shadowgraph is a technique in which light through the fluid—air in this case—shows the variations in fluid density. This was the first time (early 1990s) that a wide-field shadowgraph flow visualization technique was used for a full-scale helicopter rotor test. The results were very promising.

Helicopter Individual Blade Control (IBC)

The blade angle for each blade on a typical helicopter rotor is controlled by a fixed-length pitch link. One end is attached to the blade and the other end is attached to a swashplate that can translate up and down or tilt. The pitch link is used to rotate the blade about its pitch axis to change its blade angle. The center part of the swashplate, in which the pitch links are attached, rotates, and the outer part does not (there is a large-diameter bearing between the two parts so that the outer part does not rotate). The swashplate and pitch links translate up and down to change the blade angle of all of the blades together (collective pitch) to vary the lift force to cause the helicopter to go up or down. In addition, the swashplate can tilt to change the cyclic pitch of the blades as they rotate about the rotor shaft so that the blade angle of each blade varies as it rotates around the rotor shaft 1/rev. This tilts the rotor thrust force so that the helicopter can translate; that is, move forward or backward or side to side. Experiments and many studies have been performed to replace the fixed-geometry pitch links with actuators. The idea is to introduce a variation in blade angle that varies several times per revolution as the blade rotates, instead of 1/rev. The purpose is to reduce noise and vibration, reduce blade loads, and increase efficiency.

MBB Bo-105 rotor IBC. The first set of experiments performed in the 40- by 80-Foot Wind Tunnel on IBC concepts was in 1993 on an MBB four-bladed, 32.2-foot-diameter, hingeless Bo-105 rotor mounted to the RTA, described above (Fig. 245, Tests 587 and 595). The experiments were an international, collaborative effort between NASA/U.S. Army Aeroflightdynamics Directorate (AFDD), ZF Luftfahrttechnik GmbH (ZFL), EuroCopter Deutschland GmbH, and the German Aerospace Laboratory (DLR), and were conducted under the auspices of the U.S./German MOU on Rotorcraft Aeromechanics. During these tests, it was found that there were very significant reductions of all vibratory rotor forces and moments as well as suppression of BVI noise [324].

Figure 246. Sikorsky UH-60 helicopter rotor in the 80- by 120-foot test section on the large rotor test apparatus (LRTA). ***(NASA AC00-0140-2)***

Reference [325] describes the results of the second test in the 40- by 80-Foot Wind Tunnel. In the second test it was found that the BVI noise could be reduced by up to 12 dB, and the dominant 4/rev hub loads could be reduced simultaneously using multi-harmonic IBC input. The data also showed that performance improvements of up to 7 percent could be obtained at high-speed forward-flight conditions using 2/rev IBC inputs.

UH-60 experiments. Because of the success of the Bo-105 studies, IBC experiments were conducted on a four-bladed, 53.7-foot-diameter Sikorsky UH-60 (Black Hawk) helicopter rotor in the 80- by 120-Foot Wind Tunnel at airspeeds up to 85 knots (Fig. 246, Test 80-0080). This test program was conducted under the authority of an International NASA Space Act Agreement. The partners were NASA Ames Research Center, ZFL, Sikorsky Aircraft Corporation, and the AFDD. The experiments were performed using the Army/NASA LRTA test stand. It was found that even though the system was not tested to its full capability, the data indicated overall vibration level reductions of 70 percent using approximately 1-degree, 3/rev IBC, and BVI noise reductions of up to 12 dB (75 percent) were achieved using 3-degree, 2/rev IBC. More information is contained in references [326] and [327].

To perform experiments at higher airspeeds (up to 170 knots), the rotor was also tested in the 40- by 80-Foot Wind Tunnel (Fig. 247, Test 40-006). The results were promising with power reductions of up to 5 percent, load reductions, and in-plane noise reductions [328]. Additional experiments are described in reference [329], along with comparisons with theories.

Sikorsky UH-60 loads tests. The primary objective of this NASA/Army-sponsored test program was to acquire a comprehensive set of validation-quality measurements on a full-scale pressure-instrumented UH-60A rotor system at conditions that challenge the most sophisticated modeling and simulation tools. Figure 248 shows the installation of the UH-60A rotor on the LRTA in the 40- by 80-Foot Wind Tunnel [330]. Key measurements included rotor performance, blade loads, blade pressures, blade displacement and deformation, and rotor wake measurements using large-field Particle Image Velocimetry (PIV) and Retro-reflective Background Oriented Schlieren (RBOS). Data were acquired at all planned flight-test conditions, including speed sweeps at 1-g level simulated flight conditions, and thrust sweeps (up to and including stall) at various combinations of shaft angle and forward speed. These conditions included airspeeds up to 175 knots, and thrusts up to 32,000 pounds. Data were also acquired to match data from a previous full-scale flight-test and small-scale DNW wind tunnel tests in the Netherlands, to assess rotor and wind tunnel scaling issues. Finally, unique slowed-rotor simulations were performed at reduced rpm, achieving advance ratios (forward speed divided by blade tip speed, normally about 0.3) up to 1. The overall goal was to improve helicopter theories and to help develop helicopters with higher cruise speeds.

Figure 247. Sikorsky UH-60 helicopter rotor in the 40- by 80-foot test section for high-speed testing.
(NASA ACD09-0020-006)

Figure 248. UH-60A main rotor on the LRTA in the 40- by 80-Foot Wind Tunnel for airloads test.
(NASA ACD10-0087-004)

Boeing Smart Material Actuated Rotor Technology (SMART) rotor. The Defense Advanced Research Projects Agency (DARPA), NASA, and Boeing conducted an investigation in the 40- by 80-Foot Wind Tunnel from February to May 2008 under the SMART development effort (Fig. 249, Test T40-009/12). DARPA, which sponsors advanced research for the DoD, was seeking to explore acoustic and vibration improvements that could be leveraged from the SMART development effort for use on future defense rotorcraft; NASA provided supplemental funding to further explore these aspects from a civilian perspective. The test featured a modified five-bladed MD-900 rotor system mounted on a Boeing-supplied test bed. The rotor blades were modified to include trailing-edge flaps, which were actuated using piezoelectric-stack actuators (small, compact actuators that can operate at high frequencies) to allow for rotor control inputs at frequencies greater than 1/rev to help mitigate noise and vibration and improve rotor performance. Control routines were attempted in both open- and closed-loop scenarios. The test demonstrated that such technology can create appreciable reductions in vibrations and noise, particularly with respect to in-plane rotor noise and BVI noise. These are two very important considerations for reducing both military and civil detectability. Test results are presented in references [331] and [332].

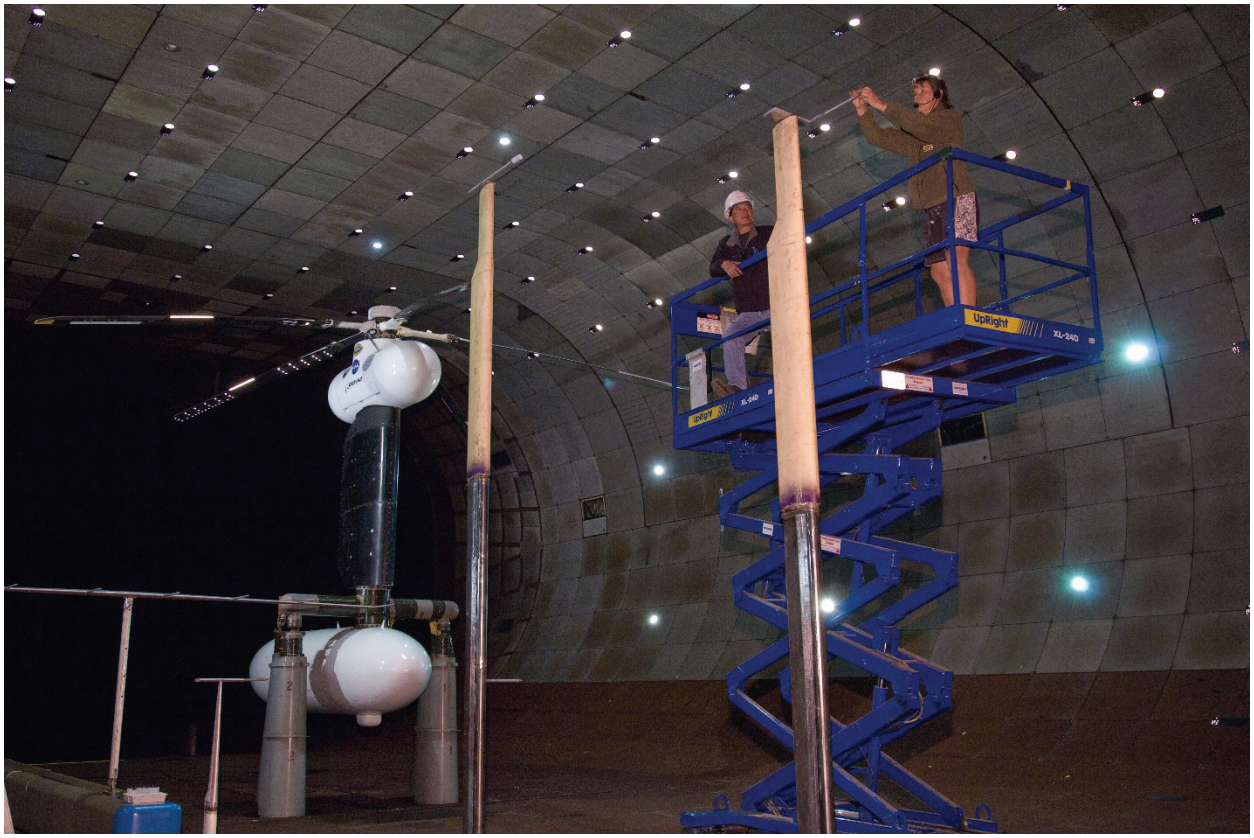

Figure 249. Boeing SMART rotor in the 40- by 80-foot test section; upstream instrumentation being installed. ***(NASA ACD08-0055-104)***

DARPA/Sikorsky active rotor. Sikorsky Aircraft Corporation modified an S-434 Fire Scout rotor system to implement active IBC for noise and vibration reduction. The system used electromechanically actuated trailing-edge flaps and a closed-loop control system on the four-bladed, 27.5-foot-diameter rotor. The rotor system was installed on the NFAC RTA and operated up to 150 knots in the 40- by 80-Foot Wind Tunnel between September 2010 and March 2011 (Fig. 250, Test 40-019). The test was a joint effort involving Sikorsky, United Technologies Research Center, Triumph Aerospace, U.S. Army (Aviation Applied Technology Directorate (AATD) and AFDD), and NASA Subsonic Rotary Wing and Arnold Engineering and Development Complex (AEDC)/NFAC personnel.

Rotorcraft theory. As a result of many experiments and studies conducted over the years in the NFAC, rotorcraft theories have been improved substantially. Because aeroelasticity effects are intimately involved when developing theories for rotorcraft, CFD must be combined with material aeroelasticity theories. See Johnson [333] for the current state of the art for rotorcraft theories.

Figure 250. DARPA/Sikorsky active rotor in the 40- by 80-foot test section. ***(NASA ACD11-0026-006)***

V/STOL

Transports

Cruise-efficient short takeoff and landing (CESTOL). California Polytechnic State University (Cal Poly) in San Luis Obispo, California, in cooperation with a NASA Research Announcement backed by the Environmentally Responsible Aviation program, tested a CESTOL fixed-wing-aircraft model to demonstrate lift enhancement technology and provide data for CFD validation and development for a typical takeoff and landing flight envelope. The purpose of the aircraft design was to reduce required landing-field lengths and reduce noise. The Advanced Model for Extreme Lift and Improved Acoustics (AMELIA) utilized leading- and trailing-edge slot blowing for wing circulation control with turbine-propulsion simulators (model jet engines) mounted above the wings. Mounting the engines above the wing has the potential for using the wing as an acoustic shield and therefore reducing noise on the ground. A 1/11-scale model was used for the design of a 100-passenger aircraft. AMELIA was mounted on the NFAC sting-pitch mechanism and tested at airspeeds up to 120 knots in the 40- by 80-Foot Wind Tunnel between November 2011 and February 2012 (Fig. 251) [334]. The test team comprised Cal Poly, NASA Subsonic Fixed Wing Branch, Georgia Tech Research Institute, Triumph Aerospace, and AEDC/NFAC personnel. Preliminary acoustic results are presented in reference [335].

Figure 251. A 1/11-scale model of AMELIA (part of the CESTOL program) sting-mounted in the 40- by 80-foot test section. ***(NASA ACD12-0003-012)***

Figure 252. SACD 23-percent-scale model in the 80- by 120-foot test section.
(110715-F-UU070-014)

Speed Agile Concept Demonstrator (SACD). The Air Force Research Laboratory (AFRL) Air Vehicle Directorate funded a multi-faceted development program for a next-generation fixed-wing military airlifter under the SACD program. This aircraft was planned as a replacement for the Lockheed C-130 transport aircraft. Part of this development program included testing a large-scale (23-percent-scale) powered model of a Lockheed Martin Company (LMC) concept in both the 40- by 80-Foot Wind Tunnel for cruise simulation and in the 80- by 120-Foot Wind Tunnel (Fig. 252) for low-speed simulation (Tests 40-017 and 80-016). The SACD program sought to create a next-generation military airlifter combining transonic-cruise capability with STOL and austere-field serviceability. The NFAC tests were designed to provide proof of concept in large scale of the LMC integrated powered-lift concept, which combined circulation control and thrust vectoring, and to collect aerodynamic performance data for a planned flight simulator model. All major test objectives were met [336, 337]. In addition, the tests served as major reactivation milestones for several key NFAC capabilities, including jet-fuel delivery, jet-engine testing, and wall-interference corrections.

Fighters

General Dynamics E-7. A full-scale powered-fighter model of the E-7 was investigated in the NFAC. It was a model of a fighter aircraft that employed a lifting-ejector system for ejector-lift/vectored-thrust short takeoff and vertical landing (STOVL) operation. This very sophisticated model was built in the Ames shops. (Unfortunately, the Ames shops have been drastically reduced and no longer have the capability to build such models.) The model is shown in Figures 253, 254, and 255, in the shop, in the 40- by 80-Foot Wind tunnel, and in the 80- by 120-Foot Wind Tunnel, respectively. Ejector-lift augmentation ratios approaching 1.6 were demonstrated during static testing. Test results are provided in reference [338].

Figure 253. General Dynamics E-7 ejector-lift/vectored-thrust full-scale model in the Ames shop.
(NASA AC87-0372-143)

Joint Strike Fighter (JSF). Several studies were undertaken to replace aging fighters. The very ambitious goals included low cost, stealth capability, supersonic airspeeds, vertical landing, commonality for the services, and a single-seat aircraft. These studies merged into the JSF program. Several airplane companies and engine manufacturers were involved in the competition. Lockheed Martin and Boeing competed for the final aircraft. Lockheed Martin was selected in 2001, and development began on the JSF, which evolved from the Lockheed X-35 and became the F-35.

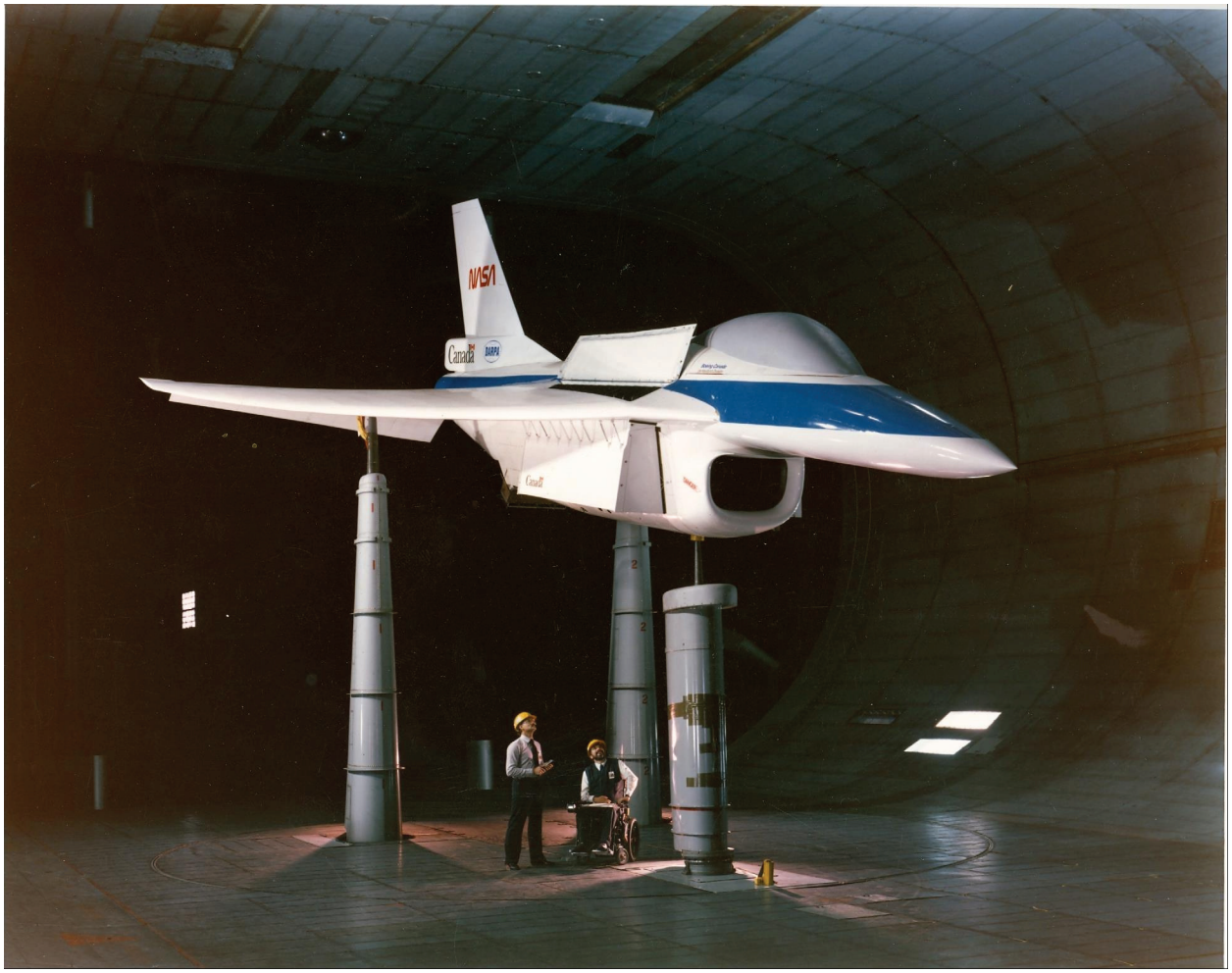

Figure 254. Three-quarter front view of General Dynamics E-7 ejector-lift/vectored-thrust full-scale model. As shown, the ejectors are along the sides of the fuselage and the inlet doors are open. ***(NASA AC88-0530-28)***

Several model studies of the JSF were done in the NFAC. Both a 12-percent-scale model (Fig. 256) and an 86-percent-scale powered model (Fig. 257) of the Lockheed version of the JSF were studied from 1996 to 1998. Static (hover) experiments were done at the OARF, and transition studies were done in the 40- by 80-Foot Wind Tunnel and the 80- by 120-Foot Wind Tunnel. Comparisons were made with the 12-percent model and the 86-percent model to define scale effects and reduce uncertainties. The 86-percent-model size was selected to allow an existing single-engine to be used. Experiments were also performed on various flow control devices. Unfortunately, research in the NFAC was limited because of increases in the overhead fees charged by Ames management; apparently the fees had not been budgeted for by the JSF program office. Studies were not performed in the NFAC after Lockheed was selected.

Figure 255. Lower front view of E-7 model at high angle of attack. ***(NASA AC89-0370-43)***

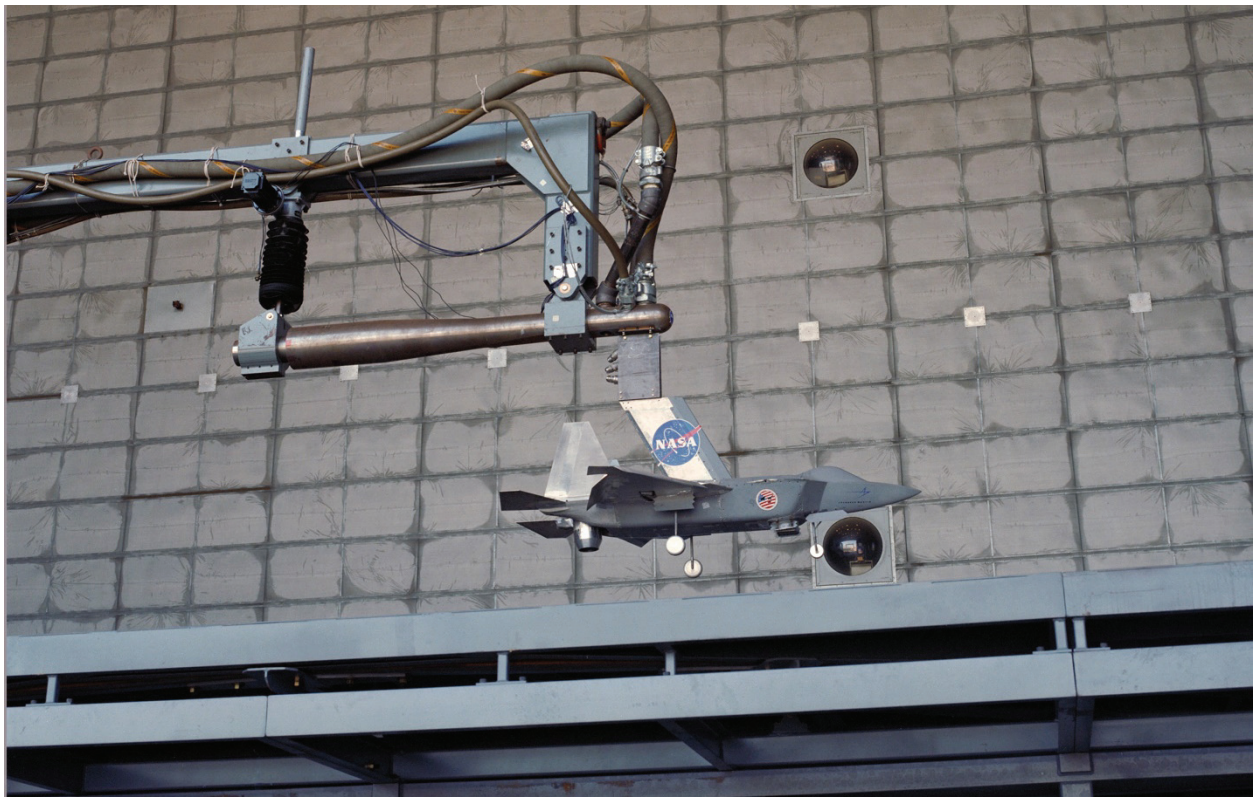

Figure 256. A 12-percent-scale model of the JSF in the 80- by 120-foot test section. ***(NASA AC97-0325-17)***

Figure 257. An 86-percent-scale model of the JSF in the 80- by 120-foot test section. ***(NASA AC96-0233-1)***

The Lockheed Martin F-35 was a very ambitious program. The airplane was to be capable of supersonic cruise and be able to land vertically as well utilize stealth technology. The long history of this aircraft has been described in many references and books [339-342]. The differences in DoD requirements resulted in three models: A, B, and C. The F-35A is a conventional takeoff and landing airplane for the Air Force; the F-35B is a STOVL airplane for the Marines, and the F-35C has a somewhat larger wing and is designed for the Navy for aircraft carriers.

The F-35B has a forward located, unique, shaft-driven lift fan just behind the pilot that produces vertical lift force, and there is an engine exhaust nozzle that can be rotated down to also produce vertical lift force to balance the pitching moment. Wing-mounted nozzles on either side of the aircraft driven by engine bypass air through the wing are used to balance and control rolling moment at low speeds.

The JSF was intended to become an affordable aircraft and an aircraft that maximized commonality to reduce parts inventory and maintenance. Despite those goals, it has become the most expensive airplane development project of all time.

Conventional Fixed-Wing Aircraft

High-Angle-of-Attack Fighters

McDonnell Douglas F-18. Over several years, studies were performed on the F-18 fighter aircraft in the 80- by 120-Foot Wind Tunnel at high angles of attack that ranged from 18 to 50 degrees and at airspeeds up to 100 knots (Fig. 258). Pneumatic and mechanical forebody flow control devices were tested and shown to produce significant yawing moments for lateral control of the aircraft at high angles of attack. Detailed measurements of the air pressures buffeting the vertical tail were made. In addition, an extensive set of data were obtained for validation and upgrade of CFD codes and for comparison with flight-test and small-scale wind tunnel test results [343].

Flow visualization studies were performed at angles of attack that ranged from about 20 to about 45 degrees and sideslip angles from –10 to 10 degrees. The purpose was to study the character of the flow at high angles of attack. Flow at high angles of attack is separated, and separated flow is not well understood. Flow studies were performed on the forebody, canopy, and wings and their leading-edge extensions. Tufts, smoke, laser light, and a video imaging system were used for flow visualization. Separated flow and vortical flow were studied [344].

Tail buffet data were obtained and analyzed for an angle-of-attack range of 20 to 40 degrees and a sideslip range of –16 to 16 degrees at wind speeds up to 100 knots. The aircraft was also equipped with a removable leading-edge-extension fence (LEF), which was intended to reduce tail-buffet loads. It was found that the LEF did reduce the loads. Comparisons with small-scale results had mixed success, however the LEF showed improvements at all model scales [345].

Figure 258. McDonnell Douglas F-18 fighter in the 80- by 120-foot test section at high angle of attack.
(NASA AC91-0255-75)

Subsonic High-Alpha (angle-of-attack) Research Concept (SHARC) model. The SHARC was a 55-percent-scale advanced-concept stealth fighter model, built in the Ames shops and tested in the 40- by 80-Foot Wind Tunnel in 1994 (Figs. 259 and 260, Tests 40-0045 and 40-0077). The U.S. Air Force Research Laboratory at Wright-Patterson Air Force Base sponsored the project. The model was a test bed for a variety of high-lift and maneuverability-enhancement devices for a next-generation fighter and attack aircraft. The model was capable of 45 degrees angle of attack, which is a high angle of attack (most aircraft do not exceed 10 to 15 degrees angle of attack) and important for a fighter aircraft for high maneuverability. The flaps were modified to increase effectiveness by using Continuous Moldline Technology (CMT); that is, there were to be no gaps at the flap hinge lines. Flap upper-surface BLC was employed to increase the maximum lift coefficient. Some of the test results are described in reference [346].

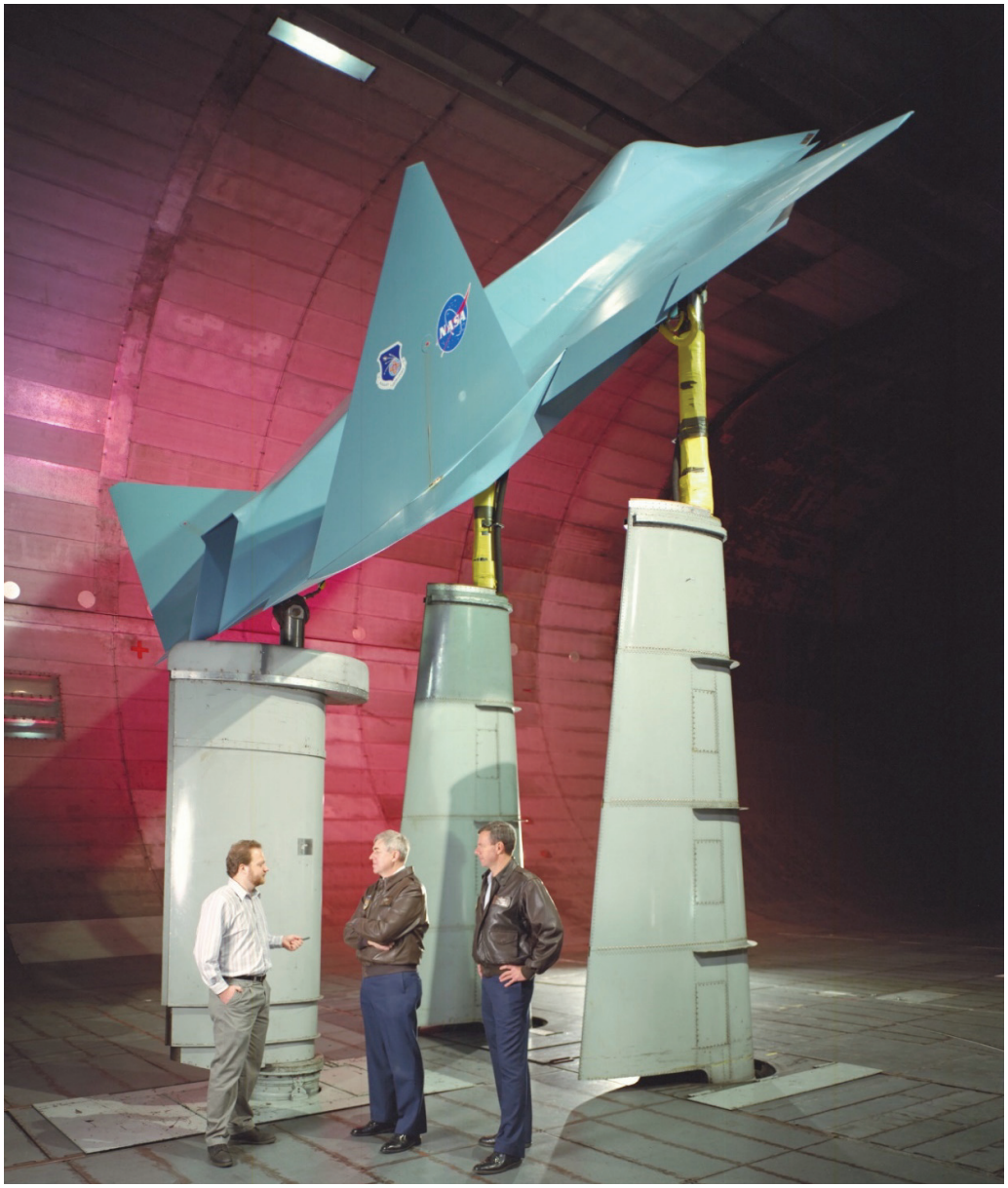

Figure 259. Side view of SHARC model at high angle of attack in the 40- by 80-foot test section. ***(NASA AC94-0480-28)***

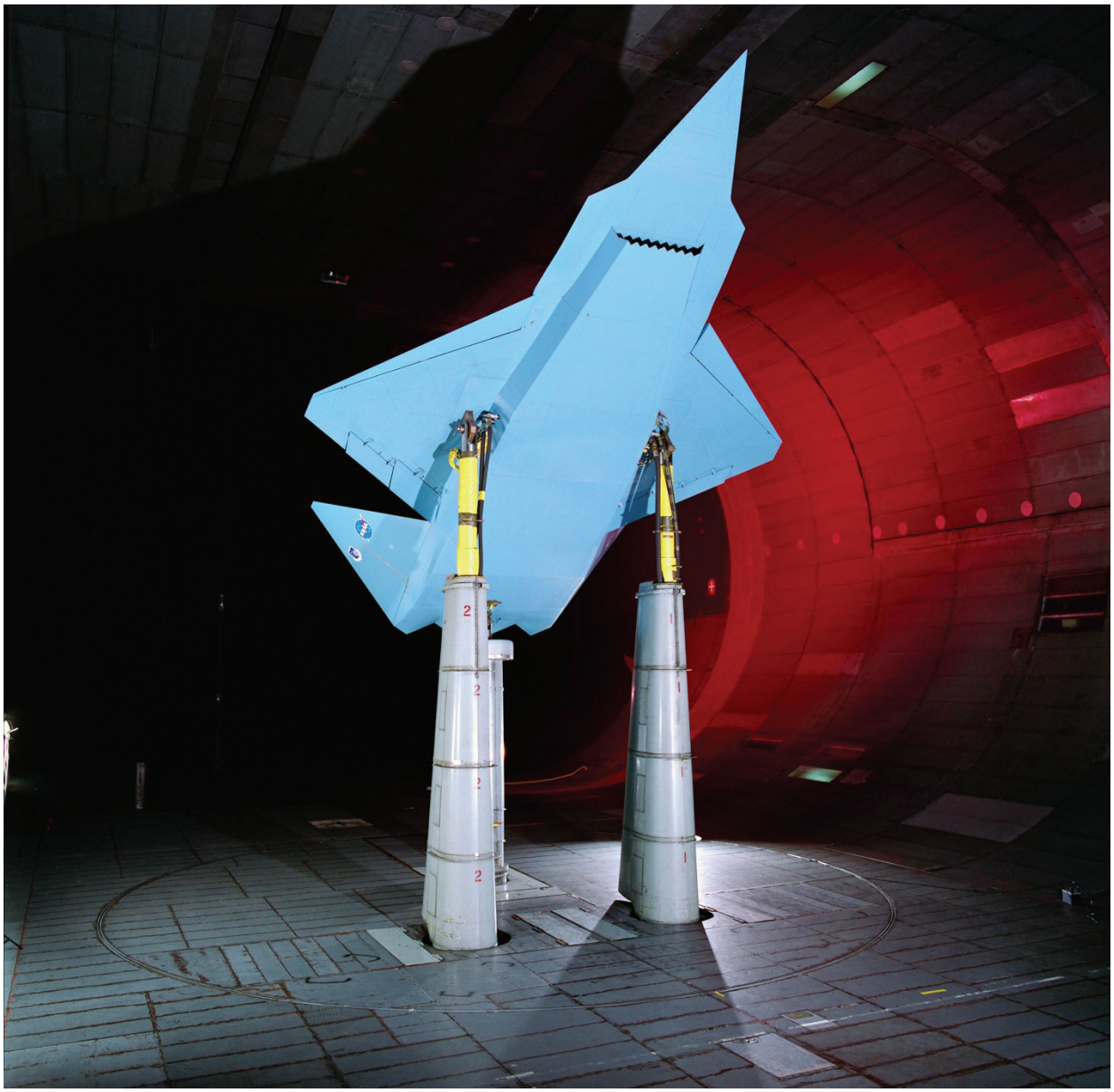

Figure 260. Three-quarter front view of SHARC model at high angle of attack. ***(NASA AC94-0480-45)***

High-Speed Civil Transport (HSCT). Model studies of the HSCT were performed in the 40- by 80-Foot Wind Tunnel (Figs. 261 and 262). These studies were in support of NASA's HSCT program, which was the focus of NASA's High Speed Research (HSR) program. The goal was to develop a 300-passenger commercial SST aircraft that would cruise at a Mach number of 2.4. It was recognized that it was essential to develop the technology required to make the transport environmentally acceptable and economically feasible. The program was started in about 1990. Excellent progress was achieved in meeting the goals, but the program was stopped in 1999 because of NASA's changing priorities.

Figure 261. Side view of HSCT model. ***(NASA AC94-0034-51)***

Figure 262. Side view of HSCT model at high angle of attack. ***(NSAS AC94-0034-52)***

Conventional Aircraft

Lift-generated tip-vortex wakes. Studies of the effects of lift-generated wakes on follower aircraft performed in the 40- by 80-Foot Wind Tunnel were continued in the 80- by 120-Foot Wind Tunnel. The wakes encountered by follower aircraft can have major effects on flying qualities; they can be disastrous for small aircraft. The objective of these tests was to expand the database of measured follower-aircraft rolling moments using the same Boeing 747 model, plus a McDonnell Douglas DC-10 3-percent-scale model of similar size, to produce the lift-generated vortex wakes. In addition, a downstream distance of both a scaled 1/2 mile and 1 mile were studied, which was allowed by the length of the 80- by 120-Foot Wind Tunnel test section. For these tests, three swept-wing follower-airplane models were used. These follower models represented the range of distances often found between a small executive jet and a jumbo jet. The installation with a Boeing 747 model is shown in Figure 263. The model was mounted upside down so the support would not interfere with the wakes.

The results of the 80- by 120-Foot Wind Tunnel tests were within about 5 percent of the results of the 40- by 80-Foot Wind Tunnel tests for the same models and test conditions, which was acceptable. The quality of the rolling moment data was good with little scatter. Two techniques to alleviate vortex wake by modifying the vortex-wake-generator aircraft were studied. One technique was to retract the landing flaps on the outboard portion of the wing, and the other was to install vortex generators (called fins) on the wing's upper surface of the vortex-wake-generator aircraft model. Both techniques were studied on the B-747 model and the DC-10 model. The substantial reduction in rolling moments on the follower-aircraft models found in the 40- by 80-Foot Wind Tunnel tests was confirmed in the 80- by 120-Foot Wind Tunnel tests for both of the vortex-wake-generator models; the results from the two tunnels were consistent [347, 348]. Results indicated that when the vortex-wake-generator aircraft was in the normal landing configuration, the rolling moment induced on the follower aircraft was substantially in excess of the rolling-moment control capability of typical, smaller, follower aircraft. The alleviated wakes studied in this program brought the induced rolling moments to within the control capability of typical follower aircraft. These results are in agreement with flight-test results where a small executive jet was uncontrollable when it encountered the vortex wake of a B-747 transport in the normal landing configuration. When a larger, four-engine jet transport was following the B-747 transport, the upset due to the vortex-wake encounter was controllable.

Both of the wake alleviation techniques studied are similar in that they introduce additional vortices into the wake, which results in a mutual interaction of the vortices downstream and accelerates decay of the vortex wakes. Aircraft designers need to determine if a practical configuration can be developed using these vortex alleviation techniques; if that is not possible, then additional alleviation techniques need to be proposed because of the seriousness of the problem.

Figure 263. Lift-generated tip-vortex wakes using a 0.03-scale Boeing 747 model in the 80- by 120-foot test section with Vernon Rossow in photo. Model is upside down to minimize model-support effects on wakes. ***(NASA AC92-0688-3)***

It was noted above that one of the objectives of the NASA program was to define safe operating distances behind landing aircraft. Further work in a flight environment is needed to evaluate additional parameters beyond the induced rolling moments measured in this wind tunnel program. These parameters include: (1) the duration of the vortex encounter, (2) the pilot response when surprised by the encounter, and (3) the response of the follower aircraft to the vortex-wake encounter. These parameters can be studied in a piloted flight simulator. Such a flight simulator study requires, as an input, the induced rolling moment and the size of the vortex wake. The rolling moment database developed in this program and discussed above provides a useful resource.

Even though the models were small (0.03 scale), the results allowed flight experiments to be more efficient by narrowing the amount and range of variables and by screening potential fixes during the wind tunnel experiments.

Often so-called "clear air turbulence" is caused by the persistence of tip vortices and is also a special hazard for small aircraft [349].

Reference [350] presents an excellent summary and overview of the status of research as of 1999. Reference [351] provides an overview of the aerodynamic mechanisms that cause the hazardous parts of lift-generated wakes to spread and move as a function of time. This reference also provides guidelines for avoiding vortex wakes during use of closely spaced parallel runways.

Lift-generated vortex wakes remain a significant problem and are an important flight safety issue. Vortex wakes affect aircraft spacing as well as runway construction spacing, therefore future research is necessary. In addition to theoretical studies, simulator studies, and flight studies, wind tunnel studies on potential aircraft modifications are required to attenuate vortex wakes. The NFAC is the best wind tunnel facility for performing these wind tunnel experiments.

North American T-39 Sabreliner high-lift research. The T-39 was a popular twin-engine business jet that had been successful in both civil and military markets since about the 1960s. The aircraft tested was going to be flown to Davis-Monthan Air Force Base in Tucson, Arizona, to be added to the aircraft "boneyard" since it had reached the end of its useful life in the early 1990s. Instead, it was detoured to Ames Research Center for testing in the 80- by 120-Foot Wind Tunnel to study lift-enhancing tabs on the wing-flap system that might increase the maximum lift of the wings (Fig. 264). The tabs were simple, small devices that could be easily added to the wing-flap system and had the potential to retrofit almost any aircraft with slotted flaps. Results of 2D studies, which had been done in the Ames 7- by 10-Foot Wind Tunnel, showed promise [352]. The results verified the 2D experiments; that is, the tabs significantly increased maximum lift. After the investigation in the 80- by 120-Foot Wind Tunnel, the aircraft was decommissioned and transported to Armstrong (Dryden) Flight Research Center to be used for spare parts for a T-39 that was still being flown at the Center.

Figure 264. Three-quarter front view of the North American T-39 Sabreliner in 80- by 120-foot test section for high-lift research. ***(NASA AC93-0233-2)***

Wright Flyer. A full-scale replica of the Wright Flyer was tested in the 40- by 80-Foot Wind Tunnel to document its flying qualities (Figs. 265 and 266, Test 40-0047). Figure 265 shows the model being installed in the tunnel, and Figure 266 shows the installed model with the test crew. This testing was done for the Los Angeles Section of the American Institute of Aeronautics and Astronautics (AIAA) that had built the replica. The purpose was to develop a historic aerodynamic stability and control database for the 1903 Wright Flyer to educate and inspire future engineers and scientists. A 45-hp electric motor was used to drive the propellers, instead of a gas engine, for more convenient control in the wind tunnel. The model was mounted on a strain-gage balance at the end of a sting to get better data sensitivity because of the low airspeed (25 knots) required. Also, because of the low airspeed, the tunnel flow was unsteady, so data sample averages over 2-minute periods were required. Airflow instrumentation was also added to improve the airspeed measurement accuracy at the low airspeeds.

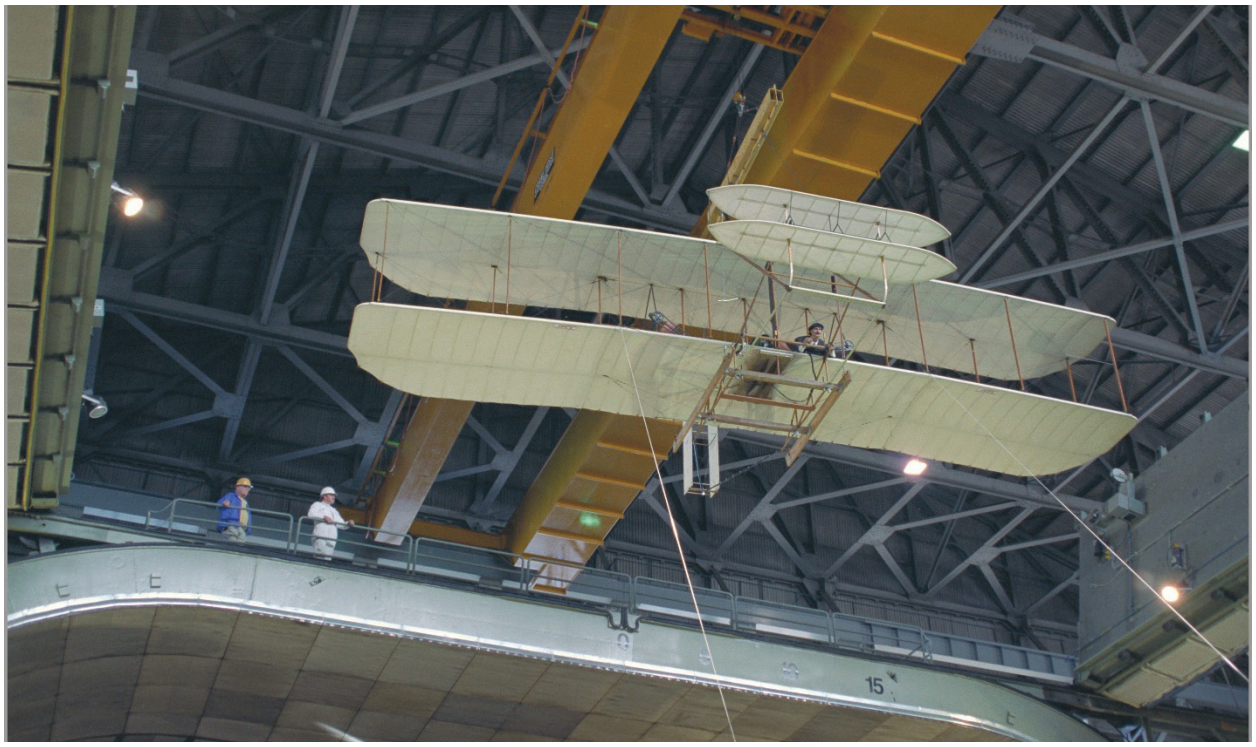

Figure 265. Full-scale replica Wright Flyer being installed in the 40- by 80-foot test section. ***(NASA AC99-0030-16)***

Figure 266. Full-scale replica Wright Flyer in the test section with the test crew. ***(NASA AC99-0030-81)***

Comparisons of full-scale replica data with small-scale unpowered-model data showed fairly close agreement at power-off conditions. The small-scale models were relatively rigid whereas the full-scale replica was flexible as was the actual Wright Flyer. Therefore, aeroelastic effects of the replica were evident when comparisons were made with the relatively rigid small-scale models.

Very severe pitch instability was found, as expected, but the canard control (forward-mounted elevons) was adequate to control the pitching moment. The airplane was marginally stable directionally but had adequate directional control using the rudders. There was enough rudder-control power to cope with the adverse yaw present due to the wing warping that was used for roll control. (There were cables that allowed the pilot to warp or distort the wing for control.) The Wright Flyer had aerodynamic deficiencies, but the wind tunnel measurements verified that the airplane was flyable and controllable. It did, however, require considerable skill and practice to fly. This did not bother the Wright brothers—they acknowledged and understood that the Flyer had to be "continuously flown," much like a bicycle needs to be "continuously controlled" [353, 354].

A second replica was to be built for flight-testing by the Los Angeles AIAA Section. The wind tunnel model had required reinforcement for the wind tunnel tests because of the mounting system and because of wind tunnel safety requirements. The flight aircraft was expected to have some minor modifications to improve flyability and safety [353], but it did not need the reinforcements required for the full-scale wind tunnel tested aircraft.

It should be mentioned that other Wright Flyer replicas were built with the goal of flight-testing. A notable amateur group was the "Wright Experience." Their replica was tested in the Langley 30- by 60-Foot Wind Tunnel in February 2003, also using an electric model motor. Flight-tests were done in December of 2003 using a reproduction of the horizontal four-cylinder Wright engine [355, 356].

There were small differences in the various replicas of the Wright Flyer for a variety of reasons. (There are many full-scale replicas in museums.) A major reason for the differences was that the Wright brothers did not produce detailed sets of drawings for their early powered aircraft. The Wright Flyer—and subsequent aircraft built by the Wright brothers—were continually undergoing improvements with minimal documentation. See reference [356] for an excellent summary of the evolution of the Wrights' aircraft from 1903 to 1912. The Wright Papers [357] are also an excellent and detailed resource. McCullough [358] is a very readable history of the development of the Wright brothers' airplanes. Creating the first airplane was an amazing accomplishment by the Wright brothers. They understood very early on the importance of having very effective controls for all three axes—pitch, roll, and yaw—and they were able to stay focused on creating a powered flying machine.

There were other experimenters who developed large man-flying gliders, but they did not produce a successful powered aircraft even though they started several years earlier than the Wright brothers. For example, John Montgomery had started building man-flying gliders about 20 years before the Wright brothers' first powered flight [359].

Bombardier Dash 8 Q400 aircraft. A Dash 8 aircraft was tested in the 80- by 120-Foot Wind Tunnel. The turboprop aircraft was flown to Ames Research Center, towed to the wind tunnel, installed in the tunnel, tested, removed from the tunnel, towed to the flight line, and flown home to Canada. The entire process only took 10 days. The purpose was to study very strong cross-wind effects (up to 65 knots) and to record propeller blade strains at these conditions for certification purposes. The effects of several yaw angles and airspeeds were studied. This was the largest aircraft ever tested in a wind tunnel; it has a wingspan of over 93 feet and a length of over 107 feet (which is larger in span and length than a Boeing 737-200). Special supports were fabricated to support the aircraft at floor level on the wind tunnel balance. The main landing gear were secured to steel pads at the tunnel floor level (Figs. 267 and 268, Test 80-0088).

While in the tunnel, the aircraft was operated by two test pilots and one flight-test engineer. Reference [360] contains some of the forces and moments for 90-degree cross-wind conditions. The test was successful in obtaining accurate force and moment data, as well as propeller blade strain-gage data, because the airspeed could be precisely controlled and measured.

Figure 267. Bombardier Dash 8 Q400 aircraft in the 80- by 120-foot test section; this was the largest airplane ever tested in a wind tunnel. ***(J. Sacco collection, airliner_80x120)***

Figure 268. Bombardier Dash 8 Q400 aircraft in the 80- by 120-foot test section with test crew.
(J. Sacco collection, DASH 8)

Navy/Boeing P-8A. A full-scale P-8A fuselage model was studied in the 40- by 80-Foot Wind Tunnel in March 2011. The P-8A is to be a replacement for the Navy anti-submarine Lockheed P-3 Orion aircraft, which is driven by four propellers. The P-8A is a twin-jet-powered aircraft and a derivative of the Boeing 737.

Space Related

Drag Devices

Space Shuttle Obiter drag parachute. The shuttle had been originally designed to use a drag parachute on landing to reduce wear and tear on the brakes and tires, to reduce sensitivity to wet runways, and to reduce landing-gear strut loads [361]. However, to reduce weight, the system was not installed for the early flights. After the Challenger disaster in 1986, a risk assessment was done, and it was recommended that the drag parachute system be used to reduce risk during landing. Preliminary parachute studies had indicated some instability and high unsteady loads. As a result, experiments were performed in the NASA Ames 80- by 120-Foot Wind Tunnel to study the stability of the drag parachute. Time varying loads and canopy position were measured. The stability was improved by increasing the porosity of the parachute canopy, which was done by removing a few sections of the canopy; an optimum was achieved with acceptable stability while retaining the required drag. Studies at the Ames Vertical Motion Simulator (VMS) were done for pilot evaluation of the drag system. Different failure scenarios with the drag parachute were performed; for example, it was found that in the event of a tire failure on landing, the drag parachute would significantly reduce pilot workload and greatly reduce risk. As a result, the parachute drag system was subsequently used on all of the following shuttle flights.

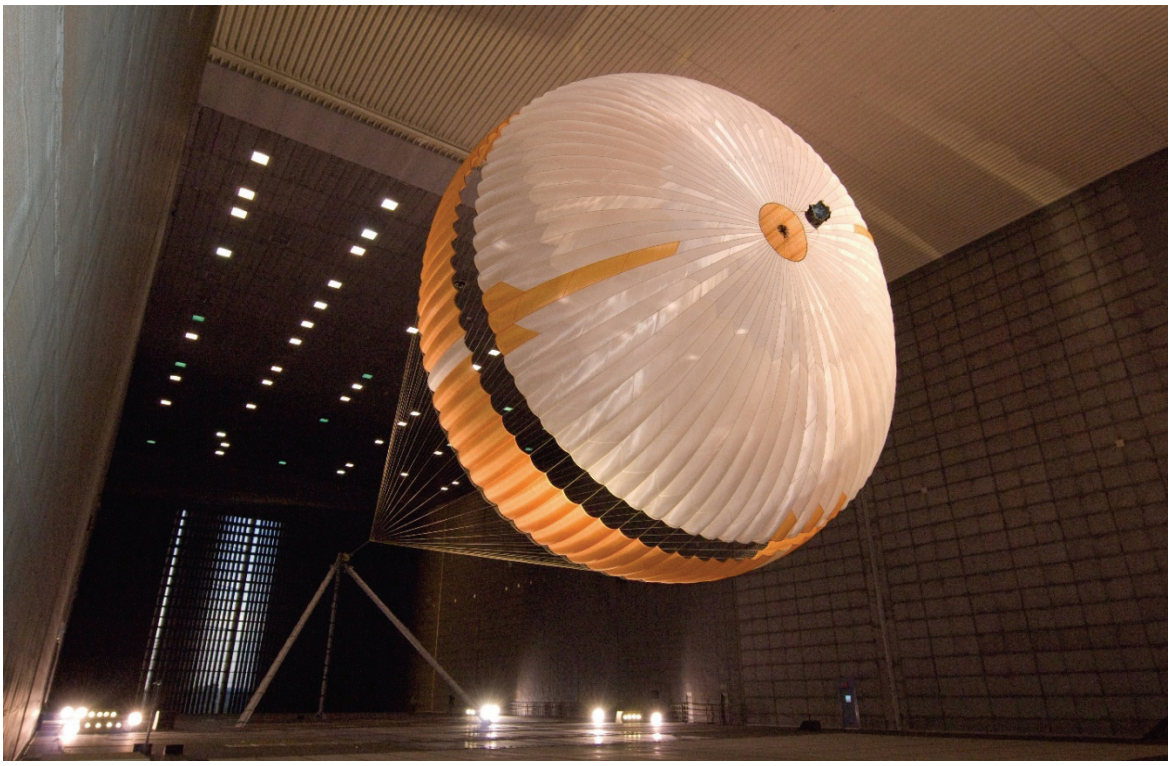

Figure 269. MSL parachute attached to a custom support in the 80- by 120-foot test section. ***(MSL_D2009_0331_TO164)***

Mars Science Laboratory (MSL) descent parachutes. NASA tested the parachutes for the Mars Exploration Rovers (MERs) Spirit and Opportunity between fall 2002 and summer 2003. These Disk-Gap-Band (DGB) parachutes ranged in nominal size from 43.2 to 50.1 feet in diameter (30 to 36 feet inflated diameter) and produced up to 30,000 pounds of drag when opening in the tunnel. The DGB parachute was developed in the late 1960s and adapted for use on the Viking missions to Mars because of its reliable operating characteristics in low-density supersonic conditions. NASA mothballed NFAC after completing the final MER parachute test in the 80- by 120-Foot Wind Tunnel on June 23, 2003. The first test in the 80- by 120-Foot Wind Tunnel after the Air Force resumed operations at NFAC was for the NASA/Jet Propulsion Laboratory (JPL) MSL program with the first run on October 11, 2007. The MSL test canopies ranged from 64.6 to 75.5 feet in nominal diameter. The final canopy diameter of 71.2 feet was roughly 52 feet in diameter when fully inflated and produced over 80,000 pounds of drag during inflation in the tunnel.

NASA/JPL conducted a series of tests in the 80- by 120-Foot Wind Tunnel from October 2007 to April 2009 to investigate and qualify the full-scale delivery parachute for the MSL rover Curiosity (Fig. 269). Testing was split into six phases of one or more weeks each, and ranged from design verification to structural qualification to flight-lot workmanship verification. Testing involved real-time development of innovative test techniques to ultimately find a way to prove that the parachutes could withstand entry into the Martian atmosphere and safely deliver the rover to the planet's surface. A completely new wind tunnel support structure was designed, built, and installed to react to the massive drag forces generated by the 52-foot-inflated-diameter full-scale test parachutes. JPL was able to fully qualify the canopy for flight in time to meet the

mission launch schedule. The flight canopy helped successfully deliver the space vehicle Curiosity to Mars in July 2012. The tests in the 80- by 120-Foot Wind Tunnel were in large part proof tests that were performed during deployment experiments. The alternative to performing these wind tunnel proof tests would have been to do drop tests using helicopters. It is much more difficult to control test conditions with helicopter drop tests, and rapid test turnaround is not possible. The tunnel tests were very successful and allowed timely optimization of configuration details under controlled conditions [362-364].

Hypersonic Inflatable Aerodynamic Decelerator (HIAD). The HIAD test was part of a parachute-replacement NASA technology development program. The model consisted of a cone-shaped stack of inflatable rings bonded and strapped together (Fig. 270). The overall objectives were to understand and characterize the behavior of the structure and validate numerical models (e.g., finite element analysis (FEA) and CFD). The primary objectives were to demonstrate the 6.0- and 8.3-meter-diameter HIAD aeroelastic response to dynamic pressure and angle of attack over a range of expected flight conditions for a representative reentry. The first series of experiments are described in reference [365]. Three-dimensional photographic data were obtained from which much of the characterizations were derived. Figure 270 shows the 6-meter-diameter model in the test section.

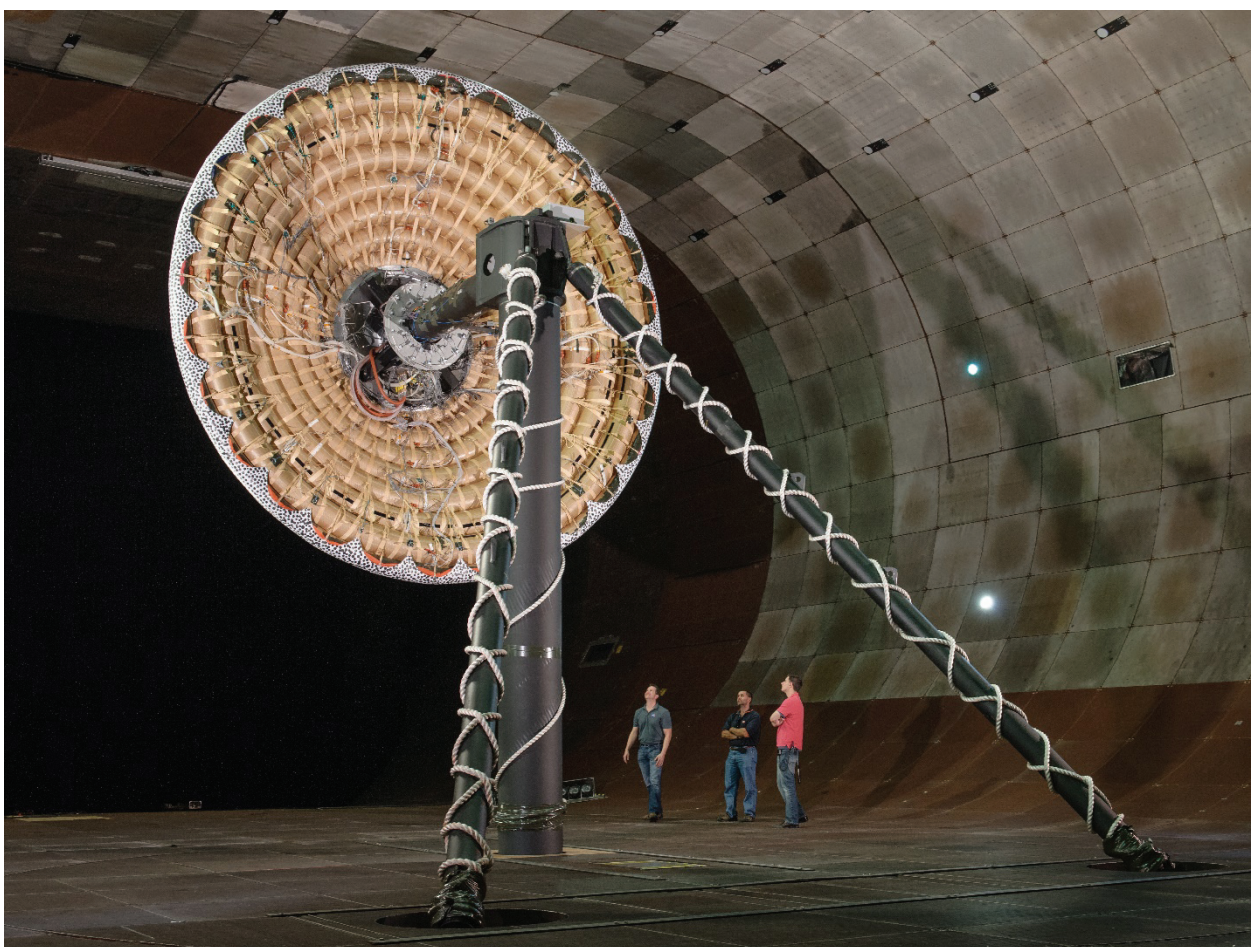

Figure 270. HIAD in the 40- by 80-foot test section. ***(NASA ACD12-0102-007)***

Ringsail parachutes. NASA/JPL is conducting a series of investigations (in the 2000s) in the 80- by 120-Foot Wind Tunnel under the Low Density Supersonic Decelerator (LDSD) program. The goal of these studies is to characterize the performance and stability improvements that Ringsail parachutes can offer over the more traditional DGB parachutes that are typically used for space-equipment recovery applications. The Ringsail parachute has a more distributed porosity than the DGB parachute. It was invented in the 1950s but had not been developed as much as the DGB parachute. Investigations of scaled canopies of various Ringsail designs began in the 2000s. Additional investigations will be performed and results compared to DGB parachute performance from the Mars Phoenix Lander program, whose drag characteristics are well understood (drag, deployment, and stability). The LDSD test parachutes will be smaller than the MSL parachutes tested from 2007 to 2009, at just 27 feet in inflated diameter or one-third scale of the full-scale parachute. A three-camera photogrammetric measurement system is used to precisely track canopy motion during deployment, and smoke visualization is utilized in conjunction with high-definition video and still photography to help qualitatively study stability and flow behavior [364].

Orion parachutes. About a dozen sub-scale Orion spacecraft parachutes were tested in the 80- by 120-Foot Wind Tunnel. The experiments were to help improve safety and reliability for Orion landings. The wind tunnel tests, as well as subsequent drop tests, will help to determine the most reliable parachute configuration for Orion landings. The Orion is currently under development by NASA; it resembles a scaled-up Apollo capsule. It is intended to facilitate human exploration of asteroids and Mars, as well as a means of delivering or retrieving crew or supplies from the International Space Station. The Orion can hold a crew of four at or beyond low Earth orbit. A cluster of three, 116-foot-diameter parachutes are required for a water landing.

Large-Scale Gliding Parachutes

Parafoils. Large-scale tests of parafoils for goods delivery were done in the 80- by 120-Foot Wind Tunnel (Fig. 271). Parafoils are parachutes that have excellent gliding capability and are commonly used by skydivers. Previously available data were for personnel-sized parafoils that are on the order of 300 square feet in area. Experiments were required to investigate scale effects to allow for the development of larger-scale parafoils. The experiments were conducted for Pioneer Aerospace Corporation, which was selected by NASA's Manned Spaceflight Center (MSFC), to investigate promising concepts for recovering launch assets such as core stages, upper stage propulsion/avionics modules, booster stages, booster P/A modules, and fuel-oxidizer tanks from next-generation space transportation systems. The experiments were conducted to determine the aerodynamic characteristics of two, scale, ram-air wings in support of air-drop testing and full-scale development of advanced recovery systems. Two models were tested: a 1/9-scale model with a wing area of 1,200 square feet (20 feet by 60 feet), and a 1/36-scale model with a 300-square-foot wing area. Both models had an aspect ratio (span-to-chord ratio) of about 3:1. Full-scale prototypes are expected to be on the order of 10,800 square feet, or 60 by 180 feet.

It was found that both models were statically stable at angles of attack from 2 to 10 degrees. The maximum lift-to-drag ratio varied from 2.9 to 2.4 [366].

The judgment was made that recovery of high-value assets would be cost-effective and warranted a significant development effort for large-scale gliding parachutes. Development of large-scale gliding parachutes for goods (such as rocket boosters) delivery has been a long-term NASA goal since the Apollo program. The 80- by 120-Foot Wind Tunnel is clearly the best wind tunnel facility for performing preliminary investigations prior to full-scale drop tests.

Figure 271. Parafoil recovery parachute in the 80- by 120-foot test section. ***(NASA AC88-0537-18)***

Acoustics

As pointed out previously, over the years more and more acoustic measurements were made until at least half of all NFAC tests included such measurements. As a result of this demand, special acoustic instrumentation was developed to eliminate microphone wind noise. Both NFAC test sections have acoustic liners to minimize reverberation and low-speed drive fans that minimize drive background noise. At much expense, the original walls of the 40- by 80-foot test section were replaced with 42-inch-thick lined walls to achieve exceptionally low acoustic reflection [367, 368].

The environmental noise of the 80- by 120-foot test-section open circuit was attenuated to low levels for excellent acoustic research, and its effect on the community was also minimized [369]. Acoustic baffles were installed at the tunnel inlet in addition to the test-section acoustic wall liner. Exhaust noise was attenuated using acoustic vanes downstream of the drive. Development of microphone instrumentation for improved noise measurements continued along with the development of the NFAC facility to reduce background noise [370-373].

The NFAC is a world-class acoustic facility. Representative research investigations are described.

Advanced Ducted Propulsor (ADP)

The ADP is a new engine that was developed for large subsonic passenger jets. The engine bypass ratio (fan-compressor air divided by core-jet air) was about 14:1. This high bypass ratio, as well as reduced fan rotational speed (compared to existing engines) is expected to cut fuel consumption 10 to 12 percent. In addition, it would significantly reduce engine noise compared to existing engines. The ADP is intended to be used in 300- to 700-seat commercial transport aircraft. The ADP has a large, variable-pitch fan system with a 40,000-hp drive system and a new, high-speed, low-pressure-ratio turbine. The engine has a maximum thrust of more than 50,000 pounds. The ADP variable-pitch fan is nearly 10 feet in diameter with 18 blades and is designed for reverse thrust as well as forward thrust. The variable-pitch fan would eliminate the need for thrust reversers. This program was a joint NASA/Pratt & Whitney project and was part of NASA's research program in subsonic aircraft to develop technologies in cooperation with the aerospace industry. The ambition was to make possible significant improvements in aircraft performance and ensure that U.S. air transportation remains competitive in a global market. The tests focused on simulated landing conditions, with primary emphasis on confirming thrust reversal using the variable-pitch fans at 120- to 140-knot airspeeds. This was the largest engine ever tested in the 40- by 80-Foot Wind Tunnel. The NFAC was the only facility capable of simulating the necessary flight conditions and thrust reversal for this size of engine (Fig. 272). Acoustic studies were also performed with this engine. Internal engine acoustic measurements were made; sensors were attached to the stators [374].

Figure 272. Pratt & Whitney ADP mounted on a wing section with engineers Pete Zell (left) and Larry Olson (right) in photo. ***(NASA AC93-0237-121)***

Jet Noise

Heated supersonic jet. The effects of forward flight on the far-field noise of a small (5-inch-diameter nozzle) heated supersonic jet was studied in the 40- by 80-foot test section at free-stream velocities up to Mach number 0.32 (Fig. 273). The jet velocities ranged from 586 to 858 meters per second. It was found that the data did not confirm the commonly used convective amplification factor to account for the effect of forward flight. The mixing noise reduction due to forward flight in the aft quadrant was much smaller than that observed in corresponding cold jets [375].

High-lift Engine Aeroacoustics Technology (HEAT). Experiments were conducted in the 40- by 80-Foot Wind Tunnel in the mid-1990s on a semispan model in cooperation with the Boeing Commercial Airplane Group, Seattle, Washington; McDonnell Douglas Aerospace, Long Beach, California; General Electric Aircraft Engines, Cincinnati, Ohio; and Pratt & Whitney, Hartford, Connecticut [376, 377]. The tests were to provide critical information to evaluate the suitability of ejector-type suppressor nozzles for high-speed civil transports (HSCTs). The goal was to make the HSCT quiet on takeoff and landing—at least as quiet as conventional subsonic jet transports. The tests were part of NASA's HSR program, which, as described previously, involved evaluating technologies needed for development of a 300-passenger SST that is both economically viable and environmentally acceptable (Fig. 274, Test 596).

Figure 273. Heated supersonic jet acoustic experiments. ***(AC94-0029-3)***

Rotor Noise

XV-15 rotor noise studies. Blade vortex interaction (BVI) noise estimates were compared with wind tunnel data [378]. The wind tunnel rotor tests were performed on a full-scale, 25-foot-diameter rotor in the 80- by 120-foot test section. BVI noise is a major contributor to rotor noise. The experiments were performed to improve the capability to predict rotorcraft noise. Significant progress has been made to improve the ability to predict rotorcraft noise based on wind tunnel experiments such as this.

Airframe Noise of Commercial Transports

McDonnell Douglas DC-10. An airframe noise study of a 4.7-percent-scale model of a DC-10 was performed in the 40- by 80-foot test section. The study identified noise sources generated by the airframe using in-flow measurements with a phased array of microphones. A dominant noise source was the flap side edges; this confirmed previous study results. The model landing gear made a small contribution to the overall noise, despite previous studies. It was thought to be due to the fidelity and low Reynolds number of the model. Scaled levels at low frequencies were comparable to full-scale DC-10 flight-test data, but there was less agreement at high frequencies [379, 380].

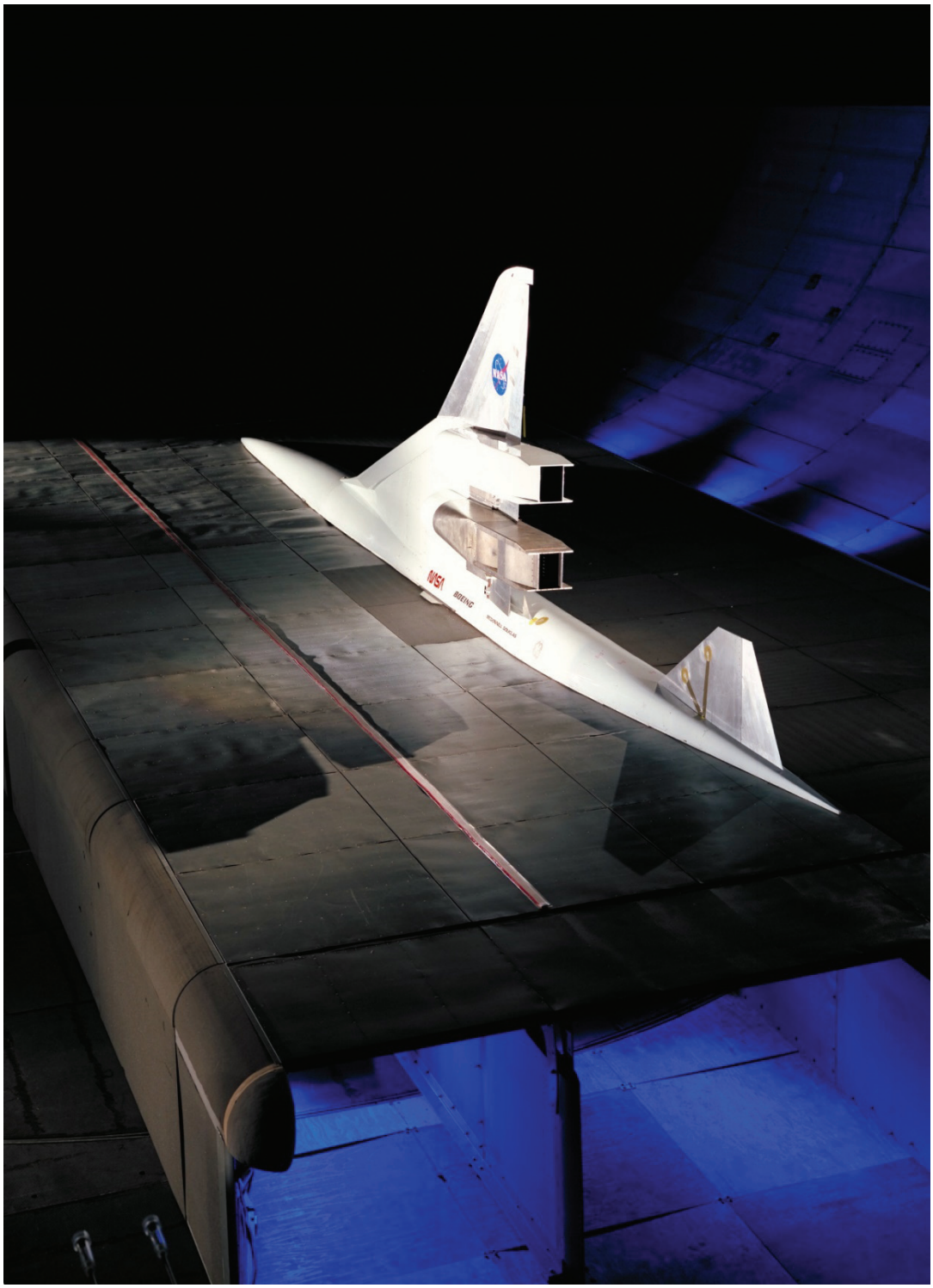

Figure 274. HEAT semispan model in the 40- by 80-foot test section. ***(NASA AC93-0186-149)***

Boeing 777. A 26-percent-scale semispan model of a Boeing 777 was studied in the 40- by 80-foot test section. This study was part of NASA's Subsonic Transport Aeroacoustic Research (STAR) program. The purpose was to investigate airframe noise in an effort to attenuate the noise. Large-scale studies were intended to validate the extensive small-scale studies that had been performed at Langley Research Center, as well as to discover new technologies at large scale. The model was fabricated at NASA Ames, based on design data provided by Boeing, and was exceptionally detailed. The 777 model had a high-lift system, main landing gear, and half-fuselage, but without empennage or nose gear. The model did not have jet engines but had flow-through nacelles (Fig. 275, Test 40-0094). Numerous airframe noise sources were identified (using unique instrumentation) that are important in reducing the approach and landing noise of the full-scale airplane. Various modifications and noise alleviation devices were evaluated. In addition to acoustic measurements, aerodynamic force data were obtained simultaneously to document any performance changes caused by the modifications. At full-scale, typical noise reductions ranged from 1 to 10 dB without significant performance losses [381]. Two 70-element arrays were developed for the study of the airframe noise. One of the 70-element arrays traversed streamwise to map the sound field.

Miscellaneous

Crew Capsules

Experiments have been performed in the 40- by 80-Foot Wind Tunnel on crew-escape capsules, which were to be used instead of ejection seats for fighter aircraft at supersonic airspeeds. The capsules include the seats and the forward section of the airplane. Ejection at supersonic airspeeds using conventional ejection seats can, at best, be problematic. Therefore, the idea was to eject the entire crew capsule, which would serve to protect the pilot and/or crew from the dynamic pressures at supersonic airspeeds. The shape of the capsule would determine the aerodynamics, and therefore the trajectory and attitude, at the time the parachute would be deployed. Examples tested in the tunnel include the F-16 crew capsule (Fig. 276) and the F-111 crew capsule (Fig. 277, Tests 505 and 571).

The F-16 fighter, which as of this writing is still a front-line fighter for the U.S. Air Force, was designed and built with a single piece, high-visibility canopy. In addition to determining the aerodynamics of the crew capsule, the Air Force was concerned about aircraft controllability during approach speeds because of pilot visibility in the event of canopy loss. NASA Ames was approached by the Air Force to test the F-16 forebody at landing approach speeds without the canopy. The request was for a sampling of experienced F-16 pilots to subjectively determine the maximum wind blast they could be subjected to and still maintain control of the aircraft and use of the cockpit instrumentation. The 40- by 80-Foot Wind Tunnel was not formally man rated, but after considerable discussion, approval was given by Ames management to allow the program to proceed (Test 505). (However this was not the first time pilots had occupied cockpits of test airplanes during wind tunnel tests.) Five different pilots were used in the experiments, and it was found that approach speeds of 140 to 150 knots could be handled by the pilots without the canopy. The program proceeded without incident, and the Air Force was extremely complimentary to the staff of the 40- by 80-Foot Wind Tunnel for the results obtained.

The F-111 was a dual-seat airplane in which the crew sat side by side in the crew capsule. Experiments were performed with the capsule mounted sideways (Fig. 277, Test 571) in the test section so that parachute deployment studies could also be performed. The entire escape module would be ejected if there were catastrophic problems with the airplane, and then the parachute would be deployed.

Figure 275. A 26-percent-scale semispan model of a Boeing 777. ***(NASA AC01-0114-116)***

Figure 276. F-16 fighter crew capsule. ***(NASA AC77-0627-1)***

Figure 277. F-111 fighter crew capsule mounted sideways with deployed parachute laying on floor.
(NASA AC89-0144-1)

Boeing 757 Aircraft Vertical Tail With Boundary Layer Control (BLC)

The vertical tail from a 757 aircraft with BLC was tested in the 40- by 80-Foot Wind Tunnel in 1998. The purpose was to improve the control capability of the vertical tail and allow its size to be reduced in order to reduce drag during cruise and to reduce the weight of the tail (Fig. 278, Test 40-043). The experiments were part of the NASA Environmentally Responsible Aviation (ERA) Project. The BLC was produced by a vertical row of sweeping jet actuators, which are devices that blow air in a sweeping motion along the span of the tail rudder to energize the boundary layer on the rudder. The model was an actual 757 tail that was refurbished and then modified for the tunnel tests. Various configurations were studied in order to select the most efficient and effective configuration for planned flight evaluation. As described earlier, the 40- by 80-Foot Wind Tunnel has been used for many years for investigating various kinds of BLC to improve the performance of aerodynamic surfaces.

Wind Turbines

The NFAC is the ideal facility to perform research on wind turbines. The facility's large size is advantageous, and the test conditions can be well controlled. Controlled conditions allow for evaluation of configurations, as well as for evaluation and development of theoretical modeling of wind-turbine aerodynamics for design development and improvement.

National Renewable Energy Laboratory (NREL) blind test. A 10-meter-diameter, stall-regulated, two-bladed rotor was tested in the 80- by 120-Foot Wind Tunnel (Fig. 279, Test 80-0072) [382, 383]. The sponsor was the NREL. Stall-regulated wind turbines use fixed-pitch blades that are designed to stall to control power output rather than employing variable blade pitch to control power output, which makes the wind turbine physically simpler, but much more difficult to model theoretically. This research turbine had been field tested in various configurations since 1989. An important goal of the wind tunnel experiments was to collect data that would enable researchers and designers to better understand how wind turbines operate during various controlled-wind conditions and to improve aerodynamic theories.

Data were collected and kept confidential and not distributed until after theoretical modeling and CFD predictions had been done—by 30 experts from 18 organizations—to evaluate the capabilities of the various codes being used for design and analysis of wind turbines (and rotorcraft). Theoretical results were compared with collected data to evaluate the various theoretical approaches. In general, the agreement was very poor; some theories overpredicted, and some underpredicted results. Even at low airspeeds (less than 16 mph), in which the blades were not stalled, the agreement was poor. Wind-turbine power predictions ranged from 25 to 175 percent of measured power, and blade bending-force predictions ranged from 85 to 150 percent of measured bending force. At higher speeds (45 mph), most of the blade surfaces were operating in stalled conditions since it was a stall-regulated wind turbine. At this airspeed, power predictions ranged from 30 to 250 percent of the measured value. It was clear that the theoretical models needed much improvement to be effective for wind-turbine design and analysis. A major part of the problem of predicting wind-turbine performance is stall prediction, both dynamic and steady state. This is especially true for stall-regulated wind turbines. Stall prediction has always been a problem for theoretical estimates and CFD, and it remains an ongoing area of research.

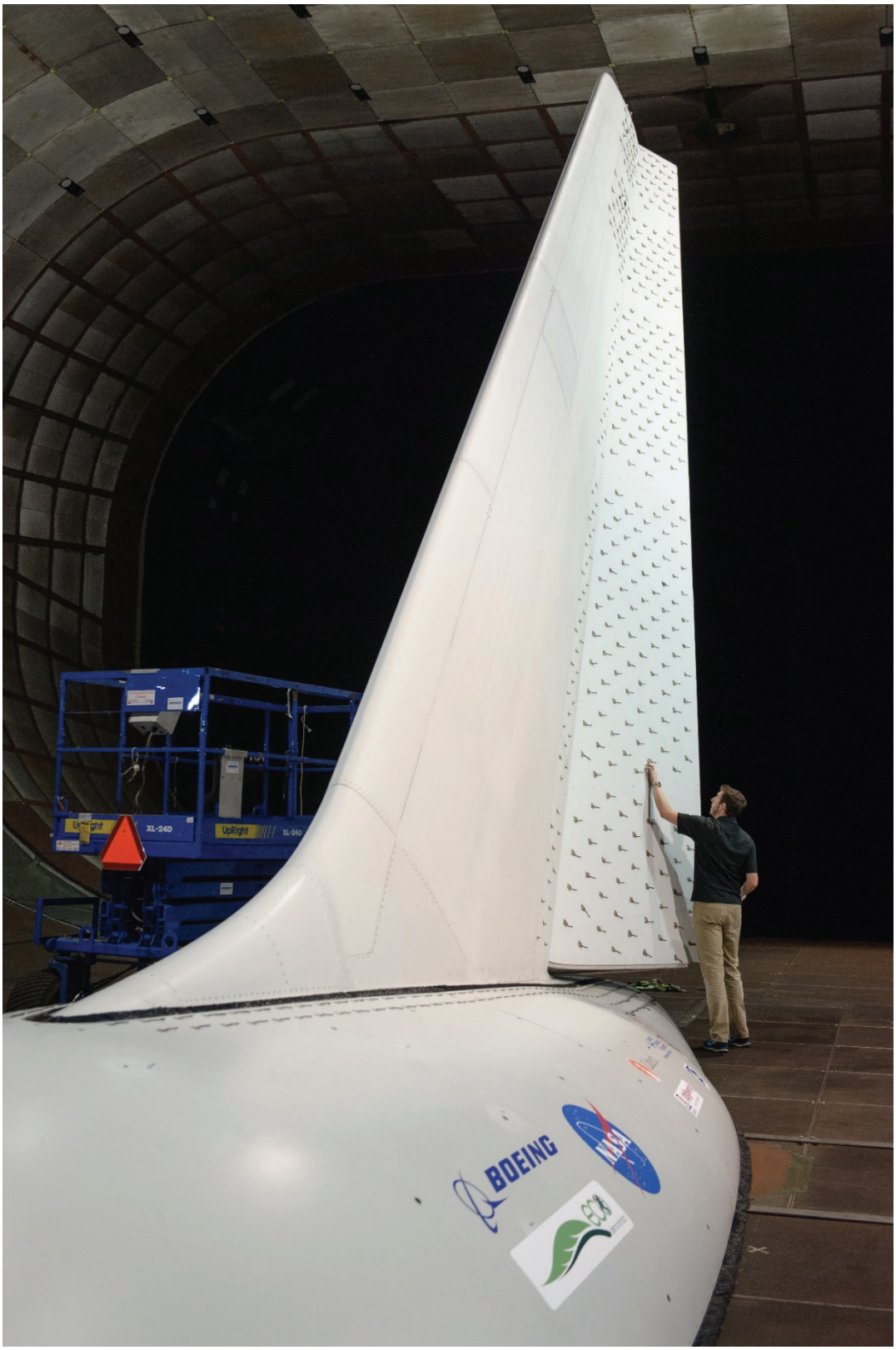

Figure 278. Boeing 757 vertical tail with BLC on the rudder in the 40- by 80-foot test section.
(NASA acd13-0172-069)

Figure 279. NREL blind-test wind turbine in the 80- by 120-foot test section. ***(NASA AC00-0010-12)***

Mecaro Spiral Magnus wind turbine. This was a very unusual 10-meter-diameter experimental horizontal-axis wind turbine that had five radial cylinders instead of blades. There were small (a fraction of cylinder diameter in height) spirally wrapped fins around each cylinder (Fig. 280, Test 40-002). The five individual cylinders were rotated about their individual axes so that the Magnus effect (airflow tends to follow around spinning surfaces) would create circulation around each cylinder similar to airfoil circulation. The power required for cylinder rotation was a small fraction of the power collected by the wind turbine. The turbine was called the "Spiral Magnus" and was tested in the 40- by 80-Foot Wind Tunnel.

The goal was to collect data that would allow for improvements in design and in theoretical modeling of this very unique wind turbine, and to allow for refinement of the design. The turbine was intended to have low rotational speed (about one-sixth that of common propeller-type wind turbines), exceptionally quiet operation, reduced bird strikes, long-lasting durability, and tolerance to high wind speeds. The research testing was performed for the Mecaro Co., Ltd. in Akita, Japan. The data were proprietary, but the company representatives were pleased with the wind tunnel results and with the excellent cooperation of the wind tunnel staff.

Truck Drag

Semi-truck and trailer drag studies were performed in the 80- by 120-Foot Wind Tunnel on actual full-size trucks. Various truck and trailer fairings were studied with excellent success. Many recommended modifications and fairings have been implemented. The 80- by 120-Foot Wind Tunnel is the ideal facility for performing these types of studies because fairings or modifications can be tried out on actual trucks. Gas savings due to the lower drag achieved have been substantial.

Truck installation is shown in Figures 281, 282, and 283. Figure 281 shows the tractor being lifted into the tunnel, and Figure 282 shows the trailer being lifted into the tunnel. Figure 283 shows the truck in the tunnel during smoke flow visualization studies. The test was funded by the Department of Energy (DOE) in a partnership with Navistar/International Trucks to complete a baseline survey of on-the-market and near-to-market aerodynamic drag-reducing devices for big-rig tractor trailers. The DOE also tested some novel under-trailer devices that it had been developing using CFD to predict results. The focus of the survey was to publish drag-reduction percentages for each device from a single controlled and unbiased wind tunnel test program, so that large trucking fleets could tailor the use of these devices to their operations, and the DOE could promote more widespread use of drag-reducing devices. In 2006 it was estimated that heavy-vehicle transportation accounted for nearly 20 percent of the nation's fuel consumption. This was a successful program; the use of the under-trailer devices as well as other aerodynamic fairings are evident on many of the trucks now traveling the highways [384].

Figure 280. Mecaro Spiral Magnus wind turbine in the 40- by 80-foot test section; note the spirally wrapped fins around the five circular "blades." ***(NASA ACD07-0242-002)***

Figure 281. Truck-tractor installation in the 80- by 120-foot test section. ***(NASA ACD10-0020-013)***

Figure 282. Truck-trailer installation in the 80- by 120-foot test section. ***(NASA ACD10-0020-023)***

Figure 283. Smoke flow visualization studies of truck with trailer in the 80- by 120-foot test section.
(NASA ACD10-0020-065)

PART IV. CONCLUDING REMARKS, REFERENCES, AND APPENDICES

Chapter 11. Concluding Remarks

The NFAC is a unique national facility that has been vitally important to the country's aeronautics programs from 1944 to the present day. There will always be subsonic aerodynamic problems that aerodynamic theory (including CFD) cannot deal with, and large- or full-scale subsonic experiments are required to reduce research and development costs, as well as to reduce risk and uncertainty before flight-tests. This has been demonstrated repeatedly over many years for conventional aircraft, but it is especially true for rotorcraft and V/STOL aircraft, and for aircraft with separated flows, multi-energy flows, dynamic effects, and aeroelastic effects.

The 40- by 80-Foot Wind Tunnel began operation in the summer of 1944 with research on fighter aircraft. Landing performance was improved by developing wing and flap designs to reduce landing and takeoff speeds. Drag was reduced to improve maximum airspeed. It was found that the models and aircraft were large enough that, by using force and moment coefficients, data could be easily corrected to subsonic cruise airspeeds. Later, experiments were performed on advanced fighter aircraft that had swept wings and were powered by jet engines. Jet engines allowed the use of wing and flap BLC to increase lift and thereby reduce aircraft landing and takeoff speeds. Jet-engine compressor bleed air can be ducted inside the wing and used to energize the wing and flap boundary layer flow.

Research on rotorcraft and V/STOL aircraft began in the 1950s. Many V/STOL configurations were studied; tilt wings, tilt propellers, tilt-rotors and ducted fans, and deflected slipstream configurations were included. Lift fans and lift engines were tried in many arrangements and locations on aircraft models. Because of the importance of reducing aircraft noise, the capability for performing acoustic research was established in the early 1960s and was subsequently improved over the years by modifying the walls of the 40- by 80-foot test section. The addition of the 80- by 120-foot test section in the 1980s improved the capability for performing large-scale low-speed research in aerodynamics and acoustics. This improved capability was a major contributor to the reduction of aircraft landing and takeoff speeds and improvements in low-speed-flight characteristics. The landing and takeoff requirements and capabilities of supersonic and hypersonic aircraft were studied using large-scale models; engineers were able to achieve major reductions in landing and takeoff airspeeds for high-speed aircraft.

Space-age requirements for recovery were met by development of parachute recovery devices in the NFAC. Lifting body research was performed that evolved into landing and control experiments on a 1/3-scale model of the space shuttle.

Despite a short-term shutdown due to changing NASA priorities in the 2000s, restoration and refurbishment were accomplished in a couple of years because of energetic pressure from the U.S. Army and the rotorcraft industry. The U.S. Air Force restored and refurbished the tunnels for the benefit of the aeronautics community. The Air Force leases the facility from NASA and rents it out for the use of industry. In addition to resumption of rotorcraft research, research on recovery parachutes and wind turbines was performed. Proprietary research became an important use of the facility by the aerodynamic industry. The NFAC started out as a NACA research facility and became a facility for hire for the aerodynamic industry.

When developing new aircraft, it has been repeatedly demonstrated that all tools should be used in the most efficient manner to produce the best aircraft, including CFD and theoretical modeling, wind tunnel experiments, simulator experiments, and flight-tests. Experienced wind tunnel research staff have been exceptionally useful and helpful in solving aerodynamic problems in the past. Just because aeronautics is a mature science, it does not mean that any of the existing research and development tools should be discarded. The way the various research tools are used can, and will, change, but it has been demonstrated that it does not make sense to eliminate any of the tools. Unanticipated aerodynamic problems still occur, and will likely continue to occur in the future, especially with the development of unique and unusual aircraft.

This history of the world's largest wind tunnels has described the development of the NFAC and summarized many of the important tests that have been conducted since 1944. The NFAC, consisting of the 40- by 80-Foot Wind Tunnel and the 80- by 120-Foot Wind Tunnel, will remain an essential aeronautical facility for our nation for many decades.

Chapter 12. References

Bibliographic Essay

For the most part only published references were used. Additional information was derived from the recollections of the author and contributors. The majority of the published information is from NACA/NASA technical reports and the NASA History Series books. American Institute of Aeronautics and Astronautics (AIAA), American Helicopter Society (AHS), and Society of Automotive Engineers (SAE) papers were also referenced and may be borrowed from technical libraries. The majority of the NACA/NASA reports can be accessed, and downloaded for free, by typing the report number into your web browser. The NASA History Series books can also be downloaded for free at http://www.nasa.gov/ebooks. A few non-NASA published books that have been helpful, and may be of general interest, were also referenced and can be borrowed from local libraries.

For those interested in more details about the aircraft tested, the online source "Virtual Aircraft Museum" is very useful.

A helpful source for Ames history materials and information is http://history.arc.nasa.gov.

List of References

1. Baals, Donald D. and Corliss, William R.: Wind Tunnels of NASA. NASA SP-440, 1981.

2. DeFrance, Smith J.: The NACA Full Scale Wind Tunnel. NACA TR-459, March 13, 1933.

3. Chambers, Joseph R.: Cave of the Winds, The Remarkable Story of the Langley Full-Scale Wind Tunnel. NASA/SP-2014-614, 2014.

4. Hartman, Edwin P.: Adventures in Research, A History of Ames Research Center, 1940-1965. NASA SP-4302, 1970.

5. Muenger, Elizabeth A.: Searching the Horizon; A History of Ames Research Center, 1940-1976. NASA SP-4304, 1985.

6. Bugos, Glenn E.: Atmosphere of Freedom; 60 Years at the NASA Ames Research Center. NASA SP-4314, 1961.

7. Bugos, Glenn E.: Atmosphere of Freedom; 70 Years at the NASA Ames Research Center. NASA SP-2010-4314, 2010.

8. Bugos, Glenn E.: Atmosphere of Freedom; 75 Years at the NASA Ames Research Center. NASA SP-2014-4314, 2014.

9. Cambra, J. M. and Tolari, G. P.: Real Time Computer Data System for the 40- by 80-Foot Wind Tunnel Facility at Ames Research Center. NASA TN D-7970, 1975.

10. Kelly, M. W.; Dickinson, S. O.; and Maynard, E. E.: Applications of the Real-Time Data Analysis System in the Ames 40- by 80-Foot Wind Tunnel. AGARD Conference Proceedings on Numerical Methods and Wind Tunnel Testing, AGARD CP-210, June 1976.

11. Grant, George R. and Orloff, Kenneth L.: A Two-Color, Dual Beam Backscatter Laser Doppler Velocimeter. NASA TM X-62,254, March 1973.

12. Orloff, K. L.; Corsiglia, V. R.; Biggers, J. C.; and Ekstedt, T. W.: Investigating Complex Aerodynamic Flows with a Laser Velocimeter. NASA TM X-73,171, Oct. 1976.

13. Orloff, Kenneth L.; Snyder, Philip K.; and Reinath, Michael S.: Laser Velocimetry in the Low-Speed Wind Tunnels at Ames Research Center. NASA TM-85885, Jan. 1984.

14. Reinath, Michael S.; Orloff, Kenneth L.; and Snyder, Philip K.: A Laser Velocimeter System for Large-Scale Aerodynamic Testing. NASA TM-84393, Jan. 1984.

15. Reinath, Michael S.: A Long-Range Laser Velocimeter for the National Full-Scale Aerodynamics Complex: New Developments and Experimental Application. NASA TM 101081, June 1989.

16. Forsyth, T. J.: Floating Frame Grounding System. ISA paper ’87-0210, 1987.

17. Kelly, Mark W.; Mort, Kenneth W.; and Hickey, David H.: Full-Scale Subsonic Wind Tunnel Requirements and Design Studies. NASA TM X-62184, Sept. 1972.

18. Mort, Kenneth W.; Eckert, William T.; and Kelly, Mark W.: The Steady-State Flow Quality in a Model of a Non-Return Wind Tunnel. NASA TM X-62170, Aug. 1972.

19. Mort, K. W.; Eckert, W. T.; and Kelly, M. W.: The Steady-State Flow Quality of an Open Return Wind Tunnel Model. Canadian Aeronautics and Space Journal, vol. 18, no. 9, Nov. 1972, pp. 285-289.

20. Structural Engineering Design Study of a Non-Return, Full-Scale Subsonic Wind Tunnel: Two Test Sections in a “Y” Configuration, John A. Blume and Associates, Engineers, San Francisco, CA, Aug. 3, 1973.

21. Eckert, William T.; Mort, Kenneth W.; and Piazza, J. E.: An Experimental Investigation of End Treatments for Nonreturn Wind Tunnels. NASA TM X-3402, June 1976.

22. Mort, K. W.; Kelly, M. W.; and Hickey, D. H.: The Rationale and Design Features for the 40- by 80-/80- by 120-Foot Wind Tunnel. AGARD CP-174, paper no. 9, presented in London, U. K., Oct. 6-8, 1975.

23. Lown, Harold: Aero-Acoustic Experimental Verification of Optimum Configuration of Variable-Pitch Fans for 40 x 80 Foot Subsonic Wind Tunnel. NASA CR-152-040, Aug. 1977.

24. Page, V. Robert; Eckert, William T.; and Mort, Kenneth W.: An Aerodynamic Investigation of Two 1.83-Meter-Diameter Fan Systems Designed to Drive a Subsonic Wind Tunnel. NASA TM 73,175, Sept. 1977.

25. Soderman, Paul T. and Page, V. Robert: Acoustic Performance of Two 1.83-Meter-

Diameter Fans Designed for a Wind-Tunnel Drive System. NASA TP 1008, Aug. 1977.

26. Soderman, P. T. and Mort, K. W.: Aeroacoustic Characteristics of a Large, Variable-Pitch Variable-Speed Fan System. Inter-Noise 83, Edinburgh, Scotland, July 13-15, 1983.

27. Eckert, William T.; Johnston, James P.; Simons, Tad D.; Mort, Kenneth W.; and Page, V. Robert: An Experimental Investigation of Two Large, Annular Diffusers with Swirling and Distorted Inflow. NASA TP 1628 and AVRADCOM-TR-79-40, Feb. 1980.

28. Eckert, William T.; Wettlaufer, Brian M.; and Mort, Kenneth W.: The Aerodynamic Performance of Several Flow Control Devices for Internal Flow Systems. NASA TP 1972 and AVRADCOM-TR-81-A-2, Dec. 1982.

29. Eckert, William T. and Mort, Kenneth W.: Earth Winds, Flow Quality, and the Minimum-Protection Inlet Treatment for the NASA Ames 80- by 120-Foot Wind Tunnel Nonreturn Circuit. NASA TM-78600 and AVRADCOM-TR-79-27, June 1979.

30. Eckert, William T. and Mort, Kenneth W.: Wind vs. Wind Tunnel: The Aerodynamics of the Inlet for NASA's New Very Large Non-Return Flow Facility. *Journal of Wind Engineering and Industrial Aerodynamics*, vol. 9, no. 3, pp. 193-205, March 1982.

31. Soderman, P. T.: Design and Performance of Resonant-Cavity Parallel Baffles for Duct Silencing. Noise Control Engineering, July-Aug. 1981.

32. Soderman, P. T.: A Study of Resonant-Cavity and Fiberglass-Filled Parallel Baffles as Duct Silencers. NASA TP 1970 and AVRADCOM-TR-81-A-2, April 1982.

33. Eckert, William T.; Mort, Kenneth W.; and Jope, Jean: Aerodynamic Design Guidelines and Computer Program for Estimation of Subsonic Wind Tunnel Performance. NASA TN D-8243, October 1976.[1]

34. Mort, K. W.; Soderman, P. T.; and Eckert, W. T.: Improving Large-Scale Testing Capability by Modifying the 40- by 80-Ft Wind Tunnel. AIAA Journal of Aircraft, vol. 16, no. 8, Aug. 1979, pp. 571-575.

35. Mort, K. W.; Engelbert, D. F.; and Dusterberry, J. C.: Status and Capabilities of the National Full-Scale Facility—40- by 80-Foot Wind Tunnel Modification. Presented at the AIAA 12th Aerodynamics Testing Conference. Williamsburg, VA, March 22-24, 1982.

36. Anon.: Report of 80- by 120-Foot Wind Tunnel Accident Investigation Board, Feb. 15, 1983.

37. Sanz, Jose M.; McFarland, Eric R.; Sanger, Nelson L.; Gelder, Thomas F.; and Cavicchi, Richard H.: Design and Performance of a Fixed, Nonaccelerating, Guide Vane Cascade That Operates Over an Inlet Flow Angle Range of 60°. NASA TM 83519, Jan. 1984.

38. Corsiglia, Victor R.; Olson, Lawrence E.; and Falarski, Michael D.: Aerodynamic Characteristics of the 40- by 80-/80- by 120-Foot Wind Tunnel at NASA Ames Research Center. NASA TM 85946, April 1984.

39. Schmidt, Gene I.; Rossow, Vernon J.; van Aken, Johannes; and Parrish, Cynthia L.: One-Fiftieth Scale Model Studies of 40- by 80-Foot and 80- by 120-Foot Wind Tunnel Complex at NASA Ames Research Center. NASA TM 89405, April 1987.

40. Dudley, M. R.; Unnever, G.; and Regan, D. R.: Two-Dimensional Wake Characteristics of Inlet Vanes for Open-Circuit Wind Tunnels. AIAA-84-0604, AIAA 13th Aerodynamic Testing Conference, San Diego, CA, March 5-7, 1984.

41. Soderman, Paul T.; Unnever, Gregory; and Dudley, Michael R.: Effect of Boattail Geometry on the Aeroacoustics of Parallel Baffles in Ducts. NASA TM 85981, July 1984.

42. Kaul, Upender K.; Ross, James C.; and Jacocks, James L.: A Numerical Simulation of the NFAC (National Full-Scale Aerodynamics Complex) Open-Return Wind Tunnel Inlet Flow. NASA TM 86724, April 1985.

43. Ross, J. C.; Olson, L. E.; and Meyn, L. A.: A New Design Concept for Indraft Wind-Tunnel Inlets with Application to the National Full-Scale Aerodynamics Complex. AIAA-86-0043, Jan. 6-9, 1986.

44. Rao, K. V.; Steger, Joseph L.; and Pletcher, R. H.: Three-Dimensional Dual-Potential Procedure for Inlets and Indraft Wind Tunnels. AIAA 87-

[1] The procedures for estimating wind tunnel performance described in this report are widely used by many wind tunnel designers.

0598, *AIAA Journal*, vol. 27, no. 7, May 17, 2012.

45. van Aken, J. M.; Lawrence, K. S.; and Scheller, N. M.: Experimental Investigation of Inlet Flow-Control Cascades for the NFAC 80- by 120-Foot Indraft Wind Tunnel. AIAA-88-0054, 26th Aerospace Sciences Meeting, Jan. 11-14, 1988.

46. van Aken, Johannes M.; Ross, James C.; and Zell, Peter T.: Inlet Development for the NFAC 80- by 120-Foot Indraft Wind Tunnel. AIAA 88-2528, 6th Applied Aerodynamic Conference, June 6-8, 1988.

47. Ross, James C.: Theoretical and Experimental Study of Flow-Control Devices for Inlets of Indraft Wind Tunnels. NASA TM 100050, Sept. 1989.

48. Ross, James C.; Olson, Lawrence E.; Meyn, Larry A.; and van Aken, Johannes M.: A New Design Concept for Indraft Wind-Tunnel Inlets with Application to the National Full-Scale Aerodynamic Complex. NASA TM 88226, Jan. 1986.

49. Rossow, Vernon J.; Schmidt, Gene I.; Meyn, Larry A.; Ortner, Kimberley R.; and Holmes, Robert E.: Aerodynamic Characteristics of an Air-Exchanger System for the 40- by 80-Foot Wind Tunnel at Ames Research Center. NASA TM 88192, Jan. 1986.

50. Rossow, Vernon J.; Schmidt, Gene I.; Reinath, Michael S.; Van Aken. Johannes M.; Parrish, Cynthia L.; and Schuler, Raymond F.: Experimental Study of Flow Deflectors Designed to Alleviate Ground Winds Induced by Exhaust of 80- by 120-Foot Wind Tunnel. NASA TM 88195, Jan. 1986.

51. Streeter, Barry G.: Simulation Investigation of the Effect of the NASA Ames 80- by 120-Foot Wind Tunnel Exhaust Flow on Light Aircraft Operating in the Moffett Field Traffic Pattern. NASA TM 86819, Feb. 1986.

52. Hicks, Raymond M.: A Recontoured, Upper Surface Design to Increase the Maximum Lift Coefficient of a Modified NACA 65 (0.82) (9.9) Airfoil Section. NASA TM-85855, Feb. 1984.

53. Signor, David B. and Borst, Henry V.: Aerodynamic Performance of Two Fifteen-Percent-Scale Wind-Tunnel Drive Fan Designs. AIAA 86-0734, March 5-7, 1986.

54. Signor, David B.: An Experimental Investigation of Two 15%-Scale Wind Tunnel Fan-Blade Designs. NASA TM 88256, April 1988.

55. Olson, Lawrence E.; Zell, Peter T.; Soderman, Paul T.; Falarski, Michael D.; Corsiglia, Victor R.; and Edenborough, H. Kipling: Aerodynamic Flow Quality and Acoustic Characteristics of the 40- by 80-Foot Test Section Circuit of the National Full-Scale Aerodynamic Complex. Presented at the 1987 SAE International Powered Lift Conference & Exposition, Santa Clara, CA, Dec. 7-10, 1987.

56. Smith, B. E.; Zell, P. T.; and Shinoda, P. M.: A Comparison of 1/50-Scale Model Studies of the 40- by 80-Foot Wind Tunnel with Full-Scale Results. AIAA-88-2536, June 6-8, 1988.

57. Soderman, Paul T.: Sources and Levels of Background Noise in the NASA Ames 40- by 80-Foot Wind Tunnel—A Status Report. NASA TM 100077, May 1988.

58. Zell, Peter T. and Flack, Karen: Performance and Test Section Flow Characteristics of the National Full-Scale Aerodynamics Complex 40- by 80-Foot Wind Tunnel. NASA TM 101065, Feb. 1989.

59. Zell, Peter T.: Performance and Test Section Flow Characteristics of the National Full-Scale Aerodynamics Complex 80- by 120-Foot Wind Tunnel. NASA TM 103920, Jan. 1993.

60. Schmitz, F. H.; Allmen, J. R.; and Soderman, P. T.: Modification of the Ames 40- by 80-Foot Wind Tunnel for Component Acoustic Testing for the Second Generation Supersonic Transport. NASA Technical Memorandum 108850, Oct. 1994.

61. Ver, Istvan L. and Howe, Michael S.: Acoustic Lining Study for the 40x80 Wind Tunnel, BBN Report No. 7739, NASA Contract No. NAS2-13461, Sept. 28, 1992.

62. Soderman, P. T.; Schmitz, F. H.; Allen, C. S.; Jaeger, S. M.; Sacco, J.; Mosher, M.; and Hayes, J. A.: Design and Development of a Deep Acoustic Lining for the 40- by 80-Foot Wind Tunnel Test Section. NASA/TP-2002-211850, Nov. 2002.

63. Soderman, P. T.; Jaeger, S. M.; Hayes, J. A.; and Allen, C. S.: Acoustic Quality of the 40- by 80-Foot Wind Tunnel Test Section After Installation of a Deep Acoustic Lining. NASA/TP-2002-211851, Nov. 2002.

64. Hunt, Rusty and Sacco, Joe: Activation and Operation of the National Full-Scale Aerodynamics Complex. AIAA 2000-1076, AIAA 38th Aerospace Sciences Meeting & Exhibit, Reno, NV, Jan. 10-13, 2000.

65. van Aken, Johannes M. and Yang, Lei: Development of a New State-of-the-Art Data Acquisition System for the National Full-Scale Aerodynamics Complex Wind Tunnels. AIAA 2009-1346, Jan. 5-8, 2009.

66. Lowrance, R. Kent and Meyer, R. David: Distributed Data System for the National Full-Scale Aerodynamics Complex Wind Tunnels. AIAA-2010-1729, Feb. 2010.

67. Harris, Roy: The first A in NASA—Lost in the Space Debate. *AIAA Aerospace*, vol. 49, no. 1, Jan. 2011.

68. Madl, Dennis O.; Trepal, Terrence A.; Money, Alexander F.; and Mitchell, James G.: Effect of the Proposed Closure of NASA's Subsonic Wind Tunnels: An Assessment of Alternatives. Institute for Defense Analyses, IDA paper P-3858, April 2004.

69. Colucci, Frank: NFAC is Back. AHS *Vertiflite*, Fall 2007, vol. 53, no. 3, pp. 40-43.

70. Flater Rhett M. E. and Smith, Kim: Advancing Vertical Flight, A History of the Vertical Flight Society; The Vertical Flight Society, Fairfax VA, May 2019.

71. Gasich, Welko E.: Experimental Verification of Two Methods for Computing the Takeoff Ground Run of Propeller-Driven Aircraft. NACA TN 1258, 1947.

72. Borchers, Paul F.; Franklin, James A.; and Fletcher, Jay W.: Flight Research at Ames; Fifty-Seven Years of Development and Validation of Aeronautical Technology. NASA/SP-1998-3300, 1998.

73. Chapman, Dean R.: Investigation of Slipstream Effects on a Wing-Inlet Oil-Cooler Ducting System of a Twin-Engine Airplane in the Ames 40- by 80-Foot Wind Tunnel. NACA MR No. A5C10, March 1945.

74. Stevens, Victor I., Jr. and McCormack, Gerald M.: Power-Off Tests of the Northrop N9M-2 Tailless Airplane in the 40- by 80-Foot Wind Tunnel. Memorandum Report for the Air Technical Service Command, U.S. Army Air Forces, MR No. A4L14, Dec. 14, 1944.

75. McCormack, Gerald M.: Tests of an Attack-Type Airplane in the Ames 40- by 80-Foot Wind Tunnel to Improve the High-Speed Maneuvering Control-Force Characteristics. NACA MR No. A5K16, Nov. 1945.

76. Hunton, Lynn W. and Dew, Joseph K.: An Investigation of the Wing and the Wing-Fuselage Combination of a Full-Scale Model of the Republic XP-91 Airplane in the Ames 40- by 80-Foot Wind Tunnel. NACA RM No. SA8F09, June 10, 1948.

77. Hunton, Lynn W.: Force Tests of the Boeing XB-47 Full-Scale Empennage in the Ames 40- by 80-Foot Wind Tunnel. NACA RM No. A7H12, Aug. 14, 1947.

78. Hunton, Lynn W. and James, Harry A.: An Investigation of the McDonnell XP-85 Airplane in the Ames 40- by 80-Foot Wind Tunnel. Force and Moment Tests. NACA RM No. SA8I23, Sept. 27, 1948.

79. Maki, Ralph L.: Full-Scale Wind-Tunnel Investigation of the Effects of Wing Modifications and Horizontal-Tail Location on the Low-Speed Static Longitudinal Characteristics of a 35° Swept-Wing Airplane. NACA RM A52B05, April 3, 1952.

80. Maki, Ralph L.: Low-Speed Wind-Tunnel Investigation of the Drag of a Lockheed F-94C Airplane. NACA RM SA52D25, April 25,1952.

81. Kelly, Mark W. and Smaus, Louis H.: Flight Characteristics of a ¼-Scale Model of the XFV-1 Airplane. NACA RM SA52J15, Oct. 15, 1952.

82. Martin, Norman J.: Tests of Submerged Duct Installation on the Ryan FR-1 Airplane in the Ames 40- by 80-Foot Wind Tunnel. NACA RM No. A7D14, April 23, 1947.

83. Martin, Norman J.: Tests of Submerged Duct Installation on a Modified Fighter Airplane in the Ames 40- by 80-Foot Wind Tunnel. NACA RM No. A7129, Dec. 11, 1947.

84. Martin, Norman J. and Holzhauser, Curt A.: An Experimental Investigation at Large Scale of Several Configurations of an NACA Submerged Air Intake. NACA RM A8F21, Oct. 19, 1948.

85. Martin, Norman J. and Holzhauser, Curt A.: An Experimental Investigation at Large Scale of Single and Twin NACA Submerged Side Intakes at Several Angles of Sideslip. NACA RM A9F20, Aug. 1, 1949.

86. Holzhauser, Curt A.: An Experimental Investigation at Large Scale of an NACA Submerged Intake and Deflector Installation on the Rearward Portion of a Fuselage. NACA RM A50F13, Aug. 30, 1950.

87. Hunton, Lynn W.; Griffin, Roy N., Jr.; and James, Harry A.: Wind-Tunnel Investigation of the Low-Speed Static Longitudinal Characteristics of the Republic RF-84F Airplane. NACA RM SA52H04, Aug. 4, 1952.

88. Maki, Ralph L.: Tests of a Northrup XSSM-A-3 Missile in the Ames 40- by 80-Foot Wind Tunnel—Stability and Control. NACA RM No. SA50D05, April 5, 1950.

89. Graham, David: Tests of the Northrup XB-62 Missile in the Ames 40- by 80-Foot Wind Tunnel. NACA RM SA54I29, Sept. 29, 1954.

90. McCormack, Gerald M. and Stevens, Victor I., Jr.: An Investigation of the Low-Speed Stability and Control Characteristics of Swept-Forward and Swept-Back Wings in the Ames 40- by 80-Foot Wind Tunnel. NACA RM No. A6K15, June 10, 1947.

91. Hunton, Lynn W. and Dew, Joseph K.: Measurements of the Damping in Roll of Large-Scale Swept-Forward and Swept-Back Wings. NACA RM No. A7D11, July 30, 1947.

92. McCormack, Gerald M. and Cook, Woodrow L.: A Study of Stall Phenomena on a 45° Swept-Forward Wing. NACA TN No.1797, Jan. 1949.

93. Walling, Walter C.: An Investigation of the Effect of Tip Shape on the Low-Speed Aerodynamic Characteristics of Large-Scale Swept Wings. NACA RM No. A7H13, Nov. 13, 1947.

94. Tolhurst, William H., Jr.: An Investigation of the Downwash and Wake behind Large-Scale Swept and Unswept Wings. NACA RM No. A7L05, Feb. 2, 1948.

95. McCormack, Gerald M. and Walling, Walter C.: Aerodynamic Study of a Wing-Fuselage Combination Employing a Wing Swept Back 63° - Investigation of a Large-Scale Model at Low Speed. NACA RM No. A8D02, Jan. 21, 1949.

96. McCormack, Gerald M.: Aerodynamic Study of a Wing-Fuselage Combination Employing a Wing Swept Back 63° - Aerodynamic Characteristics in Sideslip of a Large-Scale Model Having a 63° Swept-Back Vertical Tail. NACA RM A9F14, Oct. 7, 1949.

97. Tolhurst, William H.: Downwash Characteristics and Vortex-Sheet Shape Behind a 63° Swept-Back Wing-Fuselage Combination at a Reynolds Number of 6.1 x 10^6. NACA TN 3175, May 1954.

98. Hunton, Lynn W. and Dew, Joseph K.: The Effects of Camber and Twist on the Aerodynamic Loading and Stalling Characteristics of a large-Scale 45° Swept-Back Wing. NACA RM A50J24, Jan. 24, 1951.

99. James, Harry A. and Dew, Joseph K.: Effects of Double-Slotted Flaps and Leading-Edge Modifications on the Low-Speed Characteristics of a Large-Scale 45° Swept-Back Wing With and Without Camber and Twist. NACA RM A51D18, July 23, 1951.

100. James, Harry A.: Low-Speed Aerodynamic Characteristics of a Large-Scale 45° Swept-Back Wing with Partial-Span Slats, Double-Slotted Flaps, and Ailerons. NACA RM A52B19, April 28, 1952.

101. Hunton, Lynn W.: Effects of Finite Span on the Section Characteristics of Two 45° Sweptback Wings of Aspect Ratio 6. NACA TN 3008, Sept. 1953.

102. Kelly, Mark W.: Low-Speed Aerodynamic Characteristics of a Large-Scale 60° Swept-Back Wing with High Lift Devices. NACA RM A52A14a, March 3, 1952.

103. Wick, Bradford H. and Graham, David: Investigation of the Flying Mock-Up of the Consolidated Vultee XP-92 Airplane in the Ames 40- by 80-Foot Wind Tunnel—Force and Moment Characteristics. NACA RM No. SA8B04, Feb.13, 1948.

104. Graham, David: Investigation of the Flying Mock-Up of the Consolidated Vultee XP-92 Airplane in the Ames 40- by 80-Foot Wind Tunnel—Pressure Distributions. NACA RM No. SA8D08, April 9, 1948.

105. Anderson, Adrien E.: An Investigation at Low Speed of a Large-Scale Triangular Wing of Aspect Ratio Two. I. Characteristics of a Wing Having a Double-Wedge Airfoil Section with Maximum Thickness at 20-Percent Chord. NACA RM No. A7F06, Nov. 13, 1947.

106. Anderson, Adrien E.: An Investigation at Low Speed of a Large-Scale Triangular Wing of

Aspect Ratio Two. II. The Effect of Airfoil Section Modifications and the Determination of the Wake Downwash. NACA RM No. A7H28, Dec. 10, 1947.

107. Wick, Bradford H.: Chordwise and Spanwise Loadings Measured at Low Sped on a Triangular Wing Having an Aspect Ratio of Two and an NACA 0012 Airfoil Section. NACA TN No. 1650, June 1948.

108. Graham, David: Chordwise and Spanwise Loadings Measured at Low Speeds on a Large Triangular Wing Having an Aspect Ratio of 2 and a Thin, Subsonic-Type Airfoil Section. NACA RM A50A04a, March 13, 1950.

109. Anderson, Adrien E.: An Investigation at Low Speed of a Large-Scale Triangular Wing of Aspect Ratio Two. III. Characteristics of Wing with Body and Vertical Tail. NACA RM A9H04, Oct. 14, 1949.

110. Wick, Bradford H. and Graham, David: Exploratory Investigation of the Effect of Skewed Plain Nose Flaps on the Low-Speed Characteristics of a Large-Scale Triangular-Wing-Fuselage Model. NACA RM A9K22, Jan. 12, 1950.

111. Graham, David and Koenig, David G.: Tests in the Ames 40- by 80-Foot Wind Tunnel of an Airplane Configuration with an Aspect Ratio 2 Triangular Wing and an All-Movable Horizontal Tail—Longitudinal Characteristics. NACA RM A51B21, April 23, 1951.

112. Graham, David and Koenig, David G.: Tests in the Ames 40- by 80-Foot Wind Tunnel of an Airplane Configuration with an Aspect Ratio 4 Triangular Wing and an All-Movable Horizontal Tail—Longitudinal Characteristics. NACA RM A51H10a, Oct. 16, 1951.

113. Franks, Ralph W.: Tests in the Ames 40- by 80-Foot wind Tunnel of an Airplane Model with an Aspect Ratio 4 Triangular Wing and an All-Movable Horizontal Tail-High-Lift Devices and Lateral Controls. NACA RMA52K13, Feb. 20, 1953.

114. Koenig, David G.: Tests in the Ames 40- by 80-Foot Wind Tunnel of an Airplane Configuration with an Aspect Ratio 3 Triangular Wing and an All-Movable Horizontal Tail—Longitudinal and Lateral Characteristics. NACA RM A52L15, April 13, 1953.

115. Franks, Ralph W.: Tests in the Ames 40- by 80-Foot Wind Tunnel of Two Airplane Models Having Aspect Ratio 2 Trapezoidal Wings of Taper Ratios 0.33 and 0.20. NACA RM A52L16, Feb. 16, 1953.

116. Graham, David: The Low-Speed Lift and Drag Characteristics of a Series of Airplane Models Having Triangular or Modified Triangular Wings. NACA RM A53D14, June 15, 1953.

117. Koenig, David G.: Tests in the Ames 40- by 80-Foot Wind Tunnel of an Airplane Configuration with a Variable-Incidence Triangular Wing and an All-Movable Horizontal Tail. NACA RM A53D21, Jun 25, 1953.

118. Koenig, David G.: Tests in the Ames 40- by 80-Foot Wind Tunnel of the Effects of Various Wing Modifications on the Longitudinal Characteristics of Two Triangular-Wing Airplane Models With and Without Horizontal Tails. NACA RM A54B09, April 15, 1954.

119. McCormack, Gerald M. and Cook, Woodrow L.: Effects of Boundary-Layer Control on the Longitudinal Characteristics of a 45° Swept-Forward Wing-Fuselage Combination. NACA RM A9K02a, Feb. 2, 1950.

120. Cook, Woodrow L.; Griffin, Roy N.; and McCormack, Gerald M.: The Use of Area Suction for the Purpose of Delaying Separation of Air Flow at the Leading Edge of a 63° Swept-Back Wing. NACA RM A50H09, Nov. 22, 1950.

121. McCormack, Gerald M. and Tolhurst, William H., Jr.: The Effects of Boundary-Layer Control on the Longitudinal Characteristics of a Swept-Back Wing Using Suction Through Streamwise Slots in the Outboard Portion of the Wing. NACA RM A50K06, Jan. 5, 1951.

122. Cook, Woodrow L. and Kelley, Mark W.: The Use of Area Suction for the Purpose of Delaying Separation of Air Flow at the Leading Edge of a 63° Swept-Back Wing-Effects of Controlling the Chordwise Distribution of Suction-Air Velocities. NACA RM A51J24, Jan. 14, 1952.

123. Kelly, Mark W. and Tolhurst, William H.: The Use of Area Suction to Increase the Effectiveness of a Trailing-Edge Flap on a Triangular Wing of Aspect Ratio 2. NACA RM A54A25, April 1, 1954.

124. Cook, Woodrow L.; Holzhauser, Curt A.; and Kelly, Mark W.: The Use of Area Suction for the

Purpose of Improving Trailing-Edge Flap Effectiveness on a 35° Sweptback Wing. NACA RM A53E06, July 2, 1953.

125. Holzhauser, Curt A. and Martin, Robert K.: The Use of a Leading-Edge Area-Suction Flap to Delay Separation of Air Flow From the Leading-Edge of a 35° Sweptback Wing. NACA RM A53J26. Dec. 10, 1953.

126. Kelly, Mark W. and Tolhurst, William H., Jr.: Full-Scale Wind-Tunnel Tests of a 35° Sweptback Wing Airplane with High-Velocity Blowing Over the Trailing-Edge Flaps. NACA RM A55I09, Nov. 15, 1955.

127. Holzhauser, Curt A. and Bray, Richard S.: Wind Tunnel and Flight Investigations of the Use of Leading-Edge Area Suction for the Purpose of Increasing the Maximum Lift Coefficient of a 35° Swept-Wing Airplane. NASA TR 1276, 1955.

128. Tolhurst, William H., Jr. and Kelly, Mark W.: Full-Scale Wind-Tunnel Tests of a 35° Sweptback-Wing Airplane with High-Velocity Blowing Over the Trailing-Edge Flaps—Longitudinal and Lateral Stability and Control. NACA RM A56E24, Oct. 5, 1956.

129. Kelly, Mark W.; Anderson, Seth B.; and Innis, Robert C.: Blowing-Type Boundary-Layer Control as Applied to the Trailing-Edge Flaps of a 35° Swept-Wing Airplane. NACA TR 1369, April 30, 1958.

130. Cook, Woodrow L.; Anderson, Seth B.; and Cooper, George E.: Area-Suction Boundary-Layer Control as Applied to the Trailing-Edge Flaps of a 35° Swept-Wing Airplane. NACA TR 1370, May 6, 1958.

131. Kelly, Mark W. and Tucker, Jeffrey H.: Wind-Tunnel Tests of Blowing Boundary-Layer Control With Jet Pressure Ratios up to 9.5 on the Trailing-Edge Flaps of a 35° Sweptback Wing Airplane. NACA RM A56G19, Oct. 26, 1956.

132. Cook, Woodrow L.; Griffin, Roy N., Jr.; and Hickey, David H.: A Preliminary Investigation of the Use of Circulation Control to Increase the Lift of a 45° Sweptback Wing by Suction Through Trailing-Edge Slots. NACA RM A54I21, Dec. 14, 1954.

133. Griffin, Roy N. and Hickey, David H.: Investigation of the Use of Area Suction to Increase the Effectiveness of Trailing-Edge Flaps of Various Spans on a Wing of 45° Sweepback and Aspect Ratio 6. NACA RM A56B27, June 22, 1956.

134. Koenig, David G.: The Use of Area Suction for Improving the Longitudinal Characteristics of a Thin Unswept Wing-Fuselage Model With Leading- and Trailing-Edge Flaps. NACA RM A56D23, July 10, 1956.

135. Holzhauser, Curt A.; Martin, Robert K.; and Page, V. Robert: Application of Area Suction to Leading-Edge and Trailing-Edge Flaps on a 44° Swept-Wing Model. NACA RM A56F01, Sept. 26, 1956.

136. Koenig, David G. and Aoyagi, Kiyoshi: Large-Scale Wind-Tunnel Tests of an Airplane Model with a 45° Sweptback Wing of Aspect Ratio 2.8 with Area Suction Applied to Trailing-Edge Modifications. NACA RM A56H08, Nov. 2, 1956.[2]

137. Koenig, David G. and Aoyagi, Kiyoshi: The Use of a Leading-Edge Area-Suction Flap and Leading-Edge Modifications to Improve the High-Lift Characteristics of an Airplane Model with a Wing of 45° Sweep and Aspect Ratio 2.8. NACA RM A57H21, Nov. 4, 1957.

138. Hickey, David H. and Aoyagi, Kiyoshi: Large-Scale Wind-Tunnel Tests of an Airplane Model with a 45° Sweptback Wing of Aspect Ratio 2.8 Employing High-Velocity Blowing Over the Leading- and Trailing-Edge Flaps. NACA RM A58A09, May 26, 1958.

139. Holzhauser, Curt A.: Wind-Tunnel Investigation of the Use of Leading-Edge and Trailing-Edge Area-Suction Flaps on a 13-Percent-Thick Straight Wing and Fuselage Model. NACA RM A57k01, Jan. 24, 1958.

140. Maki, Ralph L. and James, Harry A.: Wind-Tunnel Tests of the Static Longitudinal Characteristics at Low Speed of a Swept-Wing Airplane with Slotted Flaps, Area-Suction Flaps, and Wing Leading-Edge Devices. NACA RM A57A24, April 30, 1957.

141. James, Harry A. and Maki, Ralph L.: Wind-Tunnel Tests of the Static Longitudinal Characteristics at Low Speed of a Swept-Wing Airplane with Blowing Flaps and Leading-Edge Slats. NACA RM A57D11, July 5, 1957.

[2] Adverse pitching moment variations in medium to high lift range were reduced by drooping the horizontal tail which became an identifying characteristic of the F-4.

142. Maki, Ralph L.: Low-Speed Wind-Tunnel Investigation of Blowing Boundary-Layer Control on Leading- and Trailing-Edge Flaps on a Large-Scale, Low-Aspect-Ratio, 45° Swept-Wing Airplane Configuration. NASA Memo 1-23-59A, Jan. 1959.

143. Maki, Ralph L. and Embry, Ursel R.: Effects of High-Lift Devices and Horizontal-Tail Location on the Low-Speed Characteristics of a Large-Scale 45° Swept-Wing Airplane Configuration. NACA RM A54E10, Aug. 18, 1954.

144. Hickey, David H. and Aoyagi, Kiyoshi: Large-Scale Wind-Tunnel Tests of a Jet-Transport-Type Model with Leading- and Trailing-Edge High-Lift Devices. NACA RM A58H12, Sept. 26, 1958.

145. Graham, David and Evans, William T.: Investigation of the Effects of an Airfoil Section Modification on the Aerodynamic Characteristics at Subsonic and Supersonic Speeds of a Thin Swept Wing of Aspect Ratio 3 in Combination with a Body. NACA RM A55D11, June 28, 1955.

146. Evans, William T.: Data From Large-Scale Low-Speed Tests of Airplane Configurations with a Thin 45° Swept Wing Incorporating Several Leading-Edge Contour Modifications. NACA RM A56B17, March 20, 1958.

147. Evans, William T.: Leading-Edge Contours for Thin Swept Wings: an Analysis of Low- and High-Speed Data. NACA RM A57B11, March 29, 1957.[3]

148. Roberts, John C. and Yaggy, Paul F.: A Survey of the Flow at the Plane of the Propeller of a Twin-Engine Airplane. NACA TN 2192, Sept. 1950.

149. Rogallo, Vernon L.; Roberts, John C.; and Oldaker, Merritt R.: Vibratory Stresses in Propellers Operating in the Flow Field of a Wing-Nacelle-Fuselage Combination. NACA TN 2308, March 1951.

150. Yaggy, Paul F.: A Method for Predicting the Upwash Angles Induced at the Propeller Plane of a Combination of Bodies with an Unswept Wing. NACA TN 2528, Oct. 1951.

151. Rogallo, Vernon L.: Effects of Wing Sweep on the Upwash at the Propeller Planes of Multiengine Airplanes. NACA TN 2795, Sept. 1952.

152. Rogallo, Vernon L. and McCloud, John L. III: Surveys of the Flow Fields at the Propeller Planes of Six 40 deg. Sweptback Wing-Fuselage-Nacelle Combinations. NACA TN 2957, June 1953.

153. Rogallo, Vernon L.; Yaggy, Paul F.; and McCloud, John L. III: An Analysis of Once-Per-Revolution Oscillating Aerodynamic Thrust Loads on Single-Rotation Propellers on Tractor Airplanes at Zero Yaw. NACA TR 1295, 1956.

154. Rogallo, Vernon L.; Yaggy, Paul F.; and McCloud, John L. III: An Investigation in the Ames 40- by 80-Foot Wind Tunnel of a YT-56A Turboprop Engine Incorporating a Decoupler and a Controlled-Feathering Device. NACA RM SA54I09, Sept. 9, 1954.

155. Hickey, David H.: Full-Scale Wind Tunnel Tests of the Longitudinal Stability and Control Characteristics of the XV-1 Convertiplane in the Autorotating Flight Range. NACA RM A55k21a, May 17, 1956.

156. McCloud, John L. III and McCullough, George B.: Wind-Tunnel Tests of a Full-Scale Helicopter Rotor with Symmetrical and with Cambered Blade Sections at Advance Ratios From 0.3 to 0.4. NACA TN 4367, Sept. 1958.

157. McCloud, John L. III; Hall, Leo P.; and Brady, James A.: Full-Scale Wind-Tunnel Tests of Blowing Boundary-Layer Control Applied to a Helicopter Rotor. NASA TN D-335, Sept. 1960.

158. Koenig, David G.; Aiken, Thomas N.; Aoyagi, Kiyoshi; and Falarski, Michael D.: Large-Scale V/STOL Testing. NASA TM X-73,231, May 1977.

159. Eckert, William T. and Maki, Ralph L.: Low-Speed Wind-Tunnel Investigation of the Longitudinal Characteristics of a Large-Scale Variable Wing-Sweep Fighter-Model in the High-Lift Configuration. NASA TM X-62,244, Aug. 1973.

160. Eckert, William T. and Maki, Ralph L.: Low-Speed Wind-Tunnel Investigation of the Lateral-Directional Characteristics of a Large-Scale Variable Sweep Fighter-Model in the High-Lift Configuration. NASA TM X-62,306, Oct. 1973.

[3] This reference contains an excellent summary of the results of these studies.

161. Eckert, William T.; Maki, Ralph L.; and Tolhurst, William H.: Low Speed Wind Tunnel Tests of the Effects of Various Configuration Changes on a ¾ Scale Unpowered Fighter Model with 45° Swept Wings. NASA TM X-62,140, May 1972.

162. Olson, L. E. and Dvorak, F. A.: Viscous/Potential Flow About Multi-Element Two-Dimensional and Infinite-Span Swept Wings: Theory and Experiment. NASA TM X-62,513, Dec. 1975.

163. Olson, Lawrence E.; McGowan, Phillip R.; and Guest, Cla:yton J.: Leading-Edge Slat Optimization for Maximum Airfoil Lift. NASA TM 78566, March 22, 1979.

164. Griffin, Roy N., Jr.; Holzhauser, Curt A.; and Weiberg, James A.: Large-Scale Wind-Tunnel Tests of an Airplane Model with an Unswept, Aspect-Ratio-10 Wing, Two Propellers, and Blowing Flaps. NASA Memo 12-3-58A, Dec. 1958.

165. Weiberg, James A.; Griffin, Roy N., Jr.; and Florman, George L.: Large-Scale Wind-Tunnel Tests of an Airplane Model with an Unswept, Aspect-Ratio-10 Wing, Two Propellers, and Area-Suction Flaps. NACA TN 4365, Sept. 1958.

166. Weiberg, James A. and Holzhauser, Curt A.: STOL Characteristics of a Propeller-Driven, Aspect-Ratio-10, Straight-Wing Airplane with Boundary-Layer Control Flaps, as Estimated From Large-Scale Wind-Tunnel Tests. NASA TN D-1032, June 1961.

167. Hickey, David H. and Aoyagi, Kiyoshi: Large-Scale Wind-Tunnel Tests and Evaluation of the Low-Speed Performance of a 35° Sweptback Wing Jet Transport Model Equipped with a Blowing Boundary-Layer-Control Flap and Leading-Edge Slat. NASA TN D-333, Oct. 1960.

168. Evans, William T.: Data From Flow-Field Surveys Behind a Large-Scale Thin Straight Wing of Aspect Ratio 3. NACA RM A58D17, June 23, 1958.

169. Aoyagi, K. and Tolhurst, W. H.: Large-Scale Wind-Tunnel Tests of a Subsonic Transport with Aft Engine Nacelles and High Tail. NASA TN D-3797, Jan 1967.

170. Soderman, P. T. and Aiken, T. N.: Full-Scale Wind-Tunnel Tests of a Small Unpowered Jet Aircraft with a T-Tail. NASA TN D-6573, Nov. 1971.

171. Rossow, V. J. and Corsiglia, V. R.: Measurements of the Vortex Wakes of a Subsonic- and a Supersonic-Transport Model in the 40- by 80-Foot Wind Tunnel. NASA TM X-62,391, Sept. 1974.

172. Rossow, Vernon J.; Corsiglia, Victor R.; Schwind, Richard G.; Frick, Juanita K. D.; and Lemmer, Opal J.: Velocity and Rolling-Moment Measurements in the Wake of a Swept-Wing Model in the 40- by 80-Foot Wind Tunnel. NASA TM X-62,414, April 1975.

173. Corsiglia, V. R.; Rossow, V. J.; and Ciffone, D. L.: Experimental Study of the Effect of Span Loading on Aircraft Wakes, *Journal of Aircraft*, vol. 13, no. 12, Dec. 1976, pp. 968-973.

174. Corsiglia, V. R.; Schwind, R. G.; and Chigier, N. A.: Rapid Scanning, Three-Dimensional Hot-Wire Anemometer Surveys of Wing-Tip Vortices. *AIAA Journal of Aircraft*, vol. 10, no. 12, 1973, pp. 752-757.

175. Corsiglia, Victor R. and Orloff, Kenneth L.: Scanning Laser-Velocimeter Surveys and Analysis of Multiple Vortex Wakes of an Aircraft. NASA TM X-73169, Aug. 1, 1976.

176. Corsiglia, Victor R.; Rossow, Vernon J.; and Ciffone, Donald L.: Experimental Study of the Effect of Span Loading on Aircraft Wakes. NASA TM X-62,431, May 1975.

177. Corsiglia, Victor R. and Rossow, Vernon J.: Wind-Tunnel Investigation of the Effect of Porous Spoilers on the Wake of a Subsonic Transport Model. NASA TM-73,091, Jan. 1976.

178. Rossow, Vernon J.: Experimental Investigation of Wing Fin Configuration for Alleviation of Vortex Wakes of Aircraft. NASA Technical Memorandum 78520, Nov. 1978.

179. Tolhurst, William H., Jr.; Hickey, David H.; and Aoyagi, Kiyoshi: Large-Scale Wind-Tunnel Tests of Exhaust Ingestion Due to Thrust Reversal on a Four-Engine Jet Transport. NASA TN D-686, Jan. 1961.

180. Hickey, David H.; Tolhurst, William H., Jr.; and Aoyagi, Kiyoshi: Investigation of the Longitudinal Characteristics of a Large-Scale Jet Transport Model Equipped with Controllable Thrust Reversers. NASA TN D-786, March 1961.

181. Tolhurst, William H. and Aoyagi, Kiyoshi: Large-Scale Low-Speed Wind-Tunnel Tests of a Delta Winged Supersonic Transport Model to Determine Aerodynamic Effects of Forward or Reverse Thrust. NASA TM-X-1017, 1964.

182. Falarski, Michael D. and Mort, Kenneth W.: Full-Scale Wind-Tunnel Investigation of a Target-Type Thrust Reverser on the A-37B Airplane. NASA TM X-1985, April 1970.

183. Reynolds, Randolph S.: An Overview of the Demise of NASA's High Speed Research Program. *Journal of Aviation/Aerospace Education & Research*, vol. 14, no. 1, Article 5, Fall 2004.

184. Conway, Erik M.: High-Speed Dreams; NASA and The Techno-Politics of Supersonic Transportation, 1945-1999. The Johns Hopkins University Press, 2005.

185. Brady, J. A.; Koenig, D. G.; and Page, V. R.: Large-Scale Low-Speed Wind-Tunnel Tests of a Delta Winged Supersonic Transport Model with a Delta Canard Control Surface. NASA TM-X-643, Jan. 1962.

186. Brady, J. A.; Koenig, D. G.; and Page, V. R.: Large-Scale Wind-Tunnel Tests at Low Speed of a Delta Winged Supersonic Transport Model in the Presence of the Ground. NASA TM-X-644, Jan. 1962.

187. Cook, Anthony M.; Grief, Richard K.; and Aoyagi, Kiyoshi: Large-Scale Wind-Tunnel Investigation of the Low-Speed Aerodynamic Characteristics of a Supersonic Transport Model Having Variable-Sweep Wings. NASA TN D-2824, May 1965.

188. Cook, Anthony M.: Wind-Tunnel Investigation of the Low-Speed High-Lift Aerodynamics of a One-Fifth Scale Variable-Sweep Supersonic Transport. NASA TN D-4844, Oct. 1968.

189. Cook, Anthony M. and Jones, Dale G.: Large-Scale Wind-Tunnel Investigation to Improve the Low-Speed Longitudinal Stability at High Lift of a Supersonic Transport with Variable-Sweep Wings. NASA TN D-5005, Jan. 1969.

190. Corsiglia, Victor R.; Koenig, David G.; and Morelli, Joseph P.: Large-Scale Tests of an Airplane Model with a Double-Delta Wing, Including Longitudinal and Lateral Characteristics and Ground Effects. NASA TN D-5102, March 1969.

191. Rolls, L. Stewart; Koenig, David G.; and Drinkwater, Fred J. III: Flight Investigation of the Aerodynamic Properties of an Ogee Wing. NASA TN D-3071, Dec. 1965.

192. Rolls, L. Stewart and Koenig, David G.: Flight-Measured Ground Effects on a Low-Aspect-Ratio Ogee Wing Including a Comparison with Wind-Tunnel Results. NASA TN D-3431, June 1966.

193. Chambers, Joseph: Modeling Flight: The Role of Dynamically Scaled Free-Flight Models in Support of NASA's Aerospace Programs. NASA SP 2009-575, 2009.

194. Feistel, T. W. and Anderson, S. B.: A Method for Localizing Wing Flow Separation at Stall to Alleviate Spin Entry Tendencies. AIAA 78-1476, AIAA Aircraft Systems and Technology Conference, Los Angeles, CA, Aug. 21-23, 1978.

195. Corsiglia, V. R.; Katz, J.; and Kroeger, R. A.: Full-Scale Wind-Tunnel Study of the Effect of Nacelle Shape on Cooling Drag. *Journal of Aircraft*, vol. 18, no 2, Feb. 1981, pp. 82-88. Also AIAA 79-1820.

196. Katz, J.; Corsiglia, V. R.; and Barlow, P. R.: Study of Cooling Air Inlet and Exit Geometries of Horizontally Opposed Piston Aircraft Engines. AIAA/SAE/ASME 16th Joint Propulsion Conference, Hartford, CT, June 1980. Also AIAA-80-1242.

197. Katz, J.; Corsiglia, V. R.; and Barlow, P.: Effect of Propeller on the Drag and Performance of the Cooling System in a General Aviation Twin-Engine Aircraft. AIAA-80-1872, *Journal of Aircraft,* vol. 19, no. 3, March 1982.

198. Corsiglia, V. R. and Katz, J.: Full-Scale Study of the Cooling System Aerodynamics of an Operating Piston Engine Installed in a Light Aircraft Wing Panel. Paper No. 810623, SAE Business Aircraft Meeting, Wichita, KS, April 1981.

199. Ross, J. C.; Vogel, J. M.; and Corsiglia, V. R.: Full-Scale Wind-Tunnel Study of Wing-Fuselage Interaction and Comparison with Paneling Method. AIAA-81-1666, AIAA Aircraft Systems and Technology Conference, Dayton, OH, Aug. 11-13, 1981.

200. Warmbrodt, William; Smith, Charles A.; and Johnson, Wayne: Rotorcraft Research Testing in the National Full-Scale Aerodynamics Complex

at NASA Ames Research Center. NASA TM 86687, May 1985.

201. Harris, Franklin D.: Introduction to Autogyros, Helicopters, and Other V/STOL Aircraft. NASA/SP-2012-215959, Vol. II, Oct. 2012.

202. Johnson, Wayne: Helicopter Theory. Dover Publications, Inc. 1994. Originally published by Princeton University Press, 1980.

203. Koenig, David G.; Grief, Richard K.; and Kelly, Mark W.: Full-Scale Wind-Tunnel Investigation of the Longitudinal Characteristics of a Tilting-Rotor Convertiplane. NASA TN D-35, 1959.

204. Quigley, Hervey C. and Koenig, David G.: A Flight Study of the Dynamic Stability of a Tilting-Rotor Convertiplane. NASA TN D-778, April 1961.

205. Weiberg, James A. and Maisel, Martin D.: Wind-Tunnel Tests of the XV-15 Tilt Rotor Aircraft. NASA TM 81177, April 1980.

206. Maisel, Martin D.; Giulianetti, Demo J.; and Dugan, Daniel C.: The History of the XV-15 Tilt Rotor Research Aircraft: From Concept to Flight. NASA History Series, SP-2000-4517, 2000.

207. Johnson, Wayne: Milestones in Rotorcraft Aeromechanics. NASA/TP-2011-215971, May 2011.

208. McCloud, John L. III; Evans, William T.; and Biggers, James C.: Performance Characteristics of a Jet-Flap Rotor. NASA Conference on V/STOL and STOL Aircraft, NASA SP-116, paper no. 3, April 4-5, 1966.

209. Watts, George A. and Biggers, James C.: Horizontal Stoppable Rotor Conversion. Presented at the 27th Annual National V/STOL Forum of the AHS, Washington, DC, May 1971.

210. McCloud, J. L. III; Biggers, J. C.; and Stroub, R. H.: An Investigation of Full-Scale Helicopter Rotors at High Advance Ratios and Advancing Tip Mach Numbers. NASA TN D-4632, July 1968.

211. La Forge, S. V. and Rohtert, R. E.: Aerodynamic Tests of an Operational OH-6A Helicopter in the Ames 40 ft x 80 ft Wind Tunnel. 369-A-8020, Hughes Tool Co., Aircraft Division, May 1970.

212. Stroub, Robert H.; Falarski, Michael D.; McCloud, John L.; and Soderman, Paul T.: An Investigation of a Full-Scale Advancing Blade Concept Rotor System at High Advance Ratio. NASA TM X-62,081, Aug. 1971.

213. Felker, Fort F. III: Performance and Loads Data From a Wind Tunnel Test of a Full-Scale, Coaxial, Hingeless Rotor Helicopter. NASA TM X-81329, Oct. 1981.

214. Peterson, Randall L. and Mosher, Marianne: Acoustic Measurements of a Full-Scale, Coaxial, Hingeless Rotor Helicopter. NASA TM 84349, July 1983.

215. Ballard, John D.; McCloud, John L. III; and Forsyth, T. J.: An Investigation of a Stoppable Helicopter Rotor with Circulation Control. NASA TM 81218, Aug. 1980.

216. Warmbrodt, William and McCloud, John L. III: A Full-Scale Wind Tunnel Investigation of a Helicopter Bearingless Main Rotor. NASA TM 82321, Aug. 1981.

217. Jepson, D.; Moffitt, R.; Hilzinger, K.; and Bissell, J.: Analysis and Correlation of Test Data From an Advanced Technology Rotor System. NASA CR 3714, Aug. 1983.

218. Mosher, Marianne: Acoustic Measurements of a Full-Scale Rotor with Four Tip Shapes. Vol. 1: Text, Appendix A, and Appendix B. NASA TM 85878, April 1984.

219. Kelly, Mark W.: Large-Scale Wind-Tunnel Studies of Several VTOL Types. NASA Conference on V/STOL Aircraft, paper no. 3, Langley Research Center, Langley Field, VA, Nov. 17-18, 1960.

220. Cook, Woodrow L. and Hickey, David: Comparison of Wind Tunnel and Flight Test Aerodynamic Data in the Transition Flight Speed Range for Five V/STOL Aircraft. NASA SP 116, paper 26, 1966.

221. Koenig, David G.: V/STOL Wind-Tunnel Testing. NASA TM 85936, May 1984.

222. Hickey, David H. and Kirk, Jerry V.: Survey of Lift-Fan Aerodynamic Technology. NASA Contractor Report 177615, Sept. 1993.

223. Deckert, Wallace H.: The Lift-Fan Powered-Lift Aircraft Concept: Lessons Learned. NASA Contractor Report 177616, 1993.

224. Cook, Woodrow L.: Summary of Lift and Lift/Cruise Fan Powered Lift Concept Technology. NASA Contractor Report 177619, Aug. 1993.

225. Greif, Richard K. and Tolhurst, William H., Jr.: Large-Scale Wind-Tunnel Tests of a Circular Plan-Form Aircraft with a Peripheral Jet for Lift, Thrust, and Control. NASA TN D-1432, Feb. 1963.

226. Greif, Richard K.; Kelly, Mark W.; and Tolhurst, William H., Jr.: Wind-Tunnel Tests of a Circular Wing with an Annular Nozzle in Proximity to the Ground. NASA TN D-317, May 1960.

227. Aoyagi, K.; Hickey, D.; and deSavigny, R.: Aerodynamic Characteristics of a Large-Scale Model with a High Disc-Loading Lifting Fan Mounted in the Fuselage. NASA TN D-775, Oct. 1961.

228. Maki, Ralph L. and Hickey, David H: Aerodynamics of a Fan-In-Fuselage Model. NASA TN D-789, May 1961.

229. Hickey, D. and Hall L.: Aerodynamic Characteristics of a Large-Scale Model of Two High Disc-Loading Fans Mounted in the Wing. NASA TN D-1650, Feb. 1963.

230. Kirk, Jerry V.; Hickey, David H.; and Hall, Leo P.: Aerodynamic Characteristics of a Full-Scale Fan-in-Wing Model Including Results in Ground Effects with Nose-Fan Pitch Control. NASA TN D-2358, 1964.

231. Cook, Woodrow L. and Hickey, David H.: Comparison of Wind-Tunnel and Flight-Test Aerodynamic Data in the Transition-Flight Speed Range for Five V/STOL Aircraft. NASA SP-116, paper 26, April 4-5, 1966.

232. Hall, Leo P.; Hickey, D. H.; and Kirk, Jerry V.: Aerodynamic Characteristics of a Large-Scale V/STOL Transport Model with Lift and Lift/Cruise Fans. NASA TN D-4092, 1967.

233. Kirk, Jerry V.; Hodder, Brent V.; and Hall, Leo P.: Large-Scale Wind Tunnel Investigation of V/STOL Transport Model with Wing-Mounted Lift Fans and Fuselage-Mounted Lift-Cruise Engines for Propulsion. NASA TN D-4233, 1967.

234. Atencio, Adolph, Jr.; Hall, Leo P.; and Kirk, Jerry V.: Low-Speed Wind Tunnel Investigation of a Large-Scale Lift Fan STOL Transport Model. NASA TM X 62,231, 1973.

235. Hodder, Brent K.; Kirk, Jerry V.; and Hall, Leo P.: Aerodynamic Characteristics of a Large-Scale Model with a Lift Fan Mounted in a 5-Percent-Thick Triangular Wing, Including the Effects of BLC on the Lift-Fan Inlet. NASA TN D-7031, 1970.

236. Kirk, Jerry V. and Barrack, Jerry P.: Reingestion Characteristics and Inlet-Flow Distortion of a V/STOL Lift Engine Fighter Configuration. NASA TN D-7014, Dec. 1970.

237. Falarski, Michael: Wind-Tunnel Investigation of Highly Maneuverable Supersonic V/STOL Fighter. NASA TM 78599, June 1979.

238. Martin, Joseph C.: A Case for VATOL Flight Demonstration. David W. Taylor NAVAL Ship Research Aero Report 1264, V/STOL Aircraft Aerodynamics Meeting, Naval Postgraduate School, Monterey, CA, May 16-18, 1979.

239. Borst, Henry V.: The Aerodynamics of the Unconventional Air Vehicles of A. Lippisch. Henry V. Borst & Associates, 203 W. Lancaster Avenue, Wayne, PA, 19087, 1980.

240. Koenig, David G. and Brady, James A.: Large-Scale Wind-Tunnel Tests of a Wingless Vertical Take-Off and Landing Aircraft–Preliminary Results. NASA TN D-326, Oct. 1960.

241. Yaggy, Paul F. and Mort, Kenneth W.: A Wind-Tunnel Investigation of a 4-Foot-Diameter Ducted Fan Mounted on the Tip of a Semispan Wing. NASA TN D-776, March 1961.

242. Yaggy, Paul F. and Goodson, Kenneth W.: Aerodynamics of a Tilting Ducted Fan Configuration. NASA TN D-785, March 1961.

243. Mort, Kenneth W. and Yaggy, Paul F.: Aerodynamic Characteristics of a 4-Foot-Diameter Ducted Fan Mounted on the Tip of a Semispan Wing. NASA TN D-1301, April 1962.

244. Mort, Kenneth W. and Yaggy, Paul F.: The Effectiveness of Three Exit Vane Cascade Configurations for Vectoring the Thrust of a Ducted Fan. NASA TN D-1688, Oct. 1964.

245. Mort, Kenneth W.: Performance Characteristics of a 4-Foot-Diameter Ducted Fan at Zero Angle of Attack for Several Fan Blade Angles. NASA TN D-3122, Dec. 1965.

246. Falarski, Michael D. and Mort, Kenneth W.: Large-Scale Wind-Tunnel Investigation of a Ducted-Fan-Deflected-Slipstream Model with an Auxiliary Wing. NASA TN D-6323, April 1971.

247. Giulianetti, Demo J.; Biggers, James C.; and Maki, Ralph L.: Longitudinal and Lateral-Directional Aerodynamic Characteristics of a Large-Scale, V/STOL Model with Four Tilting

Ducted Fans Arranged in a Dual Tandem Configuration. NASA TN D-3490, June 1966.

248. Giulianetti, Demo J.; Biggers, James C.; and Maki, Ralph L: Longitudinal Aerodynamic Characteristics in Ground Effect of a Large-Scale, V/STOL Model with Four Tilting Ducted Fans Arranged in a Dual Tandem Configuration. NASA TN D-4218, Oct. 1967.

249. Mort, Kenneth W. and Gamse, Berl: A Wind-Tunnel Investigation of a 7-Foot-Diameter Ducted Propeller. NASA TN D-4142. Aug. 1967.

250. Giulianetti, Demo J.; Biggers, James C.; and Corsiglia, Victor R.: Wind-Tunnel Test of a Full-Scale, 1.1 Pressure Ratio, Ducted Lift-Cruise Fan. NASA TN D-2498, Nov. 1964.

251. Mort, Kenneth W.: Summary of Large-Scale Tests of Ducted Fans. NASA Conference on V/STOL and STOL Aircraft, SP-116, paper no. 8, April 4-5, 1966.

252. Full-Scale Tests of Grumman Design 698-111 Tilt-Nacelle V/STOL Model at NASA Ames, Grumman Aerospace Corporation Report for NAVAL Air Systems Command, N00019-80-C-0116.

253. James, Harry A.; Wingrove, Rodney C.; Holzhauser, Curt A.; and Drinkwater, Fred J. III: Wind-Tunnel and Piloted flight Simulator Investigation of a Deflected-Slipstream VTOL Airplane, the Ryan VZ-3RY. NASA TN D-89, Nov. 1959.

254. Page, V. Robert; Dickinson, Stanley O.; and Deckert, Wallace H.: Large-Scale Wind-Tunnel Tests of a Deflected Slipstream STOL Model with Wings of Various Aspect Ratios. NASA TN D-4448, March 1968.

255. Page, V. Robert and Aiken, Thomas N.: Stability and Control Characteristics of a Large-Scale Deflected Slipstream STOL Model with a Wing of 5.7 Aspect Ratio. NASA TN D-6393, Oct. 1971.

256. Page, V. Robert and Aiken, Thomas N.: Large-Scale Wind-Tunnel Tests of Propeller-Driven Deflected Slipstream STOL Model in Ground Effect. NASA TM X-2313, Oct. 1971.

257. Weiberg, James A. and Holzhauser, Curt A.: Large-Scale Wind-Tunnel Tests of an Airplane Model with an Unswept, Tilt Wing of Aspect Ratio 5.5, and with Four propellers and Blowing Flaps. NASA TN D-1034, June 1961.

258. Weiberg, James A. and Giulianetti, Demo J.: Large-Scale Wind-Tunnel Tests of an Airplane Model with an Unswept Tilt Wing of Aspect Ratio 5.5 and with Various Stall Control Devices. NASA TN D-2133, Feb. 1964.

259. Deckert, Wallace H.; Page, V. Robert; and Dickinson, Stanley O.: Large-Scale Wind-Tunnel Tests of Descent Performance of an Airplane Model with a Tilt Wing and Differential Propeller Thrust. NASA TN D-1857, Oct. 1964.

260. Dickinson, Stanley O.; Page, V. Robert; and Deckert, Wallace H.: Large-Scale Wind-Tunnel Investigation of an Airplane Model with a Tilt Wing of Aspect Ratio 8.4, and Four Propellers, in the Presence of a Ground Plane. NASA TN D-4493, April 1968.

261. Yaggy, Paul F. and Rogallo, Vernon L.: A Wind-Tunnel Investigation of Three Propellers Through an Angle-of-Attack Range From 0° to 85°. NASA TN D-318, May 1960.

262. Yaggy, Paul F. and Mort, Kenneth W.: Wind-Tunnel Tests of Two VTOL Propellers in Descent. NASA TN D-1766, March 1963.

263. Mort, Kenneth W. and Yaggy, Paul F.: Aerodynamic Characteristics of a Full-Scale Propeller Tested with both Rigid and Flapping Blades and with Cyclic Pitch Control. NASA TN D-1774, May 1963.

264. Fluk, Harold, et al.: The X-19 V/STOL Technology—A Critical Review. AFFDL-TR-66-195, Curtiss-Wright Corporation, May 1967.

265. Deckert, Wallace H.; Koenig, David G.; and Weiberg, James A.: A Summary of Recent Large-Scale Research on High-Lift Devices. NASA SP-116, paper no. 6, Conference on V/STOL and STOL Aircraft, Ames Research Center, Moffett Field, CA, April 4-5, 1966.

266. Weiberg, James A. and Gamse, Berl: Large-Scale Wind-Tunnel Tests of an Airplane Model with Two Propellers and Rotating Cylinder Flaps. NASA TN D-4489, March 1968.

267. Kirk, Jerry V. and Hickey, David H.: Full-Scale Wind-Tunnel Investigation of a VTOL Aircraft with a Jet-Ejector System for Lift Augmentation. NASA TN D-3725, Nov. 1966.

268. Aiken, T. A.; Aoyagi, K.; and Falarski, M. D.: Aerodynamic Characteristics of a Large-Scale Model with a Swept-Wing and a Jet Flap Having

an Expandable Duct. NASA TM-X-62,281, Sept. 1973.

269. Falarski, M. D.; Aiken, T. N.; and Aoyagi, K.: Acoustic Characteristics of a Large-Scale Wind Tunnel Model of a Jet Flap Aircraft. NASA TM-X-3263, July 1975.

270. Laub, Georgene H.: Low Speed Wind Tunnel Tests on a One-Seventh Scale Model of the H.126 Jet Flap Aircraft. NASA TM X-62,433, 1975.

271. Aiken, Thomas N. and Cook, Anthony: Results of Full-Scale Wind Tunnel Tests on the H.126 Jet Flap Aircraft. NASA TN-D7252, April 1973.

272. Kimberlin, Ralph D.: A Flight Test Evaluation of the Ball-Bartoe Jetwing Propulsive Lift Concept. University of Tennessee Space Institute report 81-1, July 1, 1981.

273. Kirk, Jerry V.; Hickey, David H.; and Aoyagi, Kiyoshi: Large-Scale Wind-Tunnel Investigation of a Model with an External Jet-Augmented Flap. NASA TN D-4278, Dec. 1967.

274. Aoyagi, K.; Falarski, M. D.; and Koenig, D. G.: Wind-Tunnel Investigation of a Large-Scale Upper Surface Blown-Flap Transport Model Having Two Engines. NASA TM X-62,296, Aug. 1973.

275. Falarski, M. D.; Aoyagi, K.; and Koenig, D. G.: Acoustic Characteristics of a Large-Scale Wind-Tunnel Model of an Upper-Surface Blown Flap Transport Having Two Engines. NASA TM X-62,319, Sept. 1973.

276. Aoyagi, K.; Falarski, M. D.; and Koenig, D. G.: Wind Tunnel Investigation of a Large-Scale Upper Surface Blown-Flap Model Having Four Engines. NASA TM X-62,419, July 1975.

277. Reed, R. Dale and Lister, Darlene: Wingless Flight, The Lifting Body Story. The NASA History Series, NASA SP-4220, 1997.

278. Thompson, Milton O. and Peebles, Curtis: Flying Without Wings, NASA Lifting Bodies and the Birth of the Space Shuttle. Smithsonian Institution Press, 1999.

279. Thompson, Milton O. and Hunley, J. D.: Flight Research: Problems Encountered and What They Should Teach Us. NASA SP-2000-4522, 2000.

280. Hoey, Robert G.: Testing Lifting Bodies at Edwards. A PAT Projects, Inc. Publication, Sept. 1994.

281. Mort, Kenneth W. and Gamse, Berl: Full-Scale Wind-Tunnel Investigation of the Longitudinal Aerodynamic Characteristics of the M2-F1 Lifting Body Flight Vehicle. NASA TN D-3330, March 1966.

282. Mort, Kenneth W. and Gamse, Berl: Low-Speed Wind-Tunnel Tests of a Full-Scale M2-F2 Lifting Body Model. NASA TM X-1347, Feb. 1967.

283. Mort, Kenneth W. and Gamse, Berl: Full-Scale Wind-Tunnel Investigation of the Aerodynamic Characteristics of the M2-F2 Lifting Body Flight Vehicle. NASA TM X-1588, 1968.

284. Gamse, Berl and Mort, Kenneth W.: Full-Scale Wind-Tunnel Investigation of the HL-10 Manned Lifting Body Flight Vehicle. NASA TM X-1476, Dec. 1967.

285. Pyle, Jon S.: Lift and Drag Characteristics of the HL-10 Lifting Body During Subsonic Gliding Flight. NASA TN D-6263, March 1971.

286. Mort, Kenneth W. and Falarski, Michael D.: Full-Scale Wind-Tunnel Investigation of the Aerodynamic Characteristics of the X-24A Lifting Body Aircraft. NASA TN D-5932, Aug. 1970.

287. Mort, Kenneth W. and Falarski, Michael D.: Large-Scale Wind-Tunnel Investigation of an M1-L Lifting Body with an Inflatable and a Rigid Afterbody. NASA TN D-5468, Oct. 1969.

288. Gamse, Berl and Yaggy, Paul F.: Wind Tunnel Tests of a Series of 18-Foot-Diameter Parachutes with Extendable Flaps. NASA TN D-1334, Aug. 1962.

289. Weiberg, James A. and Mort, Kenneth W.: Wind-Tunnel Tests of a Series of Parachutes Designed for Controllable Gliding Flight. NASA TN D-3960, May 1967.

290. Falarski, Michael D. and Mort, Kenneth W.: Wind-Tunnel Investigation of Several Large-Scale All-Flexible Parawings. NASA TN D-5708, March 1970.

291. Gamse, Berl; Mort, Kenneth W.; and Yaggy, Paul F.: Low-Speed Wind-Tunnel Tests of a Large-Scale Inflatable Structure Paraglider. NASA TN D-2859, June 1965.

292. Hickey, David H.; Soderman, Paul T.; and Kelly, Mark W.: Noise Measurements in Wind Tunnels. Proceedings of the NASA Conference

on Basic Aerodynamic Noise Research. NASA SP-207, July 14-15, 1969, pp. 399-408.

293. Falarski, M. D.; Koenig, D. G.; and Soderman, P. T.: Aspects of Investigating STOL Noise Using Large-Scale Wind-Tunnel Models. *Canadian Aeronautics and Space Journal*, vol. 19, no. 2, Feb. 1973 (also NASA TMX-62164).

294. Soderman, Paul T. and Noble, Stephen C.: A Four-Element End-Fire Microphone Array for Acoustic Measurements in Wind Tunnels. NASA TM X-62331, Jan. 1974.

295. Soderman, Paul T. and Noble, Stephen C.: Directional Microphone Array for Acoustic Studies of Wind Tunnel Models. *Journal of Aircraft*, vol. 12, no. 3, March 1975, pp. 168-173.

296. Mosher, M: Phased Arrays for Aeroacoustic Testing: Theoretical Development. AIAA paper 96-1713, 2nd Aeroacoustic Conference, State College, PA, May 1996.

297. Soderman, P. T. and Allen, C. S.: Microphone Measurements In and Out of Airstream. Aeroacoustic Measurements, Ch 1, Thomas J. Mueller, ed., Springer-Veriag, Berlin, 2002.

298. Atencio, A., Jr. and Soderman, P. T.: Comparison of Wind Tunnel and Flyover Noise Measurement of the YOV-10A STOL Aircraft. NASA TM X-62166, June 1972.

299. Atencio, A., Jr.; Kirk, J. V.; Soderman, P. T.; and Hall, L. P.: Comparison of Flight and Wind Tunnel Measurements of Jet Noise for the XV-5B Aircraft. NASA TM X-62182, Oct. 1972.

300. Falarski, Michael; Aoyagi, Kiyoshi; and Koenig, David G.: Acoustic Characteristics of Large-Scale STOL Models at Forward Speed. NASA TM X-62,251, 1972.

301. Falarski, Michael D.: Acoustic Characteristics of a Semispan Wing Equipped with an Externally Blown Jet Flap Including Results at Forward Speed. NASA TM X- 2749, March 1973.

302. Falarski, M. D.: Large-Scale Wind-Tunnel Investigation of the Noise Characteristics of a Semispan Wing Equipped with an Externally Blown Jet Flap. NASA TM X-62154, May 1972.

303. Falarski, Michael D.; Aiken, Thomas N.; and Aoyagi, Kiyoshi: Acoustic Characteristics of a Large-Scale Model of a Jet Flap Aircraft. NASA TM X-3263, July 1975.

304. Falarski, M. D., and Koenig, D. G.: Acoustic Characteristics of a Large-Scale Augmentor Wing Model at Forward Speed. NASA TM X-2940, Nov. 1973.

305. Edenborough, H. Kipling: Research at NASA's NFAC Wind Tunnels. NASA TM 102827, June 1990.

306. U.S. Air Force: National Full-Scale Aerodynamics Complex, AFD-070426-024.

307. Betzina, Mark D.: Rotor Performance of an Isolated Full-Scale XV-15 Tiltrotor in Helicopter Mode. AHS Technical Specialists' Meeting, San Francisco, CA, Jan. 23-25, 2002.

308. Kitaplioglu, C.: Blade-Vortex Interaction Noise of a Full-Scale XV-15 Rotor Tested in the NASA Ames 80- by 120-Foot Wind Tunnel. NASA TM 1999-208789, July 1999.

309. Kitaplioglu, C.; Betzina, M.; and Johnson, W.: Blade-Vortex Interaction Noise of an Isolated Full-Scale XV-15 Tilt-Rotor. AHS 56th Annual Forum, Virginia Beach, VA, May 2-4, 2000.

310. Nguyen, Khanh; Betzina, Mark; and Kitaplioglu, Cahit: Full-Scale Demonstration of Higher Harmonic Control for Noise and Vibration Reduction on the XV-15 Rotor. AHS 56th Annual Forum, Virginia Beach, VA, May 2-4, 2000.

311. Felker, Fort F.; Shinoda, Patrick R.; Heffernan, Ruth M.; and Sheehy, Hugh F.: Wing Force and Surface Pressure Data From a Hover Test of a 0.658-Scale V-22 Rotor and Wing. NASA TM 102244, Feb. 1990.

312. Felker, Fort F.: Results From a Test of a 2/3-Scale V-22 Rotor and Wing in the 40- by 80-Foot Wind Tunnel. AHS 47th Annual Forum Phoenix, AZ, May 6-8, 1991.

313. Acree, C. W., Jr.: JVX Proprotor Performance Calculation and Comparisons with Hover and Airplane-Mode Test Data. NASA/TM-2009-215380, April 2009.

314. Whittle, Richard: The Dream Machine, the Untold History of the Notorious V-22 Osprey. Simon and Schuster, NY, April 2010.

315. Young, Larry A.: TiltRotor Aeroacoustic Model (TRAM): A New Rotorcraft Research Facility. AHS International Meeting on Advanced Rotorcraft Technology and Disaster Relief, Gifu, Japan, April 21-23, 1998.

316. McCluer, Megan S. and Johnson, Jeffrey L.: Full-Span Tiltrotor Aeroacoustic Model (FS TRAM) Overview and Initial Testing. AHS International Aerodynamics, Acoustics, and Test and Evaluation Specialists' Conference, San Francisco, CA, Jan. 23-25, 2002.

317. Young, L. A.; Lillie, D.; McCluer, M.; Yamauchi, G. K.; and Derby, M. R.: Insights Into Airframe Aerodynamics and Rotor-on-Wing Interactions From a 0.25-Scale Tiltrotor Wind Tunnel Model. AHS International Aerodynamics, Acoustics, and Test and Evaluation Specialists' Conference, San Francisco, CA, Jan. 23-25, 2002.

318. Nguyen, Khanh; McNulty, Michael; and Lauzon, Dan: Aeroelastic Stability of the McDonnell Douglas Advanced Bearingless Rotor. AHS 49th Annual Forum, St. Louis, MO, May 19-21, 1993.

319. Wang, James M.; Duh, James; Fuh, Jon-Shen; and Kottapalli, Sesi: Stability of the Sikorsky S-76 Bearingless Main Rotor. NASA TM 112345, 1993.

320. Peterson, Randall L.: Full-Scale Hingeless Rotor Performance and Loads. NASA TM 110356, June 1995.

321. Shinoda, Patrick M. and Johnson, Wayne: Performance Results From a Test of an S-76 Rotor in the NASA Ames 80- by 120-Foot Wind Tunnel. AIAA-93-3414-CP, 1993.

322. Shinoda, Patrick M.: Full- Scale S-76 Rotor Performance and Loads at Low Speeds in the NASA Ames 80- by 120-Foot Wind Tunnel. NASA TM 1110379, April 1996.

323. Swanson, Alexandra A.: Application of the Shadowgraph Flow Visualization Technique to a Full-Scale Helicopter Rotor in Hover and Forward Flight. AIAA-93-3411, Aug. 9-11, 1993.

324. Jacklin, Stephen A.; Nguyen, Khanh Q.; Blaas, Achim; and Richter, Peter: Full-Scale Wind Tunnel Test of a Helicopter Individual Blade Control System. AHS 50th Annual Forum, May 11-13, 1994.

325. Jacklin, Stephen A.; Blaas, Achim; Swanson, Stephen M.; and Teves, Dietrich.: Second Test of a Helicopter Individual Blade Control System in the NASA Ames 40- by 80-Foot Wind Tunnel. AHS 2nd International Aeromechanics Specialists' Conference, Oct. 11-13, 1995.

326. Haber, Axel; Jacklin, Stephen A.; and deSimone, Gary: Development, Manufacturing, and Component Testing of an Individual Blade Control System for a UH-60 Helicopter Rotor. AHS Aerodynamics, Acoustics, and Test and Evaluation Technical Specialists' Meeting, San Francisco, CA, Jan. 23-25, 2002.

327. Jacklin, Stephen A.; Haber, Axel; deSimone, Gary; Norman, Thomas R.; Kitaplioglu, Cahut; and Shinoda, Patrick: Full-Scale Wind Tunnel Test of an Individual Blade Control System for a UH-60 Helicopter. AHS 58th Annual Forum, June 11-13, 2002.

328. Norman, Thomas R.; Theodore, Colin; Shinoda, Patrick; Fuerst, Daniel; Arnold, Uwe T. P.; Makinen, Stephen; Lorber, Peter; and O'Neill, John: Full-Scale Wind Tunnel Test of a UH-60 Individual Blade Control System for Performance Improvement and Vibration, Loads, and Noise Control. AHS 65th Annual Forum, May 27-29, 2009.

329. Yeo, Hyeonsoo; Romander, Ethan A.; and Norman, Thomas R.: Investigation of Rotor Performance and Loads of a UH-60A Individual Blade Control System. AHS 66th Annual Forum, May 11-13, 2010.

330. Norman, T. R.; Shinoda, P.; Peterson, R. L.; and Datta, A.: Full-Scale Wind Tunnel Test of the UH-60A Airloads Rotor. AHS 67th Annual Forum, Virginia Beach, VA, May 2011.

331. Straub, Friedrich K.; Anand, Vaidyanathan R.; Birchette, Terrence S.; and Lau, Benton H.: SMART Rotor Development and Wind Tunnel Test. Presented at 45th European Rotorcraft Forum, Hamburg, Germany, Sept. 22-25, 2009.

332. Lau, Benton H.; Obriecht, Nicole; Gasow, Tanner; Hagerty, Brandon; and Cheng, Kelly C.: Boeing-SMART Rotor Wind Tunnel Test Data Report for DARPA Helicopter Quieting Program (HQP) Phase 1 B. NASA/TM-2010-216404, Sept. 2010.

333. Johnson, Wayne: Rotorcraft Aeromechanics. Cambridge University Press, 2013.

334. Jameson, Kristina; Marshall, David; Ehrmann, Robert; Paciano, Eric; Englar, Robert J.; and Horne, William C.: Part 2: Preparation for Wind Tunnel Model Testing and Verification of Cal Poly's AMELIA 10 Foot Span Hybrid Wing-Body Low Noise CESTOL Aircraft. AIAA 2011-1307, 2011.

335. Burnside, Nathan J. and Horne, William C.: Acoustic Surveys of a Scaled-Model CESTOL Transport Aircraft in Static and Forward Speed Conditions. AIAA 2012-2231, 2012.

336. Zeune, Cale H.: An Overview of the Air Forces' Speed Agile Concept Demonstration Program. AIAA 2013-1097, 2013.

337. Shweyk, Kamal M. and Hyde, David C.: Overview of the Aerodynamic Model and Flight Control System of a Speed Agile Concept Demonstrator. AIAA 2013-1101, 2013.

338. Smith, Brian E.; Garland, Doug; and Poppen, William A.: Aerodynamic Performance of a Full-Scale Lifting Ejector System in a STOVL Fighter Aircraft. AIAA 92-3094, 1992.

339. Maddock, Ian A.: From JAST to JSF: The Evolution of the Joint Strike Fighter. Analytic Services, Inc. (ANSER), copyright 2012, AHS International.

340. Wardwell, Douglas A.; Naumowicz, Tim; Hange, Craig E.; Arledge, Thomas K.; and Margason, Richard J.: Test Techniques for STOVL Large-Scale Powered Models. SAE paper 962251, 1996 International Powered Lift Conference, Jupiter, FL, Nov. 18-20, 1996.

341. Naumowicz, T.; Wardwell, D. A.; Hange, C. E.; Margason, R.; and Arledge, T. K.: Transition Performance of a Joint Strike Fighter Configuration. SAE 96-2252, International Powered Lift Conference, Nov. 1996.

342. Sweetman, Bill: Ultimate Fighter: Lockheed Martin F-35 Joint Strike Fighter. Zenith Press, MBI Publishing Co., 2004.

343. Meyn, Larry A.; Lanser, Wendy R.; and James, Kevin D.: Full-Scale High Angle-of-Attack Tests of an F/A-18. AIAA paper 92-2676, 10th Applied Aerodynamics Conference, Palo Alto, CA, June 22-24, 1992.

344. Lanser, Wendy R.; Botha, Gavin J.; James, Kevin D.; and Crowder, James P.: Wind Tunnel Visualization of the Flow Over a Full-Scale F/A-18, SAE 20010046989, April 1994.

345. James, Kevin D. and Meyn, Larry A.: Analysis of F/A-18 Tail Buffet Data Acquired in the 80- by 120-Foot Wind Tunnel, SAE 20010051288, Jan. 1994.

346. Langan, Kevin J. and Samuels, Jeffrey, Jr.: Wing Jet Blowing on the Subsonic High Alpha Research Concept Fighter Configuration. *Journal of Aircraft*, vol. 36, no. 2, March-April 1999, pp. 413-420 (also AIAA 97-0039).

347. Rossow, V. J.; Sacco, J. N.; Askins, P. A.; Bisbee, L. S.; and Smith, S. M.: Wind-Tunnel Measurements of Hazard Posed by Lift-Generated Wakes, *Journal of Aircraft*, vol. 32, no. 2, March-April, 1995.

348. Rossow, V. J.; Fong, R. K.; Wright, M. S.; and Bisbee, L. S.: Vortex Wakes of Two Transports Measured in 80- by 120-Foot Wind Tunnel. *AIAA Journal of Aircraft*, vol. 33, no. 2, March-April 1996, pp. 399-406.

349. Rossow, V. J. and James, K. D.: Overview of Wake-Vortex Hazards During Cruise, *Journal of Aircraft*, vol. 37, no. 6, Nov.-Dec. 2000.

350. Rossow, Vernon J.: Lift-Generated Vortex Wakes of Subsonic Transport Aircraft, *Progress in Aerospace Sciences*, vol. 35, no. 6, Aug. 1999, pp. 507-660.

351. Rossow, Vernon J. and Meyn, Larry A.: Guidelines for Avoiding Vortex Wakes During Use of Closely Spaced Parallel Runways. NASA TM-2012-215985, Jan. 2012.

352. Storms, Bruce L. and Ross, James C.: Experimental Study of Lift-Enhancing Tabs on a Two-Element Airfoil. *Journal of Aircraft*, vol. 32, no. 5, Sept.-Oct. 1995.

353. Cherne, J.; Culick, F. E. C.; and Zell, P.: The AIAA 1903 Wright Flyer Project Prior to Full-Scale Tests at NASA Ames Research Center, AIAA paper 2000-0511, 38th AIAA Aerospace Sciences Meeting, Reno, NV, Jan 10-13, 2000.

354. Jex, H. R.; Grimm, R.; Latz, J.; and Hange, C.: Full-Scale 1903 Wright Flyer Wind Tunnel Test Results From the NASA Ames Research Center. AIAA paper 2000-0512, 38th AIAA Aerospace Sciences Meeting, Reno, NV, Jan 10-13, 2000.

355. Kochersberger, K; Crabill, N.; Player, J.; Britcher, C.; Dominguez, K.; and Hyde, K.: Flying Qualities of the Wright 1903 Flyer: From Simulation to Flight Test. AIAA-2004-0105, 42nd AIAA Aerospace Sciences Meeting and Exhibit, Reno, NV, Jan. 5-8, 2004.

356. Culick, Fred E. C.: What the Wright Brothers Did and Did Not Understand About Flight Mechanics—In Modern Terms. AIAA-2001-3385, 37th AIAA/ASME/SAE/ASEE Joint Propulsion Conference and Exhibit, Salt Lake City, UT, July 8-11, 2001.

357. McFarland, Marvin W., (Ed.): The Papers of Wilbur and Orville Wright, McGraw-Hill, 2001, originally published in 1953.

358. McCullough, David: The Wright Brothers, Simon and Schuster, 2015.

359. Harwood, Craig S. and Fogel, Gary B.: Quest for Flight, John J. Montgomery and the Dawn of Aviation in the West. University of Oklahoma Press: Norman, OK, 2012.

360. Lye, J. D.; Buchholz, S.; and Nickison, D.: Testing of a Dash 8 Q400 in the NASA Ames 80X120' Wind Tunnel. ICAS 2002 Congress.

361. Myerson, Robert E.: Space Shuttle Orbiter Drag Parachute Design. AIAA 2001-2051, 16th AIAA Aerodynamic Decelerator Systems Technology Conference, Boston, MA, May 21-24, 2001.

362. Cruz, J. R.; Kandis, M; and Witkowski, A.: Opening Loads Analyses for Various Disk-Gap-Band Parachutes. AIAA 2003-2131, May 19-22, 2003.

363. Witkowski, Allen; Kandis, Mike; Sengupta, Anita; and Long, Kurt: Comparison of Subscale Versus Full Scale Wind Tunnel Tests of MSL Disk Gap Band Parachutes. AIAA 2009-2914, May 2009.

364. Gonyea, Keir C.; Tanner, Christopher L.; Clark, Ian G.; Kushner, Laura K.; Schairer, Edward T.; and Braun, Robert D.: Aerodynamic Stability and Performance of Next-Generation Parachutes for Mars Descent. AIAA 2013-1356, AIAA Aerodynamic Decelerator Systems (ADS) Conference, March 25-28, 2013.

365. Kazemba, Cole D.; Cassell, Alan M.; Kushner, Laura K.; Tran, Kevin; Quach, Bill T.; Li, Lin; Van Norman, John W.; Littell, Justin D.; Johnson, R. Keith; Hughes, Stephen J.; Calomino, Anthony M.; and Cheatwood, F. McNeil: Determination of the Deformed Structural Shape of HIADS From Photogrammetric Wind Tunnel Data. AIAA 2013-1286, AIAA Aerodynamic Decelerator Systems (ADS) Conference, March 25-28, 2013.

366. Geiger, R. H. and Wailes, W. K.: Avanced Recovery Systems Wind Tunnel Test Report. NASA CR-177563, Aug. 1990.

367. Soderman, P. T.: Sources and Levels of Background Noise in the NASA Ames 40- by 80-Foot Wind Tunnel—A Status Report. NASA TM 100077, May 1988.

368. Allen, C. S.; Jaeger, S. M.; and Soderman, P. T.: Background Noise Sources and Levels in the NASA Ames 40- by 80-Foot Wind Tunnel at the Turn of the Century: A Status Report. NASA/TP-2003-212259, Nov. 2003.

369. Soderman, Paul T. and Phillips, J. D.: Noise Radiation Directivity From a Wind Tunnel Inlet with Inlet Vanes and Duct Wall Linings. AIAA paper 86-1896, 10th Aeroacoustic Conference, Seattle, WA, July 1986.

370. Allen, C. and Soderman, P.: Aeroacoustic Probe Design for Microphones to Reduce Flow-Induced Self Noise. AIAA paper 93-4343, AIAA 15th Aeroacoustics Conference, Long Beach, CA, Oct 25-27, 1993.

371. Allen, C. S. and Soderman, P. T.: Effect of Freestream Turbulence on the Flow-Induced Background Noise of In-Flow Microphones. AIAA/CEAS-98-2297, 4th AIAA/CEAS Aeroacoustics Conference, Toulouse, France, Jun 2-4, 1998.

372. Fields, R. S.; Tso, J.; and Soderman, P. T.: Experimental Investigation of Cavity Flow Oscillations and Tones of an In-flow Microphone. *International Journal of Aeroacoustics*, vol. 5, no. 2, 2006, pp. 173-191.

373. Jaeger, S. M.; Horne, W. C.; and Allen, C. S.: Effect of Surface Treatment on Array Microphone Self Noise. AIAA-2000-1937, 6th AIAA/CEAS Aeroacoustics Conference, Lahaina, HI, 2000.

374. Santa Maria, O. L.; Soderman, P. T.; Horne, W. C.; Jones, M. G.; and Bock, L. A.: Internal Acoustics Measurements of a Full Scale Advanced Ducted Propulsor Demonstrator. AIAA-95-3034. 31st AIAA/ASME/SAE/ASEE Joint Propulsion Conference, San Diego, CA, July 1995.

375. Krothapalli, A; Soderman, P. T.; Hayes, J. A.; and Jaeger, S. M.: Effects of Forward Flight on the Far-Field Noise of a Heated Supersonic Jet. AIAA 96-1720, 2nd AIAA/CEAS Aeroacoustics Conference, State College, PA, May 1996.

376. Soderman, P. T.: HEAT Installed Suppressor Performance. High-Lift Engine Aeroacoustic Technology (HEAT) NASA/Industry Workshop. Vol. II, NASA CDCP-21010, March 1996.

377. Smith, Brian E.; Soderman, P. T.; and Zuniga, Fanny A.: Summary of HEAT 1 Aeroacoustics Installation Effects. First NASA/Industry High-

Speed Research Configuration Aerodynamics Workshop. NASA/CP-1999-209690/PT3, Dec. 1, 1999, pp. 1407-1452.

378. Kitaplioglu, C. and Johnson, W.: Comparison of Full-Scale XV-15 Blade Vortex Interaction Noise Calculations with Wind Tunnel Data. Presented at the AHS International Technical Specialists' meeting on Aerodynamics, Acoustics, and Test and Evaluation, San Francisco, CA, Jan. 23-25, 2002.

379. Rackl, Robert G.; Miller, Gregory; Guo, Yueping; and Yamamoto, Kingo: Airframe Noise Studies—Review and Future. NASA/CR-2005-213767, 2005.

380. Hayes, J.; Horne, W. C.; Soderman, P.; and Bent, P.: Airframe Noise Characteristics of a 4.7% DC-10 Model. AIAA-97-2594, AIAA/CEAS 3rd Aeroacoustics Conference, Atlanta, GA, May 1997.

381. Horne, W. Clifton; Burnside, Nathan J.; Soderman, Paul T.; Jaeger, Stephen M.; Reinero, Bryan R.; James, Kevin D.; and Arledge, Thomas K.: Aeroacoustic Study of a 26%-Scale Semispan Model of a Boeing 777 Wing in the NASA Ames 40- by 80-Foot Wind Tunnel. NASA/TP-2004-212802, Oct. 2004.

382. Simms, D.; Schreck, S.; Hand, M.; and Fingersh, L. J.: NREL Unsteady Aerodynamics Experiment in the NASA-Ames Wind Tunnel: A Comparison of Predictions to Measurements, NREL/TP-500-29494, June 2001.

383. Leishman, J. Gordon: Challenges in Modeling the Unsteady Aerodynamics of Wind Turbines, 21st ASME Wind Energy Symposium and the 40th AIAA Aerospace Sciences Meeting, Reno, NV, AIAA 2002-0037, Jan 14-17, 2002.

384. Salari, Kambiz: DOE's Effort to Reduce Truck Aerodynamic Drag Through Joint Experiments and Computations. Lawrence Livermore National Laboratory, LLNL-PRESS-473472, May 9-13, 2011.

Appendix A. Dates of Important Events

Date	Event
1940 July	Test piles driven.
1942 March	Construction began.
1944 June	Dedication of the 40- by 80-Foot Wind Tunnel.
1944 July	40- by 80-Foot Wind Tunnel became operational.
1947	Test-section survey rig installed.
1958	National Aeronautics and Space Act passed on July 29, 1958; became effective October 1, 1958.
1961	Height-control simulator attached to outside of wind tunnel south wall.
1964	Failure of upper middle motor (FM2) bearing.
1965	Woodrow Cook leaves division to start Advanced Aircraft Projects Office.
1965 September	Paul F. Yaggy leaves branch to become technical director of the new Army Aeronautical Research Laboratory at Ames.
1967 to 1974	Studies of new full-scale subsonic wind tunnels.
1969 September	Cheyenne helicopter accident; test-section armor plate installed.
1970 to 1974	Wind tunnel diagnostic tests performed.
1971 June	Survey rig removed.
1971 December	Failure of upper east motor (FM1) bearing.
1972 February	Flat-plate vortex generators designed by Bob Page installed at end of test section to improve test-section flow quality.
1973	Scale-head digitizers installed to improve data-acquisition efficiency.
1973 August	New large-scale facility proposed: two open-circuit test sections in a Y-configuration, but instead modification of 40- by 80-Foot Wind Tunnel judged cost-effective.
1973 September	Dr. Hans Mark established the 40- by 80-Foot Wind Tunnel modification team with Ben Beam, project manager.
1974 January	Charles Hermach appointed project manager of modification team; Ben Beam retires.
1974	15-ton overhead crane replaced with 35-ton crane.
1974	40- by 80-Foot Wind Tunnel test-section yaw system replaced with a turntable system.
1974	Height-control simulator removed from south wall of 40- by 80-Foot Wind Tunnel, and roll doors installed for engine and hot-air exhaust.
1974 August	Preliminary engineering report (PER) issued for tunnel modification.
1976 June	NASA HQ shifts helicopter research charter from Langley Research Center to Ames Research Center.
1977 March	Organizational changes to accommodate Ames lead role in rotorcraft by Dr. Hans Mark.
1977 June	Environmental impact statement (EIS) completed for tunnel modification.
1978 July	Ames acquired approximately 5 acres from Pacific Gas and Electric Company (PG&E) in exchange for an equal parcel of NASA property to accommodate wind tunnel modifications.
1978 August	Dave Englebert appointed project manager for tunnel modification; Charles Hermach retires.
1978 November	Ground breaking for 80- by 120-Foot Wind Tunnel construction.
1979 September	John Dusterberry appointed systems integration manager of tunnel modification project.
1980 July	Tunnel shut down for modification project.
1981 December	Ken Mort appointed project manager for modification project; David Englebert becomes chief of systems engineering division.

Date	Event
1981 December to 1982 December	Integrated systems testing (IST) of modified wind tunnel.
1982 December	Accident during IST.
1983 January	New modification project established with Lee Stollar, project manager; Ken Mort becomes assistant chief of systems engineering division.
1983 February	Accident report issued.
1983 February	Replacement blades ordered.
1983 March to 1987 December	Repairs and reliability improvements.
1986 September to 1987 March	IST.
1987 March	NASA research performed.
1987 December	Dedication of repaired and modified facility named the National Full-Scale Aerodynamics Complex (NFAC).
1994	50th reunion of the 40- by 80-Foot Wind Tunnel.
1995	Langley Research Center closes 30- by 60-Foot Wind Tunnel so NFAC becomes the only full-scale facility.
1995 to 1996	Wind tunnel and simulator operation organizations at Ames combined.
1996 March	Fan blade cracking discovered and causes studied.
1996 July to 1998 November	42-inch-deep acoustic walls installed in 40- by 80-foot test section.
1997 January to 1999 February	Fan blade fatigue test; terminated before blade failure because new blades ordered.
1997 August to 1998 January	Fan blade repair and reinforcement.
1998 May to 1998 July	80- by 120-Foot Wind Tunnel IST.
1998 June	Contractor selected to perform design and construction of new carbon-fiber composite fan blades.
1998 August to 1998 November	40- by 80-Foot Wind Tunnel IST.
1998 November	Acoustic wall project operational readiness review (ORR).
1999	Full-cost accounting implemented to study effects.
2000	Drive motor repair.
2001 November	Replacement blade order cancelled because of changing NASA programs and budget reductions in aeronautics research.
2002	NASA rotorcraft program terminated then reinstated at very reduced funding.
2003	NFAC shut down because of changing NASA programs and drastic reductions in NASA aeronautics budget.
2003 October	NASA implements full-cost recovery so all wind tunnel users (including NASA) must pay full costs including inflated overhead costs.
2005	NFAC operation to be resumed to support Army rotorcraft research; Air Force to lease NFAC from NASA and operate NFAC.
2005 to 2006	Repair, maintenance, and checkout testing of NFAC by Air Force.
2007	Research resumed on rotors and V/STOL aircraft, as well as NASA programs such as recovery and drag devices. Proprietary studies performed on wind turbines and miscellaneous aerodynamic research.
2007 March	Fatigue testing resumed on partially fatigued blade since new blade order cancelled.
2009 April	Fatigue failure of blade and blade life predictions.
2012 December	25th anniversary of the NFAC.

Appendix B. List of NFAC Tests

The following two tables contain lists of tests performed in the 40- by 80-foot test section and the 80- by 120-foot test section.

Over the years several test numbering systems were used. The first research test was for the Douglas XSB2D-1; the test was not listed, however data were collected and reported. A few times, the same test numbers were repeated. The test numbers were more or less in sequence until the 40- by 80-Foot Wind Tunnel was shut down for repowering and the addition of the 80- by 120-foot test section. After the repowering and addition of the 80- by 120-foot test section, the test numbers continued for tests in the 40- by 80-foot test section, but there were no test numbers assigned for tests in the 80- by 120-foot test section until about 1995. At that time the NFAC operators started using a prefix to identify which test section was used for the tests. This system continued until the NFAC was shut down in about 2003. The test numbering system was modified again, but the identifying prefix was retained when the Air Force took over operation in 2007. Often test numbers were preassigned and were not corrected if the test was delayed or cancelled. The practice early on was to simply use initials rather than names for the test engineers, but an attempt was made herein to replace the initials with names wherever possible.

Table B1. History of Tests in the 40- by 80-Foot Wind Tunnel

Item No.	Test No.	Test Title	Start Date	Finish Date	Objectives	Engineer(s)/Test Director
1	A	Surveys of Test Sections	Jul-44	Jul-44		McCamael
2	B	Tests of Standard Low-Drag Wing	Aug-44	Aug-44		Norman J. Martin
3	C	Tests of 8 X 48 Clark Y Wing	Aug-44	Aug-44		Lynn W. Hunton
4	1	BTD-1 Airplane	Aug-44	Sep-44		Davidsen
5	2	F7F-1 Airplane	Sep-44	Sep-44		Charles W. Harper
6	1	BTD-1 Airplane	Sep-44	Oct-44		Davidsen
7	3	N9M Airplane	Oct-44	Oct-44		Victor I. Stevens
8	2	F7F-1 Airplane	Dec-44	Dec-44		Charles W. Harper
9	4	P75 Airplane	Dec-44	Jan-45		Summers
10	2	F7F-1 Airplane	Jan-45	Mar-45		Lynn W. Hunton
11	5	FR-1 Airplane	Mar-45	Apr-45		Victor I. Stevens
12	5	FR-1 Airplane	May-45	May-45		Victor I. Stevens
13	7	A-26 Airplane	May-45	Jun-45		McCamael
14	8	FR-1 Engineering Installation	Jun-45	Jul-45		Conway
15	9	BT2D-1 Airplane	Jul-45	Aug-45		Bradford H. Wick
16	10	XB-36 Airplane	Aug-45	Nov-45		Summers
17	11	Static Bomb Calibration	Nov-45	Nov-45		LBB
18	12	FR-1 Drag Tests	Dec-45	Dec-45		Conway
19	12	FR-1 I-16 Duct Tests	Jan-46	Jan-46		Conway
20	13	Radar Truck	Jan-46	Jan-46		RC Masa
21	14	BTD-1	Jan-46	Apr-46		ARA, RHC
22	15	Swept Wing	Apr-46	May-46		DRJ
23	16	Swept Wing	Jun-46	Sep-46		LWM
24	17	Wingtip Bodies of Revolution	Sep-46	Oct-46		Walter C. Walling
25	18	Ryan FR-1 Inlet	Oct-46	Oct-46		Norman J. Martin
26	19	Swept Tail	Nov-46	Nov-46		Walter C. Walling
27	20A	Delta Wing	Jan-47	Feb-47		Adrien E. Anderson
28	21	BT2D	Feb-47	Feb-47		
29	20B	Delta Wing	Feb-47	Mar-47		Adrien E. Anderson
30	22	45-deg Swept Fwd Wing with BLC	Apr-47	Apr-47		Gerald M. McCorrmak
31	20C	Delta Wing	Apr-47	Apr-47		Adrien E. Anderson
32	23	XP-91 Wing	Apr-47	May-47		Lynn W. Hunton
33	24	Pipe Tests	Jun-47	Jun-47		Bradford H. Wick
34	20D	Wick's Test Delta Wing	Jun-47	Jun-47		Gerald M. McCorrmak
35	25	XB-47 Tail	Jul-47	Jul-47		Lynn W. Hunton
36	26	Flush Ducts Martin	Jul-47	Aug-47		Norman J. Martin
37	27-A	63-deg Swept Wing	Aug-47	Aug-47		Walter C. Walling
38	20 E	Delta Wing + Fuselage	Aug-47	Sep-47		Adrien E. Anderson

Item No.	Test No.	Test Title	Start Date	Finish Date	Objectives	Engineer(s)/Test Director
39	27-B	63-deg Swept Wing	Sep-47	Sep-47		Walter C. Walling
40	20F	Delta Wing I & II	Sep-47	Sep-47		Adrien E. Anderson
41	23A	XP-91	Sep-47	Oct-47		Lynn W. Hunton, Joseph K. Dew
42	28	XP-92, 63-deg Swept Wing	Dec-47	Jan-48		Bradford H. Wick, Gerald M. McCormack
43	30	XP-85	Feb-48	May-48		Lynn W.Hunton, Joseph K. Dew, Norman J. Martin, Gerald M. McCormack
44	23B	XP-91	May-48	Jun-48		Joseph K. Dew
45	30	-45-deg Wing	Jul-48	Jul-48		Gerald M. McCorrmak
46	31	Survey (F7F)	Aug-48	Aug-47		John C. Roberts
47	32	Agine Fuselage	Aug-48	Sep-48		David Graham
48	34	Droop - Skewed Nose	Sep-48	Sep-48		David Graham
49	35	First-order Propeller	Sep-48	Sep-48		Vernon L. Rogallo
50	34	Skewed Droop Nose	Oct-48	Oct-48		David Graham
51	22E	45-deg Swept Forward	Oct-48	Oct-48		Woodrow L. Cook
52	36	F-84	Oct-48	Nov-48		Lynn W. Hunton
53	33	Delta Wing #3 (NACA 0005) Section	Nov-48	Nov-48		David Graham
54	22F	45-deg Swept-Forward Wing	Dec-48	Dec-48		Woodrow L. Cook
55	37	63-deg Swept Back (Downwash)	Dec-48	Dec-48		William H. Tolhurst
56	38	Propeller Vibration	Jan-49	Feb-49		Vernon L. Rogallo
57	22G	45-deg Swept Forward	Feb-49	Mar-49		Woodrow L. Cook
58	39	Semispan	Mar-49	Mar-49		Harry A. James
59	39	Wing #1	Mar-49	Apr-49		Harry A. James, Joseph K. Dew
60	40	63-deg Boundary Layer Wing	Apr-49	May-49		Woodrow L. Cook
61	41	Wing #2	May-49	Jun-49		DW
62	39A	Wing #1	Jun-49	Jun-49		DW
63	42	Wing #4	Jun-49	Jun-49		Joseph K. Dew
64	43	Wing #5	Jun-49	Jun-49		DW
65	44	Wing #6	Jun-49	Jun-49		Joseph K. Dew
66	45	Wing #3	Jun-49	Jul-49		Joseph K. Dew
67	40A	63-deg Swept-Back-Wing Fuselage, Inflow Survey 2X5	Jul-49	Aug-49		Woodrow L. Cook, Vernon L. Rogallo, RDS
68	46	Prop. Vibrations	Aug-49	Oct-49		John C. Roberts, Vernon L. Rogallo
69	47	MX-775A Missile, Heat Transfer	Oct-49	Dec-49		David Graham
70	48	Delta Wing 0005 Section	Dec-49	Jan-50		Paul F. Yaggy
71	49	63-deg Wing	Jan-50	Mar-50		William H. Tolhurst
72	50	Delta Wing	Mar-50	Apr-50		David Graham
73	51	Nacelle	Apr-50	Apr-50		John C. Roberts
74	49	63-deg Tip Suction Wing	Apr-50	May-50		Gerald M. McCorrmak
75	52	Semispan Wing Swept 45 Degrees	May-50	May-50		Harry A. James

Item No.	Test No.	Test Title	Start Date	Finish Date	Objectives	Engineer(s)/Test Director
76	53	Semispan Wing Swept 45 Degrees	May-50	Jun-50		Harry A. James
77	54	Delta Wing #4, Slotted Flap	Jun-50	Jun-50		David Graham, Woodrow L. Cook
78		**Ames Inspection**	Jun-50	Jul-50	Inspection	
79	55	Boundary Layering Porous Nose	Jul-50	Aug-50		Woodrow L. Cook
80	56	63-deg Wing Downwash Survey	Aug-50	Sep-50		William H. Tolhurst
81	57	Delta Wing, Fuselage - Tail	Sep-50	Nov-50		David Graham
82	55	Boundary-Layer Wing, Porous Nose	Nov-50	Jan-51		Woodrow L. Cook
83	58	45-deg Delta Wing	Jan-51	Jan-51		David Graham
84	59	F6U-1 Wing	Jan-51	Feb-51		Roy N. Griffin
85	58,60,61	A = 4 Delta Wing Fuselage, Tips Off, etc.	Feb-51	Mar-51		David Graham
86	62	F-86A	Mar-51	May-51		Ralph L. Maki
87	61	45-deg Delta Wing, Cutoff Tips	May-51	Jun-51		David Graham
88	63	Semispan 45-deg, Slat & Flap P.D.	Jun-51	Jul-51		Harry A. James
89	64	High-Lift Devices, 60-deg W.	Jul-51	Jul-51		Woodrow L. Cook
90	63B	45-deg Swept Semispan, Cambered Airfoil	Jul-51	Aug-51		Harry A. James
91	65	Wing-Nacelle-Fuselage: Plain Wing, 40-deg Sweep	Aug-51	Aug-51		Vernon L. Rogallo
92	59	F6U-1 Wing	Sep-51	Oct-51		Roy N. Griffin
93	58F	Aspect Ratio 4 Delta Wing	Oct-51	Nov-51		David Graham
94	66	Area Suction - F-86	Nov-51	Jan-52		Charles W. Harper
95	67	Aspect Ratio 3 Delta Wing	Jan-52	Jan-52		David Graham
96	68	45-deg Porous Leading Edge	Jan-52	Feb-52		Woodrow L. Cook
97	69	F84F Prototype	Feb-52	Feb-52		Lynn W. Huinton
98	70	F94C	Feb-52	Mar-52		Ralph L. Maki
99	69	F84	Mar-52	Apr-52		Lynn W. Huinton
100	72	Variable Incidence, A-2, Delta Wing	Apr-52	May-52		David G. Koenig
101	71	XFV-1 Lockheed	May-52	Jun-52		Woodrow L. Cook, Mark W. Kelly
102	73	F-86 Area Suction LE & Flap	Jun-52	Sep-52		Charles W. Harper
103		**1952 Inspection**	Jun-52	Jul-52		
104	74	Aspect Ratio 2, Delta Wing	Sep-52	Sep-52		David Graham
105	75	Aspect Ratio 3, 45-deg SW.W	Nov-52	Nov-52		David Graham
106	76	Aspect Ratio 6, 45 Sigma Circulation Control	Nov-52	Dec-52		Roy N. Griffin
107	74B	Inves. Ch. ext., AR 3 Delta Wing	Dec-52	Jan-53		David Graham
108	75	45-deg Swept Wing	Jan-53	Feb-53		David Graham
109	77	45-deg Sweep, AR 3.5, TR 3	Feb-53	Feb-53		Ralph L. Maki
110	78	F-86 Area Suction	Feb-53	Mar-53		Charles W. Harper

Item No.	Test No.	Test Title	Start Date	Finish Date	Objectives	Engineer(s)/Test Director
111	79	45-deg Full-Span, Camber & Twist	Mar-53	Apr-53		Lynn W. Huinton
112	80	AR2 Delta Wing, Suction Flap	Apr-53	Apr-53		Mark W. Kelly
113		Repairs to MG Room	Apr-53	May-53	Electrical repairs	
114	78A	F-86 Area Suction	May-53	Jun-53		Woodrow L. Cook
115	80	AR2 Delta Wing, J Suction Flap	Jun-53	Jun-53		Mark W. Kelly
116	75B	A = 3, 45-deg Sigma	Jun-53	Jul-53		David Graham
117	82	A = 3, Unswept Wing	Jul-53	Jul-53		David Graham
118	83	McDonnell 82 convertiplane	Jul-53	Sep-53		Vernon L. Rogallo
119	75D	A = 3, 45-deg Sigma	Sep-53	Sep-53		David Graham
120	82B	A = 3, Unswept Wing, Body & Tail	Sep-53	Oct-53		David Graham
121	84	A = 6, Sigma 45-deg, Area-Suction Flap Lead Edge	Oct-53	Dec-53		Roy N. lGriffin
122	85	Lockheed YC-130 Tests	Feb-54	Feb-54		Vernon L. Rogallo
123	75 E	AR3 45-deg Sweep	Feb-54	Feb-54		David Graham
124	86	AR3.74, S 44-deg, BLC	Mar-54	Mar-54		Curt A. Holzhauser
125	75F	AR3, 45-deg Sweep	Mar-54	Mar-54		David Graham
126	87	Northrop N-69 Missile	Mar-54	Apr-54		David Graham
127	88	MCDonnell XV-1 Conv.	Apr-54	May-54		Vernon L. Rogallo
128	75G	AR3, 45-deg Sweep	Jun-54	Jun-54		David Graham
129	86A	BLC to AR3, Sw 44-deg, TR 4	Jun-54	Jul-54		Curt A. Holzhauser
130	75G-2	AR3, 45-deg Sweep	Jul-54	Jul-54		David Graham
131	89	AR3, Str. W, Suction Moll	Jul-54	Sep-54		David G. Koenig
132	90	F-86D - Blowing Flap	Sep-54	Oct-54		Mark W. Kelly
133	91	T-33 AS LE & TE Flaps	Oct-54	Nov-54		Curt A. Holzhauser
134	75H	AR3, 45-deg SW. W	Nov-54	Dec-54		William T. Evans
135	92	45-deg Swble AR6 Low Drag	Dec-54	Dec-54		David H. Hilckey
136	89-2	AR3 Str. W, W. Por. Suction Flaps	Jan-55	Jan-55		David G. Koenig
137	90-A	F-86D Blowing Flap	Jan-55	Mar-55		
138	91	T-33, Lockheed	Mar-55	Apr-55		Curt A. Holzhauser
139	75H-2	AR3, 45-deg Swept Wing	Apr-55	Apr-55		William T. Evans
140	94	FJ-3, Ejector Flap	May-55	May-55		Ralph L. Maki
141	95	A6, 45-deg Sigma, DSF, Tail & Fences	May-55	Jul-55		Harry A. James
142	92A	A6, 45-deg Sigma Drag Test	Jul-55	May-55		David H. Hickey
143	96	XA30-1 Airplane	Jul-55	Aug-55		Ralph L. Maki
144	86B	44-deg Sw, W, As Tests	Aug-55	Aug-55		Roy N. Griffin
145	91	T-33	Aug-55	Sep-55		Curt A. Holzhauser
146	97	45-deg Sw, AR 2.8	Sep-55	Oct-55		David G. Koenig
147	92B	45-deg Sw bkw, AR 6, Area Sec	Nov-55	Nov-55		David H. Hickey
148	96	XA3D-1 with BLC	Dec-55	Jan-56		Ralph L. Maki

Item No.	Test No.	Test Title	Start Date	Finish Date	Objectives	Engineer(s)/Test Director
149	75J	AR3,45-deg Sw. W	Jan-56	Jan-56		William T. Evans
150	91 -C	T-33 W, A,S Flaps	Jan-56	Feb-56		Curt A. Holzhauser
151	98	Blowing Flaps, F-93	Feb-56	Mar-56		Mark W. Kelly
152	75K	AR3,45-deg Sw. W	Mar-56	Mar-56		William T. Evans
153	99	Air Sampler	Mar-56	Mar-56		Curt A. Holzhauser
154	100	As BLC to C-123, 4-Sc mdl	Mar-56	Apr-56		Roy N. Griffin
155	97-B	As one le of F4H-like mdl R-306T	Apr-56	May-56		David G. Koenig
156	96-C	Blow BLC on A3D	May-56	May-56		Ralph L. Maki
157	102	F-86-D shroud bl. flap	May-56	Jul-56		William H. Tolhurst
158	103	Propeller Stall Flutter	Jul-56	Aug-56		Vernon L. Rogallo
159		**Wind Tunnel Shut Down August 13, 1956**				
160		All Changed to "Parasite Pwr" (2x2, 6" H.T.)	Aug-56	Oct-56		
161	104	F4H-like model	Oct-56	Nov-56		David H. Hickey
162	107	C-123 (Mod) High Airspeeds	Dec-56	Jan-57		Roy N. Griffin
163	105	BLC to Helicopter Rotor	Jan-57	Jan-57		John L. McCloud III
164		**Wind Tunnel Shut Down January 23,1957**				
165	102	F-86	Feb-57	Feb-57		William H. Tolhurst
166	108	F-100 Blowing Wing	Feb-57	Mar-57		Ralph L. Maki
167	109	F-93	Mar-57	Apr-57		David H. Hickey
168	110	C-123 Blowing	Apr-57	May-57		Roy N. Griffin
169	105-B	BLC Helicopter Rotor	Jun-57	Jul-57		John L. McCloud III
170	111	45-deg -6-.5 Slotted Lip Flap	Jul-57	Jul-57		Harry A. James
171	112	F-86 Thrust Reverser	Jul-57	Aug-57		Mark W. Kelly
172	113	C-123 Suction Flaps, w.a. Nacelles	Aug-57	Aug-57		James A. Weiberg
173	113A	C-123 Suction Flaps, w.a. Nacelles	Aug-57	Aug-57		Harry A. James
174	114	XV-3 (Bell) Convertiplane	Sep-57	Oct-57		Mark W. Kelly
175	109-B	F-93	Oct-57	Nov-57		David H. Hickey
176	115	F8U	Nov-57	Dec-57		Ralph L. Maki
177	112	Thrust Reverser	Dec-57	Jan-58		Mark W. Kelly
178	116	Hughes Antenna	Jan-58	Jan-58		Harry A. James
179	105	BLC Helicopter	Jan-58	Jan-58		John L. McCloud III
180	117	Vertol 76 Articulated Prop.	Feb-58	Feb-58		Vernon L. Rogallo
181	118	C-123 Blowing Flaps, 4 Props	Feb-58	Apr-58		James A. Weiberg
182	121	C-123 Bl. Flaps & Load Cells & Dynamic Aileron	Apr-58	Apr-58		Harry A. James
183	120	Curtis VTOL Propeller	Apr-58	May-58		Paul F. Yaggy

Item No.	Test No.	Test Title	Start Date	Finish Date	Objectives	Engineer(s)/Test Director
184	119	Jet Transport	May-58	Jun-58		David H. Hickey
185	122	Ryan Mdl 92 Deflected Slipstream	Jun-58	Jul-58		Curt A. Holzhauser
186	120	Curtis VTOL Propeller	Jul-58	Jul-58		Paul F. Yaggy
187	123	F-104 - BLC	Jul-58	Aug-58		Mark W. Kelly
188	122A	Ryan Model 92	Sep-58	Sep-58		Curt A. Holzhauser
189	124	GE Missile Nose Recovery	Sep-58	Sep-58		Gerald M. McCormack
190	116	Hughes Radar	Sep-58	Sep-58		Harry A. James
191	120	Curtis Wright VTOL Prop	Sep-58	Oct-58		Paul F. Yaggy
192	125	XV-3	Oct-58	Oct-58		David G. Koenig
193	126	Jet Transport	Oct-58	Dec-58		David H. Hickey
194	128	F5D-1	Dec-58	Dec-58		Ralph L. Maki
196	127	C-123 Blowing Tail	Jan-59	Feb-59		James A. Weiberg
197	129	F-100F Thrust Reverser	Feb-59	Mar-59		Mark W. Kelly
198	130	Helicopter w/Forced Blowing	Mar-59	Mar-59		John L. McCloud III
199	131	Ryan Propeller	Mar-59	Apr-59		Paul F. Yaggy
200	132	Doak Ducted Fan	Apr-59	May-59		Paul F. Yaggy
201	132	Doak Ducted Fan	May-59	May-59		Paul F. Yaggy
202	133	Ingestion Studies	Jul-59	Jul-59		David H. Hickey
203	134	Helicopter Boundary-Layer Control	Jul-59	Jul-59		John L. McCloud III
204	132	Doak Ducted Fan	Jul-59	Aug-59		Paul F. Yaggy
205	135	Jet Transport Thrust Reverser	Aug-59	Sep-59		David H. Hickey
206	136	Collins Aerodyne	Sep-59	Oct-59		David G. Koenig
207	137	VTOL Prop Descent Conditions	Oct-59	Nov-59		Paul F. Yaggy
208	138	Tilt Wing	Nov-59	Dec-59		James A. Weiberg
209	139	Collins Aerodyne	Dec-59	Jan-60		David G. Koenig
210	140	Vanguard 2C	Jan-60	Mar-60		Ralph L. Maki
211	141	Avrocar	Mar-60	May-60		James A. Weiberg
212	142	Tilt Wing	May-60	Jun-60		James A. Weiberg
213	140	Vanguard 2C	Jun-60	Jul-60		Demo J. Giulianetti
214	143	G. E. Lift Fan	Jul-60	Sep-60		David H. Hickey
215		**Wind Tunnel Shut Down July 22, 1960**				
216	144	Doak Ducted Fan	Sep-60	Oct-60		Paul F. Yaggy
217	145	G.E. Lift Fan	Nov-60	Nov-60		David H. Hickey
218	146	VTOL Prop. Descent Conditions	Dec-60	Dec-60		Demo J. Giulianetti
219	147	Subsonic Jet Transport Model with BLC	Dec-60	Jan-61		David H. Hickey, RAD
220	148	Tests of Vertol Model 76 Prop.	Jan-61	Feb-61		Paul F. Yaggy, Kenneth W. Mort

Item No.	Test No.	Test Title	Start Date	Finish Date	Objectives	Engineer(s)/Test Director
221	149	Landing and Takeoff Problems SST	Feb-61	Mar-61		David G. Koenig, William H. Tolhurst
222	141	Avrocar with Tail	Mar-61	Apr-61		William H. Tolhurst, Richard K. Greif
223	150	Tilt Wing Prop. Model with BLC Flaps and Slats	Apr-61	May-61		James A. Weiberg
224	151	G.E. Fan-in-Fuselage	May-61	May-61		David H. Hickey
225	149	SST Landing and Takeoff Problems	May-61	May-61		David G. Koenig
226	152	Full-scale Test of Grumman YAO-1	May-61	Jun-61		James A. Weiberg
227	153	Bell HU-1	Jun-61	Jul-61		John L. McCloud III
228	154	Tilt Wing/Prop. Model with BLC Flaps	Jul-61	Aug-61		James A. Weiberg
229	155	SST Landing/Takeoff Problems-Ground Effects	Aug-61	Sep-61		David G. Koenig
230	156	Steerable Parachutes for Apollo	Sep-61	Sep-61		Paul F. Yaggy
231	157	Tests of Vertol Model 76 Prop.	Sep-61	Sep-61		Paul F. Yaggy
232	156	Steerable Parachutes for Apollo	Oct-61	Oct-61		Paul F. Yaggy
233	158	High-Disc-Loading Fan-in-Wing	Oct-61	Oct-61		David H. Hickey
234	160	Rotor Performance (Bell H-40/ HU-1)	Oct-61	Nov-61		John L. McCloud III
235	161	SST-Landing & Takeoff	Nov-61	Dec-61		David G. Koenig
236	162	Recovery Device for Minuteman	Dec-61	Dec-61		Mark W. Kelly
237	163	Prop. Tilt Wing Prop. w/BLC Flaps	Jan-62	Jan-62		James A. Weiberg
238	164	Hi-Disc-Loading Fan-in-Wing	Jan-62	Jan-62		David H. Hickey
239	159	Vanguard 2D VTOL	Jan-62	Feb-62		Ralph L. Maki
240	156	Steerable Parachutes for Apollo	Feb-62	Feb-62		Paul F. Yaggy
241	165	Lockheed Rigid Helicopter Rotor	Feb-62	Feb-62		John L. McCloud III, Paul F. Yaggy
242	166	Doak Ducted Fan with Exit Vane Cascade	Mar-62	Mar-62		Paul F. Yaggy, Kenneth W. Mort
243	168	Subsonic Jet Transp.	Mar-62	Apr-62		David H. Hickey, Kyoshi Aoyagi
244	169	Blow to Canard Cont. Wing Flap for SST	Apr-62	May-62		David G. Koenig, James A. Brady
245	170	Paraglider and Manned Space Capsule	May-62	Jun-62		Paul F. Yaggy, Kenneth W. Mort
246	171	Hamilton Standard VTOL Props.	Jun-62	Jun-62		Paul F. Yaggy, William H. Tolhurst
247	172	XV-3 Rotor System	Jun-62	Jul-62		David G. Koenig, James A. Brady
248	173	Fan-in-Wing VTOL (VZ-11) Ground Effects	Jul-62	Jul-62		David H. Hickey, Leo P. Hall, Anthony M. Cook
249	170-2	Gemini Paraglider	Jul-62	Jul-62		Berl Gamse

Item No.	Test No.	Test Title	Start Date	Finish Date	Objectives	Engineer(s)/Test Director
250	165-2	Rigid Helicopter Rotor (Lockheed XH-51)	Jul-62	Aug-62		John L. McCloud, James C. Biggers
251	174	Parachute Cluster	Aug-62	Aug-62		Paul F. Yaggy, Berl Gamse, Kenneth W. Mort
252	175	Kaman K-16B	Sep-62	Sep-62		James A. Weiberg, Demo J. Giulianetti
253	171-2	Hamilton Standard VTOL Props.	Sep-62	Sep-62		Paul F. Yaggy, William H. Tolhurst
254	176	Tri-Service VTOL 0.6-Scale Model	Oct-62	Nov-62		Wallace H. Deckert, Virgil R. Page
255	171-2	Hamilton Standard VTOL Props.	Nov-62	Nov-62		William H. Tolhurst
256	177	VZ-11 with Pitch-Fan	Dec-62	Jan-63		David H. Hickey, Leo P. Hall, Jerry V. Kirk
257	178	Tri-Service VTOL	Jan-63	Jan-63		Wallace H. Deckert, Virgil R. Page, James C. Biggers
258	179	Ryan VZ-3 on Ground plane	Jan-63	Feb-63		James A. Weiberg, Demo J. Giulianetti
259	180	SST-SCAT-14	Feb-63	Mar-63		Richard K. Greif, Anthony M. Cook
260	181	M2-F1 Lifting Body	Mar-63	Mar-63		Paul F. Yaggy
261	182	Radome	Mar-63	Mar-63		Demo J. Giulianetti
262	183	Supersonic Transport	Mar-63	Apr-63		David G. Koenig
263	184	Curtiss X-100 Airplane	Apr-63	Apr-63		James A. Weiberg
264	185	Variable Wing-Sweep SST	Apr-63	May-63		Richard K.Greif
265	186	M-1L	May-63	May-63		Paul F. Yaggy, Berle Gamse
266	187	SCAT 17-SST with Thrust Reverser	May-63	Jun-63		William H. Tolhurst, David H. Hickey
267	188	Gliding Parachutes	Jun-63	Jun-63		Paul F. Yaggy, Kenneth W. Mort, Berl Gamse
268	189	Cruise Fan Model	Jun-63	Jul-63		Ralph L. Maki, Demo Giulianetti
269	190	Paraglider	Jul-63	Aug-63		Paul F. Yaggy, Kenneth W. Mort
270	191	SST-SCAT 16	Aug-63	Aug-63		Richard K. Greif, Anthony M. Cook
271	192	F5D with Ogee Wing	Aug-63	Sep-63		David G. Koenig
272	193	Hamilton Standard Lt. Wt. Propeller	Sep-63	Sep-63		William H. Tolhurst
273	194	M-2 Model	Oct-63	Oct-63		Kenneth W. Mort
274	195	Apollo Parachute	Oct-63	Oct-63		James A. Weiberg
275	196	Half-Scale Gemini Paraglider	Oct-63	Oct-63		Berl Gamse
276	197	Boeing 720-tail	Oct-63	Nov-63		DHA
277	198	Hamilton Std. Light. Wt. Propeller	Nov-63	Nov-63		William H. Tolhurst
278	199	SST-SCAT-16	Nov-63	Dec-63		Richard K. Greif
279	200	Paraglider	Dec-63	Dec-63		PIP
280	201	M-2 Lifting Body Model	Dec-63	Dec-63		JB
281	202	SCAT-17 SST	Dec-63	Jan-64		Victor R. Corsiglia
282	203	Tilt Wing VTOL (XC-142)	Jan-64	Jan-64		NHD
283	204	M-2 Lifting Body Model	Jan-64	Feb-64		Kenneth W. Mort
284	205	Steerable Parachutes	Feb-64	Feb-64		James A. Weiberg

Item No.	Test No.	Test Title	Start Date	Finish Date	Objectives	Engineer(s)/Test Director
285	206	Apollo Parachutes	Feb-64	Feb-64		James A. Weiberg
286	205	Steerable Parachutes	Feb-64	Feb-64		James A. Weiberg
287	207	Ducted Cruise Fan	Feb-64	Mar-64		Demo J. Giulianetti
288	198-1	Hamilton Standard Lt. Wt. Propeller	Mar-64	May-64		William H. Tolhurst
289	208	M-2 Model	May-64	May-64		Berl Gamse
290	209	Delta Wing Transport	May-64	May-64		David G. Koenig
291	210	XV-5A	May-64	May-64		Jerry V. Kirk
292	211	M-I-L Solid & Inflatable Lifting Body	May-64	Jun-64		Paul F. Yaggy
293	210	XV-5A	Jun-64	Jun-64		Jerry V. Kirk
294	212	Bell X-22 Ducted Fan	Jul-64	Jul-64		Kenneth W. Mort
295	213	Variable Sweep SST	Aug-64	Aug-64		Anthony M. Cook
296	214	Bell High-Speed Rotor	Aug-64	Aug-64		James C. Biggers
297	215	XV-4A Hummingbird VTOL	Sep-64	Sep-64		Jerry V. Kirk
298	216	Sikorsky Rotor	Oct-64	Oct-64		John L. McCloud III
299	217	M-2 Lifting Body Model	Oct-64	Oct-64		Kenneth W. Mort
300	218	Tandem, Dual, Ducted Fan V/STOL	Oct-64	Nov-64		Ralph L. Maki
301	219	Turbo Lift Engine Configuration	Nov-64	Dec-64		William H. Tolhurst
302	220	M-2 F1 Flight Vehicle	Dec-64	Dec-64		Kenneth W. Mort
303	221	Variable Sweep Wing SST	Dec-64	Dec-64		Anthony M. Cook
304	222	X-22A Full-Scale Ducted Fan	Dec-64	Dec-64		Kenneth W. Mort
305	F	Tunnel Q Survey	Dec-64	Dec-64		James A. Weiberg
306	223	Deep Stall Transport	Jan-65	Jan-65		David H. Hickey
307	224	Tilt Wing Transport	Jan-65	Feb-65		Stanley O. Dickenson
308	225	Turbo Lift Engine Configuration	Feb-65	Feb-65		William H. Tolhurst
309	226	Tandem, Dual, Ducted Fan V/STOL	Feb-65	Mar-65		Demo J. Giulianetti
310	227	Delta Calibration Wing	Mar-65	Mar-65		David G. Koenig
311	227B	Delta Calibration Wing	Apr-65	Apr-65		David G. Koenig
312	228	Lockheed SST	Apr-65	Apr-65		David G. Koenig
313	229	XC-142 Model	Mar-65	Apr-65		Stanley O. Dickenson
314	203	Variable Sweep (Phase II)	Apr-65	Apr-65		Anthony M. Cook
315	231	Jet Augmented Flap	Apr-65	May-65		Jerry V. Kirk
316	232	Calibrate Wing with Load Cells	May-65	May-65		David G. Koenig
317	233	F5D Ground Effect	May-65	May-65		David G. Koenig
318	234	Lockheed SST Ground Effect	May-65	May-65		David G. Koenig
319	235	COIN Model with Conventional Flaps on Ground Plane	May-65	May-65		James A. Weiberg
320	236	Lockheed SST	May-65	Jun-65		David G. Koenig
321	237	Variable Sweep (Phase II SST)	Jun-65	Jun-65		Anthony M. Cook

Item No.	Test No.	Test Title	Start Date	Finish Date	Objectives	Engineer(s)/Test Director
322	238	Jet Augmented Flap	Jun-65	Jun-65		Jerry V. Kirk
323	239	Jet Flap Rotor	Jun-65	Jul-65		John L. McCloud III
324	240	M2-F2 Aircraft	Jul-65	Aug-65		Kenneth W. Mort
325	241	COIN Model w/Conventional Flaps	Aug-65	Aug-65		James A. Weiberg
326	242	Hamilton Std Light Weight Prop	Aug-65	Aug-65		William H. Tolhurst
327	243	Variable Sweep (Phase II SST)	Aug-65	Sep-65		Jerry V. Kirk
328	244	Lockheed SST	Sep-65	Sep-65		David G. Koenig
329	245	4 Fan V/STOL Transport	Sep-65	Oct-65		Leo P. Hall
330	246	Kaman KRC-6 Rotochute	Oct-65	Oct-65		Ralph L. Maki
331	247	M1-L	Oct-65	Nov-65		Kenneth W. Mort
332	248	De Havilland Augmentor Wind Model	Nov-65	Nov-65		David G. Koenig
333	249	COIN Model with Rotating Cylinder Flaps	Nov-65	Nov-65		James A. Weiberg
334	250	Parachutes	Nov-65	Dec-65		Kenneth W. Mort
335	251	Lockheed Stoppable Rotor	Dec-65	Dec-65		John L. McCloud III
336	252	XC-142 Tilt Wing	Dec-65	Jan-66		Stanley O. Dickenson
337	253	Variable Sweep SST with BLC	Jan-66	Jan-66		Anthony M. Cook
338	254	Northrop Lift-Engine VTOL (Flight Line)	Jan-66	Jan-66		
339	255	Deep Stall Study Transport No. 2	Jan-66	Jan-66		Kyoshi Aoyagi
340	256	Full-Scale X-22A Ducted Fan	Jan-66	Feb-66		Kenneth W. Mort
341	257	Lockheed SST	Feb-66	Feb-66		David G. Koenig
342	258	Boeing SST (Phase 2)	Feb-66	Feb-66		Anthony M. Cook
343	259	Rotating Cylinder Flap Model	Feb-66	Feb-66		James A. Weiberg
344	260	De Havilland Augmentor Wing Model	Mar-66	Mar-66		David G. Koenig
345	261	Fixed-Wing SST	Mar-66	Mar-66		David G. Koenig
346	262	HL-10	Mar-66	Mar-66		Kenneth W. Mort
347	263	Tests of F111 A, B Parachutes	Apr-66	Apr-66		James A. Weiberg
348	264	Bell Re-entry Rotor	Apr-66	Apr-66		David G. Koenig
349	265	Lockheed Stoppable Rotor	Apr-66	Apr-66		John L. McCloud III
350	266	SST Lockheed Fixed Wing	May-66	May-66		David G. Koenig
351	267	Advanced Tilting Rotor	May-66	May-66		David G. Koenig
352	268	Barrish Flexirotor	May-66	Jun-66		Ralph L. Maki
353	269	Barrish Parachutes	Jun-66	Jun-66		Kenneth W. Mort
354	270	CX-6 Model	Jun-66	Jun-66		Jerry V. Kirk
355	271	North American OV-10A	Jun-66	Jul-66		James A. Weiberg
356	272	Deep Stall Study Transport 2	Jun-66	Jul-66		Kyoshi Aoyagi
357	273	Short-Haul Transport	Jul-66	Jul-66		Virgil R. Page

Item No.	Test No.	Test Title	Start Date	Finish Date	Objectives	Engineer(s)/Test Director
358	274	Bell High-Speed Rotor	Jul-66	Aug-66		John L. McCloud III
359	275	Variable-Sweep SST	Aug-66	Sep-66		Anthony M. Cook
360	276	Sikorsky High-Speed Rotors	Sep-66	Sep-66		John L. McCloud III
361	277	Fixed-Wing SST	Sep-66	Oct-66		David G. Koenig
362	278	Variable-Sweep SST	Oct-66	Oct-66		Anthony M. Cook
363	279	Short Haul Transport	Oct-66	Oct-66		Virgil R. Page
364	280	Lift-Fan Fighter	Nov-66	Nov-66		Jerry V. Kirk
365	281	Lift-Engine Fighter	Nov-66	Dec-66		Jerry V. Kirk
366	282	X22A Ducted Fan Tip Clearance Studies	Dec-66	Dec-66		Kenneth W. Mort
367	283	COIN Model with Double-Slotted Flaps	Dec-66	Jan-67		Berl Gamse, Stanley O. Dickenson
368	284	367-80B Airplane Model with Jet-Augmented Flaps	Jan-67	Jan-67		Kyoshi Aoyagi
369	285	Variable Sweep SST Inlet Studies	Feb-67	Feb-67		Anthony M. Cook
370	286	Inflatable Antenna	Feb-67	Feb-67		Michael D. Falarski
371	287	Lift-Engine Fighter Model	Feb-67	Mar-67		Jerry V. Kirk
372	288	Bell High-Speed Rotor	Mar-67	Mar-67		John L. McCloud, James C. Biggers
373	289	Sideways Mounting (Bell X-14 Airplane)	Apr-67	Apr-67		James A. Weiberg, Berl Gamse
374	290	Forward Flight Mounting (Bell X-14 Airplane)	Apr-67	Apr-67		James A. Weiberg, Berl Gamse
375	291	Prop., STOL	Apr-67	Apr-67		Virgil R. Page, Stanley O. Dickenson
376	292	Lift-Fan Fighter	Apr-67	May-67		Brent K. Hodder, Leo P. Hall
377	293	Jet Augmented Flap	May-67	May-67		Kyoshi Aoyagi, Paul T. Soderman
378	294	Augmentor Wing	May-67	Jun-67		David G. Koenig, Victor R. Corsiglia
379	295	4 Propeller Rotating Cylinder Flap	Jun-67	Jul-67		James A. Weiberg
380	296	Cornell Stopped Rotor	Jul-67	Jul-67		John L. McCloud, James C. Biggers
381	297	Variable-Sweep SST Main Drive Repair	Jul-67	Jul-67		Anthony M. Cook
382	298	Variable-Sweep SST	Aug-67	Aug-67		Anthony M. Cook
383	299	Deflected Slipstream Model	Aug-67	Aug-67		Virgil R. Page
384	300	Lockheed Stoppable Rotor, Phase III	Aug-67	Sep-67		James C. Biggers, John L. McCloud III, Robert H. Stroub
385	301	Lift Fan Transport with BLC Inlets	Sep-67	Sep-67		Berl Gamse, Brent K. Hodder, Jerry V. Kirk
386	302	Tandem-Dual Ducted Fan	Sep-67	Oct-67		Demo J. Giulianetti, Ralph L. Maki
387	303	X-22A Ducted Fan	Oct-67	Oct-67		MIchael D. Falarski
388	304	Deflected Slipstream Model	Oct-67	Nov-67		Virgil R. Page, Stanley O. Dickenson
389	305	Hypersonic Transport Model	Nov-67	Nov-67		Victor R. Corsiglia
390	306	Variable-Sweep SST	Nov-67	Dec-67		Anthony M. Cook

Item No.	Test No.	Test Title	Start Date	Finish Date	Objectives	Engineer(s)/Test Director
391	307	Deflected Slipstream Model	Dec-67	Dec-67		Virgil R. Page
392	308	Lift-Engine Fighter	Dec-67	Jan-68		Jerry V. Kirk, Jerry P. Barrack, Brent K. Hodder
393	309	Lift-Fan Transport	Jan-68	Jan-68		Stanley O. Dikenson, Kyoshi Aoyagi
394	310	Bell High-Advance-Ratio Rotors	Jan-68	Jan-68		James C. Biggers, Michael D. Falarski
395	311	4 Propeller Rotating Cylinder Flap	Feb-68	Feb-68		James A. Weiberg
396	312	Langley Parawings	Feb-68	Feb-68		Kenneth W. Mort
397	313	SV5 Lifting Body	Feb-68	Mar-68		Kenneth W. Mort
398	314	Hypersonic Transport	Mar-68	Mar-68		Victor R. Corsiglia
399	315	Air Bus Inlet Distortion	Mar-68	Apr-68		Kyoshi Aoyagi
400	316	Hughes LOH	Apr-68	May-68		Robert H. Stroub
401	317	M2-F2 Aircraft	May-68	May-68		Kenneth W. Mort
402	318	Lear Jet	May-68	Jun-68		Paul T. Soderman
403	319	Delta Wing Lift-Fan Fighter	Jun-68	Jun-68		Brent K. Hodder
404	320	OV-10	Jun-68	Jul-68		Terrence W. Feistal
405	321	Jet Transport with Jet Flaps	Jul-68	Aug-68		Kyoshi Aoyagi
406	322	Cessna A-37 with Thrust Reverser	Jul-68	Aug-68		Michael D. Falarski
407	323	2 Propeller Rotating Cylinder Flap	Aug-68	Sep-68		Ralph L. Maki
408	324	Hughes Inflatable Shelter	Sep-68	Sep-68		Ralph L. Maki
409	325	Lift-Fan Transport	Sep-68	Oct-68		Stanley O. Dikenson
410	326	V/STOL Prop.	Oct-68	Oct-68		William H. Tolhurst
411	327	Tilt Rotor (AAPO)	Oct-68	Nov-68		David G. Koenig
412	328	SST-SCAT 15	Nov-68	Dec-68		Victor R. Corsiglia, Virgil R. Page
413	329	Deflected Slipstream Model	Dec-68	Dec-68		Virgil R. Page
414	330	Rotating Cylinder Flap COIN Model	Dec-68	Dec-68		Terrence W. Feistal
415	331	Inverting Flap COIN Model	Jan-69	Jan-69		Terrence W. Feistal
416	332	SCAT 15	Jan-69	Jan-69		Virgil R. Page
417	333	F-111 B	Feb-69	Mar-69		Jerry P. Barrack
418	334	De Havilland Augmentor Wing Model	Mar-69	Mar-69		David G. Koenig, Thomas N. Aiken
419	335	Stopped Rotor-Cornell Aero. Lab.	Mar-69	Apr-69		James C. Biggers
420	336	Bell Instrumented Rotor Blades	Apr-69	Apr-69		James C. Biggers
421	337	COIN Inverting Flaps	Apr-69	Apr-69		Terrence W. Feistal, Joseph P. Morelli
422	338	SST SCAT 15-F	Apr-69	May-69		David G. Koenig
423	339	Semispan Ducted Fan Deflected Slipstream model	May-69	May-69		Kenneth W. Mort, Michael D. Falarski
424	340	Lear Jet	May-69	Jun-69		Paul T. Soderman, Thomas N. Aiken
425	341	M2 Model	Jun-69	Jun-69		Kenneth W. Mort, Michael D. Falarski
426	342	SCAT 15	Jun-69	Jun-69		David G. Koenig, Virgil R. Page
427	343	H-126 Jet Flap Aircraft	Jun-69	Jul-69		Thomas N. Aiken, Leo P. Hall

Item No.	Test No.	Test Title	Start Date	Finish Date	Objectives	Engineer(s)/Test Director
428	344	High-Pressure-Ratio Lift Fans	Jul-69	Jul-69		Jerry V. Kirk, Brent K. Hodder
429	345	External Flow Jet Augmented Triple Slotted Flap	Jul-69	Aug-69		Kyoshi Aoyagi, Leo P. Hall
430	346	Hamilton Standard Cyclic Prop. Test	Aug-69	Aug-69		William H. Tolhurst
431	347	High-Pressure-Ratio Lift Fans	Aug-69	Sep-69		Jerry V. Kirk, Brent K. Hodder
432	348	AH-56 Helicopter	Sep-69	Sep-69		James C. Biggers, Leo P. Hall
433	349	High-Pressure-Ratio Lift Fans	Oct-69	Oct-69		Jerry V. Kirk, Brent K. Hodder, Leo P. Hall
434	350	Advanced Fighter Model	Oct-69	Nov-69		Demo J. Giulianetti
435	351	Cyclic Pitch Prop.	Nov-69	Nov-69		William H. Tolhurst
436	352	De Havilland Augmented Wing Model	Nov-69	Nov-69		David G. Koenig, Thomas N. Aiken
437	353	Prop. STOL-Low Struts	Nov-69	Dec-69		Virgil R. Page
438	354	Prop. STOL-High Struts	Dec-69	Dec-69		Virgil R. Page
439	355	Ducted Fan - Semispan	Dec-69	Jan-70		MIchael D. Falarski
440	356	Cyclic Pitch Prop.	Jan-70	Jan-70		William H. Tolhurst
441	357	Augmentor Wing in Ground Effect	Feb-70	Feb-70		Thomas N. Aiken
442	358	Advanced Fighter No. 2, F-14A	Feb-70	Mar-70		Joseph P. Morelli
443	359	V/STOL Lift Fan Transport	Mar-70	Mar-70		Jerry V. Kirk
444	360	Advanced Fighter No. 2	Mar-70	Apr-70		Joseph P. Morelli
445	361	Advanced Fighter No. 2	Apr-70	Apr-70		Joseph P. Morelli
446	362	ABC Rotor	May-70	Jun-70		Robert H. Stroub
447	363	Model of a V/STOL Wind Tunnel	Jun-70	Jul-70		Kenneth W. Mort
448	364	Tilt Rotor Dynamic Model	Jul-70	Jul-70		David G. Koenig, Kyoshi Aoyagi
449	365	F-14	Jul-70	Aug-70		Ralph L Maki, Demo J. Giulianetti
450	366	Lockheed Slowed/Stopped Rotor	Aug-70	Aug-70		James C. Biggers, Leo P. Hall
451	367	Kaman Aercab Test	Aug-70	Sep-70		Terrence W. Feistal, Demo J. Giulianetti
452	368	Fairchild/Strator AERCAB Test	Sep-70	Sep-70		Michael D. Falarski, Jeff G. Bohn
453	367A	Kaman Aercab Test	Sep-70	Sep-70		Terrence W. Feistal, Demo J. Giulianetti
454	369	Cyclic Pitch Prop.	Sep-70	Sep-70		William H. Tolhurst, Jeff G. Bohn
455	370	F-14	Sep-70	Oct-70		Demo J. Giulianetti, William T. Eckert
456	371	High-Pressure-Ratio Lift-Fan Semispan Model	Oct-70	Oct-70		Jerry V. Kirk, Leo P. Hall
457	372	Ducted-Fan Semispan Sound Study	Oct-70	Oct-70		Michael D. Falarski, Virgil R. Page
458	373	Lift-Fan Semispan Mode	Nov-70	Nov-70		Jerry V. Kirk, Leo P. Hall
459	374	Tilt Rotor (AAPO)	Nov-70	Dec-70		William H. Tolhurst, Jeff G. Bohn
460	375	OV-10 Propeller Driven	Dec-70	Dec-70		James A. Weiberg, William H. Tolhurst
461	376	High Wing Externally	Dec-70	Dec-70		Kyoshi Aoyagi
462	377	Model of a V/STOL Wind Tunnel	Dec-70	Jan-71		Kenneth W. Mort
463	378	Adv. Fighter Model No. 3, F-15	Jan-71	Jan-71		Rallph L. Maki, Terrence W. Feistal

Item No.	Test No.	Test Title	Start Date	Finish Date	Objectives	Engineer(s)/Test Director
464	379	Swept Augmentor Wing	Jan-71	Feb-71		David G. Koenig, Michael D. Falarski
465	380	Wind Tunnel Noise Study	Feb-71	Feb-71		Paul T. Soderman
466	381	Fighter No. 3 Ground Effect	Feb-71	Feb-71		Ralph L. Maki, William H. Tolhurst
467	381B	Pressure Survey of 40x80	Feb-71	Mar-71		Kenneth W. Mort, Joseph E. Piazza
468	382	Prop. STOL Model	Mar-71	Mar-71		Virgil R. Page, Thomas N. Aiken
469	383	Jet Flap Rotor	Mar-71	Mar-71		John L. McCloud III, Robert H. Stroub
470	383B	Pressure Survey of 40x80	Apr-71	Apr-71		Kenneth W. Mort, William T. Eckert
471	384	Fighter No. 2	Apr-71	Apr-71		Ralph L. Maki, Jeff G. Bohn
472	385	Model of V/STOL Wind Tunnel	Apr-71	Apr-71		Kenneth W. Mort, William T. Eckert
473	386	DC-9 Based STOL Lift-Fan Transport	Apr-71	May-71		AT, Leo P. Hall, Jerry V. Kirk
474	386B	Pressure Survey of 40x80	Jun-71	Jun-71		Kenneth W. Mort
475	387	Advanced Fighter No. 3	Jun-71	Jun-71		William H. Tolhurst, William T. Eckert
476	387B	Pressure Survey of 40x80	Jun-71	Jun-71		Kenneth W. Mort
477	388	Y OV-10A RCF Airplane AAPO	Jun-71	Jul-71		Demo J. Giulianetti, James A. Weiberg
478	389	Advanced Fighter No. 3	Jul-71	Jul-71		Rallph L. Maki, Terrence W. Feistal
479	389B	Pressure Survey of 40x80	Jul-71	Jul-71		Kenneth W. Mort
480	390	High Wing 25-deg Sweep EEF Model	Jul-71	Aug-71		David G. Koenig, Michael D. Falarski
481	391	Model of V/STOL Wind Tunnel	Aug-71	Aug-71		Kenneth W. Mort, Joseph E. Piazza, William T. Eckert
482	392	DC9-Based V/STOL Transport Model	Aug-71	Sep-71		Jerry V. Kirk, Leo P. Hall
483	393	Advanced Fighter #3 Powered	Sep-71	Oct-71		Laura E. Gregg, William H. Tolhurst
484	394	40x80 Pressure Survey	Oct-71	Oct-71		Kenneth W. Mort, Joseph E. Piazza, William T. Eckert
485	395	Swept Augmentor Wing Model	Oct-71	Nov-71		David G. Koenig, Michael D. Falarski
486	395B	Pressure Survey of 40x80	Nov-71	Nov-71		Kenneth W. Mort, Joseph E. Piazza
487	396	Power Section Inspection & Repair	Nov-71	Jan-72		
488	397	Fan-in-Wing Model	Jan-72	Jan-72		Kenneth W. Mort, Joseph E. Piazza, William T. Eckert
489	397B	Pressure Survey of 40x80	Jan-72	Jan-72		Kenneth W. Mort, Joseph E. Piazza, William T. Eckert
490	398	Wake Turbulence	Jan-72	Jan-72		Victor R. Corsiglia, Norman Chigier
491	399	Bell Folding Proprotor	Feb-72	Feb-72		John P. Rabbott, Jeff G. Bohn, James C. Biggers
492	400	Advanced Fighter #3 Powered in G-Effect	Feb-72	Mar-72		Laura E. Gregg, William H. Tolhurst, Ralph L. Maki
493	401	External Blowing Flap Model with JT 15D-1 Engines	Mar-72	Mar-72		Kyoshi Aoyagi, Michael D. Falarski, David G. Koenig

Item No.	Test No.	Test Title	Start Date	Finish Date	Objectives	Engineer(s)/Test Director
494	402	Model of V/STOL Wind Tunnel	Apr-72	Apr-72		Kenneth W. Mort, Joseph E. Piazza, William T. Eckert
495	403	Lift Fan Semispan Model	Apr-72	Apr-72		Jerry V. Kirk, Brent K. Hodder, Leo P. Hall
496	404	Swept Augmentor Wing in Ground Effect	May-72	May-72		David G. Koenig, Michael D. Falarski
497	405	Wake Turbulence	May-72	Jun-72		Victor R. Corsiglia, Jeff G. Bohn
498	406	XV-5B Wind Tunnel Test	Jun-72	Jun-72		Jerry V. Kirk
499	407	Basic High-Lift Study	Jun-72	Jun-72		Larry E. Olson, Jeff G. Bohn
500	408	Lear Jet STOL Study	Jun-72	Jun-72		Paul T. Soderman
501	409	QUESTOL Model	Jul-72	Jul-72		Kyoshi Aoyagi, Michael D. Falarski
502	410	Boeing-Vertol Tilt Rotor Dynamics	Aug-72	Sep-72		Jeff G. Bohn, James C. Biggers, John P. Rabbott
503	411	Basic High-Lift Study	Sep-72	Oct-72		Larry E. Olson, William H. Tolhurst, Laura E. Gregg
504	412	Wind Tunnel Wall Corrections	Oct-72	Oct-72		Kenneth W. Mort, William T. Eckert, Joseph E. Piazza
505	413	Wake Turbulence	Oct-72	Oct-72		Victor R. Corsiglia, Robert H. Stroub
506	414	Correlation Study	Oct-72	Nov-72		Paul T. Soderman
507	415	Expanding Duct Jet Flap	Nov-72	Nov-72		Kyoshi Aoyagi, Thomas N. Aiken, David G. Koenig
508	416	Vertol Power Tilt Rotor	Nov-72	Dec-72		Jeff G. Bohn, James C. Biggers, Robert H. Stroub
509	417	F-14 Stall/Spin Study	Dec-72	Jan-73		Ralph L. Maki, Laura E. Gregg, William H. Tolhurst
510	418	Expanding Duct Jet Flap	Jan-73	Jan-73		Thomas N. Aiken, Michael D. Falarski
511	419	Fire Bee (AF-AM-148)	Feb-73	Feb-73		Ralph L. Maki, Laura E. Gregg, William H. Tolhurst
512	420	Wake Turbulence	Feb-73	Feb-73		Victor R. Corsiglia, Vern R. Rossow, William T. Eckert
513	421	Statorless Lift-Fan Semispan	Feb-73	Feb-73		Leo P. Hall, Michael D. Falarski
514	422	Deployable Rigid Wing	Feb-73	Mar-73		Terrence W. Feistal, Laura E. Gregg, RJ
515	423	AST Propulsion Noise	Mar-73	Mar-73		Paul T. Soderman, Adolph Atencio
516	424	Wake Turbulence	Mar-73	Mar-73		Vernon J. Rossow, Victor R. Corsiglia, William T. Eckert
517	425	AST Propulsion Noise	Mar-73	Mar-73		Paul T. Soderman, Adolph Atencio
518	426	Twin-Engined USB Model	Apr-73	Apr-73		Kyoshi Aoyagi, David G. Koenig, Michael D. Falarski
519	427	Wake Turbulence	Nov-73	Nov-73		Victor R. Corsiglia, Vernon J. Rossow
520	428	AST	Nov-73	Jan-73		Adolph Atencio, Warren F. Ahtye
521	429	JT-15	Dec-73	Dec-73		Michael D. Falarski, Thomas N. Aiken

Item No.	Test No.	Test Title	Start Date	Finish Date	Objectives	Engineer(s)/Test Director
522	430	Noise Survey	Dec-73	Dec-73		Kenneth W. Mort
523	431	Army Tents	Dec-73	Dec-73		Michael D. Falarski
524	432	Wake Turbulence	Dec-73	Dec-73		Victor R. Corsiglia
525	433	Separated Flow Studies	Dec-73	Feb-74		Larry E. Olson
526	433A	Air Frame Noise	Dec-73	Jan-74		Warren F. Ahtye
527	434	USB Model	Feb-74	Mar-74		Kyoshi Aoyagi
528	435	Noise Survey	Mar-74	Mar-74		Kenneth W. Mort
529	436	Wake Turbulence	Mar-74	Mar-74		Victor R. Corsiglia
530	437	Bell Tip Shape	Mar-74	Apr-74		Robert H. Stroub
531	438	Wake Turbulence	Apr-74	Apr-74		Victor R. Corsiglia
532	439	Semispan Augmentor Wing	Apr-74	May-74		Thomas N. Aiken, Mark D. Betzina
533	440	Wake Turbulence	May-74	May-74		Vernon J. Rossow, Victor R. Corsiglia
534	441	Upper Surface Blowing	Jun-74	Jun-74		Kyoshi Aoyagi, David G. Koenig
535	442	Semispan Augmentor Wing Tare Correction	Jun-74	Jun-74		Thomas N. Aiken, David G. Koenig
536	443	Wake Turbulence	Jul-74	Jul-74		Vernon J. Rossow, Victor R. Corsiglia
537	444	High-Aspect-Ratio Wing	Jul-74	Jul-74		Larry E. Olson
538	445	XV5B	Oct-74	Nov-74		Leo P. Hall, Adolph Atencio
539	446	Wind Tunnel Noise & Temperature Measurements	Nov-74	Nov-74		Kenneth W. Mort
540	447	QSRA Model	Nov-74	Dec-74		Kyoshi Aoyagi
541	448	Helicopter Test Rig	Dec-74	Dec-74		James C. Biggers, Leo P. Hall
542	449	Torpedo Recovery System	Dec-74	Dec-74		David H. Brown, Mark D. Betzina
543	450	Yawed Wing	Dec-74	Jan-75		Larry E. Olson
544	451	YOV-10A	Jan-75	Jan-75		Ralph L. Maki
545	452	Airframe Noise	Jan-75	Jan-75		Warren F. Ahtye, Leo P. Hall
546	453	Wind Loads on False Work in Tunnel	Jan-75	Jan-75		Ralph L. Maki, Mark D. Betzina, David H. Brown
547	454	Wake Turbulence	Jan-75	Feb-75		Victor R. Corsiglia, Vernon J. Rossow
548	455	OWRPRA-Oblique Yawed Wing RPV	Feb-75	Feb-75		Ralph L. Maki
549	456	Acoustic Calibration	Feb-75	Feb-75		Adolph Atencio, Leo P. Hall
550	457	JT8D	Feb-75	Mar-75		Adolph Atencio, Leo P. Hall
551	458	Helicopter Test Rig	Mar-75	Apr-75		Wayne R. Johnson, Jeff G. Bohn, David H. Brown, JH
552	459	Lift-Fan Transport	Apr-75	May-75		Kyoshi Aoyagi, Leo P. Hall, Mark D. Betzina
553	460	Swept Augmentor Wing	May-75	May-75		Michael D. Falarski, Mark D. Betzina, David H. Brown
554	461	Tunnel Flow Survey	May-75	May-75		William H. Tolhurst

Item No.	Test No.	Test Title	Start Date	Finish Date	Objectives	Engineer(s)/Test Director
555	462	Space Shuttle	May-75	Jun-75		Ralph L. Maki, Leo P. Hall, Mark D. Betzina
556	463	Controllable Twist Rotor, CTR, Test	Jun-75	Jul-75		John L. McCloud III, Robert H. Stroub, Mark D. Betzina, Leo P. Hall
557	464	Battle Damage	Jul-75	Aug-75		
558	465	Flow Survey Rig	Aug-75	Aug-75		William H. Tolhurst, Mark D. Betzina, David H. Brown
559	466	Semispan Augmentor	Aug-75	Sep-75		Thomas N. Aiken, Michael D. Falarski, Leo P. Hall, David H. Brown
560	467	B77 Lifing Parachutes	Sep-75	Sep-75		Ralph L. Maki, Mark D. Betzina, David H. Brown
561	468	OWRPRV Oblique Wing RPV	Sep-75	Oct-75		Ralph L. Maki, Mark D. Betzina, David H. Brown
562	469	Propeller Test Rig Checkout T-4947	Oct-75	Oct-75		William H. Tolhurst, Leo P. Hall, Joseph E. Piazza, Robert H. Stroub
563	470	Wake Turbulence	Oct-75	Oct-75		Vernon J. Rossow, Victor R. Corsiglia, David H. Brown
564	471	Flow Survey Rig	Oct-75	Nov-75		William H. Tolhurst, David H. Brown
565	472	XV-15 Rotor	Nov-75	Nov-75		Robert H. Stroub, Leo P. Hall, David H. Brown
566	473	Space Shuttle	Nov-75	Dec-75		Ralph L. Maki, David H. Brown
567	474	Small-Scale Jet Noise	Dec-75	Dec-75		Adolph Atencio, Mark D. Betzina
568	475	Acoustic Calibration	Dec-75	Dec-75		Michael D. Falarski, David H. Brown
569	476	High-Lift Model	Dec-75	Jan-76		Larry E. Olson, Mark D. Betzina
570	477	Tunnel Flow Calibration	Jan-76	Jan-76		William H. Tolhurst, Mark D. Betzina, David H. Brown
571	478	Fan Noise in Tunnel	Jan-76	Jan-76		Brent K. Hodder, David H. Brown
572	479	Space Shuttle	Feb-76	Feb-76		Ralph L. Maki, Mark D. Betzina, David H. Brown
573	480	Correlation Microphone	Mar-76	Mar-76		Warren F. Ahtye
574	481	Model 80X120 Wind Tunnel Test	Mar-76	Mar-76		William T. Eckert, Terry Oesch
575	482	Multimission Lift-Fan Model	Mar-76	Apr-76		Kyoshi Aoyagi, KH, Mark D. Betzina
576	483	Wake Turbulence	Apr-76	Apr-76		Victor R. Corsiglia, Vernon J. Rossow
577	484	Airframe Noise	Apr-76	May-76		Warren F. Ahtye
578	485	Navy Control Tower	May-76	May-76		William H. Tolhurst, David H. Brown
579	486	Parachutes, Pioneer	May-76	May-76		Ralph L. Maki, Leo P Hall
580	487	De Havilland Augmentor Wing	May-76	Jun-76		David G. Koenig, Michael D. Falarski, Mark D. Betzina
581	488	JT15-D Fan Noise	Jun-76	Jun-76		
582	489	B-77 Parachutes	Jun-76	Jun-76		Ralph L. Maki, Leo P Hall

Item No.	Test No.	Test Title	Start Date	Finish Date	Objectives	Engineer(s)/Test Director
583	490	Multimission Lift-Fan Model	Jun-76	Jul-76		Kyoshi Aoyagi, David H. Brown
584	491	Rotor Test Apparatus	Jul-76	Jul-76		John L. McCloud III, Robert H. Stroub
585	492	Q Fan	Jul-76	Jul-76		Michael D. Falarski, Mark D. Betzina
586	493	AV8B	Aug-76	Sep-76		Thomas N. Aiken, David H. Brown, Leo P. Hall
587	494	B-77 Lifting Chutes Phase	Sep-76	Sep-76		Ralph L. Maki, David H. Brown
588	495	Q-Fan	Sep-76	Oct-76		Michael D. Falarski, Mark D. Betzina, Terry Oesch
589	496	Multicyclic Twist Rotor	Oct-76	Nov-76		John L. McCloud III, Robert H. Stroub, Leo P. Hall, Mark D. Betzina
590	497	Wake Turbulence	Nov-76	Dec-76		Vernon J. Rossow, David H. Brown
591	498	Ball-Bartoe Jet Flap Ac	Dec-76	Dec-76		Thomas N. Aiken, Leo P. Hall
592	499	QSRA Model	Jan-77	Jan-77		Kyoshi Aoyagi, Leo P. Hall, Terry Oesch
593	500	Space Shuttle	Jan-77	Feb-77		Ralph L. Maki, Terry Oesch, David H. Brown
594	501	High-Lift Model	Feb-77	Feb-77		Larry E. Olson, David H. Brown, Terry Oesch
595	502	Sikorsky Rotor S-76	Feb-77	Apr-77		Robert H. Stroub, Mark D. Betzina, David H. Brown
596	503	B-77 Parachutes	Apr-77	Apr-77		Ralph L. Maki, David H. Brown
597	504	Wake Turbulence	Apr-77	Apr-77		Vernon J. Rossow, Terry Oesch
598	505	F-16 Forebody	Apr-77	May-77		Leo P. Hall, David H. Brown
599	506	Acoustic Calibration	May-77	May-77		Michael D. Falarski, Mark D. Betzina
600	507	QSRA Model	May-77	Jun-77		Kyoshi Aoyagi, Terry Oesch
601	508	JT8D	Jun-77	Jun-77		Adolph Atencio, David H. Brown
602	509	J-79	Jun-77	Jul-77		Adolph Atencio, Mark D. Betzina
603	510	Small-Scale Nozzles	Jul-77	Aug-77		Adolph Atencio, Leo P. Hall, Mark D. Betzina
604	511	British Nozzles	Aug-77	Aug-77		Adolph Atencio, Leo P. Hall, Mark D. Betzina
605	512	Hybrid Inlet	Aug-77	Sep-77		Michael D. Falarski, David H. Brown, Terry Oesch
606	513	Q Fan	Sep-77	Oct-77		Mark D. Betzina
607	514	Q Fan (Lewis)	Oct-77	Oct-77		Mark D. Betzina
608	515	QSRA	Oct-77	Nov-77		Kyoshi Aoyagi, Leo P. Hall, Terry Oesch
609	516	Parachutes B-77	Nov-77	Nov-77		David H. Brown, Terry Oesch
610	517	Helicopter Drag	Nov-77	Nov-77		DRS, Leo P. Hall, Terry Oesch
611	518	Grumman VTOL (Q Fan)	Dec-77	Dec-77		Mark D. Betzina
612	519	Wake Turbulence	Dec-77	Jan-79		Vernon R. Rossow
613	520	Strut Shake	Jan-78	Jan-78		Wayne R. Johnson, David H. Brown

Item No.	Test No.	Test Title	Start Date	Finish Date	Objectives	Engineer(s)/Test Director
614	521	Stall Spin	Feb-78	Feb-78		Terrence W. Feistal, David H. Brown
615	522	De Havilland VTOL Ejector	Feb-78	Mar-78		Thomas N. Aiken, Mark D. Betzina
616	523	High-Lift Model	Mar-78	Apr-78		Lawrence E. Olson
617	524	Propulsion Drag	Apr-78	Apr-78		Victor R. Corsiglia, Terrence W. Feistal, David H. Brown
618	525	XV-15 Tilt Rotor	May-78	Jun-78		Wayne R. Johnson, Jeff G. Bohn, Mark D. Betzina
619	526	Stall-Spin Test	Jun-78	Jul-78		Terrence W. Feistal, David H. Brown
620	527	Circulation Control	Jul-78	Aug-78		James C. Ross, Alfred A. Lizak, David H. Brown
621	528	JT15D Fan Noise	Aug-78	Sep-78		Warren F. Ahtye, Mark D. Betzina
622	529	Hybrid Inlet	Sep-78	Oct-78		Michael D. Falarski, Mark D. Betzina
623	530	JT15D Fan Noise	Oct-78	Oct-78		Michael D. Falarski, Mark D. Betzina, Warren F. Ahtye
624	531	Stall-Spin Model	Nov-78	Nov-78		Victor R. Corsiglia, David H. Brown, Terrence W. Feistal
625	532	Airframe Noise	Nov-78	Nov-78		Warren F. Ahtye, Michael R. Dudley
626	533	Experimental Wind Turbine	Dec-78	Dec-78		William T. Eckert, Michael R. Dudley
627	534	Heliostat	Dec-78	Dec-78		Mark D. Betzina
628	535	JT15D Aft Quadrant Noise	Dec-78	Jan-79		Warren F. Ahtye, Michael R. Dudley
629	536	Cooling Drag	Jan-79	Feb-79		Victor R. Corsiglia, Michael R. Dudley
630	537	VTOL Fighter Model	Feb-79	Mar-79		Michael D. Falarski, Mark D. Betzina
631	538	De Havilland VTOL Ejector	Feb-79	Mar-79		Kyoshi Aoyagi, Michael R. Dudley
632	539	X-Wing Rotor	Mar-79	May-79		John L. McCloud III, Leo P. Hall
633	540	AST Jet Noise	May-79	Jun-79		Adolph Atencio, Leo P. Hall
634	541	Mitre Communication Antenna	Jun-79	Jun-79		David H. Brown, Michael R. Dudley
635	542	De Havilland Augmentor	Jun-79	Jul-79		Kyoshi Aoyagi, Michael R. Dudley
636	543	VTOL Fighter	Jul-79	Aug-79		Michael D. Falarski, Paul T. Soderman
637	544	Cooling Drag	Aug-79	Sep-79		Victor R. Corsiglia, Michael R. Dudley, Philip R. Barlow
638	545	Research Rotor	Sep-79	Oct-79		Wayne R. Johnson, Alfred A. Lizak, Raymond Piziali
639	546	VTOL Fighter	Oct-79	Nov-79		Michael D. Falarski
640	547	Wing-Fuse Interaction	Nov-79	Dec-79		Victor R. Corsiglia, Philip R. Barlow, Terrence W. Feistal
641	548	Cooling Drag	Dec-79	Jan-80		Victor R. Corsiglia, Philip R. Barlow
642	549	Fan Inlet Distortion	Jan-80	Jan-80		Michael R. Dudley
643	550	Bearingless Main Rotor	Jan-80	Mar-80		William G. Warmbrodt, John L. McCloud III, Mark D. Betzina
644	551	JT15D Noise (Langley)	Mar-80	Mar-80		AK, CH

Item No.	Test No.	Test Title	Start Date	Finish Date	Objectives	Engineer(s)/Test Director
645	552	JT15D Acoustics (GE)	Mar-80	Mar-80		AK, CH, Adolph Atencio
646	553	Turbulence Studies	Mar-80	Apr-80		Philip P. Barlow, Victor R. Corsiglia
647	554	ABC Rotor	Apr-80	May-80		Alfred A. Lizak, Fort F. Felker, Jeff G. Bohn
648	555	698 Tilt Nacelle VTOL	May-80	Jul-80		Michael D. Falarski, Michael R. Dudley
649	556	VATOL	Jul-80	Jul-80		David G. Koenig, Fred Stoll
650	557	Sandia Parachutes	Jul-80	Jul-80		Victor R. Corsiglia, Philip P. Barlow, James C. Ross
651	558	High-Angle-of-Attack Studies				
		Wind Tunnel Shut Down July 1980				
652	558	Grumman Small-Scale Hover	Mar-83	May-83		Susan Braden
653	559	Bearingless Main Rotor	May-83	May-83		William G. Warmbrodt
654		**Wind Tunnel Shut Down June 1983**				
655	560	BO-105 Rotor - Hover	Jul-83	Jul-83	Test cancelled	
656	561	Balance Calibration-RTR	Oct-83	03/04/1984		Robert H. Stroub
657	562	Rotor Wing - Noise RTR - Hover	Mar-84	08/30/1984		Robert H. Stroub
658	563	Alperin Ejector Model	Sep-84	10/30/1984		GA
659	564	40x80 IST	Sep-86	Mar-87	Facility perf./flow calibration	Michael D. Falarski, Thomas N. Aiken
660	565	IST/Flow Calibration	May-87	Jun-87	Facility perf./flow calibration	Peter T. Zell, Robert D. McMahon
661	566	Mini Drogue Test	Jul-87	Jul-87	Drougue dynamics	Lawrence A. Meyn, Nina M. Scheller
662	567	Balance Calibration	Aug-87	Oct-87		Trent J. Thrush
663	568	V-22 Performance	Oct-87	Jun-88	Forward-flight performance and hover download	Fort F. Felker, Nina M. Scheller
664	569	E-7A	Nov-88	Dec-88	Transition performance	Brian E. Smith, Robert D. McMahon
665	570	Hose Drogue	Jan-89	Feb-89	Drougue dynamics	Lawrence M. Meyn, Nina M. Scheller
666	571	F-111 Crew Capsule with Parachute	Mar-89	Apr-89	Crew capsule chute ejection trajectory	Robert E. Faye
	572	Facility Diffuser Column Evaluation Test	Apr-89	Apr-89		Ruth M. Heffernan
667	573	Interactional Aerodynamics	May-89	Jul-89	Rotor performance	Gloria K. Yamauchi, Thomas R. Norman
668	574	LHX	Jul-89	Oct-89	Rotor performance and airframe aerodynamics	Larry A. Young, Randall L. Peterson
669	575	Interactional Aerodynamics 2	Jan-90	Apr-90	Rotor performance	Gloria K. Yamauchi, Alexander W. Louie
670	576	NOTAR (no tail rotor)	Apr-90	Jul-90	Rotor performance and airframe aerodynamics	Randall L. Peterson, Larry A. Young
671	577	Model Support	Nov-90	Nov-90	Facility systems check	Janet E. Beegle
672	579	V-22	Nov-90	Mar-91	Forward-flight performance	Stephen E. Dunagan, Jeffrey S. Light
673	580	Unsteady Flow Quality/IFC Acoustics	Jun-91	Jul-91	Flow quality/acoustic performance	Janet E. Beegle, Thomas N. Aiken

Item No.	Test No.	Test Title	Start Date	Finish Date	Objectives	Engineer(s)/Test Director
674	582	CRW (canard rotor wing)	Nov-91	Jan-91	Aerodynamic force and moment	Steven D. Christensen, Stephen M. Swanson, Joseph N. Sacco
675	583	MDART	Jan-92	Apr-92	Rotor performance for MD Explorer	Steven A. JackIlin
676	585	SBMR	Jun-92	Oct-92	Rotor performance, structural loads, acoustics	Thomas R. Norman, Robert D. McMahon
	586	SBMR Shake Test	Oct-92	Oct-92		Sesi B.R. Kottapalli, Robert K. Fong
677	587	BO-105	Dec-92	Feb-93	Rotor performance, wind tunnel to flight	Randall L. Peterson, Scott M. Larwood
678	588	BO-105	Feb-93	Apr-93	Rotor loads	Steven A. Jacklin, Robert K. Fong
679	589	Acoustic Calibration	May-93	Jun-93	Acoustic performance	Janet E. Beegle
680	590	ADP (advanced ducted propulsion)	Jun-93	Sep-93	Thrust reversal rejected take-off acoustics	Peter T. Zell
681	591	Acoustic Coupon	Sep-93	Nov-93	Acoustic performance of new liner	Scott M. Larwood, Joseph N. Sacco, Sandy R. Liu
682	592	HSR (high-speed research)	Nov-93	Jan-94	Jet acoustics	Janet E. Beegle, Thomas N. Aiken
683	594	HSCT (high-speed civil transport)	Feb-94	Mar-94	Performance/S&C	Peter T. Zell
684	595	BO-105 IBC (individual blade control)	Mar-94	Jun-94	Rotor performance, wind tunnel to flight	Steven A. Jacklin, Scott M. Larwood
685	596	HEAT ISO	Jun-94	Nov-94	Baseline propulsion acoustics for HEAT SS	Mariano M. Perez, Brian E. Smith
686	597	SHARC 1	Nov-94	Mar-95	Stealth aero performance and maneuverability	Stephen J. Craft, Paul A. Askins, Lawrence M. Meyn, Jeffrey J. Samuels
687	598	Acoustic Coupon	Jan-95	Jan-95	Acoustic performance of new liner	Joseph N. Sacco
688	599	HEAT Semispan	Mar-95	May-95	Airframe/propulsion acoustics	Janet E. Beegle, Brian E. Smith
689	600	SHARC 2	Jun-95	Aug-95	Stealth aero performance and maneuverability	Leo DeGreef, Mariano M. Perez
690	601	DC-10 Noise Studies	Aug-95	Sep-95	Airframe noise	Ross Shaw, William C. Horne
		Wind Tunnel Shut Down September 1995				
691	40-0043	IST	08/24/98	11/13/98		Paul A. Askins, Joseph N. Sacco
692	40-0045	SHARC CMT Test	11/09/98	02/16/99		Mariano M. Perez
693	40-0047	1903 Wright Flyer	02/19/99	03/18/99		Peter T. Zell
694	40-0071	Tailplane Icing Test	06/14/99	08/23/99		Paul A. Askins
695	40-0070	Acoustic IST	09/06/99	10/12/99		Paul A. Askins, Joseph N. Sacco
696	40-0075	JSF Validation	10/18/99	10/28/99		Paul A. Askins
697	40-0077	SHARC CMT Test II	11/01/99	12/02/99		Mariano M. Perez
698	40-0062	TRAM	08/01/00	12/19/00		Janet E. Beegle
699	40-0098	CEi Drone	06/04/01	07/02/01		Janet E. Beegle, Joseph N. Sacco

Item No.	Test No.	Test Title	Start Date	Finish Date	Objectives	Engineer(s)/Test Director
700	40-0094	STAR	08/03/01	10/01/01		Thomas K. Arledge
701	40-0104	TX RX Antenna Test	03/06/02	03/14/02		Thomas K. Arledge
702	40-0105	LRTA UH-60 Wide Chord Blades with IBC	08/01/02	01/30/03		Thomas R. Norman, Patrick M. Shinoda, Thomas K. Arledge
		End of NASA Operation				
		Start of AF Operation				
1	40-001	40x80 IST 1	01/22/07	01/26/07		Joseph N. Sacco
2	40-002	Magnus Wind Turbine	02/01/07	02/07/07	Proof of concept	Jeffrey L. Johnson, Joseph N. Sacco
3	40-003	IST 2	04/09/07	04/19/07	Integrated system testing (checkout)	Joseph N. Sacco
4	40-003	NSMS for Tunnel Drive Fans	07/18/07	07/18/07	Non-intrusive stress measurement system	Joseph N. Sacco
7	40-005	LRTA Training	10/29/07	01/28/08	Large rotor test apparatus	Thomas R. Norman, Jeffrey L. Johnson
12	40-009/12	DARPA/Boeing SMART Rotor	03/13/08	04/28/08		Benton H. Lau, Patrick W. Goulding
16	40-006	NASA/Army LRTA UH-60 IBC	07/01/08	04/04/09		Thomas R. Norman, Patrick M. Shinoda, Jeffrey L. Johnson
20	40-010	NASA/Army LRTA UH-60 Airloads	01/15/10	05/15/10		Thomas R. Norman, Patrick M. Shinoda, Justin W. McLellan
24	40-019	DARPA/Sikorsky Active Rotor Control	10/18/10	03/11/11		Charles R. Rogers
26	40-030	Navy/Boeing P-8A	03/14/11	04/22/11	P8A, Antisub P-3 replacement	Jonathon D. Gesek
28	40-017	Air Force/Lockheed Speed Agile Concept Demo (40x80)	06/06/11	10/14/11	C130 replacement	Patrick W. Goulding
29	40-038a	NASA Hypersonic Inflatable Aerial Decelerator	10/17/11	10/21/11		Stephen J. Lee
30	40-021	NASA/Cal Poly CESTOL Aircraft	10/29/11	02/22/12	Cruise efficient short takeoff & landing	Charles R. Rogers, Christopher S. Hartley
31	40-038	NASA Hypersonic Inflatable Aerial Decelerator	04/03/12	09/07/12		Stephen J. Lee, Patrick W. Goulding
	40-057	Sikorsky S-97 Coaxial Rotor	02/06/13	06/24/13		Stephen J. Lee
	40-043	NASA/Boeing AFC Vertical Tail	07/01/13	12/04/13	767 tail with active flow control	Charles R. Rogers
	40-063	High-Frequency Acoustic Cal	12/02/13	12/19/13		Arturo R. Zamora
	40-073	NFAC 40x80 BMS Runs	04/14/14	04/15/14	Fan drive blade monitoring system	Hudson L. Brower
	40-078	NASA ERA Hybrid Wing Body (HWB)	11/24/14	03/04/15		Hudson L. Brower, Adam R. Tupis
	40-070	Sikorsky CARTR 2 (S-97)	03/03/15	05/29/15		Arturo R. Zamora, Hudson L. Brower
	40-053	DARPA-Sikorsky TER (S-76 Type on RTA)	09/01/15	04/01/16		Christopher S. Hartley, Christopher J. Northrup

Item No.	Test No.	Test Title	Start Date	Finish Date	Objectives	Engineer(s)/Test Director
	40-091	RTA Checkout with S-76 Rotor	04/04/16	07/01/16		Christopher S. Hartley, Christopher J. Northrup
	40-062	Army-Sikorsky CARTR Propulsor	07/05/16	11/11/16		Adam R. Tupis, Justin M. Ellerbee
	40-089	40x80 Flow Calibration Part 1	11/14/16	02/10/17		Ryan Tatro, Justin M. Ellerbee, Barry J. Porter
	40-092	NASA TTR Checkout with 609 Rotor	02/13/17	12/11/18	Tiltrotor test rig	Christopher S. Hartley, William B. Bartow
		Wind Tunnel Shut Down June 2017				
	40-101	40x80 Return-to-Service Systems Tests	09/29/17	05/15/18		Justin M. Ellerbee
	40-102	40x80 Return-to-Service Integrated Systems Test	05/15/18	07/24/18		Adam R. Tupis
	40-099	Army Sikorsky CARTR FVL	12/03/18	06/25/19		David W. Wang, Justin M. Ellerbee
	40-097	Navy/AMA Actively Stabilized Refueling Drogue	07/15/19	08/06/19		Kevin S. Boyce, Barry J. Porter
	40-055	40x80 Low-Frequency Acoustic Calibration (Army)	08/19/19	11/29/19		William R. Bartow
	40-080	AATD-Sikorsky Rotor Prop	12/02/19	07/24/2020		William R. Bartow, Scott B. Edwards
	40-111	F-16 Canopy Water Pooling Test	7/27/2020			Kyle S. Lukacovic, Kevin S. Boyce

Table B2. History of Tests in the 80- by 120-Foot Wind Tunnel

Item No.	Test No.	Test Title	Start Date	Finish Date	Objectives	Engineer(s)/Test Director
1		IST/Flow Calibration	10/21/1987	3/14/1988	Facility performance/flow calibration	Thomas N. Aiken, Robert D. McMahon
2		Advanced Recovery System Parafoil	9/1/1988	9/30/1988	Parafoil performance	Fred Elliot
3	805	Base Drag (truck)	10/1/1988	11/12/1988	Tractor trailer	Wendy R. Lanser, James C. Ross
4		Personnel Stand	11/12/1988	11/15/1988	Airport aircraft access stands under wind loads	Wendy R. Lanser
5		E-7A	7/5/1989	10/15/1989	Transition performance	Brian E. Smith, Tim Naumowicz, Peter T. Zell
6		Model Effects	12/4/1989	2/28/1990	Jet engine effects on the facility	Thomas N. Aiken, Wendy R. Lanser
7		Advanced Recovery System Parafoil	3/1/1990	4/30/1990	Parafoil performance	Fred Elliot, James C. Ross
8		IFC	11/8/1990	4/22/1991	Induction frequency control system performance	Fred Elliot, Michael G. Herrick
9		F-18 Fighter at High Angle of Attack	5/30/1991	12/30/1991	High angle of attack, tail buffet, high lift	Peter T. Zell, Lawrence A. Meyn
10	815	S-76 (RTA)	2/1/1992	5/1/1992	Rotor performance and acoustics	Patrick M. Shinoda, David B. Signor
11		Parafoil Glide Enhancement	7/1/1992	8/10/1992	Parafoil performance	Paul A. Askins, James C. Ross
12		BVI (blade vortex interaction)	8/13/1992	8/27/1992	Basic rotor acoustic research	Janet E. Beegle
13		S-76 Blade Fold	9/11/1992	9/16/1992	S-76 blade fold under wind loads	Steven D. Christensen, David B. Signor
14		Wake Vortex	12/1/1992	1/15/1993	Wingtip vortex measurements	Joseph N. Sacco, Vernon J. Rossow
15		BVI (blade vortex interaction)	1/19/1993	4/2/1993	Basic rotor acoustic research	Steven D. Christensen, Cahit Kitaplioglu, Stephen J. Craft
16		Shuttle Drag Chute	4/1/1993	4/30/1993	Chute stability on landing	Mariano M. Perez, Thomas N. Aiken
17		T-39	5/1/1993	6/15/1993	High-lift research	Paul A. Askins, James C. Ross, Bruce L. Storms, Joseph N. Sacco
18		F-18 Fighter at High Angle of Attack, Phase 2	7/6/1993	10/30/1993	Forebody vortex control, tail buffet	Wendy R. Lanser, Gavin Botha
19		Wake Vortex 2	8/8/1994	10/19/1994	Wingtip vortex measurements	Robert K. Fong, Vernon J. Rossow
20		Base Drag (truck)	10/22/1994	11/30/1994	Tractor trailer	James C. Ross, Karlin Roth Toner
21		CALF (common affordable lightweight fighter)	10/18/1995	2/28/1996	Transition performance, ground effects	Paul A. Askins, Tim Naumowicz
22	828	XV-15 (RTA)	3/1/1996	3/25/1996	Tilt rotor performance and noise reduction	Jeffrey S. Light, Robert K. Fong

Item No.	Test No.	Test Title	Start Date	Finish Date	Objectives	Engineer(s)/Test Director
		Wind Tunnel Shut Down March 1996				
23	80-0028	JSF Hover 1 Lockheed/Martin (LMCO)	11/25/1996	1/11/1997		Paul A. Askins
24	80-0034	JSF Hover 2 Lockheed/Martin (LMCO)	7/14/1997	8/14/1997		Paul A. Askins
25	80-0040	JSF Hover 3 Lockheed/Martin (LMCO)	1/20/1998	2/23/1998		Paul A. Askins, Mariano M. Perez
26	80-0042	IST	5/18/1998	7/30/1998	IFC drive tuning	Janet E. Beegle, Joseph N. Sacco, Michael G. Herrick
27	80-0048	XV-15 Noise Reduction Test	10/15/1998	11/9/1999		Mark D. Betzina, Robert K. Fong
28	80-0076	Flow Calibration	11/15/1999	12/9/1999		Paul A. Askins
29	80-0072	Unsteady Aero Pre Test Phase. NREL Wind Turbine	1/4/2000	4/14/2000	10-m wind turbine installation	Janet E. Beegle, Joseph N. Sacco
30	80-0072	Unsteady Aero Test Phase. NREL Wind Turbine	4/17/2000	6/6/2000	10-m wind turbine test	Janet E. Beegle, Joseph N. Sacco
31	80-0087	Tilt-Rotor Descent Aero Test	6/26/2000	8/11/2000	Ring vortex state	Mark D. Betzina, David E. Jordan
32	80-0088	Dash 8 Crosswind Test	9/7/2000	9/14/2000	Measure dynamic strain gage loads for 2 propeller blades on the left-hand engine and record nacelle temperature data for the right-hand engine.	Steven J. Buchholz
33	80-0080	LRTA Checkout Phase I	9/21/2000	4/20/2001	Test bed validation	Thomas R. Norman, Patrick M. Shinoda, Alfred A. Lizak, David E. Jordan
34	80-0080	LRTA Checkout Phase II	4/23/2001	2/13/2002	Forward flight validation and IBC test	Thomas R. Norman, Patrick M. Shinoda, Stephen A. Jacklin, Alfred A. Lizak
35	80-0106	NRL Antenna Test	6/17/2002	7/1/2002	Qualification testing for SPQ-9B antenna array	Thomas K. Arledge
36	80-0111	Parachute Test Entry I & II	9/9/2002	6/23/2003	Entry I: 8/28/03 through 10/31/2002	Peter T. Zell
		End of NASA Operation				
		Start of AF Operation				
5	80-004	80x IST 1	06/27/07	10/15/07		Joseph N. Sacco
6	80-007	MSL Phase 1	10/16/07	10/19/07		Joseph N. Sacco
8	80-011	Sikorsky S-92	11/05/07	11/09/07		David E. Morrison, Joseph N. Sacco
9	80-008	NASA MSL Parachute Phase II	11/27/07	12/03/07		Justin W. McLellan, Joseph N.Sacco
10	80-004a	NSMS	02/27/08	02/28/08		Joseph N. Sacco
11	80-014	NASA MSL Parachute Phase III	03/10/08	03/14/08		Justin W. McLellan

Item No.	Test No.	Test Title	Start Date	Finish Date	Objectives	Engineer(s) / Test Director
13	80-004b	80x IST 2/ NSMS	05/09/08	05/21/08		Joseph N. Sacco
14	80-015	NASA MSL Parachute Phase IV	06/02/08	06/06/08		Charles R. Rogers, Joseph N. Sacco
15	80-018	NASA MSL Parachute Phase V	07/01/08	07/17/08		Charles R. Rogers
17	80-004c	80x IST 3 (drive bus)	12/19/08	01/05/09		Joseph N. Sacco
18	80-022	NASA MSL Parachute Phase VI	03/30/09	04/09/09		Patrick W. Goulding
19	80-004d	80x IST 4/ NSMS	08/28/09	10/01/09		Joseph N. Sacco
21	80-004e	80x IST 5	01/06/10	01/06/10		Joseph N. Sacco
22	80-020	DOE/LLNL Tractor/Trailer	01/25/10	03/15/10		Christopher S. Hartley
23	80-033	NASA Acoustic Array Survey	03/22/10	03/26/10		Christopher S. Hartley
25	80-040	NFAC Fan Drive System IST	01/03/11	01/14/11		Christopher S. Hartley
27	80-016	Air Force/Lockheed Speed Agile Concept Demo (80x120)	04/12/11	05/31/11		Patrick W. Goulding
	80-050	NASA Low-Density Supersonic Decelerator (80x120)	10/01/12	03/07/13		Patrick W. Goulding
	80-072	NFAC Drive IST	04/04/14	04/09/14		Hudson L. Brower
	80-074	NFAC 80x120 BMS Runs	04/16/14	04/17/14		Hudson L. Brower
	80-077	NFAC 1/50th-Scale Inlet Efficiency Study	10/04/14	11/26/14		Alan J. Wadcock, Arturo R. Zamora
	80-076	NASA Orion CPAS Parachute Stability	12/08/14	01/23/15		Patrick W. Goulding
	80-071	NASA JPL InSIGHT Parachute	02/09/15	02/13/15		Ary J. Glantz
	80-084	NASA ESA ExoMars Parachute Assembly System	06/22/15	08/21/15		Joseph N. Sacco, Patrick W. Goulding
	80-086	NASA JPL InSIGHT Parachute Phase 2	10/05/15	11/20/15		Patrick W. Goulding, Ary J. Glantz
	80-075	DARPA-Northrop Grumman TERN PIE-1	10/03/16	01/13/17		Hudson L. Brower, David W. Wang, Patrick W. Goulding
	80-046	DOE/LLNL Super Truck	01/16/17	03/31/17		Christopher M. Nykamp, Patrick W. Goulding, Christopher S. Hartley
	80-082	Army Natick Ram Air Parachute	04/03/17	05/04/17		Justin M. Ellerbee, Charles R. Rogers
	80-088	NASA JPL Mars 2020	05/08/17	06/09/17		Adam R. Tupis, Christopher M. Nykamp
		Wind Tunnel Shut Down June 2017				

National Aeronautics and
Space Administration

Ames Research Center
Moffett Field, California 94035-1000

ISBN 978-0-578-81608-1
90000>
9 780578 816081